Potential impacts of late-Quaternary environmental changes - from the Last Glacial Maximum to the Little Ice Age - on migratory birds in the Americas

OLGUIN-VILLA, MONICA,CECILIA

Potential impacts of late-Quaternary environmental changes – from the Last Glacial Maximum to the Little Ice Age – on migratory birds in the Americas

by

Monica Cecilia Olguin Villa

Durham University

Department of Biosciences

This thesis is submitted in candidature for the degree of

Master of Science

DECLARATION

The material contained within this thesis has not previously been submitted for a degree at Durham University or any other University. The research reported within this thesis has been conducted by the author unless indicated otherwise.

ABSTRACT

The aim of the study was to explore how climatic changes during the last twenty six thousand years may have impacted upon the potential breeding and non-breeding distributions of a range of predominantly migratory bird species that breed in the Americas. The period examined encompasses both the Last Glacial Maximum and the Holocene thermal optimum, the two extremes of climate during the recent geological past. Two contrasting groups of birds were chosen for study: shorebirds in the families Charadriidae, Haematopodidae, Recurvirostridae, Scolopacidae that feed principally on invertebrates and predominantly breed in areas of open vegetation and/or around water bodies; and hummingbirds in the family Trochilidae that are predominantly nectar feeders and occupy a variety of terrestrial habitats, including forests. Climate Response Surface (CRS) models were fitted describing the relationship between each species' current breeding/non-breeding distribution and a limited set of bioclimatic variables. The models were then used to predict potential past distributions using climate scenarios derived from a series of general circulation model experiments. In all cases a small number of bioclimatic variables with known mechanistic relationships to species' distributions were selected *a priori*. Model performance was assessed using AUC, TSS and Kappa values and was generally high. The principal exception was for the non-breeding ranges of many shorebirds that are restricted to coastal areas but which the models projected to be extensive also in inland areas. The results showed that most species' distributions have potentially shifted, in many cases quite substantially, in response to past climatic changes, but that for most species examined the extent of potentially suitable area had changed relatively little. Greatest impacts were predicted for Arctic-breeding shorebirds, including most members of the Scolopacidae, distributions of which were reduced in extent and shifted during the glacial, extending only as the Laurentide ice sheet decayed during the late-glacial and early Holocene. Climate scenarios for Heinrich events had greater impacts than had that for the glacial maximum, potential distributions of many North American breeding species being shifted to northern South America under these scenarios. The results provide evidence of the vulnerability of many Arctic-breeding species to past climatic changes, whereas species with breeding distributions in tropical regions likely did not change their distributions or range extents to any marked degree.

ACKNOWLEDGMENTS

Firstly, I would like to thank Durham University and especially to the Department of Biosciences for becoming my second home, accepting me and allowing me to do research. Also, to CONACyT for providing the scholarship that allowed me to work abroad.

I would like to especially thank my supervisor Professor Brian Huntley for all the help, the attention and kindness he has provided since day one, it has made my work enjoyable and enthusiastic to learn new things. I'll look forward to future conversations and acquiring more knowledge from you.

The people in lab 12, Ali, Dr. Judy Allen, and of course Polly, have provided me with very good memories and knowledge about the British culture. I also would like to thank Yvonne Collingham for her help when using the models and doing the maps, thank you for allowing me to learn from you.

To my friends and second family in Durham, especially to Diana, Jaime, Ary, Ernesto, Camila, Biagio, Annalisa, Consuelo, Nico, Sergio, Elba, Karis, Andreanna, Michelle, Shelley, Menno, Vania, Xiao… You are so many! And I am so glad I met you, you have made my time in Durham enjoyable and especially a learning experience when cooking.

To my 'mapaches' Santos, Henry, Nava. I love you guys! Also, to Jovita, Mamá Eva, Pablo, Marem for accepting me in your family and for all your advice and support in this process.

To my parents Rita and Roberto, and my brothers Angel and Andrés, this is for you and for supporting me in every aspect, -even if my goals sometimes are weird ones-; thanks to you I have achieve a beautiful life goal that makes me believe that dreams do come true.

To Erandi, without your support I could have not achieved this, thank you for embarking in this journey with me, I am eternally grateful for all you have done.

Lastly, to all the people who directly or indirectly help me and supported me during this time, I am truly grateful for everything.

CONTENTS LIST

LIST OF TABLES

LIST OF FIGURES

CHAPTER 1 INTRODUCTION

The present study aims to understand how climatic changes of the last around (*ca*.) 25,000 years, spanning both the Last Glacial Maximum (LGM, *ca*. 21ka) and the Holocene thermal maximum (*ca*. 7 thousand years i.e. 'ka'), have influenced the distributions of migratory birds in the Americas. This is addressed by focusing on two groups of birds that migrate within the Americas, the Shorebirds (families Charadriidae, Haematopodidae, Recurvirostridae, Scolopacidae) and the Hummingbirds (family Trochilidae), both spending either their breeding season in North America, i.e. Canada, United States of America and Mexico, and their non-breeding season mostly in Mexico, and Central and/or South America, for a total of 63 species.

The background to the study is described in Chapter 2, beginning with a summary of how climate in the Americas has varied in the past, especially between the LGM and 1 ka. Particular attention is given to significant climatic changes associated with Heinrich events H2 (24 ka), H1 (17 ka) and H0 (13 ka), the latter coinciding with the onset of the Younger Dryas stadial *ca*. 12.9 ka. Although this stadial seems to have been expressed differently in the Americas than in Europe, where it was first recognised and is most clearly expressed, it will nonetheless be considered.

Descriptions of the two study groups of birds Hummingbirds (Family Trochilidae) and Shorebirds (Families Charadriidae, Haematopodidae, Recurvirostridae and Scolopacidae) then follow, outlining for each species to be studied its natural history and records (when available) of where it might have occurred in the past. The history of development of the modelling approaches used is then outlined, including consideration of how this has influenced research in the field of biogeography.

Attention focuses upon Species Distribution Models (SDMs) and General Circulation Models (GCMs), especially coupled Atmosphere–Ocean GCMs, these being the principal modelling approaches used. Whereas GCMs are used to provide simulations of past (or future) climatic conditions, given knowledge of the relevant forcing factors, SDMs are used to make projections of species' potential distributions under changed climatic conditions in the past or future. It is important to consider that uncertainties arise with all such modelling approaches. This is discussed especially in relation to SDMs where the nature and number of variables

used when fitting the models is important if robust models are to be obtained that are accurate whilst avoiding the dangers of over-fitting.

Chapter 3 provides descriptions and explanations of the data and methods employed in this study. The sources of the bird distribution and climatic data and of the palaeo-climatic simulations are described, along with the methods used to transform these into the forms required for fitting and applying SDM. The SDM approach used is outlined, including the approach used to select the variables used to fit these models.

The results of the modelling are presented in Chapter 4 as a series of maps for each species showing their present and potential past seasonal distributions (from 1 to 26 ka) as projected by the SDMs used. This enables comparison of the models used, as well as showing how past climatic changes may have shifted the distributions of the birds. The maps are used to explore whether the impacts of past climatic changes may have differed between Hummingbirds and Shorebirds, as well as between individual species, and especially to consider how species' migratory behaviours may have been influenced.

In Chapter 5 the discussions are presented, from the model performance for each range species to the patterns of the projections made, with a comparison between species of each family and given insight to similar studies using SDMs models and the climate from the Late Pleistocene until current time. There is also a discussion about how using one modelling approach potentially could be over-fitted with no cross- validation analysis. It is important to state the awareness of the limitations of the modelling approach and the study itself, however, it does give insight into what could potentially happen to species suitable climatic areas, with comparisons made with other studies.

The conclusions of the study are presented in Chapter 6, where the main points given by the results and discussion section are described, from the CRS model performance to the projected bird ranges over the last 26,000 years which gives hindsight of the key role of climate over the migratory preferences of birds, hence, concluding the study.

CHAPTER 2 BACKGROUND TO THE STUDY

2.1 Climate history

I will begin by describing the climatic history of the American continent, from Heinrich event 2 (*ca*. 24 ka) to 1,000 years ago. Climate can be defined as a description of the average variability of weather (i.e. temperature, precipitation, wind) generally during a period of 30 years as set by the World Meteorological Organization (WMO), meaning: a description of the state of the climate system (Marshall and Plumb 2008).

Given the climatic history of the Earth it is well known that climate has not remained static; instead, it appears constantly to fluctuate on all timescales (Adams et al. 1999). Numerous studies have tried to understand the climatic history of the Earth, specifically the events that caused greater changes in the ecosystems (Hawkins and Porter 2003, Clark et al. 2012).

For many millennia climate has been one of the key factors in changing conditions, mainly transforming the structure and composition of the flora and fauna around the world (Delcourt and Delcourt 1988, Graham and Grimm 1990); this can be supported by the understanding of the climate system, which is ruled by several factors (Bartlein 1997), primarily by insolation -as a response of orbital forcing-, that occurs during a particular timescale, between 20 to 100 ka, as it has been proven by fossil records (Hays et al. 1976). In addition, it is important to mention the Thermohaline Circulation (THC), meaning the temperature and salinity of the seawater that plays an important role in rapid climate changes, only that with a very different time scale of every 1,000 years (Bartlein and Prentice 1989, Huntley et al. 2014).

One of the most discussed periods given its ‘sudden’ climate variability (especially during the Pleistocene) is the Quaternary (Lowe and Walker 2015). The term Quaternary was first introduced by J. Desnoyers in 1829 as a geological term for the younger deposits that corresponds to the last 2.588 million years (Ma). The Quaternary Period is widely recognized as an interval with many large-scale environmental fluctuations (Bradley 2014); it is divided into two epochs named Pleistocene and Holocene.

The Pleistocene corresponds to the first part of the Quaternary 2.588 Ma to 11.7 ka, a well-studied epoch given the records of climate, with radical changes that have been identified as

glacial and interglacial stages in which mainly the temperature shifted drastically affecting ecosystems and species around the world.

During the late Pleistocene and especially after the LGM (*ca.* 21 ka), the climate began to be less variable than most of the Pleistocene epoch and gave way to more settled conditions, accordingly to the evidence of fossils, ice cores, and other indicators that suggest that these adjustments on the environment, were key elements that enhance the development of how the flora and fauna is distributed nowadays.

The Holocene epoch then covers the remaining time from 11.7 ka until the present day. During this period, climatic changes have also been registered, but on a different and smaller scale than the Pleistocene (Adams et al. 1999). The late Holocene has significant importance in the settlement of human populations given that promoted the development of agriculture, livestock and more recently industry (Hannes 1998, Mayewski et al. 2004, Singarayer and Davies-Barnard 2012).

2.1.1 Pleistocene

The Pleistocene epoch, as mentioned above, corresponds to the interval between 2.588 Ma and 11.7 ka, covering almost entirely the Quaternary Period. It is described as the most dynamic epoch because of its radical changes in global temperatures (Bradley 2014).

These variations in climate have been registered all around the world through the study of paleoclimates and paleovegetation, although most of the evidence is from regions with temperate and relatively humid climates that promote the preservation of the palaeoclimatic archives and provide clearer indication of such changes (Hendrickson and Minckley 1985, Cowardin et al. 1992).

The records studied include pollen from lake sediment cores and mires, remains of various planktonic organisms from ocean sediments, ice cores, coral growth rings, tree rings and packrat (*Neotoma*) middens, among others (Meyer 1973, Betancourt et al. 1990, Brunelle et al. 2010, Bradley 2011) that seems to indicate a correlation between the climatic conditions and the records.

It is important to understand that even though nowadays the vegetation and landscape of North America and South America are very distinct, during the late Pleistocene conditions

were considerably more similar in both hemispheres. For example, some of the records for North America suggests that conditions were colder and arid in the regions that were not covered by ice (Whitlock and Bartlein 1997), and for South America, conditions were consistent and indicative of cooler and drier climate (Markgraf 1993).

2.1.2 Last Glacial Maximum

The Last Glacial Maximum (LGM) corresponds to the time of maximum global ice volume during the most recent glacial period of the Pleistocene and corresponds to a global expansion of ice sheets (Rutter et al. 2012).

Over the past few years the beginning of the LGM has been in debate; several studies have proposed the beginning of the LGM at around 26.5 ka BP to 19 ka BP (Clark et al. 2009, Shakun and Carlson 2010); however, some studies still considered the maximum reach of the ice sheets would be around 21 ka BP (Brunelle et al. 2010, Bartlein et al. 2014).

The ice sheets during the LGM covered large parts of the Northern Hemisphere, including most of Alaska and Canada, northern parts of the conterminous United States and much of north-west Europe.

In North America, the ice sheet has been divided into three main component ice sheets: the Cordilleran ice sheet which covered the Canadian Rockies, Western Canada and Alaska; the Laurentide ice sheet extending from the Central and Eastern parts of Canada to the Central United States; and the Greenland ice sheet which covered Greenland (Clark and Mix 2002).

Given the growth of the glaciers, extensive volumes of water were extracted from the oceans, the climate system changed dramatically, and shorelines were altered substantially as mean sea level fell by up to *ca*. 120 m (Lambeck et al. 2000, Clark and Mix 2002).

For the vegetation during this period, a study suggests for the east region of Canada the landscape was covered by polar desert, and on the east-southeast by tundra; the rest of the territory was covered by ice (Whitlock and Bartlein 1997).

For the south-central part of the United States during the LGM, the vegetation tendency was mainly dry alpine tundra and polar desert (Whitlock and Bartlein 1997). For the remainder of the United States, even though an ice sheet did not cover it there is evidence that in the southeast (including Florida), the land was a mixed vegetation of desert dunes and sparse

scrub (Wells 1992); contrasting the evidence found in the study of (Watts and Stuiver 1980) with vegetation of open woodland for the region. This condition continued through the southwest of United States until it became a treeless steppe (Adams 1996), resulting in a cooler but drier climate.

In the north of Mexico, conditions were similar to the southwest United States, being colder and dryer, although in highlands conditions have remained quite analogous to the present (Markgraf 1993). Conditions around 11 ka BP then quickly became warmer and moister, though with an interruption by cold and aridity in many areas (Adams 1996).

Some comparisons of glacial climates over the American continent suggest that glacial climatic fluctuations in Mexico are different from those in northern parts of North America which were covered by ice, the climatic behaviour in Mexico being inferred to have been controlled more by precipitation than by temperature (Bradbury 1989).

On the other hand, little is understood about the conditions during this time in the Southern Hemisphere (Clapperton 1993, Sylvestre 2009), maybe because of the wider range of ecosystems and geophysical features between latitudes 12°N and 56°S (Clapperton 1993). Precipitation and fire activity were significant during the LGM in South America (Sylvestre 2009, Correa-Metrio et al. 2012).

For instance in Central America (mostly Panama records) and south Mexico in the Peninsula of Yucatan which are characterized by tropical rainforest and warm mixed forest, the sediment cores for the period of the LGM registered 5°C colder than present, with mesic temperate forest vegetation, followed by a rapid increased of *ca.* 3.5°C resulting in warmer conditions (Correa-Metrio et al. 2012).

More evidence of cooler conditions are shown in the study by Hulton et al. 2002, where using a climate model that mimics the LGM conditions, it was possible to inferred that in the Andes, where ice-fields nowadays cover a small proportion of the Patagonia and Cordillera of Darwin, the conditions were *ca.* 6°-5°C colder than current conditions.

There is evidence presented of the complex climatic history for South America (Coronato and Rabassa 2011), differing somewhat from the climatic history in North America with more relatable patterns (Coltrinari 1993). For example, the work from Marchant et al. (2009) in which they used biomisation (methods to reconstruct vegetation types such as biomes) to

reconstruct the paleovegetation is considered to be a key on the understanding of the LGM in this part of the continent. The study presents records from *ca*. 18 ka BP in South America that allows the interpretation of predominant cooler and drier conditions, with a vegetation of grassland and at a minor scale and mostly in the Amazonian vegetation tends to a tropical dry forest.

These characteristics of the environment during the LGM have evolved into stable or constant conditions for the vegetation, climate and species distributions. Regarding the fauna that was living during the LGM, most of the species are similar to the ones found today, only the changes were in their ranges of distribution (Huntley and Webb 1989, Prentice et al. 1991, Davis and Shaw 2001, MacDonald et al. 2008). Even more, some species became extinct during this period mainly in terrestrial species of mammals such as mastodon like the American Mastodon (*Mammut americanum*), mammoths like the Columbian Mammoth (*Mammuthus columbi*), Dwarft Mammoth (*M. exilis*), Wooly Mammoth (*M. primigenius*) and the sabre-toothed cat (*Smilodon fatalis*) (Grayson 1991, Martin 2005).

According to the climate records, the process of deglaciation began with the rapid rising of the summer insolation in the Northern Hemisphere (as established before by the Milankovitch cycle) which in turn led to increased atmospheric CO_2 concentrations (Shakun and Carlson 2010) causing major warming (Labeyrie et al. 2007) at around 19 ka BP (Lambeck et al. 2000).

2.1.3 The Younger Dryas

The Younger Dryas began around 12.9 ka BP and ended about 11.7 ka BP (Broecker et al. 2010). It is recognized as an important event in Earth's history, given that dramatic changes occur around the world, altering the climatic conditions (a cooling event) and interrupting the natural transition from the LGM to the Holocene (Reeder et al. 2011).

This event was triggered by a re-routing of the main meltwater flow from the Laurentide Ice Sheet (Broecker et al. 1989, Teller et al. 2002) that led to a slowing in the Atlantic Meridional Overturning Circulation (AMOC) and what has come to be referred to as Heinrich Event 0 (H0) (Broecker et al. 2010), as discussed later.

The name Younger Dryas comes from the episodes called Older Dryas and Oldest Dryas that refer to fossil leaves of *Dryas octopetala* found in core sediments from Sweden and Denmark. This Arctic–Alpine species is considered a significant indicator of cold climate conditions, hence the event came to be called the Younger Dryas *ca*. 13 ka BP (Straus and Goebel 2011, Carlson 2013); However, studies have shown that the Younger Dryas climatic fluctuation increased in magnitude towards higher latitudes and in the North Pole (Carlson 2013), which could mean that high latitudes are more sensitive to a given climate change (Shakun and Carlson 2010).

2.1.4 Holocene

The Holocene is the most recent epoch, considered to begin around 11,700 years ago and to extend to the present day (Lowe and Walker 2015). During this time, climatic conditions like the events during the Pleistocene did not take place; nevertheless, there are worldwide records that show more modest fluctuations in climate (Bond et al. 1997, Mayewski et al. 2004, Lowe and Walker 2015).

The term ‘stable’ and ‘modern conditions’ for climate have been used in studies of conditions during the Holocene which are interpreted as a contribution to the development of the modern vegetation as well as the modern distribution of animals, and to the rapid advancement of human settlements (Mayewski et al. 2004, Lowe and Walker 2015).

Some studies on global temperature reconstructions suggest how during the beginning and until the middle of the Holocene (9.5-5.5 ka) the climatic conditions began to be established as ‘a modern state’ with warming temperatures of about 0.6°C, often referred to as Altithermal (Lowe and Walker 2015). Studies suggest that during the Holocene the climatic variations were driven mainly by the influence of orbital forcing (Wanner et al. 2011), as well as by variability in solar input (Bond et al. 2001) and by volcanism.

It is also important to mention that there is a diversity and complexity of climatic history shown around the world, mainly in places with very different geomorphological features and with contrasts between the Northern and Southern Hemispheres, known as bipolar see-saw (Lowe and Walker 2015). As a result, in many cases, a clear correlation cannot be observed.

In the Northern Hemisphere at the start of the Holocene between 9-6 ka, through the study of pollen, a prairie and oak savannah vegetation is interpreted as evidence of warmer and drier conditions in some regions of the Midwest of the United States (Wanner et al. 2011). A similar interpretation has been made of pollen analytical data from southwest Arizona (United States) during the early Holocene, suggesting arid conditions (Chenopodiaceae-*Amaranthus* dominance) accompanied by desiccation periods that led to the poor preservation of the pollen spectra (Martin and Mehringer 1966).

In the case of the Southern Hemisphere, global climate reconstructions during the time of the 'Altithermal' in the early Holocene (11-7 ka) appeared to be less warm and even cooler (*ca*. 0.4°C), than the Northern Hemisphere, which is attributed to orbital forcing (Lowe and Walker 2015). However, another study using pollen analysis in Arizona (Moctezuma) suggests moist and cooler conditions for the early Holocene (ca. 8.4 ka), with the presence of *Quercus,* Poaceae and aquatic vegetation being interpreted as an indicator of much greater rainfall than today (Davis and Shafer 1992).

There is evidence that the Holocene has had very shifting and abrupt climatic conditions, in fact, Mayewski et al. (2004) discuss that in this period, at least, six rapid climate change events are recognized, from 9-8 ka, 6-5 ka, 4.2-3.8 ka, 3.5-2.5 ka, 1.2-1 ka, 0.6- ka. Conditions are apparently different for North America and South America during these events, where the first remained cooler and the second drier.

Much more recently a warm period referred to as the Medieval Warm Period (MWP), occurred between about 800 and 1200 A. D. (Broecker 2001). This warm period corresponds to the time of the expansion of the Viking populations into Northern territories (Uriarte-Cantolla 2003).

Whether or not this period was registered globally as a warm interval is very controversial, with considerable discussion of how it was recorded in different parts of the world and varying interpretations of a more regional event rather than a global phenomenon, with most evidence concentrated in the Northern Hemisphere and especially around the Atlantic (Hughes and Diaz 1994, Broecker 2001).

One of the most recent changes registered during the Holocene is the Little Ice Age (LIA) that extended between the 16th and 19th centuries. This event appears also to be most evident in Europe, where it was captured in paintings and historical documents, as well as in the

history of human populations (Mann 2007). During this period there was glacial expansion and the atmospheric circulation was altered (Grove and Switsur 1994), with consequences that in some cases were fatal to human populations (Mann 2007).

2.1.5 Heinrich Events

Heinrich events, named after their discoverer Hartmut Heinrich (Labeyrie et al. 2007), are events that occur in the Atlantic during glacial periods and reflect large-scale ice rafting of rock debris (Heinrich 1988). The ice-rafted debris, or IRD, consists of sediment carried by icebergs or sea ice that settled to the ocean floor when the ice melted (Hemming 2004).

During such events the ocean surface salinity is reduced by the input of fresh water from the melting ice, resulting in slowing or cessation of the AMOC that in turn leads to a rapid shift to a much colder conditions (Heinrich 1988). Such rapid cooling has been recorded in many regions, including the western United States where conditions during such events have been characterised by markedly cold temperatures (Clark and Bartlein 1995, Hostetler et al. 1999).

Six Heinrich Events are recognized during the last glacial period; these events are referred to as H6 (~60 ka), H5 (45 ka), H4 (38 ka), H3 (~31 ka), H2 (24 ka) and H1 (16.8 ka) (Hemming 2004). More recently the Younger Dryas has been recognised to have been a similar event and is now also referred to as H0 (13 ka) (Broecker et al. 2010). As mentioned before, for this study we will only focus on the last three Heinrich events H2, H1 and H0.

2.2 Birds

The first evidence of birds in the fossil record is that of *Archaeopteryx* in the Late Jurassic (around 150 million years ago), firstly found in Solnhofen, Germany in 1861 by Von Meyer which showed how birds radiated from dinosaurs (Ruben 2010). Many years later more fossils of *Archaeopteryx* were found in China (Xu et al. 2011).

It is suggested that birds radiated even before the Tertiary period (Cox 2010), with the modern families have been in existence since the Pliocene epoch before the beginning of the Quaternary, during which the glacial and interglacial periods, as well as continental and sea-level movements, have shaped how birds are distributed around the world today (Newton 2003).

It is important to mention the historical significance of birds: In many ancient civilizations birds have played a significant role as magical or healing organisms, shown in ancient ruins and writings, such as the Quetzals (Family Trogonidae), Hummingbirds (Family Trochilidae) and Eagles (Family Falconidae) in Mesoamerican (pre-Columbian) civilizations such as the Aztecs (Arizmendi and Berlanga 2014).

Current knowledge of birds groups them into 40 Orders, 238 Families, 2297 Genera and around 10,694 species of birds (Gill and Donsker 2018). Birds are one of the most remarkable vertebrates, their varied adaptations allowing them to colonize almost every ecosystem in the world, from terrestrial to marine-coastal environments (Floyd 2008), as well as from Polar Regions to the Tropics (Cox 2010). This is due to their morphology, especially their main feature, namely feathers, and their aerodynamic body shapes that enable their capacity for flying, making traveling relatively easy (Floyd 2008).

Also, birds are influenced by the type of habitat and landscapes where they live. Given that birds are widely spread around the world, they have become important players in ecosystems' natural dynamics, many being specialized in how they feed; for example, hummingbirds feed on the nectar of flowers, thus playing an important role as pollinators, whilst trogons disperse seeds, and vultures consume carrion (Floyd 2008).

Migration is a vital element in the cycle of life of many bird species; large numbers of birds travel every year from North America to South America in the non-breeding season, returning to the north in the breeding season (Floyd 2008). Mostly migratory movements are made to acquire the resources that the species needs for survival and reproduction (Dingle 1996).

Migrant birds are generally classified as long, medium and short distance migrants, according to the distance they travel for the breeding of wintering season. For example, a long distance migrant bird can travel between different continents or hemispheres almost every year in order to reach suitable places for feeding and nesting (Floyd 2008).

It is important to consider the potentially very great implications of past climatic changes for the migration of birds, given that birds are dependent upon particular habitats and resources in different geographical areas (Cox 2010) and during different parts of their annual cycle.

Climatic history has had obvious effects and has influenced how birds are geographically distributed and the patterns of their present migratory behaviour, (Newton 2007). Additionally, as weather might change within a year, species could experience different conditions that are not tolerable for them (Sinclair et al. 2010).

Staging areas used during the migration of birds are a very important key to their success, their importance lies on the fact that they need to rest and refuel for periods of time, that could be from a few days to a few weeks in order to restore the energy lost during the flight (Arizmendi and Berlanga 2014) and/or to gain the body mass excess necessary to sustain the next part of their migration.

2.2.1 Shorebirds

Shorebirds include some of those species making the longest migrations, some species travelling from the Arctic to the Southern limits of Australia, Asia, Africa and South America (Hayman et al. 1991). Although many nest solitarily, most shorebirds during the non-breeding season feed and migrate in flocks, and can be found principally in habitats near water, whether inland or near the oceans (Message and Taylor 2016).

Shorebirds have developed various strategies to enable them to migrate great distances, often traveling at speeds of 60-70 km hr^{-1} (Myers 1983). It is important to mention that, given their reliance upon what are often inherently spatially restricted aquatic and wetland habitats, shorebirds are one of the species groups most negatively affected by habitat loss, especially when migrating (Floyd 2008). In California, for example, at least 70% of wetlands have been destroyed by human activities (Myers 1983). According to past studies it has been suggested that shorebirds can provide important indications of the health of wetlands around the globe (Hayman et al. 1991).

Shorebirds breeding in North America belong to four families: Charadriidae (Plovers); Haematopodidae (Oystercatchers); Recurvirostridae (Stilts and Avocets); and Scolopacidae (Sandpipers, Snipes and Phalaropes). The evolutionary affinities of shorebirds traditionally have been determined on the basis of the morphology they exhibit, although recently behaviour, ecology and DNA analysis have also all been applied to understand their evolutionary relationships (Floyd 2008).

2.2.1.1 Family Charadriidae

Usually known as plovers, this family globally includes 12 genera, 71 species and 112 taxa, of which 17 species are identified as threatened and one species recognized as extinct since de 1600. It is known that Plovers have originated during the late Eocene, around 40 million years ago, (Piersma and Bonan 2018).

Members of this family are characteristically powerful runners and fliers, adapted to harsh habitats and being opportunists. They are small to medium-sized shorebirds; their main features include long legs, rounded head with big eyes and a stubby pointed bill (Piersma and Bonan 2018).

Found mainly in habitats such as open wetlands, mudflats, sandbars and sometimes in dry habitats such as grasslands and tundra, all of which they share mostly with sandpipers (Family Scolopacidae), being the two families that together account for the larger part of shorebirds (Floyd, 2008).The relationship between the families has been studied by many workers as they share the same ecosystems, but unfortunately, there is still no direct evidence that proves their relationship, only that they might have shared the same 'shorebird ancestor' (Piersma and Bonan 2018).

Nearly all plovers feed by plucking invertebrates on or just beneath the ground (hence the pointed bill) like earthworms and also spiders, flies, beetles, ants, among other insects (Hayman et al. 1991). Also, the time when they feed varies depending on the presence of predators, but mostly they search for food during day and night (Piersma and Bonan 2018).

Plovers are migratory species that spend the breeding season mainly in the northern hemisphere, and they usually can travel alone or within several hundred individuals for great distances (Floyd 2008), which seem to be more diversified below the equator (Hayman et al. 1991). For most of the plovers, their behaviour can be considered territorial especially during the breeding season, as well as in stopovers for some species (Piersma and Bonan 2018).

Table 1. Species of Charadriidae studied, including sub-species.

Scientific name	Common name	Breeding range	Non-breeding range
Charadrius collaris	Collared Plover	Resident Central Mexico to South America (Central Argentina).	Same as breeding range.
C. falklandicus	Two-banded Plover	Coasts of South Chile and Argentina.	N of Chile, Uruguay and S of Brazil.
C. melodus including *C. m. melodus* and *C. m. circumcinctus*	Piping Plover (Near Threatened)	*C. m. melodus* Atlantic coast from Newfoundland to the S of Carolina. *C. m. circumcinctus* in Great Plains and Great Lakes, SC Canada and NC USA.	*C. m. melodus* from Carolina to S Florida and the Caribbean. *C. m. circumcinctus* to the coast of Gulf of Mexico.
C. modestus	Rufous-chested Plover	Central and S Chile and Argentina. Falkland Islands too.	N of Chile, Argentina, Uruguay and S Brazil.
C. montanus	Mountain Plover (Near Threatened)	Central America (Great Plains) to the E Colorado and S-W Texas. NE Mexico (Nuevo León).	Central California to Baja California; E to S Texas and NE Mexico.
C. nivosus including *C. n. nivosus* and *C. n. occidentalis*	Snowy Plover (Near Threatened)	*C. n. nivosus* W, Central, South Central USA, to NW, E Central Mexico; Bahamas, Greater Antilles and Leeward Antilles. *C. n. occidentalis* coast of SW Ecuador, Peru and S Central Chile.	*C. n. nivosus* on the S of Panama. *C. n. occidentalis* same as breeding range.
C. semipalmatus	Semipalmated Plover	Mostly arctic regions of Canada (British Columbia, Nova Scotia) and Alaska, part in E Newfoundland.	West coast of USA, Mexico onto Peru and N of Chile. In the East coast of USA, Mexico onto S Argentina, and, in the Caribbean.
C. vociferus including *C. v. vociferus, C. v. ternominatus* and *C. v. peruvianus*	Killdeer	*C. v. vociferus* SE Alaska, S Central Canada, USA, Mexico. *C. v. ternominatus* and *C. v. peruvianus* considered resident to Central America (Caribbean Islands to Peru and NW Chile)	*C. v. vociferus* from S Mexico, Honduras, Guatemala, Belize and NW South America (Colombia, Ecuador and Venezuela).

Table 1. Species of Charadriidae studied, including sub-species (continued**).**

Scientific name	Common name	Breeding range	Non-breeding range
C. wilsonia including *C. w. wilsonia, C. w. beldingi, C. w. cinnamominus* and *C. w. crassirostris*	Wilson's Plover	*C. w. wilsonia* E USA, Mexico and Belize; also in the Bahamas, Greater Antilles and N of Lesser Antilles. *C. w. beldingi* NW Mexico in Pacific coast to S Panama and Ecuador. *C. w. cinnamominus* mainly resident to N of South America. *C. w. crassirostris* resident to NE Brazil.	*C. w. wilsonia* S to N South America. *C. w. beldingi* in S to C Peru.
Oreopholus ruficollis including *O. r. pallidus* and *O.r. ruficollis*	Tawny-throated Dotterel	*O. r. pallidus* resident in N Peru. *O. r. ruficollis* from S Peru to W Bolivia, Chile, Argentina to Tierra del Fuego.	*O. r. ruficollis* E to Argentina and SE Brazil.
Pluvialis dominica	American Golden Plover	Arctic region of North America from Alaska, N of Canada.	South America from SE Brazil, Paraguay to NE Argentina. Some to Tierra del Fuego and Patagonia.
P. squatarola cynosurae	Grey Plover	Arctic North America in coast and islands of Canada.	From coasts of and South America (USA, Mexico, Caribbean to Chile, Brazil and Uruguay).

2.2.1.2 Family Haematopodidae

Commonly known as Oystercatchers, this family includes one genus, nine species and 15 taxa, of which three species are under the category of threatened and one probably extinct. They have a worldwide distribution (mainly in coastal regions) with the exception of the Poles and tropical parts of Africa and Asia (Hockey et al. 2018).

Oystercatchers have specialized compressed bills (Floyd 2008) that are developed to enable them to open bivalve molluscs or crabs on which they feed, and also the bills composed with nerves that allow them to feel when foraging along the shores (Samaniego-Herrera et al. 2007, Message and Taylor 2016).

The birds are medium size, 40-46 centimetres long, the males weighing around 550-650 grams and females from 500-700 grams, usually with black or black and white plumage, long and pinkish legs, and an orange-red dagger bill (Hockey et al. 2018).

Most of the species are distributed in the Southern Hemisphere, where they are also sedentary or with only a few local movements, in contrast to the species breeding in the Northern Hemisphere that usually migrate (Hockey et al. 2018). The species studied are indicated in Table 2.

Table 2. Species of Haematopodidae studied, including sub-species.

Scientific name	Common name	Breeding range	Non-breeding range
Haematopus ater including: *H. a. ater*; and *H. a. bachmani*	Blackish Oystercatcher	*H. a. ater* from N of Peru and all the coastal area of Chile until Tierra del Fuego and S Argentina. *H. a. b.* Aleutian Island, Alaska, W of Canada and USA onto NW of Mexico.	*H. a. ater* NE of Argentina and S Uruguay. *H. a. bachmani* S British Columbia, S California and N of Baja California in Mexico.
H. leucopodus	Magellanic Oystercatcher	SC Chile, Argentina and S of Cape Horn.	Same as breeding going NC of Chile and Argentina in the coast.
H. palliatus including *H. p. palliatus* and *H. p. galapagensis*	American Oystercatcher	*H. p. palliatus* USA East coast, West coast of Mexico, and all coasts of South America *H. p. galapagensis* only in the Galapagos Island.	*H. p. palliatus* from SE USA (Florida), the Caribbean Islands, SE Mexico and SW Guatemala and Honduras.

2.2.1.3 Family Recurvirostridae

Usually known as Stilts and Avocets, this family comprises three genera, seven species and 11 taxa, distributed worldwide (Pierce and Bonan 2016), even though they mainly occur in areas with warm or hot climates (Marchant et al. 2010). Unfortunately, there is not much fossil record of this family that presumably appeared during the early-middle Cenozoic era (Farner et al. 1985).

The birds are characterized by having very long legs and very slender bills (Peterson and Chalif 1999), with slim bodies and small heads. Males weigh between 200-400 grams and are 35-45 centimetres long (Beaman and Madge 1998). They feed mostly on insects, crustaceans and other small aquatic life (Peterson 1960), even in some instances on vegetable matter (Pierce and Bonan 2016). Both the thin-billed stilts and the avocets feed by plucking tiny invertebrates from the surface of shallow and often saline waters (Floyd 2008); avocets also feed sing a scything motion, sweeping their upcurved bills through the water (Message and Taylor 2016).

Given that this family is distributed worldwide they have very distinct movements as well, some being migratory, others partially migratory and some almost sedentary. The species studied are migratory in the Americas and are described in Table 3.

Table 3. Species of Recurvirostridae studied, including sub-species.

Scientific name	Common name	Breeding range	Non-breeding range
Himantopus including *H. h. melanurus* and *H. h. mexicanus*	Black-winged Stilt	*H. h. melanurus* local movements in Chile, E Central Peru, Bolivia, Paraguay, Brazil to S Argentina. *H. h. mexicanus* breeds in W Central USA and small part in E coast USA. The rest mostly local in Mexico, Central America, Caribbean Islands, Galapagos, Colombia, Venezuela, Ecuador, SW Peru and N Brazil.	*H. h. melanurus* local movements in Chile, E Central Peru, Bolivia, Paraguay, Brazil to S Argentina. *H. h. mexicanus* winters in Nicaragua. Species move to South America on local movements in Mexico, Central America, Caribbean Islands, Galapagos, Colombia, Venezuela, Ecuador, SW Peru and N Brazil
Recurvirostra americana	American Avocet	Small part in S Canada (British Columbia and Ontario), Central USA, from Montana, South Dakota to Central Texas and SW in California.	Winters in the coast of California, through N and Central Mexico and Guatemala. Small parts in Honduras, El Salvador and Nicaragua.

2.2.1.4 Family Scolopacidae

Known as Sandpipers, Snipes and Phalaropes, this is considered the largest and most varied family of shorebirds, with 16 genera, 91 species and 146 taxa globally although most of them are restricted to the Northern Hemisphere in their breeding grounds and migrating almost to the edges of the South Pole (Marchant et al. 2010). This is the reason most of them are long-distance migrants with some of the most extraordinary journeys of bird species (Message and Taylor 2016).

They usually are found in the interior of wetlands, coastal salt marshes and ocean beaches, and as with other shorebirds they mainly feed on aquatic invertebrates (Floyd 2008). Birds of medium size (15-66 centimetres), 33 species of this family breeding in the Americas will be studied (Table 4).

Table 4. Species of Scolopacidae studied, including sub-species.

Scientific name	Common name	Breeding range	Non-breeding range
Actitis macularius	Spotted Sandpiper	Almost all Canada (except Nunavut), Alaska and USA until S California, E Arizona, W New Mexico and E Carolina.	From S USA, Mexico, Caribbean Islands and Central America from Colombia to N Argentina and along the coast of Chile.
Arenaria interpres including *A. i. interpres* and *A. i. morinella*	Ruddy Turnstone	*A. i. interpres* breeds in N Canadian Arctic, Greenland, Alaska and N Eurasia. *A. i. morinella* from Alaska to Arctic Canada.	*A. i. interpres* in the coasts of Europe, Africa, Asia, N Australia and Pacific Islands until reaching California and N Mexico. *A. i. morinella* from SE USA (South Carolina), Gulf of Mexico, Argentina and Chile.
A. melanocephala	Black Turnstone	Coast of W and S Alaska.	Pacific coast of SE Alaska through USA until NW Mexico).
Bartramia longicauda	Upland Sandpiper	Central Alaska and Great Plains in USA (NE to Central).	Mainly in Bolivia, Paraguay, Uruguay, S Brazil, and N Argentina.
Calidris alba including *C. a. alba* and *C. a. rubida*	Sanderling	*C. a. alba* Canadian Arctic and Greenland, small part in Alaska. *C. a. rubida* NE Siberia, N Alaska and NW Canada.	*C. a. alba* coasts of Europe, Africa, across Asia and Pacific Islands. *C. a. rubida* on coast E Asia, North America and S America.

Table 4. Species of Scolopacidae studied, including sub-species (continued**).**

Scientific name	Common name	Breeding range	Non-breeding range
C. alpina hudsonia	Dunlin hudsonia*	Central Canada in Manitoba and part of Ninavut until Hudson Bay.	Winters mostly on the E coast USA and a small portion in E Mexico.
C. a. pacifica	Dunlin pacifica*	SW Alaska in the S of Seward Peninsula.	W coast USA and small portion on W Mexico (Baja California).
C. bairdii	Baird's Sandpiper	Canadian Arctic Islands, Alaska and small part in N Canada.	Central S South America in Peru to Chile, Argentina and Tierra del Fuego.
C. canutus including *C. c. roselaari* and *C. c. rufa*	Red Knot	*C. c. roselaari* in the NW Alaska. *C. c. rufa* in the Canadian low Arctic.	*C. c. roselaari* SE coast USA (Florida) to S Panama and N Venezuela. *C. c. rufa* in the NE of South America to the south.
C. fuscicollis	White-rumped Sandpiper	Breeds in Canadian Arctic, N Alaska and N Canada.	SE of South America, from Central Brazil to Tierra del Fuego.
C. himantopus	Stilt Sandpiper	NE Alaska, NW Canada reaching Hudson Bay.	From SE coast USA, Central-S Mexico, across Central America, South America in Colombia, Venezuela, Bolivia, Brazil, Peru, to N Argentina.
C. mauri	Western Sandpiper	N and W coast of Alaska.	From S British Columbia along the Pacific coast USA, almost all Mexico (Pacific and Gulf), Caribbean Islands and N of South America.
C. melanotos	Pectoral Sandpiper	N and W Alaska, low Canadian Arctic and reaching Hudson bay in Central Canada.	Winters in South America from Bolivia, Paraguay, Argentina, Chile and small part in S Brazil.
C. minutilla	Least Sandpiper	From Alaska, NW Central and NE Canada (Yukon, Alberta, Manitoba, Hudson Bay, Ontario and Quebec).	Winters from S USA, Mexico, Caribbean Islands, and N of South America, Colombia, Venezuela, Ecuador, Peru and S Brazil.
C. pusilla	Semipalmated Sandpiper	Along W and N Alaska, NW to NE Canada (Yukon to Labrador).	Atlantic and Pacific coast of Mexico, Central America and N Central South America (Ecuador, Peru, Venezuela, Brazil).
C. subruficollis	Buff-breasted Sandpiper (Near Threatened)	Breeds in N Alaska and low Canadian Arctic.	Winters in South America from SE Bolivia, Paraguay, NE Argentina, S Brazil and Uruguay.

Table 4. Species of Scolopacidae studied, including sub-species (continued**).**

Scientific name	Common name	Breeding range	Non-breeding range
C. virgata	Surfbird	From Central and S Alaska to the W Canada in Yukon.	Along the Pacific coast of Canada, USA, Mexico and South America (from British Colombia to Chile).
Gallinago delicata	Wilson's Snipe	Breeds from Alaska, Canada to NW and NE USA. Aleutians Islands to Maine in USA and Labrador in Canada.	From the NW, Central and E USA, all Mexico, Central America, Caribbean Islands and N of South America (N Colombia and Venezuela).
Limnodromus griseus including: *L. g. caurinus*; *L g. hendersoni*; and *L. g. griseus*	Short-billed Dowitcher	*L. g. caurinus* from S Alaska to S Yukon and NW British Columbia. *L. g. hendersoni* Central Canada in Alberta, Manitoba, S Nunavut and N Ontario. *L. g. griseus* James Bay to Quebec and W Labrador.	*L. g. caurinus* from the Pacific coast in Central USA to Peru and the Galapagos Island. *L. g. hendersoni* SE coast USA to Panama. *L. g. griseus* S USA, the Caribbean Islands to Venezuela and Brazil.
L. scolopaceus	Long-billed Dowitcher	Breeds in the north-western region of North America from NW Canada to W Alaska and in NE Siberia.	Winters in Mexico, Guatemala and S USA.
Limosa fedoa including: *L. f. beringiae*; and *L. f. fedoa*	Marbled Godwit	*L. f. beringiae* part in SW Alaska (Ugashik Bay to Port Heiden). *L. f. fedoa* Central-S Canada (Alberta, Saskatchewan and Manitoba), N USA (Montana, Dakota and Minnesota).	*L. f. beringiae* from the Pacific coast USA, Washington to Central California. *L. f. fedoa* from S California to Mexico on the W coast, and from Carolina to Panama on the E coast.
L. haemastica	Hudsonian Godwit	Breeds in W and S Alaska, NW and Central Canada (Yukon to Hudson Bay).	Winters in South America from S Brazil to Tierra del Fuego and Chile on the Pacific coast.
Numenius americanus including: *N. a. parvus*; and *N. a. americanus*	Long-billed Curlew	*N. a. parvus* S Central Canada (British Columbia and Saskatchewan) to Dakota and California in USA. *N. a. americanus* from Nevada, New Mexico, Texas and Oklahoma to South Dakota in USA.	*N. a. parvus* winters in the coast of California to the E coast in Louisiana and S Mexico. *N. a. americanus* from California to Texas, almost all Mexico, and small portion in Guatemala and El Salvador.

Table 4. Species of Scolopacidae studied, including sub-species (continued)**.**

Scientific name	Common name	Breeding range	Non-breeding range
N. phaeopus hudsonicus	American Whimbrel	Central Canada around Hudson Bay in Manitoba and Ontario.	On the coast of S USA to the Caribbean and South America.
Phalaropus lobatus	Red-necked Phalarope	Alaska and low Canadian Arctic, from NE to NW Canada (Yukon to Labrador).	Winters on the Pacific coast of SW Mexico (Jalisco to Chiapas) and Central America to the W of South America.
Scolopax minor	American Woodcock	Breeds from S-SE Canada (Manitoba to Ontario and Quebec), to the E USA (from the Great Plains to the Atlantic coast).	From the SE USA reaching the Atlantic and the Gulf in Florida and Texas.
Steganopus tricolor	Wilson's Phalarope	S-Central Canada (Alberta and Saskatchewan) to NW USA (Washington, Montana, South and Dakota).	South America from Ecuador, Peru, Galapagos Is., Chile, Argentina, Bolivia, Uruguay and Tierra del Fuego.
Tringa flavipes	Lesser Yellowlegs	From Alaska to NW-NE Canada (Yukon, British Columbia, Alberta to Hudson Bay).	Winters from New Jersey and California in the USA through Mexico and all Caribbean and South America.
T. incana	Wandering Tattler	Alaska and W Canada in Yukon and N British Columbia.	Wintering across the Pacific coast of S USA (California), Mexico, Central America and South America until N Chile.
T. melanoleuca	Greater Yellowlegs	Small portion in S Alaska. Mostly across Central Canada, from British Columbia to Labrador.	Winter season across S USA, Mexico, Central America, the Caribbean and South America.
T. semipalmata including: *T. s. inornata*; and *T. s. semipalmata*	Willet	*T. s. inornata* breeds in Central Canada (Alberta, Manitoba), NE California, Nebraska, South and Dakota. *T. s. semipalmata* in the E coast USA and the Caribbean.	*T. s.inornata* on the Pacific coast from S USA (California) across Mexico, Central America and South America (N Chile). *T. s. semipalmata* from the E coast USA in Atlantic, the Caribbean, Gulf of Mexico, Central America and N Brazil.
T. solitaria including *T. s. cinnammomea* and *T. s. solitaria*	Solitary Sandpiper	*T. s. cinnammomea* breeds across Alaska, NE-NW and Central Canada (above 60°N). *T. s. solitaria* across SE-SW and Central Canada (below 50°N).	*T. s. cinnammomea* winters in South America (Colombia to Central Argentina). *T. s. solitaria* from Central Mexico, Caribbean, Central America, to South America (N Argentina).

2.2.2 Hummingbirds

2.2.2.1 Family Trochilidae

Better known as Hummingbirds, this family belongs to the Order Apodiformes and comprises 105 genera, 363 species and 712 taxa (Schuchmann and Bonan 2016). See Table 5.

Distributed throughout the Americas, in almost every ecosystem from coasts to arid zones, wet, dry and temperate forests; they are even found in urban areas such as parks and gardens (Kaufman et al. 2005, Arizmendi and Berlanga 2014) and are absent only from areas with very cold climates. Most species are endemic to South America, but some species migrate throughout North America (Schuchmann and Bonan 2016).

The species that breed in North America are mostly migratory birds that travel to tropical ecosystems, mainly in Southern Mexico, Central and South America (Williamson 2001), during the non-breeding season.

Hummingbirds are a very specialized group; they have an amazing morphology, their chest muscles and low body weight (ranging from 2 to 24 grams) allowing them to fly in any direction, including sideways and backwards, as well as to remain suspended in the air, beating their wings at between 80 and 200 beats per second when in courtship flight (Arizmendi and Berlanga 2014).

Their ecological importance arises from their being the principal pollinators of many plants, thus contributing to the shaping of landscapes such as forests, woodlands and deserts, which in some cases would not be possible without them (Williamson 2001).

Table 5. Species of Trochilidae studied, including sub-species.

Scientific name	Common name	Breeding range	Non-breeding range
A. violiceps including *A. v. ellioti and A. v. violiceps*	Violet-crowned Hummingbird	*A. v. ellioti* local to SE Arizona and SW New Mexico in USA. *A. v. violiceps* from Guerrero to Oaxaca along S in the Pacific.	*Amazilia v. ellioti* to SE Sonora and N of the Pacific. *A. v. violiceps* Guanajuato To Hidalgo in S Pacific of Mexico.
A. yucatanensis including *A. y. chalconota*, *A. y. cerviniventris* and *A. y. yucatanensis*	Buff-bellied Hummingbird	Partial migrant. *A. y. chalconota* SE Texas in Rio Grande. *A. y. cerviniventris* in E Mexico (Veracruz to Chiapas). *A. y. yucatanensis* SE Mexico (Tabasco to Yucatan).	*A y. chalconota* Gulf of Mexico (Veracruz to Florida). *A y. cerviniventris* similar to breeding grounds. *A y. yucatanensis* NE of Texas in the Gulf Coast.
Archilochus alexandri	Black-chinned Hummingbird	From British Columbia, S and W USA (to Texas) to N of Mexico (Baja California, Sonora, Tamaulipas, Zacatecas y San Luis Potosi).	N and Central Mexico on the Pacific side, to the S in Guerrero, Morelos and Veracruz.
A. colubris	Ruby-throated Hummingbird	S Central Canada (Alberta and Nova Scotia) to Central E USA (Dakota to Maine, Texas and Florida).	Central Mexico to SW Panama. Small part in S Florida too.
Calypte anna	Anna's Hummingbird	From SW British Columbia to W USA (Arizona) and NW Mexico (Baja California).	Currently expanding non-breeding range. From N Mexico, along the W, SE USA, and Alaska.
C. costae	Costa's Hummingbird	SW USA (Nevada, California and Utah) to NW Mexico (Baja California and Sonora).	SW USA (California and Arizona) to NW Mexico (Baja California to Sinaloa and Nayarit).
Calothorax lucifer	Lucifer Hummingbird	From SW USA (Arizona), along the Sierra Madre Occidental and reaches Mexico's city.	Central and SW Mexico (Jalisco, Guanajuato, Queretaro, Guerrero and Oaxaca).

Table 5. Species of Trochilidae studied, including sub-species (continued)**.**

Scientific name	Common name	Breeding range	Non-breeding range
Cynanthus latirostris including *C. l. magicus, C. l. latirostris* and *C. l. propinquus*	Broad-billed Hummingbird	*C. l. magicus* SW USA (Arizona and New Mexico) to Central Mexico (Nayarit). *C. l. latirostris* resident in Central and E Mexico (San Luis Potosi to Veracruz). *C. l. propinquus* resident in Central Mexico (Guanajuato and Michoacan).	*C. l. magicus* to the S of Mexico in Guerrero and small parts in Oaxaca. *C. l. latirostris* resident in Central and E Mexico (San Luis Potosi to Veracruz). *C. l. propinquus* resident in Central Mexico (Guanajuato and Michoacan).
Eugenes fulgens including *E. f. fulgens* and *E. f. spectabilis*	Magnificent Hummingbird	*E. f. fulgens* mostly resident in N and Central Mexico, Guatemala, El Salvador, Honduras and Nicaragua; small part migrate SW USA (Arizona) and N Mexico (Sonora). *E. f. spectabilis* resident in Costa Rica and Panama.	*E. f. fulgens* resident Central Mexico, Guatemala, El Salvador, Honduras and Nicaragua. *E. f. spectabilis* resident in Costa Rica and Panama.
Lampornis clemenciae including *L. c. bessophilus, L. c. phasmorus* and *L. c. clemenciae*	Blue-throated Hummingbird	*L. c. bessophilus* SW USA (Arizona and New Mexico) to NW Mexico (Sonora, Chihuahua and Durango). *L. c. phasmorus* mostly resident in SW Texas. *L. c. clemenciae* NE, S and Central Mexico (Sierra Madre Oriental to Oaxaca).	*L. c. bessophilus* SW USA (Arizona and New Mexico) to NW Mexico (Sonora, Chihuahua and Durango). *L. c. phasmorus* mostly resident in SW Texas. *L. c. clemenciae* NE, S and Central Mexico (Sierra Madre Oriental to Oaxaca).
Selasphorus calliope	Calliope Hummingbird	SW Canada (British Columbia and Alberta), W USA (Washington, Oregon to Wyoming and Colorado) to NW Mexico (Baja California).	W Central Mexico from Sinaloa to Oaxaca.
S. platycercus	Broad-tailed Hummingbird	In Mexico and Guatemala is resident. Breeds in W and Central USA (from Idaho to Arizona and California).	Across Mexico reaching Guatemala.

Table 5. Species of Trochilidae studied, including sub-species (continued)**.**

Scientific name	Common name	Breeding range	Non-breeding range
Selasphorus rufus	Rufous Hummingbird	Coastal area of SW Alaska to SW Canada (British Columbia and Alberta) and NW USA (Washington, Idaho, Montana and small part in California).	Non-breeding all through Mexico (only not in Chihuahua and Coahuila) and small part in SE USA on the coast.
Selasphorus sasin including *S. s. sasin* and *S. s. sedentarius*	Allen's Hummingbird	*S. s. sasin* along coast from Oregon to California. *S. s. sedentarius* is resident to islands of S California, Malibu and San Clemente.	*S. s. sasin* in Central Mexico. *S. s. sedentarius* is resident.

2.3 Modelling Approaches

A model is defined as a representation of a complex phenomenon, process or system that is constructed in order to improve understanding, facilitate prediction or perform simulations (Barnsley 2007). Models have enabled significant advances in the study of nature, especially for natural phenomena that it are complex to measure or difficult to observe, and less likely to be manipulated (Clark 2007). In the present study one principal type of model is applied to simulate each of climate and species' distributions, respectively.

2.3.1 Climate models

The palaeoclimate information discussed above, in the background about climate history was derived from various records around the Americas, such as pollen, tree rings and fossils like corals, which provide a general view of climate from the late Pleistocene to the present day. This type of information is essential to learn how complex climate history has been, especially during this time when plants and animals began to establish their modern distributions (Newton 2003). An alternative way of obtaining this information is using mathematical models that simulate the general circulation of the atmosphere and the three-dimensional circulation of the oceans, i.e. Atmosphere–Ocean General Circulation Models (AOGCMs), one of the principal model types used.

General Circulation Models (GCMs) have been widely applied to the reconstruction of past climate conditions. An example of this is the BIOME 6000 project (Prentice and Webb 1998) that attempted to reconstruct the global vegetation at 6000 ^{14}C yr BP using paleovegetation data and biogeographic data, and compared the results with vegetation simulated by the BIOME model (Prentice et al. 1992) when driven using the palaeoclimatic conditions simulated for that time using a GCM.

HadCM3 is an example of an AOGCM. It was developed by the UK Meteorological Office and included by the IPCC in the assessment reports of 2001 and 2007. This model, which comprises fully-coupled general circulation models of the atmosphere and ocean, as well as a sea-ice model, has been used to simulate the variability in Quaternary climates, including that associated with Heinrich events (Singarayer and Valdes 2010). Using as forcing the combination of orbital configuration, greenhouse gas concentrations, ice-sheet volumes and

locations, and sea-level changes, HadCM3 provided estimates of climatic changes during the last glacial–interglacial cycle (Singarayer and Valdes 2010).

The results from the simulations made by Singarayer and Valdes (2010) have been used in previous studies exploring, for example, the Last Glacial vegetation, from the late Pleistocene to the Holocene on the northern continents (Allen et al. 2010, Huntley et al. 2013). They have also been used in studies of how the diversity of birds may have responded to the past and potential future climatic changes.

A study of birds distributed in southern Africa using the HadCM3 results, including those from experiments mimicking Heinrich Events, showed a correspondence between present diversity of species associated with the Karoo or Fynbos biomes and locations that were persistently suitable for the greatest number of these species, even under the most extreme climatic changes that were associated with the Heinrich Events (Huntley et al. 2014).

2.3.2 Species distribution models

Species Distribution Models (SDMs), sometimes also referred to as Climatic Envelope Models, Ecological Niche Models, Habitat Suitability Models or Environmental Niche Models (Elith and Leathwick 2009), have become an important tool for the exploration of how species may respond to environmental, and especially to climatic, changes. Understanding how species of flora and fauna may potentially behave under circumstances of climatic change, and especially how they may potentially be distributed in the future, provides information vital to the design of conservation efforts that take into account the potential impacts of climatic change (Loiselle et al. 2003, Elith and Leathwick 2009, Sinclair et al. 2010, Zhang et al. 2012).

SDMs have been used in recent years as a tool for understanding how species might respond to potential future climatic changes. However, when using SDMs in this way it is important that their limitations, and especially the differing assumptions inherent in different approaches to fitting such models, are taken into account. These limitations and varying assumptions lead to varying degrees of uncertainty in the model predictions, including in some cases predicting a species' presence where it does not, in reality, occur (Guisan and Thuiller 2005, Svenning et al. 2011), Such uncertainties should, as with the uncertainties inherent in all statistical modelling methods, be taken into account when applying the models.

Limitations are present in most of the models used to make past or future predictions, hence the importance of knowing the behaviour of the model(s) used. Several studies have suggested that the use of a combination of several distinct types of model can result in a better assessment, whereas other studies point out that some model types make less appropriate, or even inappropriate, assumptions and/or have greater limitations (Loiselle et al. 2003, Huntley et al. 2004, Elith and Leathwick 2009), recommending instead the use of just one or a small number of modelling approaches that make only appropriate assumptions and that have been shown to have no serious limitations. Ideally the modelling method(s) used should have been validated using spatially and/or temporally independent data.

When using a model to make predictions of species' potential distributions under environmental change, the results represent only a possible scenario. They thus should not be interpreted as a fixed prediction, but instead as a guide to assessing and representing a potential future scenario (Huntley et al. 2004, Pearson et al. 2006). Nonetheless, the application of SDMs has been important in identifying species that face the greatest extinction risk as a consequence of projected climatic changes (Thomas et al. 2004, Guisan and Thuiller 2005).

There has been some analysis of the possible limitations of SDMs, especially when predicting species' potential future ranges in regions where the projected future climatic conditions are 'novel', i.e. have no current analogue, and hence there are no observational data to support or refute the predictions (Williams and Jackson 2007). Challenging simulations of the potential responses of species to the historical climate with palaeoecological evidence of their past range extents and abundances, as well as their interactions within the ecosystem, is fundamental to better assessments of model outputs for no-analogue ecosystems or communities associated with no-analogue climates (Elith et al. 2006, Hobbs et al. 2009).

Given that the use of SDMs can contribute to conservation efforts, it is important to know where to implement these efforts, for example whether these should be focused on protected areas or extend to the wider landscape. Such decisions represent the first step in formulating conservation strategies, as suggested in a study using SDMs to model the potential future distributions of European breeding birds in which the future predictions under climatic change are of an average reduction in the extent of species' distributions (Huntley et al. 2008).

The importance of model choice is key when designating conservation areas, as has been shown in a study on West African vertebrates, with a local approach to meet the regional conditions potentially reducing the uncertainty of the projections (Baker et al. 2015). We must be aware of the choice of climate data that is also important when trying to reduce the uncertainty of the models, especially when using historical data that could misrepresent regional patterns (Baker et al. 2016).

The use of SDMs in studies of species' past ranges offers predictions on species' palaeoecology, showing how community changes were driven by climate, especially the dynamics of climate change, and offering a higher spatial and/or temporal resolution, as well as greater continuity, than generally is available from palaeoecological data (Svenning et al. 2011). There is also an increase in the application of SDMs in phylogenetics, allowing investigations of geographical and environmental correlations with the evolution of a species (Graham et al. 2004, Alvarado-Serrano and Knowles 2014).

Different types of species' distribution data are available when using SDMs, although these most commonly are records of the species' occurrences, with/without inferred absences, that may originate from survey data, museum specimens or online data bases that collect observations made by citizen scientists (Elith et al. 2006).

Different types of models use different types of data. Some approaches use only presence records. One of the most commonly used of such modelling methods is BIOCLIM, which uses the range of values of a series of environmental variables at localities where a species occurs to predict the overall potential climatically suitable area for the species, (Booth et al. 2014).

Generalised Linear Models (GLMs) were one of the first model types used as SDMs, given that they can be based on presence–absence or count data (Elith and Leathwick 2009). Generalised Additive Models (GAMs) model the relationship between the mean of the response variable and explanatory variable(s) as a smooth function, the form of which is driven more by the data than by any prior assumption about its form; they hence can establish the relationship between the response and the set of explanatory variables rather than assuming the form of that relationship (Guisan et al. 2002).

Biomod2 is a package that implements several modelling methods (10 models) for fitting SDMs and predicting species' distributions under changed climate projections. The ensemble

of models can potentially give different predictions (Thuiller 2003), some of the model types making much less appropriate assumptions and/or being likely to have much greater uncertainties.

It is important when modelling with presence–absence data to consider the confusion matrix for the evaluation of the model (Liu et al. 2013); this contains the numbers of true positive, false positive, false negative and true negative results. Furthermore, from the confusion matrix two measures can be derived, sensitivity and specificity, that together are used to compute the True Skill Statistic (TSS) that is highly recommended when evaluating a model (Allouche et al. 2006).

Sensitivity, defined as the proportion of true presences in relation to the total number of presences predicted by the model, is one measure of model performance that can be considered. Higher sensitivity indicates a 'better' model that is thus likely to give more reliable predictions (Gurgel Costa et al. 2014).

Specificity is the measurement that predicts commission errors, i.e. the observed absences given by the true negatives in relation to the false positive of the confusion matrix (Allouche et al. 2006).

In a study using museum records of bird species in Brazil for conservation planning, several model approaches were used. Taking into account the uncertainty levels, especially the possible false-negative and false-positive errors, as well as the true-negatives and true-positives, of the different models enabled a better interpretation of the results when making conservation decisions (Loiselle et al. 2003).

Model validation is one of the main issues when using SDMs because some degree of correlation between a species' distribution and one or more climatic variables is to be expected even when there is no causal relationship, direct or indirect. There are several approaches to model validation and to the avoidance of model over-fitting. Some statistical methods allow overall assessment of the model predictions, for example the Area Under a Receiver Operating Characteristic curve (AUC) assesses the model's ability successfully to discriminate sites where a species is present from those where it is absent (Elith et al. 2006); others compute the degree to which the accuracy of the model's predictions exceeds that of a random model, for example Cohen's kappa that takes into account both the omission and commission errors of the predictions (Cohen 1960). For quantitative predictions the Pearson

correlation coefficient (COR) is a measure of the agreement between the predicted and observed values (Elith et al. 2006).

All of these measures essentially compare the predictions of the model to the observations used to fit the model, and thus do not represent a validation against independent data. In order systematically to establish the accuracy of a model, however, its ability correctly to predict presence/absence observations not used in model fitting must be assessed. However, finding independent data with which to make such tests is generally very difficult given the nature of the data to be used (Araujo et al. 2005).

As a result, most model validations have used cross-validation methods that operate by partitioning the available data set. A common approach consists of splitting the data set into two sub-sets, a training set that usually comprises 70–75% of the available data, and a test set comprising the remaining 25–30% of the data. The model is fitted to the training set and then used to predict the test set, model performance being assessed using one of the above-mentioned statistics (i.e. AUC, TSS, etc.) calculated only for the test set (Moreno-Torres et al. 2012).

A marked improvement on this approach is *k*-fold validation, in which the data are split into *k* random subsets, model fitting and testing is repeated *k* times, each in turn of the subsets being omitted from the training set and used for testing, and each test resulting in a value of whichever model performance statistic is being used. The results can be summarised as a mean value of the performance statistic across the *k* models (Moreno-Torres et al. 2012), as a distribution of the values of that statistic, or by computing a single overall assessment of the statistic for a comparison of the combined predictions for the *k* test sets with the observations (Huntley et al 2007).

Another cross-validation method is the jack-knife or leave-one-out technique. In this approach the model is fitted repeatedly, either removing one randomly selected data point each time, or removing each data point in turn, the models being tested by assessing their ability correctly to predict the omitted data points (Pearson et al. 2007). This approach suffers from two important drawbacks: firstly, it will rarely be the case that the omitted data point lies outside the environmental space spanned by the remainder used to fit the model, thus rendering it likely that the model will predict that point correctly, hence giving an over-optimistic measure of model performance; and secondly, for many species' distribution

datasets, particularly the extensive presence–absence datasets offered by many distribution atlases, leaving out each data point in turn will often be computationally prohibitive.

A small number of studies have used truly independent data to undertake model validation. Beerling et al. (1995), for example, assessed the performance of a model fitted to the European distribution of *Fallopia japonica*, an introduced but now widely naturalised alien plant species, by using the model to predict its native range in eastern Asia. Comparison of the resulting prediction with an independent mapping of its native range based on herbarium specimens and other records showed the model to perform extremely well.

Green et al. (2008) showed that models fitted to the European distributions of a series of bird species that breed in limited numbers in the British Isles successfully predicted 25-year trends in the species' breeding numbers as responses to climatic variations over the same period, the breeding abundance data being quite independent of those data used to fit the models.

Not only are all models imperfect simplifications of the system being modelled, but considerable uncertainties in inputs, most notably with respect to future emissions paths and the resulting projected climatic changes (Bagchi et al. 2013), mean that SDM predictions must be considered only as scenarios of potential change in species' distributions and not as predictions of what will actually occur (Stralberg et al. 2015).

Many studies suggest that, given the projected changes in climate, most notably the increase in global mean temperature, species response will be to move to cooler areas, whether to higher altitudes or nearer the poles (Huntley et al. 2008, Bagchi et al. 2013). This might result in the extinction of some species if they are not able to make such movements, either because they are already close to the highest elevations, or are already restricted to the maximum latitude land areas, available in the region where they occur (Hughes 2000). It is important also to remember that human modifications of the landscape have resulted in severely fragmented habitats in many regions that have already led to the modification of many species' distributions.

In Europe, studies using SDMs suggest that birds' distributions and richness will be affected by climate change which will lead to birds to shape their diets and feeding behaviours (Thuiller et al. 2014). Long distance migrants will reduce their population size and in particular birds species with distribution ranges in northern Europe will most likely present a

turnover on their distributions as a result of climate change and anthropogenic land degradation resulting in the change of bird communities (Virkkala and Lehikoinen 2017).

More evidence for the use of SDMs as an important tool in management and conservation planning is shown in the study of the reproductive fitness of red-backed shrikes (*Lanius collurio*) in Italy, by evaluating the suitability of the environment and the presence of the species. Results show how well SDMs are able to predict the red-backed shrike distribution that helps to analyse their reproductive success (Brambilla and Ficetola 2012).

In a study of bird species in California, simulations of their potential distributions under future climatic scenarios were made to inform conservation efforts in areas with intense urban development. These simulations gave mixed results, with different predictions for different species, although with a general pattern of a predicted 27 to 66% reduction in the extent of distribution of the birds (Jongsomjit et al. 2013).

Another study focused on birds with boreal forest distributions in Canada using Boosted Regression Tree SDMs and GCM simulations of future climatic scenarios. The results predicted that species with more northern distributions would become scarce in comparison with species occurring in more southern areas and using grassland habitats (Stralberg et al. 2015).

There has been a recent set of papers published from the Audubon Society of America regarding the conservation status of breeding birds in North America and the impacts that climate change can have on their distributions. In this set of studies more than 500 species that breed and spend the non-breeding season in North America are considered to have a climatic sensitivity under future climatic scenarios. The studies shed light on what could potentially happen if there is no management of the areas at risk; this could potentially lead to the disappearance of species' range (Distler et al. 2015, Langham et al. 2015, Schuetz et al. 2015).

In these studies, they used historical climate data from the Canadian Forest Service (CFS) that matched the bird data counts (North American Breeding Bird Survey and Audubon Christmas Bird Count) records for each year, and led them to use 17 bioclimatic variables; by doing this they accounted the reduction of correlation. As for the future climate scenarios they used World-Clim climate grids for 13 combinations of emissions scenarios, GCMs and the IPCC Fourth Assessment (Distler et al. 2015, Langham et al. 2015).

Given the focus of the present study, it seems that the choice of Climate Envelope Models to assess potential shifts in the geographic distribution of the species is a relevant decision, given a series of climate scenarios spanning a period of time (Huntley and Green 2012).

To assess the simulated responses of species to these long-term climatic changes, we have applied the modelling approach of fitting Climatic Response Surfaces (CRSs), fitted by locally-weighted regression using a series of FORTRAN programs, following the approach of Huntley et al. (2007).

The results of this study will be of relevance to understanding species' present patterns of breeding distribution and migratory behaviour, as well as to predicting the potential impacts of future climatic change on these important components of many North American ecosystems.

2.4 Hypothesis

Given the fluctuating climate history of the late Quaternary, specifically from the Last Glacial Maximum until the Little Ice Age, and taking into account relevant climatic events (Heinrich events and Younger Dryas), the migratory routes and seasonal ranges of Hummingbirds and Shorebirds would have been affected by such climatic shifting. Hence both the breeding/non-breeding distributions and migrations of species would differ from those seen today.

2.5 General Aims

The main objective of this study is to understand how the breeding and non-breeding ranges in migratory species of Hummingbirds and Shorebirds in the Americas were influenced by the climate during the late Quaternary, specifically from the LGM to the Little Ice Age. Additionally, the impacts of important climatic events such as the Heinrich Events (H2, H1 and H0) and the Younger Dryas will be considered.

The study is based on the use of species distributions modelling, consisting in the use of Climate Response Surfaces model (CRS), which is used to simulate and project several scenarios.

To be able to achieve this overall objective, the specific study objectives are:

1. To project each species' range (breeding and non-breeding) for past climates (LGM to Little Ice Age) using CRS.

2. Compare the different values of True Skill Statistics (TSS), Area Under the Curve (AUC) and Cohen's Kappa (Kappa) for each species given by the CRS model.

3. Compare the CRS modelling approach for current and past climates.

4. Compare also the projected distributions between Shorebirds and Hummingbirds.

CHAPTER 3 MATERIALS AND METHODS

3.1 Study Area

The area of study is the American continents, with the most Northern point at 83°40′ N 29°50′ W in Greenland and the most Southern point of 56°32′ S 68°43′W in the Chilean Islands.

The American continents cover 35 countries; North America encompasses Canada, the Greater Antilles, Mexico and the United States of America. Central America includes Belize, Costa Rica, El Salvador, Guatemala, Honduras, Nicaragua and Panama. South America comprises Argentina, Bolivia, Brazil, Chile, Colombia, Ecuador, French Guiana, Guyana, Paraguay, Suriname, Uruguay and Venezuela (Figure 3.1).

Figure 3.1. Map of the American Continent divided in North America, Central America and South America.

3.2 Study Methodology

The methodology of this study begins with data recording the present distributions of the species examined. These data were transformed, modelled in relation to current climate variables and the models obtained used to project potential distributions under various climates of the past. Further detailed descriptions of the data and methods are given below.

3.3 Species Data

As the main aim of this study is to learn how different migratory bird species have been distributed in the past in the Americas, and given the impracticality of examining all such migrants, the decision was made to investigate species from two separate ecologically contrasting groups of birds. Hence the choice to study Hummingbirds (Family Trochilidae) and Shorebirds (Families Charadriidae, Haematopodidae, Recurvirostridae and Scolopacidae). The scientific and common names of the birds studied are based on the classification used by the Handbook of Birds of the World (online version).

63 species of birds have been considered for this study (Table 6). BirdLife International provided the geographical distribution information for the species studied in ArcGIS (ESRI, 2010) shapefile format. Each species' distribution was divided into breeding and non-breeding ranges.

The shapefiles were gridded, using grid cells of 0.5° degrees longitude x latitude, using ArcGIS tools. The result was a list of the coordinates and an index number for each grid cell overlapped by the species' distribution. The seasonal ranges were gridded separately in order to obtain the species' geographical breeding and non-breeding distributions. These are presented as presence only data which has been proven to be adequately accurate when used to predict species distributions (Elith et al. 2006).

3.4 Climatic Data

Different climate datasets were used for this study. Firstly, the climatic variables from the period of 1961-1990 (corresponding to the present climate) were used for the 'present projection' and were obtained from the Climate Research Unit (CRU) of the School of Environmental Sciences at the University of East Anglia ((New et al. 1999). For the historical

climate, the dataset was taken from the study of Singarayer & Valdes (2010) which consists in transient simulation from the last glacial cycle (ca. 120 ka) that has been modified by Huntley et al. (2013) with projections of the last 30 years for each period of 500 years, on nine variables for each 0.5° grid cell of the world's land surfaces.

The derivation and selection of bioclimatic variables used for modelling followed Huntley et al. (2007) in which according to the species broad geographical distribution, the most appropriate variables can be pre-selected, to use and have some biologically-relevant and meaningful predictor variables for the modelling, hence they represent some of the climatic drivers influencing bird's distributions (Virkkala and Lehikoinen 2017).

Two sets of bioclimatic predictor variables were used. The first set is appropriate to species that breed in temperate regions (see Table 6) and comprises: annual thermal sum above 5°C (GDD5); mean temperature of the coldest month (MTCO) in °C; and the annual ratio of actual to potential evapotranspiration (AET/PET). The second set, used for species of tropical and sub-tropical regions comprises: mean temperature of the coldest month (MTCO) in °C; mean temperature of the warmest month (MTWA) in °C; the annual ratio of actual to potential evapotranspiration (AET/PET); and dry season duration (DRYDUR) in days. A decision for using this small set of bio-variables was made following past literature) that is it known to work when using the CRS model (Huntley et al. 2007). Following the literature, the set of variables was established for every species range (breeding and non-breeding) to suit their current distribution, for example the species Violet-crowned Hummingbird (*Amazilia violiceps*) range its mainly located in Mexico between the 0° and 30° degrees given its position on Earth, therefore a set of tropical bio-variables is selected when modelling.

Table 6. Species studied, divided by family, showing the variable set used to model their seasonal (breeding and non-breeding) distributions.

Species name	Set of variables	
Family	**Breeding**	**Non-breeding**
Charadriidae		
Charadrius collaris	Tropical	Tropical
C. falklandicus	Temperate	Temperate
C. melodus	Temperate	Tropical
C. modestus	Temperate	Temperate
C. montanus	Temperate	Tropical
C. nivosus	Tropical	Tropical
C. semipalmatus	Temperate	Tropical
C. vociferus	Temperate	Tropical
C. wilsonia	Tropical	Tropical
Oreopholus ruficollis	Temperate	Temperate
Pluvialis dominica	Temperate	Temperate
P. squatarola cynosurae	Temperate	Tropical
Recurvirostridae		
Himantopus h. mexicanus	Tropical	Tropical
Recurvirostra americana	Temperate	Tropical
Haematopodidae		
Haematopus ater	Temperate	Temperate
H. leucopodus	Temperate	Temperate
H. palliatus	Tropical	Tropical
Scolopacidae		
Actitis macularius	Temperate	Tropical
Arenaria interpres	Temperate	Tropical
A. melanocephala	Temperate	Temperate
Bartramia longicauda	Temperate	Tropical
Calidris alba	Temperate	Tropical
C. a. hudsonia	Temperate	Temperate
C. a. pacifica	Temperate	Temperate
C. bairdii	Temperate	Temperate
C. canutus	Temperate	Tropical
C. fuscicollis	Temperate	Temperate
C. himantopus	Temperate	Tropical
C. mauri	Temperate	Tropical
C. melanotos	Temperate	Temperate

Tropical = MTWA, AET/PET, DRYDUR, WETINT. Temperate = GDD5, MTCO, AET/PET.

Table 6. Species studied, divided by family, showing the variable set used to model their seasonal (breeding and non-breeding) distributions (continued**).**

Species name	Set of variables	
Family	**Breeding**	**Non-breeding**
Scolopacidae		
C. minutilla	Temperate	Tropical
C. pusilla	Temperate	Tropical
C. subruficollis	Temperate	Temperate
C. virgata	Temperate	Tropical
Gallinago delicata	Temperate	Tropical
Limnodromus griseus	Temperate	Tropical
L. scolopaceus	Temperate	Tropical
Limosa fedoa	Temperate	Tropical
L. haemastica	Temperate	Temperate
Numenius americanus	Temperate	Tropical
N. phaeopus hudsonicus	Temperate	Tropical
Phalaropus lobatus	Temperate	Tropical
Scolopax minor	Temperate	Temperate
Steganopus tricolor	Temperate	Tropical
Tringa flavipes	Temperate	Tropical
T. incana	Temperate	Tropical
T. melanoleuca	Temperate	Tropical
T. semipalmata	Temperate	Temperate
T. solitaria	Temperate	Tropical
Trochilidae		
A. violiceps	Tropical	Tropical
A. yucatanensis	Tropical	Tropical
Archilochus alexandri	Temperate	Tropical
A. colubris	Temperate	Tropical
Calothorax lucifer	Tropical	Tropical
Calypte anna	Temperate	Temperate
C. costae	Tropical	Tropical
Cynanthus latirostris	Tropical	Tropical
Eugenes fulgens	Tropical	Tropical
Lampornis clemenciae	Tropical	Tropical
Selasphorus calliope	Temperate	Tropical
S. platycercus	Temperate	Tropical
S. rufus	Temperate	Tropical
S. sasin	Temperate	Tropical

Tropical = MTWA, AET/PET, DRYDUR, WETINT. Temperate = GDD5, MTCO, AET/PET.

3.5 Modelling method

3.5.1 Climate Response Surface Model

The model used to project the potentially suitable conditions for the 63 species of Shorebirds and Hummingbirds that breed in the Americas using 27 past climate scenarios from 26 ka BP until 1 ka BP (26 ka BP, 24 ka BP, 22 ka BP, 21 ka BP, 20 ka BP, 19 ka BP, 18 ka BP, 17 ka BP, 16 ka BP, 15 ka BP, 14 ka BP, 13 ka BP, 12 ka BP, 11 ka BP, 10 ka BP, 9 ka BP, 8 ka BP, 7 ka BP, 6 ka BP, 5 ka BP, 4 ka BP, 3 ka BP, 2 ka BP, 1 ka BP) and also taking into account the Heinrich events H0 at 13 ka BP, H1 at 17 ka BP and H2 at 24 ka BP and the current range. This past climate scenarios consists in a snapshot of time from the last 30 years of a 500-year projection followed by the work done previously by Singarayer & Valdes (2010), modified as well by Huntley et al. (2013).

The CRS model is based on the use of presence and absence data to predict the potential occurrence of a species in a climatic suitable area. It is a robust model used for the projection of species distributions as it has been shown by previous studies (Huntley et al 2012). To do this the model is fitted using locally-weighted regression that allows a prominent projection of the realised range, with no assumptions relating the species environment as discussed by Huntley et al. (2007). The only assumption of the model is made before when selecting the bioclimatic variables that are going to be fitted to predict the species potential range. For this reason, two sets of bioclimatic variables were used for the model, the set of 'temperate' variables and the set of 'tropical' variables, as discussed before.

The CRS model methodology is based on the probability of a species to occur under a given set of variables, working as a 'moving window' that weights the nearest points to the centre of the window as more strongly than the ones farther than the centre of the window, then the probability of each cell is obtained by including the fitted surface of the nodes in the designated window. The fact that each point in the window is weighted indicates the roughness of the model when predicting the occurrence of a species, based on the bioclimatic variables (Doswald 2009).

For the evaluation of the performance of the model, AUC, TSS and Kappa values were used, given as an output of the model for each species range and under the 27 past climate

scenarios and the current projected range. No independent data was used in this study as it was decided to follow the literature from previous works.

CHAPTER 4 RESULTS

Using the CRS modelling approach the distributions of the 63-species studied were simulated using the past climates defined earlier in the Materials & Methods section. In total, 27-time frames were used, from 26 ka BP until 1 ka BP (26 ka BP, 24 ka BP, 22 ka BP, 21 ka BP, 20 ka BP, 19 ka BP, 18 ka BP, 17 ka BP, 16 ka BP, 15 ka BP, 14 ka BP, 13 ka BP, 12 ka BP, 11 ka BP, 10 ka BP, 9 ka BP , 8 ka BP, 7 ka BP, 6 ka BP, 5 ka BP, 4 ka BP, 3 ka BP, 2 ka BP, 1 ka BP) and considering the Heinrich events H0 at 13 ka BP, H1 at 17 ka BP and H2 at 24 ka BP.

As mentioned before in Methods, the species' overall ranges were divided into breeding and non-breeding, according to their natural history, and, they were modelled using either 'temperate' or 'tropical' variables according to where they are distributed.

The total of simulations using the temperate variables was 1836, divided in 1377 for the breeding range, 459 for the non-breeding range. 51 species breed in temperate regions and 17 species spend the non-breeding season in temperate regions.

For the simulations using the tropical variables the total was of 1566, for which 324 correspond to the breeding range and 1242 to the non-breeding range. 12 species breed in tropical regions and 46 species spend the non-breeding season in tropical regions.

4.1 Simulations maps

The simulations are displayed by families, with each distributional range (breeding, non-breeding and passage range), their AUC, TSS and Kappa values for each range, and their conservation status according to IUCN Red List (2016). Within the maps the blue dots represent the prediction of occurrence and the yellow dots the absence of the species. The ice sheets, shaded pink, are from the modelled data ICE-6G- by Peltier et al. (2015).

The maps from 26 ka BP to 1 ka BP display some areas with white dots that indicate 'missing' climatic data, particularly in the areas of coast Greenland, south coast of Alaska, north Canadian islands and a few in the south of Chile. This is due to not having AET/PET data available for those regions. On the maps showing the projected range for the current climate, more extensive white areas in some instances indicate regions beyond the extent of the grid used when fitting the CRS model to the observed range.

4.1.1 Family Charadriidae

*4.1.1.1 Collared Plover (*Charadrius collaris*). Conservation status: Least Concern. Current known range Figure 4.1.1.1.*

Figure 4.1.1.1. Current known range of Collared Plover.

Breeding range (AUC: 0.981; TSS: 0.881; Kappa: 0.886): This species has a year-round range from the west and east coast of central Mexico to the coasts of Central America and towards South America covering the coasts of Colombia, Ecuador and the north of Peru, which then extends to central-east of South America until central Argentina. There is a small breeding range recognized in central-east Chile.

From the projection at 26 ka BP (kiloannum as used when referring to thousand years), the area is extended in almost all the territory in South America except for the Andean Cordillera from south Ecuador, Peru, Bolivia and towards Chile, central south Argentina and a small proportion in the north-east of Brazil. The 26 ka BP projection also extends to Central America, south of Mexico (Yucatan and Veracruz) and even in the central-north part in Durango and Zacatecas; additionally, the range is projected in the Greater Antilles (Cuba, Puerto Rico, Dominican Republic) and the south of Florida. See Figure 4.1.1.1.a.

A similar pattern persists with small shifts in central Argentina and central Mexico mostly until 16 ka BP when the range in Argentina begins shifting towards the north, having a

scattered projected area as well as in central Mexico where the range is slightly reduced to a few points and almost exclusively to the south.

The projection at 13 ka BP shows a gradual decrease in the Greater Antilles and Florida in USA, also in the south of Mexico the area is fragmented as well as in South America, specifically on the north-east coast of Brazil moving to central Brazil where a patchy area is shown. This magnifies towards 10 ka BP, when the territory projected in Brazil is restricted to the east coast, the north-west and a small proportion on central and southern Brazil. The rest of South America remains scarcely altered. However after 8 ka BP, the projection shows the area in Brazil to be recovered primarily from the north and east coast which seems fully restored at 1 ka BP.

There is an interesting contrast between the projections for the Heinrich events; at H2 the territory projected shows a fragmented area in the region of north-central Brazil, continuing towards the north of South America in Colombia and Venezuela, and restricted to the coasts in Central America. Also in the south of Mexico the range follows the coast on the Gulf of Mexico and there is a projected area in the north-east of Mexico (Tamaulipas) as well. This contrasts with the 24 ka BP projection as this does not show the fragmented area in Brazil and Central America.

The same pattern remains during H1, although the unoccupied area in the central part of Brazil moves to the northern coast of Brazil, Colombia and Venezuela which differs from the range presented in the 17 ka BP projection. At H0 the northern part of South America is not occupied, and the area is restricted from the west towards the south and east coasts of South America as far as the north of Argentina. The projection at 13 ka BP does not show the same behaviour, instead there is a projected range in the north of South America and only a small proportion around the area of Ceará and Piauí is not present.

For the recognized current breeding range in central Chile, the projection at 26 ka BP show a small proportion in the area which reduces from 20 ka BP to 16 ka BP, probably as a result of the LGM; later at 15 ka BP the area seems to recover and expand to the Andean Cordillera in the same region of Chile and north-west Argentina. This remains and expands briefly from 15 ka BP to 1 ka BP. The current breeding range projection resembles the known current range, and also projects suitable habitat in the Greater Antilles and the south of Florida, although there is no recognized range in those areas.

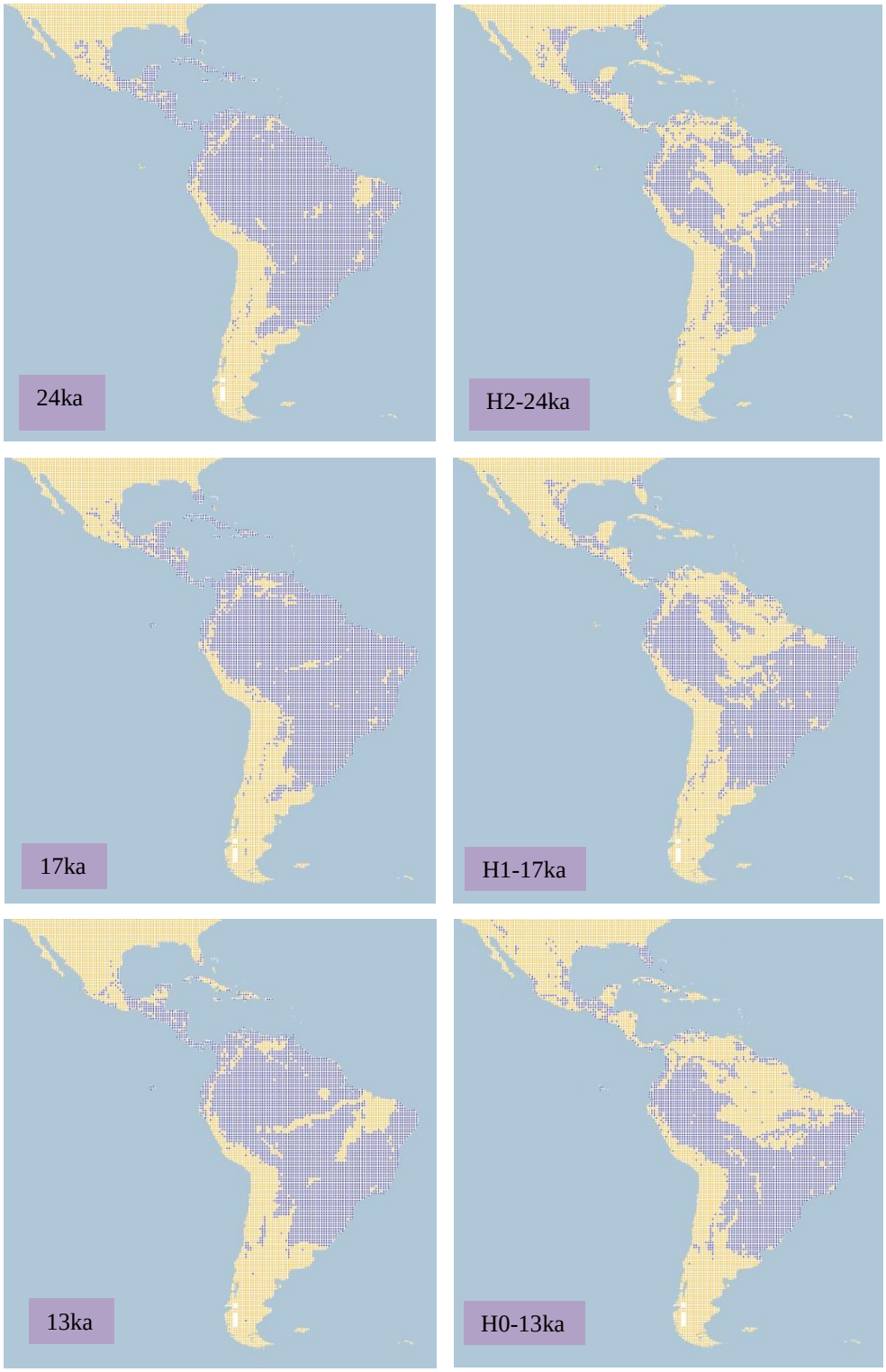

Figure 4.1.1.1.a. Simulation maps of Collared Plover breeding range.
Maps are shown for ten-time slices: 24ka, H2 (24ka), 17ka, H1 (17ka), 13ka, H0 (13ka), 9ka, 5ka, 3ka and present (1961–90).

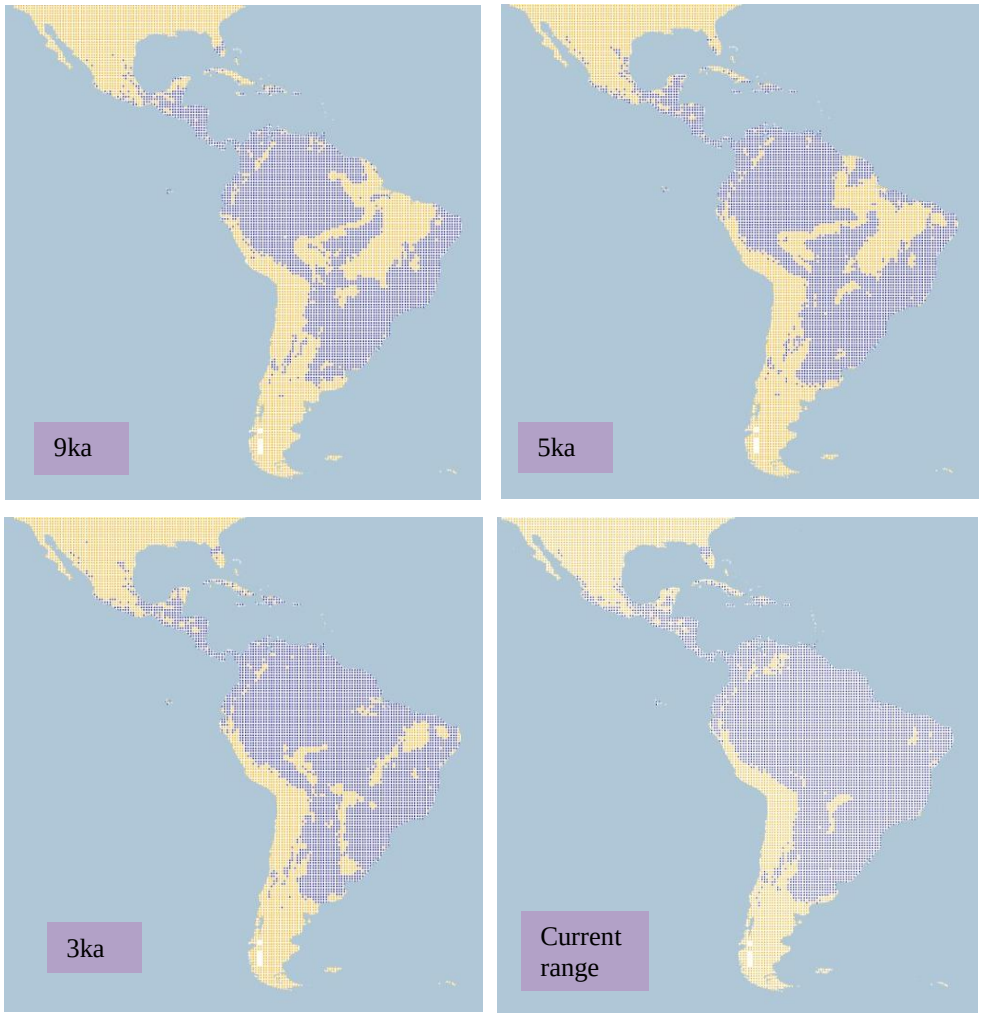

Figure 4.1.1.1.a. Simulation maps of Collared Plover breeding range (continued).

Non-breeding range (AUC: 0.982; TSS: 0.883; Kappa: 0.864): As this is predominantly a resident species it has the same range as described before in the breeding range section, with only a small non-breeding range currently known on the central-west coast of Chile, and therefore the projections for this range are almost analogous to the breeding range shown before. It is important to mention that the variables used for the projections were different in this range (tropical variables). The non-breeding range is only shown in this section.

The projected range at 26 ka BP for the non-breeding area is very restricted to the central coast of Chile and it is maintained until the 21ka projection, when there is an increase of territory projected along the coast. This similar pattern continues until the 6 ka BP projection, when the north part of the projected area in Chile is reduced and focused in the central part instead, although this is recovered by 5 ka BP and maintained until the1 ka BP and current range projections. See Figure 4.1.1.1.b.

When comparing the H2 and 24 ka BP projections, the areas shown are similar with restriction to a few points along the central coast of Chile. For the H1 and 17 ka BP projections, the area is extended towards the north of Chile, shown parallel patterns as well. For both the H0 and 13 ka BP projections, the territory seems to be settled in the coastal area of Chile.

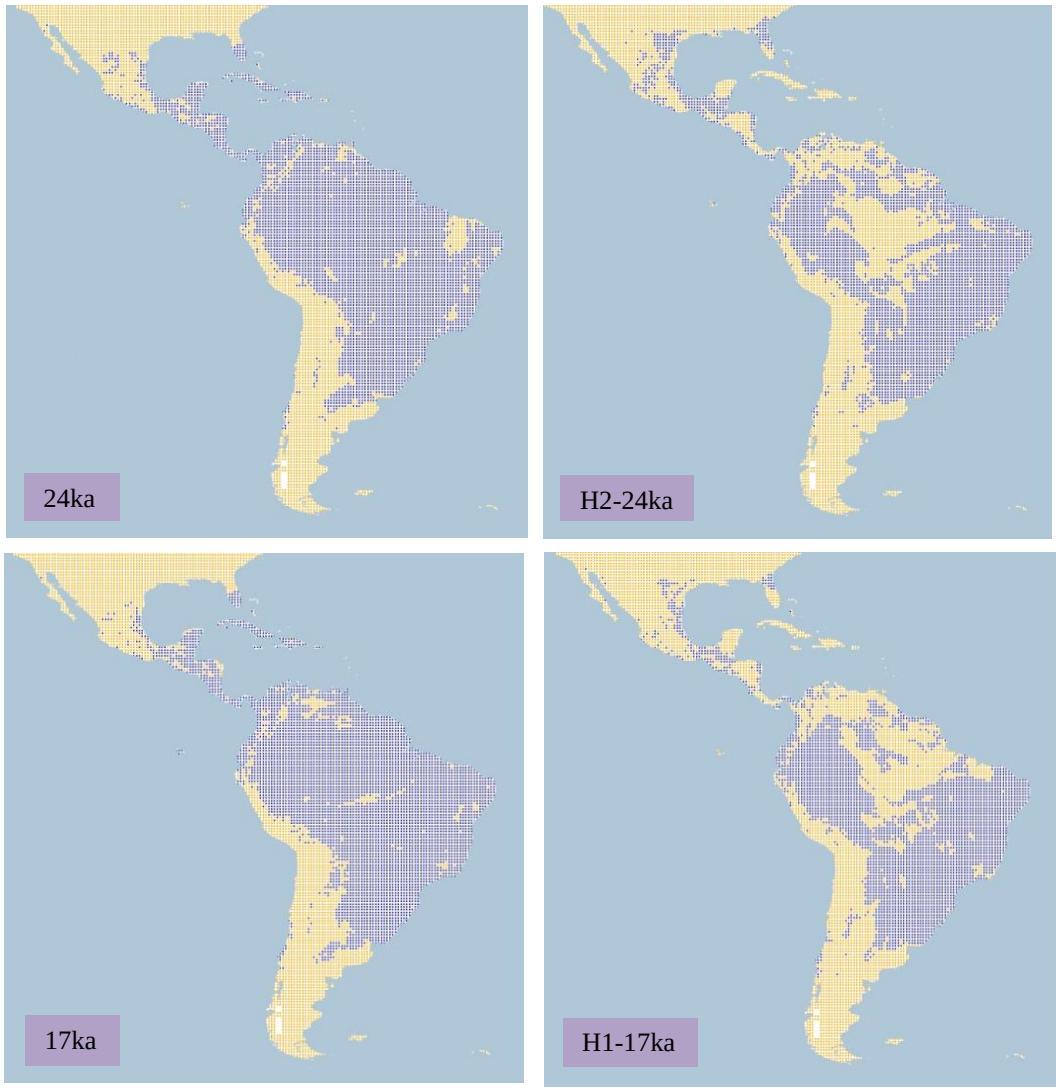

Figure 4.1.1.1.b. Simulation maps of Collared Plover non-breeding range.
Maps are shown for ten-time slices: 24ka, H2 (24ka), 17ka, H1 (17ka), 13ka, H0 (13ka), 9ka, 5ka, 3ka and present (1961–90).

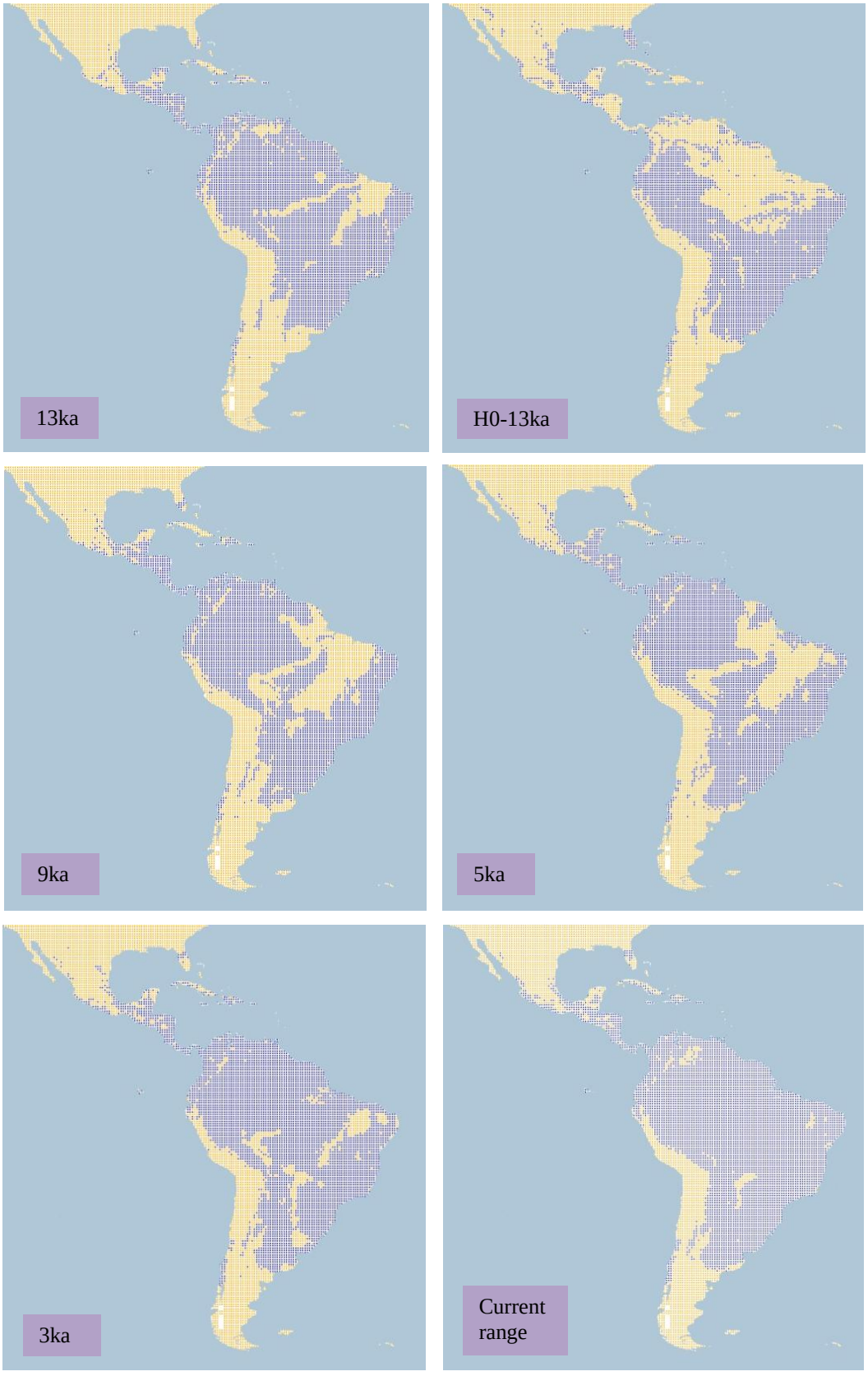

Figure 4.1.1.1.b. Simulation maps of Collared Plover non-breeding range (continued)**.**

*4.1.1.2 Two-banded Plover (*Charadrius falklandicus*). Conservation status: Least Concern. Current known range Figure 4.1.1.2.*

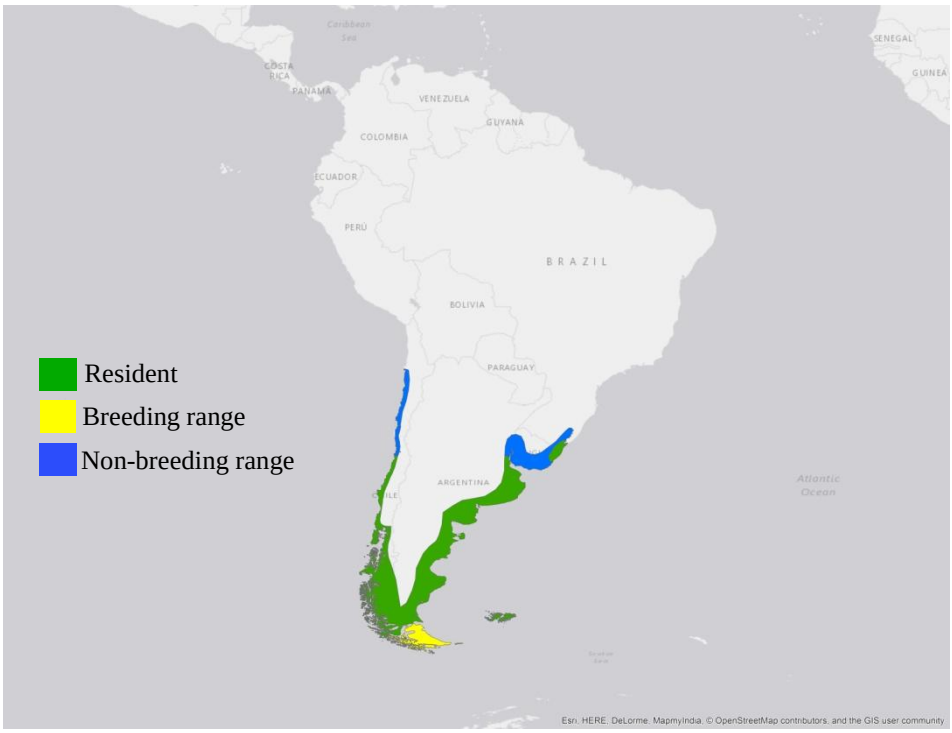

Figure 4.1.1.2. Current known range of Two-banded Plover.

Breeding range (AUC: 0.978; TSS: 0.849; Kappa: 0.770): This species has a year-round range in the Falkland Islands and on the coasts of central-south Chile and Argentina; also, a small area is recognized on the coastal boundary between Brazil and Uruguay. Further breeding grounds are documented in Tierra del Fuego territory.

From the 26 ka BP projection until the 21 ka BP, the distribution of the species in shown mainly in the south of Chile with a growing proportion located in Uruguay and the south of Brazil; there is also a fragmented area predicted in the Andean Cordillera and central Argentina. After this at 20 ka BP, the projected area located in Uruguay shifts inland towards the central and northern region of Argentina, which reduces slightly after this from 19 ka BP to 17 ka BP. At the time slice of 16 ka BP the projected territory extends again to the central northern part of Argentina. See Figure 4.1.1.2.a.

The range located in central Argentina starts increasing from 15 ka BP onwards, when the range located in the central northern part of Argentina grows to central and southern

Argentina, overlapping with the established area in that region. After this, by the beginning of the Holocene (11ka and 10 ka BP projections) the area projected is shown homogeneously on the coasts of Chile and Argentina, increasing inland, displaying a similar pattern in the remaining projections until the current projected range. For the area projected in the central northern part of Argentina at 19 ka BP shifts towards Uruguay, reducing its area at the 7 ka BP projection, to then expand at 6 ka BP and persisting towards the current range projection.

When comparing the Heinrich event H2 with the 24 ka BP projection a similar pattern is shown for the south of Chile and in the Andean Cordillera. The H2 projection predicts suitable area in central Argentina, moving to the north-east near the Andean Cordillera, contrasting the 24 ka BP projection with a fragmented ranged projected in the Andean region and a larger area in the central-east coastal part of Argentina. For the H1 projection a similar pattern persists as in H2, except it begins fragmenting along the central area of Argentina near the Andean Cordillera, moving to the south of Argentina. This is consistent with the 17 ka BP period predicted, except for the area in the central-east of Argentina, that it is not projected. For the H0 and 13 ka BP projections, a similar area is shown from the south of Chile and Argentina, only differing in central Argentina with 13 ka BP projected a wider area towards central Argentina.

Although there is no current evidence that the species occurs in North America, throughout the time slices the projections showed an appropriate area for the species to inhabit, especially in USA and Canada.

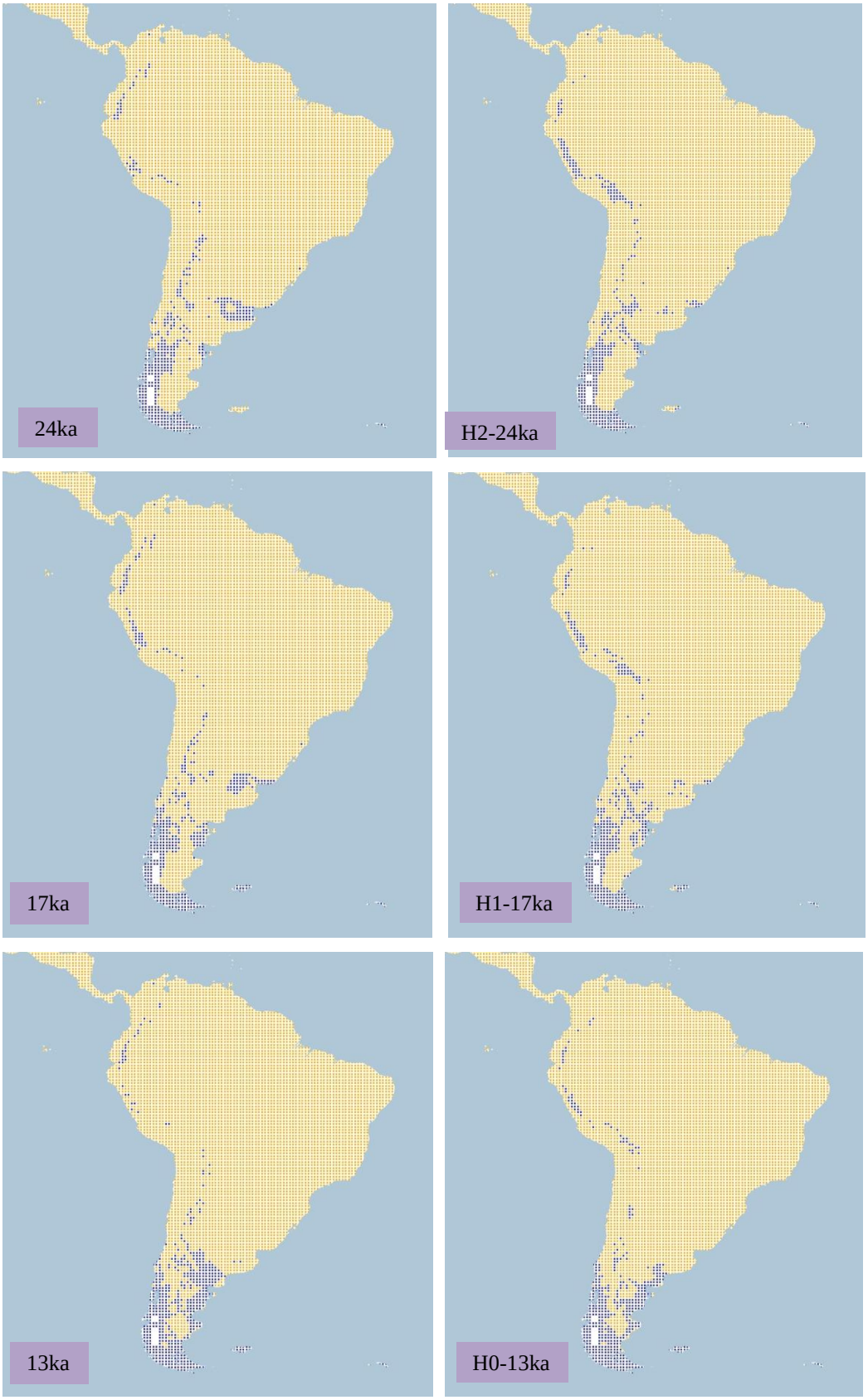

Figure 4.1.1.2.a. Simulation maps of Two-banded Plover breeding range.
Maps are shown for ten-time slices: 24ka, H2 (24ka), 17ka, H1 (17ka), 13ka, H0 (13ka), 9ka, 5ka, 3ka and present (1961–90).

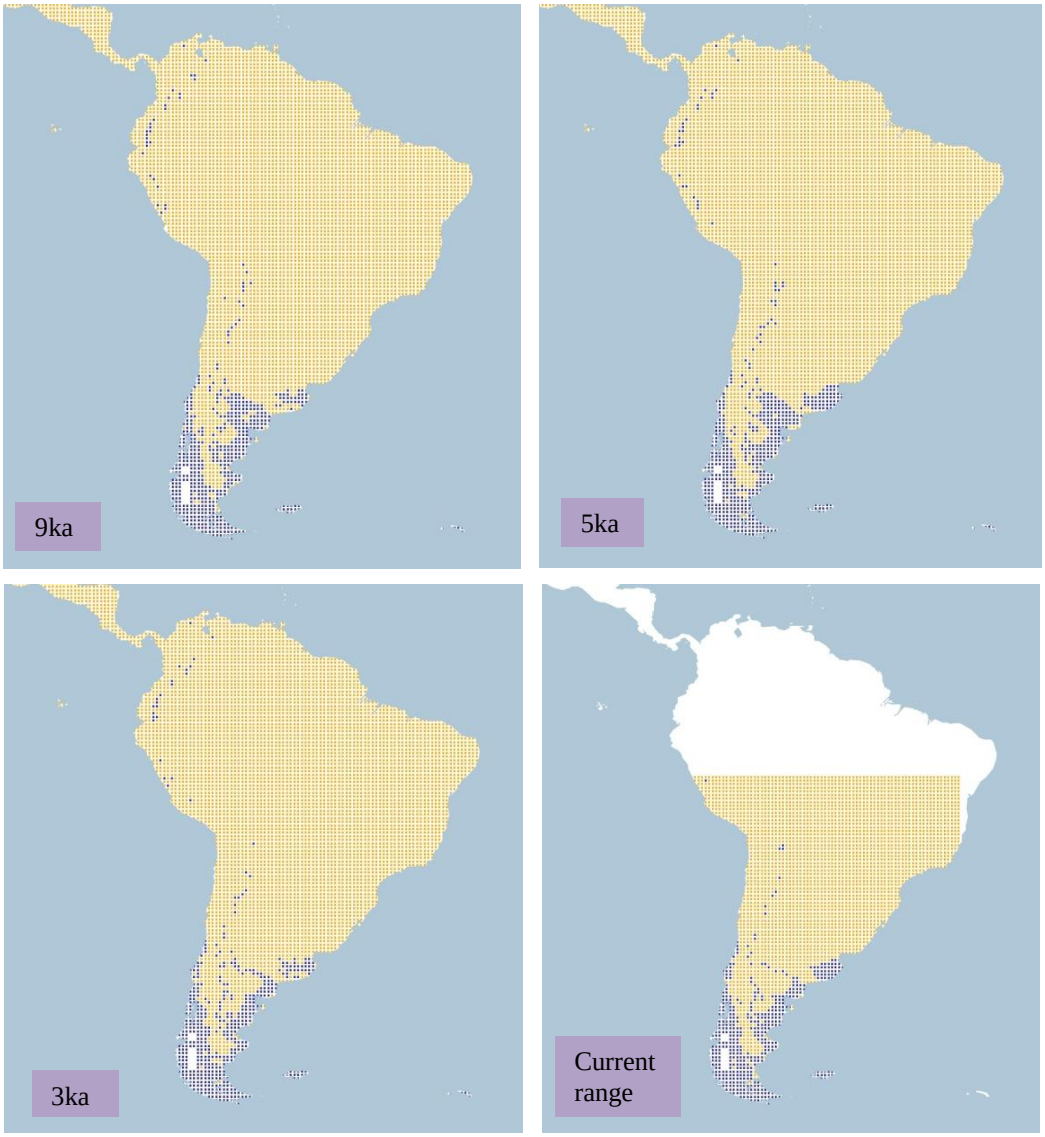

Figure 4.1.1.2.a. Simulation maps of Two-banded Plover breeding range (continued**).**

Non-breeding range (AUC: 0.970; TSS: 0.826; Kappa: 0.731): Mainly distributed on the coast of central and northern Chile, the east coast of Argentina and the central-southern coast of Uruguay and Brazil. As mentioned before the species is resident in central south Chile and Argentina, south Uruguay and Brazil, as well as the Falkland Islands.

From 26 ka BP the area projected extends from the coast to inland southern Chile, towards the Andean Cordillera, between Argentina, Peru and Ecuador. A wide region is also projected in the region of southern Brazil and in Uruguay, extending to the eastern central Argentina and a small fragmented proportion on the south-east coast of Argentina. This pattern changes

at the 22 ka BP projection, when the range in Brazil shifts to the north, reaching central Brazil where several rives are located currently. See Figure 4.1.1.2.b.

The projected area reduces at 21ka to the south of Brazil and to the east coast of Argentina with a shift in the 20 ka BP projection to central Argentina as well. At 15 ka BP this projected area starts reducing towards Uruguay and to the east coast of Argentina. However, on the south-east coast of Argentina the range beings increasing from 17 ka BP until the current range projection, overlapping with the area projected in southern Chile.

In the 6 ka BP projection there is an increase in the area predicted, moving to the central-eastern coast of Brazil and remaining until 3 ka BP. This progression may reflect the 'Alti-thermal' (between 9 ka BP and 6ka). Although the species does not have a recognized range in North America, the predictions indicate a favourable non-breeding area for this species across USA, Canada and Alaska.

A comparison between the Heinrich event H2 and the 24 ka BP projections shows a similar predicted region in the Andean Cordillera and southern Chile; differences are seen, however, around central Argentina and southern Brazil where the 24 ka BP projections predicts a large area that the H2 projection does not. The same comparison can be made between the H1 and 17 ka BP projections. Similarly, the H0 and 13 ka BP projections present parallel projected areas, except in the area of Central Argentina with a most inland rather than coastal predicted range.

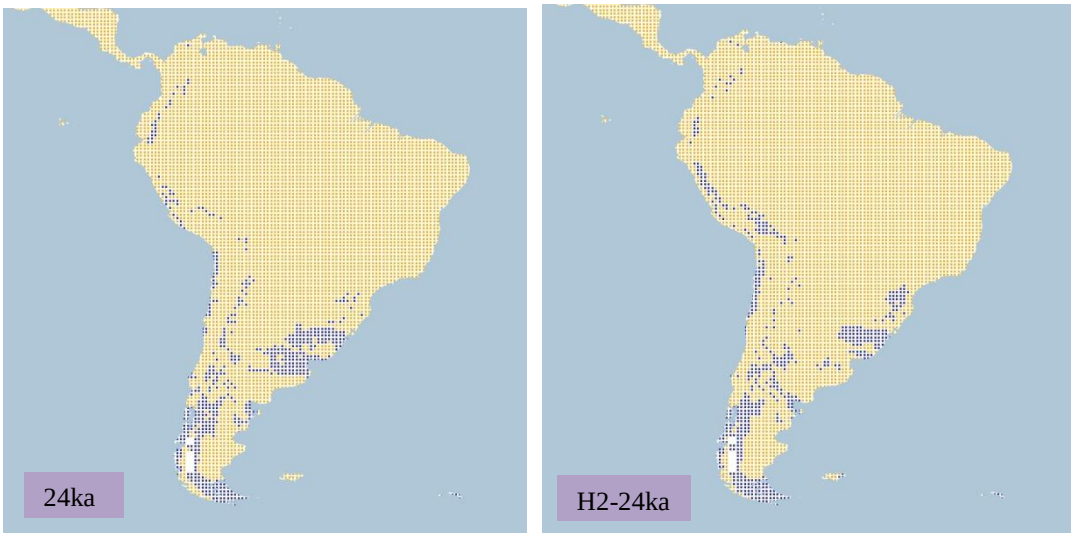

Figure 4.1.1.2.b. Simulation maps of Two-banded Plover non-breeding range.
Maps are shown for ten-time slices: 24ka, H2 (24ka), 17ka, H1 (17ka), 13ka, H0 (13ka), 9ka, 5ka, 3ka and present (1961–90).

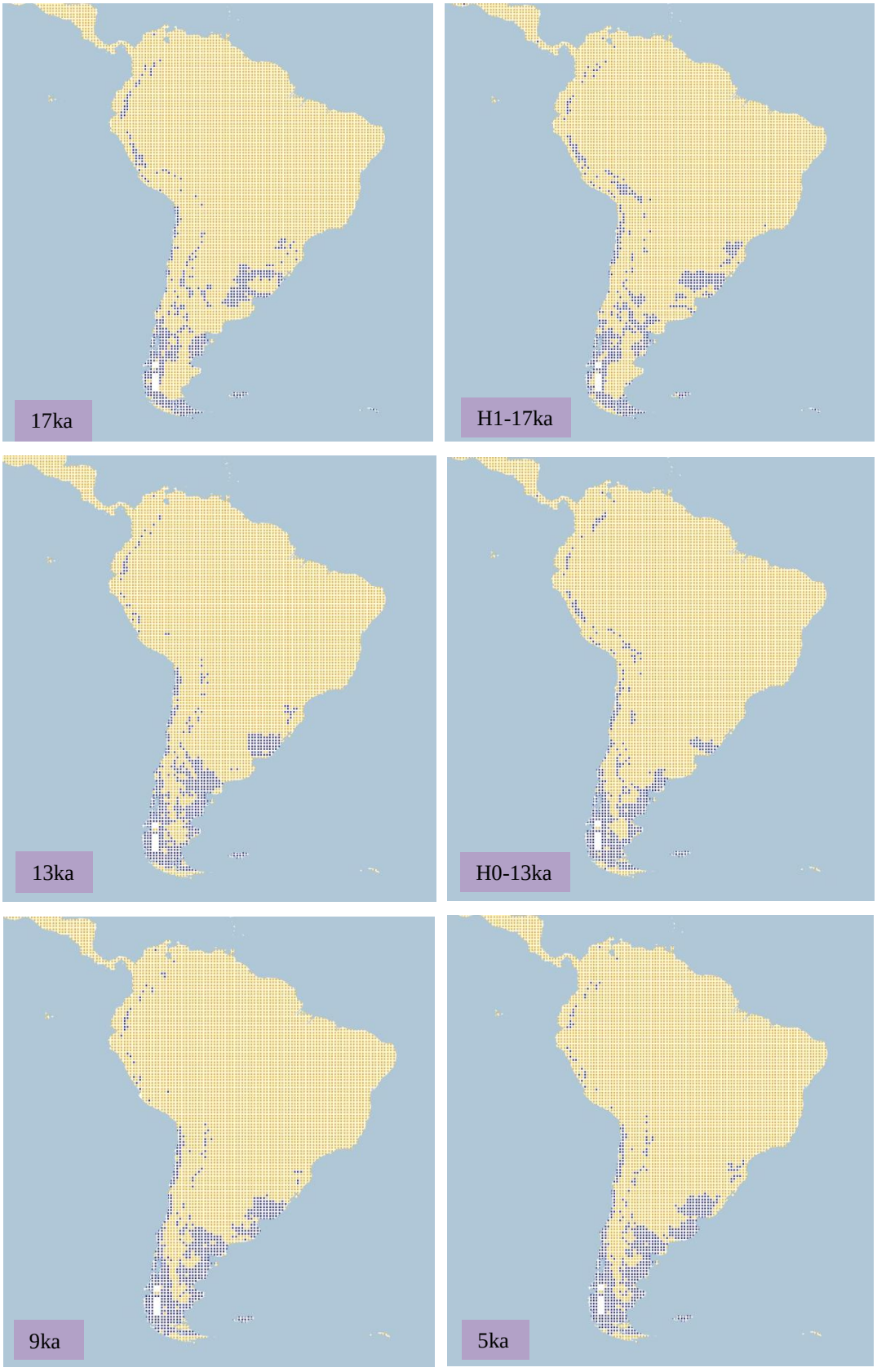

Figure 4.1.1.2.b. Simulation maps of Two-banded Plover non-breeding range (continued**).**

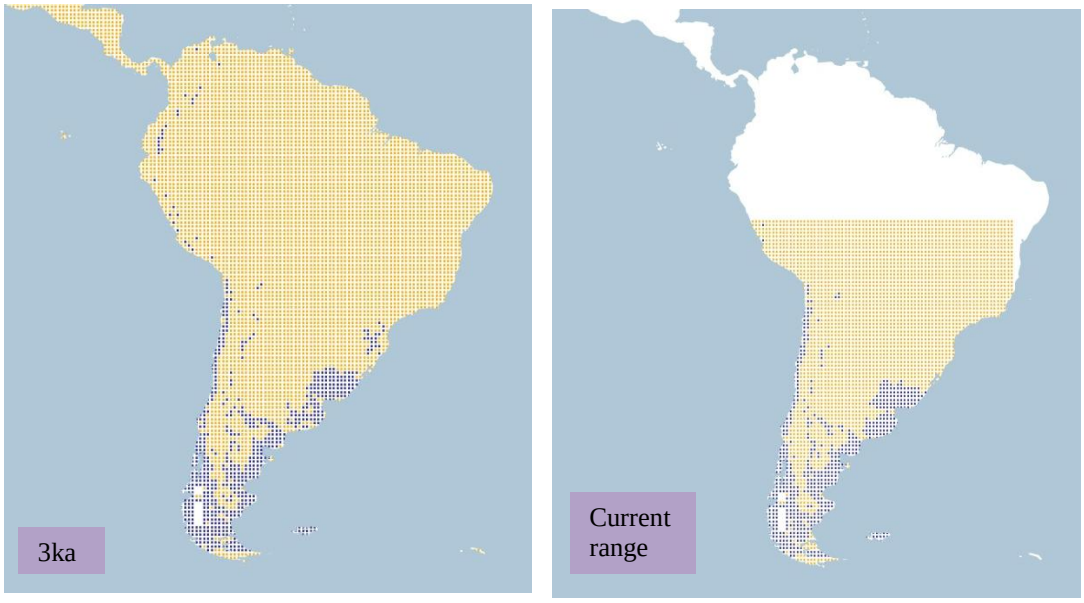

Figure 4.1.1.2.b. Simulation maps of Two-banded Plover non-breeding range (continued**).**

*4.1.1.3 Piping Plover (*Charadrius melodus *including* C. m. melodus *and* C. m. circumcinctus*). Conservation status: Near Threatened. Current known range Figure 4.1.1.3.*

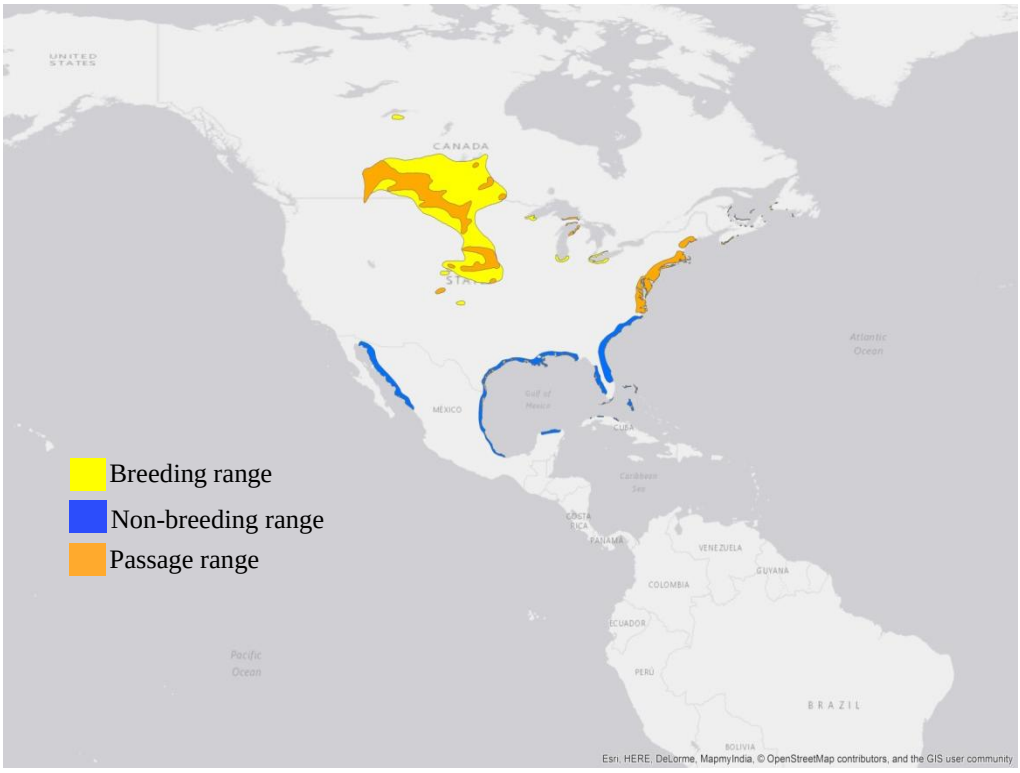

Figure 4.1.1.3. Current known range of Piping Plover.

Breeding range (AUC: 0.988; TSS: 0.903; Kappa: 0.788): The subspecies *C. m. melodus* breeds around the isles of the Gulf of St. Lawrence in Canada, extending to the east coast of USA (from Maine to North Carolina). The subspecies *C. m. circumcinctus* breeds inland in central southern Canada and central northern USA mainly, with a small proportion around the Great Lakes.

At 26 ka BP the projected area begins with a defined area in the Great Plains of central USA, with a projection in the north-western part of Canada where the glacial ice sheet was not covering the area. This pattern remains in the northern part, varying slightly, but contrasting the increasing in the central part of USA, moving to the northern and southern region, with an overlap from both areas in at the 16 ka BP projection. See Figure 4.1.1.3.a.

As the ice sheet retreats at the 13 ka BP projections, the area expands toward central Canada. After this, from 12 ka BP to 10 ka BP (the end of the Pleistocene), the range begins decreasing towards the northern and central part of Canada as well as in northern USA.

From 9 ka BP to1 ka BP the territory projected remains uniformly in the central region of Canada and USA, with a slight increase in the north-western part of Canada and to some Canadian islands located at the north. This is different from the current known range, as there is no recognized population in the northern parts of Canada. Also, the range along the Atlantic coast of USA is not predicted in any time period.

The H2 and 24 ka BP projections display similar ranges in the northern part of Canada but differ in the central part of USA and Canada with a minimal predicted area at H2, contrasting with the 24 ka BP period, when a wider range in the central region is projected. For the H1 and 17 ka BP projections, there are differences shown at H1, with an area predicted to the south of USA and less extensive than for the 17 ka BP projection. On the contrary, when comparing the H0 and 13 ka BP projections, they seem similar with the extended range towards central Canada and a reduced range in the northern parts, although H0 also predicts a southern expansion reaching the north of Mexico.

The current range is also focused in the central part of North America, mainly in the Great Plains, with no predicted range along the Atlantic coast.

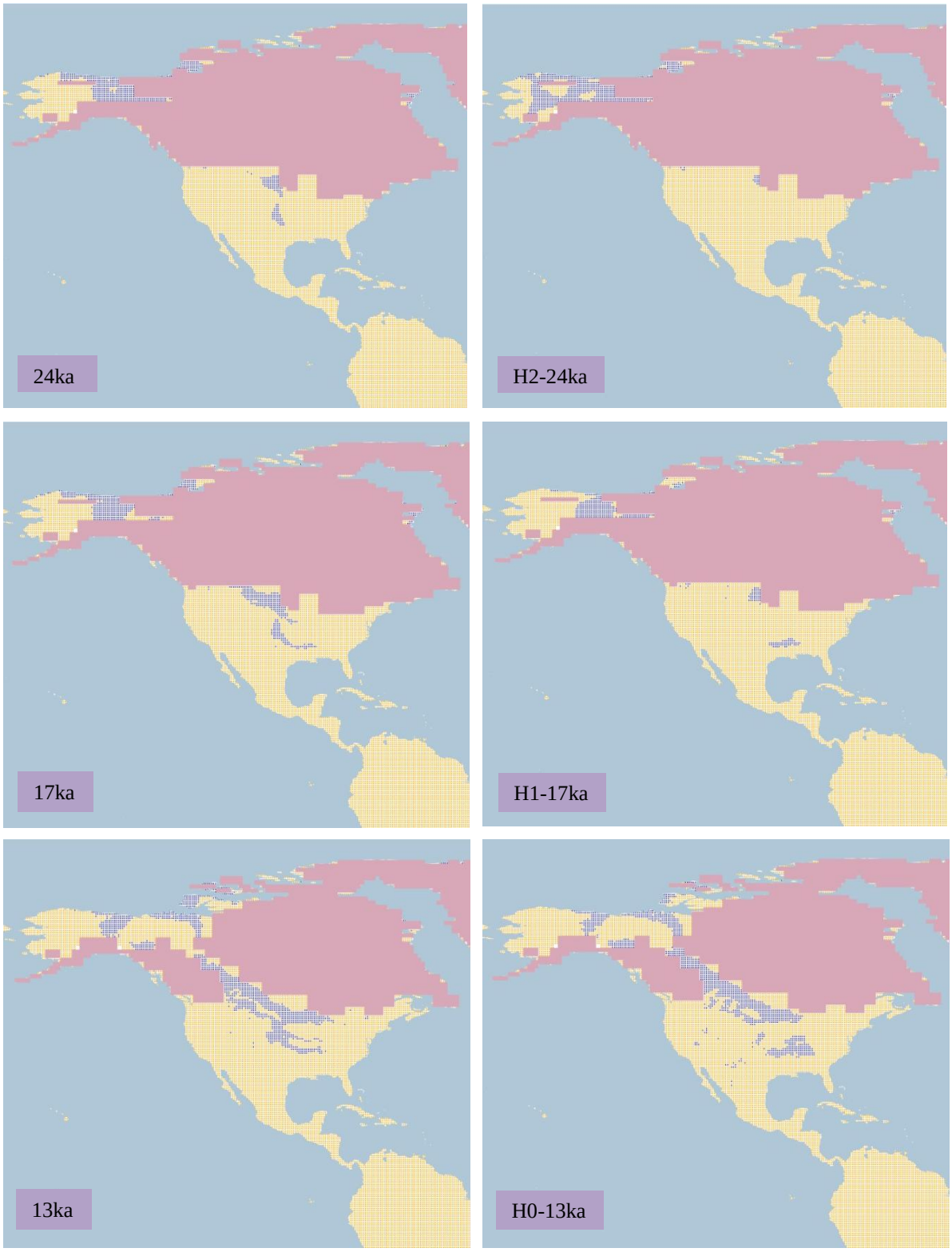

Figure 4.1.1.3.a. Simulation maps of Piping Plover breeding range.
Maps are shown for ten-time slices: 24ka, H2 (24ka), 17ka, H1 (17ka), 13ka, H0 (13ka), 9ka, 5ka, 3ka and present (1961–90).

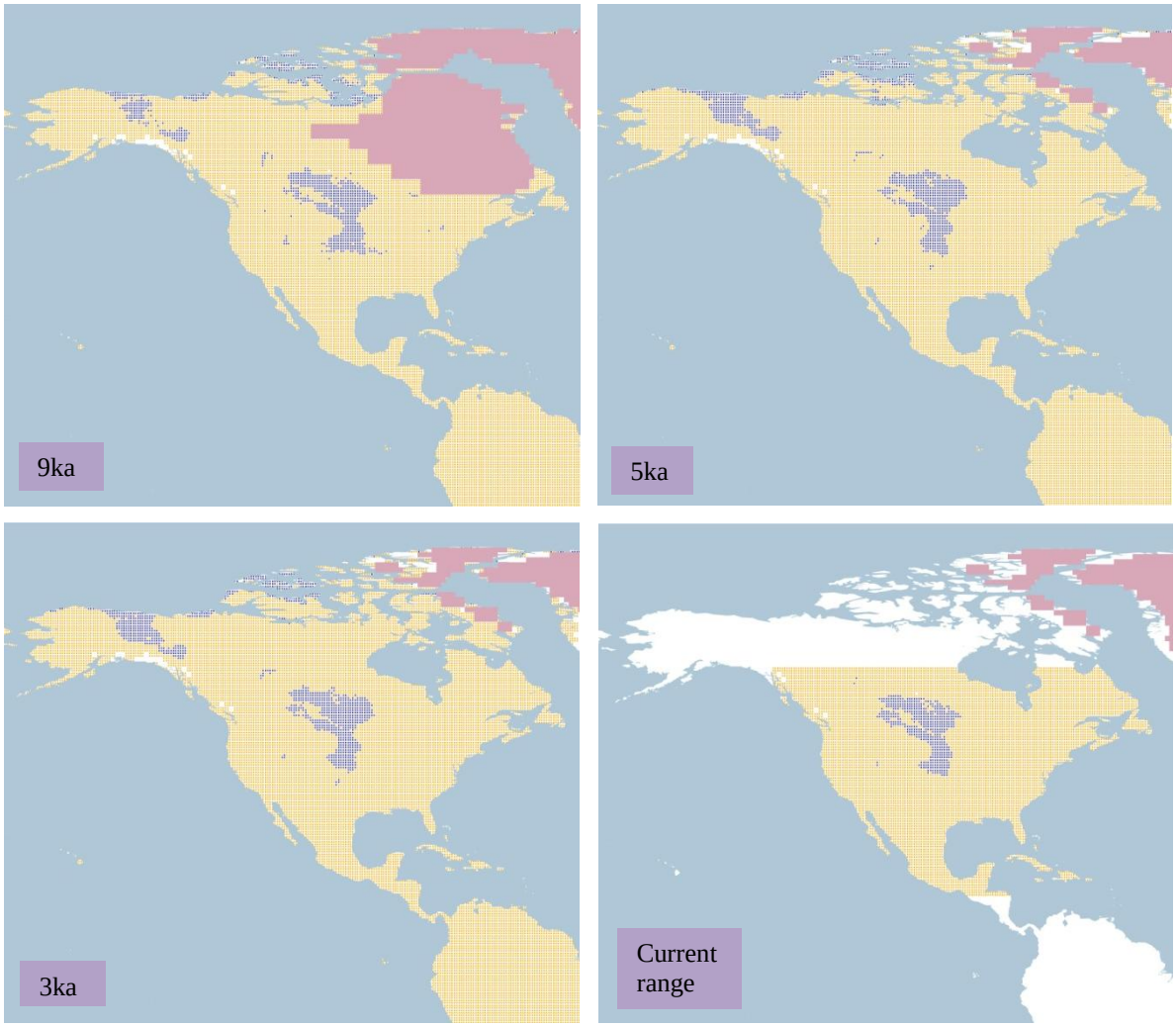

Figure 4.1.1.3.a. Simulation maps of Piping Plover breeding range (continued)**.**

Non-breeding range (AUC: 0.988; TSS: 0.930; Kappa: 0.690): the wintering grounds recognized for both subspecies are mainly located on the south-eastern coast of USA and the east coast of Mexico around the Gulf of Mexico, with small areas in the Bahamas, Cuba and the north-western part of Mexico (Sonora).

Starting at 26 ka BP the projected range is restricted to three areas, the west coast of Mexico on the Gulf of California (Sonora), the central-southern Gulf of Mexico (Veracruz) and to the south of Florida. This projected range extends to the west and eastern coast of Mexico at the 20 ka BP projection, reaching the coast of Jalisco in the Pacific Ocean and Yucatan in the Atlantic Ocean. See Figure 4.1.1.3.b.

At the 12 ka BP projection as mall area extends to the side of Baja California on the Gulf of California in Mexico with an extended area to Cuba as well. After this, there is a contraction

towards the northern part of the west coast of Mexico at the 10 ka BP projection, which is reversed at 8 ka BP, when it starts increasing again and moving also to a continental region. This differs from the east coast of Mexico, where the projected region reduces during that period.

From 7 ka BP the projected territory in Florida begins expanding to the coasts of Louisiana and Texas, and by 3 ka BP the projected area intersects with the range on the east coast of Mexico, expanding also in the continental side. This remains until the1 ka BP projection and it is similar to the current projected range, from the west coast of Mexico (from Sonora to Sinaloa) and on the east coast of USA and Mexico. Although the known current range it is not as extended as the projection, there is suitable habitat simulated.

There seems to be no correlation between the projections of H2 and 24 ka BP, given that the projection at H2 is very restricted to a small area on the west coast of Sinaloa in Mexico; the range in Florida and on the east coast of Mexico it is not projected. However, the range projected in South America at H2 is very similar to the one projected at 24ka. The same behaviour is seen for the H1 projection, with the area remaining restricted to the coat of Sinaloa with an increase on the east coast of Mexico, albeit scattered. Also, in South America the range increases in the north of Brazil for the H1 projection. In the H0 and 13 ka BP projections the region looks similar for the areas of the west coast of Mexico, even moving to the south reaching part of Central America (coast of Belize and Honduras).

It is important to mention that there is a projected range from 26 ka BP until1 ka BP in South America, even though the species is not currently located in the area. Suitable climatic conditions for this species extend from Paraguay to the north of Argentina in South America and on the east coast of Brazil. This projection remains through all the time frames, reducing slightly during 19 ka BP to increase again at 16 ka BP and persisting until the1 ka BP projection.

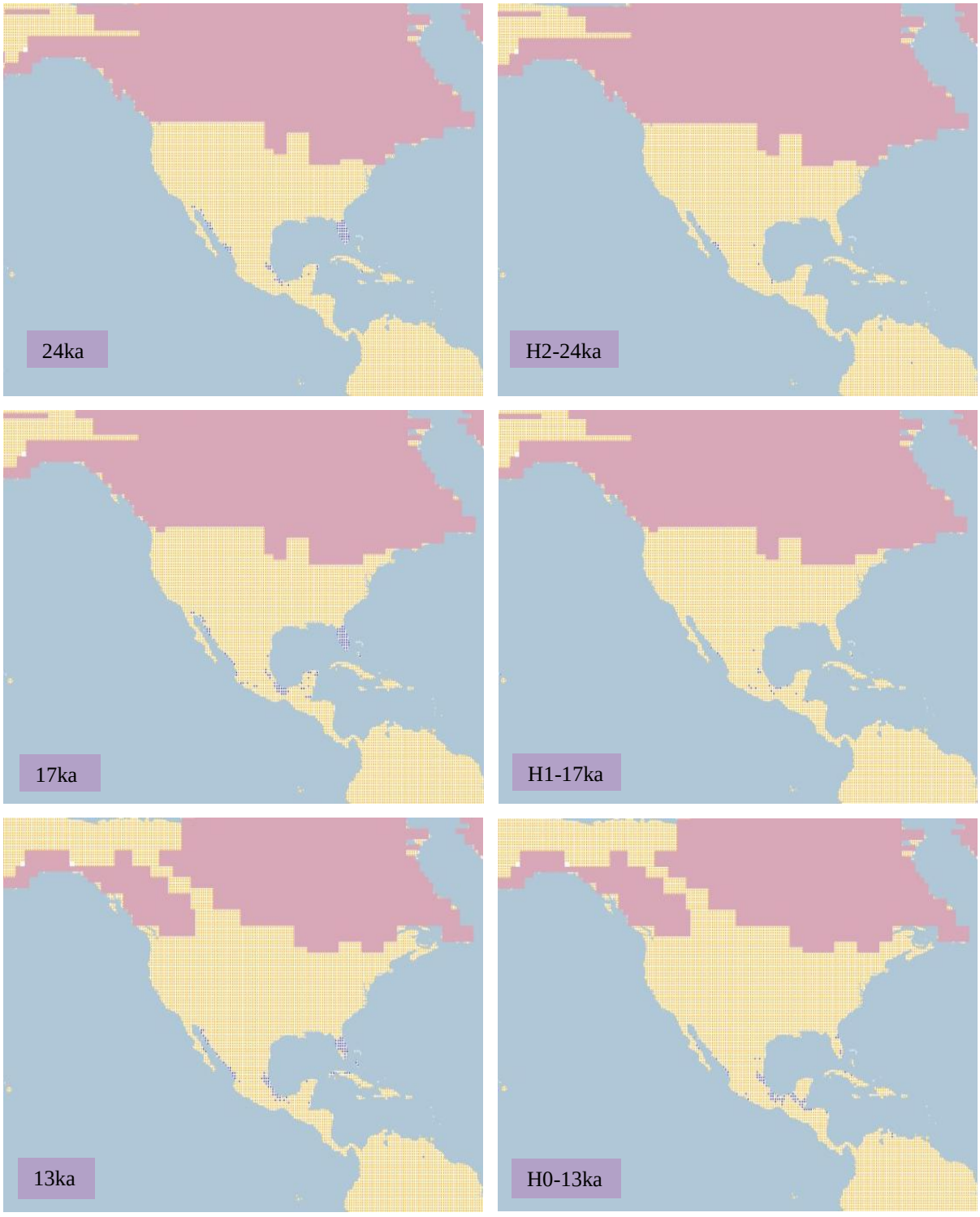

Figure 4.1.1.3.b. Simulation maps of Piping Plover non-breeding range.
Maps are shown for ten time slices: 24ka, H2 (24ka), 17ka, H1 (17ka), 13ka, H0 (13ka), 9ka, 5ka, 3ka and present (1961–90).

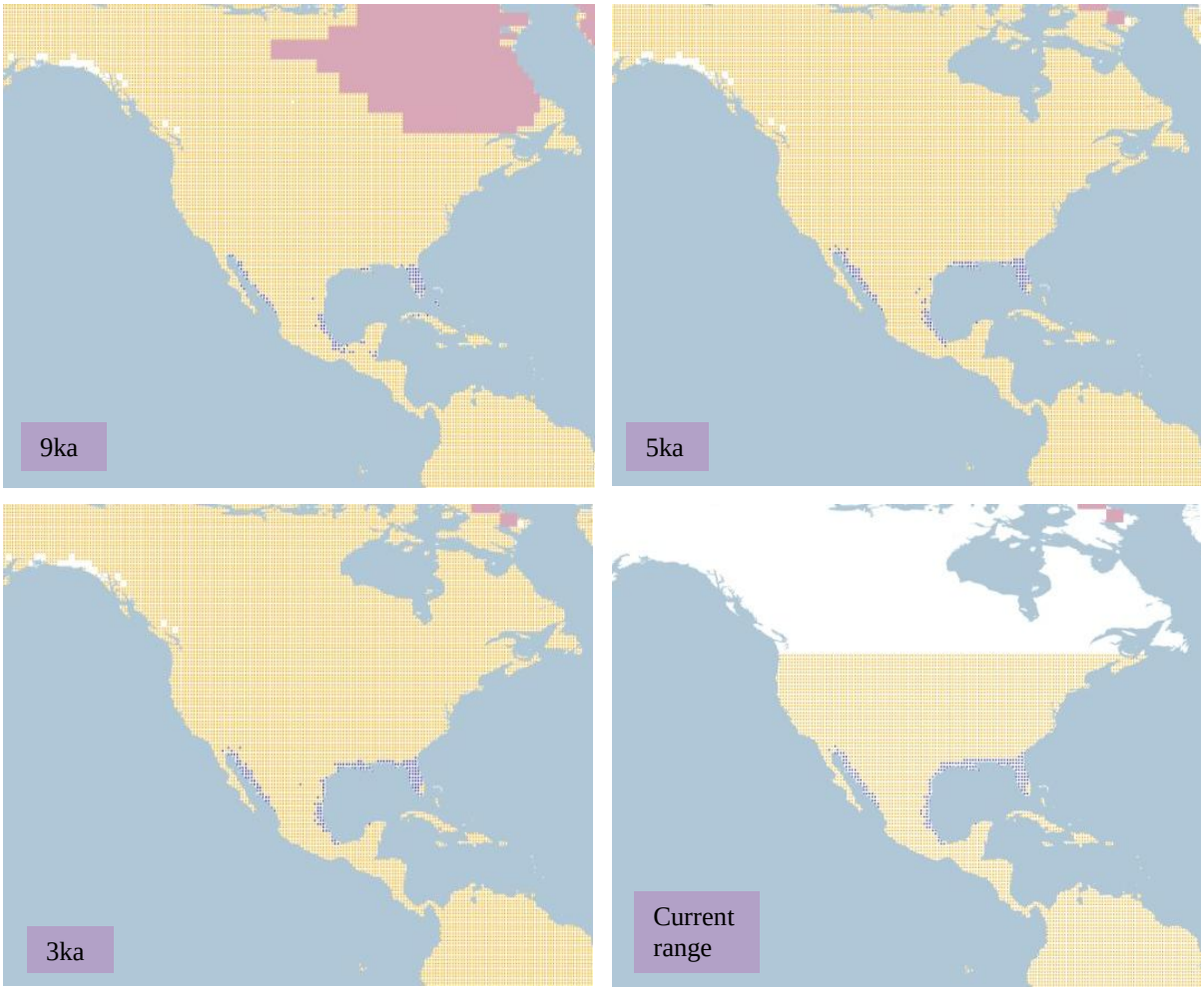

Figure 4.1.1.3.b. Simulation maps of Piping Plover non-breeding range (continued)**.**

4.1.1.4 Rufous-chested Plover (Charadrius modestus). Conservation status: Least Concern. Current known range Figure 4.1.1.4.

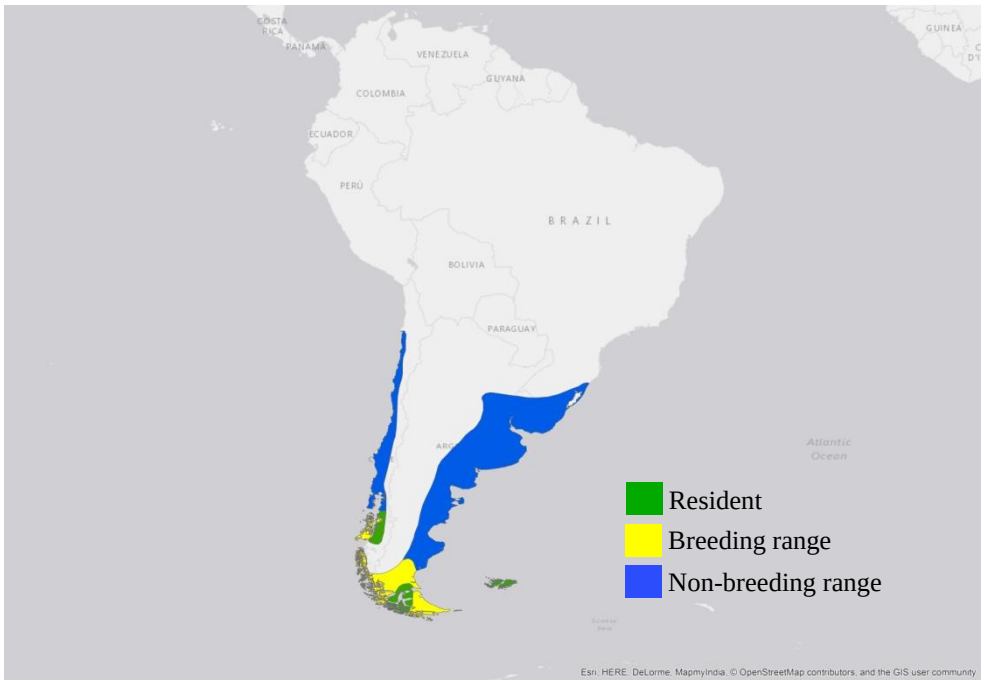

Figure 4.1.1.4. Current known range of Rufous-chested Plover.

Breeding range (AUC: 0.994; TSS: 0.691; Kappa: 0.821): the species breeds in south Chile and Argentina towards the eastern coast and reaching Tierra del Fuego. It is considered a year-round resident in the area of inland south-west coast and southern Chile, around the area of Punta Arenas and the Falkland Islands.

From the 26 ka BP simulation the range is shown at the south of Chile with a minimal proportion in the Andean Cordillera. The projected region remains more or less the same until the 17 ka BP projection. After this at 16 ka BP, the range increases to the south of Argentina and begins moving inland, increasing over time, and then remaining unaltered until 1 ka BP. The current range also looks consistent with the projection of 1 ka BP. See Figure 4.1.1.4.a.

For the Heinrich event H2 when comparing it with 24 ka BP both projections seem similar with the same area in the south of Chile. This behaviour remains when comparing H1 to 17 ka BP and H0 to 13 ka BP, with no striking differences.

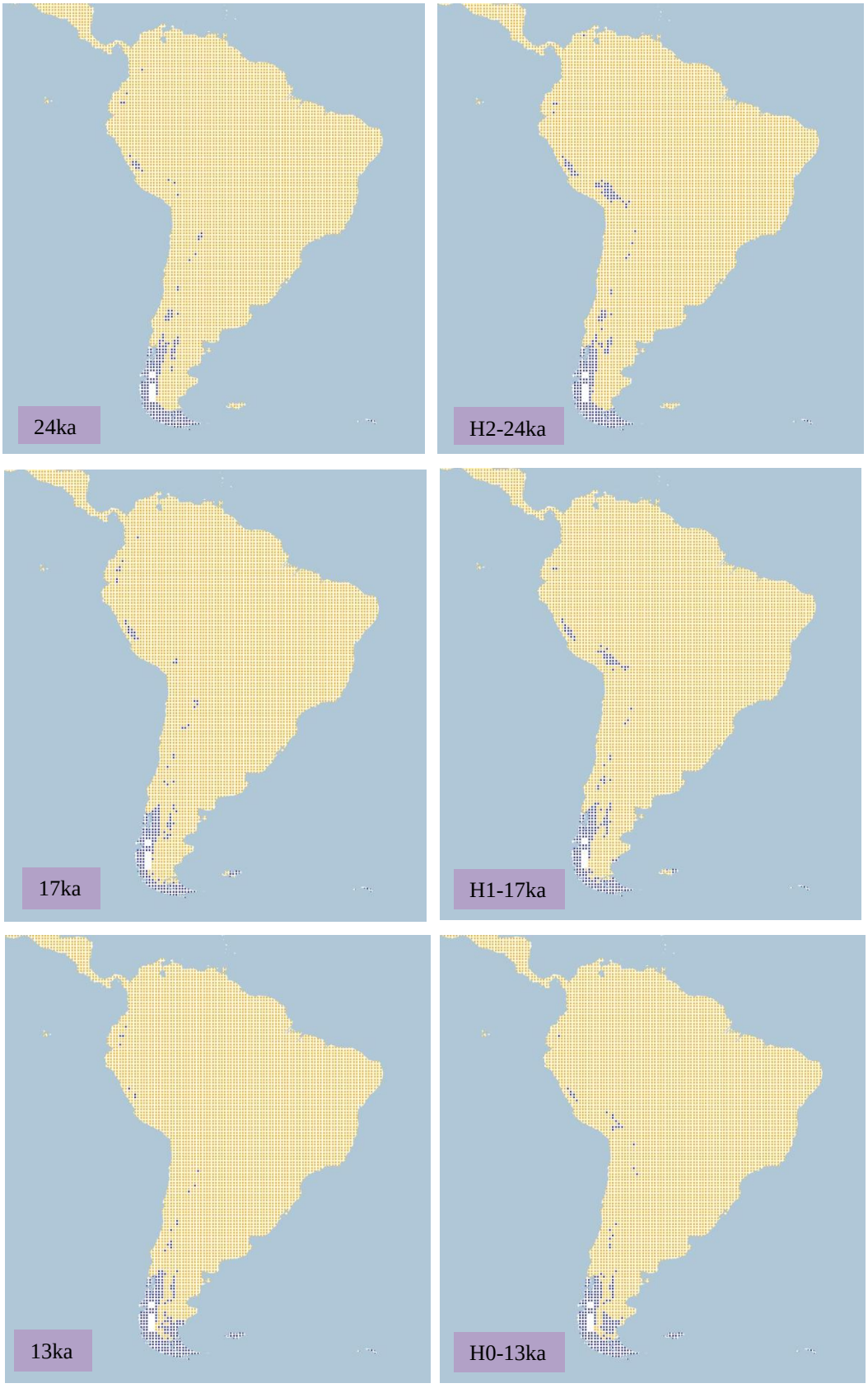

Figure 4.1.1.4.a. Simulation maps of Rufous-chested Plover breeding range.
Maps are shown for ten-time slices: 24ka, H2 (24ka), 17ka, H1 (17ka), 13ka, H0 (13ka), 9ka, 5ka, 3ka and present (1961–90).

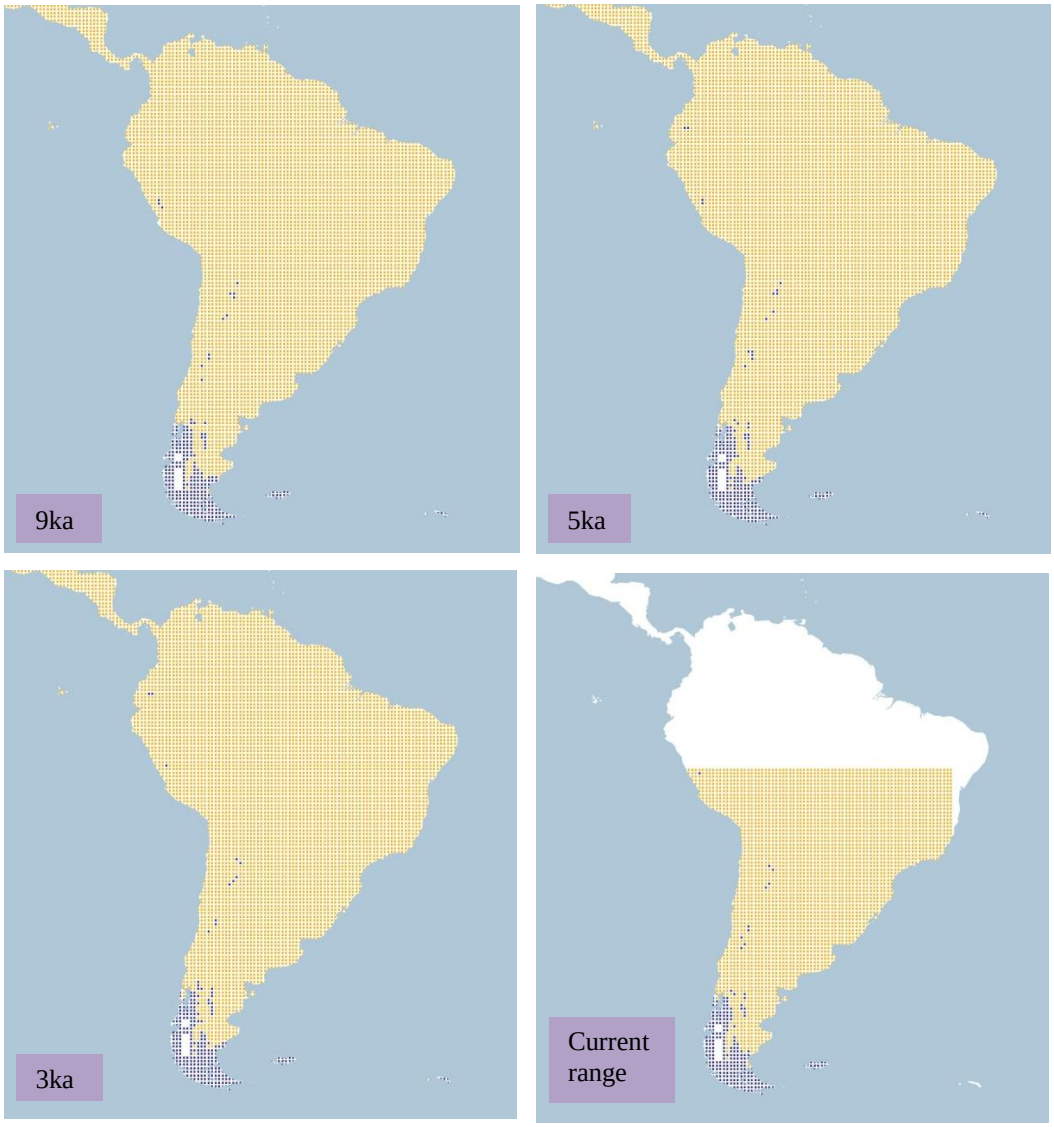

Figure 4.1.1.4.a. Simulation maps of Rufous-chested Plover breeding range (continued**).**

Non-breeding range (AUC: 0.988; TSS: 0.808; Kappa: 0.759): This range extends along the west coast of Chile, the east coast and inland Argentina, as well as Uruguay and southern Brazil. It has a year-round range in the Falkland Islands and a small range on the south of Chile.

From 26 ka BP the projected area is located mostly to the south part of Brazil, Uruguay, central-southern Paraguay and northern Argentina, extending on a smaller scale over the Andean Cordillera and reaching central Argentina and the Chilean coast. At 24 ka BP the range reduces over Brazil, moving south, towards central Argentina to grow again at 22 ka BP. See Figure 4.1.1.4.b.

At 16 ka BP there is a movement to the south over Brazil, Paraguay and Uruguay, and the area in central Argentina moves to the south as well, while the projected range in the Andean Cordillera remains the same. At the 15 ka BP projection both range areas intercalate to become a larger range from southern Brazil to southern Argentina and moving inland towards the Andean Cordillera. This lasts until the 12 ka BP projection, when the inland range begins moving to the east coast in South America, with a decrease in the territory predicted on the Andean Cordillera.

At the start of the Holocene, between 1lka and 9 ka BP, the range continues to extend from south Brazil, Uruguay and mainly in Argentina and at a smaller scale on the coast of Chile. By 8 ka BP and 6 ka BP there is an increase in range for the same region that could be related to the Alti-thermal, although at 7 ka BP the predicted area is reduced for the south of Brazil and Uruguay where the range is fragmented.

From 6 ka BP until the1 ka BP projection the range remains similar on both coasts of South America and there are several points predicted suitable around the Andean Cordillera. The current range projection is also displayed with similar patterns as the1 ka BP projection.

Currently there is a year-round range in the Falkland Islands, however, the range on the projections it is not present from 26 ka BP until 17 ka BP; after 16 ka BP the projection begins to simulated suitable areas in the Falkland Islands and moving from the east to the western region.

For the Heinrich event H2 and the 24 ka BP projection there are similar ranges shown, only at H2 the area on the Andean Cordillera and on the eastern region of South America is less fragmented than what is projected at 24 ka BP. For H1 and 17 ka BP there is also an analogous projected range for South America. Only between the H0 and 13 ka BP projections differences are presented, specifically on the eastern part of South America; in the projection for H0 the range is more restricted to the coast than for 13 ka BP.

It is important to mention than even though the species is only distributed in South America, the projections show suitable conditions for the species in North America, mainly from central-east to the coast in USA. This is seen for all the time slices but grows towards the present, with a small range also on the north-western coast of British Columbia and Alaska.

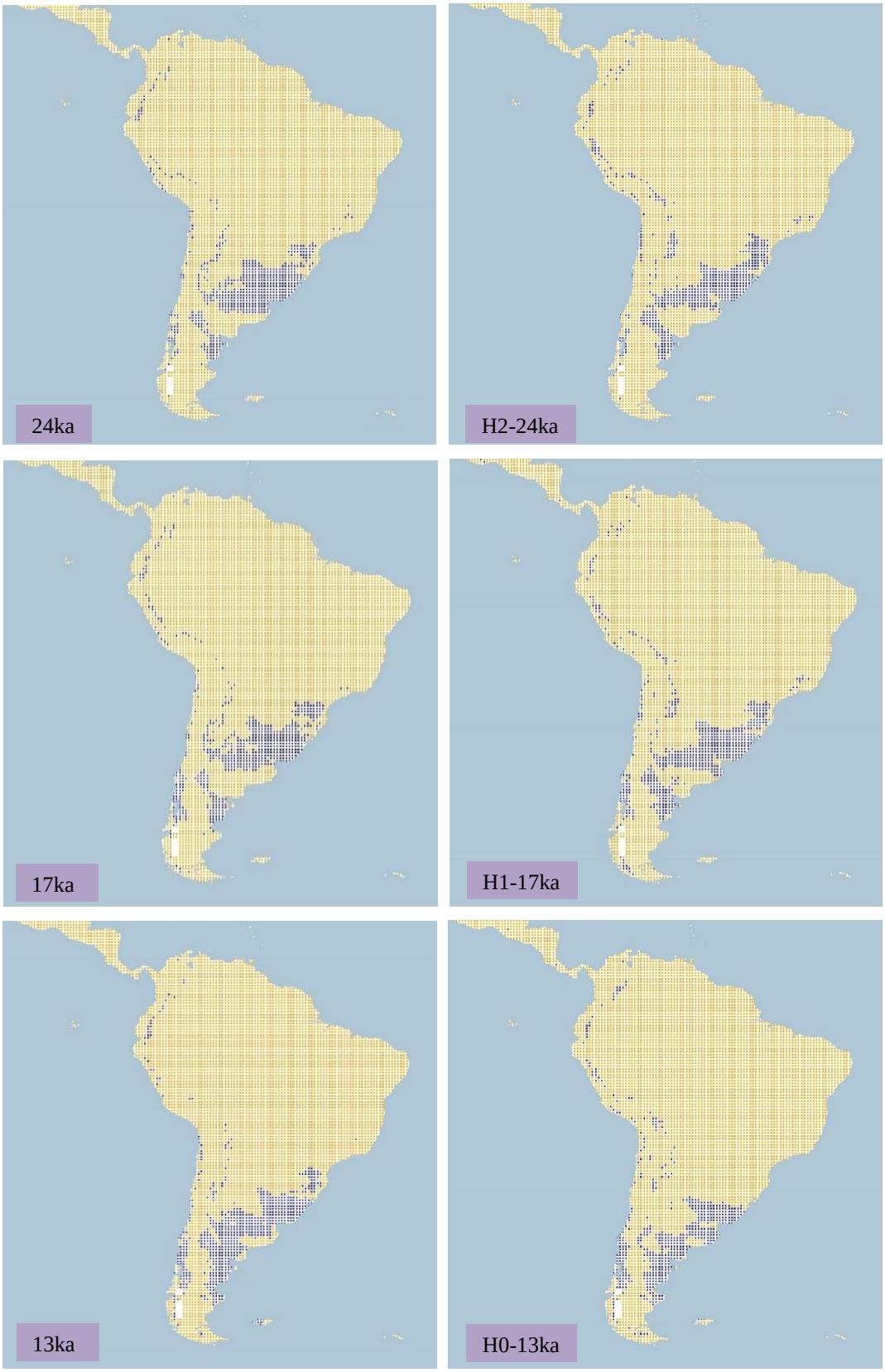

Figure 4.1.1.4.b. Simulation maps of Rufous-chested Plover non-breeding range. Maps are shown for ten-time slices: 24ka, H2 (24ka), 17ka, H1 (17ka), 13ka, H0 (13ka), 9ka, 5ka, 3ka and present (1961–90).

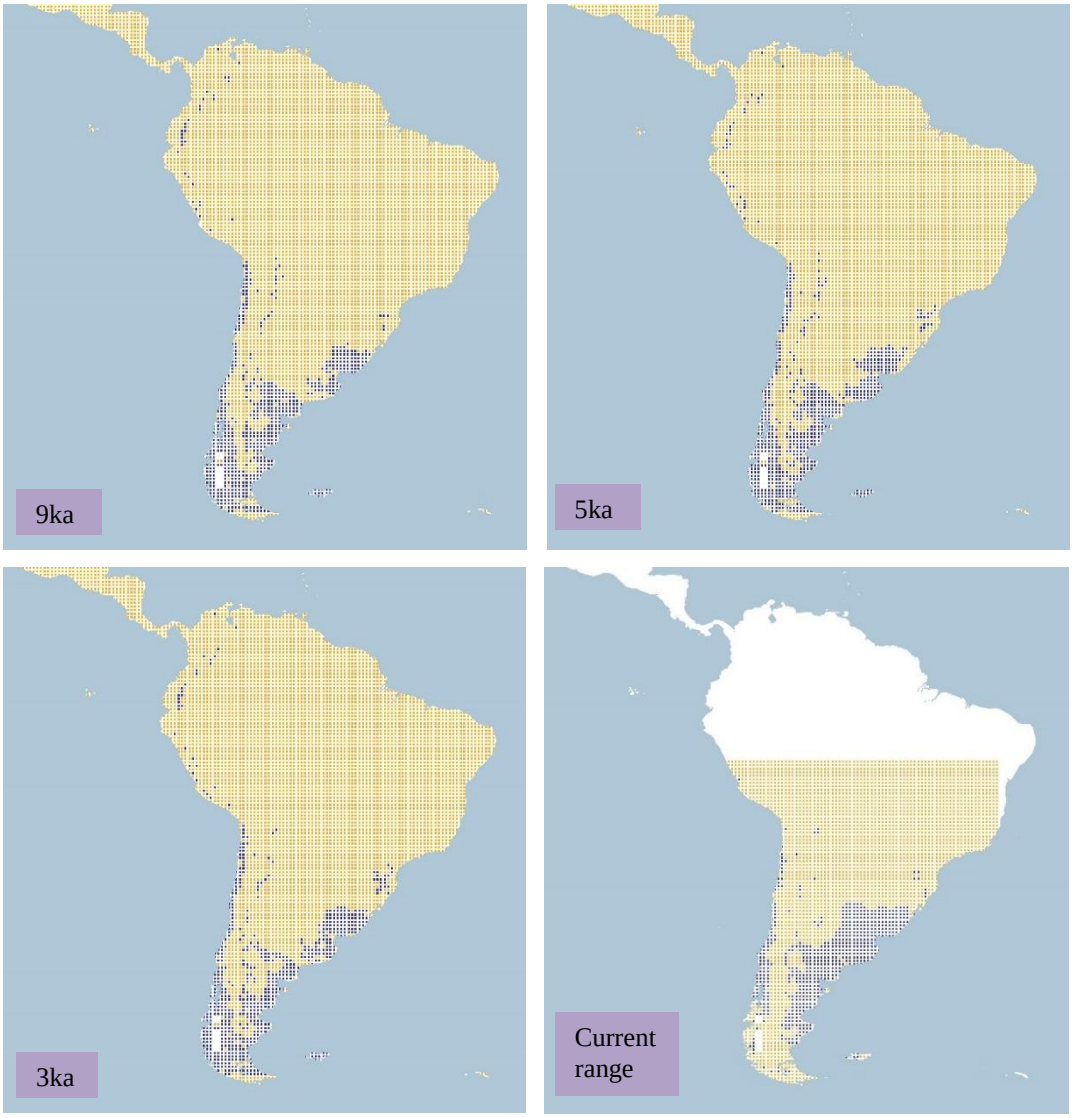

Figure 4.1.1.4.b. Simulation maps of Rufous-chested Plover non-breeding range (continued**).**

*4.1.1.5 Mountain Plover (*Charadrius montanus*). Conservation status: Near Threatened. Current known range Figure 4.1.1.5.*

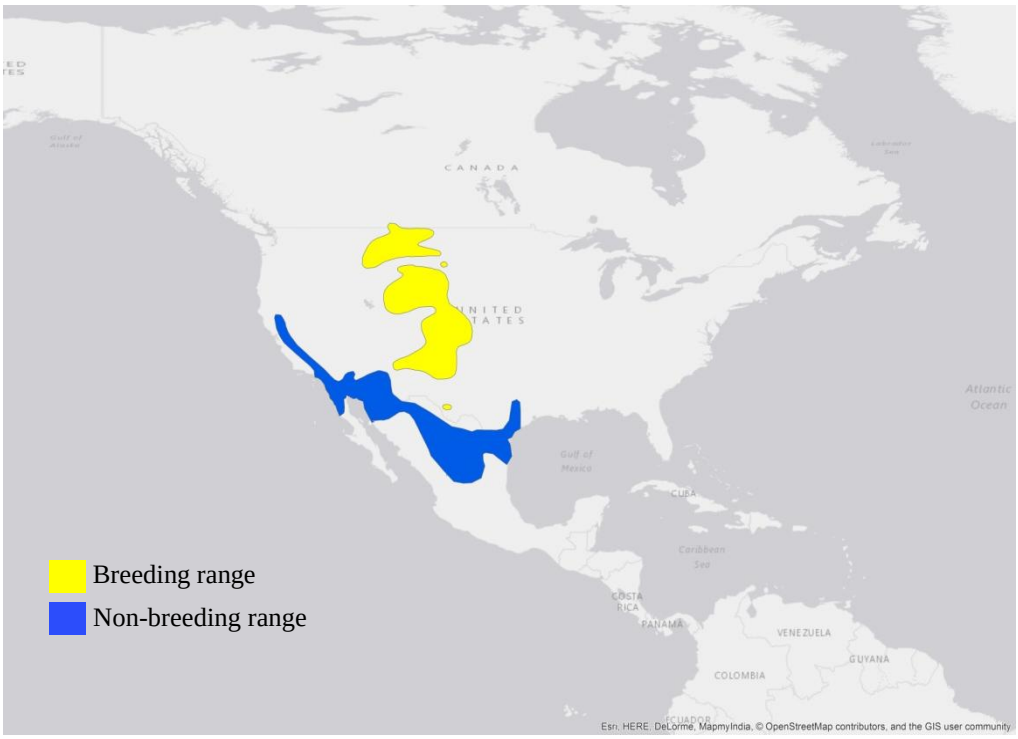

Figure 4.1.1.5. Current known range of Mountain Plover.

Breeding range (AUC: 0.987; TSS: 0.897; Kappa: 0.775): Current breeding range in the central part of USA in the region of the Great Plains, from Montana to New Mexico, with a small extension into the south of Canada (Alberta and Saskatchewan) and a small area in the north of Mexico (Nuevo Leon).

The projection at 26 ka BP shows a range mainly in the central part of USA, with a small area in the north-western part between Washington and Montana. The range gradually expands after 26 ka BP, especially in the projection for 17 ka BP when the territory extends uninterruptedly from the central USA to the north-west, and a small range is projected in the western part of Mexico between Sonora and Sinaloa. The range begins shifting to the west of USA at 16 ka BP and at 14 ka BP it disperses again towards central USA. See Figure 4.1.1.5.a.

As the ice sheet retreats to the Arctic region at 12 ka BP, the range expands to western Canada, and a small range appears in central Canada, near the ice sheet. Subsequently, the

range in western Canada fades and the range in central-eastern Canada grow; this pattern lasts until the 9 ka BP projection.

At 8 ka BP the ranges in central-eastern Canada and in the north of Mexico disappear, leaving only the range in central-western USA, which persist until the 6 ka BP projection. After this, the range begins fragmenting in central-western USA and moves toward the central region of the USA only, remaining similarly until 1 ka BP and the current range projection.

The prediction at H2 shows a very limited range in North America, with only small areas in the north-west USA and west Alaska, contrasting with the projection of a large range in the central USA at 24 ka BP. A similar projection is seen at H1 and 17 ka BP in the north-west USA, with a new area predicted in central-west Mexico between Durango and Sinaloa. At H0 there is an increase of the north-west range in the USA, although this projection shows differences from the 13 ka BP projection, showing a larger range in central USA.

Even though there is no breeding range known in South America, the projections from 26 ka BP to 12 ka BP show suitable conditions in the Andean Cordillera of Chile and south of Argentina. Subsequently, only the suitable area on the Andean Cordillera remains until the1 ka BP projection, and the same behaviour is shown on the Heinrich events H2 to H0.

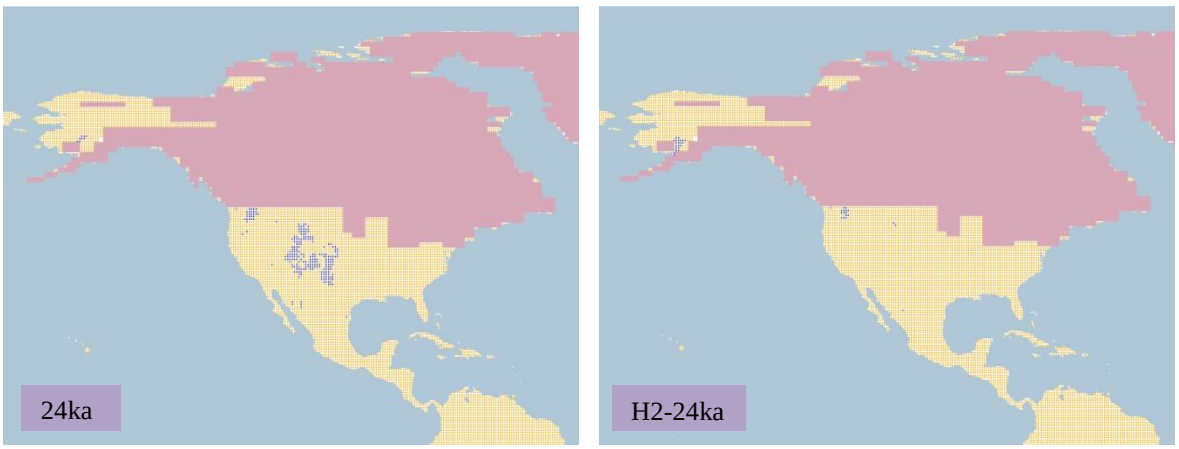

Figure 4.1.1.5.a. Simulation maps of Mountain Plover breeding range.
Maps are shown for ten-time slices: 24ka, H2 (24ka), 17ka, H1 (17ka), 13ka, H0 (13ka), 9ka, 5ka, 3ka and present (1961–90).

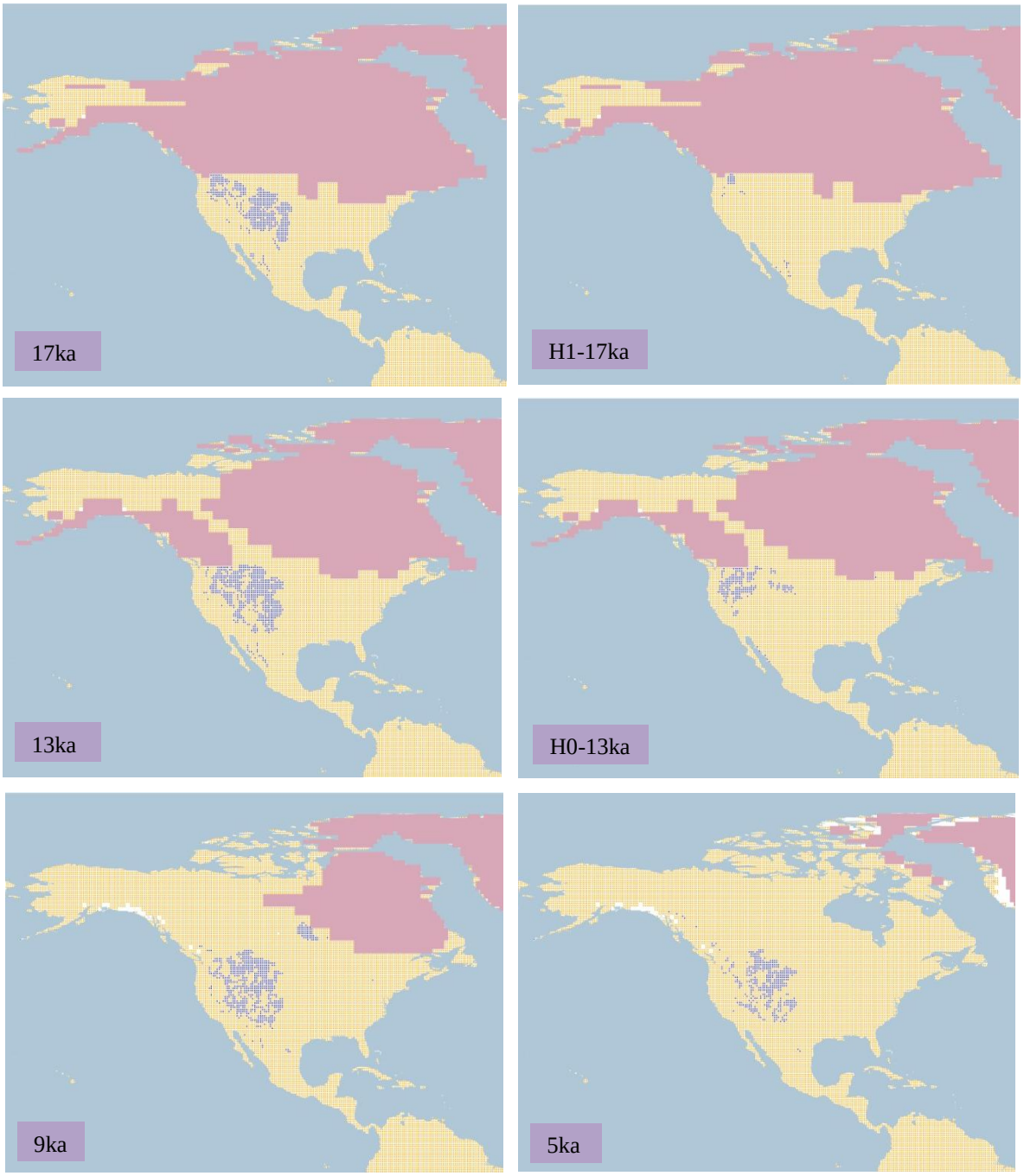

Figure 4.1.1.5.a. Simulation maps of Mountain Plover breeding range (continued**).**

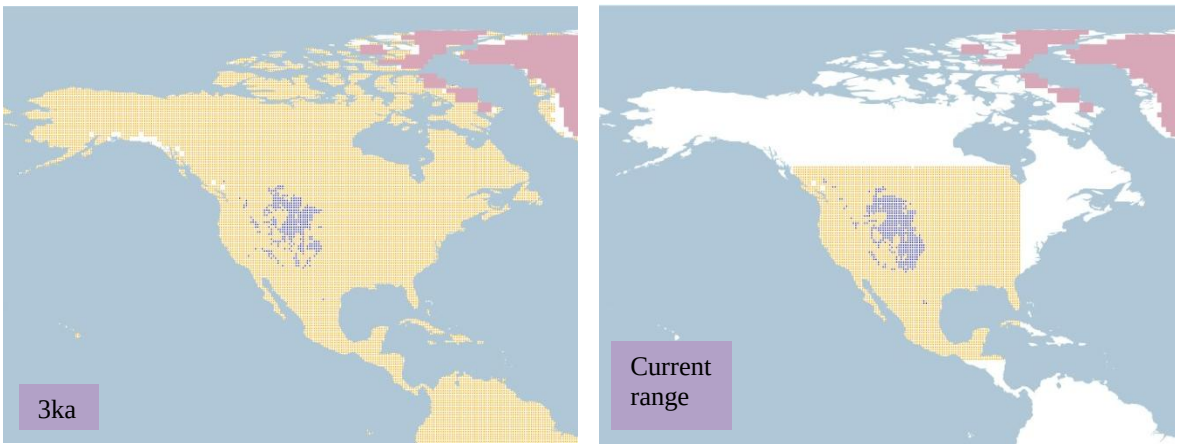

Figure 4.1.1.5.a. Simulation maps of Mountain Plover breeding range (continued**).**

Non-breeding range (AUC: 0.988; TSS: 0.936; Kappa: 0.618): the species spends the non-breeding season in an area extending from central California, central-southern Arizona and south-eastern Texas in the USA, to the north of Mexico from the north of Baja California, across Sonora, Chihuahua, Coahuila, Nuevo Leon and Tamaulipas.

Given the known non-breeding range and analysing the projections there is a larger area simulated for South America than for Mexico, therefore a description is included also for that region.

The 26 ka BP projection displays a particularly fragmented range, extending from the south-west USA in California to Baja California and Sonora on the Gulf of California, with areas projected also in central Mexico, and in South America on the Andean cordillera and from central to north-east Brazil. In addition, a larger area is projected on the east coast of Brazil reaching also Uruguay and north Argentina. The same pattern is seen at 22 ka BP, but at 21ka there is a change in the range in south Brazil with contraction to the central coast. See Figure 4.1.1.5.b.

After this at 20 ka BP the range in Mexico continues to be fragmented around the central part and in South America the range in north-east Brazil is seen steadily and there is a growing range from Bolivia to north Argentina. The same trends continue at 19 ka BP when the ranges in south Brazil and north Argentina intersect.

At 15 ka BP the range in north Brazil shifts to the central region and the range from Bolivia to Argentina reduces slightly. This continues at 14 ka BP and by 11 ka BP the range is

restricted to south Brazil and Uruguay. Also, in Mexico the range starts decreasing and is focused on the central region only.

By 8 ka BP the range increases in central Mexico and remains the same in South America, decreasing after 7 ka BP to the east coast, central Brazil and the Andean cordillera. This pattern remains until1 ka BP and on the current range the projection indicates a growth in central Mexico towards the south, contrasting with the known current range, which can be found from California to Texas in the USA and the north-central part of Mexico.

The H2 projection indicates a similar extent to that at 24 ka BP, although the range is more widespread in the south of USA, from Arizona to Florida, and also in the north-west part of South America. This pattern is shown also for H1 with an increase of range in Florida and the north of Mexico (Sonora), and at H0 the territory in Mexico shifts to the south-west on the Pacific coast.

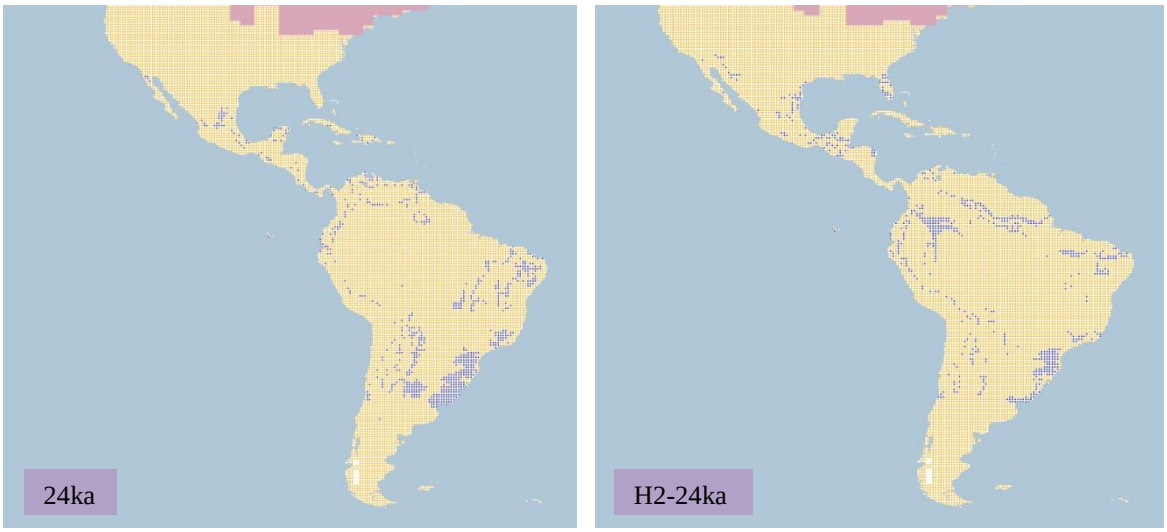

Figure 4.1.1.5.b. Simulation maps of Mountain Plover non-breeding range.
Maps are shown for ten-time slices: 24ka, H2 (24ka), 17ka, H1 (17ka), 13ka, H0 (13ka), 9ka, 5ka, 3ka and present (1961–90).

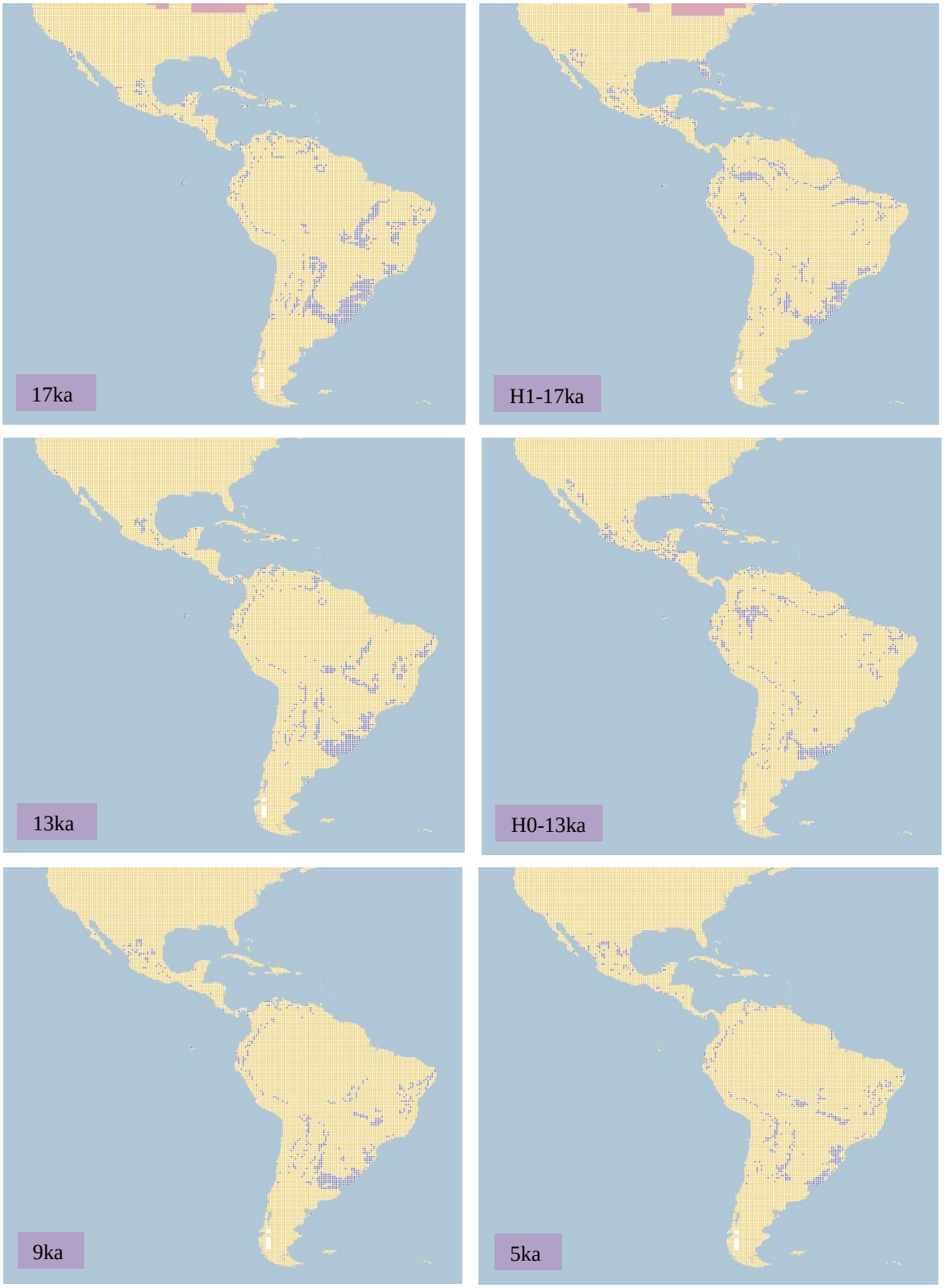

Figure 4.1.1.5.b. Simulation maps of Mountain Plover non-breeding range (continued**).**

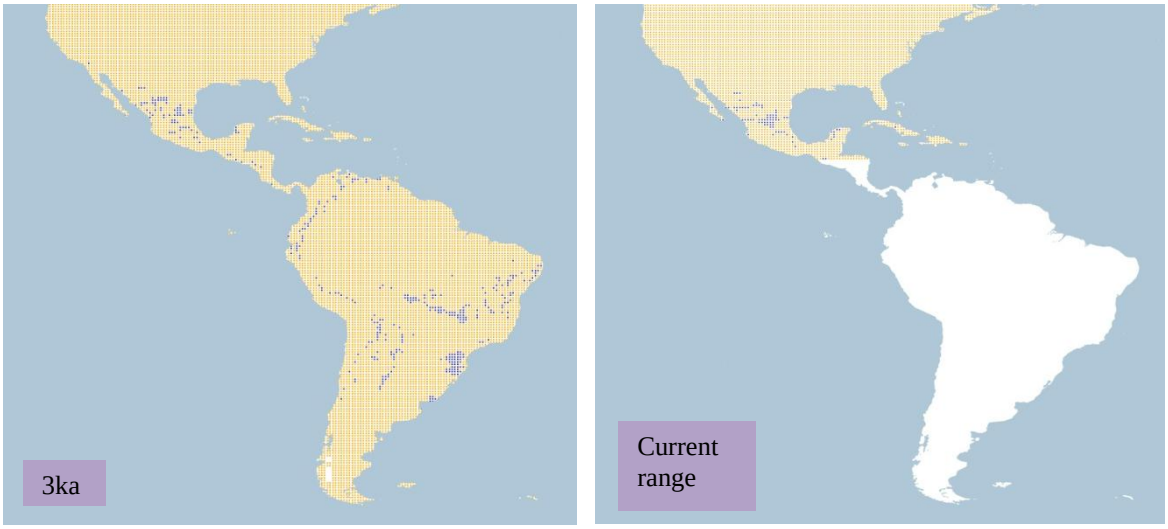

Figure 4.1.1.5.b. Simulation maps of Mountain Plover non-breeding range (continued**).**

*4.1.1.6 Snowy Plover (*Charadrius nivosus including C. n. nivosus and C. n. occidentalis*). Conservation status: Near Threatened. Current known range Figure 4.1.1.6.*

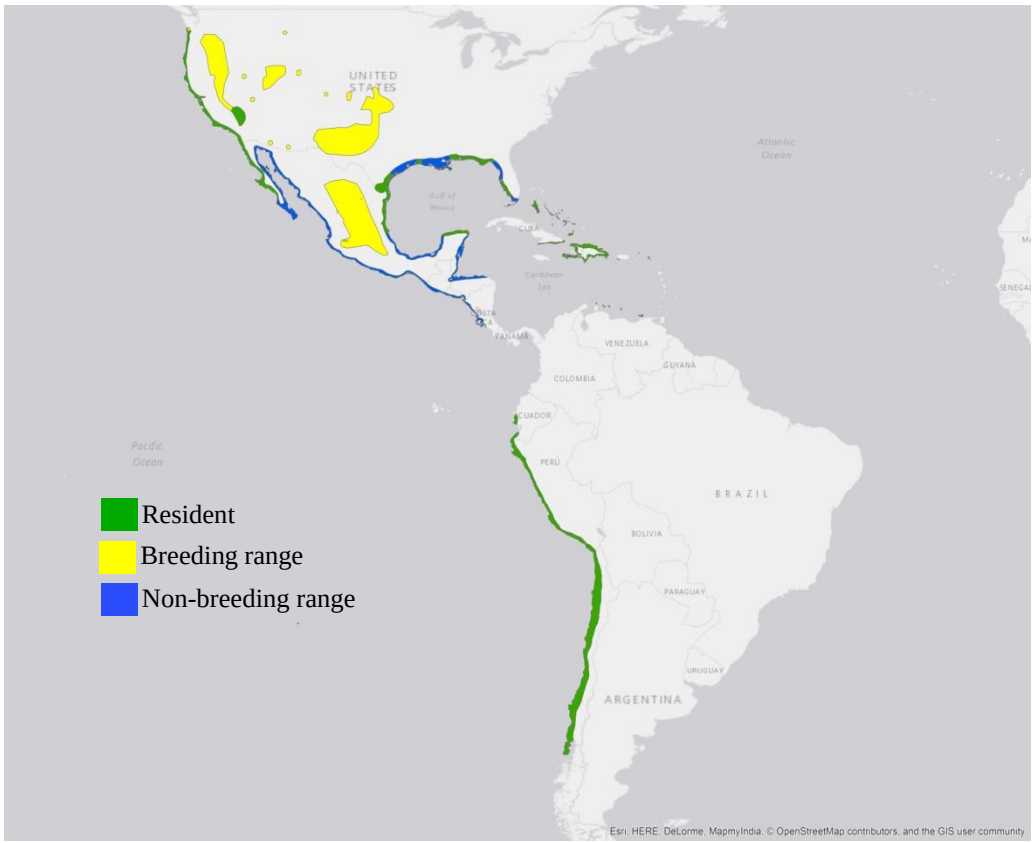

Figure 4.1.1.6. Current known range of Snowy Plover.

Breeding range (AUC: 0.982; TSS: 0.838; Kappa: 0.802): The subspecies *C. n. occidentalis* has a year-round range on the west coast of South America, from south Ecuador to central-south Chile. *C. n. nivosus* also has year-round grounds on the west coast of North America from Washington to Baja California in Mexico, and on the Gulf of Mexico from Florida to Tamaulipas and a small part in the Yucatan peninsula and Caribbean islands. *C. n. nivosus* also breeds in several areas from the western USA to south-central (Texas) and across central Mexico.

The projection for 26 ka BP predicts a range across the south and west coast of USA, extending to the coasts of Baja California and central Mexico, and along the west coast of South America, reaching the Andean cordillera and on a smaller scale in the north-east of Brazil. See Figure 4.1.1.6.a.

At 20 ka BP the range in the southern USA extends to the north of Mexico (Chihuahua), the same pattern being seen until 17 ka BP when the range shifts to the south-east USA and to the west coast in Sonora and Sinaloa. At 14 ka BP there is a distinct range in the south-east region of the USA that by the beginning of the Holocene (11ka) contracts to the central USA and extends to the north-west. The range remains unaltered in Mexico.

As the ice sheet retreats at 10 ka BP a range is projected in the area of central Canada around the Great Lakes, but this disappears again at 9 ka BP. At 8 ka BP the range is concentrated in central-south USA, north-central Mexico and along the west coasts of North and South America. This pattern persists until 2 ka BP, but at1 ka BP the range is fragmented in the western USA, contrasting with the current more continuous range in the west and south of the USA.

The projection for H2 represents a different prediction from 24 ka BP, given that the range is focused in Mexico, Central America, the Caribbean islands, and the north of South America from Colombia to French Guyana. The same range pattern appears for H1 and H0, contrasting with the 17 ka BP and 13 ka BP predictions of a range focused in the USA and Mexico.

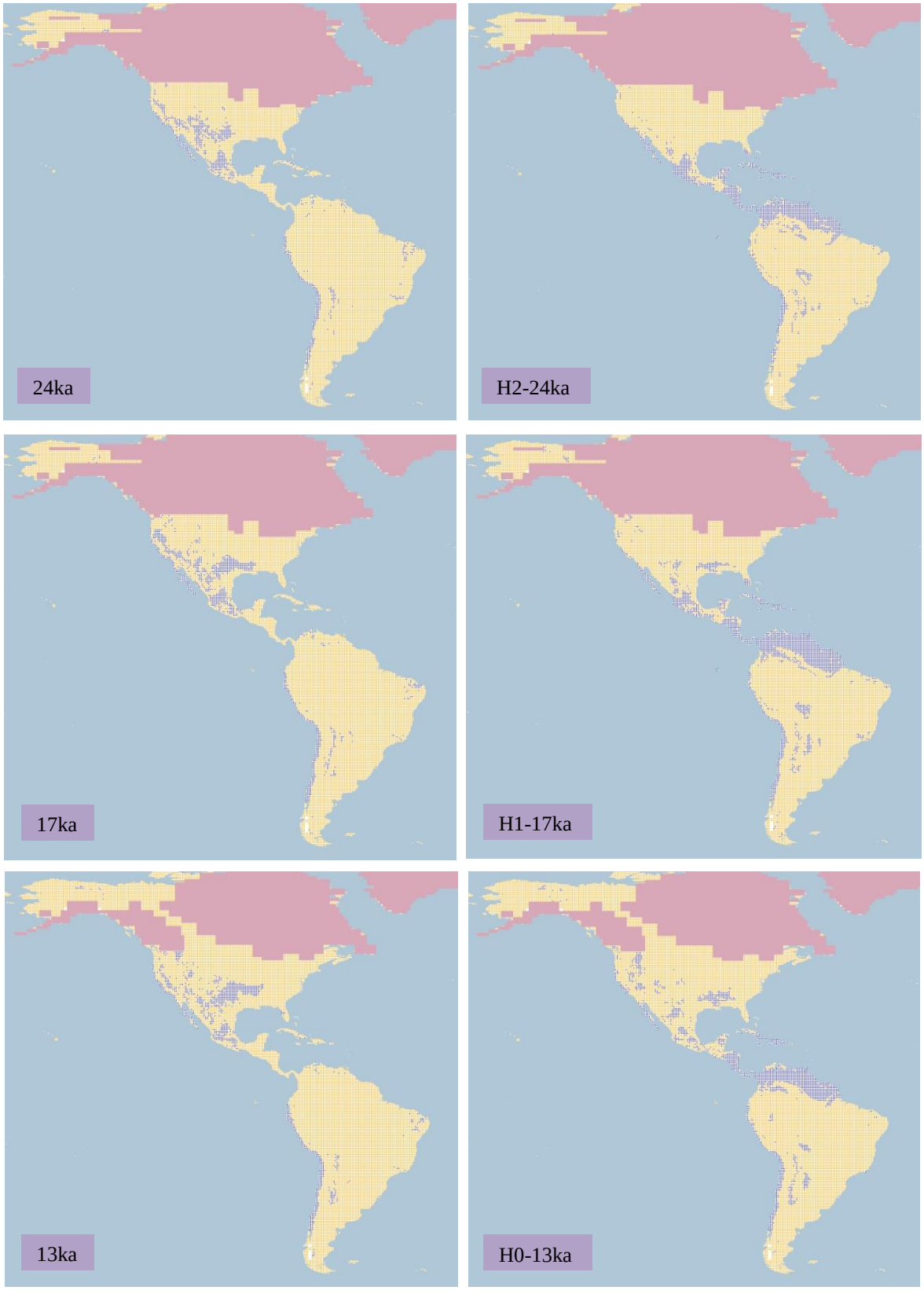

Figure 4.1.1.6.a. Simulation maps of Snowy Plover breeding range.
Maps are shown for ten-time slices: 24ka, H2 (24ka), 17ka, H1 (17ka), 13ka, H0 (13ka), 9ka, 5ka, 3ka and present (1961–90).

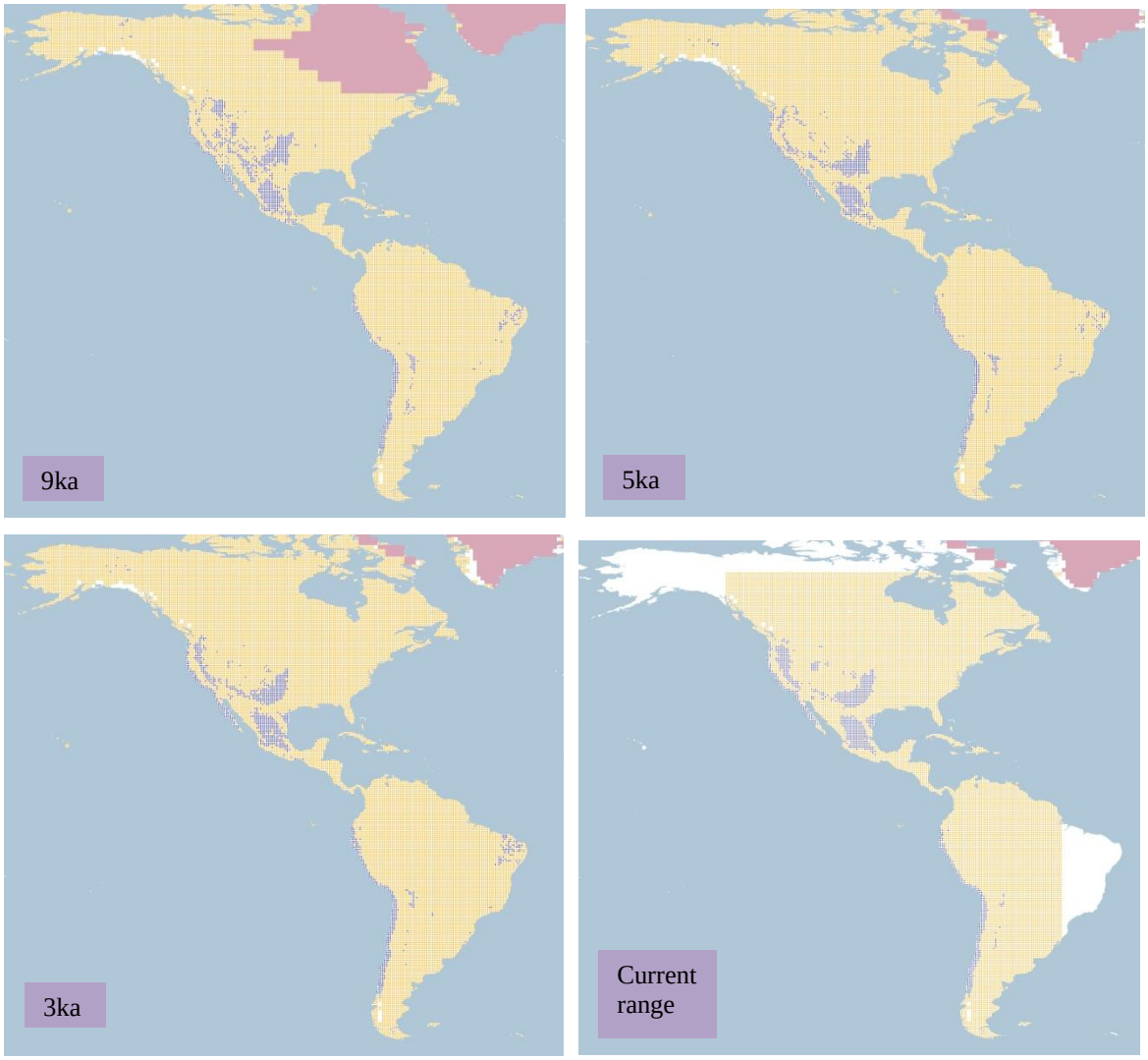

Figure 4.1.1.6.a. Simulation maps of Snowy Plover breeding range (continued**).**

Non-breeding range (AUC: 0.986; TSS: 0.892; Kappa: 0.749): A distinct non-breeding range is recognized only for *C. n. nivosus*, extending from the Pacific coast of Mexico, beginning at the Gulf of California, to Panama, and on the Gulf of Mexico coast from Florida to Campeche with small areas in Belize and Honduras.

At 26 ka BP the projection shows a range extending from the west coast of the USA towards Baja California in Mexico, with an area on the Pacific coast and in central Mexico, extending to the west coast of South America from south Ecuador to central Chile. Small areas are also projected in central Florida, Venezuela and north-east Brazil. The 22 ka BP projection shows an emerging area in the south of Brazil. At 20 ka BP the range decreases in both North and South America. See Figure 4.1.1.6.b.

At 19 ka BP the range in central Mexico shifts to the south, to then decrease after this period, becoming restricted only to the Pacific coast, but increasing in the north-east of Brazil. This pattern remains until 8 ka BP when the range grows in central Florida and central-west Mexico, and extends to the north-west coast of the USA. This pattern persists until 1 ka BP, being reduced only to the coastal areas of North America and the Pacific coast of South America for the current climate.

It is important to mention that the range does not currently extend to north-east Brazil, although the projections indicate suitable conditions in the region until 1 ka BP.

The same pattern as with the breeding range is shown for the Heinrich events H2, H1 and H0, with projected range mainly in the northern part of South America, reaching Central America and the southern part of Mexico. The only similarity with the projections for the 24 ka BP, 17 ka BP and 13 ka BP time slices is seen on the west coast of South America.

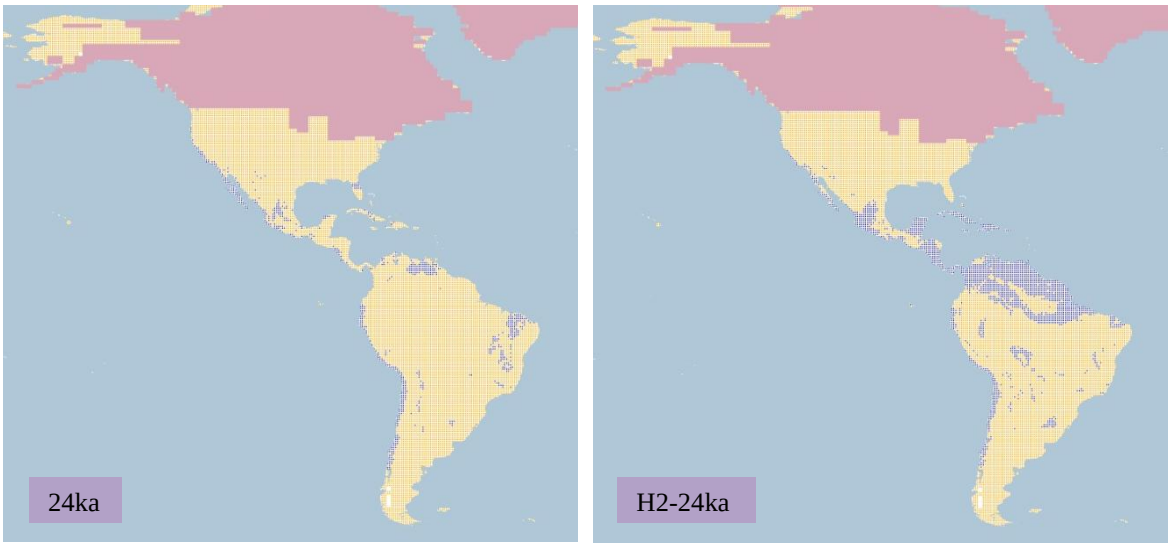

Figure 4.1.1.6.b. Simulation maps of Snowy Plover non-breeding range.
Maps are shown for ten-time slices: 24ka, H2 (24ka), 17ka, H1 (17ka), 13ka, H0 (13ka), 9ka, 5ka, 3ka and present (1961–90).

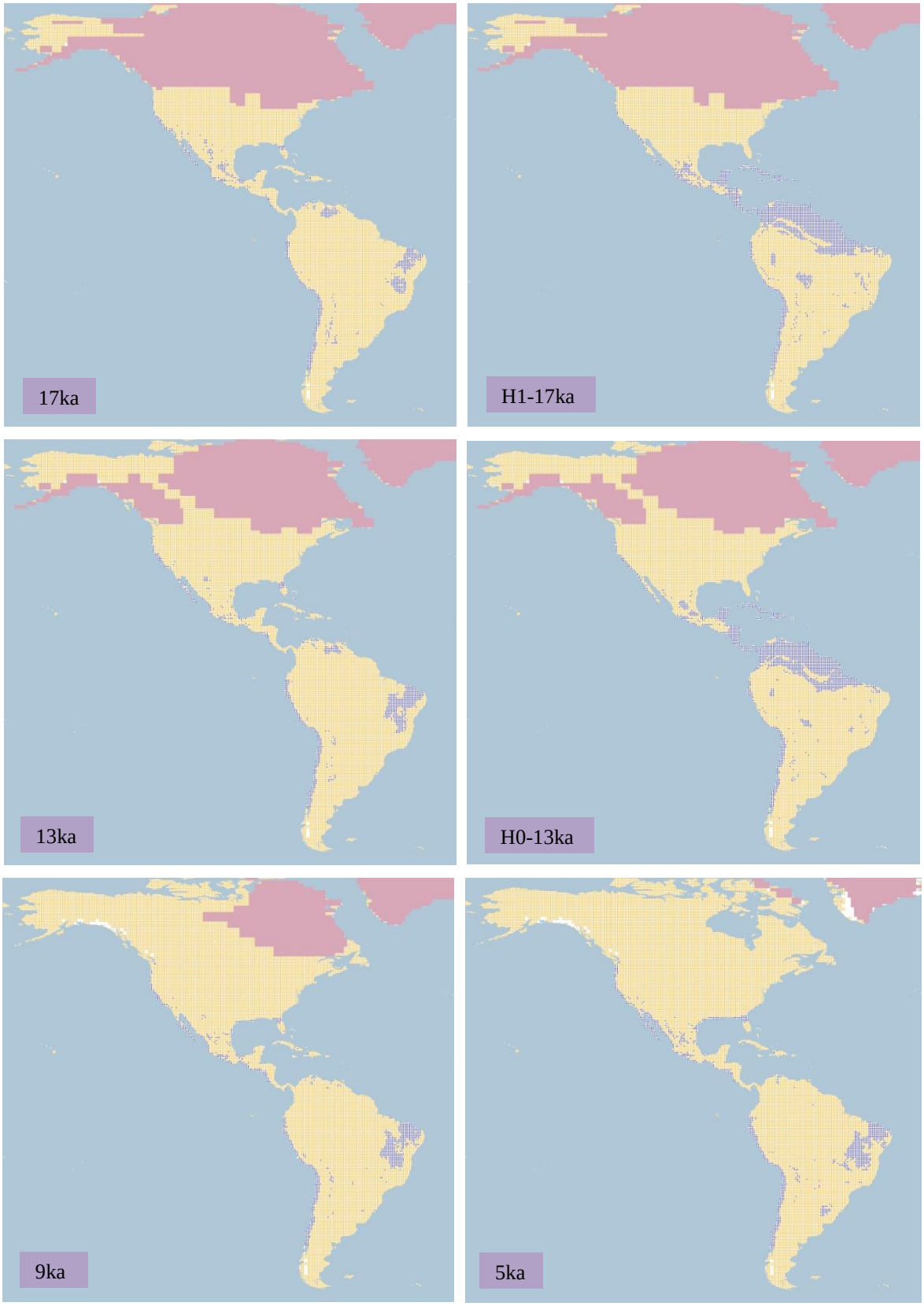

Figure 4.1.1.6.b. Simulation maps of Snowy Plover non-breeding range (continued**).**

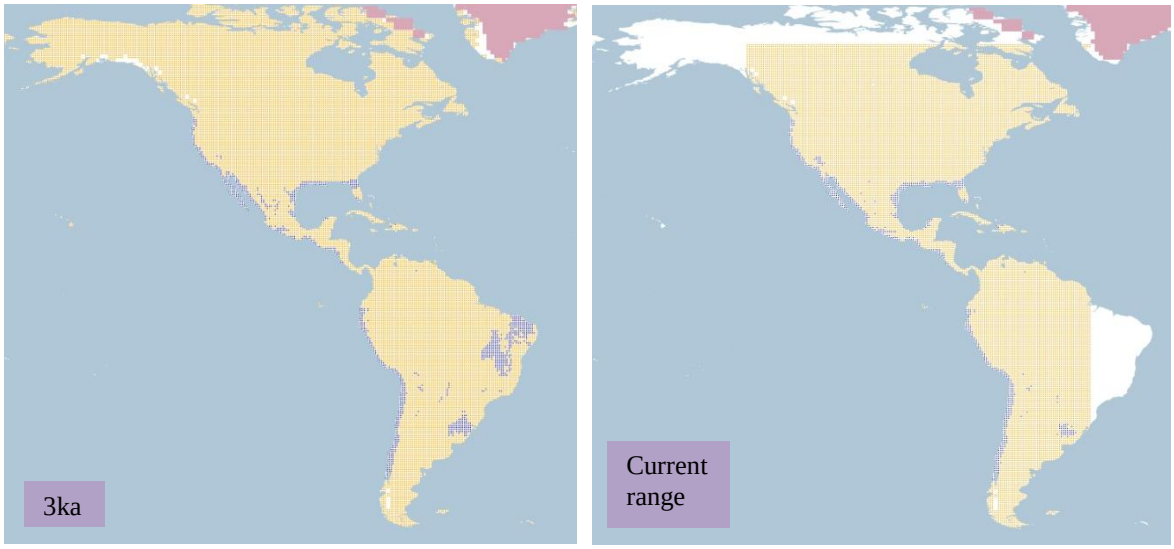

Figure 4.1.1.6.b. Simulation maps of Snowy Plover non-breeding range (continued**).**

*4.1.1.7 Semipalmated Plover (*Charadrius semipalmatus*). Conservation status: Least Concern. Current known range Figure 4.1.1.7.*

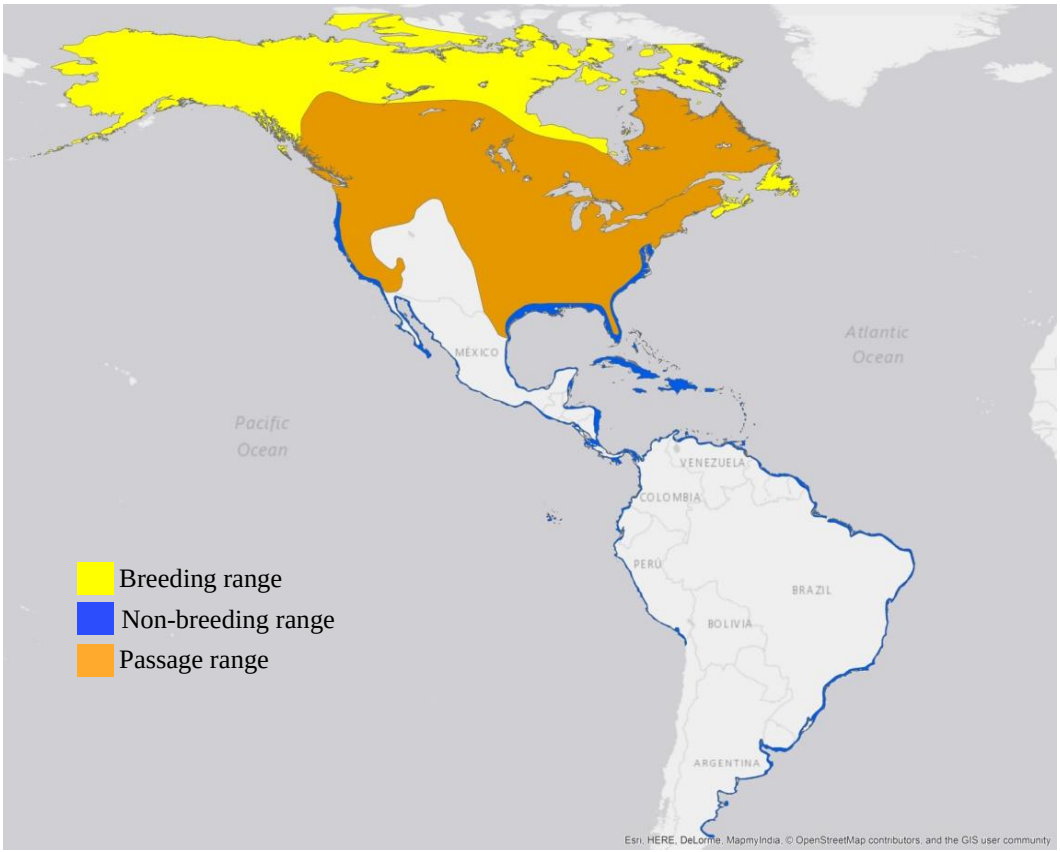

Figure 4.1.1.7. Current known range of Semipalmated Plover.

Breeding range (AUC: 0.945; TSS: 0.726; Kappa: 0.701): This species breeds in the northern part of North America, from Alaska to the northern part of Canada, reaching a part of the Canadian Arctic Archipelago, specifically Banks Island, Victoria Island, King William Island and the south-central part of Baffin Island, as well as extending around Hudson Bay and the Gulf of St. Lawrence on the east coast.

The range at 26 ka BP is projected to cover much of the area of Alaska and north-west Canada not covered by the ice sheet, mainly from the west coast to central parts, plus a small area across the north of USA south of the ice sheet. This pattern continues until 19 ka BP when the range in west Alaska and north-west Canada narrows. See Figure 4.1.1.7.a.

After this at 17 ka BP the range in the northern conterminous USA near the ice sheet is also reduced, following the same pattern until 14 ka BP when the range in Alaska shifts to the east extending across Canada in the area no longer covered by the ice sheet. As the ice sheet retreats further at 13 ka BP the northern range in the USA and that in Canada coalesce. Slowly after this the range in the northern conterminous USA shifts towards northern Canada and Alaska.

By the beginning of the Holocene the range is restricted to the northern part of North America, increasing as the ice sheets retreat, and at 7 ka BP the projection predicts areas on the east coast of Canada and north-east USA. At 4 ka BP there is an increased are near Hudson Bay, further increasing towards 1 ka BP, and being similar to the current range projection.

Even though there is no range known in South America all the projections showed suitable conditions in the mainly in south-central Chile from 26 ka BP onwards which expanded at 16 ka BP to Tierra del Fuego and the Falkland Islands. Also, there is a small range projected in Andean Cordillera of Peru, around the Lake Junin.

The projection for Heinrich events H2 and H1 show a wider range on the conterminous USA, extending from west to east south of the ice sheet, unlike the projections for 24 ka BP and 17 ka BP. Although there are similarities between H0 and 13 ka BP, with predicted range over the northern part of Canada, only H0 predicts range in the central USA. The Heinrich event projections also show suitable range in the south of Chile.

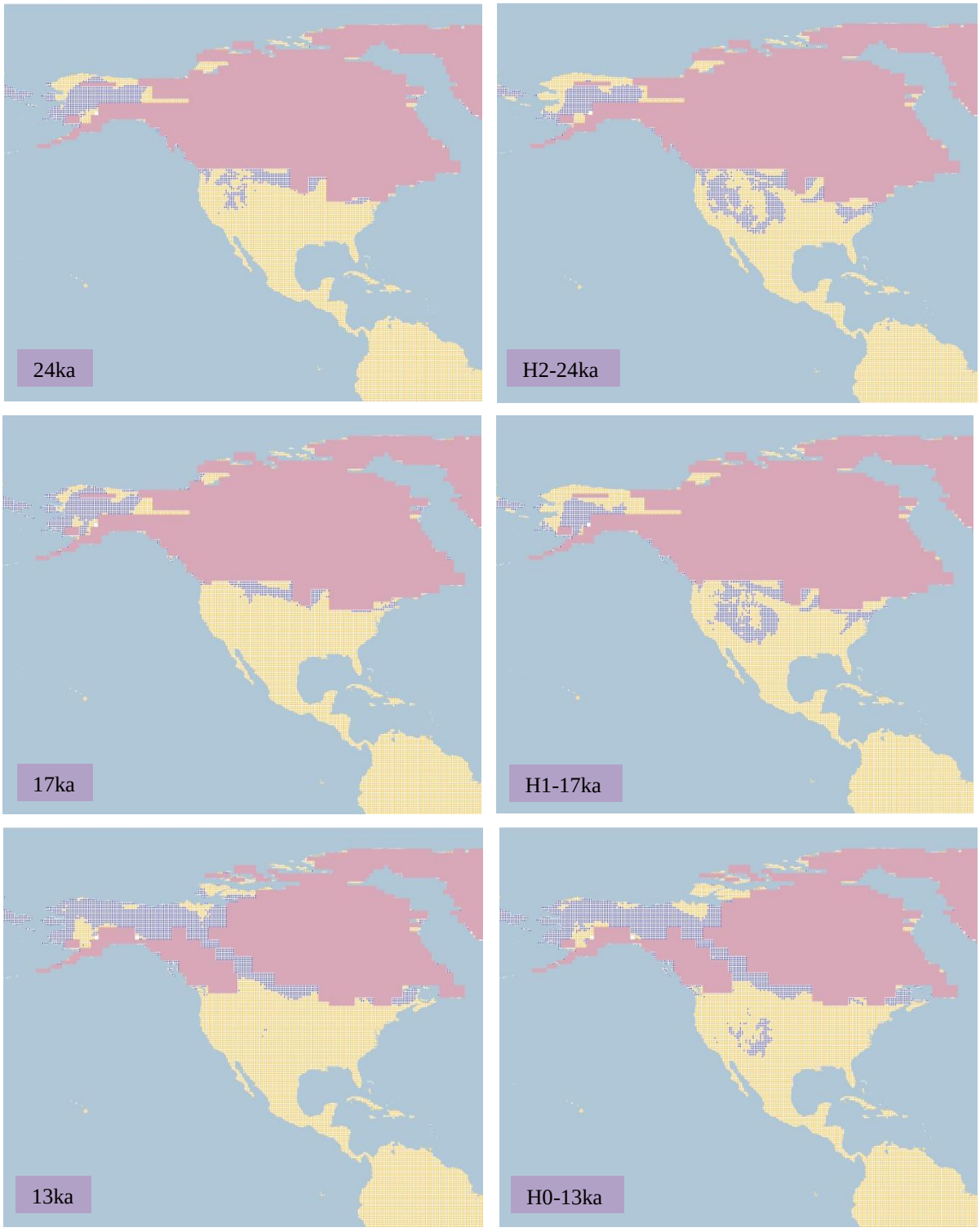

Figure 4.1.1.7.a. Simulation maps of Semipalmated Plover breeding range.
Maps are shown for ten-time slices: 24ka, H2 (24ka), 17ka, H1 (17ka), 13ka, H0 (13ka), 9ka, 5ka, 3ka and present (1961–90).

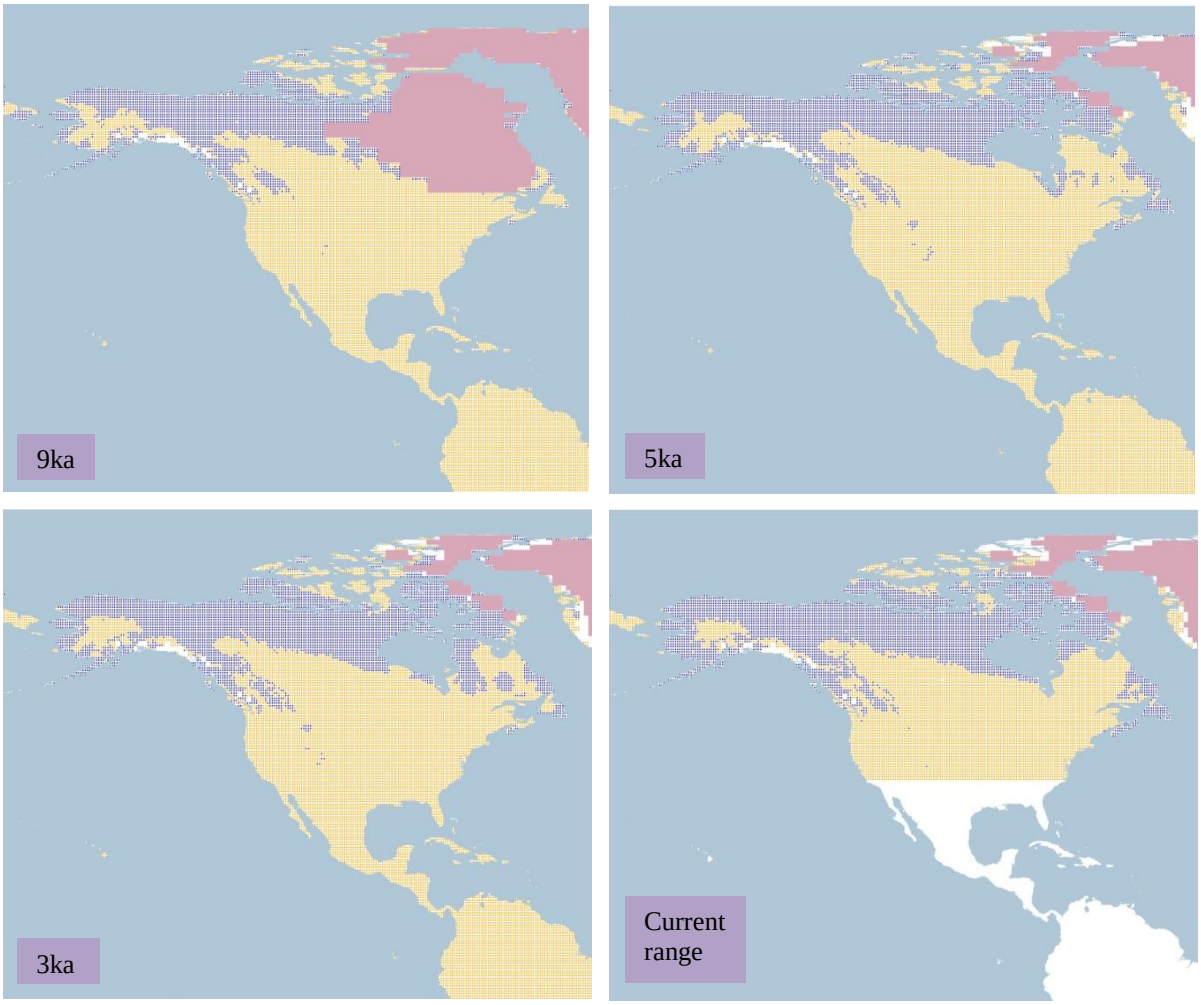

Figure 4.1.1.7.a. Simulation maps of Semipalmated Plover breeding range (continued**).**

Non-breeding range (AUC: 0.921; TSS: 0.681; Kappa: 0.547): The species spends the non-breeding season on the west and east coasts of North and South America, reaching southern Peru on the west coast and southern Argentina on the east coast. It is also found around the Caribbean islands and the Galapagos Islands.

At 26 ka BP the projected range is around the Pacific coasts of the USA, Mexico, Central America, Ecuador and Peru, as well as on the east and north coasts of South America and around the Caribbean islands. Moving inland the projected range extends across central Florida, south-central Mexico and around South America mainly in the north, in Bolivia, north Argentina and south Brazil. The projected range decreases at 22 ka BP in South America and is focused on the Pacific coasts of the USA, Mexico and Central America. See Figure 4.1.1.7.b.

As the ice sheet retreats the range in South America increases, mainly from 15 ka BP, in the region of north-west Brazil in Amazonia, decreasing after 11 ka BP in the north of Brazil, Guyana, French Guiana and Suriname.

At 6 ka BP the projected range is along the coasts of the USA, Mexico and the Caribbean islands. The range in Brazil shifts towards the south-central part, decreasing until only a small area remains at 1 ka BP. The range on the east coast of the USA increases towards 1 ka BP and presents a similar projected extent to that for the current climate.

Comparing the Heinrich events H2 and H1 with the time slices 24 ka BP and 17 ka BP they are significantly different. The Heinrich projections display a wider range in the northern-central part of South America. The region on the Pacific coasts of the USA and Mexico remains similar. The projections for H0 and 13 ka BP also show differences, but to a lesser degree, H0 having a larger extent predicted in the south of Mexico and towards Central America.

It is interesting that the current range is not known to cover inland territories across the Americas, whereas the predictions show suitable climatic conditions for the species to inhabit these areas.

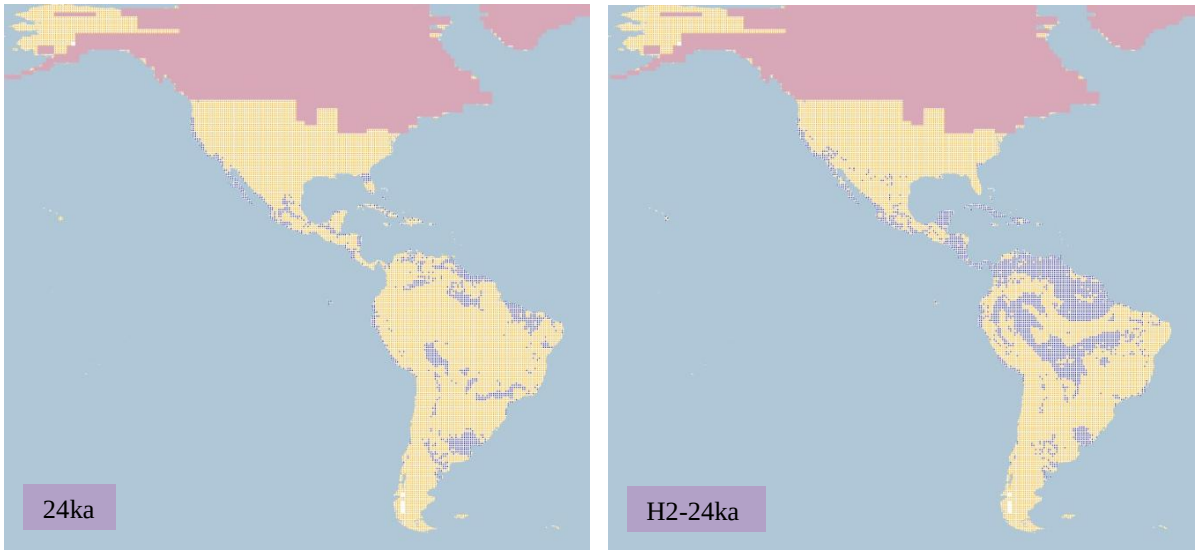

Figure 4.1.1.7.b. Simulation maps of Semipalmated Plover non-breeding range.
Maps are shown for ten-time slices: 24ka, H2 (24ka), 17ka, H1 (17ka), 13ka, H0 (13ka), 9ka, 5ka, 3ka and present (1961–90).

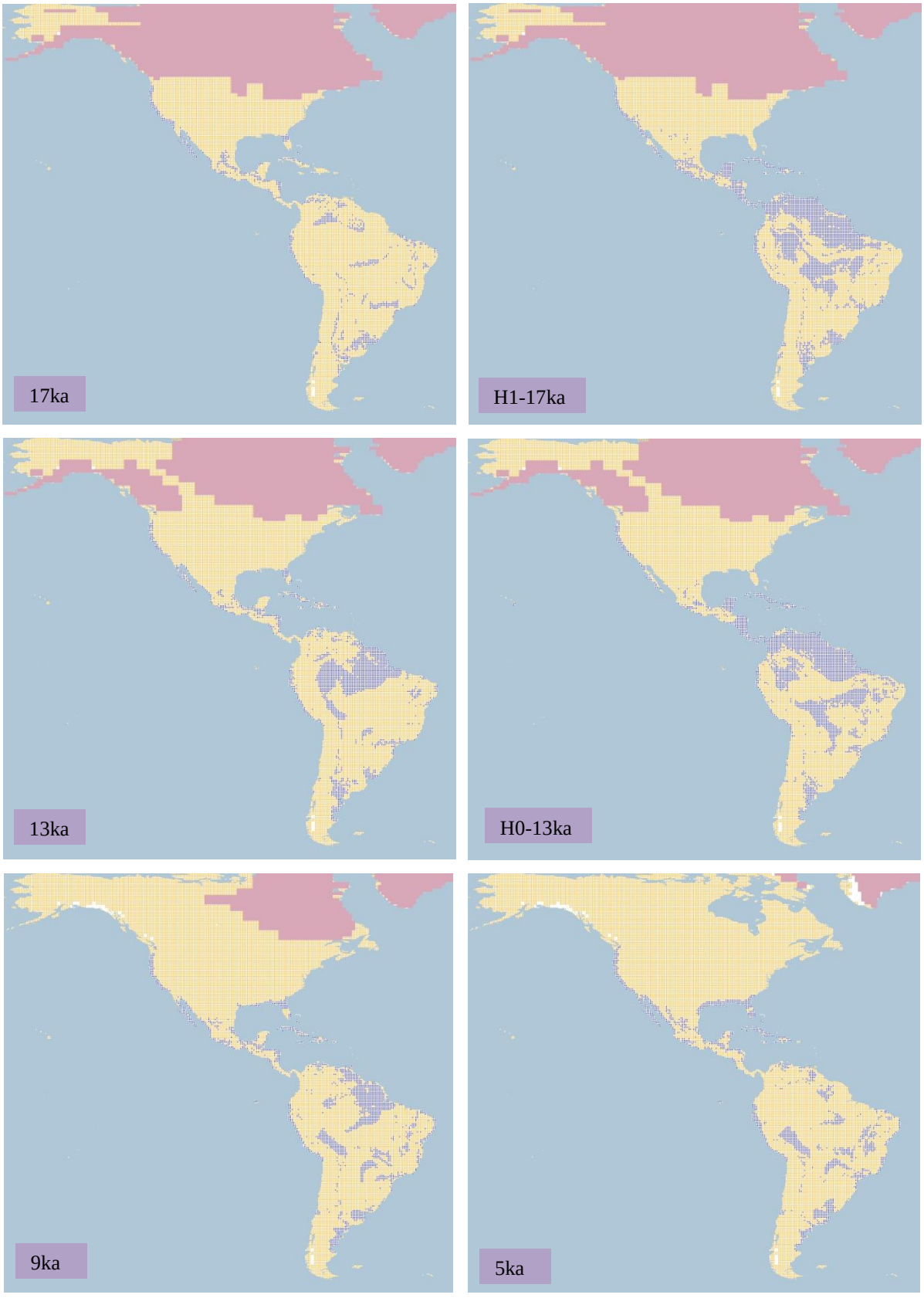

Figure 4.1.1.7.b. Simulation maps of Semipalmated Plover non-breeding range (continued**).**

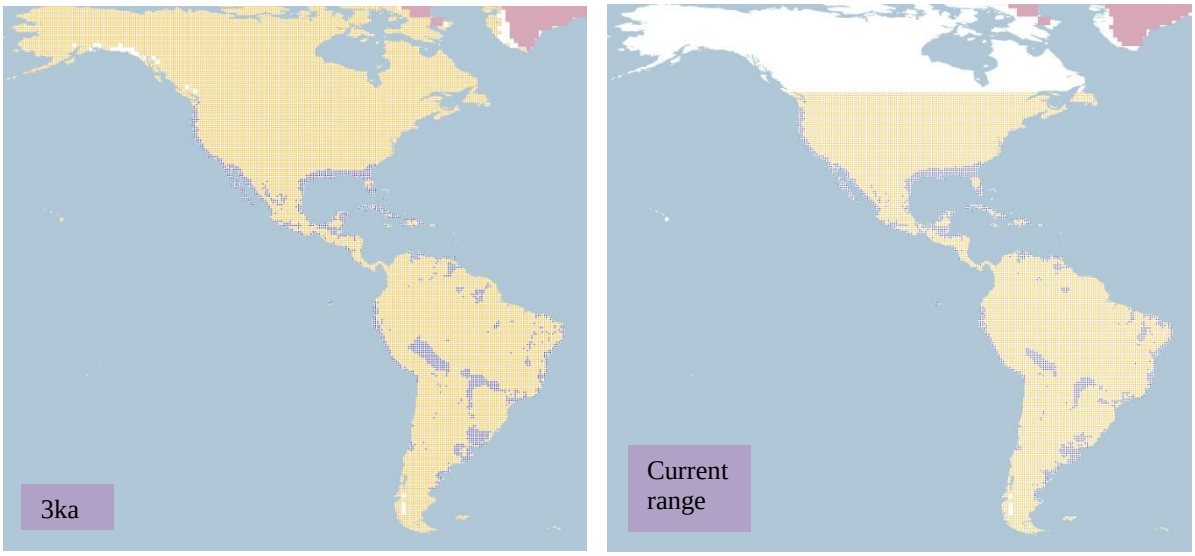

Figure 4.1.1.7.b. Simulation maps of Semipalmated Plover non-breeding range (continued**).**

*4.1.1.8 Killdeer (*C. vociferus *including* C. v. vociferus, C. v. ternominatus, C. v. peruvianus*). Conservation status: Least Concern. Current known range Figure 4.1.1.8.*

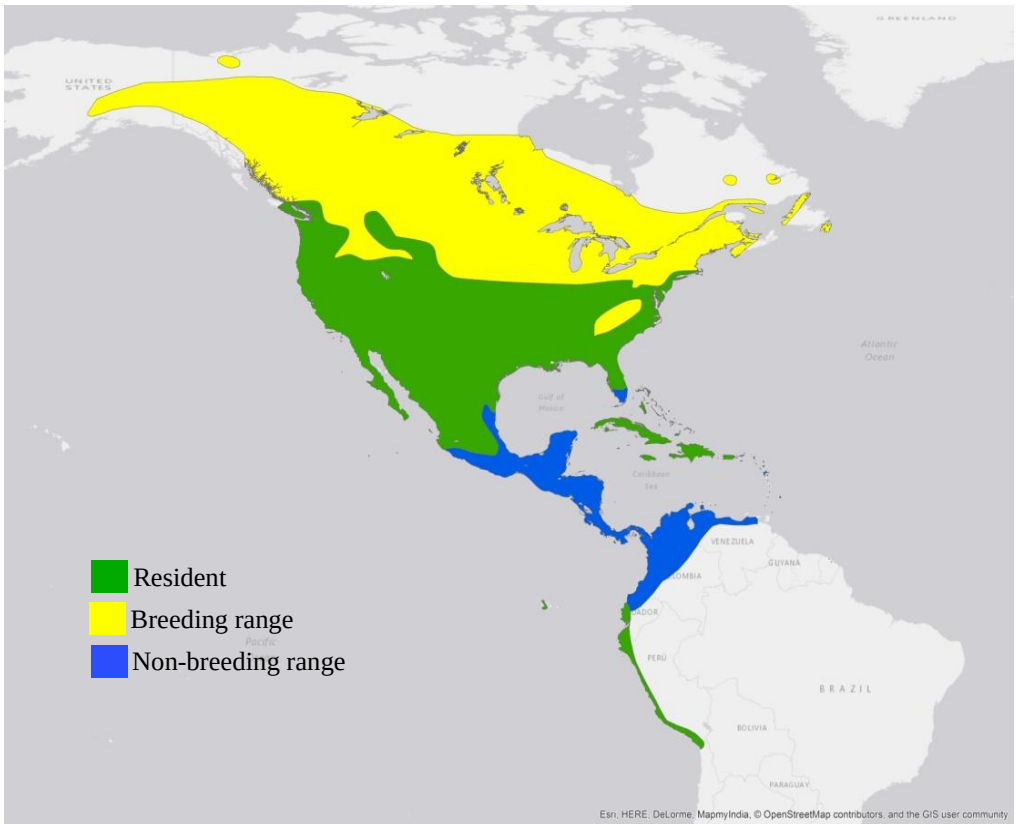

Figure 4.1.1.8. Current known range of Killdeer.

Breeding range (AUC: 0.978; TSS: 0.841; Kappa: 0.844): This species breeds from central Alaska south to the northern conterminous USA and Appalachia. It also, has a year-round distribution in the remainder of the conterminous USA and extending to central-south Mexico, the Caribbean islands, and a small area along the coasts of Ecuador and Peru.

The range at 26 ka BP extends across most of the conterminous USA, except south Florida and extends to central-south Mexico. A small range is also projected in central Alaska where the ice sheet is absent. At 19 ka BP and 18 ka BP there is a change in the extent projected in Alaska that is reduced to a minimal proportion of the ice-free area. The range then again expands to northern Alaska by 17 ka BP and the rest of the range (in USA and Mexico) remains constant and growing to the north as the ice sheet retracts. See Figure 4.1.1.8.a.

Following this, there is an increase in the north-west part of Canada where the range covers most of the territory not covered by the ice sheet. By 12 ka BP after the ice sheet is divided in Canada the range starts moving to the north and at 12 ka BP the northern range in Alaska and Canada meets the expanding range in south Canada and USA.

At the beginning of the Holocene the range covers most of North America from Alaska to Canada, USA and central Mexico; this continues expanding as the ice sheet contracts. By 4 ka BP the range in north Canada, and especially in Alaska, reduces slightly in extent, persisting until 1 ka BP. It is important to mention the range occurring on the coasts of Ecuador and Peru remains unaltered during the projections. The projection of the current breeding range remains similar to the1 ka BP with a slight decrease in the north-west of Canada and near Alaska.

The current breeding range is not known to extend to southern South America; however, throughout the projections a range is simulated from south Bolivia towards Argentina, Chile and small areas in Uruguay and east Brazil.

The simulation for Heinrich event H2 presents a different pattern of distribution from that for 24 ka BP, particularly in the western USA where the range is reduced, with complementary range expansion in southern Mexico and through Central America, the Caribbean islands, and the northern part of South America (Colombia, Venezuela, Guyana, Suriname, French Guiana and north-west Brazil). Similar contrasts are seen for H1 compared to 17 ka BP and H0 compared to 13 ka BP, although the range in the western USA is reduced less, especially in the H0 simulation.

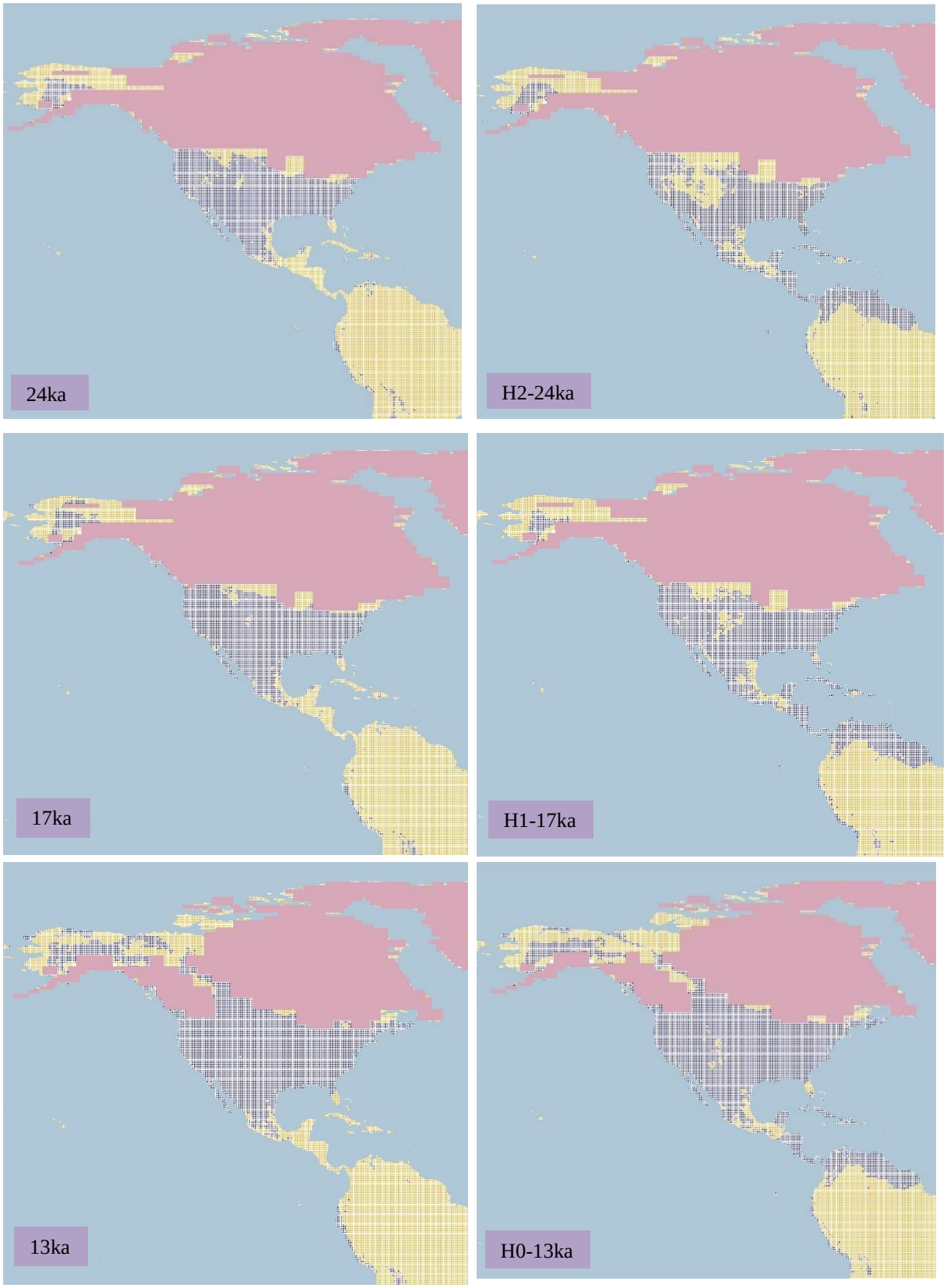

Figure 4.1.1.8.a. Simulation maps of Killdeer breeding range.
Maps are shown for ten-time slices: 24ka, H2 (24ka), 17ka, H1 (17ka), 13ka, H0 (13ka), 9ka, 5ka, 3ka and present (1961–90).

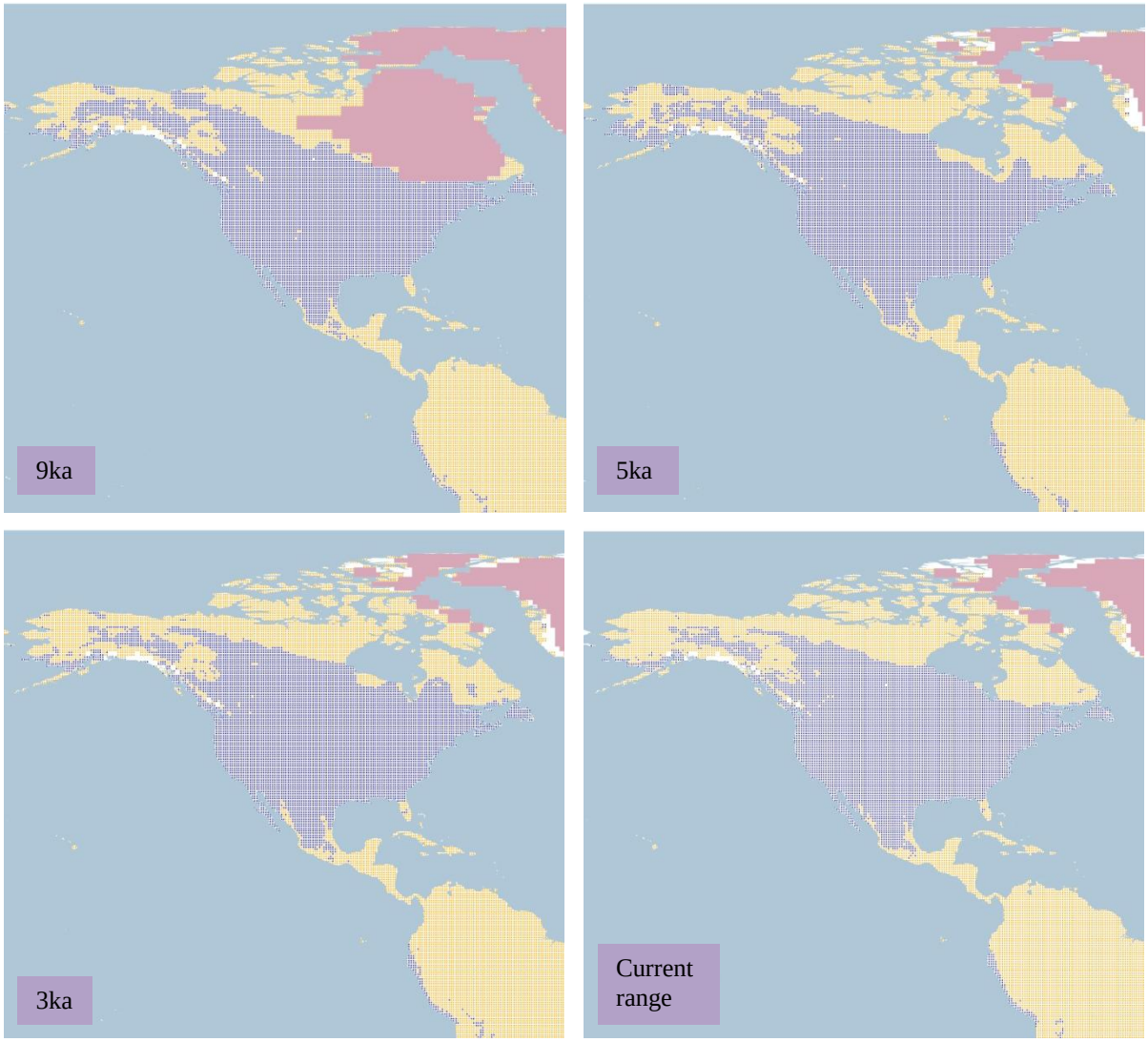

Figure 4.1.1.8.a. Simulation maps of Killdeer breeding range (continued**).**

Non-breeding range (AUC: 0.978; TSS: 0.835; Kappa: 0.816): In addition to its extensive year-round range, the species' non-breeding range includes an area extending from central-south Mexico to Central America and reaching the northern part of South America in Colombia, Venezuela and northern Ecuador. A small area is also occupied in the south of Florida and the southern islands in the Caribbean Sea.

The range at 26 ka BP is simulated to cover the west and south of the USA (except Florida), extending to Mexico, discontinuously through Central America and following the west coast and the Andean Cordillera in South America from Colombia to southern Chile. A large range is also projected in Argentina and a fragmented area across Brazil, both territories where the species does not occur currently. The pattern continues uniformly with a slight increase of the

range in west and south USA at 24 ka BP, 20 ka BP and particularly from 18 ka BP the range extends towards the north-west USA near the ice sheet and reaches the coast of Virginia in the east USA. See Figure 4.1.1.8.b.

From 17 ka BP to 12 ka BP the range remains similar, although expanding to the north as the ice sheet retreats in North America. The simulated range in South America also remains similar on the west coast and the Andean Cordillera, only growing in the north of Brazil and in Argentina (at 12ka).

At the beginning of the Holocene the simulated range grows covering almost all USA and additionally an area of occurrence is projected near Hudson Bay and the ice sheet in North America, although this area is reduced at 9 ka BP and disappears at 8 ka BP. From 6 ka BP onwards the projected extent is concentrated mainly in the USA and Mexico, with smaller suitable areas in the Andean Cordillera and Argentina, reducing the range projected across Brazil. From 3 ka BP the range in Mexico grows towards Central America and the whole range remains constant until 1 ka BP, when it is essentially identical to the current non-breeding range projection.

There is a larger difference between the H2 and 24 ka BP simulations, mainly in the area of the USA where the range is concentrated from the south of the USA to Mexico, Central America and mainly in the northern part of South America in the H2 projection. A similar pattern is seen for H1 that differs from 17 ka BP mainly by extending to the north only close to the west coast of the USA and by reaching south Florida and the Caribbean islands. In the H0 projection the range in the USA extends to the east coast and in South America there is an expansion in the central part of Brazil, again contrasting with the 13 ka BP projection.

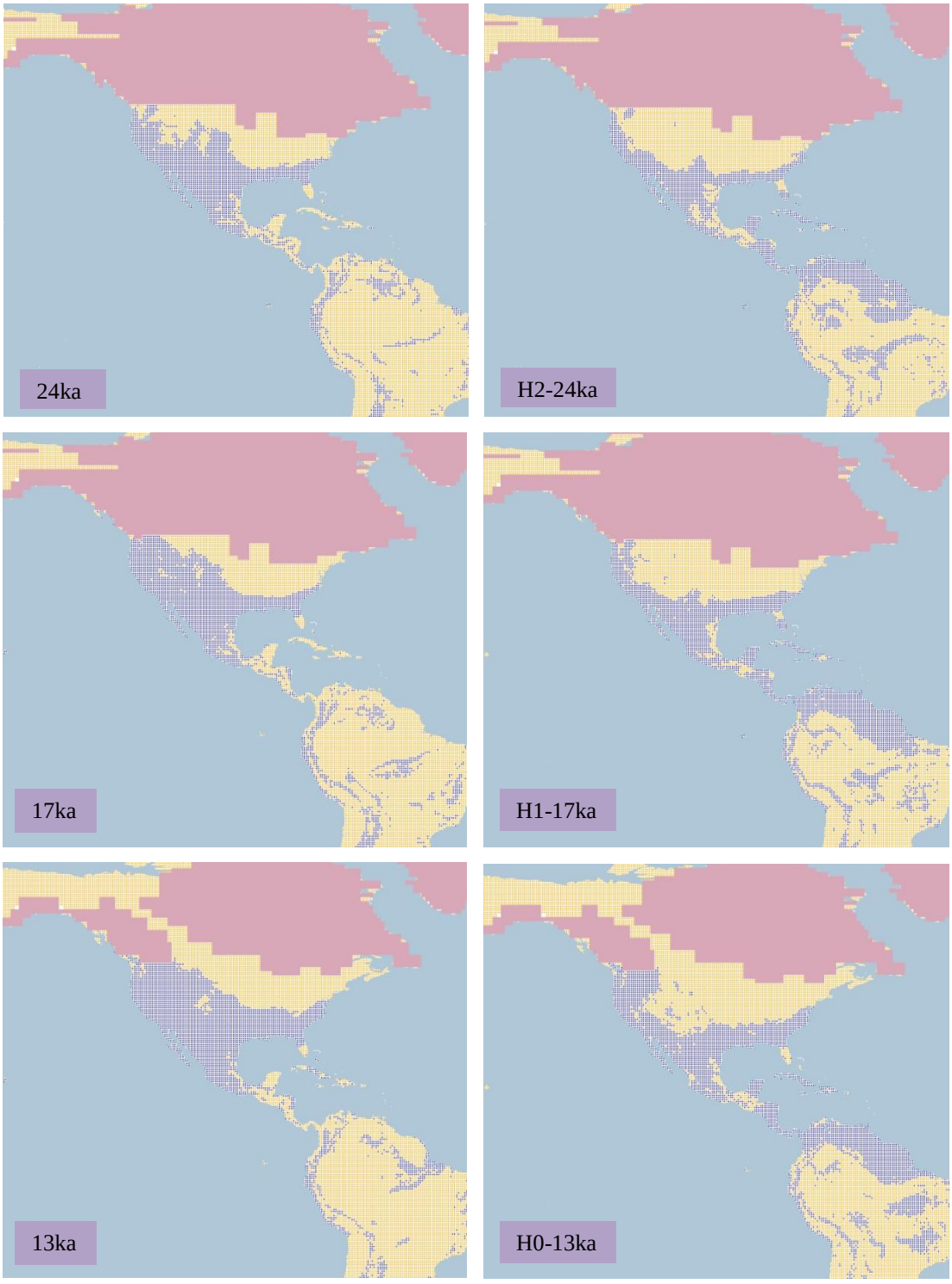

Figure 4.1.1.8.b. Simulation maps of Killdeer non-breeding range.
Maps are shown for ten-time slices: 24ka, H2 (24ka), 17ka, H1 (17ka), 13ka, H0 (13ka), 9ka, 5ka, 3ka and present (1961–90).

Figure 4.1.1.8.b. Simulation maps of Killdeer non-breeding range (continued**).**

4.1.1.9 Wilson's Plover (C. wilsonia including C. w. wilsonia, C. w. beldingi, C. w. cinnamominus, *and* C. w. crassirostris*). Conservation status: Least Concern. Current known range Figure 4.1.1.9.*

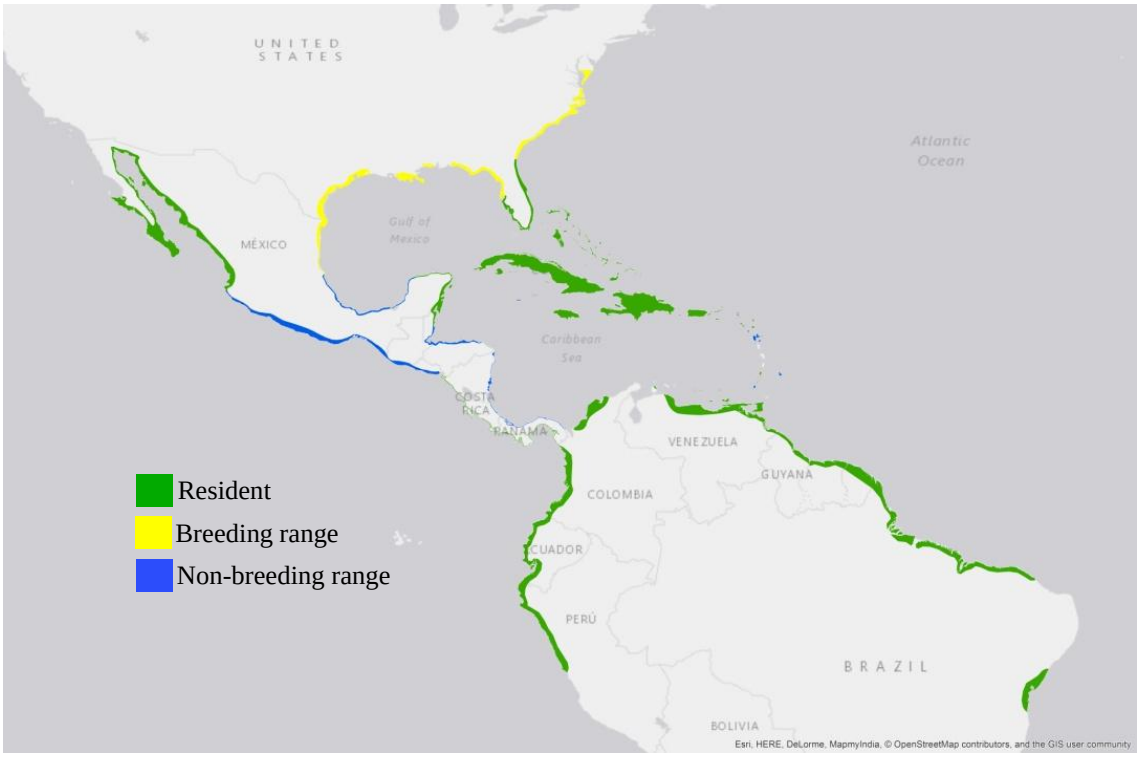

Figure 4.1.1.9. Current known range of Wilson's Plover.

Breeding range (AUC: 0.916; TSS: 0.667; Kappa: 0.484): A resident on the coasts of Baja California, Sonora and Sinaloa in the Gulf of California and in the Yucatan peninsula in Mexico; as well as on the south-east coast of Florida, the Caribbean islands, the south-west coast of Central America and the northern coasts of South America south to central Peru in the west and to the central coast of Brazil in the east, this species also has a breeding range in the USA on the coast of the Gulf of Mexico and on the east coast north to Virginia.

At 26 ka BP a scattered range is simulated across the coasts of Mexico, Ecuador and Peru mainly, with small areas in central Florida, the north of Brazil and in Paraguay. Between 21 and 20 ka BP the projected area decreases, increasing again from 19 ka BP onwards, especially in the south of Florida. See Figure 4.1.1.9.a.

As the ice sheet retreats the simulated breeding range remains more or less unchanged along the coasts of Mexico and South America. At 15 ka BP the range extends to the Caribbean islands and increases in extent towards the beginning of the Holocene between 12 ka BP and 11ka. The scattered range projected in the north-west and on the north coast of Brazil increases in extent from 13 ka BP onwards, and the two areas have merged by 11ka.

Similar patterns are shown after 11 ka BP, although with a dramatic change at 8 ka BP with the reduction in extent of the simulated range in north-west Brazil that has almost disappeared at 7 ka BP. This range, however, shifts to southern territories near Bolivia, Paraguay and the north of Argentina, although on a smaller scale, increasing only at 4 ka BP and decreasing again until 1 ka BP.

The rest of the simulated range shows minimal changes during the Holocene, being restricted to coastal areas from the north of Mexico to the north of South America between 7 ka BP and 2 ka BP. At1 ka BP there is a shift in the area located in the northern part of Mexico that moves to the central-south coastal regions instead; there is also an increased extent in Central America. This differs from the current range projection which shows an extension into the northern parts of Mexico, as well as to the south-east coast of the USA (from Texas to Florida). However, the range located in South America seems to remain constant.

The H2 projection shows a larger range than the 24 ka BP projection, extending from the central south coasts of Mexico, inland to Central America and northern regions of South America from Colombia to the north of Brazil, and with a large area also in the Caribbean islands. The range simulated for H1 is even more extensive in the north of South America and from Central America to the Yucatan peninsula in Mexico. The H0 projection shows similar patterns, contrasting markedly with the 13 ka BP projection.

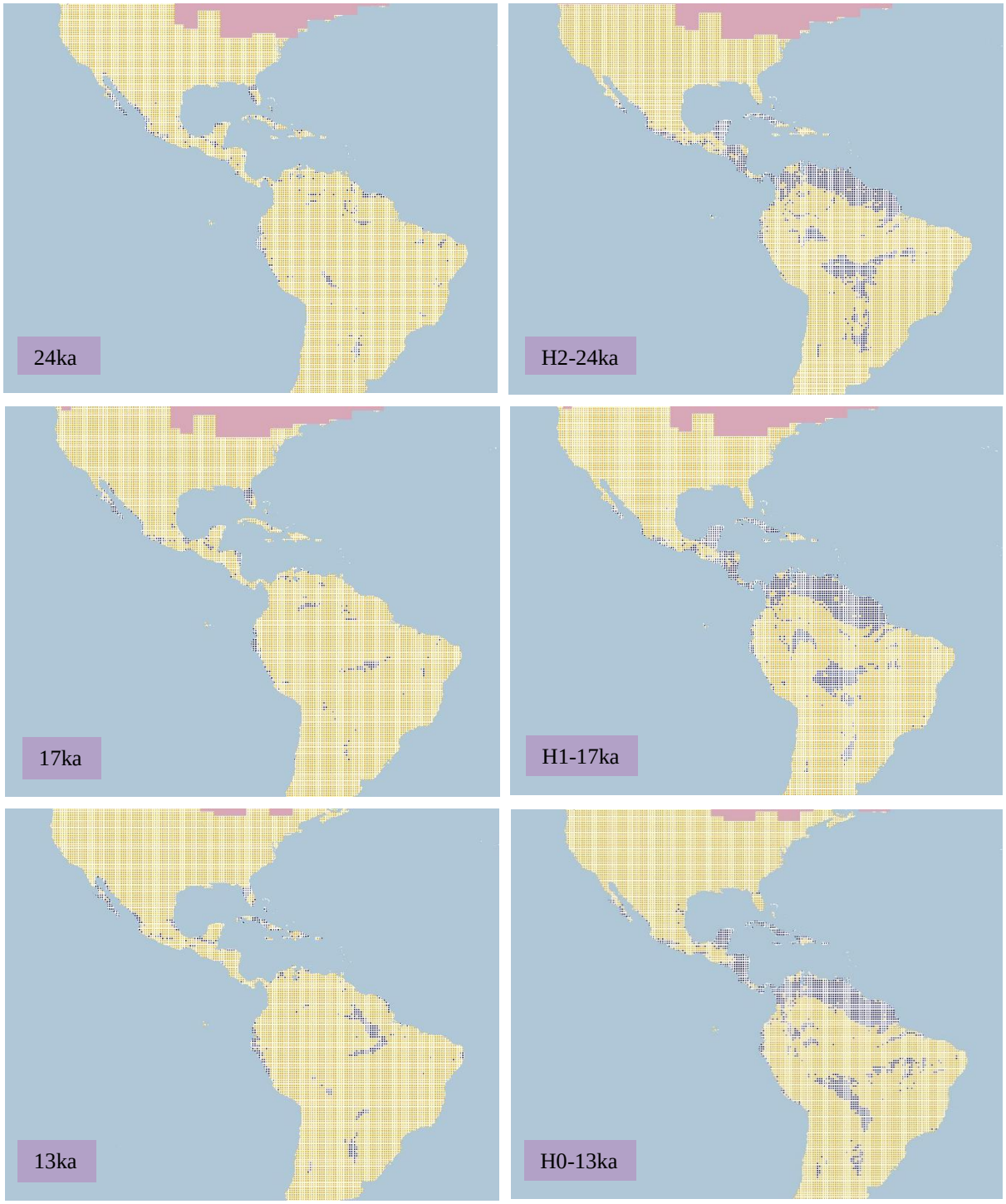

Figure 4.1.1.9.a. Simulation maps of Wilson's Plover breeding range.
Maps are shown for ten-time slices: 24ka, H2 (24ka), 17ka, H1 (17ka), 13ka, H0 (13ka), 9ka, 5ka, 3ka and present (1961–90).

Figure 4.1.1.9.a. Simulation maps of Wilson's Plover breeding range (continued**).**

Non-breeding range (AUC: 0.925; TSS: 0.669; Kappa: 0.518): In addition to its resident range on the north Pacific coasts of Mexico, the south of Florida, the Caribbean islands, the west coast from Central America to central-north South America (from Colombia to central Peru) and the east coast from Venezuela to the north of Brazil, the species also has a non-breeding range on the south Pacific coast of Mexico and in the Gulf of Mexico, as well as on the east coast of Central America and in the southern islands of the Caribbean.

At 26 ka BP the non-breeding range is projected to extend from the north-west coast of Mexico in Sonora and Baja California towards Central America, with a smaller area on the north-west coast of South America in Ecuador and Peru. In addition, areas are simulated on the north coast of South America and extending inland, as well as small areas on the Gulf of Mexico and the Caribbean islands. See Figure 4.1.1.9.b.

The simulated extent increases at 24 ka BP, mainly inland in north Brazil and in Central America, decreasing again at 22 ka BP and shifting to the east in Brazil, a pattern that persists until 16ka.

At 15 ka BP and 14 ka BP the simulated range in South America shifts to the north-west of Brazil in the area of the present Amazon rainforest, and increases in extent in southern Florida. This pattern is maintained until the beginning of the Holocene at 11 ka BP when the simulated range extent begins to decline and shifts to the north coast in Brazil.

From 8 ka BP onwards, and especially at 5 ka BP, the area projected in the north-west of Brazil decreases and shifts towards the south-west of Brazil, Bolivia and Paraguay. The simulated range in the Caribbean islands and Florida increases during this time, whereas the rest of the range in Mexico remains constant and mainly on the coasts until 1 ka BP.

The projection for H2 differs markedly from that for 24 ka BP, the range being mainly projected to occupy the central part of the north of South America, Central America and reaching the Yucatan peninsula in Mexico, as well as the coasts of Mexico from Sinaloa to Chiapas and a small area on the south coast of Baja California Sur. A similar pattern is seen for H1, although with a larger area in Brazil, again contrasting strongly with the 17 ka BP projection. The H0 and 13 ka BP projections both show potential range in the north-west of Brazil, but on a different scale; for 13 ka BP a concentrated range in the area of the present Amazon forest is simulated, whereas for H0 the range is in central-east Brazil with a larger extension to the north from Colombia to north Brazil.

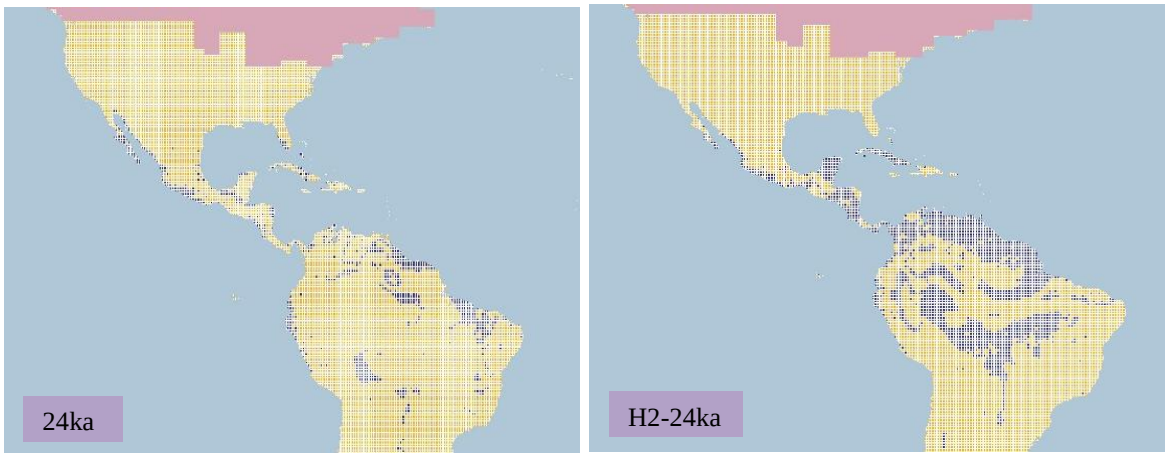

Figure 4.1.1.9.b. Simulation maps of Wilson's Plover non-breeding range.
Maps are shown for ten-time slices: 24ka, H2 (24ka), 17ka, H1 (17ka), 13ka, H0 (13ka), 9ka, 5ka, 3ka and present (1961–90).

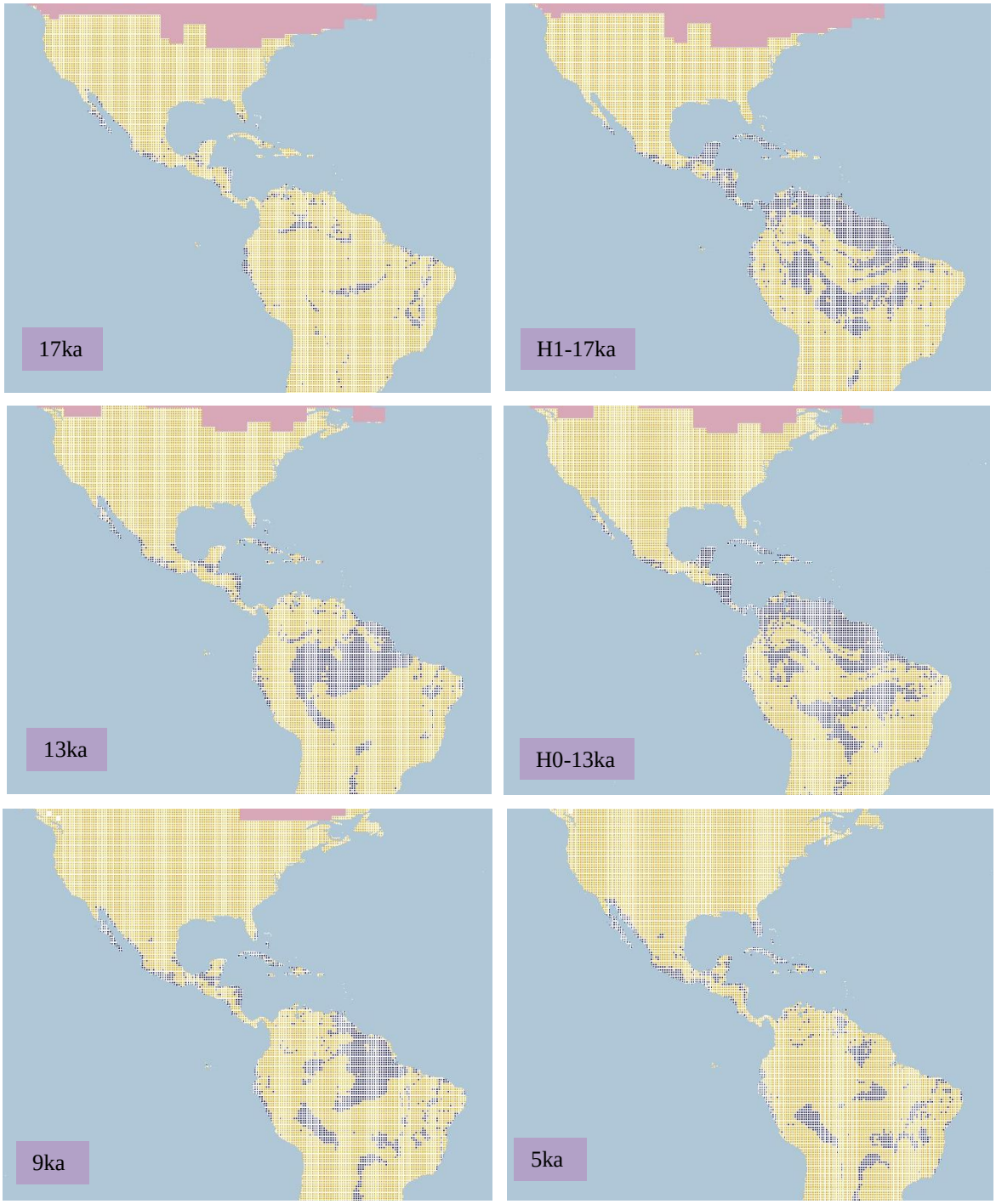

Figure 4.1.1.9.b. Simulation maps of Wilson's Plover non-breeding range (continued**).**

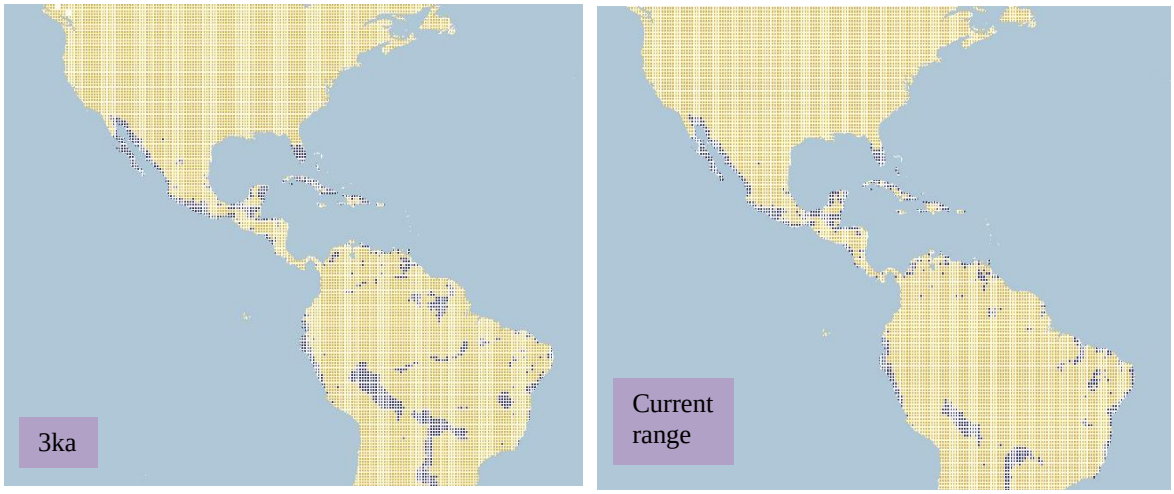

Figure 4.1.1.9.b. Simulation maps of Wilson's Plover non-breeding range (continued**).**

*4.1.1.10 Tawny-throated Dotterel (*Oreopholus ruficollis including O. r. pallidus *and* O. r. ruficollis*). Conservation status: Least Concern. Current known range Figure 4.1.1.10.*

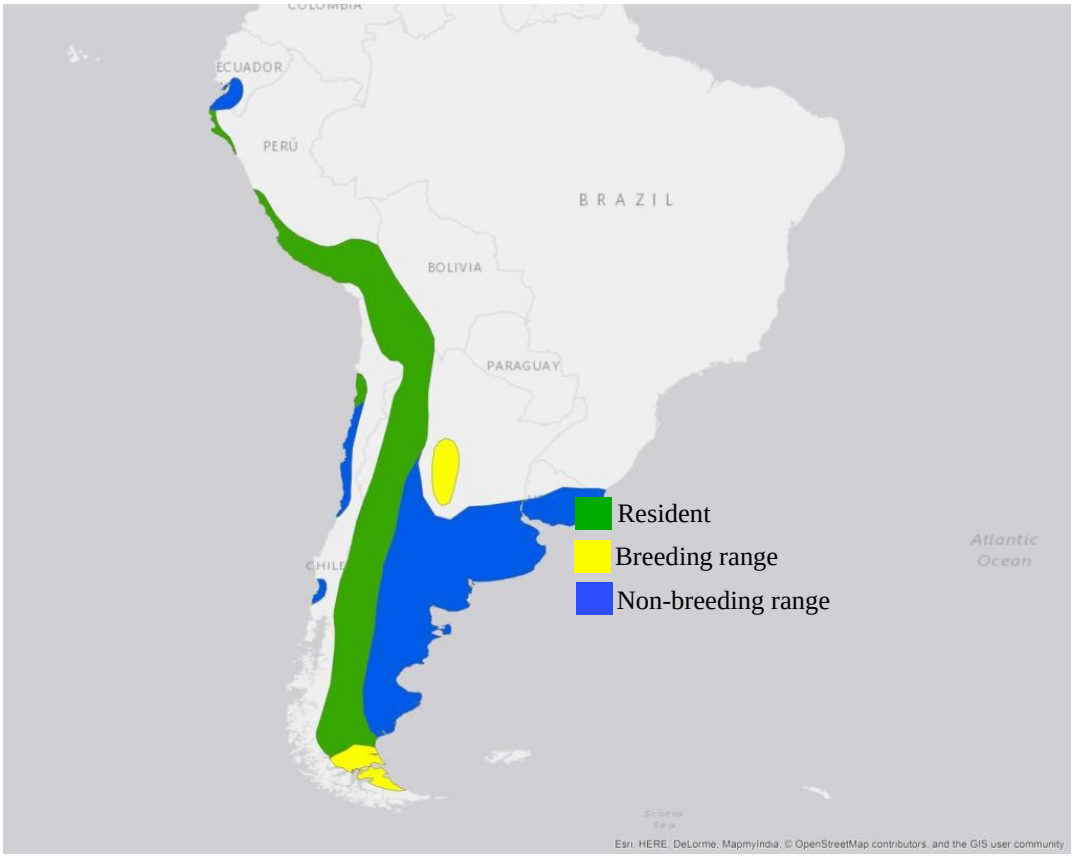

Figure 4.1.1.10. Current known range of Tawny-throated Dotterel.

Breeding range (AUC: 0.994; TSS: 0.942; Kappa: 0.826): Resident species along the coast of Peru, following the Andean Cordillera as far as south Argentina and a small proportion on the coast of Chile between south Antofagasta and north of Taltal. The breeding range is located in north-central Argentina (Salinas Grandes) and Tierra del Fuego.

At 26 ka BP a range is simulated in the Andean Cordillera from south Peru to south Argentina a small area extending to central-north Argentina and the Falkland Islands as well as a scattered range along the coast of Peru. The same pattern continues until 21ka when the range in south Argentina decreases, which increases again at 18 ka BP. Between 17 ka BP and 16 ka BP the range in central-north Argentina reduces and at 15 ka BP increases again and extending towards the east of Argentina until 13 ka BP. Also at 13 ka BP the range on the coast of Peru expands to a constant range. See Figure 4.1.1.10.a.

By the beginning of the Holocene the range is maintained with minimal differences until 7 ka BP, when the range starts narrowing to the Andean Cordillera until 1 ka BP. The current range also presents the same pattern as 1 ka BP, maintaining the same conditions.

The Heinrich event H2 and the 24 ka BP projection have a similar range across the Andean Cordillera and central Argentina, also, the H2 projection shows suitable conditions at the south of Central America and the north of South America from Colombia to Venezuela and Guyana, with a scattered range in Mexico. The same pattern is maintained between the H1ka and 17 ka BP projections from the Andean Cordillera, and the range projected in the north of South America is as well predicted, increasing to the north of Brazil as well. At last, the H0 projection shows a similar range to the 13 ka BP projection across the Andean Cordillera; however it also shows suitable conditions in the south of Central America and the north of South America mainly from the east Venezuela to Guyana, Suriname and French Guiana, and on a smaller scale in north-west Colombia and the Caribbean islands.

Even though, the breeding range of the species is focused to South America, suitable conditions were predicted in North America as well, from the north of Mexico to the south-west of the USA, between 26 ka BP and 18 ka BP.

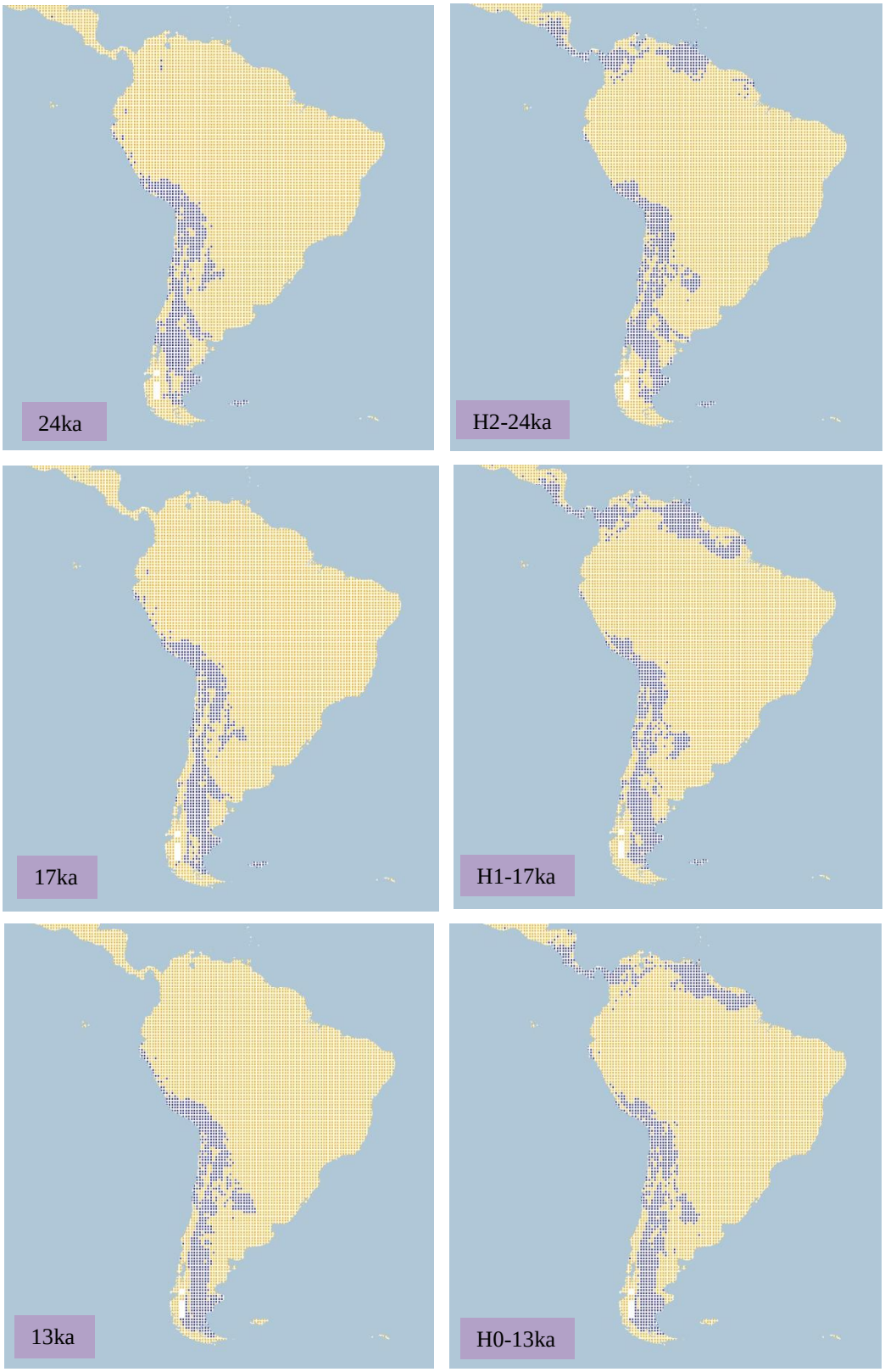

Figure 4.1.1.10.a. Simulation maps of Tawny-throated Dotterel breeding range.
Maps are shown for ten-time slices: 24ka, H2 (24ka), 17ka, H1 (17ka), 13ka, H0 (13ka), 9ka, 5ka, 3ka and present (1961–90).

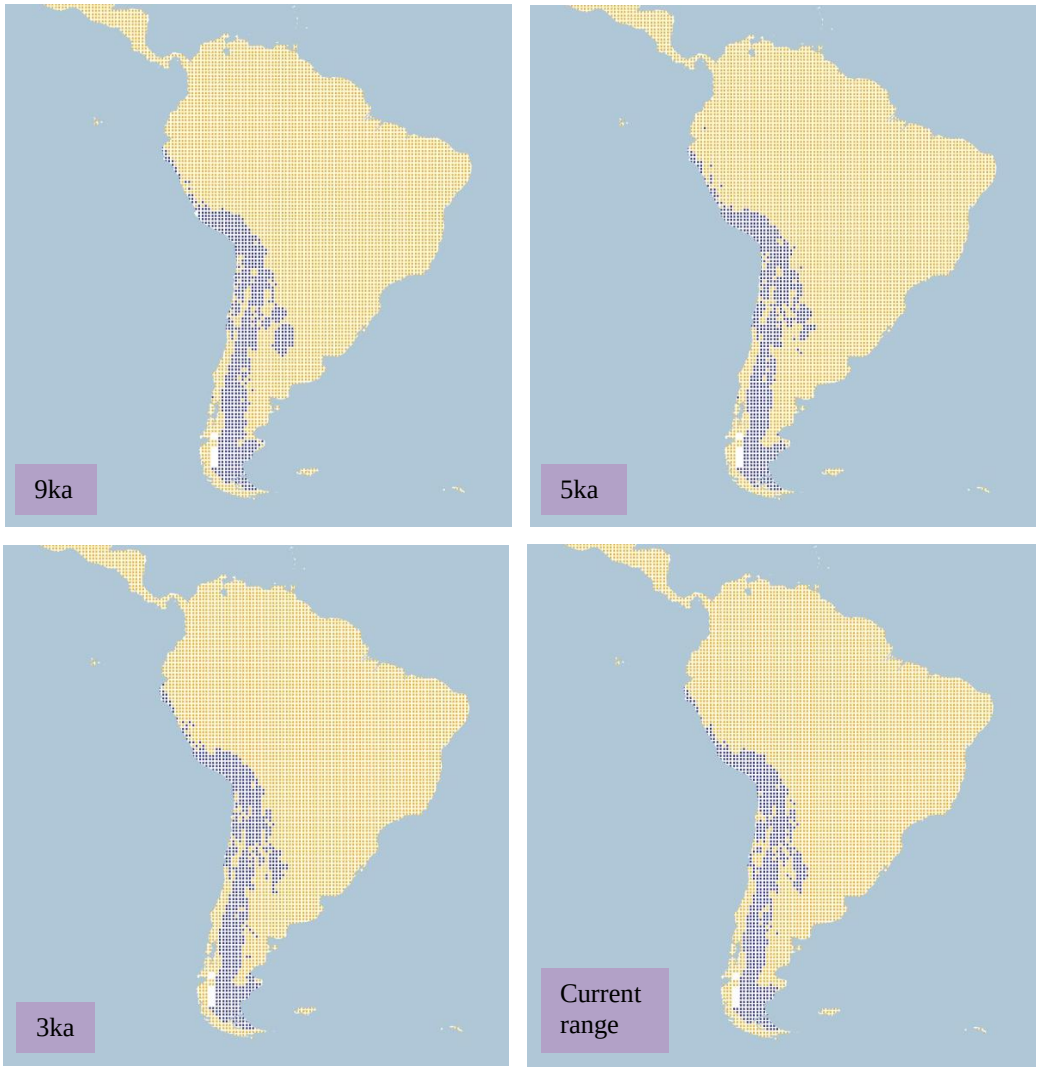

Figure 4.1.1.10.a. Simulation maps of Tawny-throated Dotterel breeding range (continued**).**

Non-breeding range (AUC: 0.994; TSS: 0.921; Kappa: 0.873): In addition to the resident range on the coast of Peru and the Andean Cordillera, the species also has a non-breeding range in central-south Argentina reaching central-south Uruguay and the south of Brazil. Also, a small range is located on the central coast of Chile and with isolated records on the south coast of Ecuador.

At 26 ka BP the range is projected along the Andean Cordillera from south Peru to south-central Argentina reaching the south coast of Argentina, and also there is a range from central to north-east Argentina, covering Uruguay and the south of Brazil as well. There is an increase on the range in south Brazil during 24 ka BP and 22 ka BP which decreases from 21ka onwards. See Figure 4.1.1.10.b.

The Andean Cordillera and the central-north Argentina to south Brazil pattern is maintained after the LGM, with slight differences, being the most notorious at 17 ka BP with a reduction on the central-north of Argentina onto south Brazil. This changes at 16 ka BP with an increase over that area, and also the range moves towards south Argentina reaching the south of Chile.

At 14 ka BP the range in central-north Argentina shifts to the south intersecting with the southern range and decreasing in the south of Brazil. This pattern continues towards the beginning of the Holocene, with a homogenous range across the Andean Cordillera, Argentina, Uruguay and south Brazil.

During the Holocene at 7 ka BP there is a reduction in the north of Argentina which increases again at 6 ka BP and its maintained until the1 ka BP projection with minimal variation. This is also consistent with the current non-breeding range projection.

For the H0 and 13 ka BP projection they present similar ranges across the Andean Cordillera and central-north Argentina, Uruguay and south Brazil, only with a larger range around the area of the Tietê River in Brazil and with a projected range in the north of South America, the west coast of Central America, a scattered range across central towards the north-west of Mexico, north of Florida and south of the Caribbean islands at the H0 projection.

The H1 projection shows a similar range to the H2 projection in the area of north South America, Central America, Mexico and the Caribbean islands. Also, the projected range in the Andean Cordillera and Argentina is similar to the 17 ka BP projection. This is changed during the H0 projection reducing at the north of South America and maintaining a similar range in the Andean Cordillera and Argentina as the 13 ka BP projection.

Although there is no evidence that the species has a non-breeding range in North America, during the projection of 26 ka BP and 17 ka BP mainly, there are suitable conditions across central-north of Mexico and the south-west of the USA.

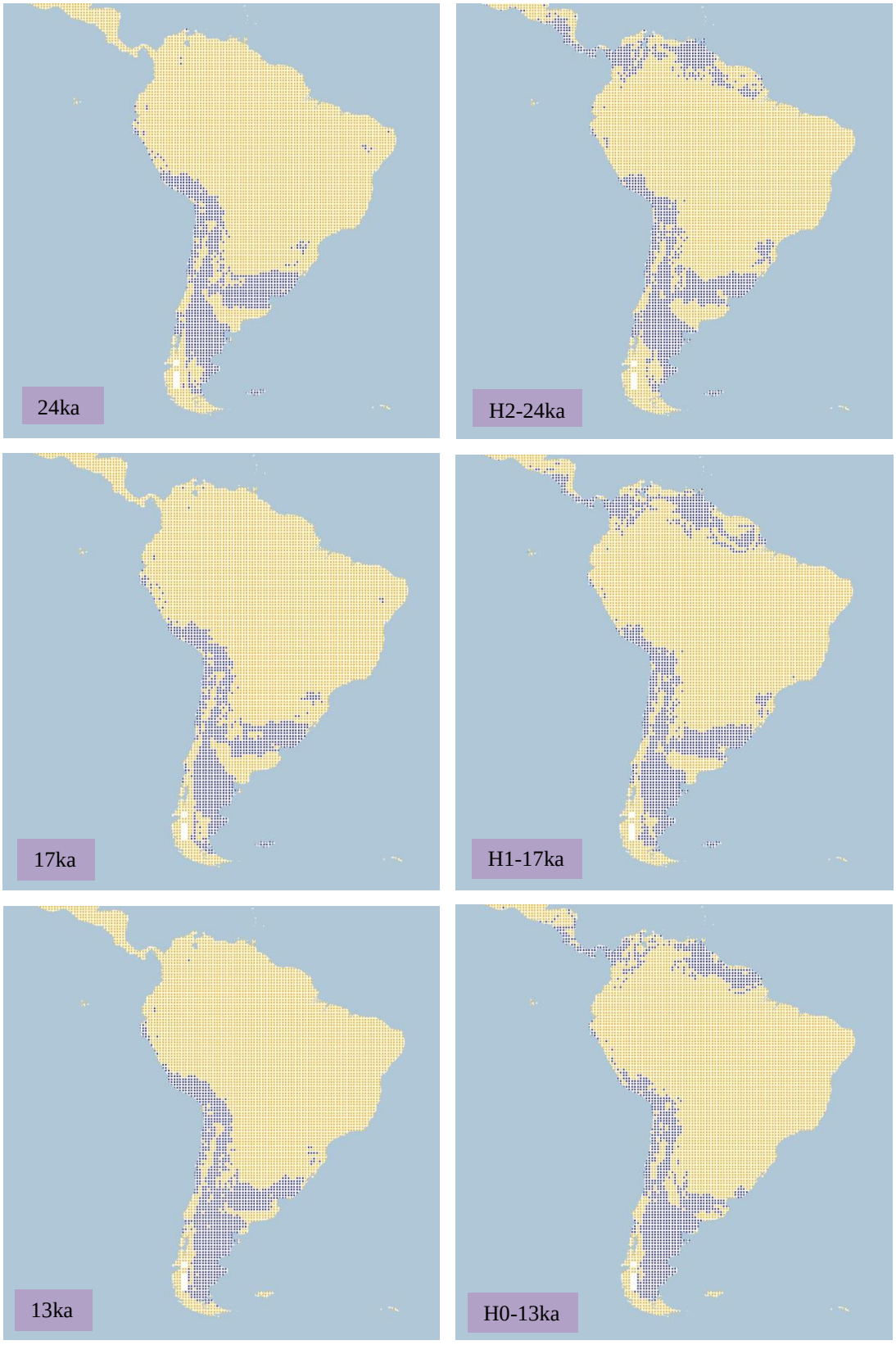

Figure 4.1.1.10.b. Simulation maps of Tawny-throated Dotterel non-breeding range. Maps are shown for ten-time slices: 24ka, H2 (24ka), 17ka, H1 (17ka), 13ka, H0 (13ka), 9ka, 5ka, 3ka and present (1961–90).

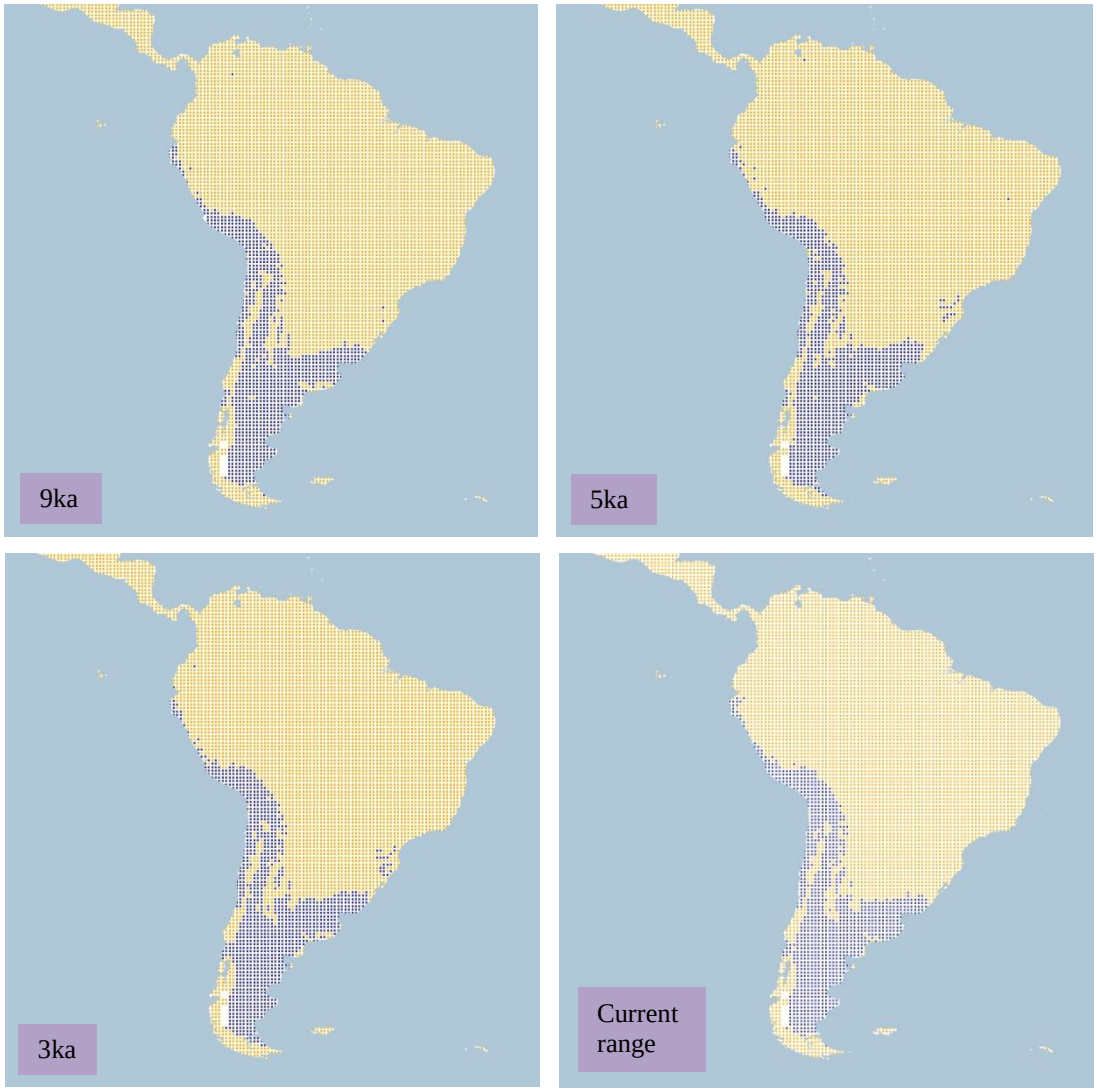

Figure 4.1.1.10.b. Simulation maps of Tawny-throated Dotterel non-breeding range (continued**).**

*4.1.1.11 American Golden Plover (*Pluvialis dominica*). Conservation status: Least Concern. Current known range Figure 4.1.1.11.*

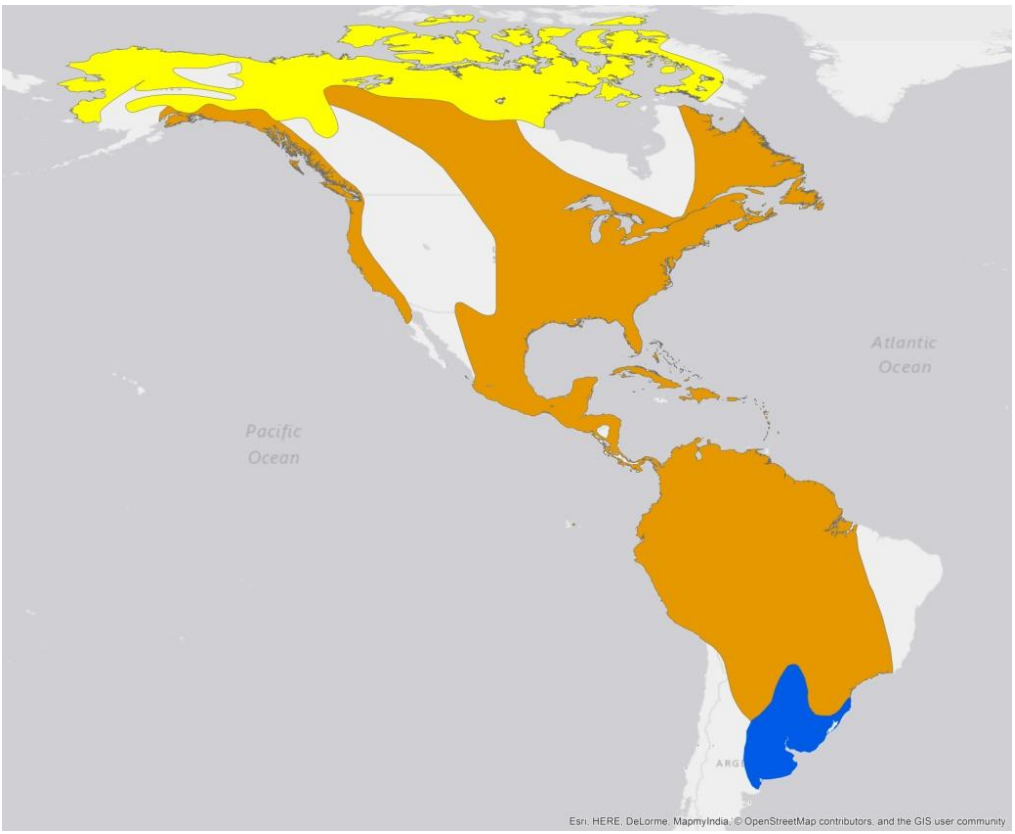

Figure 4.1.1.11. Current known range of American Golden Plover.

Breeding range (AUC: 0.965; TSS: 0.803; Kappa: 0.788): At the north of North America across Alaska and northern parts of Canada from Yukon to Devon and Baffin Island.

At 26 ka BP the range is projected across Alaska and the north-west of Canada not covered by the ice sheet and at a smaller scale in the north of the USA between Montana, North Dakota and Minnesota. This pattern continues with minimal differences until 17 ka BP when the range in the north of conterminous USA expands and the range in the central-south of Alaska not covered by ice decreases. See Figure 4.1.1.11.a.

As the ice sheet is melted the range in conterminous USA follows to the north reducing at 15 ka BP and also, the range in Alaska reduces as well, focusing mostly along the west and northern areas. In the north of Canada, the range increases as well as the ice sheet retreats.

At 13 ka BP the range the ice sheet is divided into two parts which lead to an increase on range in the west of Canada reaching the northern ranges and disappearing at 12 ka BP, focusing on the northern areas.

By the beginning of the Holocene the range on the west coast of Alaska decreases to a scattered range and is mainly located on the northern coast of Alaska, north-west of Canada and the Canadian islands not covered by ice. This increase as the ice retreats, following the northern parts of Canada.

From 8 ka BP onwards the range begins settling in the northern territories of Alaska and Canada with minimal differences only at 4 ka BP and1 ka BP with an inland expansion of the range. This also is complementary to the current breeding range projection.

The H2 and 24 ka BP projections show similar ranges in the conterminous north of the USA, and in the areas of Alaska and Canada not covered by the ice sheet. A minimal difference is shown at H1, where there is a shift on the western range of Alaska to an inland range, as well as an increase in the conterminous north of the USA, being is similar to the 17 ka BP projection except in the area of Alaska where the southern range decreases. The H0 and 13 ka BP projection present analogous ranges as well, with small differences.

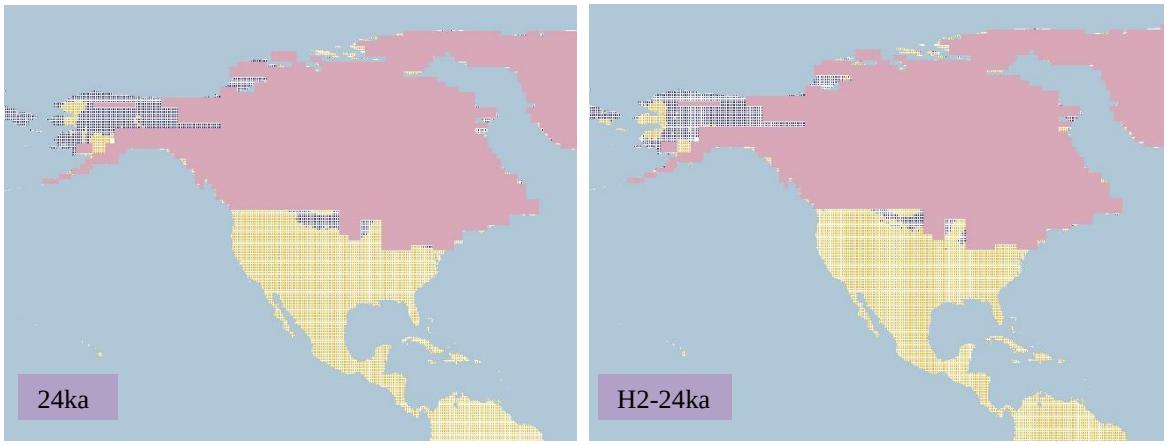

Figure 4.1.1.11.a. Simulation maps of American Golden Plover breeding range.
Maps are shown for ten-time slices: 24ka, H2 (24ka), 17ka, H1 (17ka), 13ka, H0 (13ka), 9ka, 5ka, 3ka and present (1961–90).

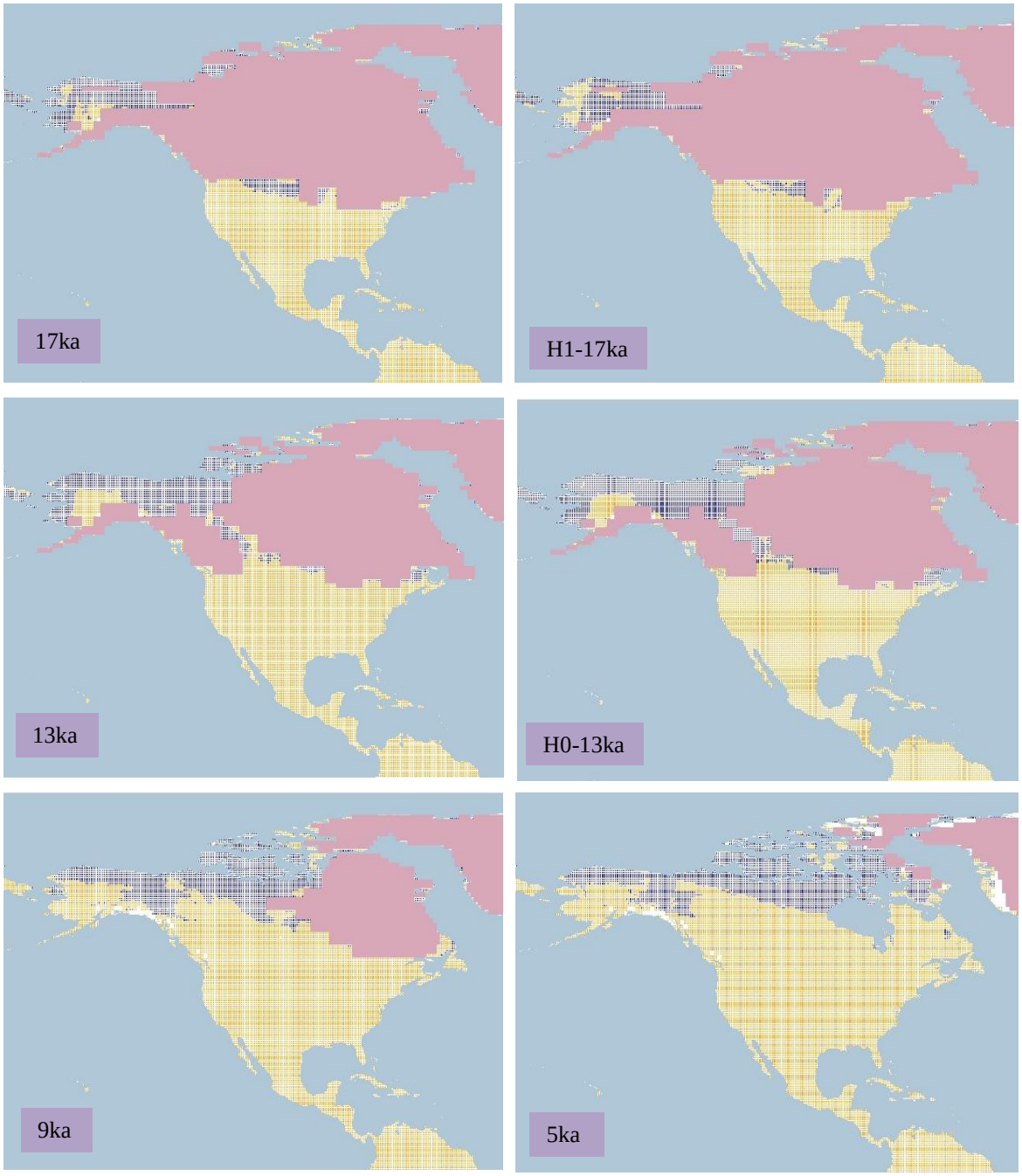

Figure 4.1.1.11.a. Simulation maps of American Golden Plover breeding range (continued**).**

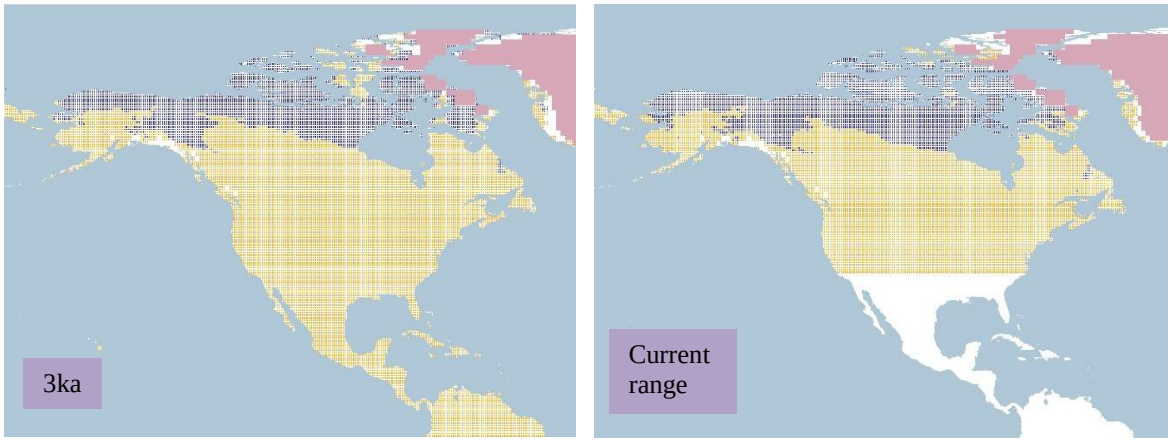

Figure 4.1.1.11.a. Simulation maps of American Golden Plover breeding range (continued**).**

Non-breeding range (AUC: 0.993; TSS: 0.928; Kappa: 0.865): This is located in the east/south-east of South America from the east of Paraguay to the north east of Argentina, following to Uruguay and a small range in the south of Brazil.

The range at 26 ka BP is projected in the area of south Paraguay, south Brazil, moving to Uruguay and the north-east of Argentina with a scattered range near the Andean Cordillera in the west of Argentina and near Rio de Janeiro in Brazil. See Figure 4.1.1.11.b.

There is an important difference presented at 24 ka BP and 21ka when the range decreases and moves to the south. At 19 ka BP the range increases at a small proportion and it's maintained until 15 ka BP when the range is expanded to the west of Argentina, and moves to the north too.

At the beginning of the Holocene the range remains similar, increasing in the south of Brazil and north Argentina at 8 ka BP, reducing at 7 ka BP and increasing from 6 ka BP onwards once more. Only at 2 ka BP there is a difference in the range projected which reduces in the south of Brazil and in Paraguay as well. This is consistent with the current non-breeding range projection, in the area covering the south Brazil.

The H2 and 24 ka BP projections have similar ranges in Paraguay, Uruguay and south Brazil, only with a larger range in Argentina, specifically in the north-west at the H2 projection. This increases at H1 in the north-west and the central part of Argentina, which contradicts the 17 ka BP projection with a smaller range in general. The H0 and 13 ka BP projections shown differences as well, especially in Argentina where the range at H0 is

restricted to the north-east, moving to Uruguay, the southern boundaries of Brazil and increasing towards north of Paraguay and reaching Bolivia.

Even though the non-breeding range is focused in South America there are suitable conditions presented in the east and south-east of the USA across all the projections, and extending to the north-west of Mexico and south-west of the USA on the Heinrich events projections.

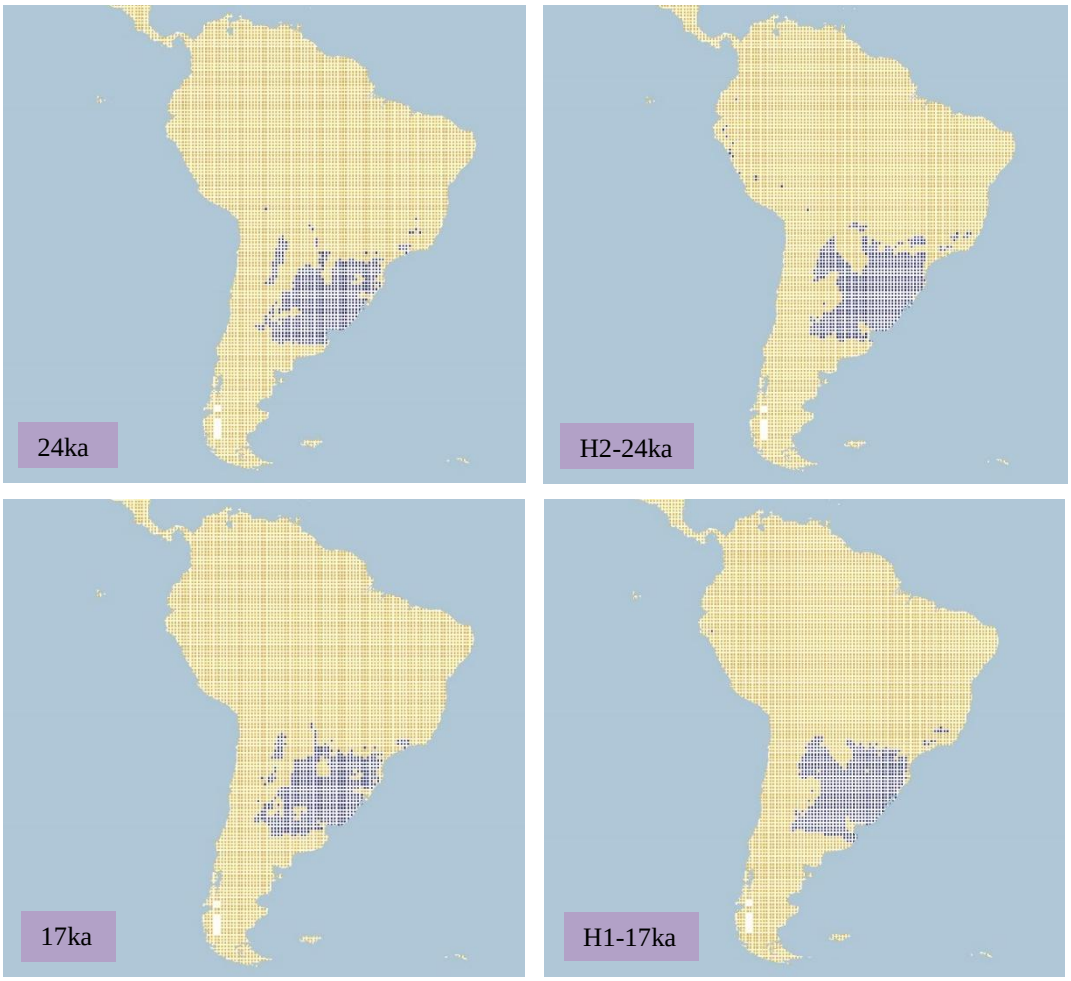

Figure 4.1.1.11.b. Simulation maps of American Golden Plover non-breeding range. Maps are shown for ten-time slices: 24ka, H2 (24ka), 17ka, H1 (17ka), 13ka, H0 (13ka), 9ka, 5ka, 3ka and present (1961–90).

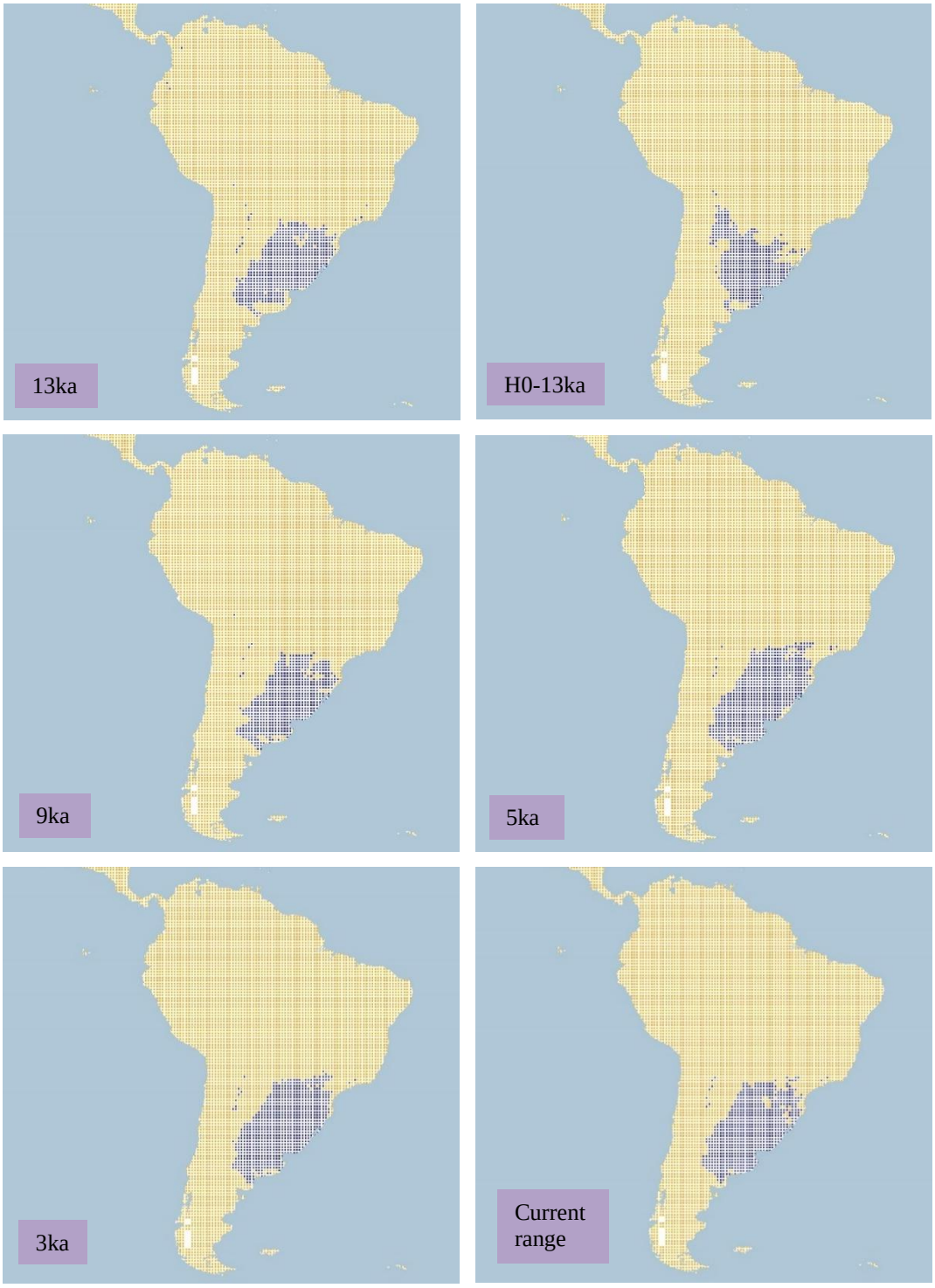

Figure 4.1.1.11.b. Simulation maps of American Golden Plover non-breeding range (continued**).**

*4.1.1.12 Grey Plover (*P. squatarola*, only subspecies* P. s. cynosurae*). Conservation status: Least Concern. Current known range Figure 4.1.1.12.*

Figure 4.1.1.12. Current known range of Grey Plover.

Breeding range (AUC: 0.935; TSS: 0.752; Kappa: 0.700): the sub-species *P. s. cynosurae* breeds on the northern coast of Canada and in the Canadian Arctic Archipelago as far as Ellef Ringnes Island to the north, and the Baffin Islands to the east.

At 26 ka BP the range is projected on the northern coast of Alaska and on the north-west of Canada in the areas not covered by ice and reaching Banks Island; a small range is also projected inland in the north of the USA from Montana to Minnesota. The range continues with minimal variations growing to the west coast of Alaska at 20 ka BP to decrease at 19 ka BP. See Figure 4.1.1.12.a.

As the ice sheet retreats at 16 ka BP the range projected in conterminous north of the USA moves to the north, and the range in the north-west of Canada and in Alaska remain stable. At 15 ka BP there is a decrease of the range in the north of the USA which moves near the ice

sheet on the border between Montana and Saskatchewan and Alberta; this range disappears at 13 ka BP, and instead is focused to the north-west of Canada near the ice sheet.

By 12 ka BP the range is restricted to the northern coasts of Alaska and Canada, also with presence from Banks Island to Borden Island; additionally, a small range is shown on the south-east coast of Canada near the ice sheet.

At the beginning of the Holocene the range shifts mainly to the Canadian Arctic Archipelago and with a scattered and small range along the northern coast of Alaska and north-west of conterminous Canada. By 9 ka BP this changes and there is a growing inland range in the north of conterminous Canada, and as the ice sheet retreats at 8 ka BP the range reaches other islands of the Canadian Arctic region.

From 6 ka BP onwards the range begins decreasing and is establish mainly in the Canadian Arctic Archipelago with a small range on the north-coast of Quebec and in the north of Alaska until 1 ka BP. The current breeding range projection shows the same range projected as 1 ka BP.

The H2 and 24 ka BP projection illustrate enormous similarities from the north of conterminous USA towards Alaska and the north-west of Canada not covered by ice, only the H2 projection has a wider range along the west of Alaska. This same pattern is shown in the H1 projection, being similar as well with 17 ka BP. Furthermore, the H0 projection is analogous to 13 ka BP only with a wider range in the north-west of Canada and on the north-west coast of Alaska.

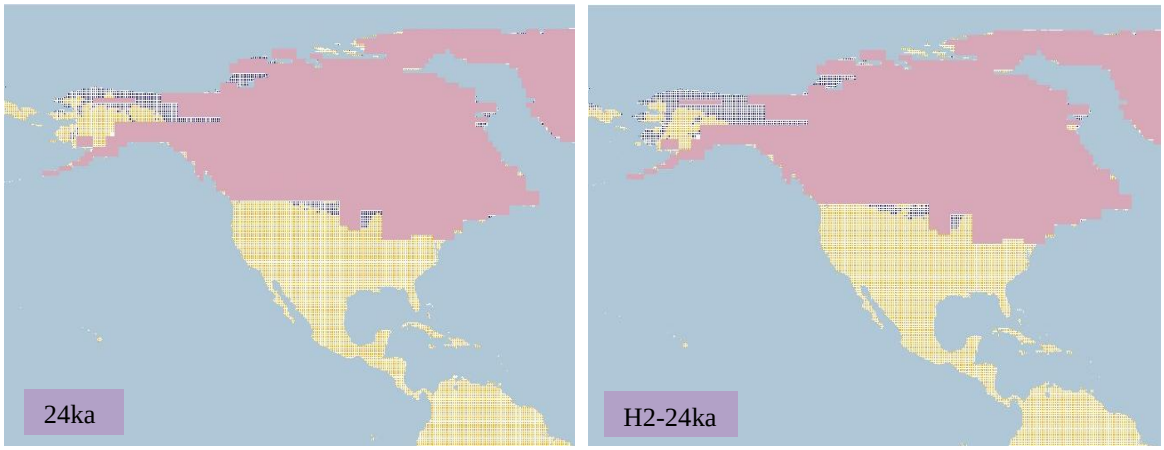

Figure 4.1.1.12.a. Simulation maps of Grey Plover breeding range.
Maps are shown for ten-time slices: 24ka, H2 (24ka), 17ka, H1 (17ka), 13ka, H0 (13ka), 9ka, 5ka, 3ka and present (1961–90).

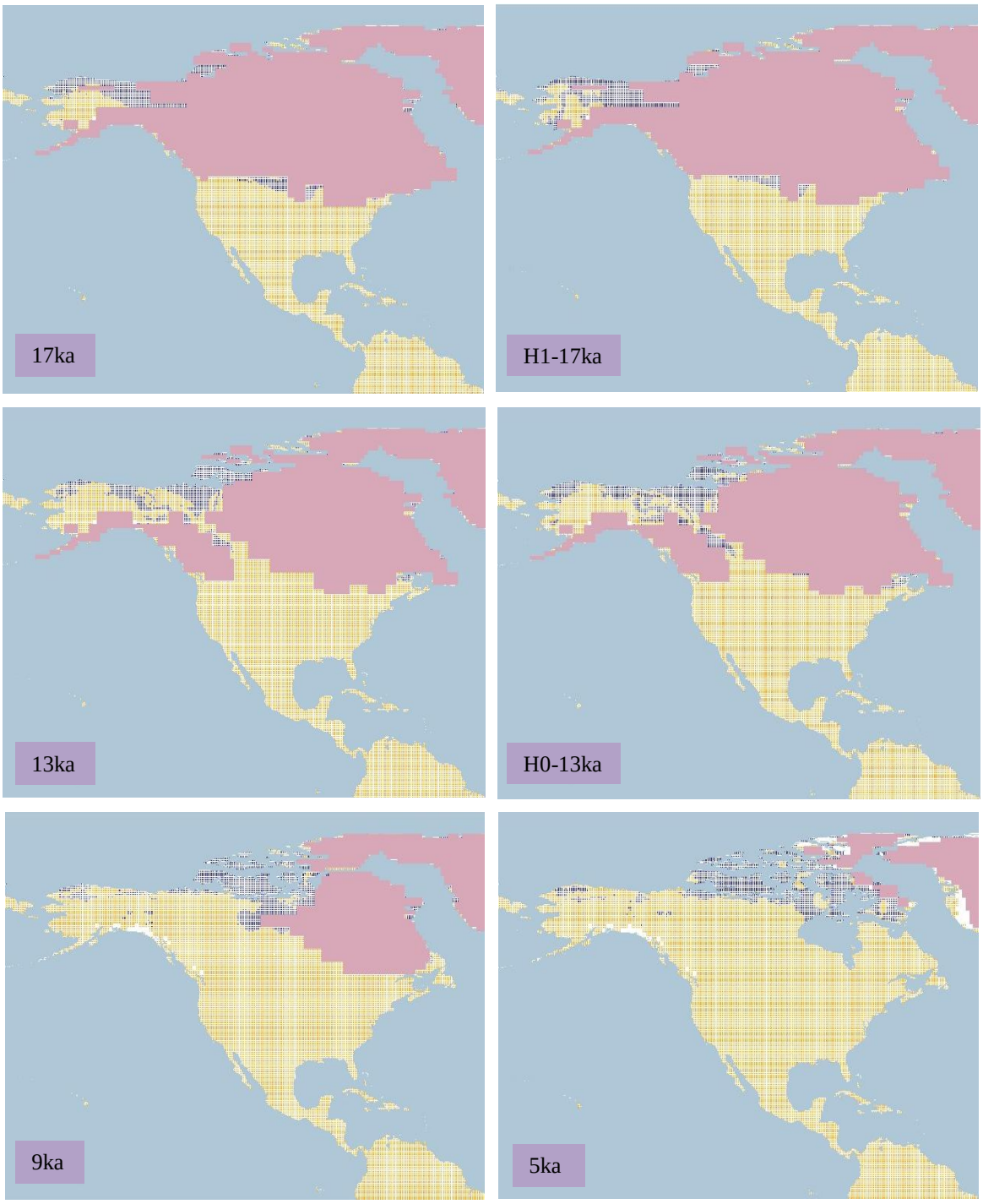

Figure 4.1.1.12.a. Simulation maps of Grey Plover breeding range (continued**).**

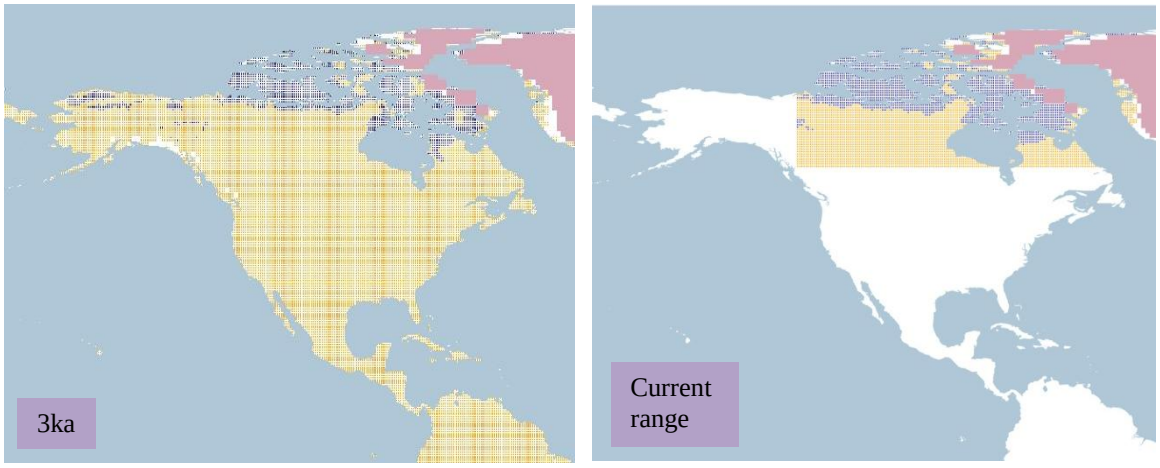

Figure 4.1.1.12.a. Simulation maps of Grey Plover breeding range (continued**).**

Non-breeding range (AUC: 0.937; TSS: 0.706; Kappa: 0.562): this sub-species presents a wide non-breeding range along the coasts of North and South America, from the south-west of Canada to Central Chile in the Pacific, and, from the north-east of the USA, along the Caribbean islands, to the south of Uruguay in the Atlantic.

At 26 ka BP the range is projected along the Pacific coasts of the USA, Mexico and in South America from Ecuador to central Chile, also, with a scattered and more inland range in the Atlantic from Florida, the Caribbean islands, and in South America from Venezuela to the north of Brazil, the north of South America. See Figure 4.1.1.12.b.

The 24 ka BP time frame has a projected range in the north of Brazil in South America increases, and then decreases at 22 ka BP, along with the range projected in the Andean cordillera. This pattern continues until 15 ka BP with an increase on the west coast of USA and the south-west coast of Canada as the ice sheet reduces; also, in South America, the range in the north-west of Brazil, Guyana, Suriname and French Guiana increases and continues increasing until 13 ka BP.

By the beginning of the Holocene the range in the north-west of inland Brazil reduces and on the east coast of Brazil increases. Also, there is an increase of the range projected from central to the north of Mexico. This pattern continues until 8 ka BP with the decrease of the range in the north-west of Brazil, increasing to the east and central areas between Goiás, Minas Gerais, state of São Paolo, and Mato Grosso do Sul, also in Uruguay and Bolivia. The range also increases on the south-east coast of the USA from Louisiana to Georgia.

At 6 ka BP the range in South America extends mainly from Bolivia to the east and north of Brazil, and on a smaller scale on the Pacific coast of Ecuador, Peru and Chile. Likewise, in North America the range is projected along the Pacific coast of southern Canada, USA, and Mexico. The inland range in South America changes at 4 ka BP with a decrease in the north and east of Brazil, but remaining in Bolivia and Uruguay. The decreasing pattern continues in South America until 1 ka BP with the rise of the range projected on the south-east coast of USA, the remainder of the range persisting with minimal variations. This also is present in the current non-breeding projection.

When compared with 24 ka BP, the Heinrich event H2 presents a different projection, mostly evident in South America, covering large areas from south-central Brazil to the north of Venezuela. This continues in Central America and to the centre and south of Mexico, as well as on the south of USA. A similar range in South America, Central America and centre to south of Mexico continues at H1, only reducing the range in the south of USA and presenting only comparisons with 17 ka BP along the Pacific coast of the Americas. At H0 the range projected in central Brazil decreases; however, the similarities persist with 13 ka BP along the Pacific coast of the Americas.

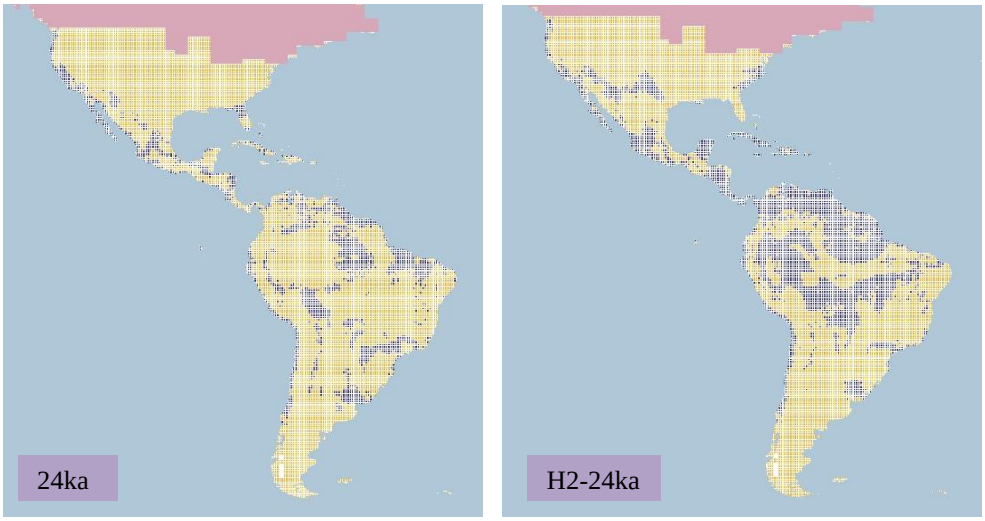

Figure 4.1.1.12.b. Simulation maps of Grey Plover non-breeding range.
Maps are shown for ten-time slices: 24ka, H2 (24ka), 17ka, H1 (17ka), 13ka, H0 (13ka), 9ka, 5ka, 3ka and present (1961–90).

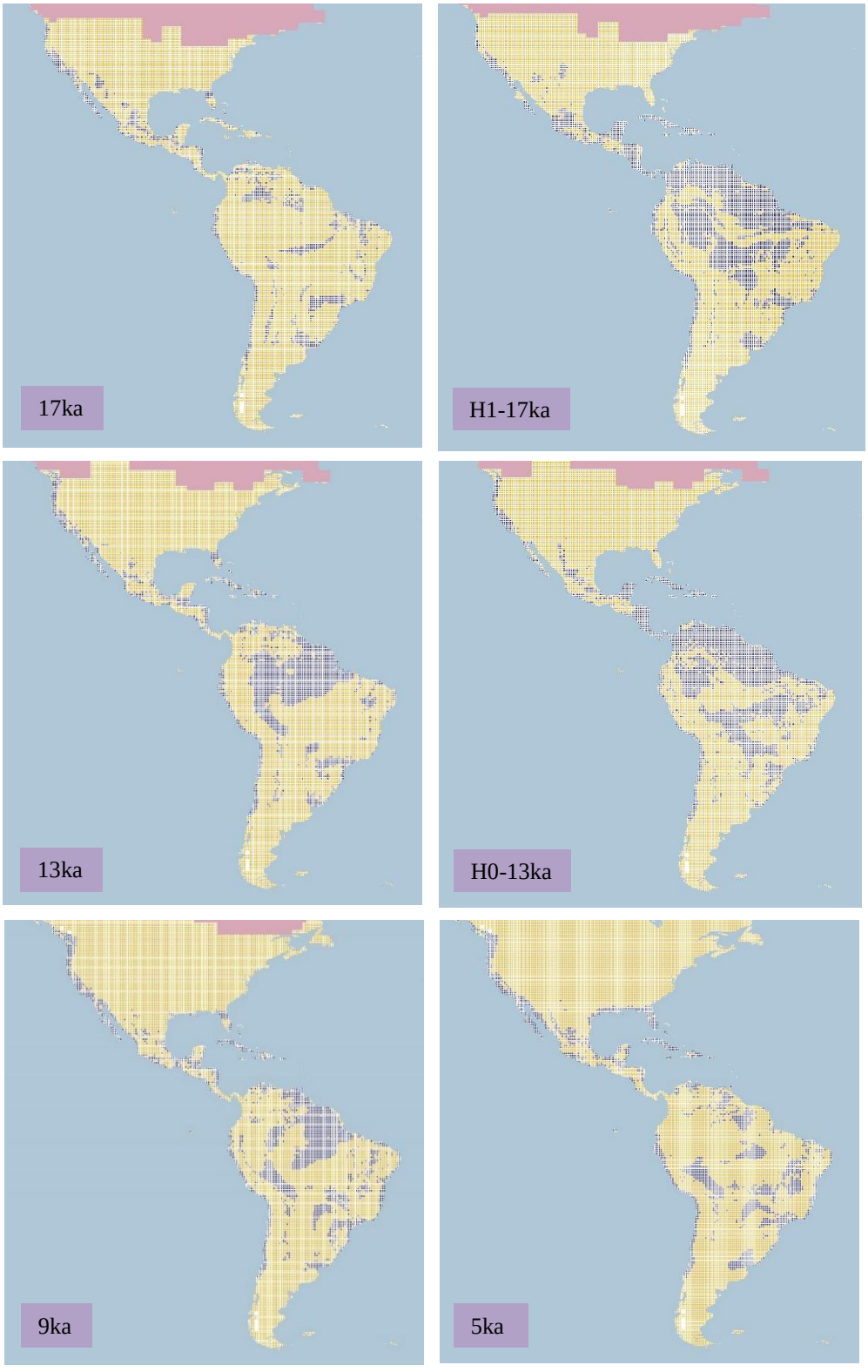

Figure 4.1.1.12.b. Simulation maps of Grey Plover non-breeding range (continued**).**

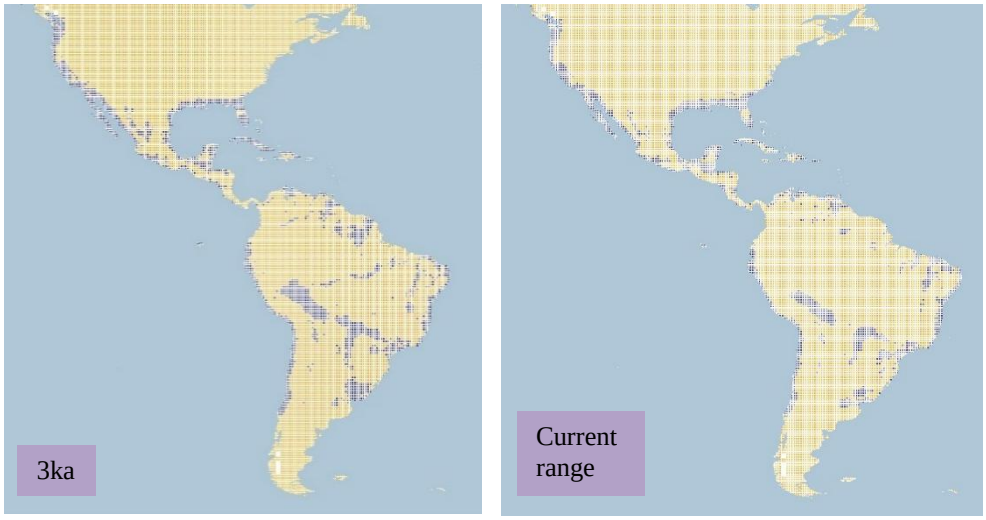

Figure 4.1.1.12.b. Simulation maps of Grey Plover non-breeding range (continued**).**

4.1.1.13 AUC, TSS, and Kappa values.

The resulted AUC, TSS and Kappa values for each species of the family Charadriidae are shown in here. These are divided in breeding and non-breeding ranges and there is an indication when temperate or tropical variables were used.

For the Charadriidae breeding ranges the measures of model accuracy indicated a high model performance with AUC values mainly >0.950 (Huntley et al. 2008), with a median of 0.980, as well as overall higher values than in comparison with TSS and Kappa; the major AUC value is 0.9945 for species Tawny-throated Dotterel (*O. ruficollis*), followed by Rufous-chested Plover (*C. modestus*) with 0.9944 and Piping Plover (*C. melodus*) with 0.988. The lowest AUC values correspond to the species Wilson's Plover (*C. wilsonia*) at 0.916 which may reflect the species' restricted coastal range. For Semipalmated Plover (*C. semipalmatus*) and Grey Plover (*P. squatarola*) AUC values were also lower, at 0.945 and 0.935 respectively, although these species breed in Arctic regions of North America and have larger ranges.

The TSS values for the breeding range projections varied from 0.803 to 0.961, with a median of 0.845, with the highest value of 0.961 for the species Rufous-chested Plover (*C. modestus*), next to Tawny-throated Dotterel (*O. ruficollis*) with 0.942 and Piping Plover (*C. melodus*) with 0.903. The lowest TSS value corresponds to species Wilson's Plover (*C. wilsonia*) with 0.667, followed by Semipalmated Plover (*C. semipalmatus*) with 0.726 and Grey Plover (*P. squatarola*) with 0.752; these results support inferences from the AUC values.

For the Kappa index of the breeding range projections the values obtained were from 0.802 to 0.861, with a median of 0.788. The highest value of 0.861 is presented from species Collared Plover (*C. collaris*), followed by Killdeer (*C. vociferus*) with 0.844 and Tawny-throated Dotterel (*O. ruficollis*) with 0.826. Again, the lowest Kappa value was for Wilson's Plover (*C. wilsonia*) with 0.484; Semipalmated Plover (*C. semipalmatus*) with 0.701 and Grey Plover (*P. squatarola*) with 0.700 again had relatively low values. Several other species also had values less than 0.800: Two-banded Plover (*C. falklandicus*) with 0.770; Mountain Plover (*C. montanus*) with 0.775; Piping Plover (*C. melodus*) with 0.788; and American Golden Plover (*P. dominica*) with 0.788. Given that Piping Plover (*C. falklandicus*) breeds along coastal regions of southern South America this relatively low value can reflect its

restricted range; although for the rest of the species that breed inland in North America with a wider range the Kappa value indicates lesser accuracy. See Figure 4.1.1.a.

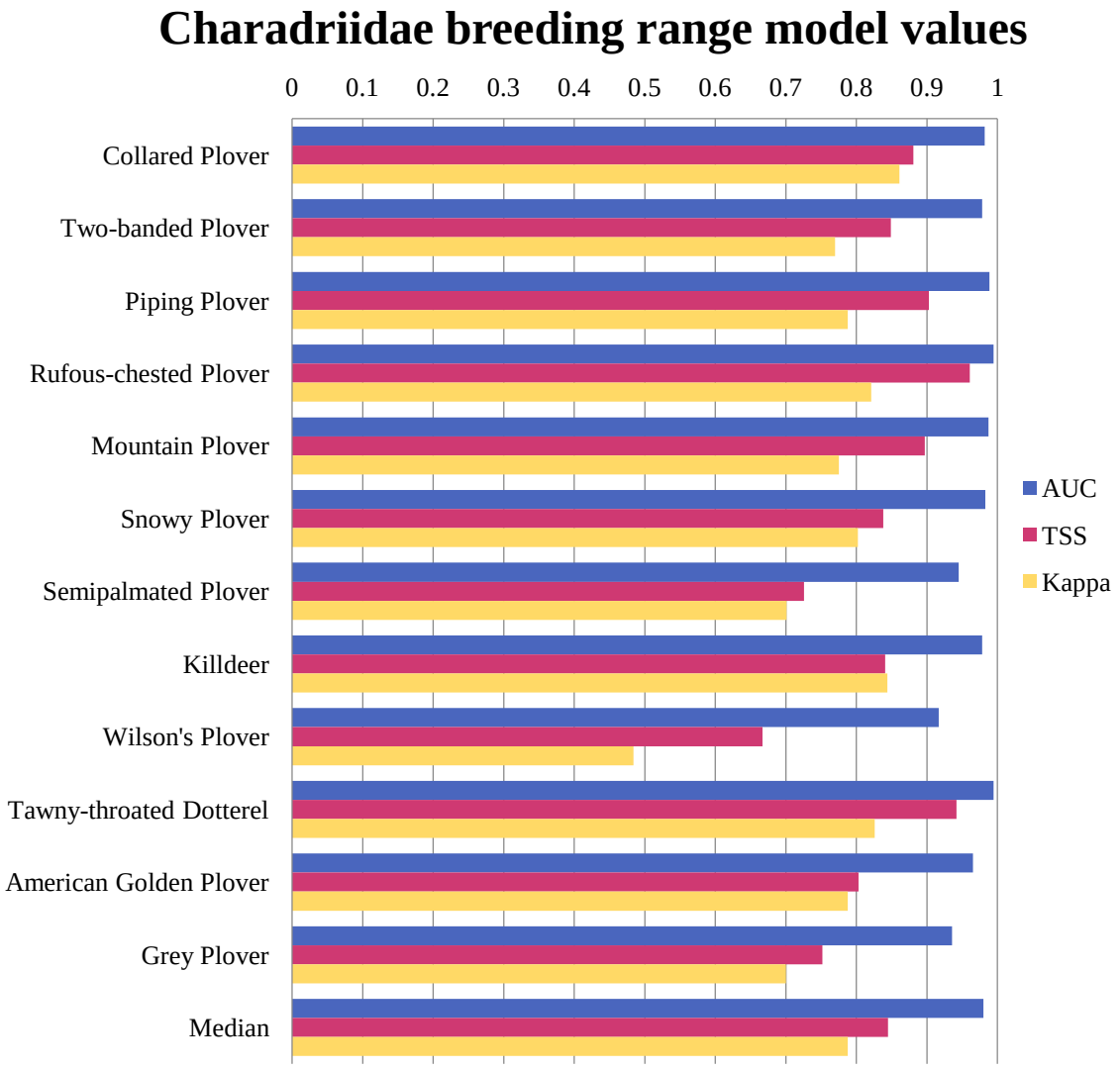

Figure 4.1.1.a. Model performance values of the family Charadriidae breeding range. The graph shows values for each species of AUC, TSS and Kappa values from the CRS model as well as the median for each statistical measurement.

For the non-breeding range models, the AUC values were mainly from 0.970 to 0.994 with a median of 0.980. The highest AUC values are presented by species Tawny-throated Dotterel (*O. ruficollis*) with 0.994, followed by American Golden Plover (*P. dominica*) with 0.993 and Mountain Plover (*C. montanus*) with 0.9887. The lowest values were for Semipalmated Plover (*C. semipalmatus*) with 0.921, Wilson's Plover (*C. wilsonia*) with 0.925 and Grey

Plover (*P. squatarola*) with 0.937. The current non-breeding ranges of these species are restricted to coastal areas, which probably explain the lower AUC values for their models.

The TSS values were mainly between 0.808 and 0.936, with a median of 0.859, a middle range between AUC and the Kappa values. The highest TSS value is presented by the species Mountain Plover (*C. montanus*) with 0.936, followed by Tawny-throated Dotterel (*O. ruficollis*) with 0.932 and Piping Plover (*C. melodus*) with 0.930. The lowest values correspond to Wilson's Plover (*C. wilsonia*) with 0.669, Semipalmated Plover (*C. semipalmatus*) with 0.681 and Grey Plover (*P. squatarola*) with 0.706, again reflecting the restriction of their current non-breeding ranges to coastal regions.

The Kappa values also indicate lower accuracy mainly for species with non-breeding ranges restricted to coastal areas, with values mainly from 0.731 to 0.873 with a median of 0.740. The highest Kappa value presented by species Tawny-throated Dotterel (*O. ruficollis*) with 0.873, followed by American Golden Plover (*P. dominica*) with 0.865 and Collared Plover (*C. collaris*) with 0.864. The lower Kappa values are presented by Piping Plover (*C. melodus*) with 0.690, Mountain Plover (*C. montanus*) with 0.618, Semipalmated Plover (*C. semipalmatus*) with 0.547, Wilson's Plover (*C. wilsonia*) with 0.518 and Grey Plover (*P. squatarola*) with 0.562. See Figure 4.1.1.b.

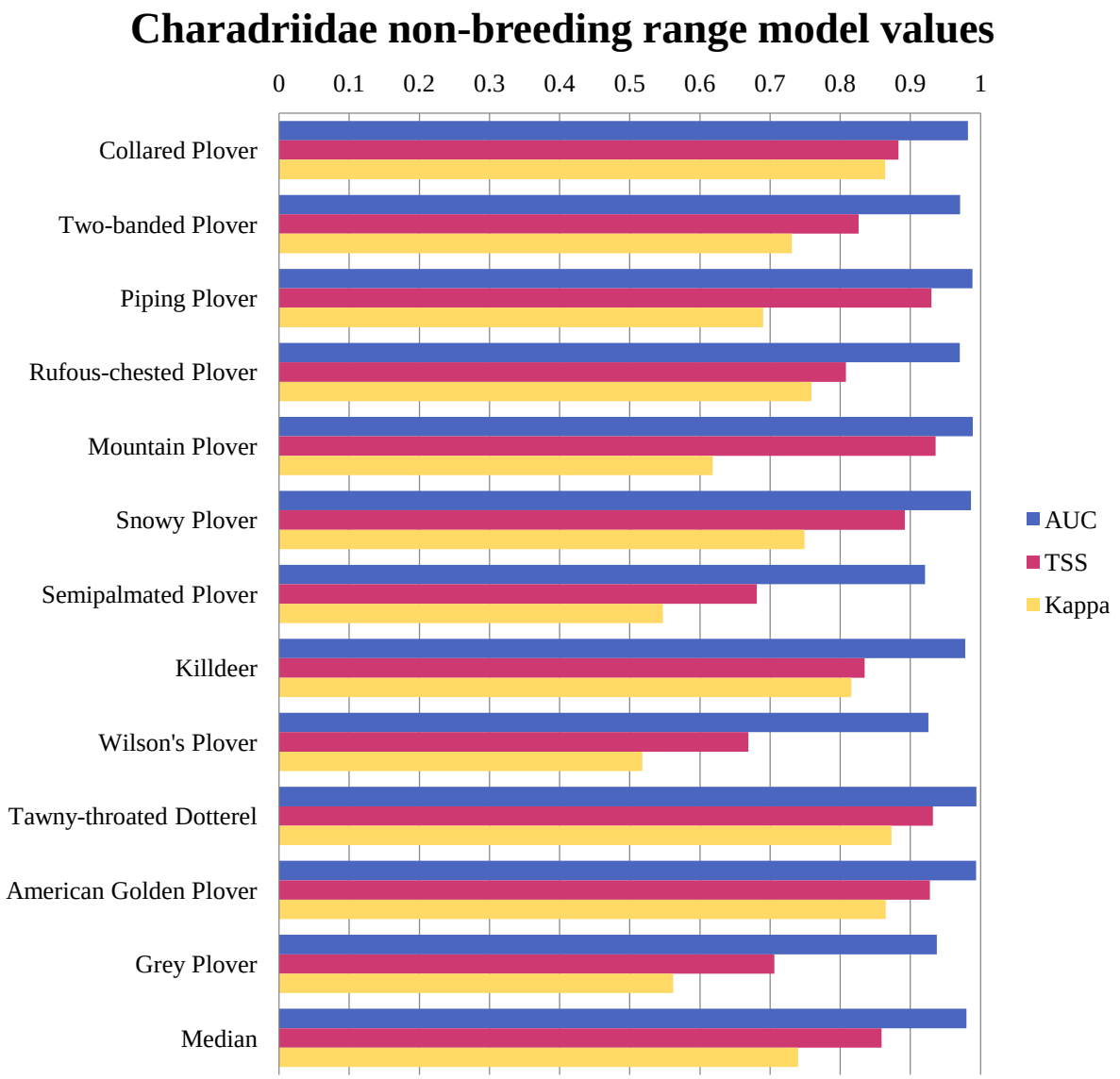

Figure 4.1.1.b. Model performance values of the family Charadriidae non-breeding range.
The graph shows values for each species of AUC, TSS and Kappa values from the CRS model as well as the median for each statistical measurement.

4.1.2 Family Haematopodidae

*4.1.2.1 Blackish Oystercatcher (*Haematopus ater*, including* H. a. ater *and* H. a. bachmani*). Conservation status: Least Concern. Current known range at Figure 4.1.2.1.*

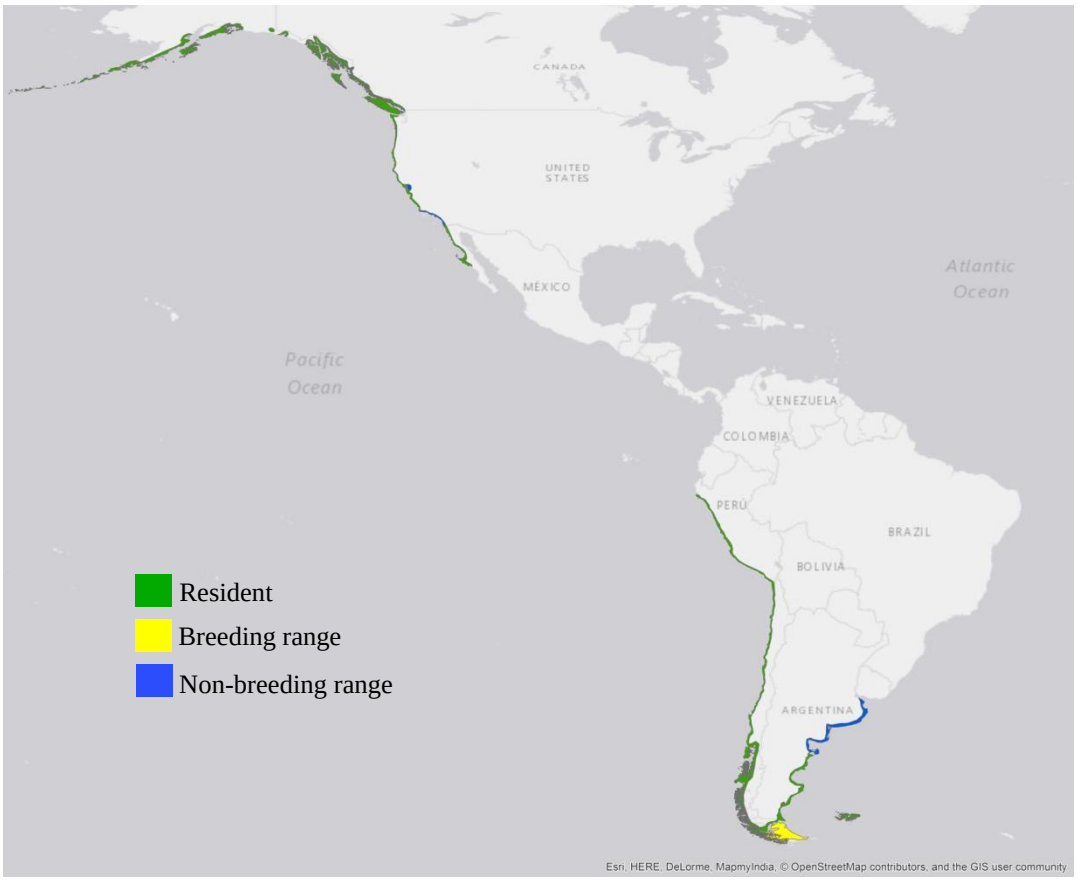

Figure 4.1.2.1. Current known range of Blackish Oystercatcher.

Breeding range (AUC: 0.995; TSS: 0.949; Kappa: 0.836): This species' current breeding range is restricted to Tierra del Fuego in Argentina with a large resident range on the west coast of the Americas, from South Alaska to southern Chile. For modelling the breeding range, the variables used were the 'temperate' set.

From 26 ka BP until 19 ka BP there is no range projected in the region of Tierra del Fuego and the Falkland Islands. The Pacific coastal range tends to be restricted and instead shifts towards inland regions. The distribution in South America moves to the centre of Ecuador, Argentina and Peru. In North America a similar shift is shown mainly to the region of Nevada, Arizona, and Utah, appearing to surround the Great Salt Lake. In the central-south

part of Mexico there is also a potential range, surrounding several lakes such as Lake Cuitzeo. This suggests that, given the climate and sea level variations during this period, before and after the LGM, the breeding range of this species may potentially have shifted inland to sites near water. See Figure 4.1.2.1.a.

The projections for 24 ka BP and H2 (24ka) show an important contrast in the area of North America. For H2 a large range is projected in the central-west part of USA, as well as in central Mexico, the Greater Antilles, Central America (from Guatemala to Panama) and reaching the north of Colombia, Venezuela and Guyana. For the rest of South America, the two projections are similar.

At 18 ka BP the range begins decreasing on the inland areas, a trend that continues at 17ka. The 17 ka BP and H1 projections are similar for the areas in South America and central Mexico, and for the small range in Baja California. In contrast, the projected North American range is smaller at 17 ka BP than at 24 ka BP, and more restricted to the coastlines, whereas the H1 and H2 projections are similar in North and Central America. At 16 ka BP the breeding range expands to include Tierra del Fuego and the Falkland Islands.

After this period, the projected inland distribution in Utah, Nevada and Arizona disappears. Towards the end of the Pleistocene 12-11ka the ice on the coastal area of Alaska and Canada disappears and the range extends into that region. The range also slightly increases in South America, specifically in southern parts of Chile and Argentina. At 10 ka BP there is a potential breeding area in central Canada, near Hudson Bay, but this disappears after 9 ka BP.

From 6 ka BP until 1 ka BP the projected range of the species is focused mainly in coastal areas and it remains much the same. During the past 26,000 years the two sub-species ranges apparently didn't intersect in any time slice, however, taking into account the projections of the Heinrich events there is a projected range in Central America and the northern part of South America which is not recognized currently, and might suggest that both subspecies connected within this area.

For the current climate the known current range is well projected, and it seems it has been unchanged over the last millennium, given the similarity with the 1 ka BP simulation.

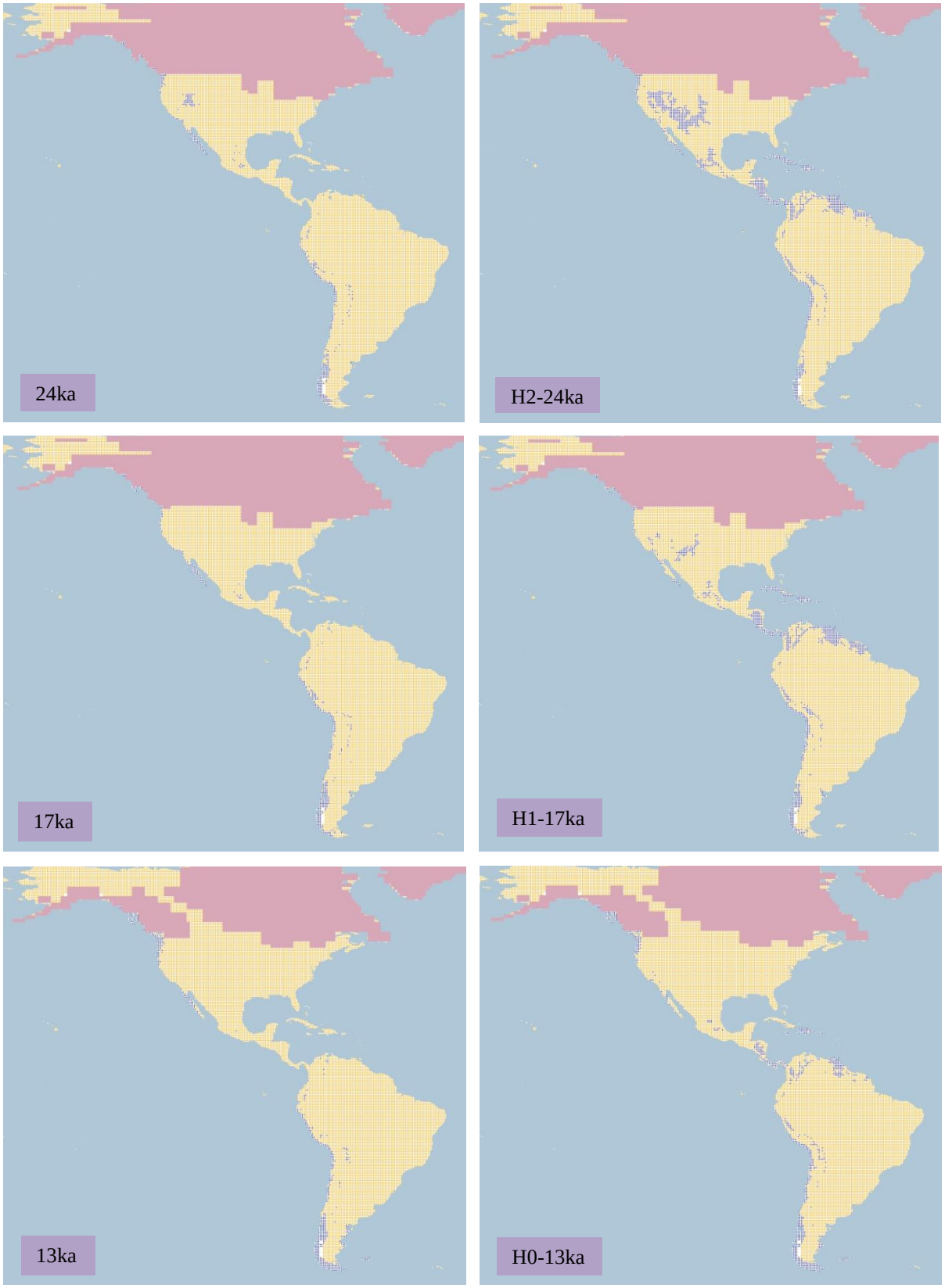

Figure 4.1.2.1.a. Simulation maps of Blackish Oystercatcher breeding range.
Maps are shown for ten-time slices: 24ka, H2 (24ka), 17ka, H1 (17ka), 13ka, H0 (13ka), 9ka, 5ka, 3ka and present (1961–90).

Figure 4.1.2.1.a. Simulation maps of Blackish Oystercatcher breeding range (continued**).**

Non-breeding range (AUC: 0.993; TSS: 0.934; Kappa: 0.796): Projected changes in this range are mostly similar to those for the breeding range, given that the species is predominantly resident. The discussion below is therefore focused only on the distinct non-breeding areas, on the south-east coast of Argentina for *H. a. ater* and in southern California for *H. a. bachmani*. The variables used to model this range were the 'temperate' set.

At 26 ka BP there is no projected range in the south-east of Argentina; instead is shifted to the northern part of Uruguay. This pattern continues until 15 ka BP when the range moves to the central part of Uruguay and Argentina. Likewise, the range in California initially is shifted south to Baja California in Mexico, with projected areas also inland towards Nevada, Utah and Arizona. This pattern continues until 18 ka BP, after which the range is focused in

Baja California. In central Mexico there is also a range extension from 26 ka BP until 15 ka BP, after which it begins to fragment. See Figure 4.1.2.1.b.

On the north-west coast of USA (Oregon and Washington) from 26 ka BP to 12 ka BP there is a projected range that, following the deglaciation at the beginning of the Holocene, extended to the west coast of Canada and south-west Alaska, persisting there until the present.

For the comparison between the 24 ka BP and H2 projections, the same contrasts as with the breeding range are seen, with a more extensive inland range in the H2 projection in the central USA, central Mexico, Central America and in the northern countries of South America (Colombia, Venezuela and Brazil).

In Argentina from 14 ka BP the projected range starts shifting to the south-east coast and remains until 12 ka BP. At 11 ka BP, the beginning of the Holocene, the distributional range for both North and South America begins to be restricted to coastal areas, and slowly decreases in extent until1 ka BP and what it is known now as the current range.

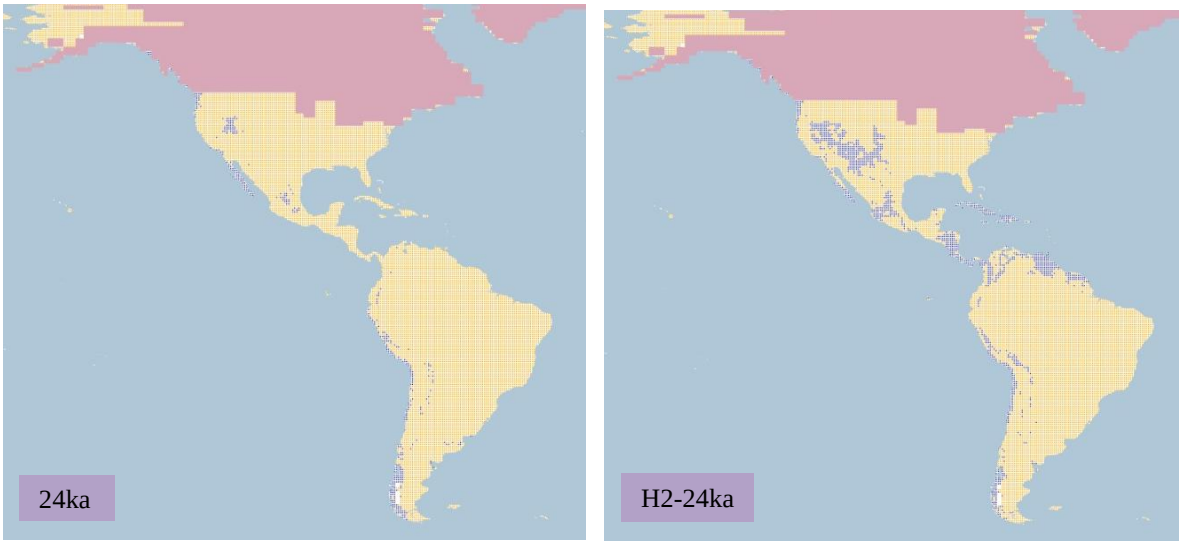

Figure 4.1.2.1.b. Simulation maps of Blackish Oystercatcher non-breeding range. Maps are shown for ten-time slices: 24ka, H2 (24ka), 17ka, H1 (17ka), 13ka, H0 (13ka), 9ka, 5ka, 3ka and present (1961–90).

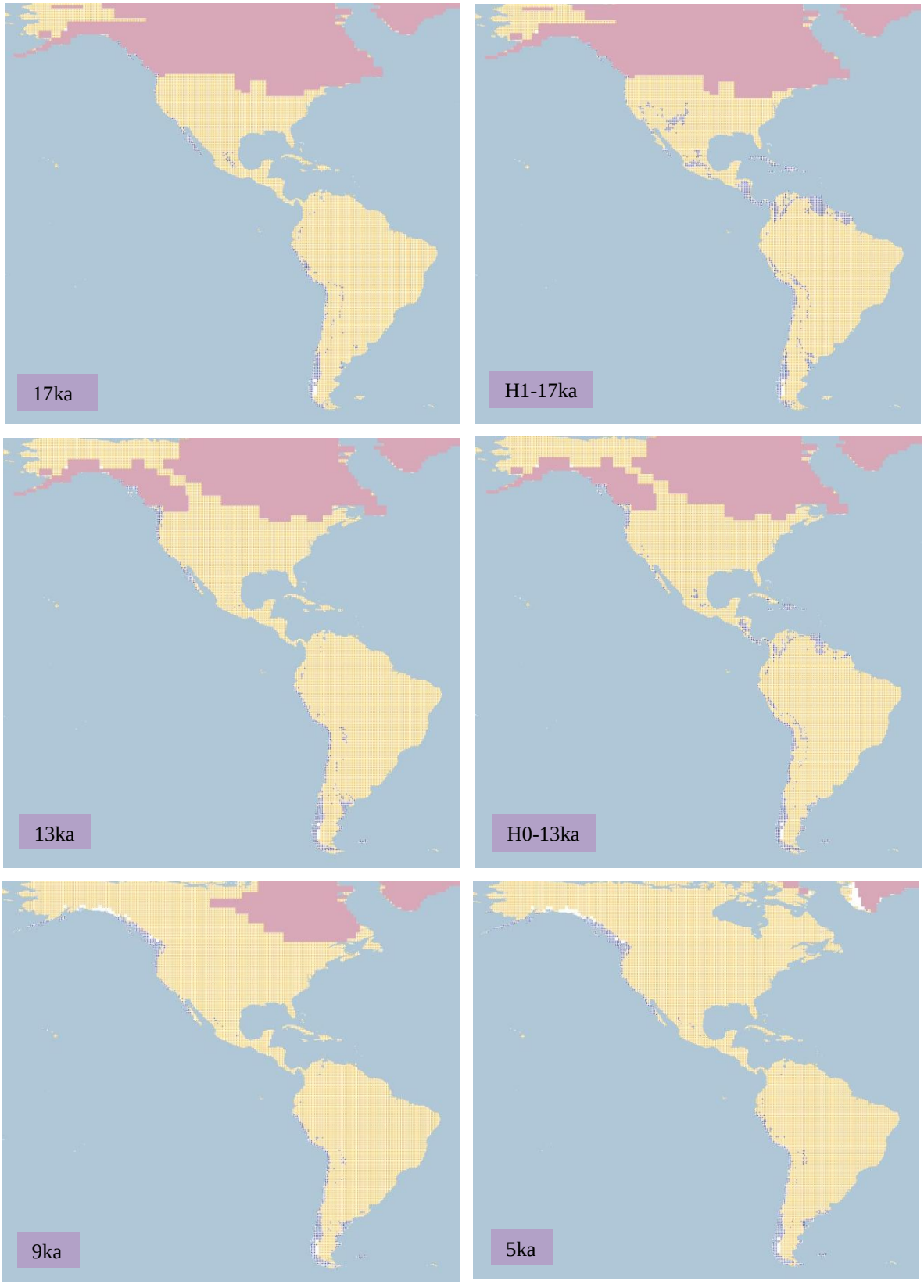

Figure 4.1.2.1.b. Simulation maps of Blackish Oystercatcher non-breeding range (continued**).**

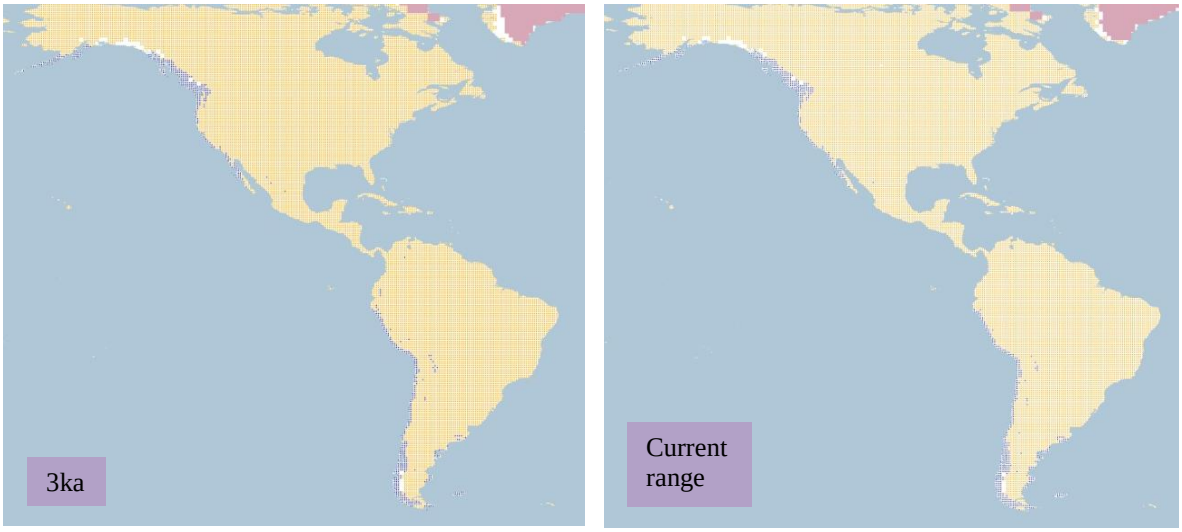

Figure 4.1.2.1.b. Simulation maps of Blackish Oystercatcher non-breeding range (continued**).**

*4.1.2.2 Magellanic Oystercatcher (*Haematopus leucopodus*). Conservation status: Least Concern. Current known range Figure 4.1.2.2.*

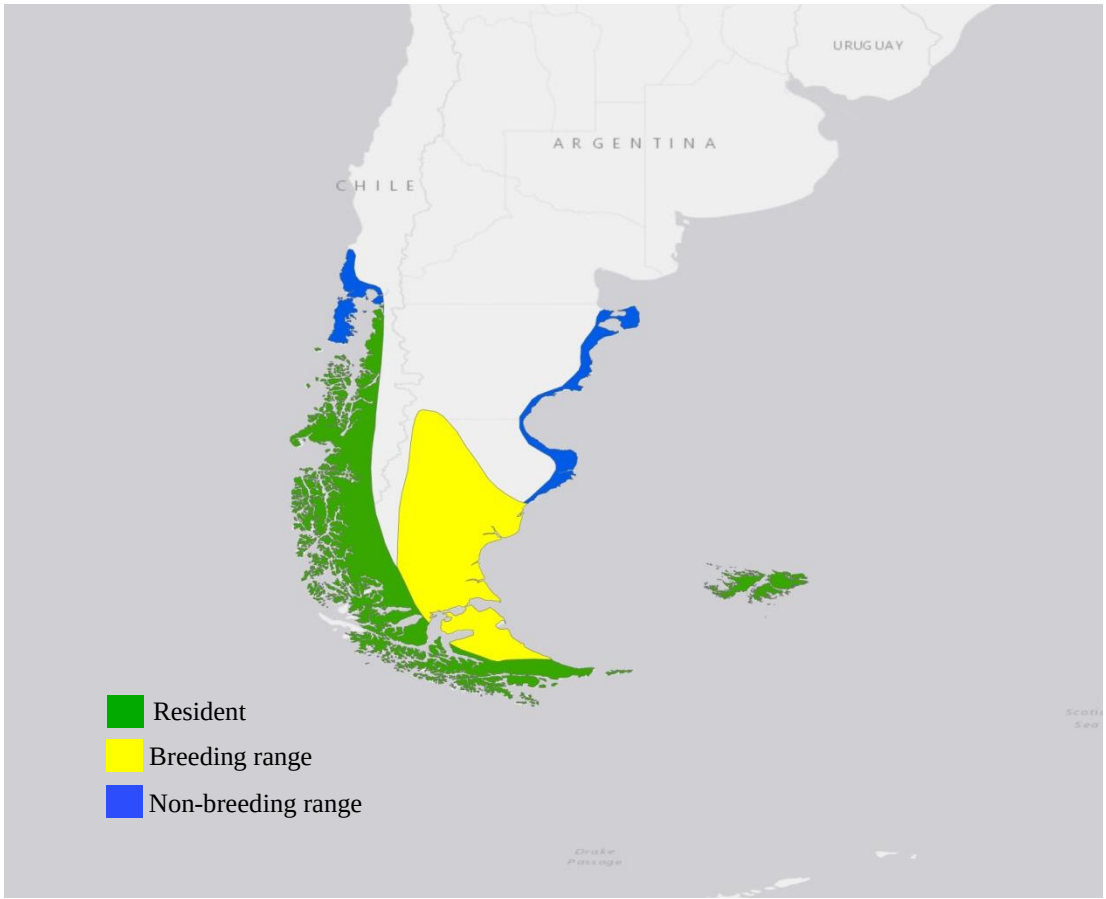

Figure 4.1.2.2. Current known range of Magellanic Oystercatcher.

Breeding range (AUC: 0.994; TSS: 0.960; Kappa: 0.858): This species currently breeds in the south of South America where it has a year-round range in the south of Chile and the Falkland Islands, and a breeding range in Tierra del Fuego and south-central Argentina. 'Temperate' variables were used to model this range.

At 26 ka BP the projected distribution is in central Argentina, southern Chile and Tierra del Fuego. Initially projected to be absent from the Falkland Islands, the species' range extends there at 20 ka BP, thereafter persisting until the present. Beginning at 16 ka BP an increasing area of occurrence is projected in the central-south part of Chile and Argentina, extending also to the Andean Cordillera. This persists until 11-10ka when the central range in Chile and Argentina gradually starts shifting to the south. From that period until the present the range remains stable without any radical changes. See Figure 4.1.2.2.a.

When comparing 24 ka BP with H2 the range remains in central Argentina and extends inland around the Andean cordillera. The 17 ka BP projection appears analogous to the H1 projection, as well as the 13 ka BP to the H0 projection.

It is important to note that a wide range is initially projected across the north and centre of USA, which fragments as the ice sheet retreats, shifting to the border with Canada. Even though there are no recognized occurrences in these regions, the model projections indicate favourable climatic conditions for the species (not shown on maps).

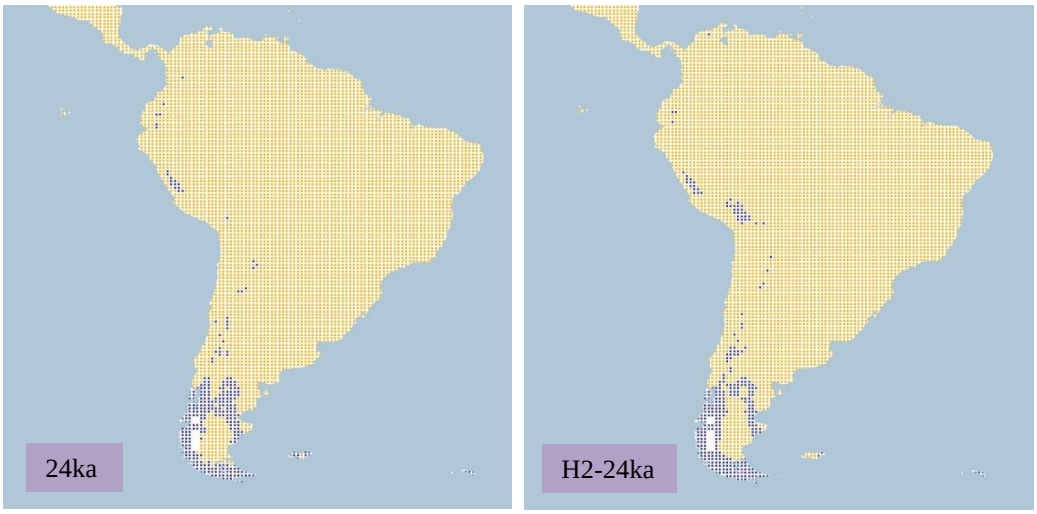

Figure 4.1.2.2.a. Simulation maps of Magellanic Oystercatcher breeding range. Maps are shown for ten-time slices: 24ka, H2 (24ka), 17ka, H1 (17ka), 13ka, H0 (13ka), 9ka, 5ka, 3ka and present (1961–90).

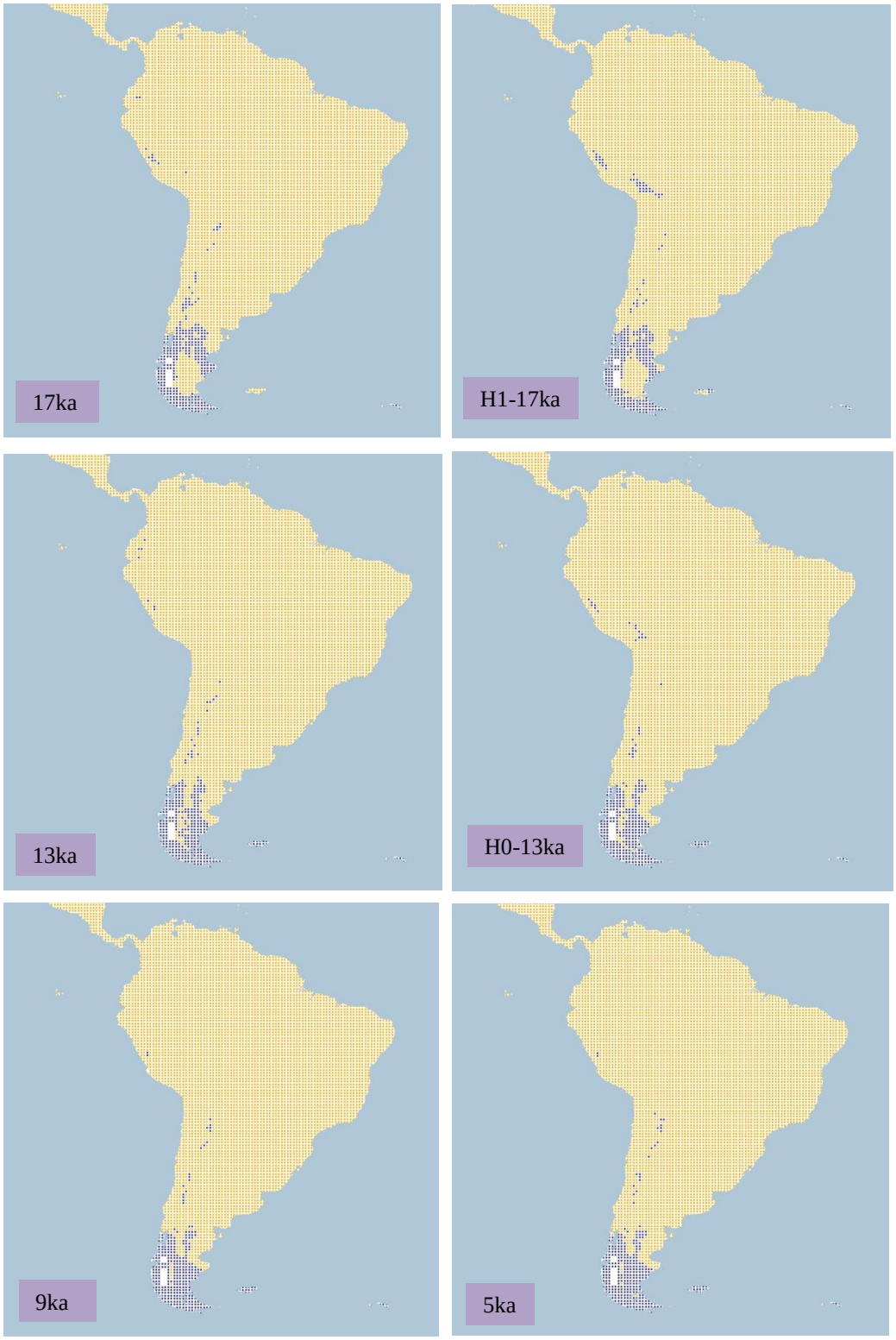

Figure 4.1.2.2.a. Simulation maps of Magellanic Oystercatcher breeding range (continued**).**

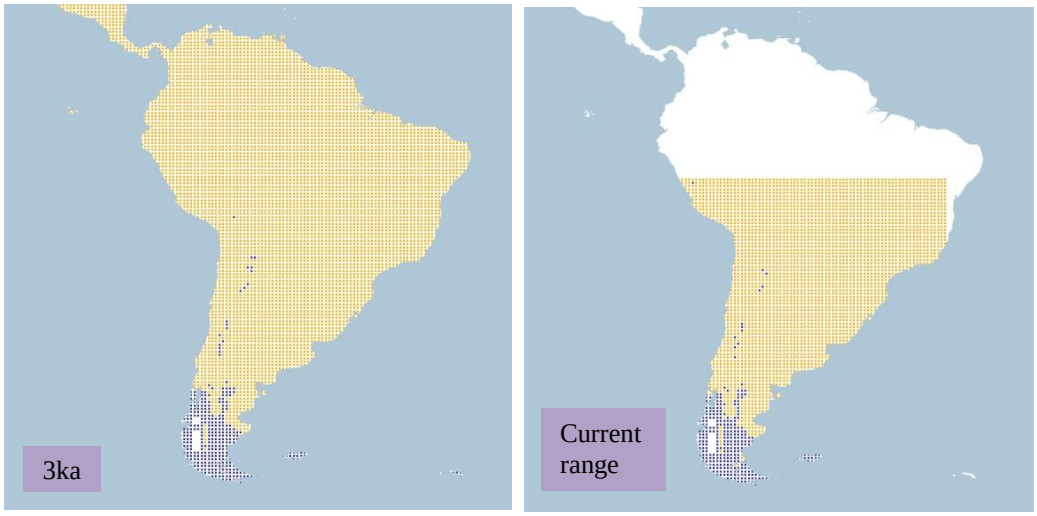

Figure 4.1.2.2.a. Simulation maps of Magellanic Oystercatcher breeding range (continued**).**

Non-breeding range (AUC: 0.995; TSS: 0.946; Kappa: 0.858): The species' wintering grounds are located on the east coast of Argentina and the central-south coast of Chile, both with a small extent and restricted to coastal areas. For this range the model also used 'temperate' variables.

The projection for 26 ka BP shows a southern range in Chile, extending to Tierra del Fuego. Small areas are also projected in the Andean cordillera of Ecuador, Peru and the western boundaries of Argentina. This pattern continues until 16 ka BP when the projected range extends to the Falkland Islands and a small area on the east coast of Argentina that from 15 ka BP to 12 ka BP expands to south-central inland Argentina. After this, at 11 ka BP the projected range decreases, becoming limited to the south-east coast of Argentina where it persists under the present climate. See Figure 4.1.2.2.b.

With reference to the non-breeding range there is a simulated area in North America with the same characteristics as with the breeding range. Although climatic conditions might have been suitable for this species in North America, no historical evidence has been found to indicate its occurrence there.

The projections for Heinrich events H2, H1 and H0 resemble the projections for 24 ka BP, 17 ka BP and 13 ka BP, except in the Andean cordillera where the range is more extensive for the Heinrich events.

Overall the projections of the non-breeding range of the Magellanic Oystercatcher from 26 ka BP to1 ka BP appear broadly similar to the current range. This may suggest that the climatic fluctuations of the late Quaternary didn't affect this species' range as much as those of many other species.

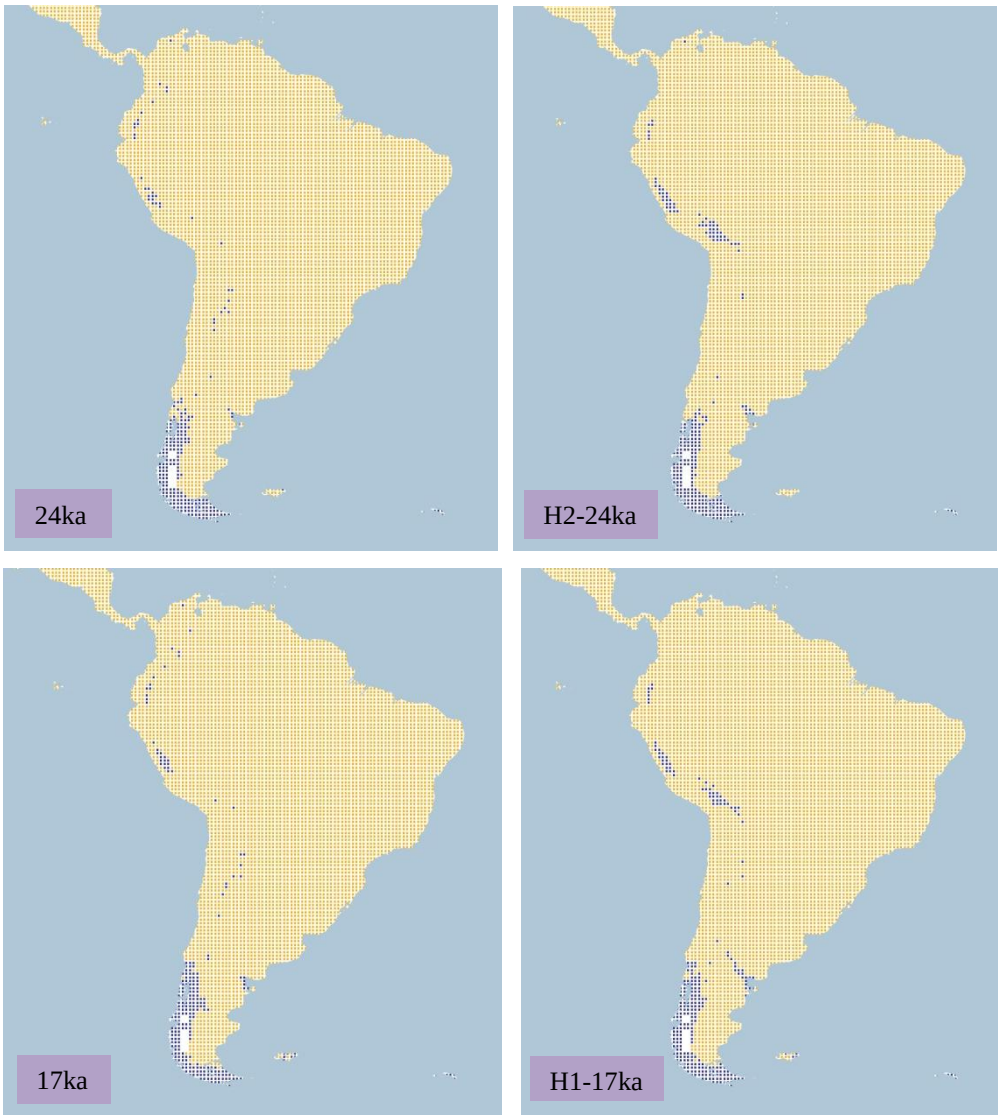

Figure 4.1.2.2.b. Simulation maps of Magellanic Oystercatcher non-breeding range. Maps are shown for ten-time slices: 24ka, H2 (24ka), 17ka, H1 (17ka), 13ka, H0 (13ka), 9ka, 5ka, 3ka and present (1961–90).

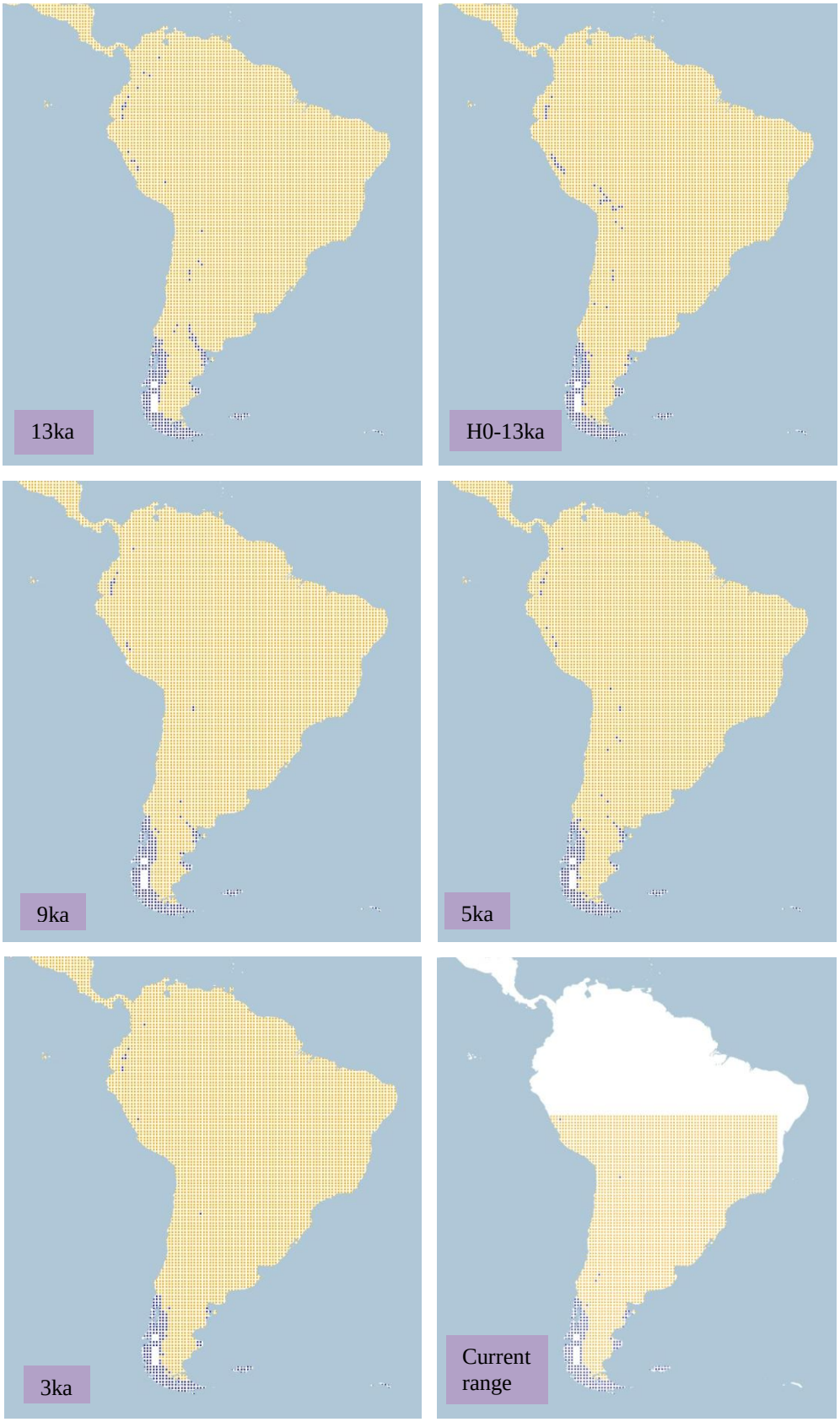

Figure 4.1.2.2.b. Simulation maps of Magellanic Oystercatcher non-breeding range (continued**).**

*4.1.2.3 American Oystercatcher (*Haematopus palliatus *including* H. p. palliatus *and* H. p. galapagensis*). Conservation status: Least Concern. Current known range Figure 4.1.2.3.*

Figure 4.1.2.3. Current known range of American Oystercatcher.

Breeding range (AUC: 0.939; TSS: 0.721; Kappa: 0.583): This species is a year-round resident of the coasts of the Americas, from the east coast to the west coast of USA, and with a smaller range on the east coast of Mexico, on the west coast of Costa Rica and Panama in Central America, and in South America from Colombia to Venezuela, from Brazil to the south of Argentina on the east coast and from Ecuador to the south of Chile on the west coast. It also breeds in the Galapagos Islands.

The range at 26 ka BP is projected along the Pacific coast of Mexico, from inland Baja California to the north of Oaxaca, and in South America from Ecuador to the south of Chile. Also in South America the range is projected inland in the south of Brazil and north of Argentina with a scattered range in the north of South America between Venezuela, French

Guiana and north of Brazil; this scattered range is also found in the Greater Antilles, in central Mexico and in Florida in USA. This pattern continues and intensifies at 22 ka BP in the south of Brazil, Uruguay and north of Argentina. See Figure 4.1.2.3.a.

At 15 ka BP the inland range of south Brazil decreases with an increase of range in central and southern Argentina, reaching the coast of Chubut and Santa Cruz provinces; the range also decreases in the north of Venezuela, as well as in central Mexico. This pattern continues until 10 ka BP with changes of the range in Argentina and Brazil where it is projected to extend to the east coast. After this at 9 ka BP the range continues with the same pattern and in North America there is range projected along the coast of Louisiana in USA.

At 6 ka BP the range along the Pacific coast of Mexico increases inland from Baja California to Chiapas and likewise on the coast of Louisiana and Florida in USA. This increases at 5 ka BP in USA, extending from the coast of Texas to Florida. The pattern continues until 2 ka BP with an increase of the range projected on the south-east coast of USA reaching the north-east of Mexico in Tamaulipas and continuing at 1 ka BP.

The current breeding range projection presents the same pattern as the1 ka BP projection, covering the Pacific coasts of Mexico, Ecuador, Peru and Chile, the south-east coast of USA and north-east of Mexico, a small range on the north coast of Venezuela and Brazil, and the southern coast of Brazil, Uruguay and Argentina.

The Heinrich event H2 when compared with 24 ka BP presents different projections, mainly with an inland range along central and southern Mexico, the Greater Antilles, and from Central America to the north of South America, from Venezuela to the north-west of Brazil. The only similarities are found in the range projected along the Pacific coast of Baja California in Mexico, Ecuador, Peru and Chile. The range in northern and central Mexico decreases at H1 with the remaining range unchanged and differing from the 17 ka BP projection. The same pattern as H1 continues at H0 in Central America and in the north of South America, which is not projected at 13 ka BP.

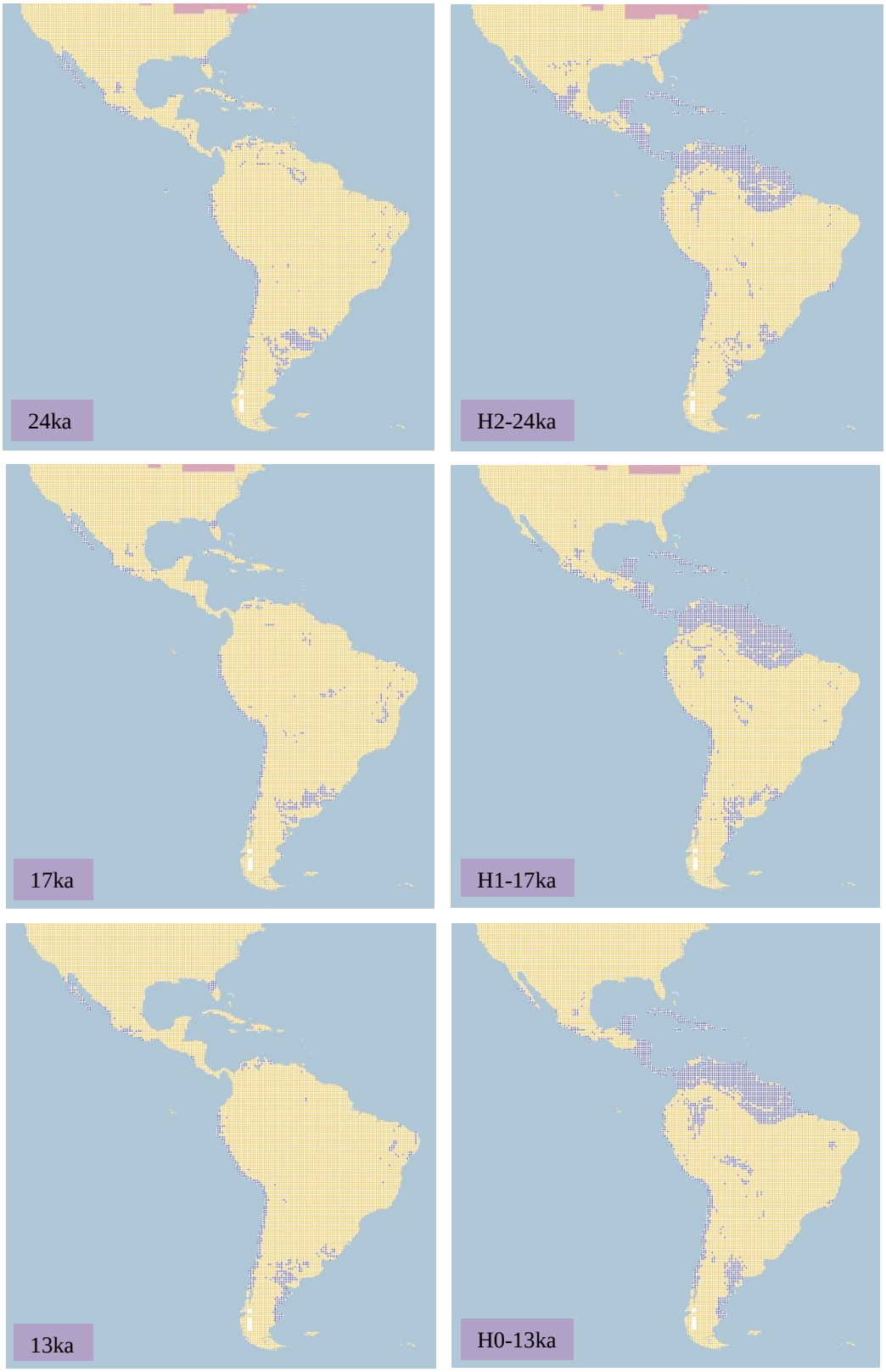

Figure 4.1.2.3.a. Simulation maps of American Oystercatcher breeding range.
Maps are shown for ten-time slices: 24ka, H2 (24ka), 17ka, H1 (17ka), 13ka, H0 (13ka), 9ka, 5ka, 3ka and present (1961–90).

Figure 4.1.2.3.a. Simulation maps of American Oystercatcher breeding range (continued**).**

Non-breeding range (AUC: 0.938; TSS: 0.731; Kappa: 0.576): This species is a year-round resident of the coasts of the Americas from the east coast of USA, to the south of Chile and Argentina in South America. It also has a non-breeding range including Florida, the Greater Antilles, the south-east coast of Mexico from Veracruz to Yucatan, the coast of Belize and on the south-west coast from Chiapas in Mexico to El Salvador in Central America.

At 26 ka BP the range is projected along the Pacific coast of Mexico from Baja California to Oaxaca, the south of Nicaragua, north of Costa Rica, and in South America from Ecuador to the south of Chile. There is also a small range projected in central Mexico, the Greater Antilles and in the north of Florida in USA. The range in the north of South America is fragmented from Venezuela to the north-east of Brazil, with a larger range projected from the

south of Brazil to central Argentina and in the west of Bolivia. The pattern continues with the range disappearing in Bolivia at 22 ka BP.

Until 14 ka BP the range projected between the south of Brazil and Argentina changes to central and southern Argentina, disappearing from the south of Brazil and Uruguay. After this at 13 ka BP, the range in the north-east of Brazil increases reaching as far as Guyana, and the range in the Greater Antilles increases as well. The pattern continues until 10 ka BP with the decrease of the range in the north of Brazil with a fragmented range projected across central Brazil.

It is until 8 ka BP that the range in the north of Brazil decreases, allowing the increase of the range in central Brazil. During this period the range on the south-east coast of USA increases from Louisiana to Florida, reaching the coast of Texas and the north of Mexico at 6 ka BP. Between 4 ka BP and 3 ka BP the range on the south-east coast of USA increases, as well as on the east coast of Mexico from Tamaulipas to the Yucatan Peninsula and on the coast of Belize and Honduras. This pattern continues at 2 ka BP and 1 ka BP, the range increasing only along the south-east coast of USA and the south of Mexico in Tabasco as far as Guatemala. This also agrees with the projection of the current non-breeding range.

Comparison between H2 and 24 ka BP can only be made on the projected range along the Pacific coast of Mexico, Central America and South America, and from the south of Brazil to central Argentina; at H2 the range inland is greater than at 24 ka BP from the centre to the north, and in the south of Mexico, in Central America and continuing in the north of South America and at a smaller scale between central Colombia and central areas of Brazil. Also, the range in the Greater Antilles is greater at H2. This pattern continues at H1 differing from the 17 ka BP projection and only with a smaller range than H2 from central to north of Mexico including the Pacific coast. Once more, the pattern is present at H0, mainly from Central America to South America, with similarities as 13 ka BP only along the Pacific coast of Mexico, Ecuador, Peru and Chile, and in Argentina.

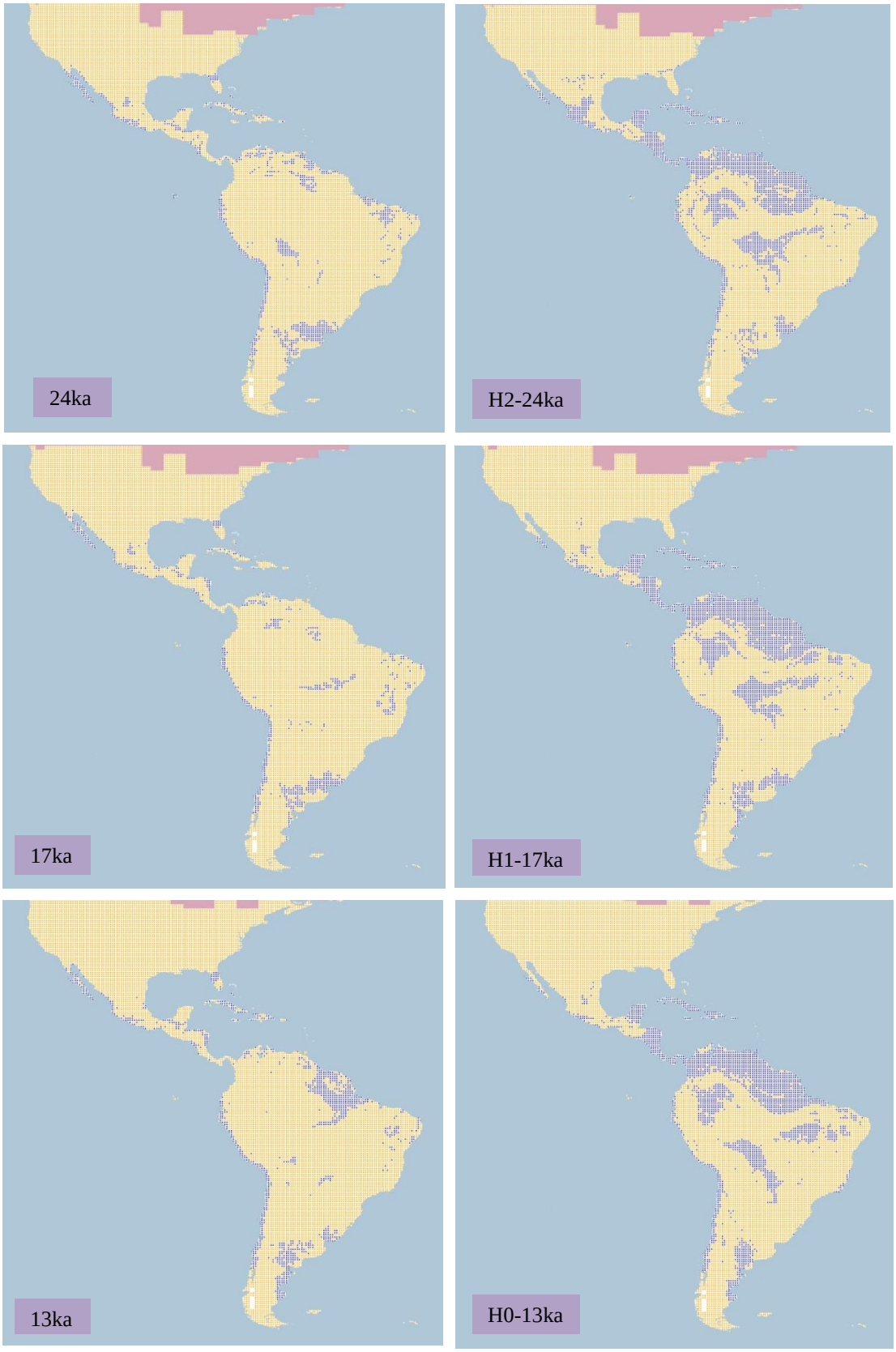

Figure 4.1.2.3.b. Simulation maps of American Oystercatcher non-breeding range. Maps are shown for ten-time slices: 24ka, H2 (24ka), 17ka, H1 (17ka), 13ka, H0 (13ka), 9ka, 5ka, 3ka and present (1961–90).

Figure 4.1.2.3.b. Simulation maps of American Oystercatcher non-breeding range (continued**).**

4.1.2.4 AUC, TSS and Kappa values.

The resulted AUC, TSS and Kappa values for each species of the family Haematopodidae are shown in here. These are divided in breeding and non-breeding ranges. Overall the AUC values for the projection were the highest in comparison with TSS and Kappa, with a median of 0.976.

The breeding range models for members of the Haematopodidae gave an AUC median of 0.994 with overall higher values than 0.950 and in comparison, with TSS and Kappa. The highest AUC value was from Blackish Oystercatcher (*H. ater*) with 0.995, followed by Magellanic Oystercatcher (*H. leucopodus*) with 0.994 and American Oystercatcher (*H. palliatus*) at last with 0.939. The latter species has a year-round resident range along the coastal areas of the Americas.

The TSS performance values for the breeding range have a median of 0.949, with the highest value for Magellanic Oystercatcher (*H. leucopodus*) with 0.960, next to Blackish Oystercatcher (*H. ater*) with 0.949 and American Oystercatcher (*H. palliatus*) at last with 0.721.

The Kappa values have a median of 0.836, the lowest of the three different measurements with the highest value for species Blackish Oystercatcher (*H. ater*) with 0.836, followed by Magellanic Oystercatcher (*H. leucopodus*) with 0.858 and the lowest value with 0.583 from American Oystercatcher (*H. palliatus*). This brings support to the argument that models for species with ranges restricted to coastal areas are generally of lower accuracy. See Figure 4.1.2.a.

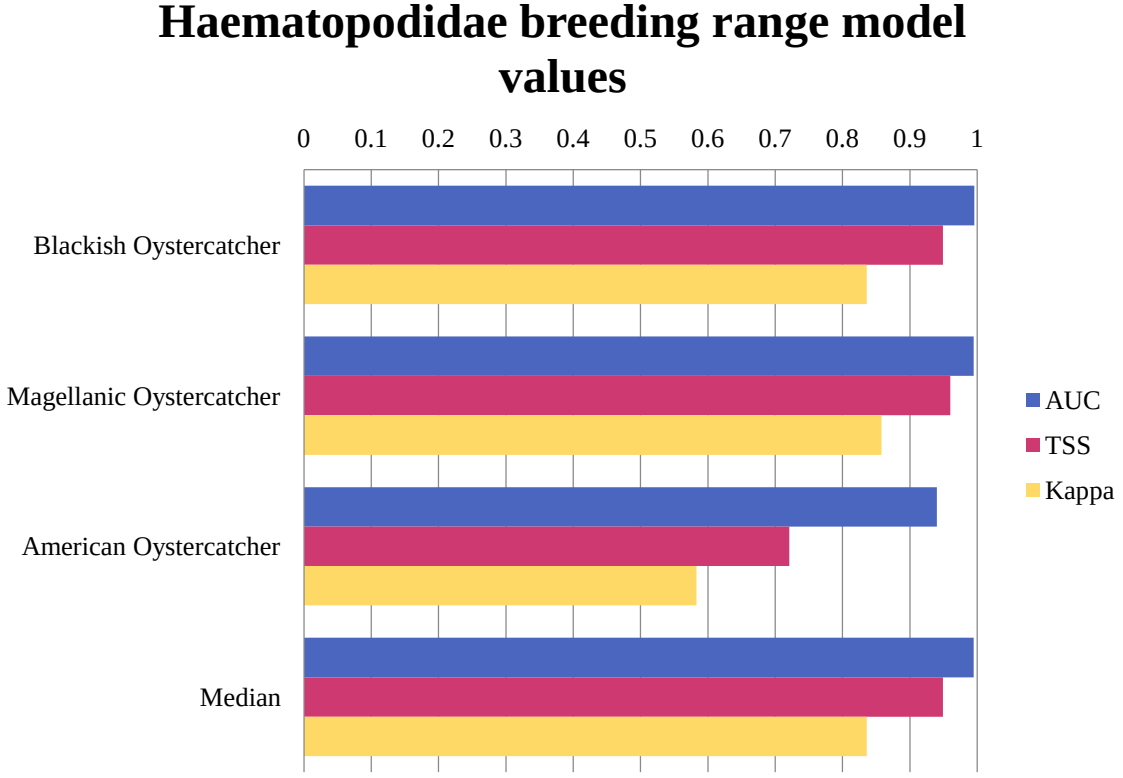

Figure 4.1.2.a. Model performance values of the family Haematopodidae breeding range.
The graph shows values for each species of AUC, TSS and Kappa values from the CRS model as well as the median for each statistical measurement.

For the non-breeding range the resulted values for the projections show a similar pattern to the breeding range values, especially the median values, only differing at Kappa. AUC displays the highest values and Kappa with the lowest.

For AUC the highest value is shown by species Magellanic Oystercatcher (*H. leucopodus*) with 0.995, followed by Blackish Oystercatcher (*H. ater*) with 0.993 and the lowest value of 0.938 for American Oystercatcher (*H. palliatus*).

The TSS values for the non-breeding modelling show species Magellanic Oystercatcher (*H. leucopodus*) with the highest value of 0.946, next to Blackish Oystercatcher (*H. ater*) with 0.934 and at last with 0.731 species American Oystercatcher (*H. palliatus*).

For Kappa the highest value for the non-breeding modelling is shown by species Magellanic Oystercatcher (*H. leucopodus*) as well with 0.858, followed by Blackish Oystercatcher (*H. ater*) with 0.796 and American Oystercatcher (*H. palliatus*) with 0.576. See Figure 4.1.2.b.

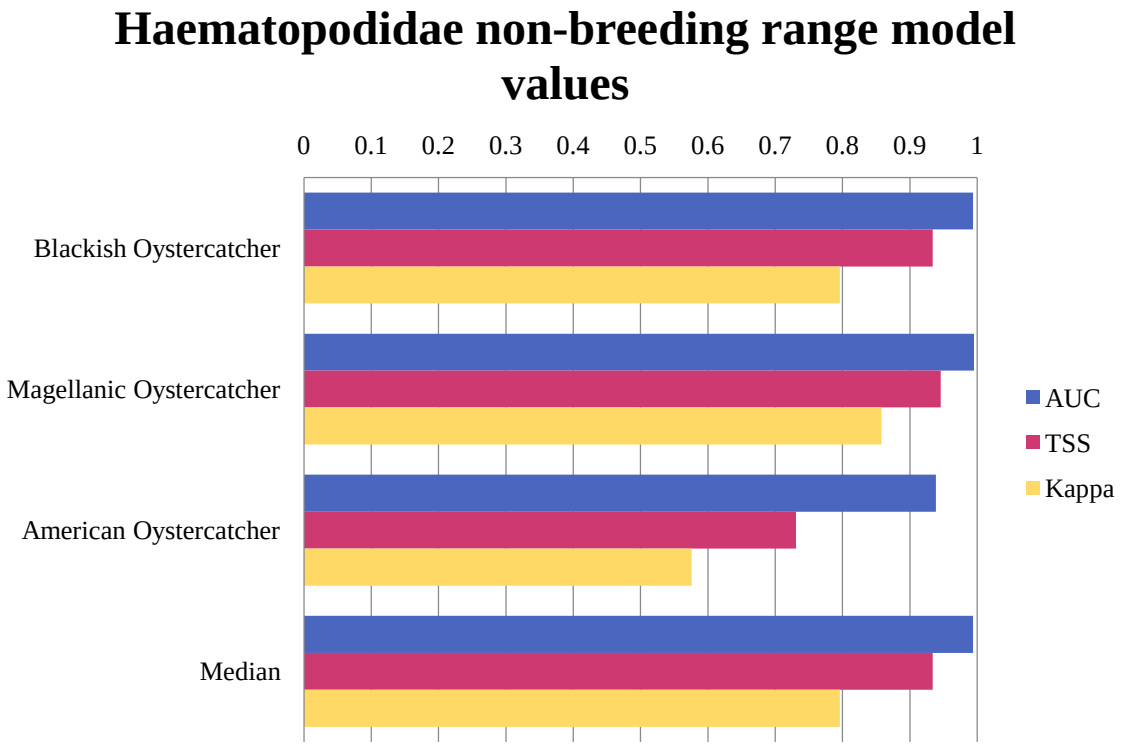

Figure 4.1.2.b. Model performance values of the family Haematopodidae non-breeding range.
The graph shows values for each species of AUC, TSS and Kappa values from the CRS model as well as the median for each statistical measurement.

4.1.3 Family Recurvirostridae

*4.1.3.1 Black-winged Stilt (*Himantopus himantopus *including* H. h. melanurus *and* H. h. mexicanus*). Conservation status: Least Concern. Current known range Figure 4.1.3.1.*

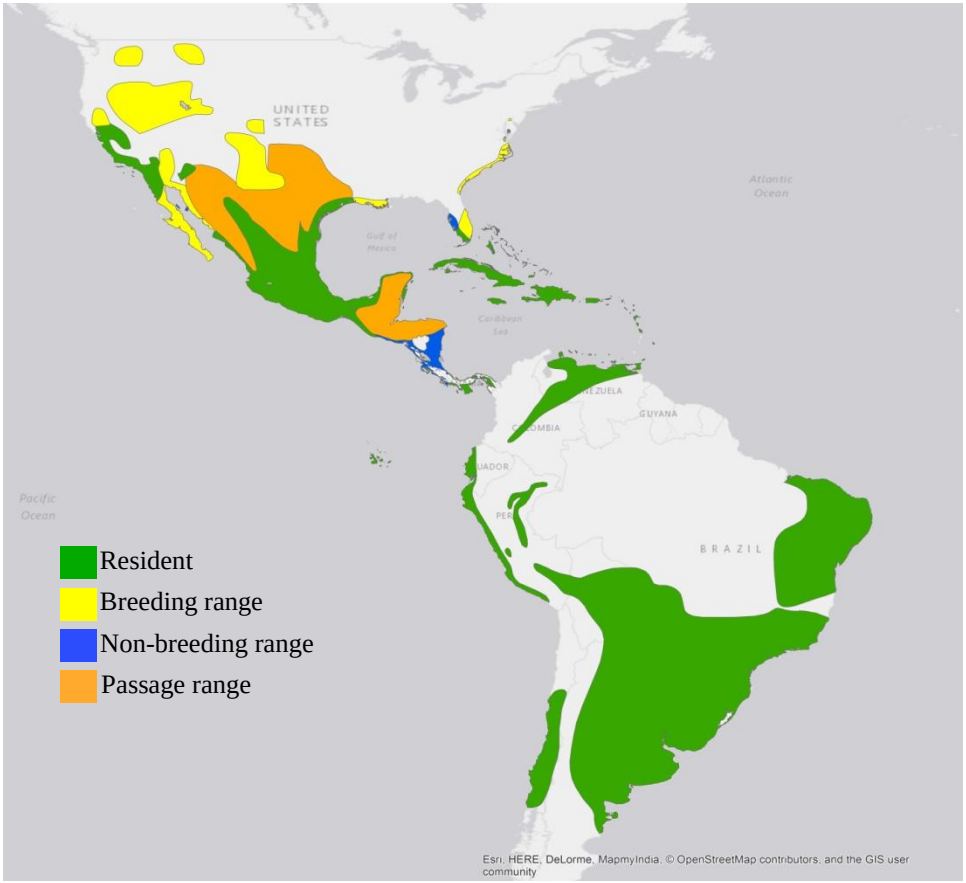

Figure 4.1.3.1. Current known range of Black-winged Stilt.

Breeding range (AUC: 0.981; TSS: 0.857; Kappa: 0.826): Breeding range in the west, south and east coast of USA. It also is a year-round resident of California, Mexico, and the Greater Antilles. In South America it breeds from Venezuela, north-eastern and southern Brazil, Bolivia, Paraguay and Uruguay, to the north and centre of Argentina, as well as in Ecuador, Peru and from the centre to the south of Chile.

At 26 ka BP the range is projected from central to western USA and south of Florida, also along Mexico, Central America, the Greater Antilles, and in almost all the territory from South America except the Amazonas, north-central Brazil, Uruguay, central to southern Argentina and in the Andean cordillera from southern Peru and along Chile. The pattern

continues only with a decrease in the projected range from Venezuela to the north of Brazil and an increase in the south of Argentina at 22 ka BP. See Figure 4.1.3.1.a.

Between 17 ka BP and 16 ka BP the range in the west of USA increases to the north near the ice sheet. This is followed by a decrease of the range projected in the north-west of USA and south-west of Canada at 14 ka BP, and by a rise in the northern part of Brazil. The same pattern continues to the beginning of the Holocene, increasing especially at 10 ka BP in the north and east of Brazil and at 8 ka BP in the central part of Brazil.

By 6 ka BP the range from Panama to the north-east of Brazil is reduced, which contrasts the increase in south-central USA. This continues until 4 ka BP when the range in the north of South America disappears, extending mainly from Bolivia to central Argentina and the east of Brazil, and in North America from the north-west of USA as far as Honduras. After this, the projected range remains with minimal differences until1 ka BP and agreeing with the current breeding projection.

The Heinrich event H2 projects a larger range than 24 ka BP, covering nearly the entire territory of South America, and with a restricted range in California, south of Texas, and Florida in USA. A similar projection is shown at H1, only with a smaller range in the west of South America and an increasing range in the north-west of USA, differing from 17 ka BP as well. The range between H0 and 13 ka BP in North America presents similarities, except in the south-central and south-east areas of USA; these similarities continue in Central America and in South America, particularly in the central and eastern regions, varying only in the northern areas.

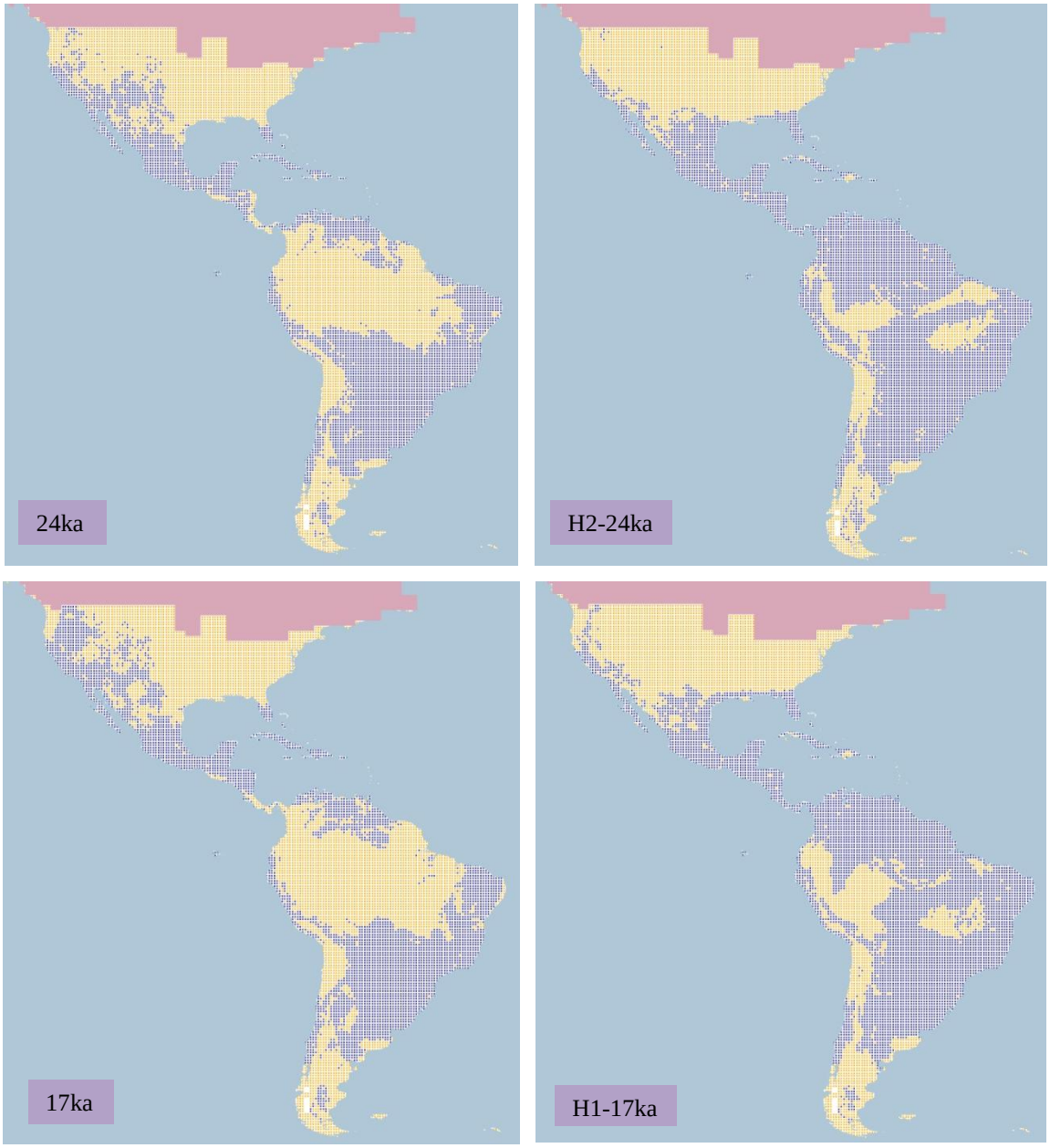

Figure 4.1.3.1.a. Simulation maps of Black-winged Stilt breeding range.
Maps are shown for ten-time slices: 24ka, H2 (24ka), 17ka, H1 (17ka), 13ka, H0 (13ka), 9ka, 5ka, 3ka and present (1961–90).

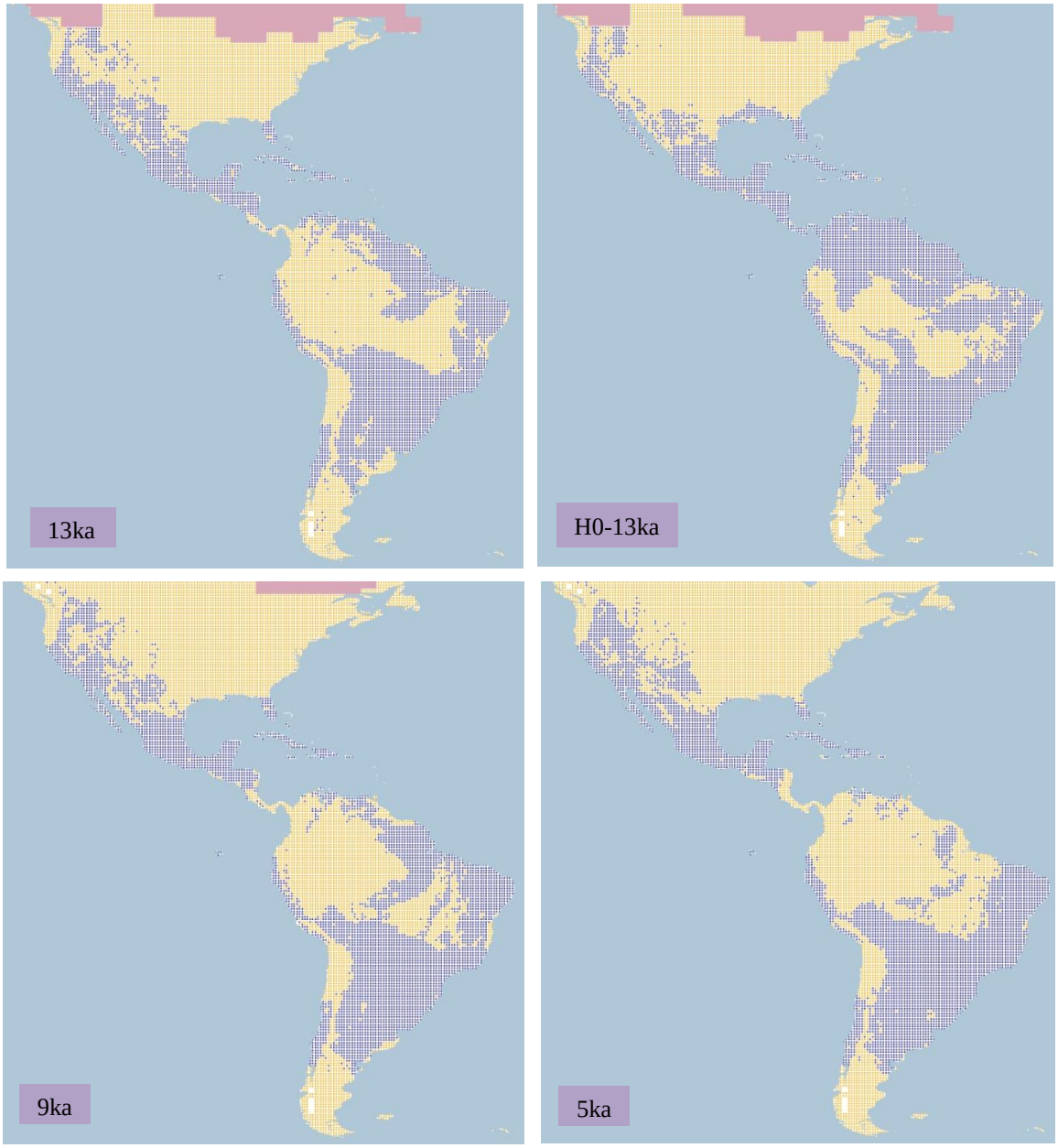

Figure 4.1.3.1.a. Simulation maps of Black-winged Stilt breeding range (continued**).**

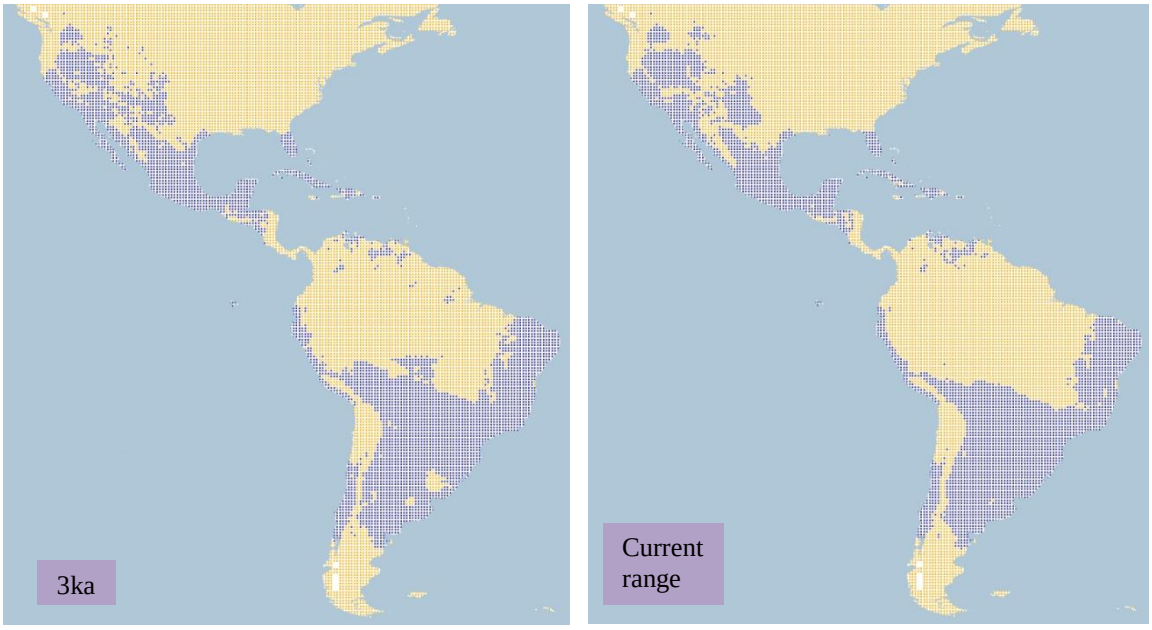

Figure 4.1.3.1.a. Simulation maps of Black-winged Stilt breeding range (continued**).**

Non-breeding range (AUC: 0.985; TSS: 0.874; Kappa: 0.839): Spends the non-breeding season in Central America mainly in Nicaragua with a smaller range in Costa Rica and the north of Panama. The species is also a year-round resident from the west of USA in California and the south-west of Arizona, in Mexico from the north-west in Baja California, in the Sierra Madre Occidental from Chihuahua to the south of Mexico, in the Greater Antilles, the north of Venezuela, along the coast of Ecuador, Peru and Chile and from Bolivia to Paraguay, Uruguay, central to the north of Argentina and in Brazil from the north-east to the south.

The 26 ka BP projection is of a range from the west of USA and south of Florida, through Mexico, Central America, the Greater Antilles, and nearly the entirety of South America, except the Amazon River, from the south of Peru to the north of Chile and from central to southern Argentina and south of Chile. There is a decrease in the range of the northern region of South America at 22 ka BP, with the remainder of the range being almost unaltered. See Figure 4.1.3.1.b.

By 19 ka BP the range increases in central-north Brazil and decreases in the north of Mexico; this is more evident from 16 ka BP onwards with a particular increase in the range in central Brazil at 13 ka BP. This pattern continues to the beginning of the Holocene with minimal variation in the west of USA and the north of South America.

From 4 ka BP onwards, the range from Nicaragua to the north of South America disappears, projecting the range from California and south of Florida in USA, to Mexico, Guatemala, Belize, El Salvador, Honduras, the Greater Antilles, and in central and east of South America with a smaller range along the coast of Ecuador, Peru and Chile. Likewise, this pattern corresponds with the current non-breeding projection.

There are similarities between the projections in H2 and 24 ka BP, mainly in USA, Mexico, Central America, and the Greater Antilles and in South America along the coasts of Ecuador, Peru and Chile and from central to east and south regions. However, H2 projects a range in the north of South America as well, hence differing from the 24 ka BP projection. This pattern is also found at H1 with a smaller range in the north-west of Mexico and the west of South America. Similar ranges in North America and Central America are observed between H0 and 13 ka BP, the remainder of the range in South America is also similar, with differences only in the north-west and central region.

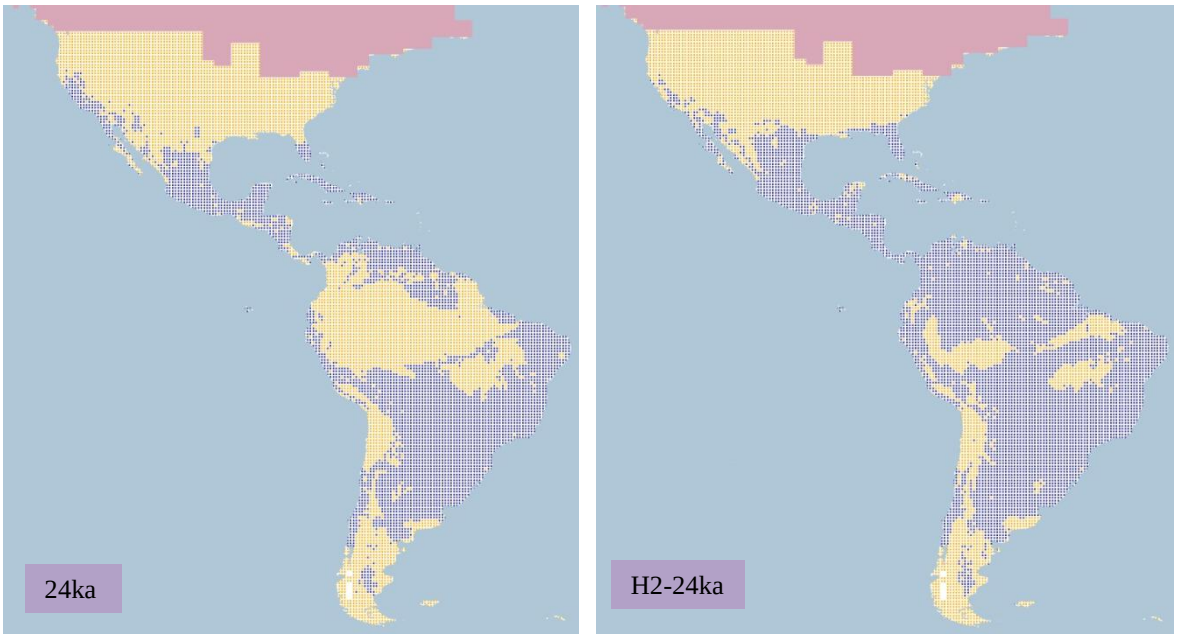

Figure 4.1.3.1.b. Simulation maps of Black-winged Stilt non-breeding range.
Maps are shown for ten-time slices: 24ka, H2 (24ka), 17ka, H1 (17ka), 13ka, H0 (13ka), 9ka, 5ka, 3ka and present (1961–90).

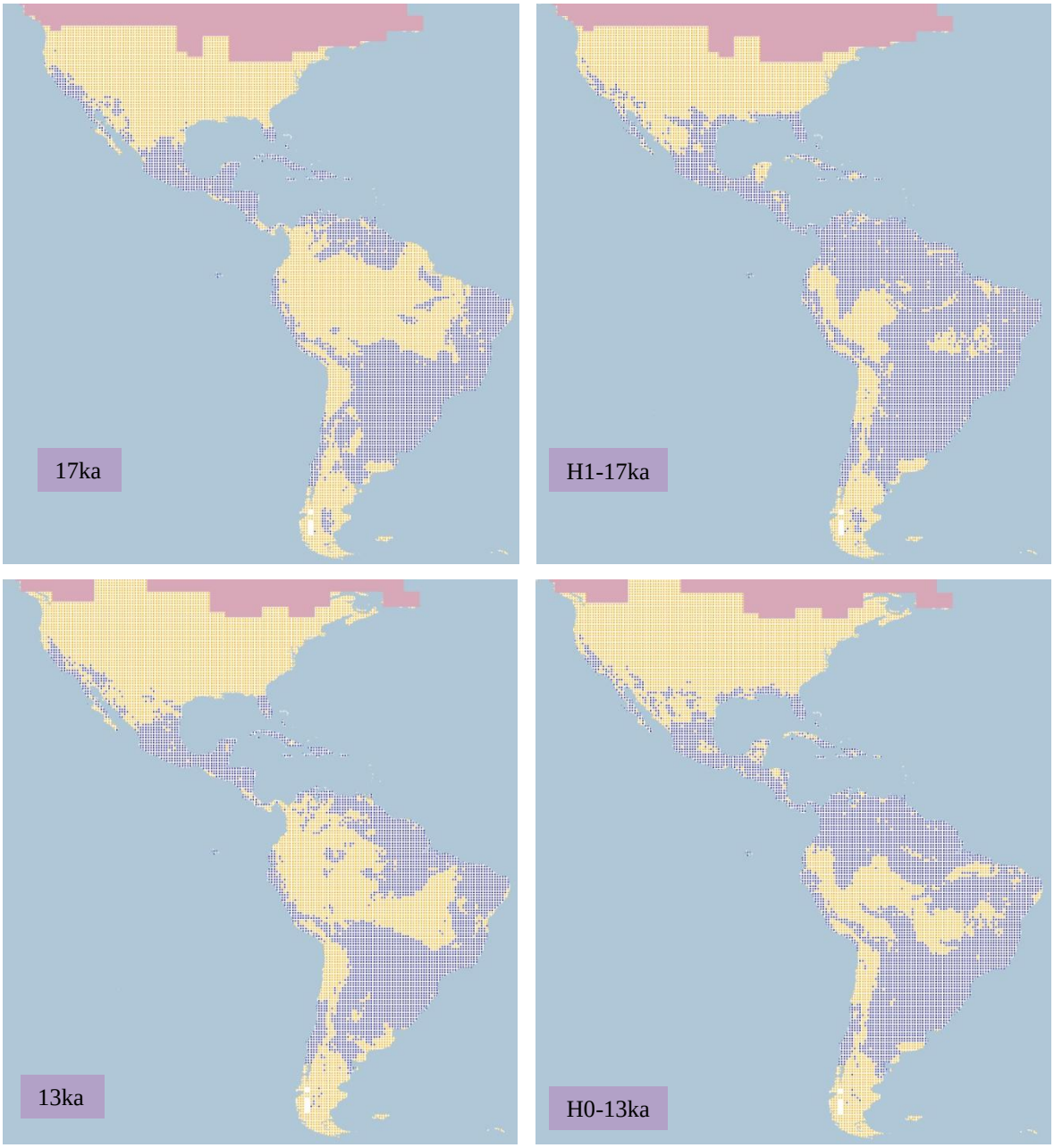

Figure 4.1.3.1.b. Simulation maps of Black-winged Stilt non-breeding range (continued**).**

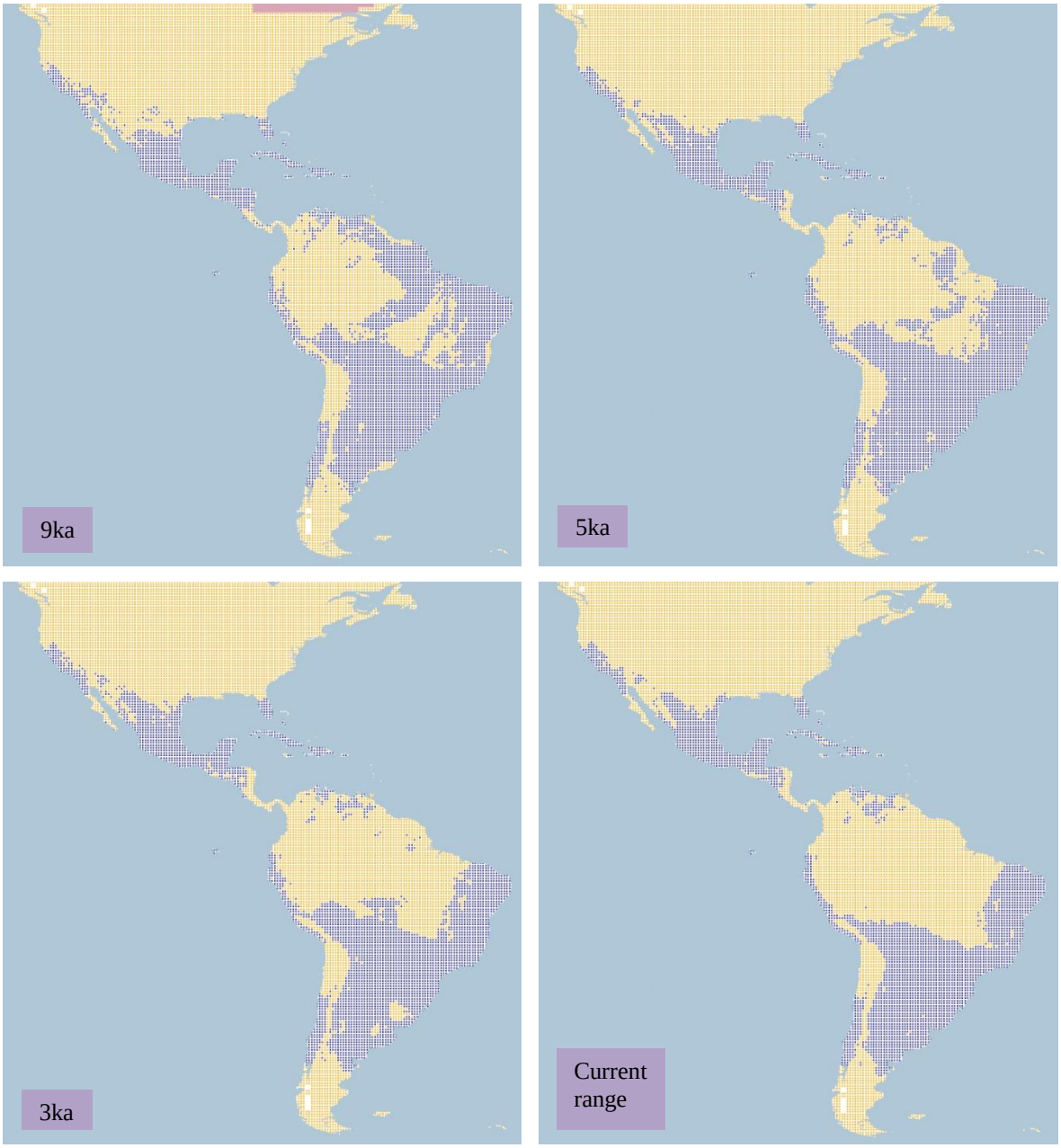

Figure 4.1.3.1.b. Simulation maps of Black-winged Stilt non-breeding range (continued**).**

*4.1.3.2 American Avocet (*Recurvirostra americana*). Conservation status: Least Concern. Current known range Figure 4.1.3.2.*

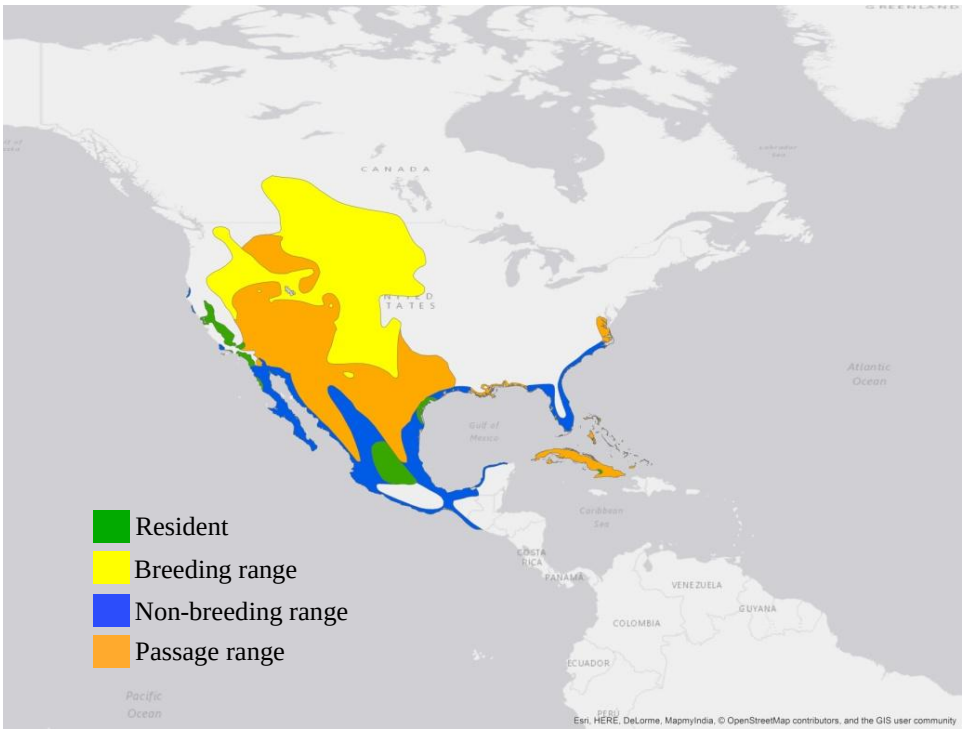

Figure 4.1.3.2. Current known range of American Avocet.

Breeding range (AUC: 0.987; TSS: 0.887; Kappa: 0.847): Spends the breeding season from south-central Canada to south-central USA with a smaller range to the north-west between Washington and the north of Nevada. The species also has a year-round resident range in California USA and in the north of Baja California, from Guanajuato to Toluca and on the north-east coast of Tamaulipas in Mexico.

At 26 ka BP a scattered range is projected in central and west USA, with a range on the coast of California, extending to Baja California in Mexico, and a scattered range as well in central areas of Mexico. The range in central USA continues growing until at 17 ka BP when the range extends from central to west of USA. After this and as the ice sheet reduces the range extends to the south of Canada, especially at 13 ka BP with the split of the ice sheet in Alberta, Canada, increasing as well on the Sierra Madre Occidental in Mexico. See Figure 4.1.3.2.a.

In the beginning of the Holocene the range is projected mainly from west to central USA and in the south and south-central of Canada, near the ice sheet. A smaller range is projected in

central Mexico and along the Sierra Madre Occidental and the coast of Baja California. Particularly at 9 ka BP there is a range projected in the south-east of Canada in Manitoba and Ontario near Hudson Bay, and the range in the Sierra Madre Occidental and central Mexico increases. After this at 8 ka BP, the range in the south-east of Canada disappears and the range in Mexico reduces.

From 7 ka BP onwards, the main projected range remains from west to central USA, with a small range projected in central Mexico. The range in the west of USA begins decreasing at 6 ka BP , and increases in the south-central part of Canada, which lasts until1 ka BP and agreeing with the current breeding range projection.

Similarities between H2 and 24 ka BP are only found in central Mexico and along the coast of Baja California, with no projected range in USA at H2, contrary to 24ka. However, a range is projected in the north-west of Canada at H2 and 24ka. This similar range continues at H1 and 17 ka BP in the north-west of Canada, and in central Mexico, with only a small range projected in the north-west of USA at H1. At H0 a range is projected in north-central and west of USA, and in Alberta, Canada, agreeing with the 13 ka BP projection for that area, although a larger range is projected in central USA at 13 ka BP, which extends to the Sierra Madre Occidental in Mexico.

Although the current breeding range of the species is located in North America, there are suitable conditions projected along the Andean cordillera and from central to southern Argentina in South America.

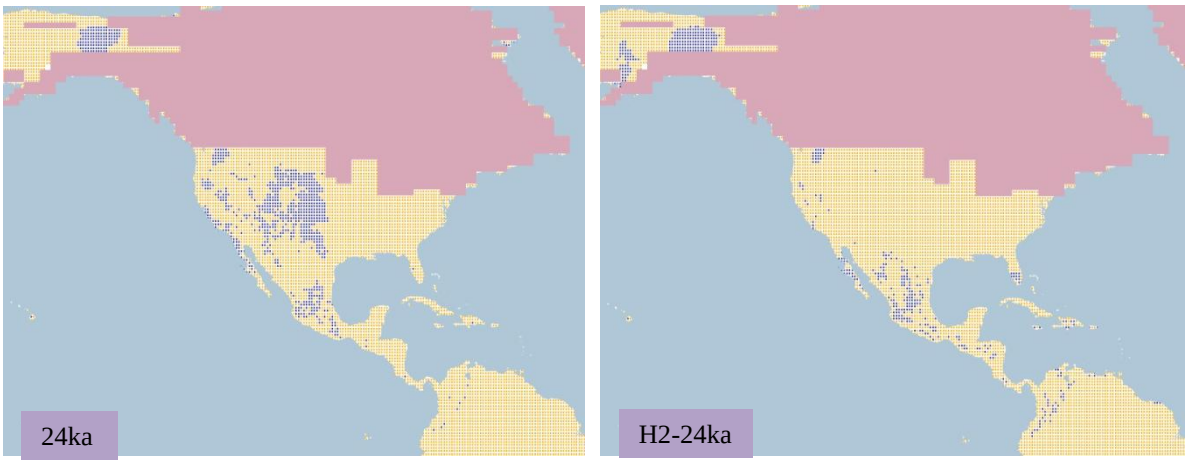

Figure 4.1.3.2.a. Simulation maps of American Avocet breeding range.
Maps are shown for ten-time slices: 24ka, H2 (24ka), 17ka, H1 (17ka), 13ka, H0 (13ka), 9ka, 5ka, 3ka and present (1961–90).

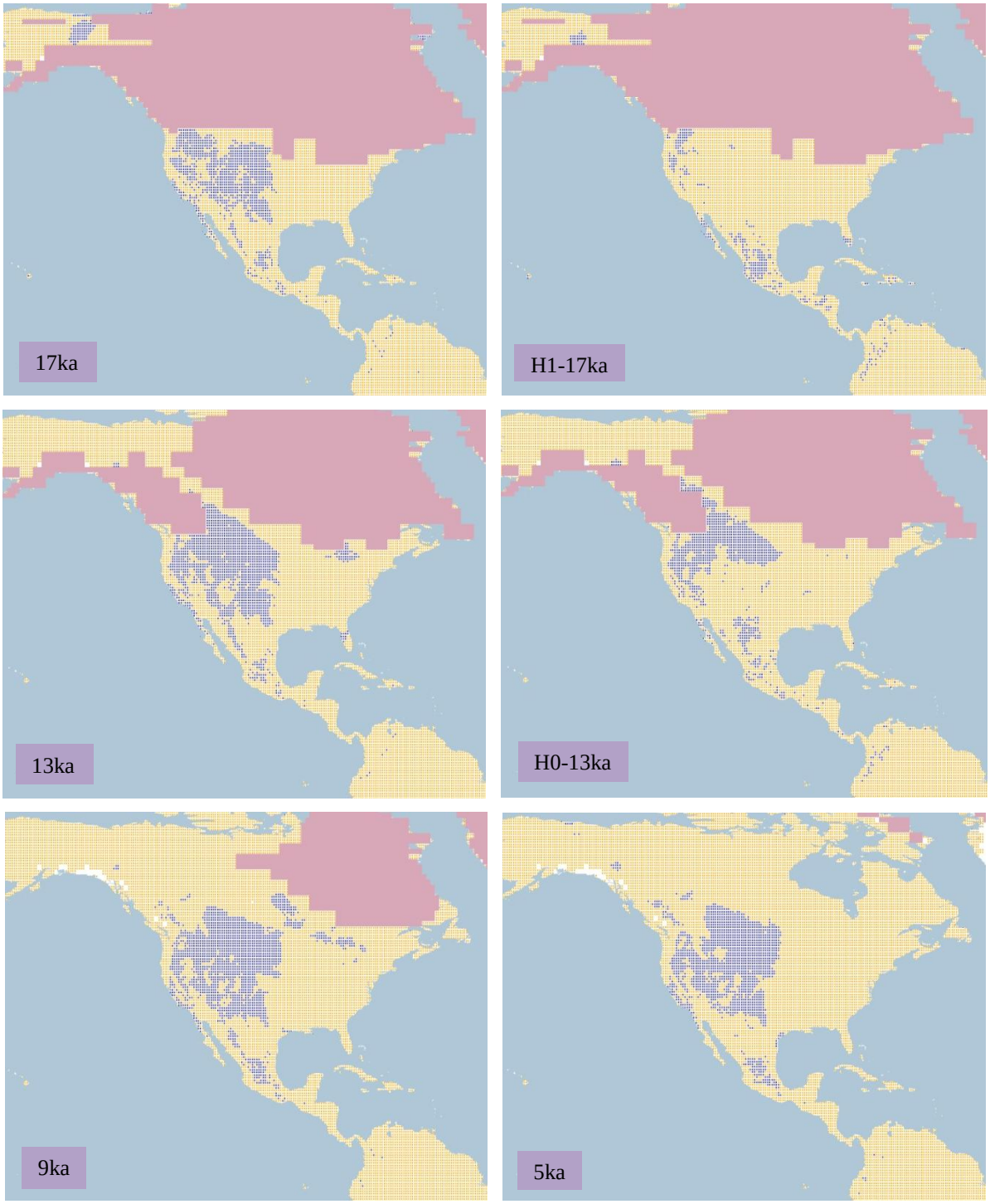

Figure 4.1.3.2.a. Simulation maps of American Avocet breeding range (continued**).**

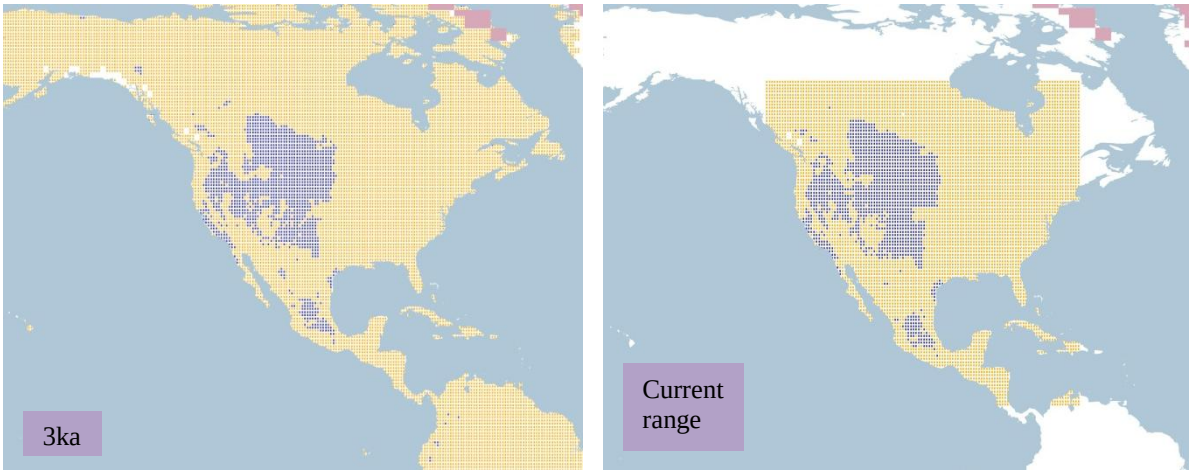

Figure 4.1.3.2.a. Simulation maps of American Avocet breeding range (continued**).**

Non-breeding range (AUC: 0.990; TSS: 0.906; Kappa: 0.821): Range in Mexico from Baja California, the coast of Sonora, Sinaloa, Jalisco, Guerrero, Oaxaca, Chiapas on the Pacific side and Tamaulipas, Veracruz, Tabasco, Campeche, Quintana Roo and Yucatan on the Gulf of Mexico, also inland from Chihuahua to Toluca. The non-breeding range also extends to the coast of Guatemala, and in the USA from Texas to Florida, South and North Carolina. As with the breeding range the year-round grounds are located in California USA, and in Mexico from northern Baja California to Guanajuato, Toluca and on the north-east coast of Tamaulipas.

At 26 ka BP a small range is projected in California and in Florida USA, with a larger range from north-western Mexico in Baja California and along the coast of Sonora as far as Jalisco, extending to a larger range inland from Nuevo Leon to Oaxaca and in northern Yucatan. This pattern continues, with an increasing range in the south of Mexico at 19 ka BP. See Figure 4.1.3.2.b.

By the end of the Pleistocene at 15 ka BP, the range reduces in the north-central part of Mexico, extending from the north-west in Baja California, on the central coast of Sonora, to central Mexico, from Zacatecas to Oaxaca with a small range in Yucatan, Campeche and Quintana Roo. This pattern continues and by 13 ka BP the range in the Yucatan peninsula disappears.

By the beginning of the Holocene at 10 ka BP, the range in central Mexico increases to the north, covering Durango and the south of Coahuila. This continues until 8 ka BP, with a rise of the range in central-north of Mexico, covering as far as central Chihuahua, and increasing

on the coast of Sinaloa and Sonora to the west. After this at 6 ka BP , the range extends from southern to northern Mexico, except between the Sierra Madre Occidental in the north, increasing on the west and east coast, following the same pattern until 1 ka BP. The current non-breeding range projection presents similarities with the 1 ka BP projection, only with a scattered range in central and north-central Mexico. In additions, neither the1 ka BP nor the current non-breeding projection display range along the east coast of USA, as it is found in literature for the current known range.

Even though the wintering grounds of the species are located in Mexico and the south of USA, there are suitable conditions projected in South America throughout the time frames, mainly from the west coast between Ecuador and Chile, to central regions from Bolivia to central-south Argentina and in central-east Brazil.

Figure 4.1.3.2.b. Simulation maps of American Avocet non-breeding range.
Maps are shown for ten-time slices: 24ka, H2 (24ka), 17ka, H1 (17ka), 13ka, H0 (13ka), 9ka, 5ka, 3ka and present (1961–90).

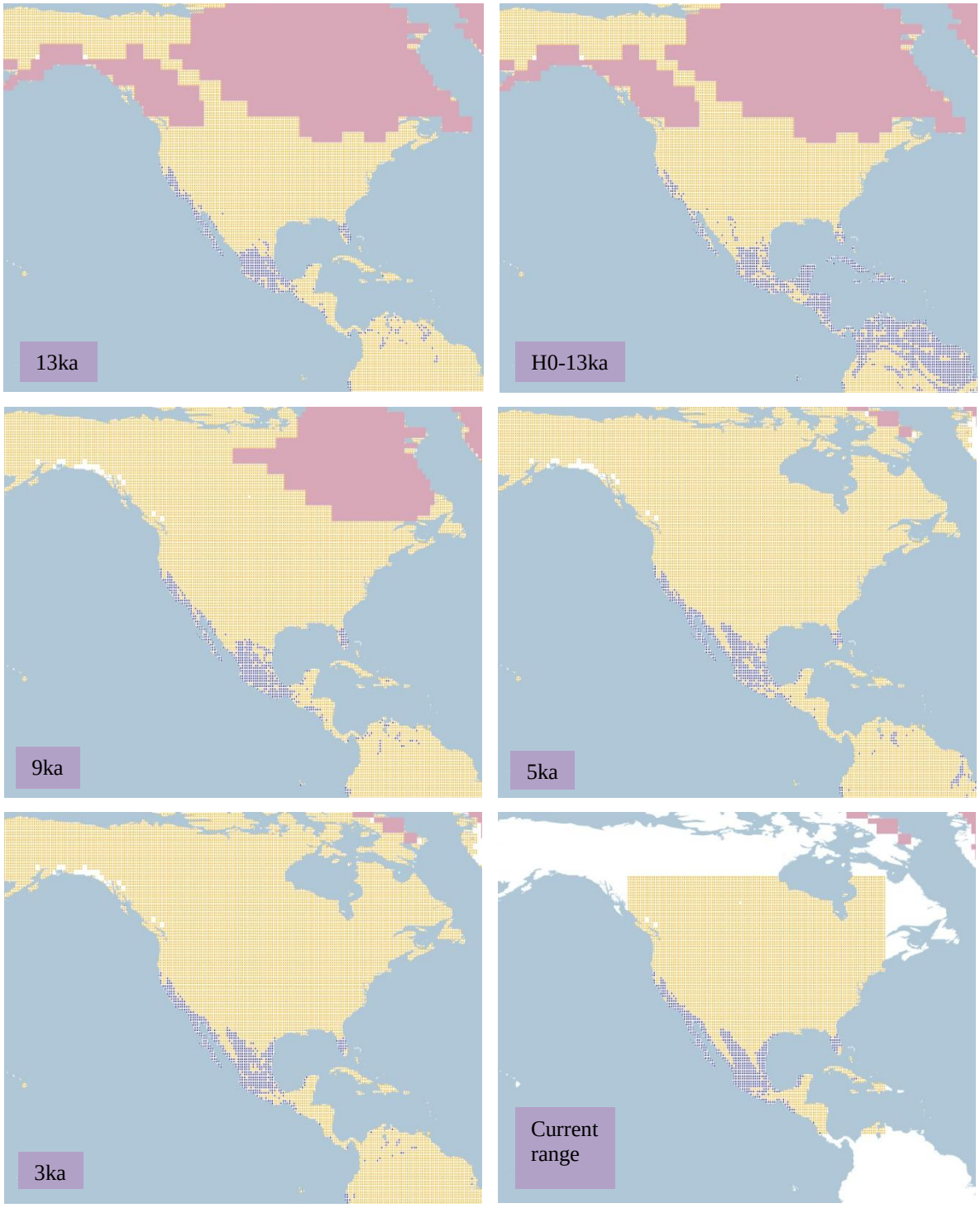

Figure 4.1.3.2.b. Simulation maps of American Avocet non-breeding range (continued**).**

4.1.3.3 AUC, TSS and Kappa values.

The resulted AUC, TSS and Kappa values for each species of the family Recurvirostridae are shown in here. These are divided in breeding and non-breeding ranges. The values for the model performance of the breeding range show AUC with the highest values for both species followed by TSS and Kappa with the lowest values.

For AUC the median is 0.984 with highest value presented by American Avocet (*R. americana*) with 0.987, followed by Black-winged Stilt (*H. h. mexicanus*) with 0.981.

The TSS median for the breeding range is of 0.872 with the highest value shown by American Avocet (*R. americana*) again with 0.887, and Black-winged Stilt (*H. h. mexicanus*) with the lowest at 0.857.

The Kappa median is 0.836 being the lowest of the three different measurements and the values follow the same trend as the highest value by American Avocet (*R. americana*) with 0.847, followed with Black-winged Stilt (*H. h. mexicanus*) with 0.826. See Figure 4.1.3.a.

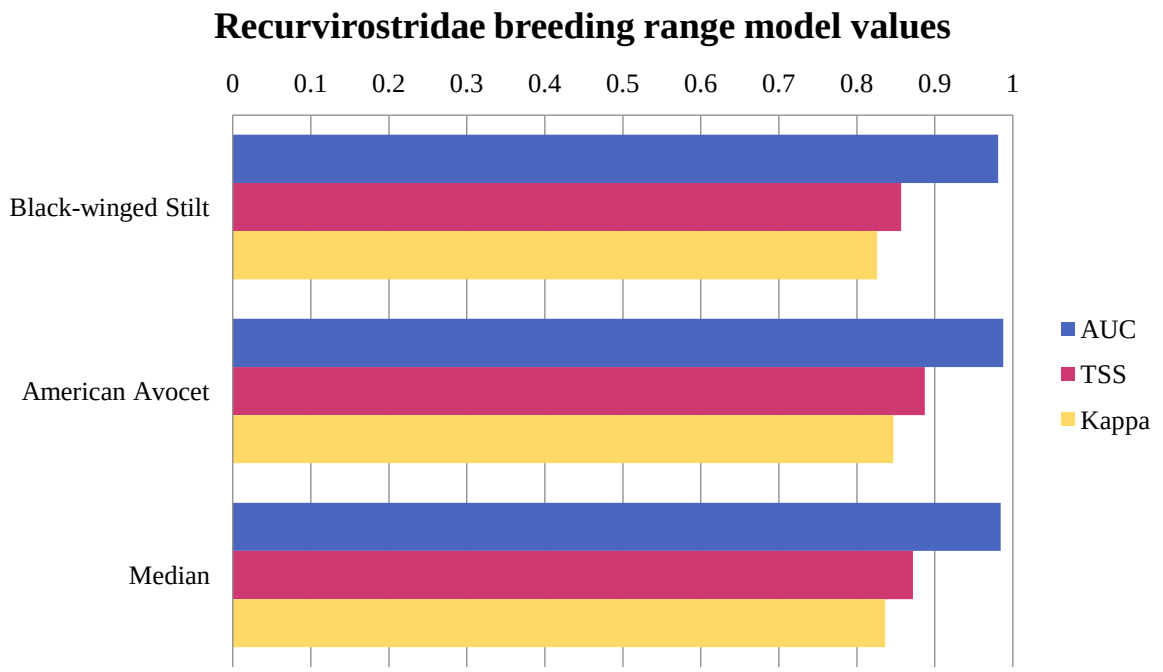

Figure 4.1.3.a. Model performance values of the family Recurvirostridae breeding range.
The graph shows values for each species of AUC, TSS and Kappa values from the CRS model as well as the median for each statistical measurement.

The values of the CRS modelling for the non-breeding range species were similar to the ones given in the breeding range, with higher values for AUC (median of 0.987), followed by TSS (median of 0.890) and Kappa (median of 0.830) with the lowest.

The AUC highest value is presented by species American Avocet (*R. americana*) with 0.990 followed by Black-winged Stilt (*H. h. mexicanus*) with 0.985.

For TSS the highest value is again from American Avocet (*R. americana*) with 0.906 and Black-winged Stilt (*H. h. mexicanus*) with 0.874.

The Kappa values for the non-breeding modelling show the highest value for Black-winged Stilt (*H. h. mexicanus*) with 0.839 followed by American Avocet (*R. americana*) with 0.821). See Figure 4.1.3.b.

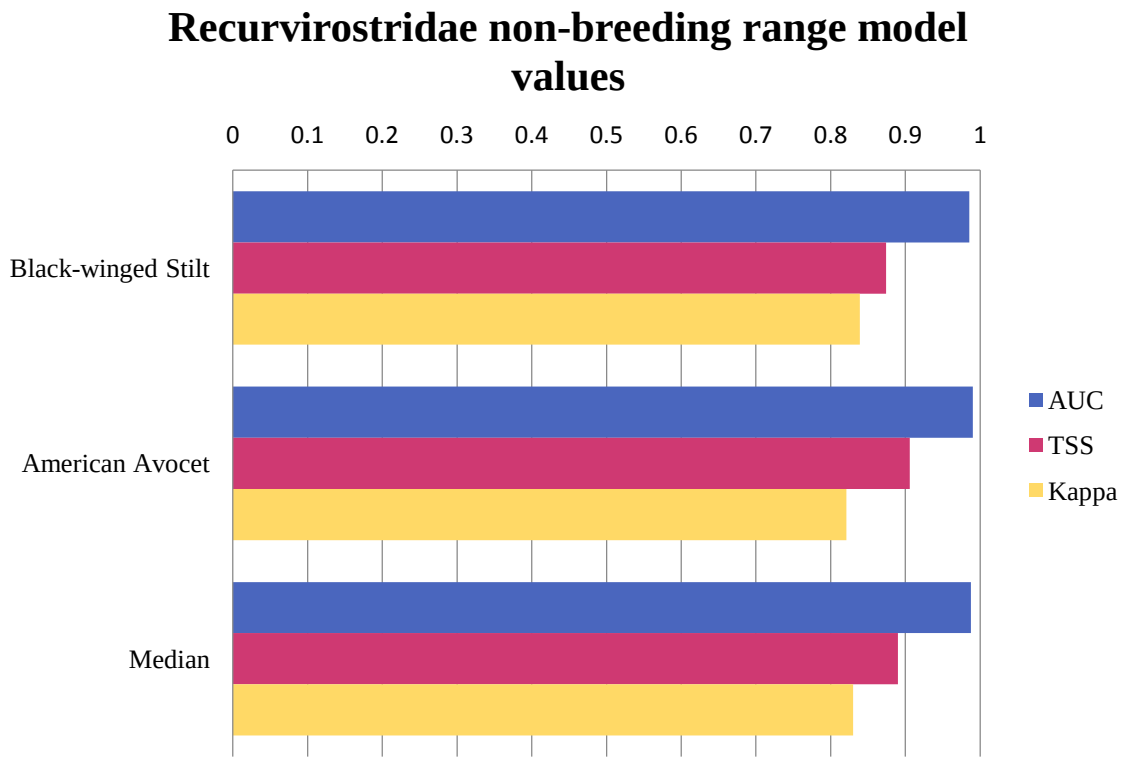

Figure 4.1.3.b. Model performance values of the family Recurvirostridae non-breeding range.
The graph shows values for each species of AUC, TSS and Kappa values from the CRS model as well as the median for each statistical measurement.

4.1.4 Family Scolopacidae

*4.1.4.1 Spotted Sandpiper (*Actitis macularius*). Conservation status: Least Concern. Current known range Figure 4.1.4.1.*

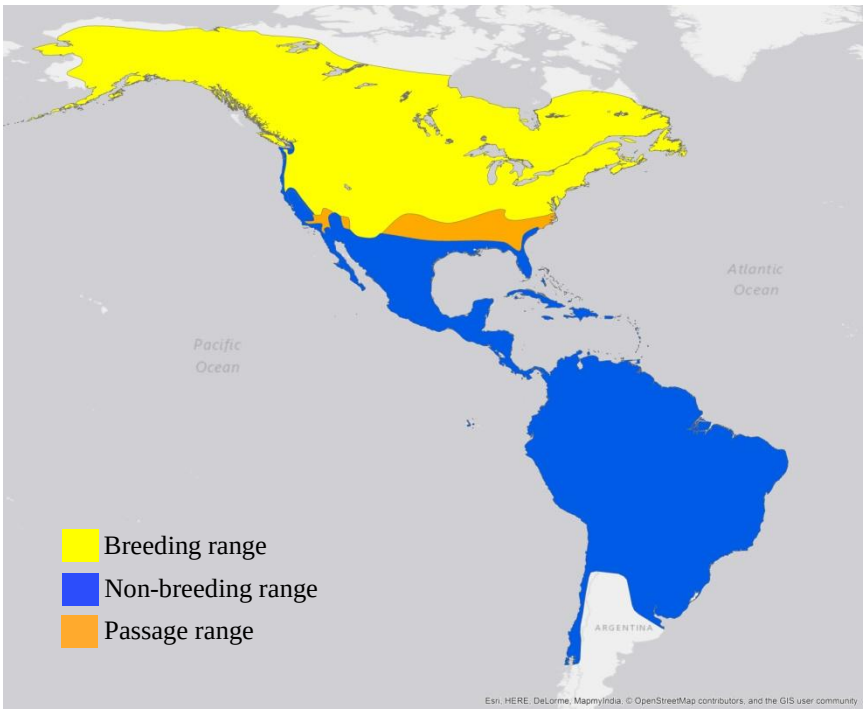

Figure 4.1.4.1. Current known range of Spotted Sandpiper.

Breeding range (AUC: 0.994; TSS: 0.932; Kappa: 0.930): This species spends the breeding season in North America, from Alaska to Canada apart from the Arctic islands, and in the USA except the southern states from California to Florida.

The projections begin at 26 ka BP with a range across the USA and extending to Mexico from Chihuahua to Durango following the Sierra Madre Occidental, also with a small range projected in Alaska. This pattern continues until 17 ka BP when the area projected in Mexico starts fragmenting and the range in the USA grows to the north as the ice sheet retreats. See Figure 4.1.4.1.a.

At 14 ka BP there is another increase in North America, specifically around north Canada and with an expansion in Alaska; additionally, the range in Mexico decreases to only a few points. After this as the ice sheet retreats at 13 ka BP the range grows towards the west of Canada and at 12 ka BP the range is uniform across the USA and Canada. This persists

towards the beginning of the Holocene at 11 ka BP and with slight increases after 10 ka BP as the ice sheet is restricted to the northern islands and Greenland. There is no change in the projections after this, being similar to the current projection.

Comparing H2 with the 24 ka BP projection they share similar ranges across the USA and central-north Mexico, with a slight difference at H2 where the range is not as uniform in the central USA. The same arrangement persists when comparing H1 to the 17 ka BP projection and H0 to the 13 ka BP projection, only with a more extensive range in central-north Mexico.

Even though the species doesn't occur in South America, according to the projections there are suitable conditions in central-south Argentina and Chile.

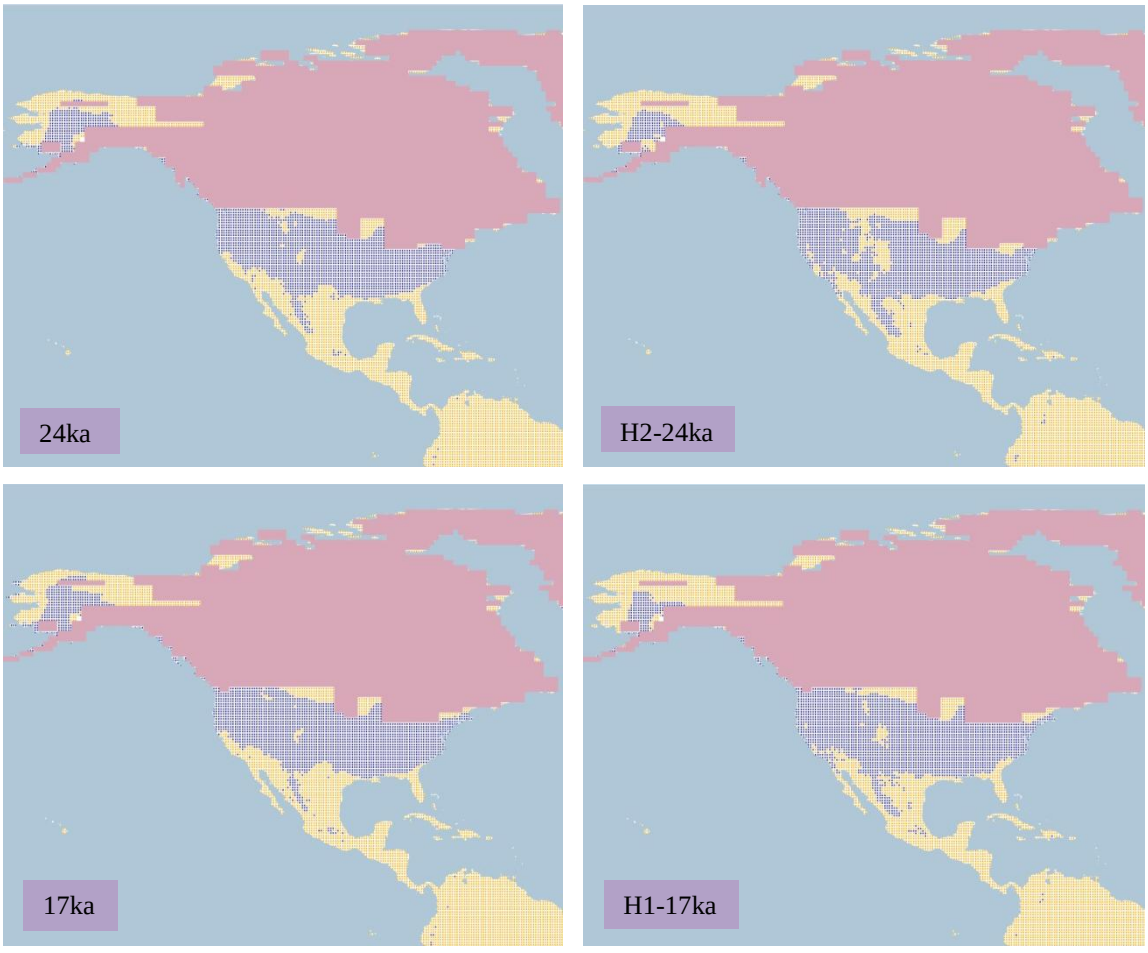

Figure 4.1.4.1.a. Simulation maps of Spotted Sandpiper breeding range.
Maps are shown for ten-time slices: 24ka, H2 (24ka), 17ka, H1 (17ka), 13ka, H0 (13ka), 9ka, 5ka, 3ka and present (1961–90).

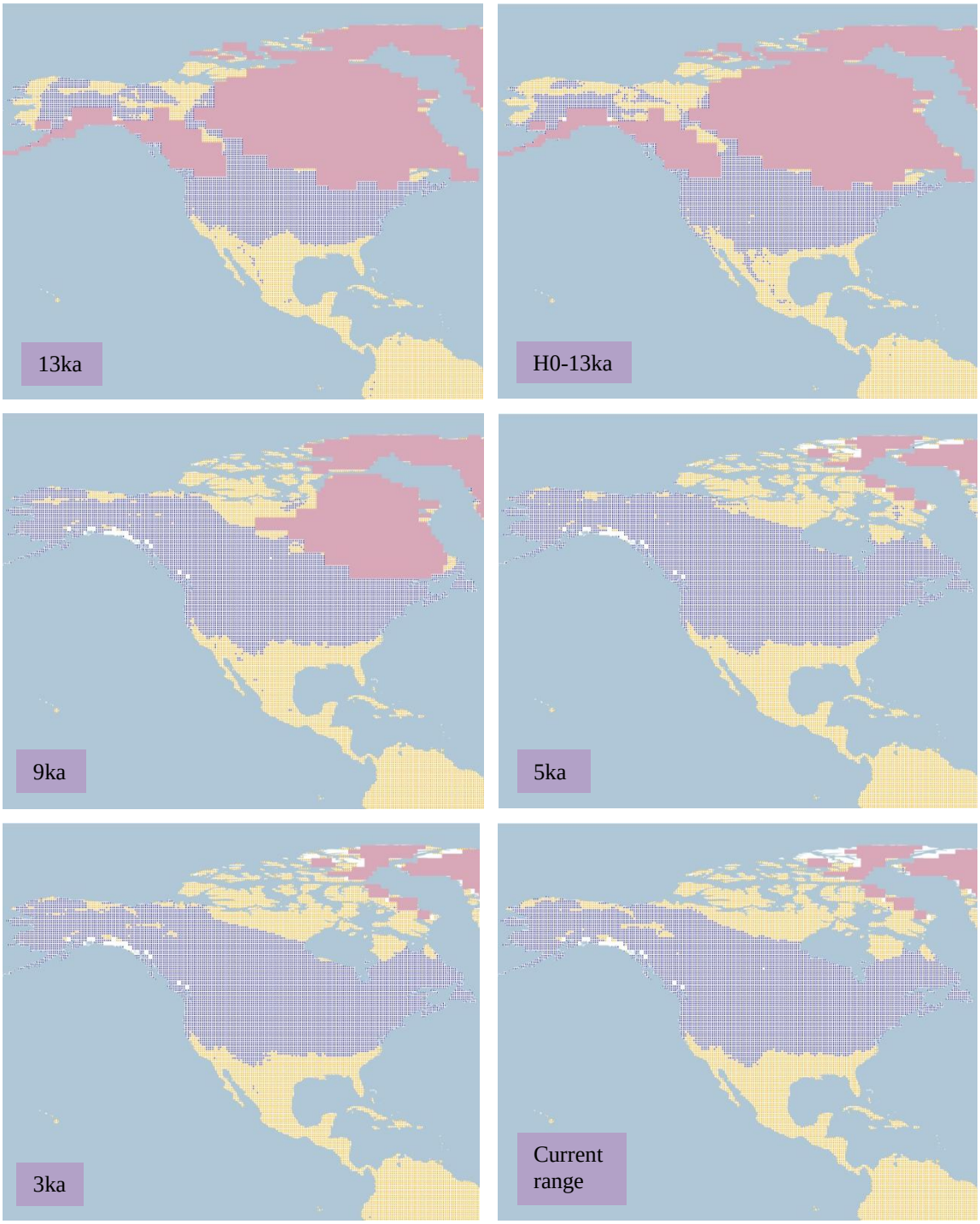

Figure 4.1.4.1.a. Simulation maps of Spotted Sandpiper breeding range (continued**).**

Non-breeding range (AUC: 0.996; TSS: 0.955; Kappa: 0.94): the wintering grounds of the species are located across Mexico, Central America, the Greater Antilles and in South America south to northern Argentina and following the coast line of Chile, as well as in southern regions of the USA, from California to Florida, and in the Galapagos Islands.

At 26 ka BP the projected range extends from Florida, south California, across Mexico except the central-northern part, south to Central America, the Greater Antilles, Galapagos Islands and South America as far as the north of Argentina. This pattern remains unaltered until 21ka when the area in central-north Mexico is also projected as suitable. See Figure 4.1.4.1.b.

From 17 ka BP the range increases along the west coast of the USA, and a small range is projected in north Argentina; this remains constant until 12 ka BP when there is a growing range across the southern part of the USA, intersecting with the range in Florida. This pattern continues to the early Holocene and until ka BP, almost unchanged.

The range in South America remains also constant until 7 ka BP when the range in the central-north part of Argentina begins to decline, continuing to do so progressively until 1 ka BP. Additionally, the current range projection remains similar to 1 ka BP.

Comparing H2 to 24 ka BP the projections are similar in almost all the range except in the area of central-north Mexico, where the H2 projection does not have a range, as well as in the area of Florida and the Greater Antilles, where the H2 projection is of a less extensive range. This changed at H1 with an increase in range in the central-north area of Mexico, however not at the same scale as 17ka. Likewise, the projection at H0 is analogous to 13 ka BP in almost the whole range except in the areas of north Mexico and the southern USA where the H0 range is more fragmented.

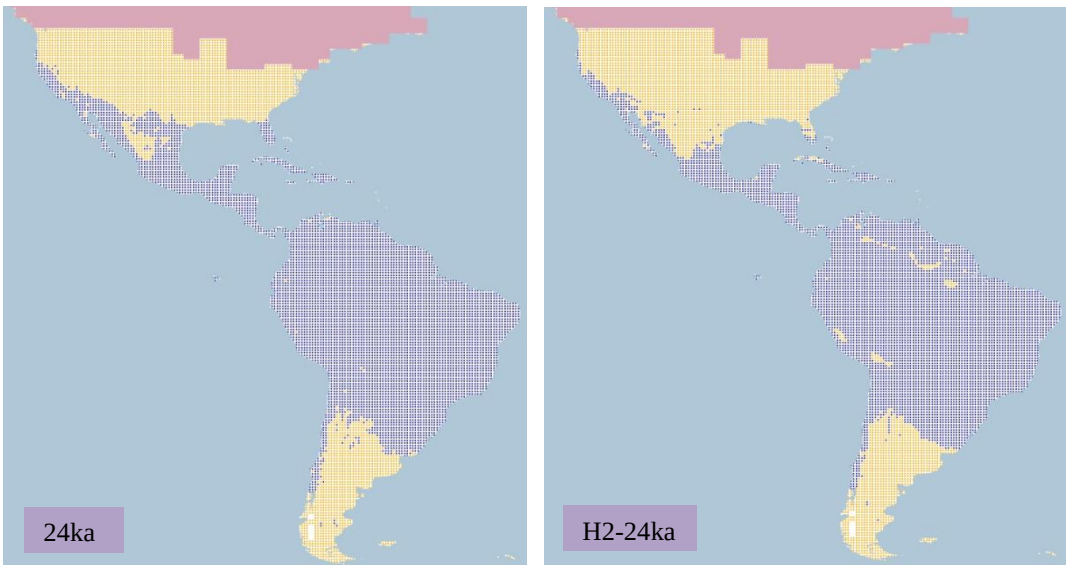

Figure 4.1.4.1.b. Simulation maps of Spotted Sandpiper non-breeding range.
Maps are shown for ten-time slices: 24ka, H2 (24ka), 17ka, H1 (17ka), 13ka, H0 (13ka), 9ka, 5ka, 3ka and present (1961–90).

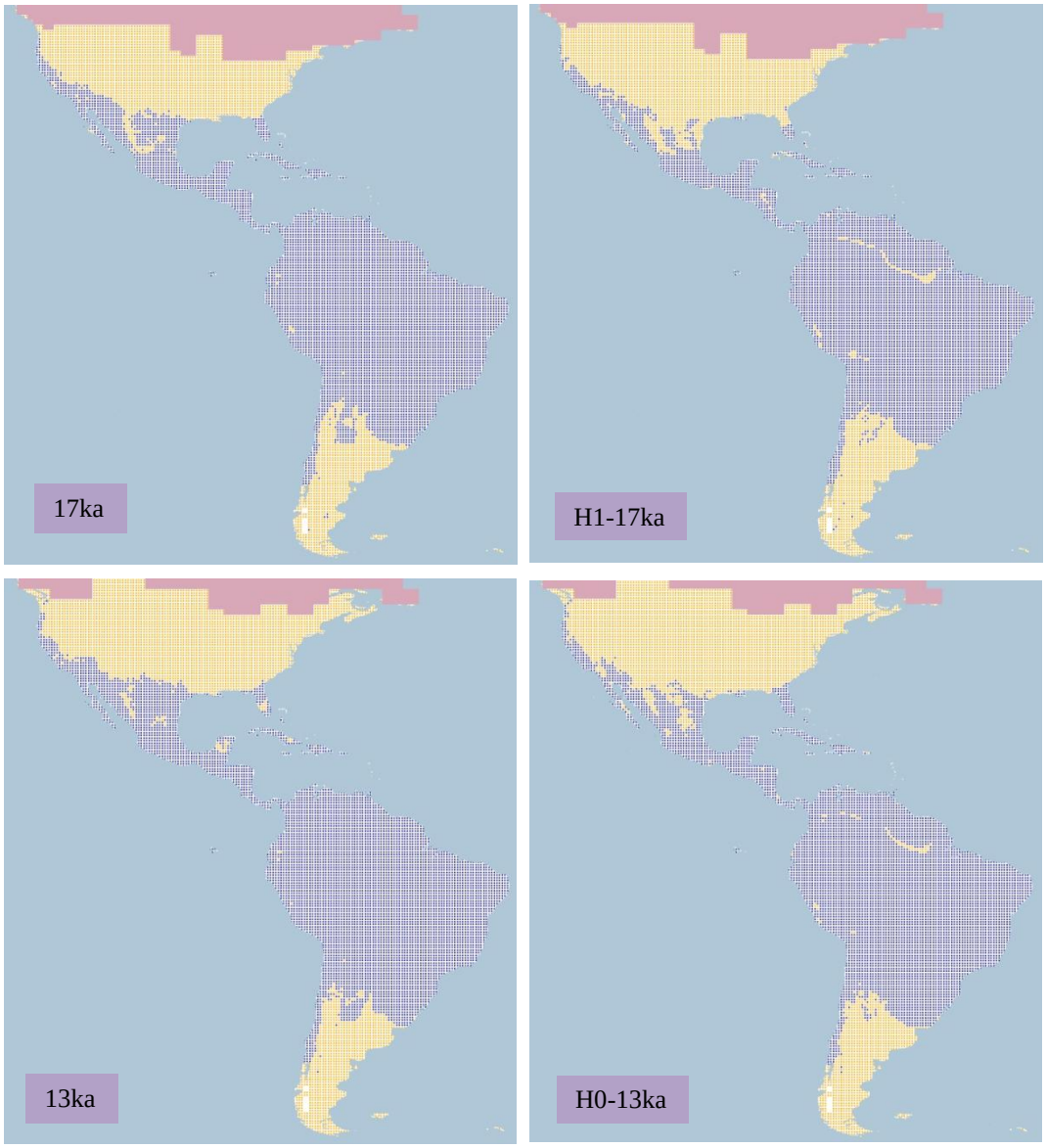

Figure 4.1.4.1.b. Simulation maps of Spotted Sandpiper non-breeding range (continued**).**

Figure 4.1.4.1.b. Simulation maps of Spotted Sandpiper non-breeding range (continued**).**

*4.1.4.2 Ruddy Turnstone (*Arenaria interpres *including* A. i. interpres *and* A. i. morinella*). Status conservation: Least Concern. Current known range Figure 4.1.4.2.*

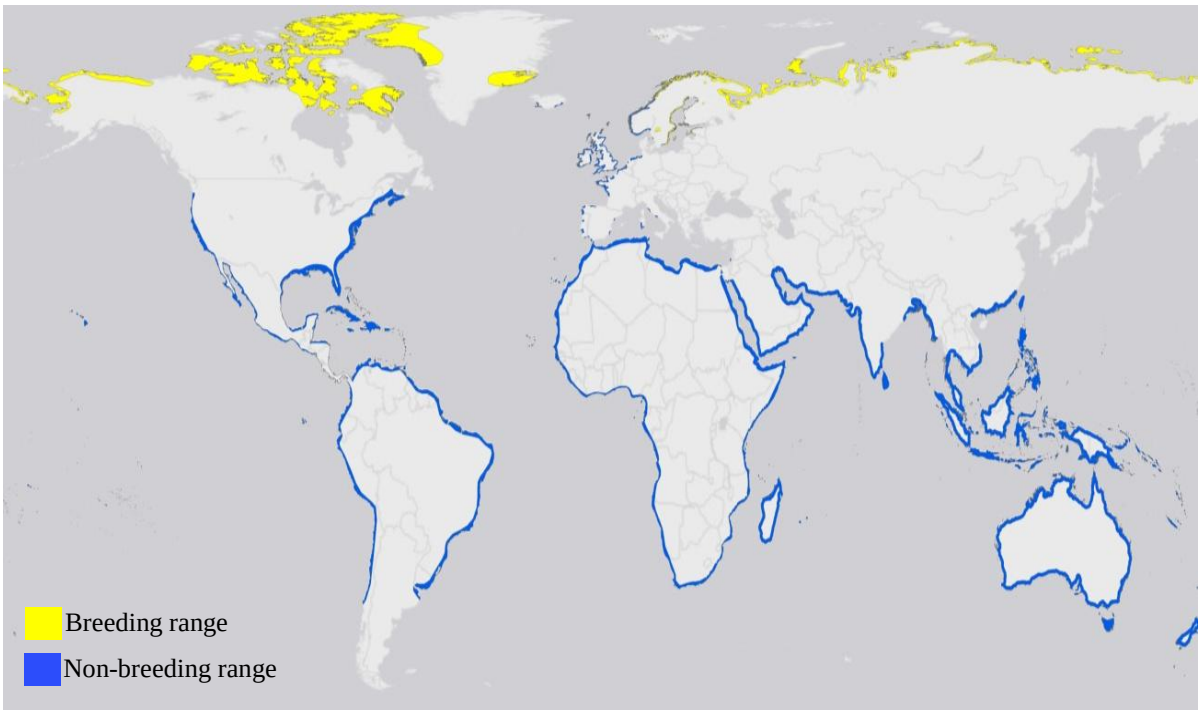

Figure 4.1.4.2. Current known range of Ruddy Turnstone.

Breeding range (AUC: 0.977; TSS: 0.884; Kappa: 0.631): This species spends the breeding season in high Arctic regions, from north Alaska, high Arctic islands of Canada, Greenland and around the north coast of Norway and Russia.

The range at 26 ka BP is projected across the Northern Hemisphere, from the north of Alaska, a small part in the south of Canada and in Russia mainly in the north-west region, and with a smaller range in central Asia and the north-west of Russia. The same pattern continues until 20 ka BP when the range in Asia reduces in extent, increasing again at 18 ka BP here as well as in North America. See Figure 4.1.4.2.a.

At 16 ka BP the projection is of a reduction in the north-east of Russia and in the south of Canada; also, the range in central Asia shifts south near central-west China. The same reducing pattern remains and at 14 ka BP there is a dramatic change with the northern

projected ranges decreasing inland and concentrating across the northern coastal areas for both Asia and North America.

As the ice sheet retreats the range moves north as well, specifically at the beginning of the Holocene between 11 ka BP and 10 ka BP when the central range in Asia is reduced to only a minor range. After this, and considering the ice sheet retreat, the range persists in northern territories where at 8 ka BP there is a projected range around the coasts of Norway, Sweden, Finland and a small part in Greenland. The general pattern continues after this period with only slight differences, increasing from 3 ka BP to 1 ka BP. The current range projection also exhibits the same pattern as 1 ka BP.

Comparison between H2 and 24 ka BP shows the same pattern in the high Arctic regions across North America and Eurasia, although the H2 projection shows a wider range around the central and east part of Asia (mainly in Russia). At H1 this reduces slightly in central Asia, but a similar pattern remains. At H0 this range again decreases but a constant range persists in north-east Russia, a pattern not shown in the 13 ka BP projection where the range is mainly restricted to northern coastal areas from North America to Eurasia.

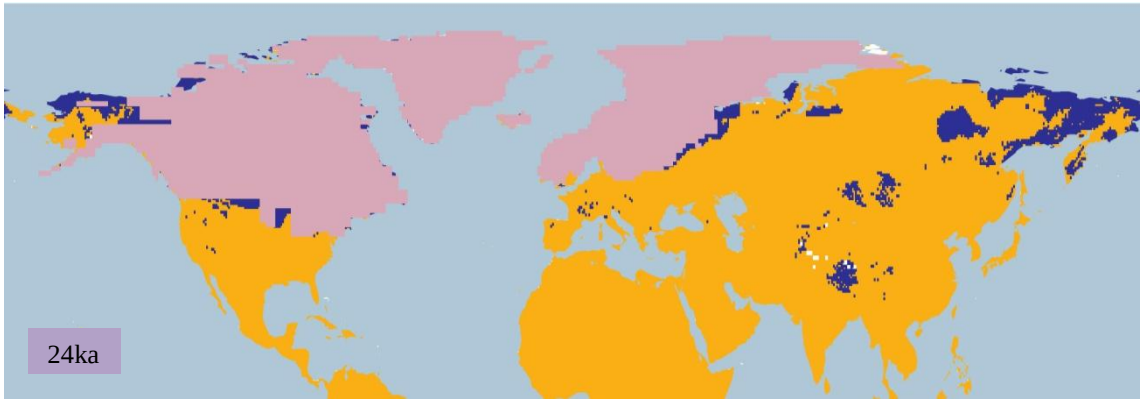

Figure 4.1.4.2.a. Simulation maps of Ruddy Turnstone breeding range.
Maps are shown for ten-time slices: 24ka, H2 (24ka), 17ka, H1 (17ka), 13ka, H0 (13ka), 9ka, 5ka, 3ka and present (1961–90).

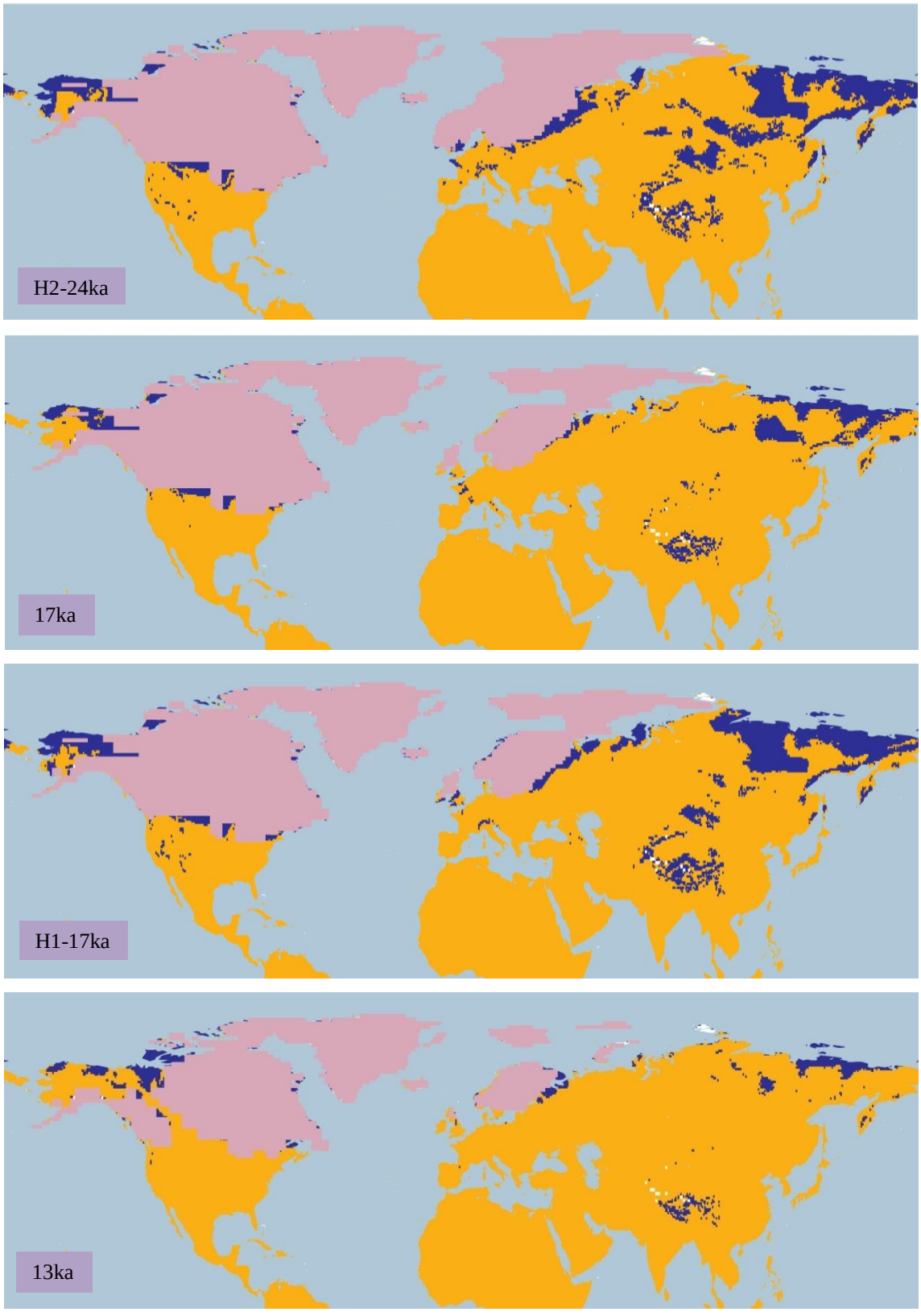

Figure 4.1.4.2.a. Simulation maps of Ruddy Turnstone breeding range (continued**).**

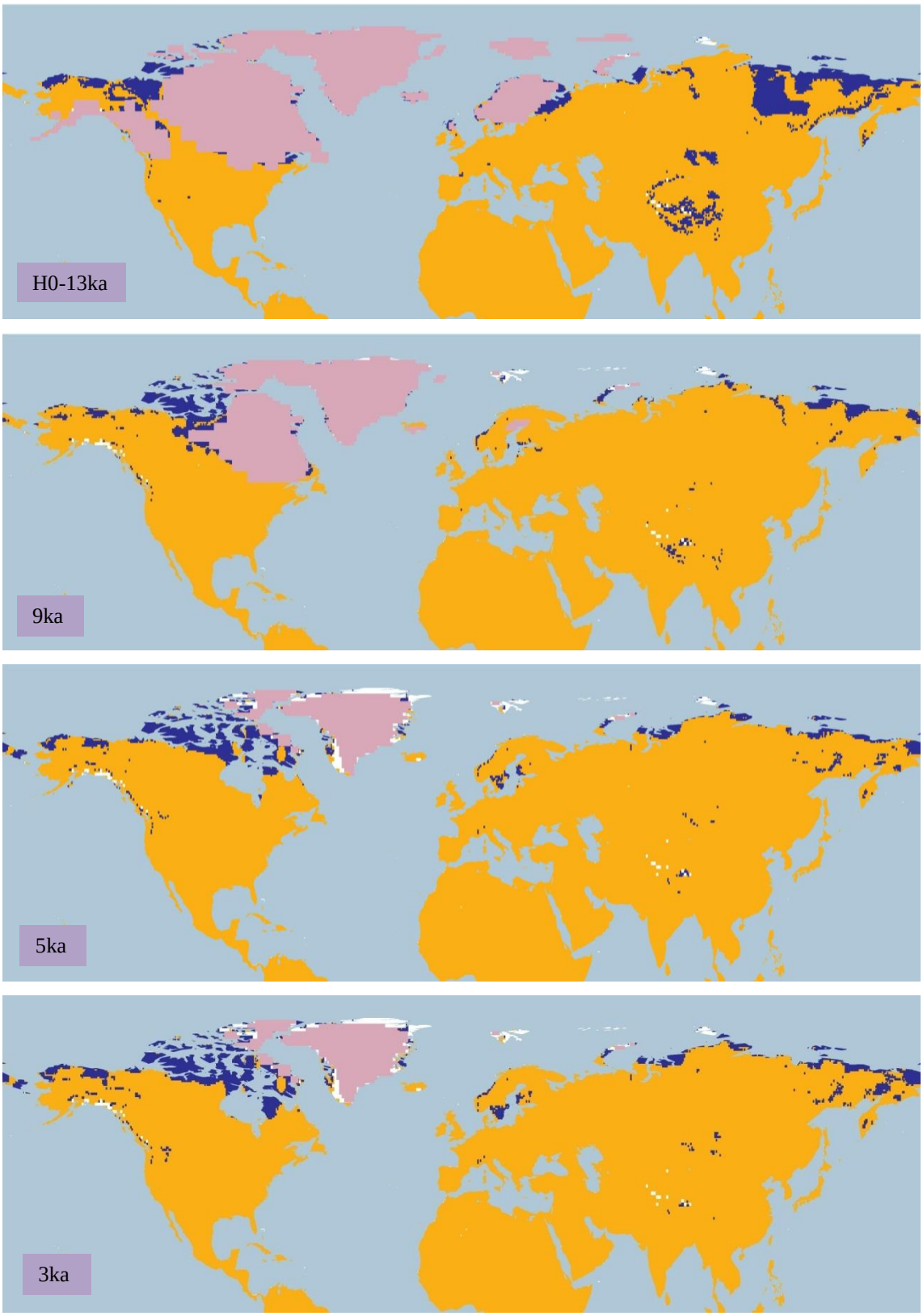

Figure 4.1.4.2.a. Simulation maps of Ruddy Turnstone breeding range (continued**).**

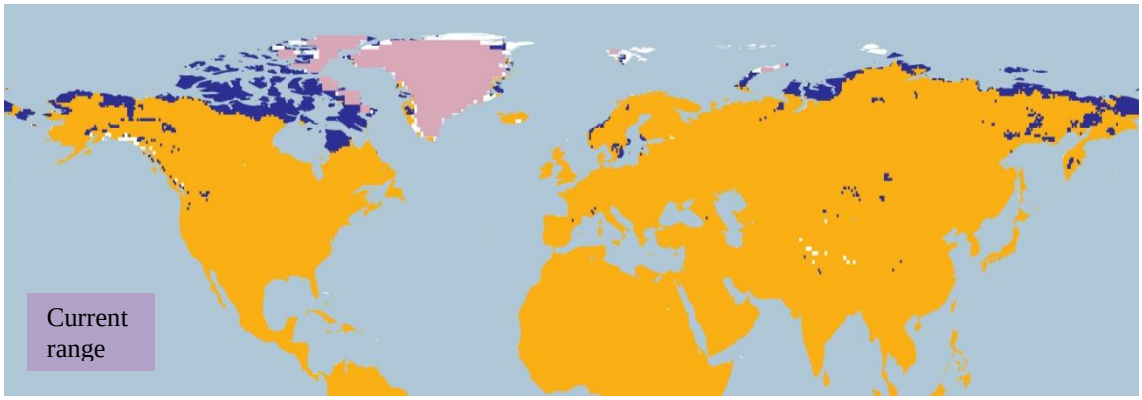

Figure 4.1.4.2.a. Simulation maps of Ruddy Turnstone breeding range (continued**).**

Non-breeding range (AUC: 0.950; TSS: 0.775; Kappa: 0.600): The species spends the non-breeding season mainly on the coasts of the Southern Hemisphere. In North America from north-western USA, along western Mexico, the coast of Guatemala and the coast of El Salvador; on the east side from Nova Scotia in Canada, along the eastern coast of USA, Mexico, Belize and Honduras, as well as the Greater Antilles. In South America on the west coast from Colombia to south-central Chile, and on the Atlantic side from northern Colombia to eastern Argentina. In Europe the wintering grounds are found along the coast of Norway, the coasts of Great Britain, the northern coast of France, Belgium, Netherlands and in north-western Germany, with a smaller range along north-western Spain, western Portugal, and on the west coast of Italy. The range extends to the coasts of the African continent, the southern coasts of the Asian continent from Saudi Arabia to southern India, and from north-eastern India to eastern Indonesia, extending also to the coasts of the Australian continent.

The range at 26 ka BP is projected along the west coast of USA and the north-west coast of Mexico, as well as the central region of Mexico and the Greater Antilles. In South America along the west coast from Ecuador to southern Chile and inland from Bolivia to northern Argentina and in south-eastern Brazil, with a smaller range in the northern region. In Europe the range is projected in the northern region from the northern Portugal to northern France, and inland between Spain and France. In Africa on the north-west coast from Libya to Guinea, also on the coast of Namibia; on the east side from South Africa to Somalia; there is also range projected inland in Africa from Guinea to Sudan and in eastern South Africa. There is also range projected in southern Asia, from the south of Saudi Arabia to India, Myanmar, south-eastern China, Indonesia and Papua New Guinea, as well as around the coast of Australia. See Figure 4.1.4.2.b.

By 19 ka BP the range in Brazil and north-central Africa increases, with the remaining range along the coasts of the Southern Hemisphere unchanged. After this between 17 ka BP and 16 ka BP with the deglaciation in Europe, the range increases on the south-west of Great Britain, with also an increase in northern South America and north of Australia. By 15 ka BP, the range in Great Britain covers the western region, following an increased range as well in the north of Australia and South America.

Particularly from 14 ka BP onwards, and by the beginning of the Holocene, there is greater range projected in the north-central part of Brazil in South America, as well as central Australia and north-central Africa, with a decrease in the range projected in the southern region of Asia. The pattern in South America changes at 8 ka BP, with the range moving to western Brazil, near the Andean cordillera, and with a decrease of the range in central-east Australia. Also, the range on the west coast of USA reaches the south-west coast of Canada, and the range covers most of Great Britain.

By 6 ka BP the range in Saudi Arabia increases in the southern region, as well as in India, with a decreasing range in central-western Brazil. The decreasing pattern continues from 6 ka BP until 1 ka BP, restricting the range around the world to mostly coastal areas, except in Great Britain, Indonesia and the Greater Antilles.

The current non-breeding range projection shows a similar range as 1 ka BP, although with a larger range projected on the northern coast of Australia, on the central and west islands of Indonesia, and in the Amazonian region of Brazil, Peru and Colombia.

There are similar ranges projected between H2 and 24 ka BP on the coastal areas of North and South America, Africa and Saudi Arabia. However, a larger range is projected in the H2 projection, from the central region of Mexico to Central America and northern and central regions of South America, with a smaller range in Portugal, Spain and France. The same pattern is present in the H1 projection for South America, central Mexico and Central America, with a smaller range in the north-central part of Africa and the southern region of Asia. Between H0 and 13 ka BP, the differing ranges are located inland, from the north-central region of South America, in the central region of Africa and in the north of Australia, projecting a smaller range at H0 than at 13 ka BP for these areas.

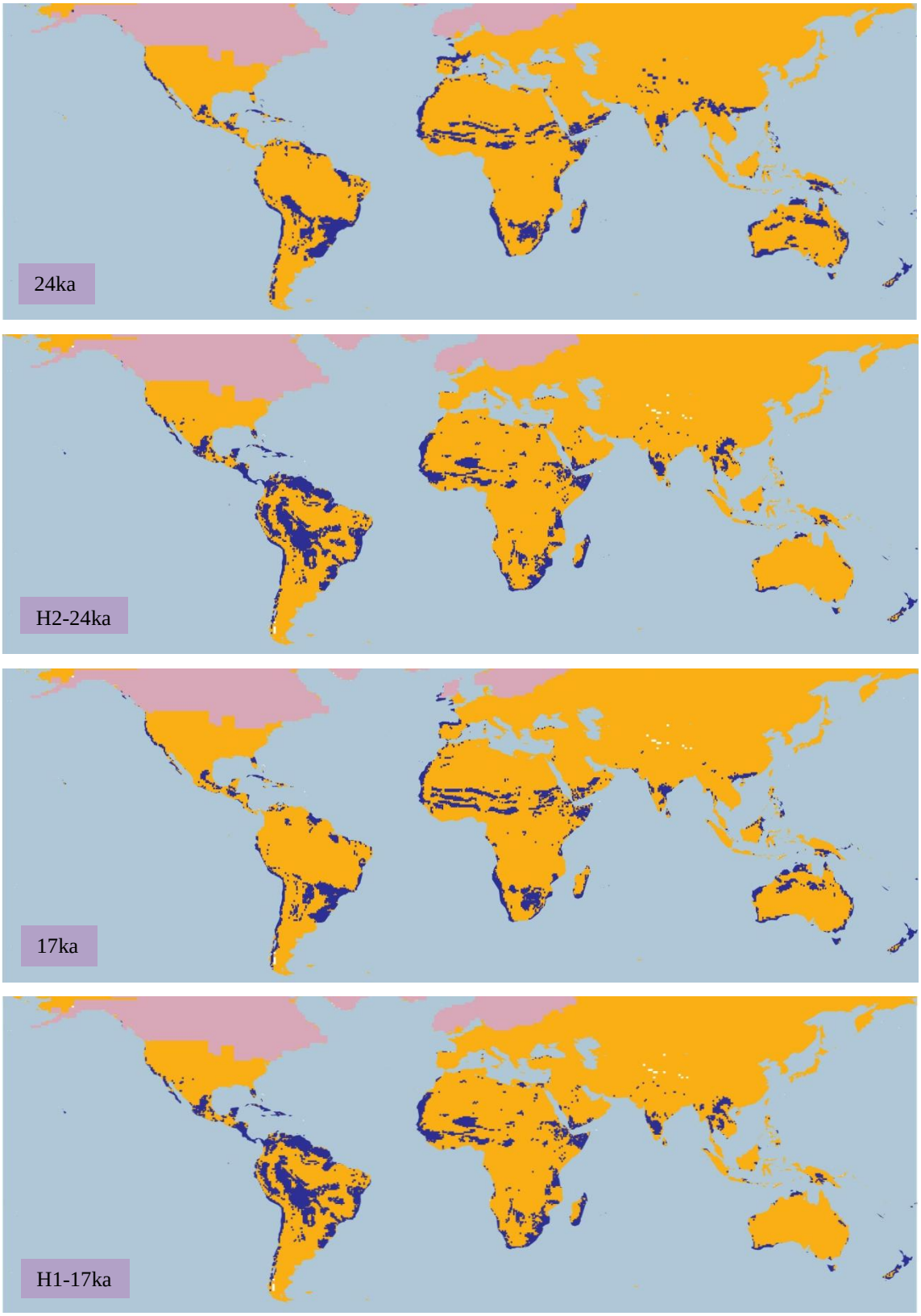

Figure 4.1.4.2.b. Simulation maps of Ruddy Turnstone non-breeding range.
Maps are shown for ten-time slices: 24ka, H2 (24ka), 17ka, H1 (17ka), 13ka, H0 (13ka), 9ka, 5ka, 3ka and present (1961–90).

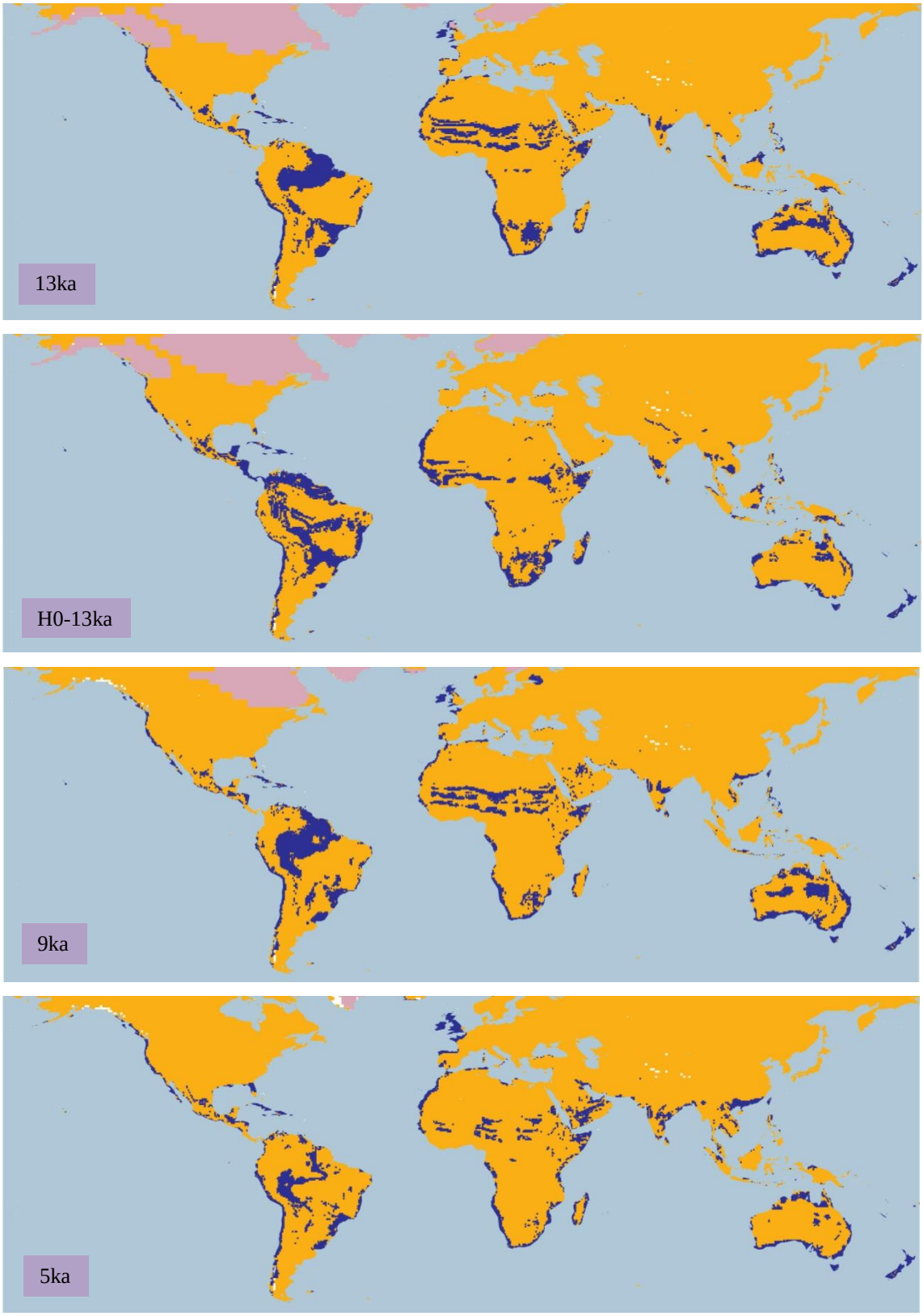

Figure 4.1.4.2.b. Simulation maps of Ruddy Turnstone non-breeding range (continued**).**

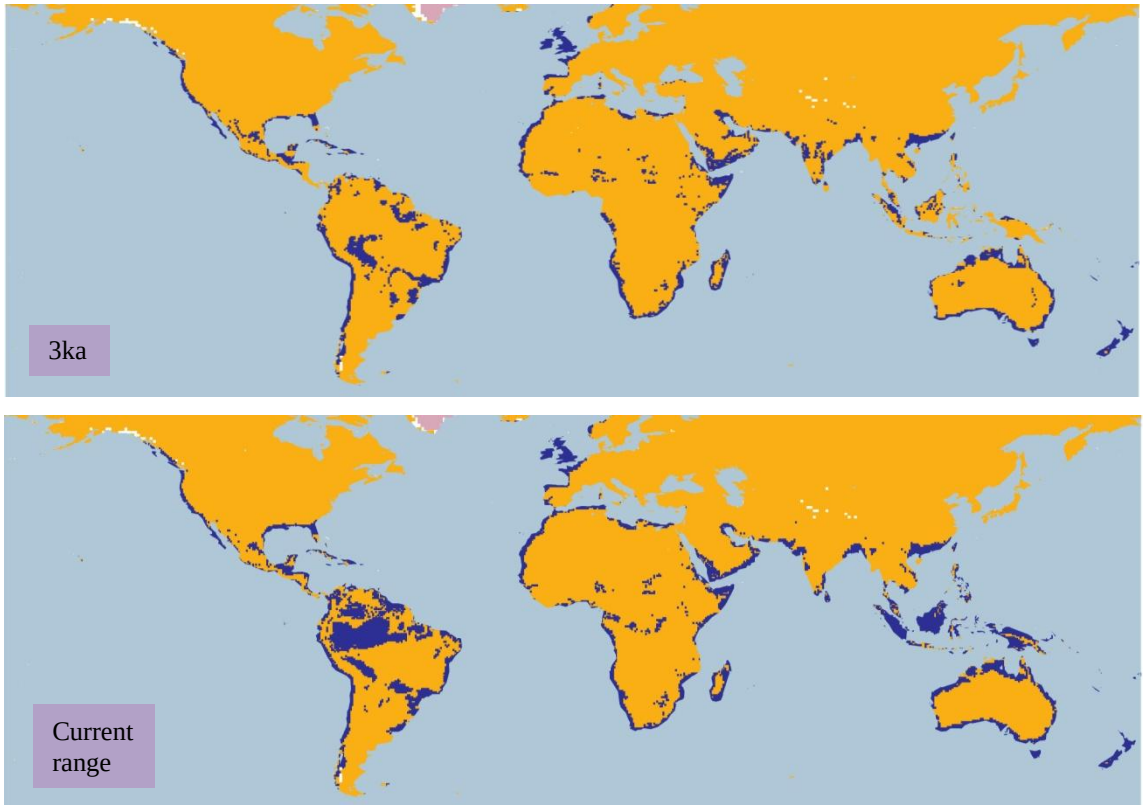

Figure 4.1.4.2.b. Simulation maps of Ruddy Turnstone non-breeding range (continued**).**

*4.1.4.3 Black Turnstone (*Arenaria melanocephala*). Conservation status: Least Concern. Current known range Figure 4.1.4.3.*

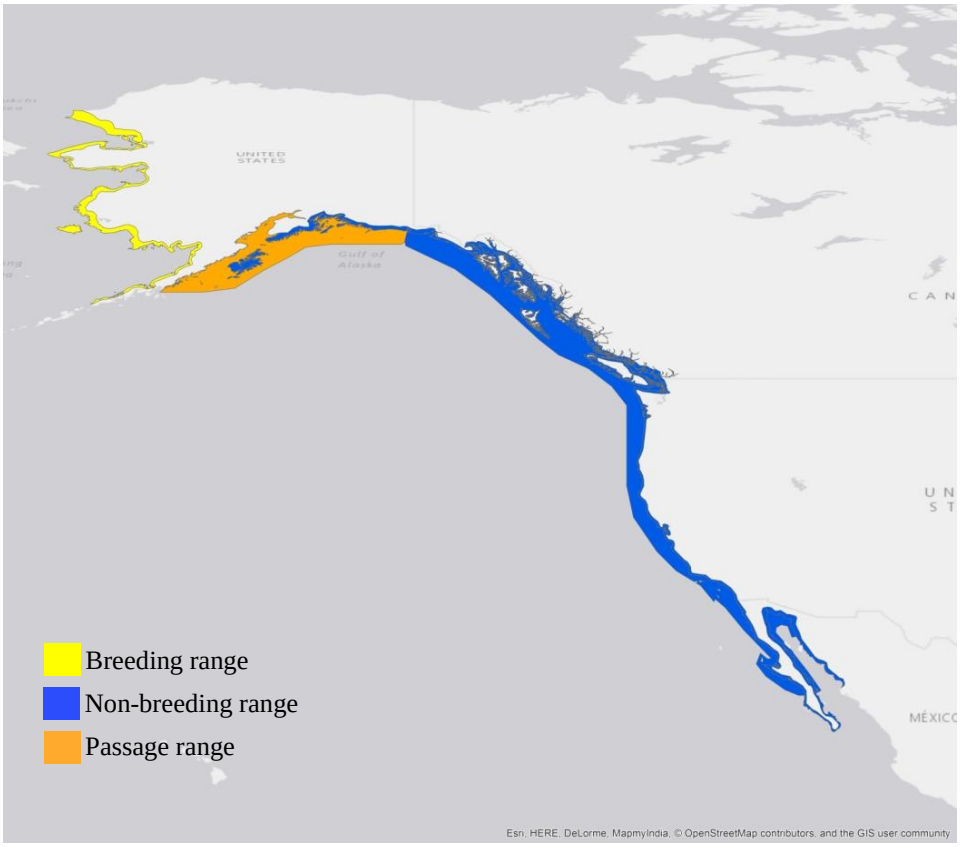

Figure 4.1.4.3. Current known range of Black Tunrstone.

Breeding range (AUC: 0.914; TSS: 0.702; Kappa: 0.523): This species has a restricted breeding range around the west coast of Alaska from Wevok to the Unimak Island.

At 26 ka BP the range is projected in south-central and central regions of Alaska and a small range in the north-central and north-western conterminous USA. This pattern continues at 24 ka BP with a small variation in the range projected in the north-central and north-east conterminous USA near the ice sheet. The pattern changes at 22 ka BP with a decrease in the range in Alaska, and in the north-central conterminous USA. In addition, the pattern continues until 19 ka BP with the increase in the north-central region of conterminous USA. See Figure 4.1.4.3.a.

In the 16 ka BP projection the range in the north-eastern conterminous USA disappears, restricting the range to the north-eastern USA near the ice sheet and to southern Alaska, also

near the ice sheet. The decrease of range continues at 15 ka BP, with the range mainly being projected in south-western Alaska near the ice sheet. After this, with the deglaciation at 13 ka BP, the range extends to northern Canada in the Northwest Territories near the ice sheet.

At 12 ka BP the range increases and extends to south-western British Columbia and the northern region of the Northwest Territories in Canada. This pattern continues at 1 ka BP, with increasing extents in south-western Alaska and southern Alberta in Canada. With the deglaciation at 10 ka BP, the range in Alaska increases to the north-west, and in southern Northwest Territories and Nunavut in Canada.

The range changes at 8 ka BP, increasing in western and southern Alaska, decreasing in the south-west of Canada and with a shifting range near Hudson Bay between Manitoba and Ontario, as well as a small range projected on the north-east coast of Newfoundland and Labrador. The range near Hudson Bay in Canada disappears from 7 ka BP onwards, and there is an increasing range along western and southern regions of Alaska, western British Columbia, near Hudson Bay in Quebec and northern Newfoundland and Labrador in Canada. This continues until ka BP, and afterwards the range in the west of Alaska and north-east of Canada decreases until 1 ka BP.

The current breeding range projection present similarities with the 1 ka BP projection, extending across western Canada in British Columbia, and the southern region of Alaska, only with a larger range in western Alaska than the 1 ka BP projection.

The Heinrich event H2 presents a different range than 24 ka BP, with a larger range projected in the north-east near the ice sheet between Indiana and Illinois, and a fragmented range in the central-west region of the conterminous USA and a small range near the ice sheet in southern Alaska. This change at H1, with an increase of the range in the north-central and north-east conterminous USA, differing also from the 17 ka BP projection that has a small range in the north and west of Montana in the conterminous USA. There are no similar ranges projected between H0 and 13 ka BP, only with a small range projected in the central conterminous USA at H0, a small range in the north of the Northwest Territories in Canada at 13 ka BP.

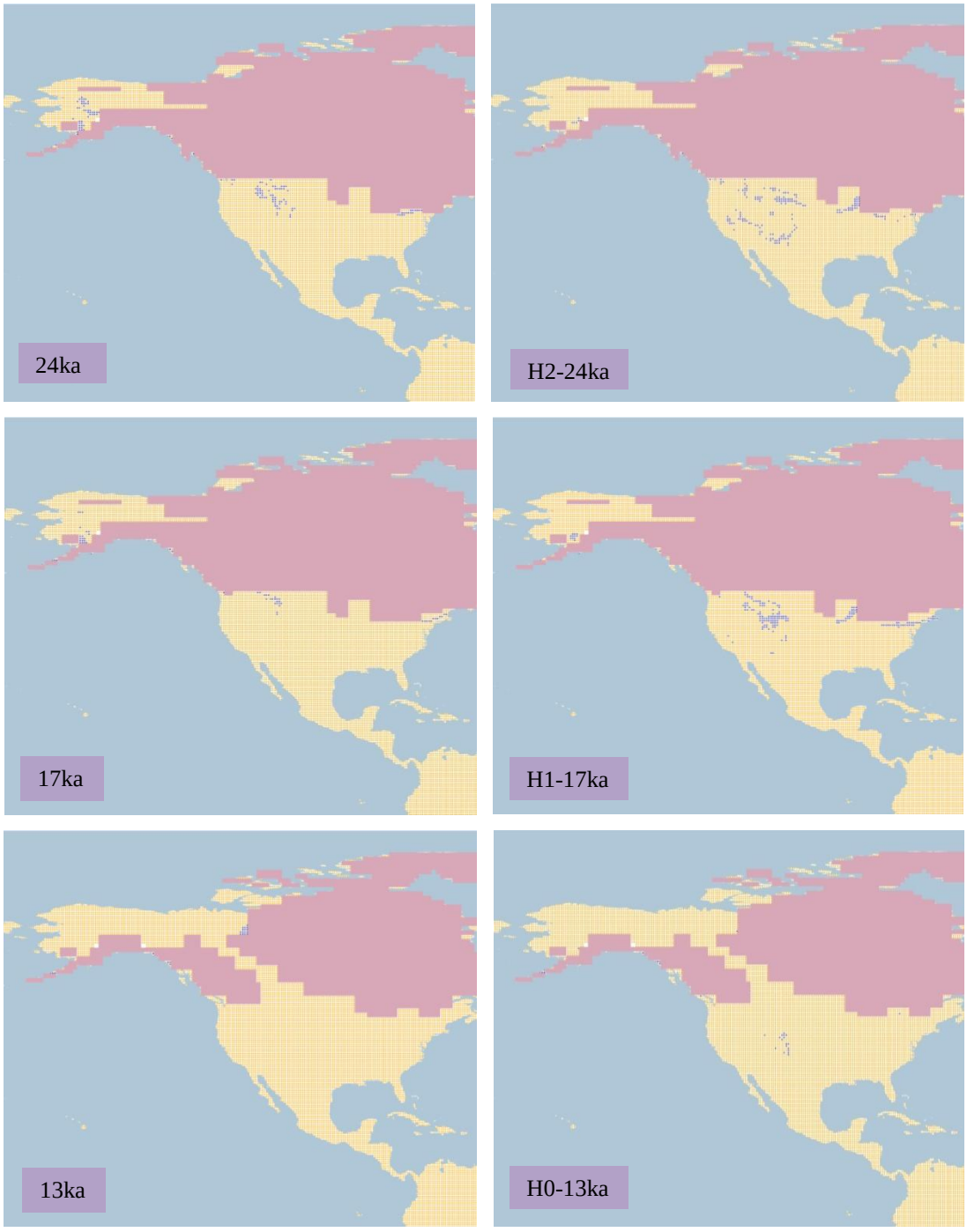

Figure 4.1.4.3.a. Simulation maps of Black Turnstone breeding range.
Maps are shown for ten-time slices: 24ka, H2 (24ka), 17ka, H1 (17ka), 13ka, H0 (13ka), 9ka, 5ka, 3ka and present (1961–90).

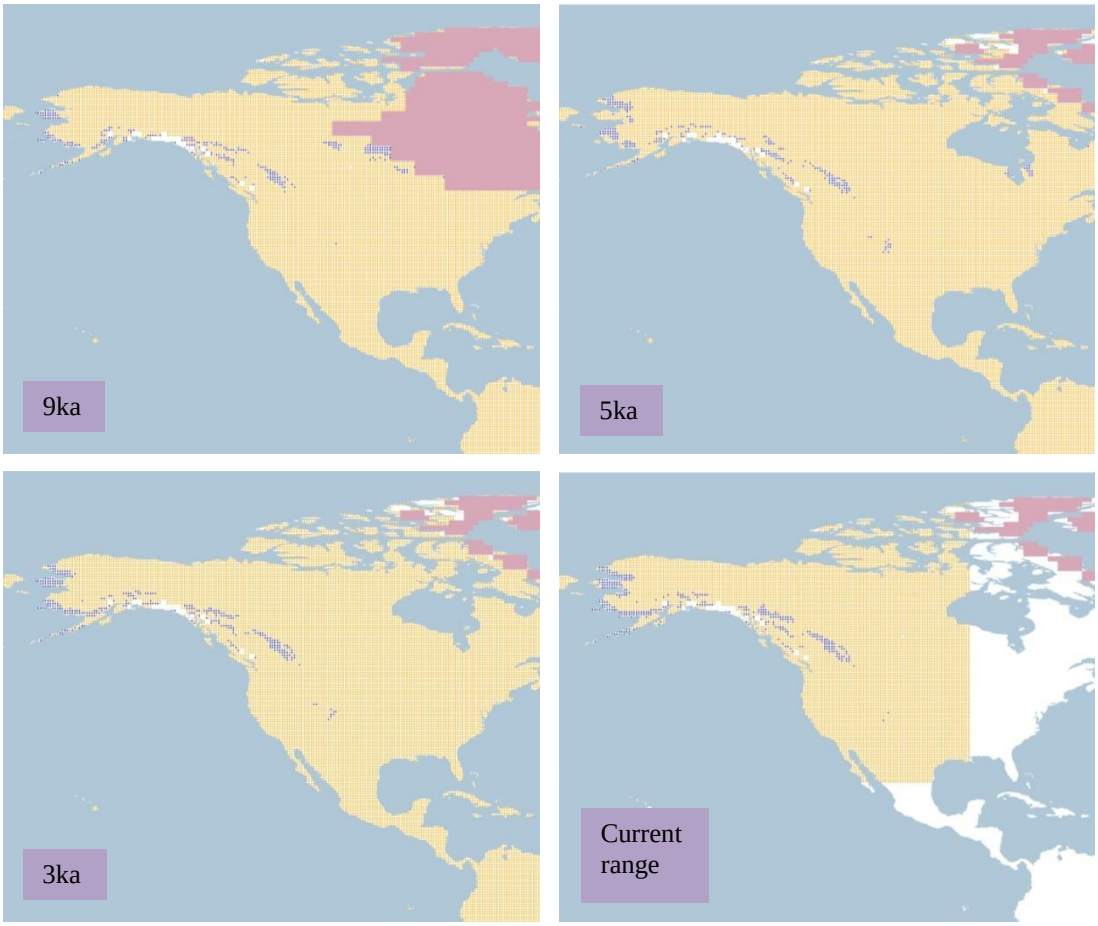

Figure 4.1.4.3.a. Simulation maps of Black Turnstone breeding range (continued**).**

Non-breeding range (AUC: 0.993; TSS: 0.920; Kappa: 0.870): This species spends the non-breeding season across the west coast of North America, from southern Alaska to north-western Mexico, and in the Gulf of California.

At 26 ka BP the projections begin with a range on the west coast of the USA, and the west coast of Mexico south to Sinaloa, also with a small inland range around the Great Salt Lake in the USA and in central Mexico. The same pattern continues only with minimal differences, and after 21ka the range projected around the Great Salt Lake and in central Mexico starts decreasing, maintaining mainly the west coast range. See Figure 4.1.4.3.b.

As the ice sheet retreats the range on the west coast of the USA moves north, specifically at the beginning of the Holocene (11ka) when the ice sheet is no longer covering the west part of Canada there is a projected range in that area. The pattern continues and at 10 ka BP there is a range covering the Aleutian Islands, followed by an increase on the west coast of Canada

and the conterminous USA at 7 ka BP. Afterwards the range remains constant until 1 ka BP and the projection of the current non-breeding range.

The H2 projection shows differences to the 24 ka BP projection having a larger extension across the central south of the USA and Mexico as well as Central America, the Greater Antilles and the north of South America. The same pattern remains at a smaller scale at H1 differing as well from 17 ka BP and at H0 the extent disappears from inland USA and Mexico but remains in the Greater Antilles, Central America and the north of South America.

Although the species does not occur in South America a range was projected across the west coast and around the Andean Cordillera in all the time slices.

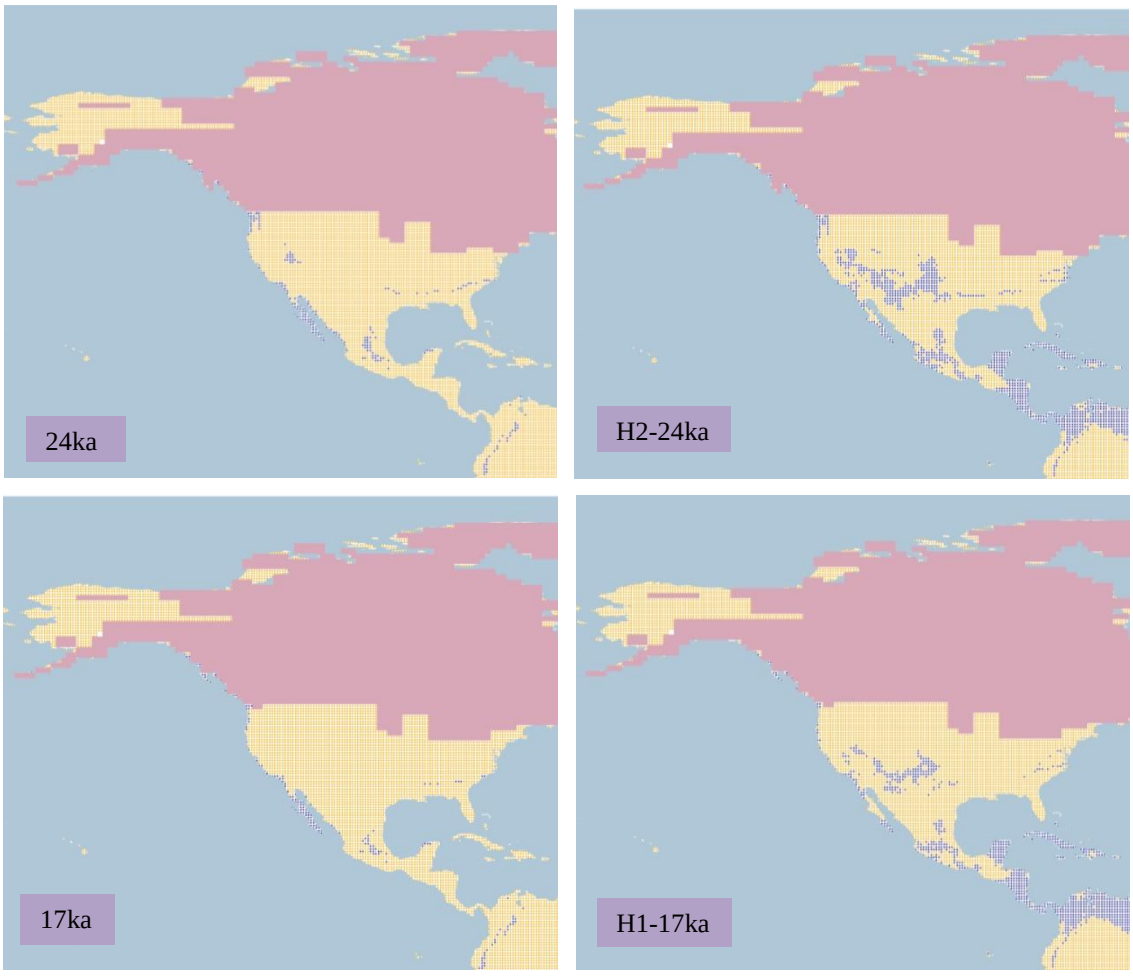

Figure 4.1.4.3.b. Simulation maps of Black Turnstone non-breeding range.
Maps are shown for ten-time slices: 24ka, H2 (24ka), 17ka, H1 (17ka), 13ka, H0 (13ka), 9ka, 5ka, 3ka and present (1961–90).

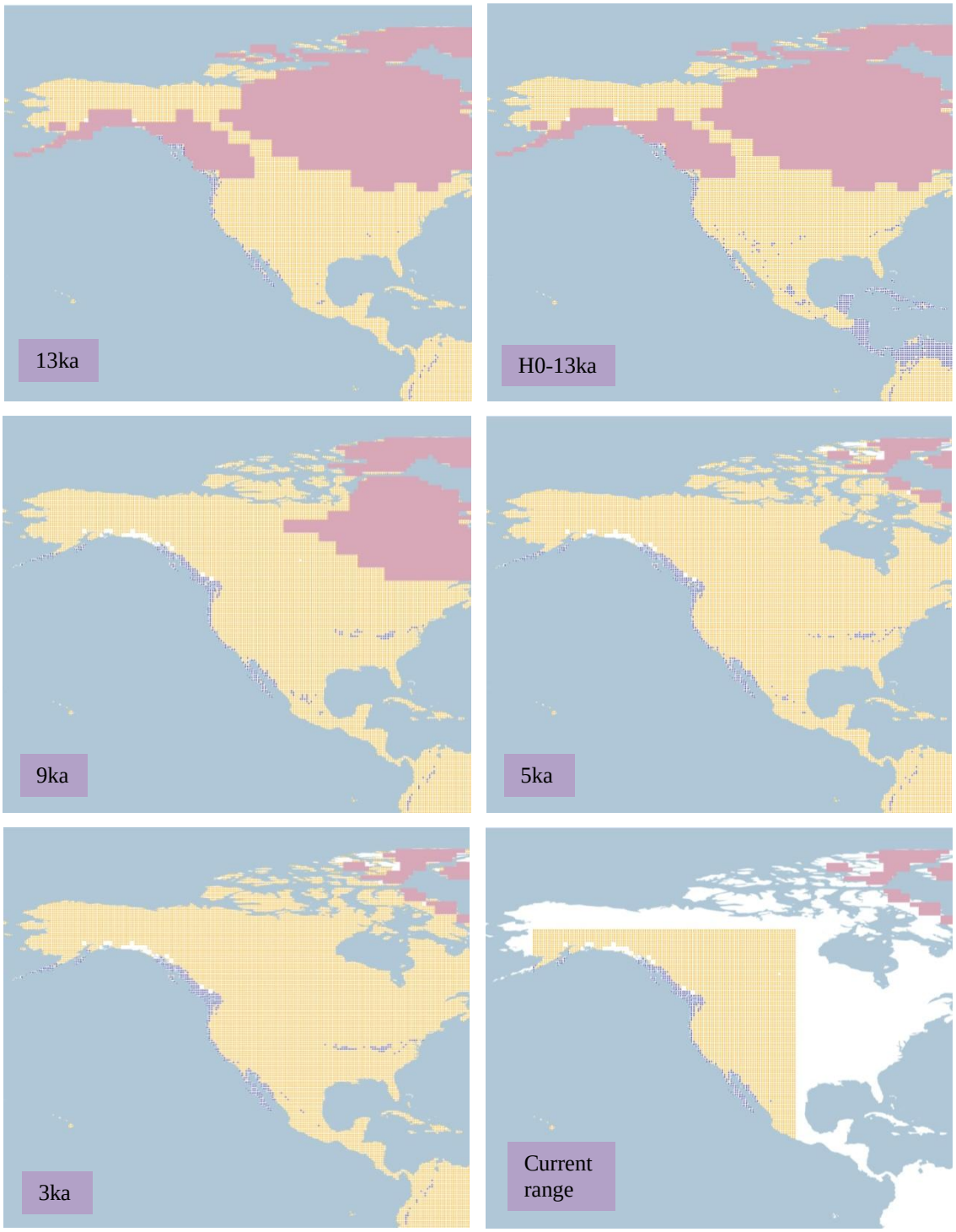

Figure 4.1.4.3.b. Simulation maps of Black Turnstone non-breeding range (continued**).**

*4.1.4.4 Upland Sandpiper (*Bartramia longicauda*). Conservation status: Least Concern. Current known range Figure 4.1.4.4.*

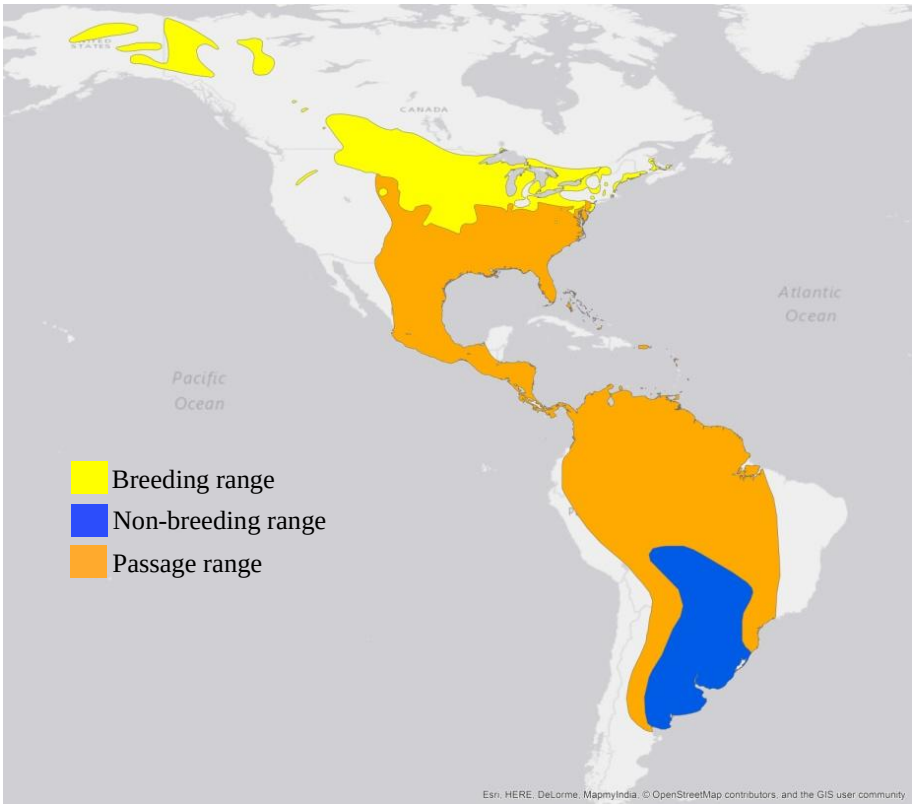

Figure 4.1.4.4. Current known range of Upland Sandpiper.

Breeding range (AUC: 0.962; TSS: 0.778; Kappa: 0.747): This species spends the breeding season in central-east Alaska, west and south-central Canada, the Great Plains in the USA, north-east to the Great Lakes and reaching southern Quebec and Pennsylvania.

The projected range at 26 ka BP extends across the central-east conterminous USA with a small extension across central Alaska. This pattern initially persists with small changes, mainly increasing in Alaska and in the north of the USA. At 18 ka BP there is a change with the Alaskan extent decreasing to a fragmented range in the north and in west Canada. Also at 17 ka BP the range across the USA increases to the north-west reaching the north of Idaho, and mainly at 14 ka BP the range increases to the central-south part of the USA as well as the north-west of Canada, and as the ice sheet retreats at 13 ka BP the range extends across the western part of Canada, decreasing in extent once again at 12 ka BP. See Figure 4.1.4.4.a.

From the beginning of the Holocene the range is focused mainly in the northern part of the conterminous USA with a smaller extension across the north-west of Canada, which begins decreasing after 9 ka BP. This pattern continues uniformly after 8 ka BP, remaining in the north-west of Canada and with a larger extent in the Great Plains of the USA, extending to reach the east coast in Maine and Nova Scotia in Canada by 1 ka BP and with the same projection in the current range.

The H2 projection shows differences with the 24 ka BP projection with a smaller extension in the east of the conterminous USA and a larger range in Alaska. This change at H1 with a decrease in the Alaskan extent and an increase in the east of the USA, differing from the 17 ka BP projection too. There are similarities between the H0 and 13 ka BP range projections, showing almost the same range only with a more extensive range in H0.

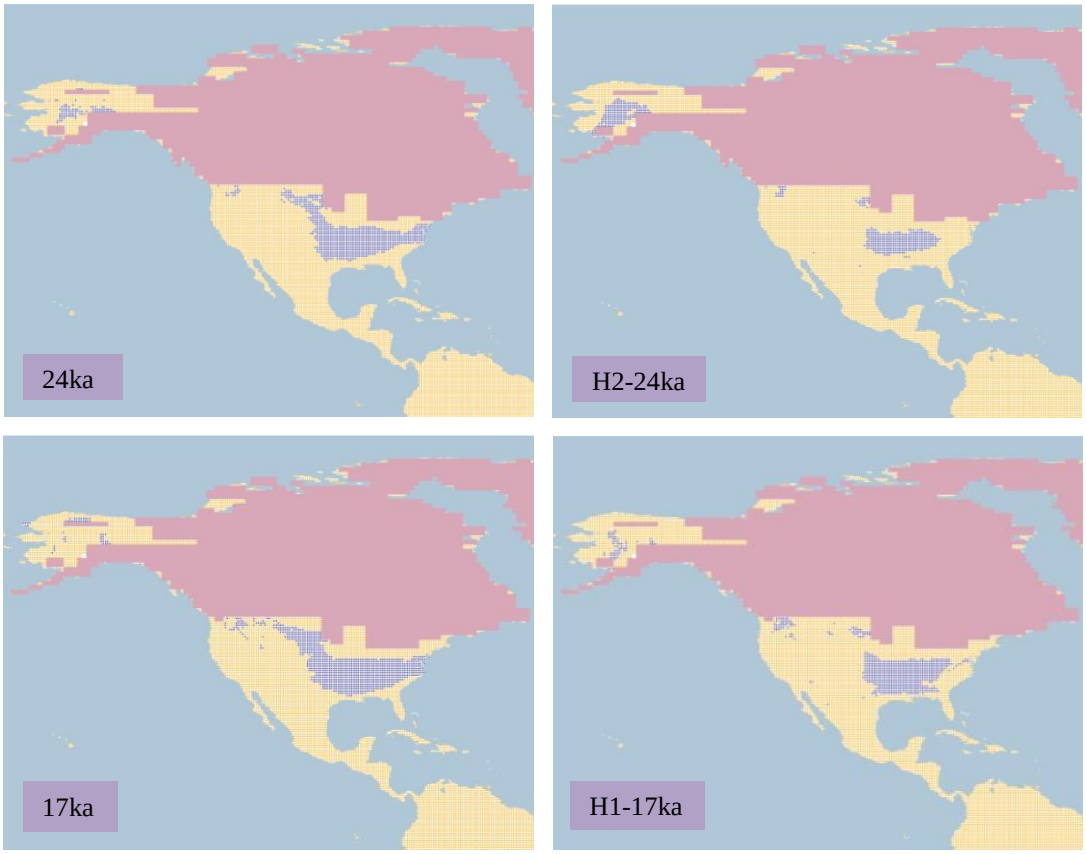

Figure 4.1.4.4.a. Simulation maps of Upland Sandpiper breeding range.
Maps are shown for ten-time slices: 24ka, H2 (24ka), 17ka, H1 (17ka), 13ka, H0 (13ka), 9ka, 5ka, 3ka and present (1961–90).

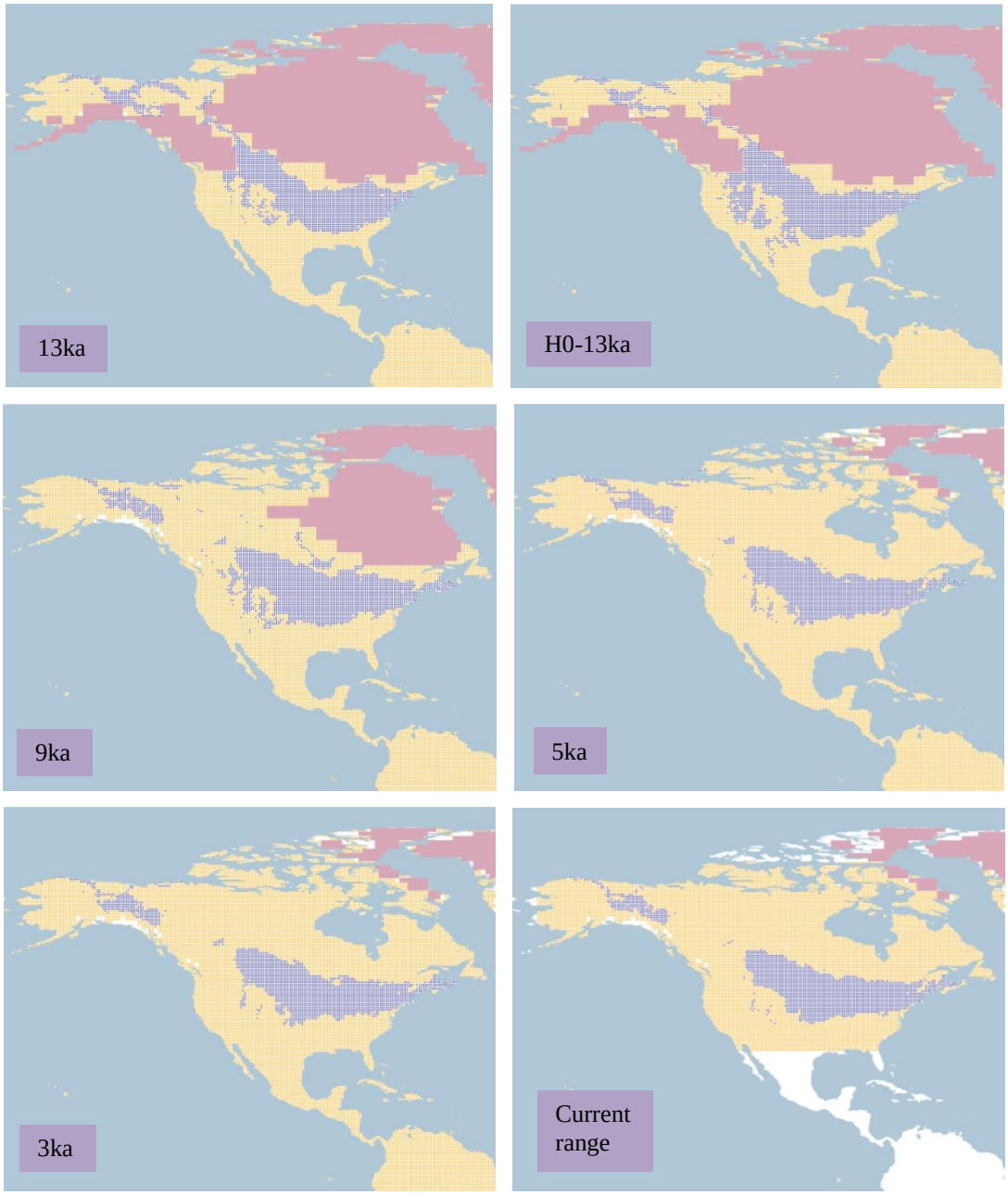

Figure 4.1.4.4.a. Simulation maps of Upland Sandpiper breeding range (continued**).**

Non-breeding range (AUC: 0.989; TSS: 0.912; Kappa: 0.800): The species winters in South America from central-east Bolivia, Paraguay, Uruguay and southern Brazil to the central-east of Argentina.

At 26 ka BP the range is projected to extend from south-central Brazil to Bolivia, Paraguay, Uruguay and as far as central Argentina. At 22 ka BP there is a decrease in this range mainly in the central part of Brazil, concentrating the extension to south Brazil instead of central. This pattern changes at 21ka growing again to central Brazil, remaining with small

changes until 18 ka BP when the range in central Brazil shifts to the north and persists until 16ka. Between 15 ka BP and 14 ka BP there is a decrease in the area projected in north-central Brazil which grows later from 13 ka BP. See Figure 4.1.4.4.b.

At the beginning of the Holocene the range remains similar to past projections and particularly at 10 ka BP the range in north Brazil reaches its northern extent in Amapá. There is an increase in the territory from 8 ka BP to 6 ka BP, with a projection across the north-central part of Brazil into central Argentina. This changes from 5 ka BP onwards when the northern range in Brazil disperses to the central region; the same pattern remains from central south Brazil to central Argentina analogous to the current non-breeding range projection.

The H2 projection seems similar to 24 ka BP in the region of South America except for a small range extending to the north part of Brazil and with a projected range over the north-east of Mexico and the south-east of USA. This pattern is shown at H1 as well only with a slightly smaller extent, and similar to 17 ka BP in the region of South America. In the H0 projection there is a dramatic change in the territory of South America, restricting the range to the central-east area from south Brazil to east Argentina, and also with a projected range across the east of Mexico and south-east of the USA.

Although the wintering grounds are located in South America there are suitable conditions predicted on the east coast of Central America and in south Florida throughout the projections.

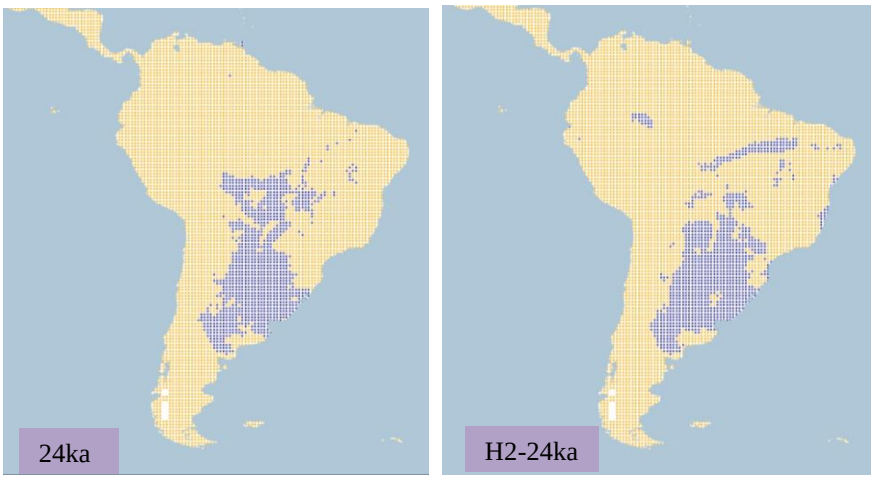

Figure 4.1.4.4.b. Simulation maps of Upland Sandpiper non-breeding range.
Maps are shown for ten-time slices: 24ka, H2 (24ka), 17ka, H1 (17ka), 13ka, H0 (13ka), 9ka, 5ka, 3ka and present (1961–90).

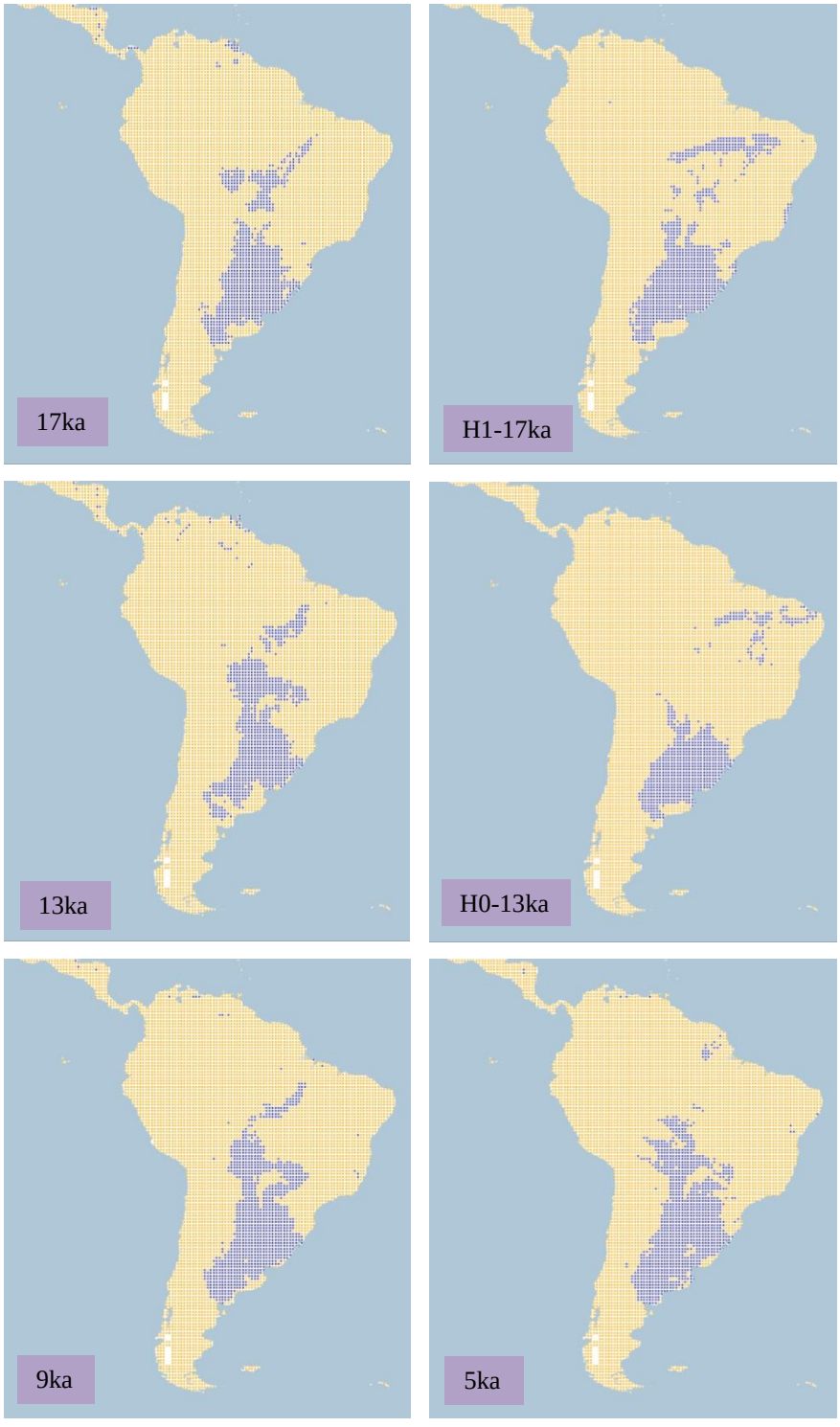

Figure 4.1.4.4.b. Simulation maps of Upland Sandpiper non-breeding range (continued**).**

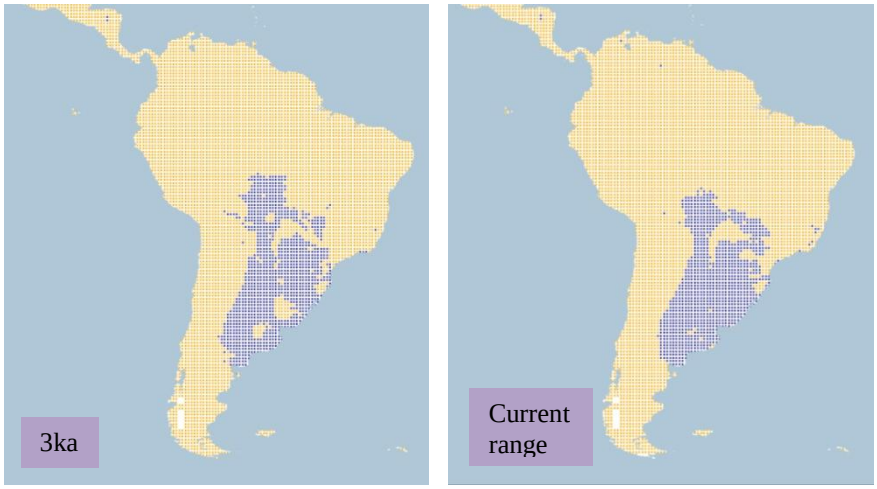

Figure 4.1.4.4.b. Simulation maps of Upland Sandpiper non-breeding range (continued**).**

*4.1.4.5 Sanderling (*Calidris alba *including* C. a. alba *and* C. a. rubida*). Conservation status: Least Concern. Current known range Figure 4.1.4.5.*

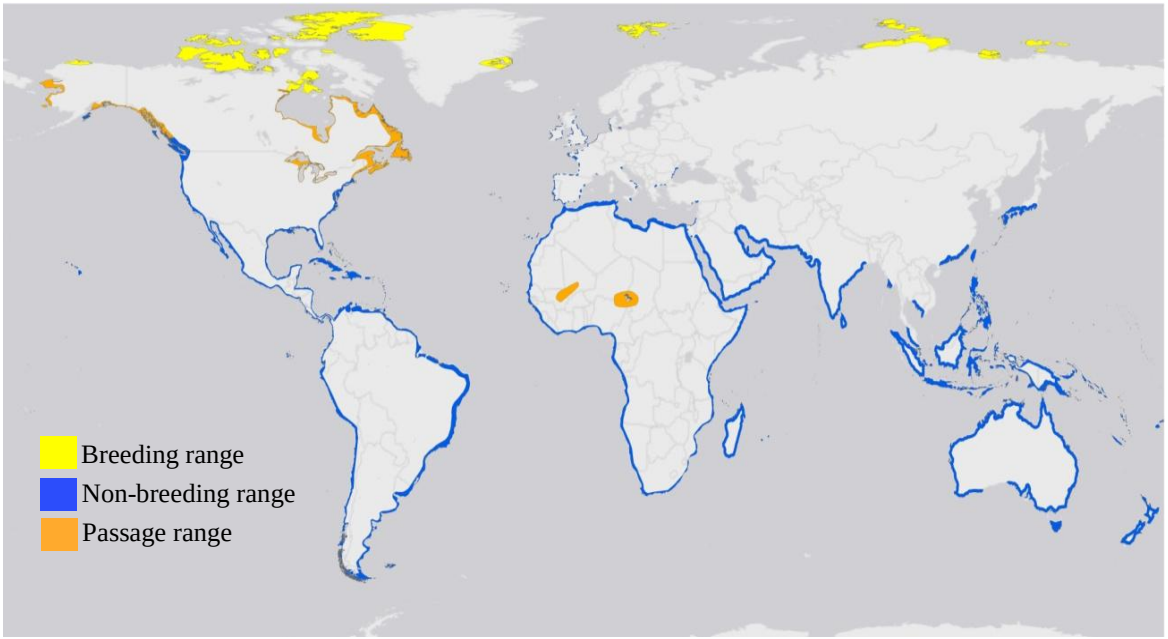

Figure 4.1.4.5. Current known range of Sanderling.

Breeding range (AUC: 0.991; TSS: 0.943; Kappa: 0.653): This species has a breeding range in high Arctic regions, from northern Alaska, the Canadian Islands and the west and east

coast of Greenland in North America and in Eurasia from the Svalbard archipelago to the north-east of Siberia.

The range at 26 ka BP is projected in the high latitude regions of the Northern Hemisphere, from the north of Alaska and Canada in the areas not covered by the ice sheet and also a small part in central-north USA. There is also a large range projected across the north of Russia, with a dispersed range moving to central territories. This pattern remains until 19 ka BP when the range in the north-west of Russia near the ice sheet starts decreasing and the central range shifts to a northern range. This specially changes at 17 ka BP when the territory is reduced in central-north and north-west of Russia with the dissipation of the range near the ice sheet at 16 ka BP and reduction of the north-east range in Russia at 15 ka BP. At this period the range in North America remains similar. See Figure 4.1.4.5.a.

At 14 ka BP there is an increase in the northern range of Russia and in North America the range declines and is restricted to the coastal areas in the north. After this there is an increase in the North American range and a decrease in the Eurasia range at 13 ka BP which is followed at 12 ka BP by a reduction of both North American and Russian ranges which become limited to the northern parts.

In the beginning of the Holocene the range follows a similar pattern and as the ice sheet retreats in North America the range covers the Canadian Islands. At 9 ka BP there is a growth in the north-east part of Russia extending inland, as well as in the north of Canada. This distribution remains constant only with minor changes until 1 ka BP and is also similar to the projection of the current breeding range.

The range in the H2 projection shows differences from 24 ka BP mainly in the area of Russia where the range is wider from central to north-east Russia. A similar pattern remains at H1 with a slightly small range over the north-east of Russia, which is different from the 17 ka BP projection. The North American range projected at H0 is similar to the 13 ka BP projection; however, the range in Russia extends across a larger area from central-east to north-east at H0 which is different from 13 ka BP.

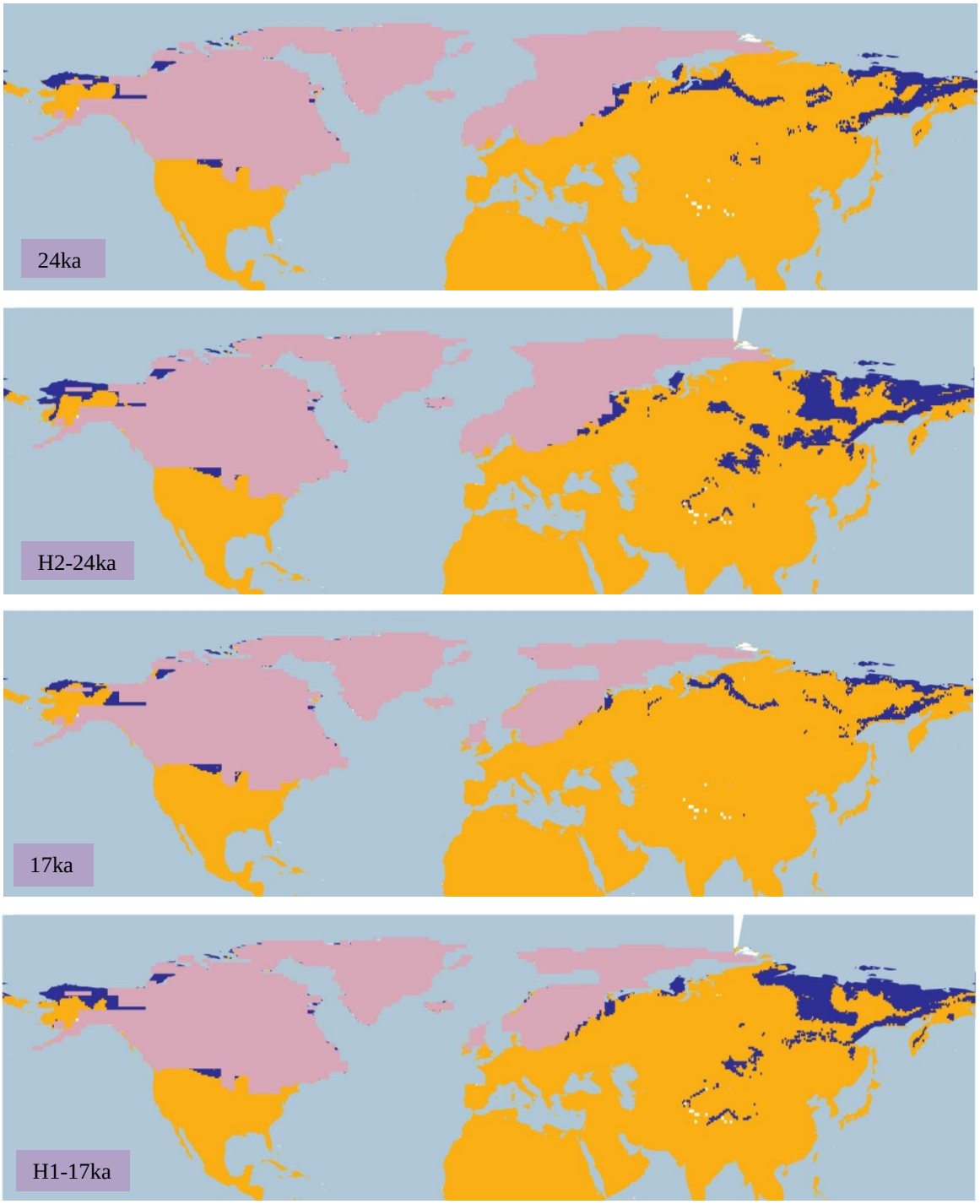

Figure 4.1.4.5.a. Simulation maps of Sanderling breeding range.
Maps are shown for ten-time slices: 24ka, H2 (24ka), 17ka, H1 (17ka), 13ka, H0 (13ka), 9ka, 5ka, 3ka and present (1961–90).

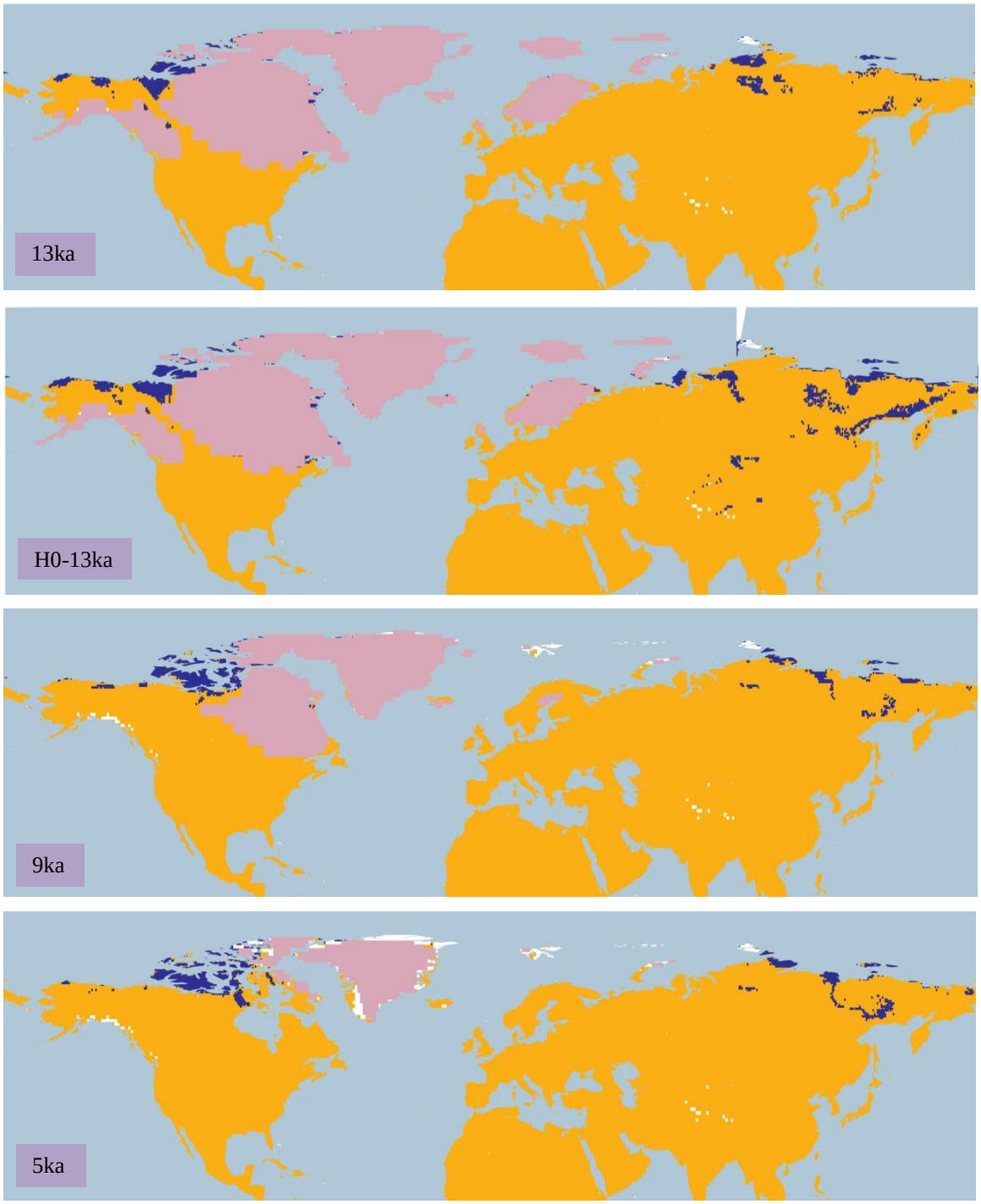

Figure 4.1.4.5.a. Simulation maps of Sanderling breeding range (continued**).**

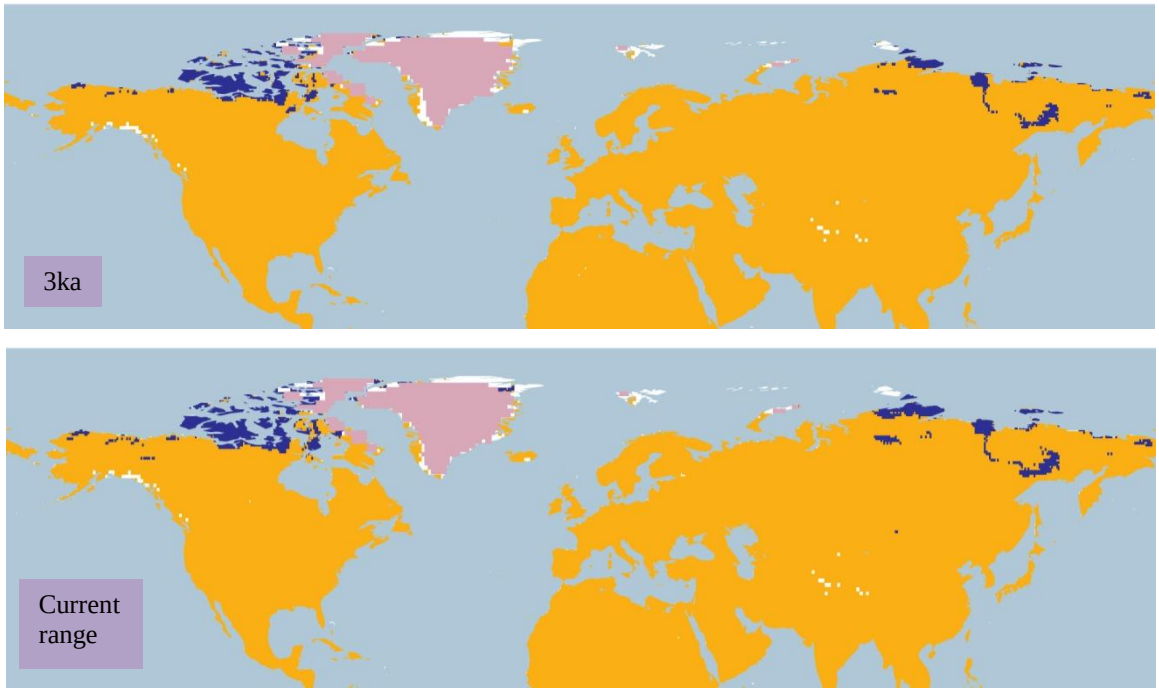

Figure 4.1.4.5.a. Simulation maps of Sanderling breeding range (continued**).**

Non-breeding range (AUC: 0.949; TSS: 0.776; Kappa: 0.592): The wintering grounds of the species are along the coastal areas of North America from the south of British Columbia in Canada and the coast of Massachusetts in the USA, as far as Tierra del Fuego in South America and including the Greater Antilles and the Galapagos Islands. Also along the coasts of the African continent, the south of Asia from Saudi Arabia to India, Indonesia and the south of Japan, as well as Papua New Guinea, Australia and New Zealand. In addition, there is a fragmented range around the coasts of Europe from Portugal to Denmark and Great Britain, and a smaller range in Italy, Greece and Ukraine.

At 26 ka BP the range is projected to extend along the west coast of the USA, Mexico and South America with a large inland range in north-western and south-eastern South America. The range is also projected in Europe, along the north-western and south-western coast of Africa, with an inland range across central-northern Africa. There is also a small range projected in southern Asia and along the coastal area of Australia. This pattern continues until 22 ka BP when the range in the Amazonian region in South America increases. After this at 17 ka BP there is a small increase in northern Australia, and a decrease in northern South America. See Figure 4.1.4.5.b.

With the deglaciation at 13 ka BP the range in South America, Africa and Australia increases, with a projected range in the United Kingdom. At 10 ka BP the ranges on the western coast of Canada and in the United Kingdom increase, covering all the territory at 8 ka BP. After this the range continues with minimal variation in the inland regions of South America and Africa until ka BP, when the range in northern South America and in central-northern Africa reduces. This pattern of decrease in the inland regions continues until 1 ka BP. A similar range is projected in the current non-breeding projection, although with a smaller range in north-western South America but a larger range in India.

When comparing H2 to 24 ka BP, a smaller range is projected in Australia, Asia, Europe and North America, with a larger range in northern South America and north-western Africa. At H1 the range increases in north-western Africa and central South America, still with a larger range projected than at 17ka. At H0 a scattered range is projected in South America, increasing in Australia, Asia and southern Africa.

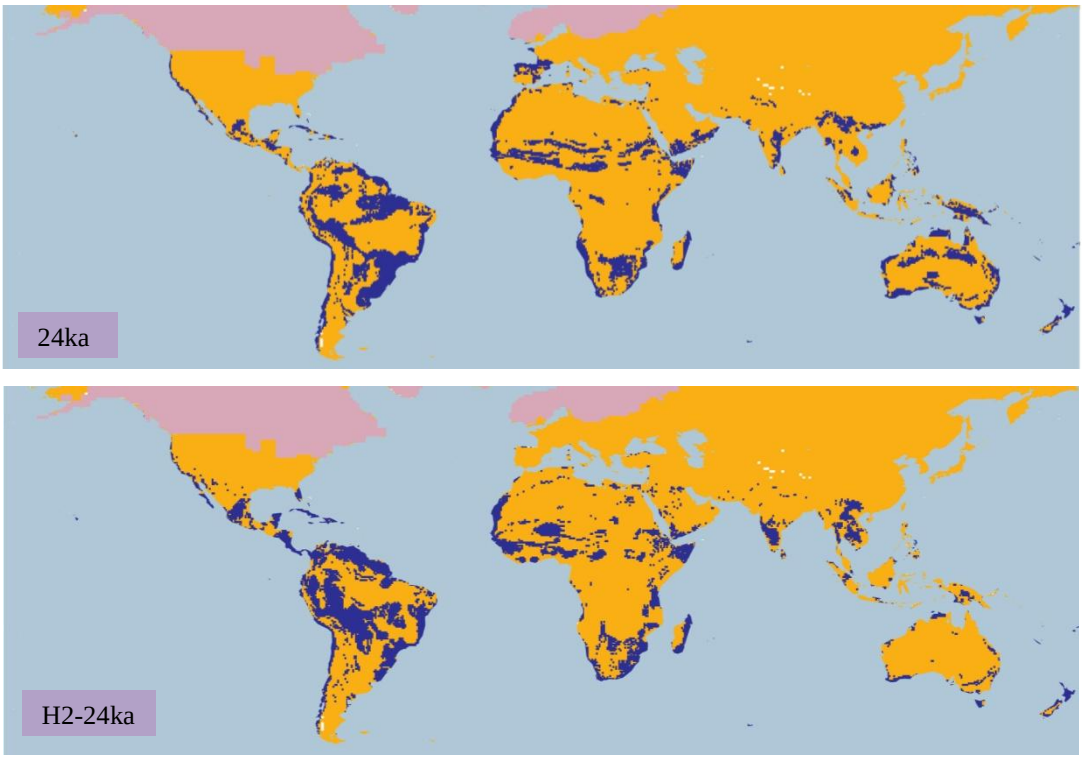

Figure 4.1.4.5.b. Simulation maps of Sanderling non-breeding range.
Maps are shown for ten-time slices: 24ka, H2 (24ka), 17ka, H1 (17ka), 13ka, H0 (13ka), 9ka, 5ka, 3ka and present (1961–90).

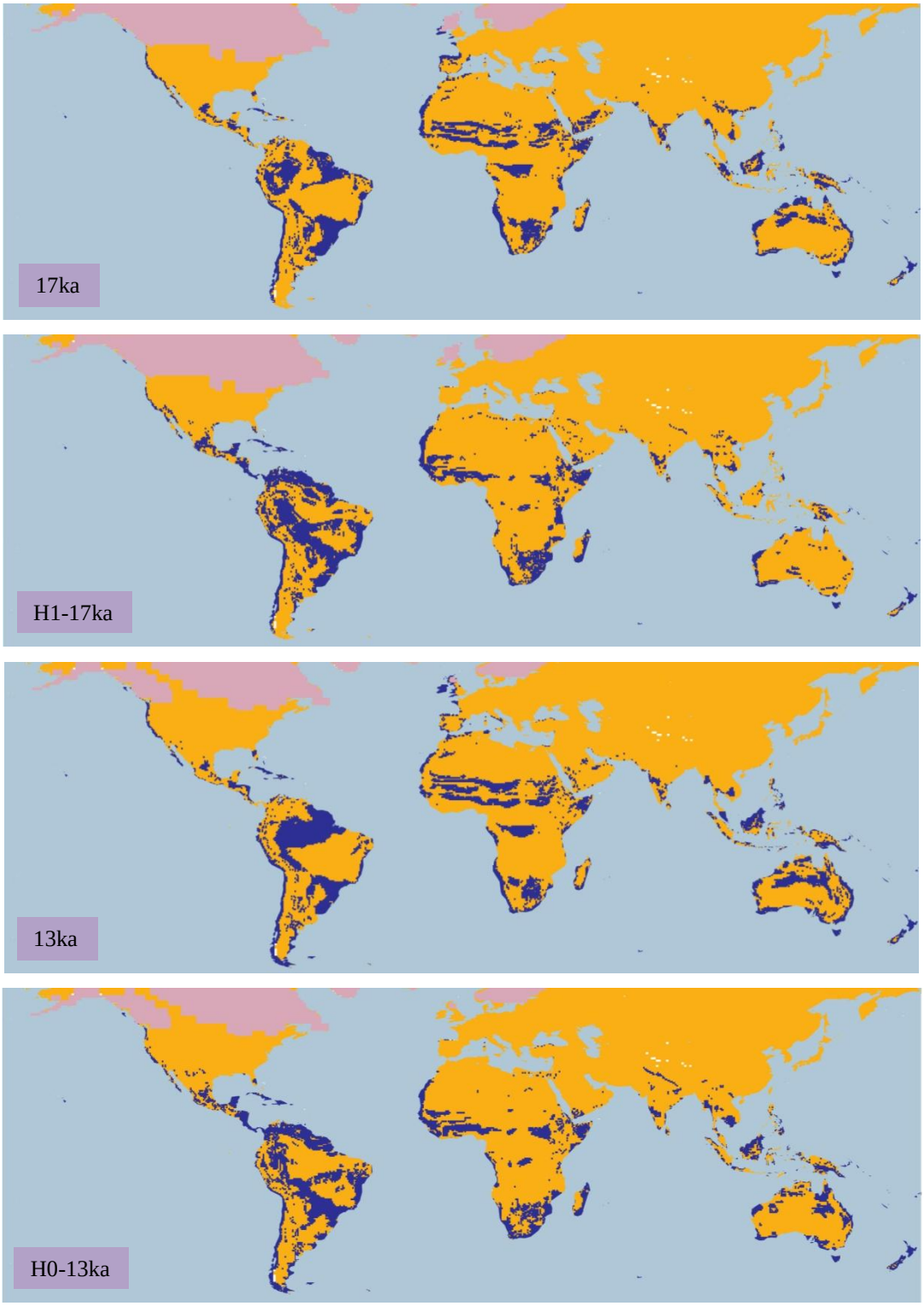

Figure 4.1.4.5.b. Simulation maps of Sanderling non-breeding range (continued**).**

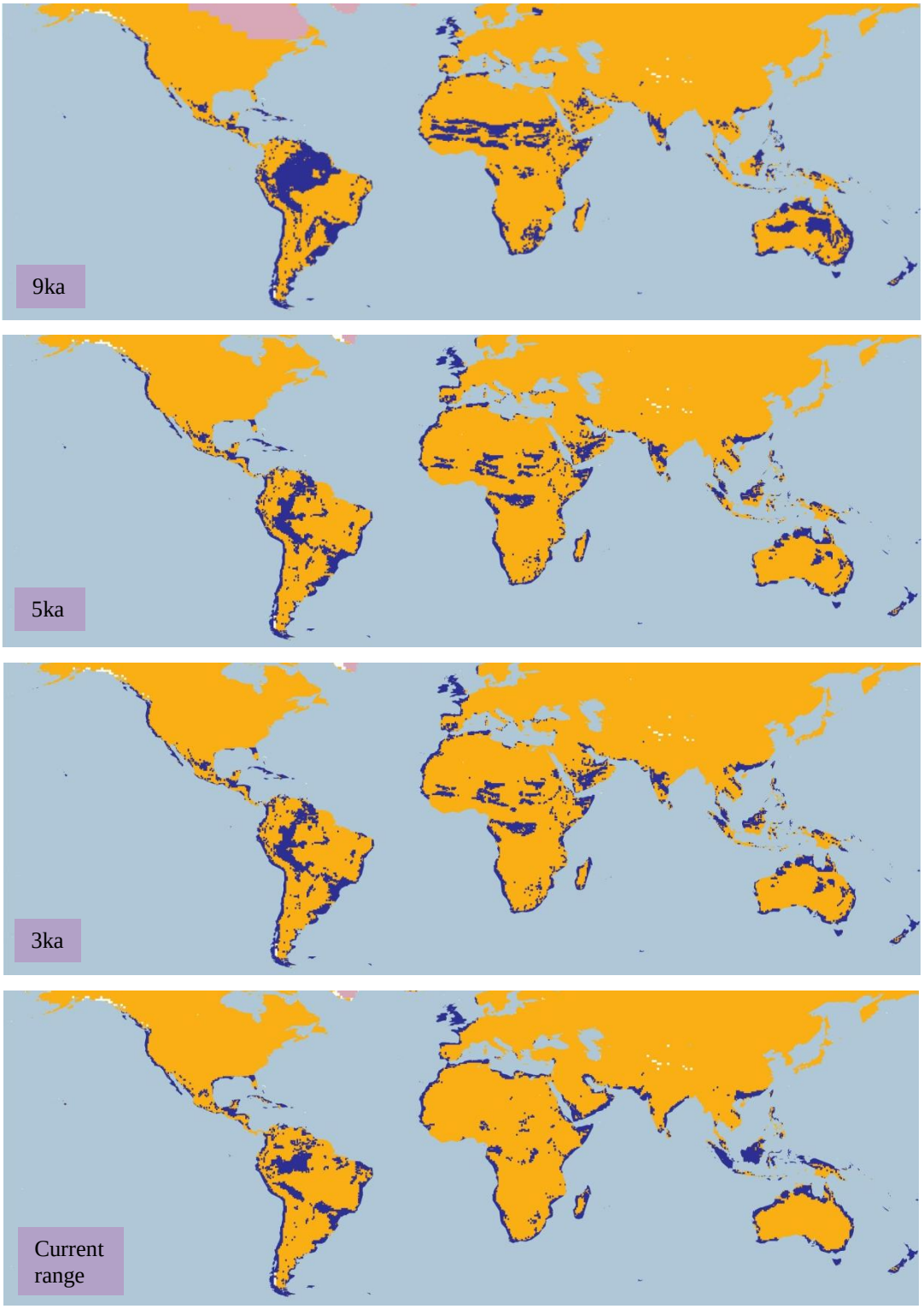

Figure 4.1.4.5.b. Simulation maps of Sanderling non-breeding range (continued**).**

*4.1.4.6 Dunlin (*Calidris alpina hudsonia*). Conservation status: Least Concern. Current known range Figure 4.1.4.6.*

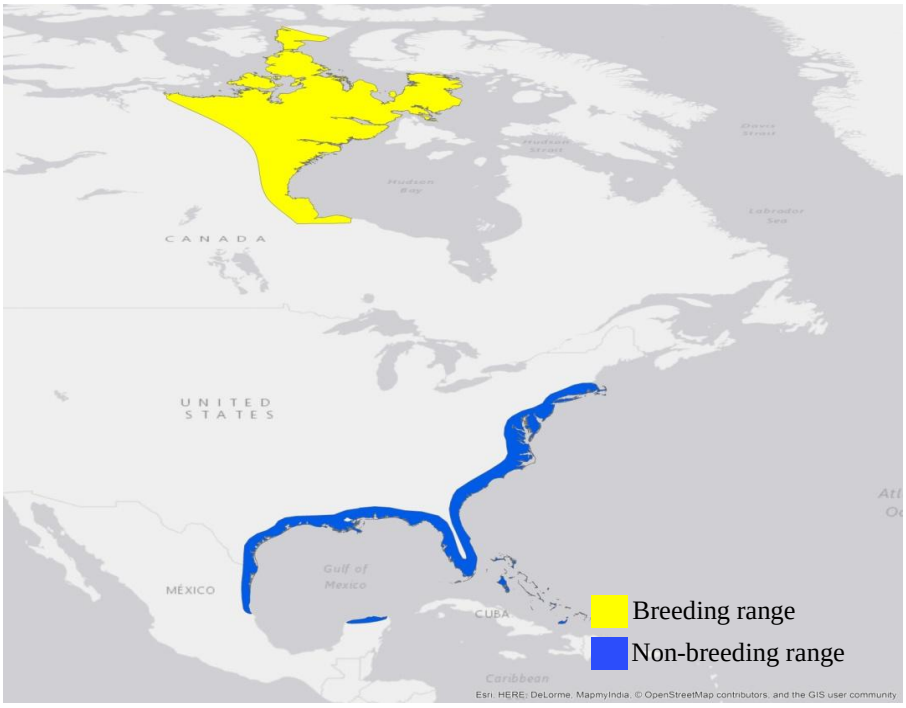

Figure 4.1.4.6. Current known range of Dunlin, subspecies *C. a. hudsonia*.

Breeding range (AUC: 0.966; TSS: 0.870; Kappa: 0.602). This sub-species has a small breeding range in the north of Canada, from the coast of Manitoba to Nunavut as far as Somerset Island.

The range at 26 ka BP is projected mainly from western Alaska in the USA to eastern Chukotka in Russia, with a smaller range near the ice sheet in the central-northern conterminous USA between North Dakota and Wisconsin. This pattern continues and at 20 ka BP the range in western Alaska and eastern Chukotka is decreased. After this at 19 ka BP the range in the region of Alaska and Chukotka increases remaining unchanged until 15 ka BP, when the range in Russia is decreased to a minimal coastal range and with the range in the central-northern conterminous USA disappearing. See Figure 4.1.4.6.a.

With the deglaciation at 13 ka BP, the range increases in Alaska and is also projected in Canada in small patches, between Yukon and Northwest Territories, in southern Ontario and in New Brunswick and southern Quebec, extending to the north-eastern USA in Maine and Vermont. At 12 ka BP this pattern continues in Canada with a projected range in northern

Northwest Territories and an increasing range in western Alaska in the USA. By the beginning of the Holocene, the range in Alaska is reduced to a small eastern range, as well as the range in northern Northwest Territories and south-eastern Canada. By 9ka, the range in northern Northwest Territories shifts to northern Nunavut and especially at 8 ka BP the inland range in Nunavut is increased as well as on some islands of the Arctic Archipelago not covered by the ice sheet.

At 7 ka BP the range in Nunavut is increased and shifts to the east near Hudson Bay, also with a large range on Baffin Island in the areas not covered by the ice sheet. By 6 ka BP the range in Baffin Island is reduced and the range in Nunavut increases covering most of the continental area and reaching the Northwest Territories boundaries. This pattern continues until ka BP, when a range is projected in eastern Canada between Quebec and Newfoundland and Labrador. The current breeding range follows the same pattern as 1 ka BP in the area of Nunavut and the Arctic Archipelago, although there is no projected range in eastern Canada.

The Heinrich event H2 and the 24 ka BP projections present similar ranges projected near the ice sheet in central-northern USA between North Dakota and Wisconsin, only with a larger range at H2 in North Dakota in the area of Lake Sakakawea. Also, a smaller range is projected in Alaska in the H2 projection. There are differences between the H1 and 17 ka BP projection, with a scattered range projected in Alaska and a smaller range in Wisconsin at H1. However, a similar pattern is displayed between the H0 and 13 ka BP projections for the areas of Canada, only with a smaller range projected in Alaska at H0.

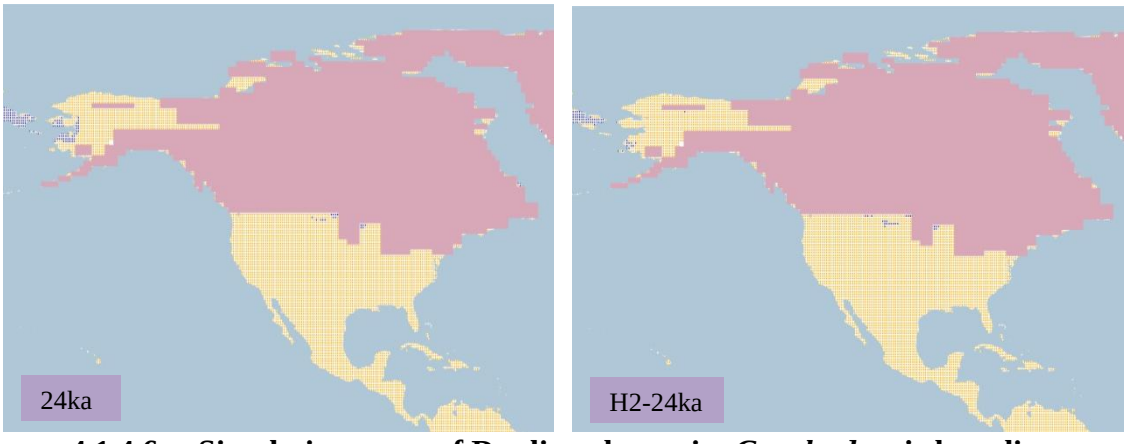

Figure 4.1.4.6.a. Simulation maps of Dunlin sub-species *C. a. hudsonia* breeding range. Maps are shown for ten-time slices: 24ka, H2 (24ka), 17ka, H1 (17ka), 13ka, H0 (13ka), 9ka, 5ka, 3ka and present (1961–90).

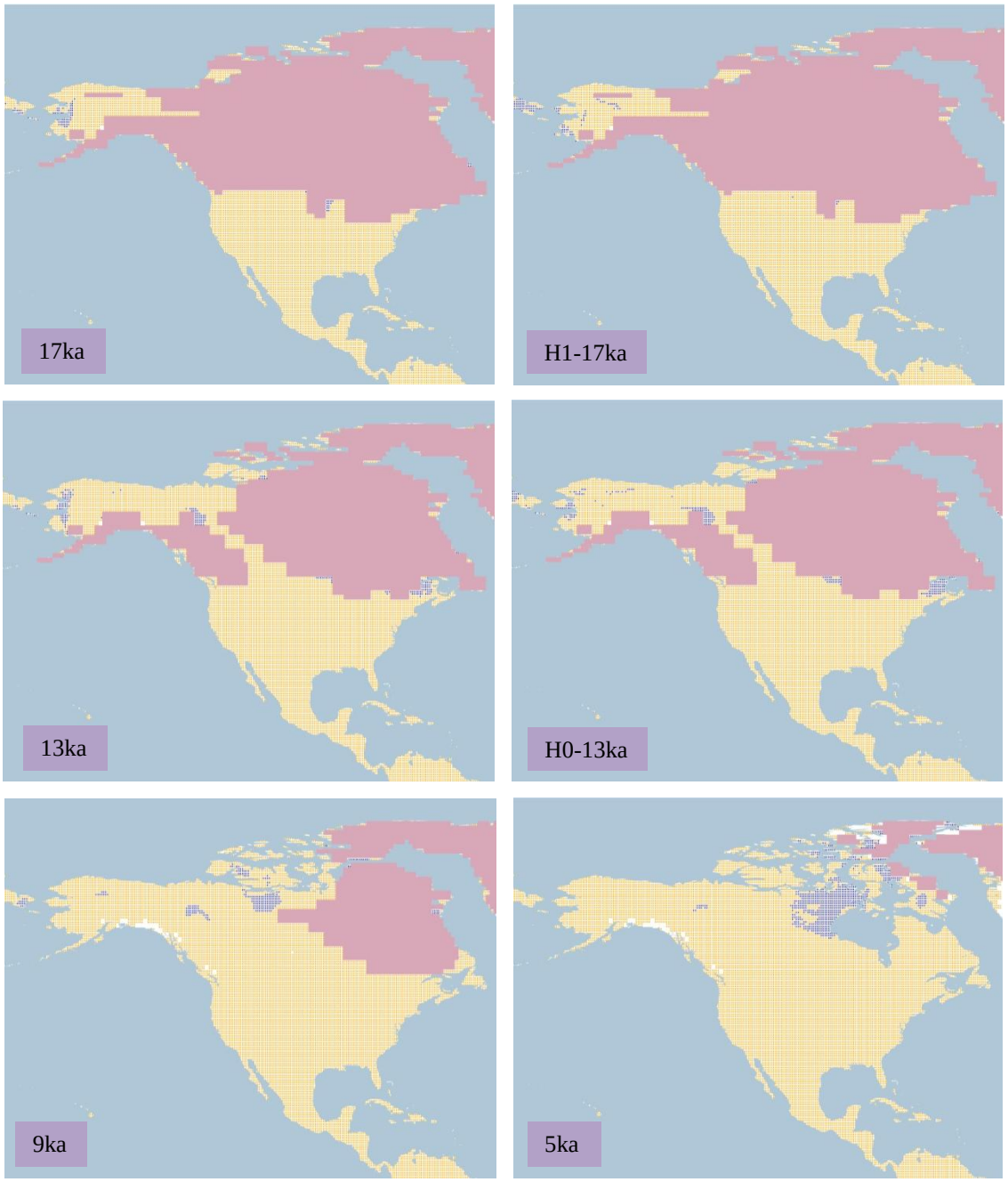

Figure 4.1.4.6.a. Simulation maps of Dunlin sub-species *C. a. hudsonia* breeding range (continued**).**

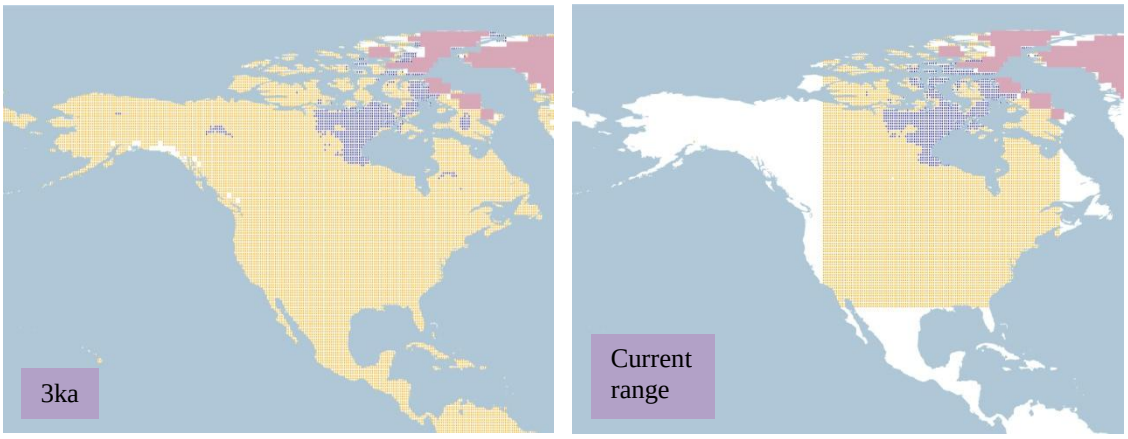

Figure 4.1.4.6.a. Simulation maps of Dunlin sub-species *C. a. hudsonia* breeding range (continued**).**

Non-breeding range (AUC: 0.960; TSS: 0.816; Kappa: 0.617): The wintering grounds of this sub-species are located along the east coast of the USA, from Massachusetts to Texas, and in the north-east of Mexico along the coast of Tamaulipas and on the north coast of Yucatan, with a small range also in the Bahamas.

At 26 ka BP the range is projected mainly in Florida in the USA, a scattered range along the eastern coast of Mexico and in central-eastern South America, between southern Brazil, Bolivia, Paraguay and northern Argentina. This pattern continues and at 22 ka BP the range in South America, especially in southern Brazil, is increased, with a reduced range after this at 21 ka BP. This reducing trend continues in South America at 19 ka BP, between Paraguay and southern Brazil. See Figure 4.1.4.6.b.

At 17 ka BP the range on the eastern coast of Mexico is increased as well as that in southern Brazil, and especially at 15 ka BP the range on the eastern coast of Mexico reaches Yucatan. This pattern continues and by the beginning of the Holocene at 11 ka BP a range is projected on the south-eastern coast of the USA. By 9ka, the range in North America covers the eastern coast of Mexico and south-eastern coast of the USA; the range in South America is increased in southern Brazil as far as northern Argentina and with a small projected range in north-eastern Brazil.

At 8 ka BP an inland eastern range is projected in the USA between Kentucky and Virginia, followed by the range on the eastern coast of the USA extending from Massachusetts to Texas and in eastern Mexico as far as Veracruz. This pattern continues until ka BP, when the range in eastern USA is increased, extending from Indiana to Massachusetts and from

Mississippi to Delaware, as well as along the eastern coast from North Carolina to Texas and as far as northern Veracruz on the eastern coast of Mexico. The range in South America continues with the same pattern. The current non-breeding range projection follows the 1 ka BP projection on the eastern coast of the USA and Mexico, with a smaller range in eastern inland USA than at the 1 ka BP projection.

A different pattern is found between the H2 and 24 ka BP projection, mainly in North America, with a scattered range at H2 in central and eastern USA, no range projected in Mexico and a larger range in central-eastern South America. These differences continue between the H1 and 17 ka BP projections, with the range in North America mainly projected in eastern USA. The H0 and 13 ka BP projections present a similar range projected on the eastern coast of Mexico only, differing from the range in south-central USA and north-western Mexico projected at H0.

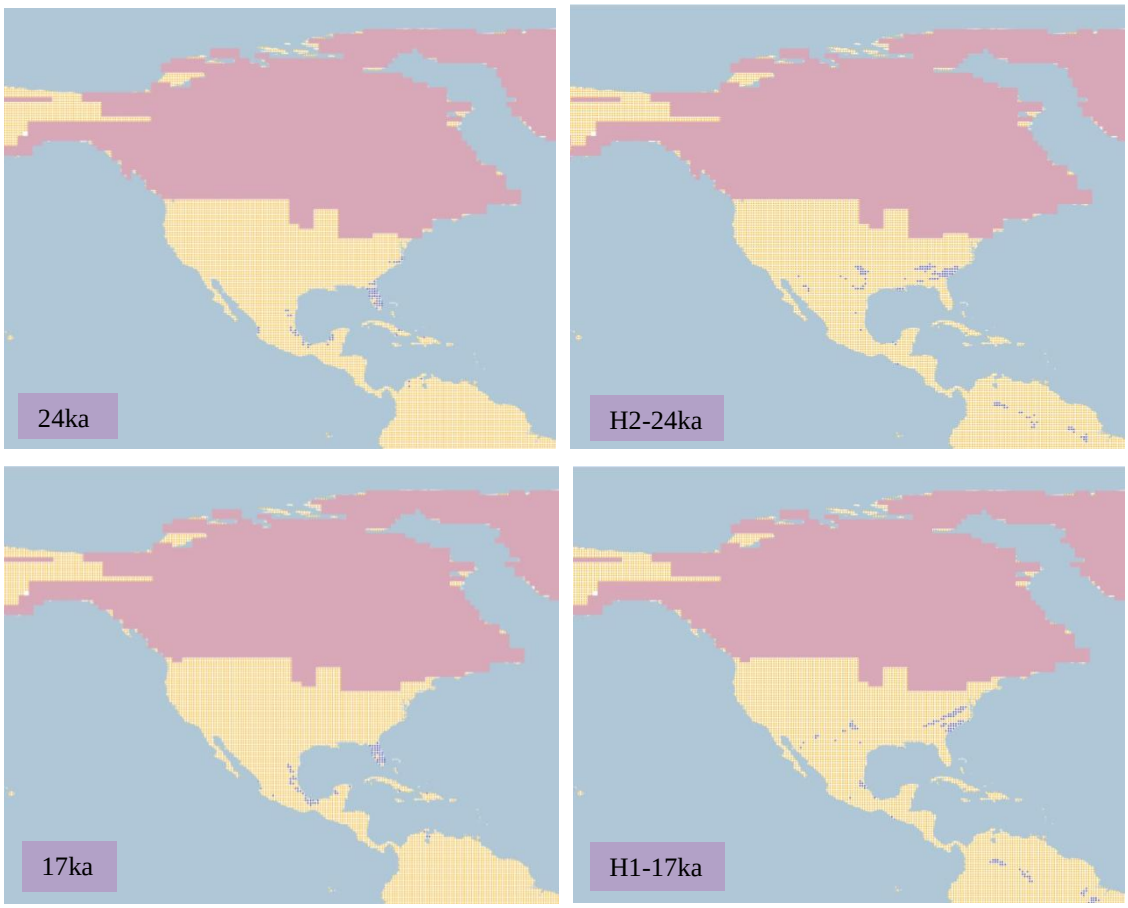

Figure 4.1.4.6.b. Simulation maps of Dunlin sub-species *C. a. hudsonia* non-breeding range.
Maps are shown for ten-time slices: 24ka, H2 (24ka), 17ka, H1 (17ka), 13ka, H0 (13ka), 9ka, 5ka, 3ka and present (1961–90).

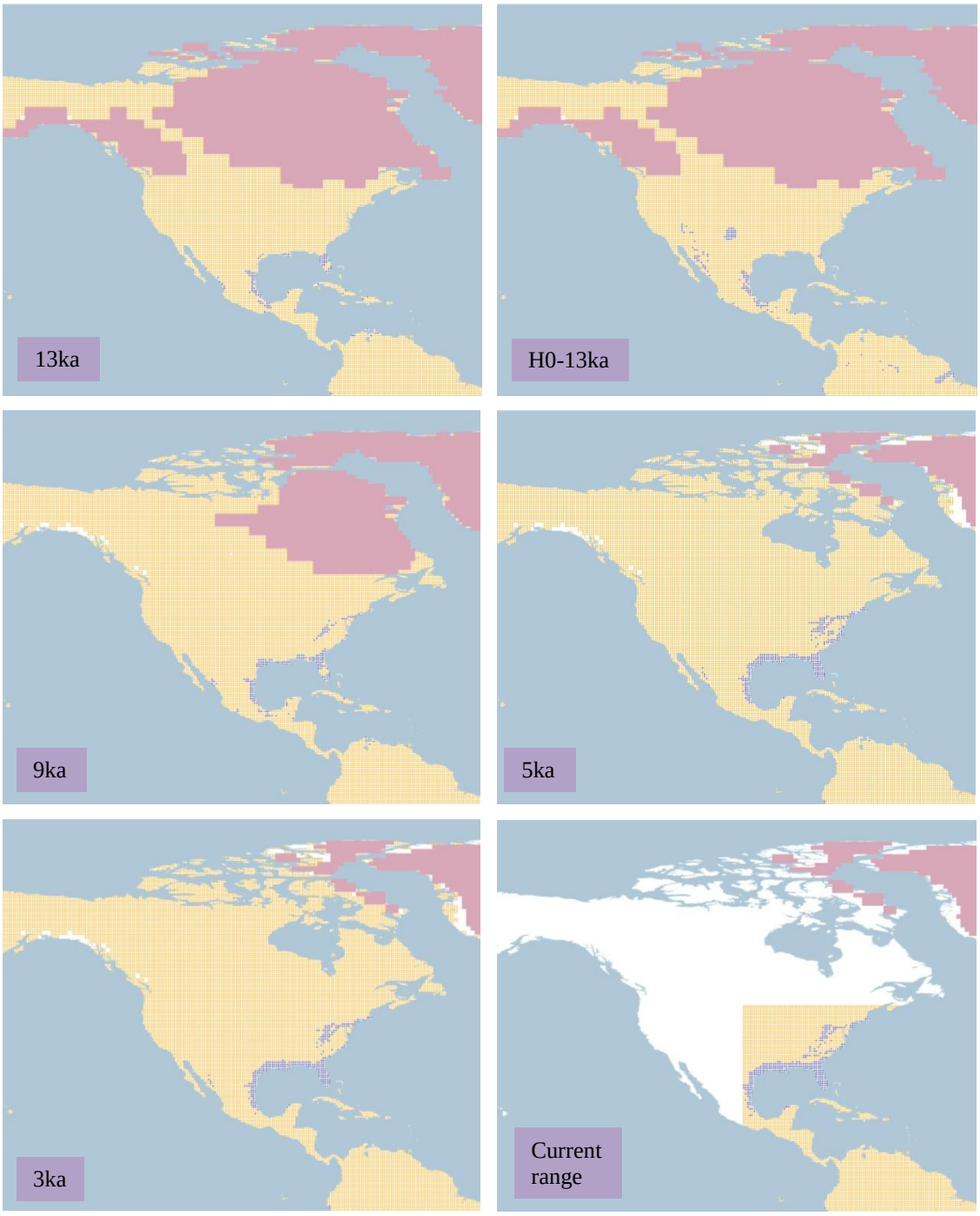

Figure 4.1.4.6.b. Simulation maps of Dunlin sub-species *C. a. hudsonia* non-breeding range (continued**).**

*4.1.4.7 Dunlin (*Calidris alpina pacifica*). Conservation status: Least Concern. Current known range Figure 4.1.4.7.*

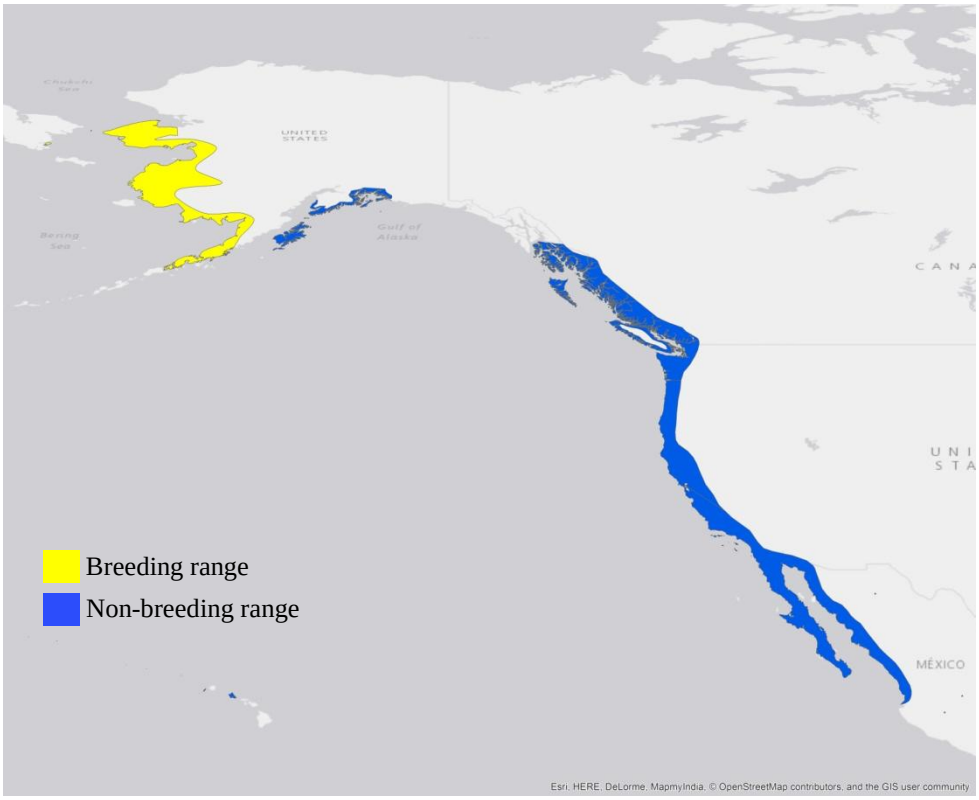

Figure 4.1.4.7. Current known range of Dunlin, subspecies *C. a. pacifica***.**

Breeding range (AUC: 0.951; TSS: 0.820; Kappa: 0.500): This sub-species' breeding range is located on the west coast of Alaska, from Nome to the south-west region as far as the Alaskan Peninsula.

At 26 ka BP a small range is projected in Utah and from Indiana to New York in the conterminous USA, with a small range in southern Alaska as well. At 24 ka BP the range in Utah disappears and returns at 22 ka BP. After 21ka the range in Utah disappears. See Figure 4.1.4.7.a.

At 19 ka BP a small range is projected along the Rocky Mountains of Montana and between Indiana and Pennsylvania. After this, as the ice sheet melts, the range in western USA decreases and the range in the eastern region shifts between Pennsylvania and Massachusetts.

The range in southern Alaska is increased during this time frame. This pattern continues and by 15 ka BP the range in the conterminous USA disappears.

During the deglaciation at 13 ka BP, the range is restricted to southern Alaska in the USA. After this, at 12 ka BP, a scattered range is projected in southern British Columbia in Canada. By the beginning of the Holocene at 11 ka BP, the range is projected from southern Alaska to northern British Columbia and southern Alberta in Canada. This pattern continues and at 9 ka BP the range projected in Alaska, British Columbia and Alberta increases.

At 8 ka BP there is a range projected between Ontario and Quebec near Hudson Bay and in Newfoundland and Labrador in Canada. This range is decreased at 7 ka BP, and instead the range projected in Alaska increases in the western region. The pattern continues with an increase in Newfoundland and Labrador at 5 ka BP.

The range projected in eastern Canada is decreased by ka BP, remaining principally in northern British Columbia and south-western Alaska. This pattern continues with a slight decrease until ka BP, covering south-western Alaska in the USA, and northern British Columbia and Newfoundland and Labrador in Canada. The current breeding range projection continues with the pattern as the 1 ka BP projection for the range in Alaska and British Columbia, although with a larger range projected in Alaska in the current breeding range.

The Heinrich event H2 and the 24 ka BP projections share only a similarity in the projected range along the Rocky Mountains in the north-western USA. The H2 projected range covers a small territory of south-western, central and eastern regions in the USA. This projected range is decreased at H1, and still differing from the 17 ka BP projection. The H0 projected range continues to decrease and shares a similar range along the territory in southern Alaska not covered by ice, with a small range projected in the central conterminous USA.

Even though the species current breeding range is located in North America, there are suitable conditions for the species among the projections in South America, from southern Chile as far as Tierra del Fuego in Argentina.

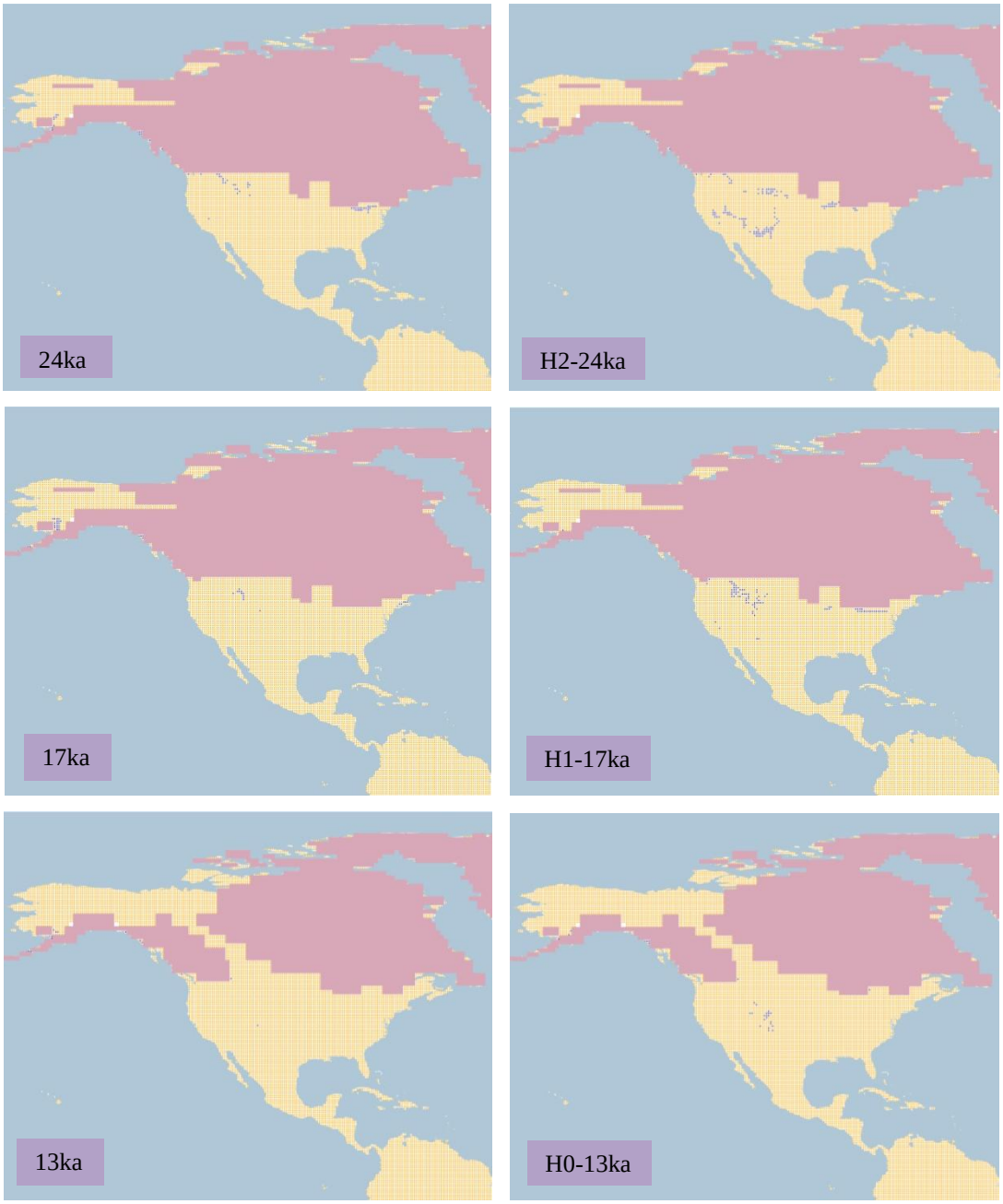

Figure 4.1.4.7.a. Simulation maps of Dunlin sub-species *C. a. pacifica* breeding range. Maps are shown for ten-time slices: 24ka, H2 (24ka), 17ka, H1 (17ka), 13ka, H0 (13ka), 9ka, 5ka, 3ka and present (1961–90).

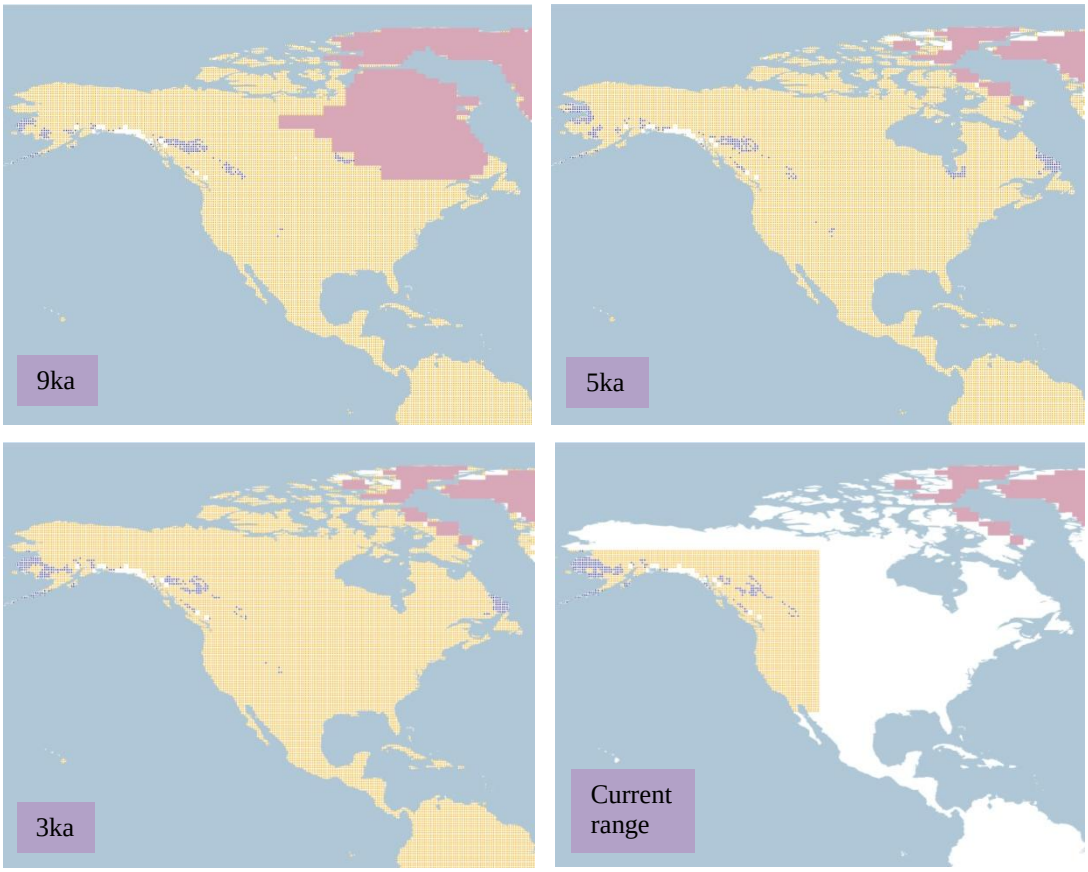

Figure 4.1.4.7.a. Simulation maps of Dunlin sub-species *C. a. pacifica* breeding range (continued**).**

Non-breeding range (AUC: 0.993; TSS: 0.930; Kappa: 0.873): This sub-specie's wintering grounds are located on the south-central and south-eastern coast of Alaska, along the western coast of British Columbia in Canada and on the west coast of the conterminous USA as far as the central-western coast of Mexico in Jalisco.

At 26 ka BP the range is projected along the western coast, western and south-eastern region of the USA, and along the central-western coast, central and southern region in Mexico, with a small range in the Greater Antilles. This pattern continues until 18 ka BP with a decrease of the range in central-western and south-eastern regions of the USA. The decrease of the range continues and at 15 ka BP the range in central Mexico is reduced as well. See Figure 4.1.4.7.b.

By the beginning of the Holocene at 11 ka BP the range is projected along the western coast of British Columbia in Canada, also on the western coast and the eastern region of the USA,

which follows to the north-east of Mexico, and along the western coast from Baja California to Jalisco. There is also a small range projected in the Aleutian Islands of Alaska in the USA.

At 7 ka BP the range in eastern USA and along the Aleutian Islands of Alaska is increased. This pattern continues with minimal differences until the 1 ka BP projection, with a range from western British Columbia, along the western coast of the USA and Mexico and in the eastern region of the USA from Texas and Kansas as far as the east coast, and following to the north-east coast and in southern Mexico. The current non-breeding range projection presents a similar range from the Aleutian Islands in Alaska as far as the western coast of the USA and Mexico.

A large range is projected at H2 in central and southern USA, extending to central-northern and southern region of Mexico, and covering the Greater Antilles as well. The range in the central and southern USA is decreased in the H1 projection, although remaining with the same range in Mexico and differing from the 17 ka BP projection. This decreasing pattern continues in the H0 projection, mainly in southern and eastern regions of the USA, with the range in Mexico remaining similar to the 13 ka BP projection.

Although the current non-breeding range is located on the western coast of North America, there are suitable conditions for the species among the projections, mainly along the Andean cordillera and in the central-southern region of South America.

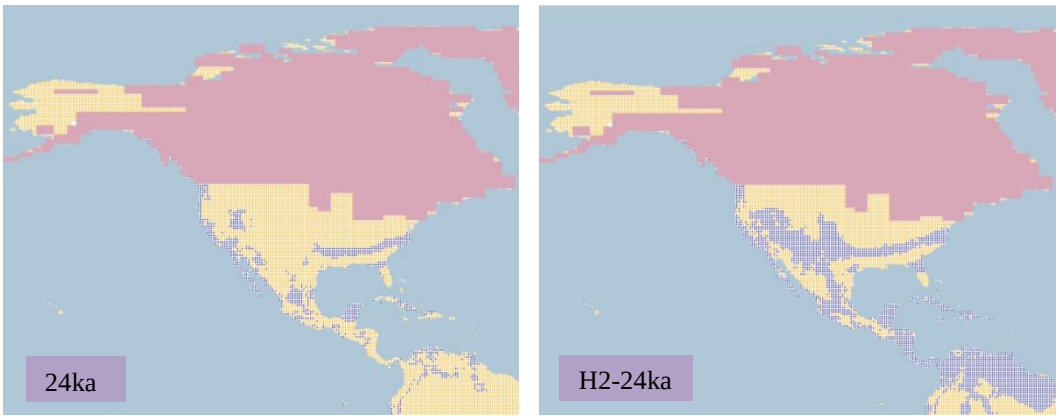

Figure 4.1.4.7.b. Simulation maps of Dunlin sub-species *C. a. pacifica* non-breeding range.
Maps are shown for ten-time slices: 24ka, H2 (24ka), 17ka, H1 (17ka), 13ka, H0 (13ka), 9ka, 5ka, 3ka and present (1961–90).

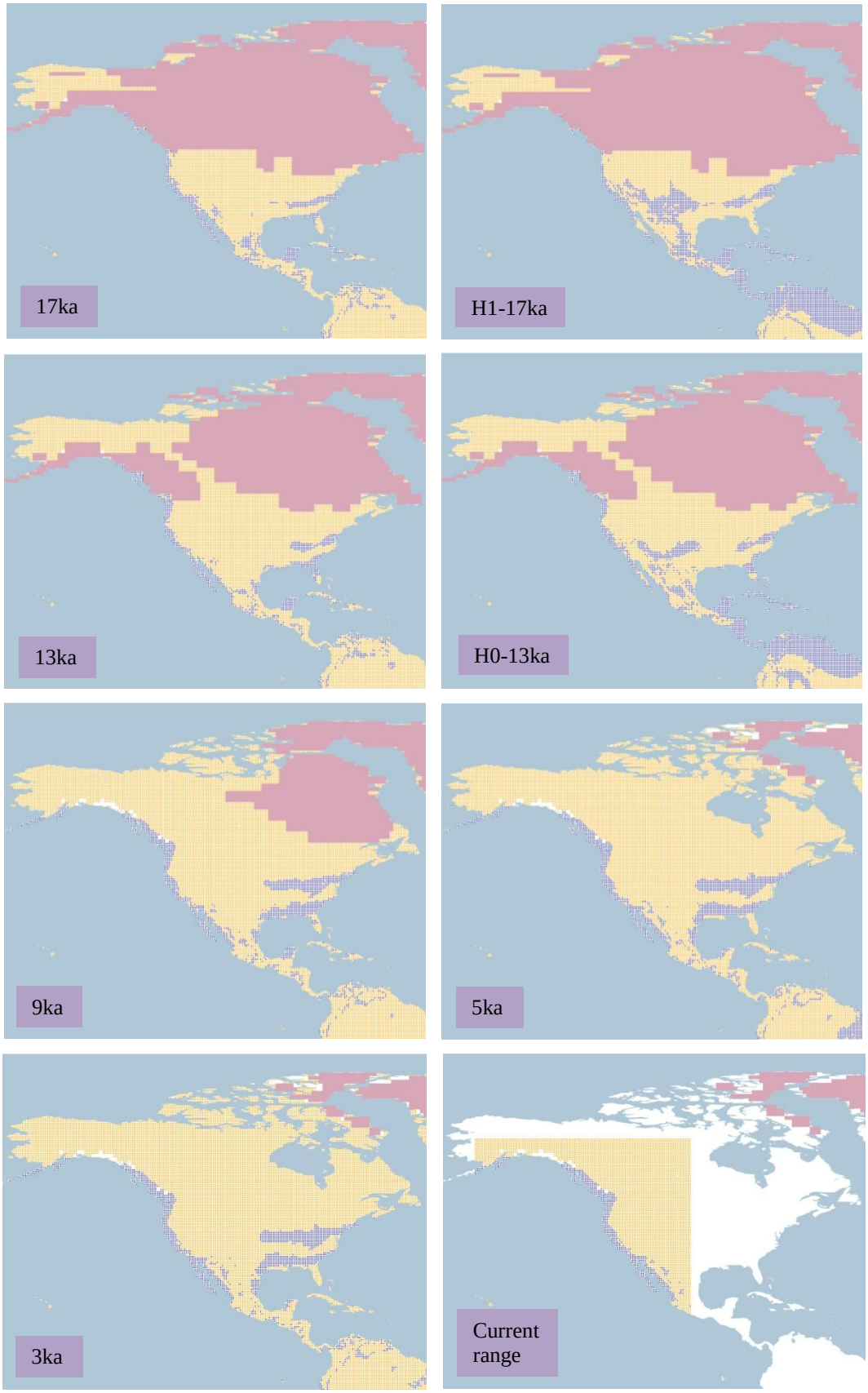

Figure 4.1.4.7.b. Simulation maps of Dunlin sub-species *C. a. pacifica* non-breeding range (continued**).**

*4.1.4.8 Baird's Sandpiper (*Calidris bairdii*). Conservation status: Least Concern. Current known range Figure 4.1.4.8.*

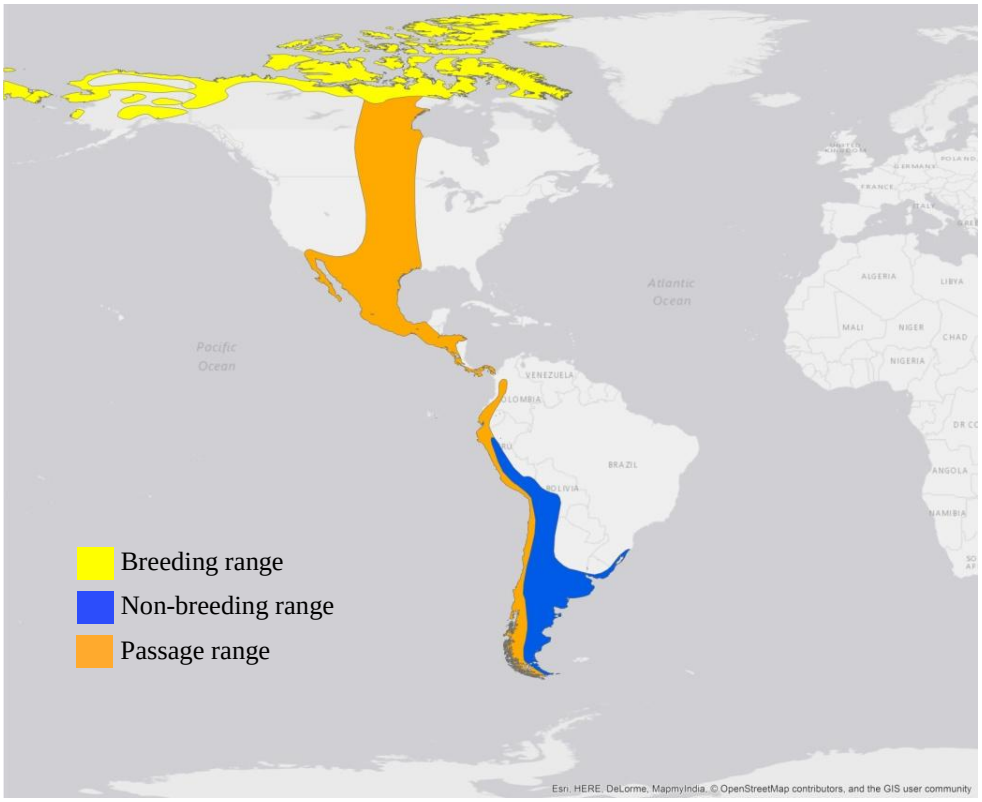

Figure 4.1.4.8. Current known range of Baird's Sandpiper.

Breeding range (AUC: 0.988; TSS: 0.901; Kappa: 0.740): The breeding range of this species is located in the high Arctic region of North America from Alaska to the north of Canada, the Canadian Islands and a small range on the coast east of Greenland.

The range starts at 26 ka BP in the area of Alaska and north-west of Canada where the ice sheet is not present, as well as in a small area in the central-north USA near the ice sheet. The same pattern continues and at 19 ka BP the range between Alaska and north-east Canada increases. See Figure 4.1.4.8.a.

At 16 ka BP the Alaskan range decreases, as does the north-central range in the USA, and there is an increase in the north-west of Canada. As the ice sheet retreats this pattern continues. Particularly at 14 ka BP the range in the conterminous USA disappears and there

is a small range near the ice sheet in central Canada and in the north-west; in addition, the Alaskan range is restricted to the northern coast.

From 13 ka BP the simulated range is restricted to the north-west of Canada and in the Canadian Islands which changes at 11 ka BP with an increase over Alaska and a decrease in the Canadian range. Following this there is an increase in both areas of Alaska and Canada, near the ice sheets at 9 ka BP that decreases at 8 ka BP concentrating the range in the north of Alaska, north-west Canada and in the Canadian Islands. The pattern gradually grows towards the 1 ka BP projection and matching the current breeding range projection.

Both projections H2 and 24 ka BP are similar in extent, only with a more uniform range at H2. At H1 the range moves inland to the west of Canada similar to the 17 ka BP projection. Finally, the H0 projection is also similar to 13 ka BP only with a slightly greater projected range.

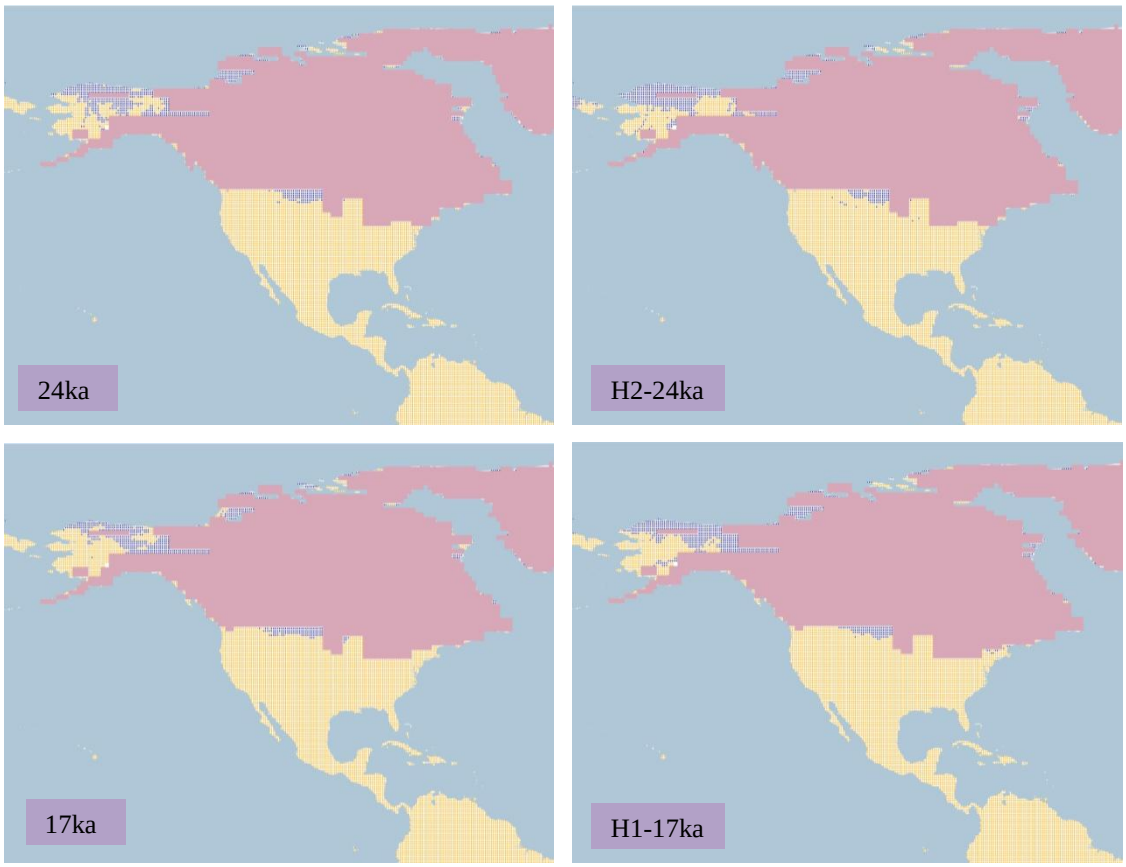

Figure 4.1.4.8.a. Simulation maps of Baird's Sandpiper breeding range.
Maps are shown for ten-time slices: 24ka, H2 (24ka), 17ka, H1 (17ka), 13ka, H0 (13ka), 9ka, 5ka, 3ka and present (1961–90).

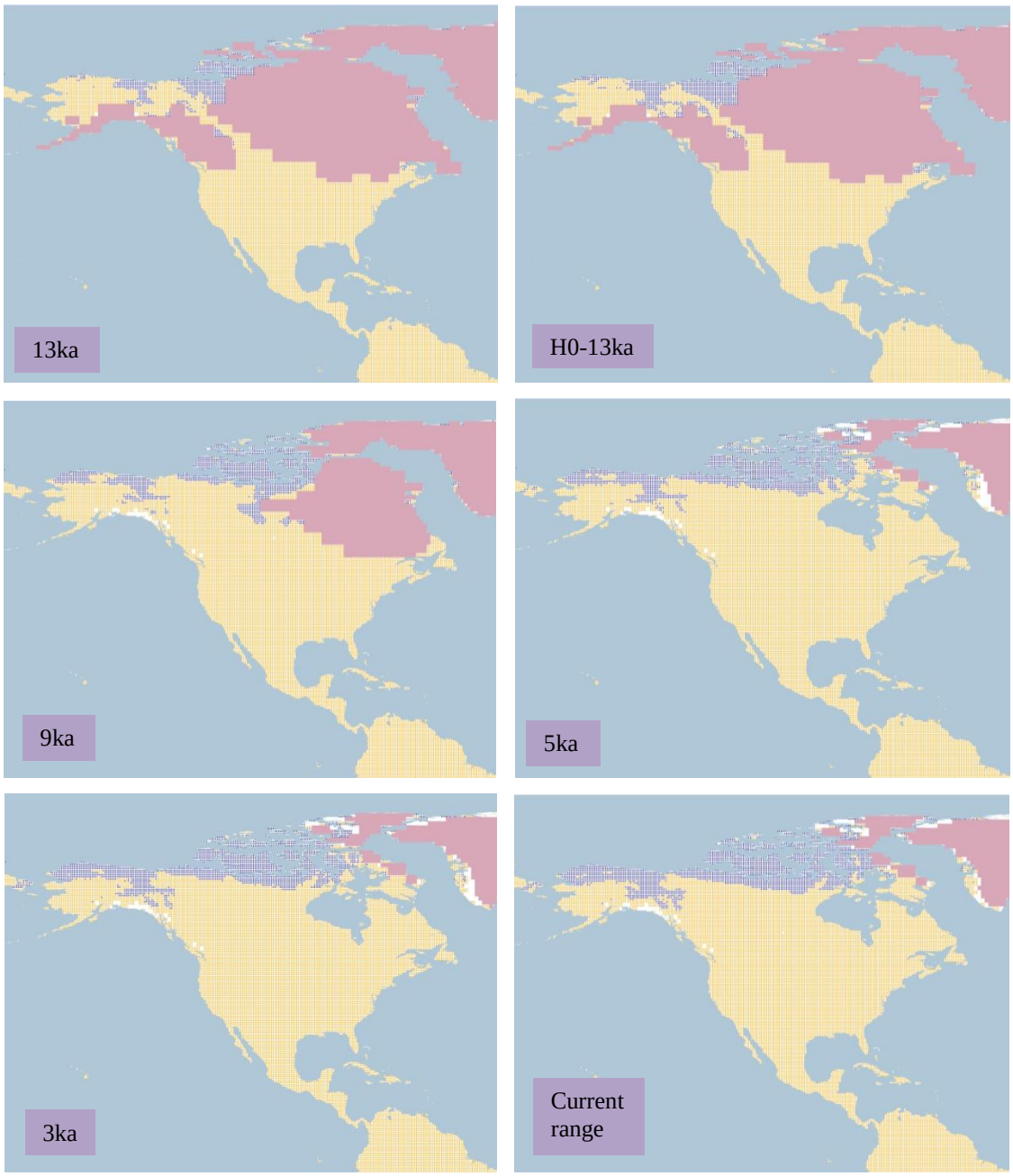

Figure 4.1.4.8.a. Simulation maps of Baird's Sandpiper breeding range (continued**).**

Non-breeding range (AUC: 0.992; TSS: 0.918; Kappa: 0.737): This species spends the non-breeding season in South America from central Peru, south-west Bolivia, across the west (following the Andean Cordillera) to the east coast of Argentina and with a small range on the south-east coast of Brazil.

The range at 26 ka BP is projected around the Andean Cordillera from Peru to the south-east and increasing in the central part of Argentina; also, a small range is projected in Uruguay and the south of Brazil. This pattern continues and grows at 22 ka BP, particularly in the south region of Brazil, declining after 19 ka BP. See Figure 4.1.4.8.b.

From 18 ka BP the range in Argentina expands to the southern region and at 15 ka BP the range in south Brazil and Uruguay begins decreasing, especially at 14 ka BP when the range in that area shifts to the north of Argentina. Following this the range in north Argentina and south Paraguay increases and meets the range in Uruguay and south Brazil, as well as the range across Argentina increasing towards the Chilean border.

By 9 ka BP the range is concentrated in the Andean Cordillera from Peru to the south of Argentina and with a smaller range in the north and in Uruguay, which presents a changing range between 7 ka BP and 6 ka BP and after this remaining uniform with the rest of the range until 1 ka BP and agreeing with the current non-breeding range projection.

The H2 and 24 ka BP projections present similar simulated ranges in South America with only small differences; in the H2 projection the range extends only from the south of Peru and is of lesser extent. The same pattern remains at H1 with similar conditions to 17 ka BP as well. The H0 and 13 ka BP projections display similar ranges as well, only with a bigger extent at 13 ka BP.

Even though the species only winters in South America there are suitable conditions presented in the projections from 26 ka BP to 18 ka BP on the Mexican plateau and in the south-west USA.

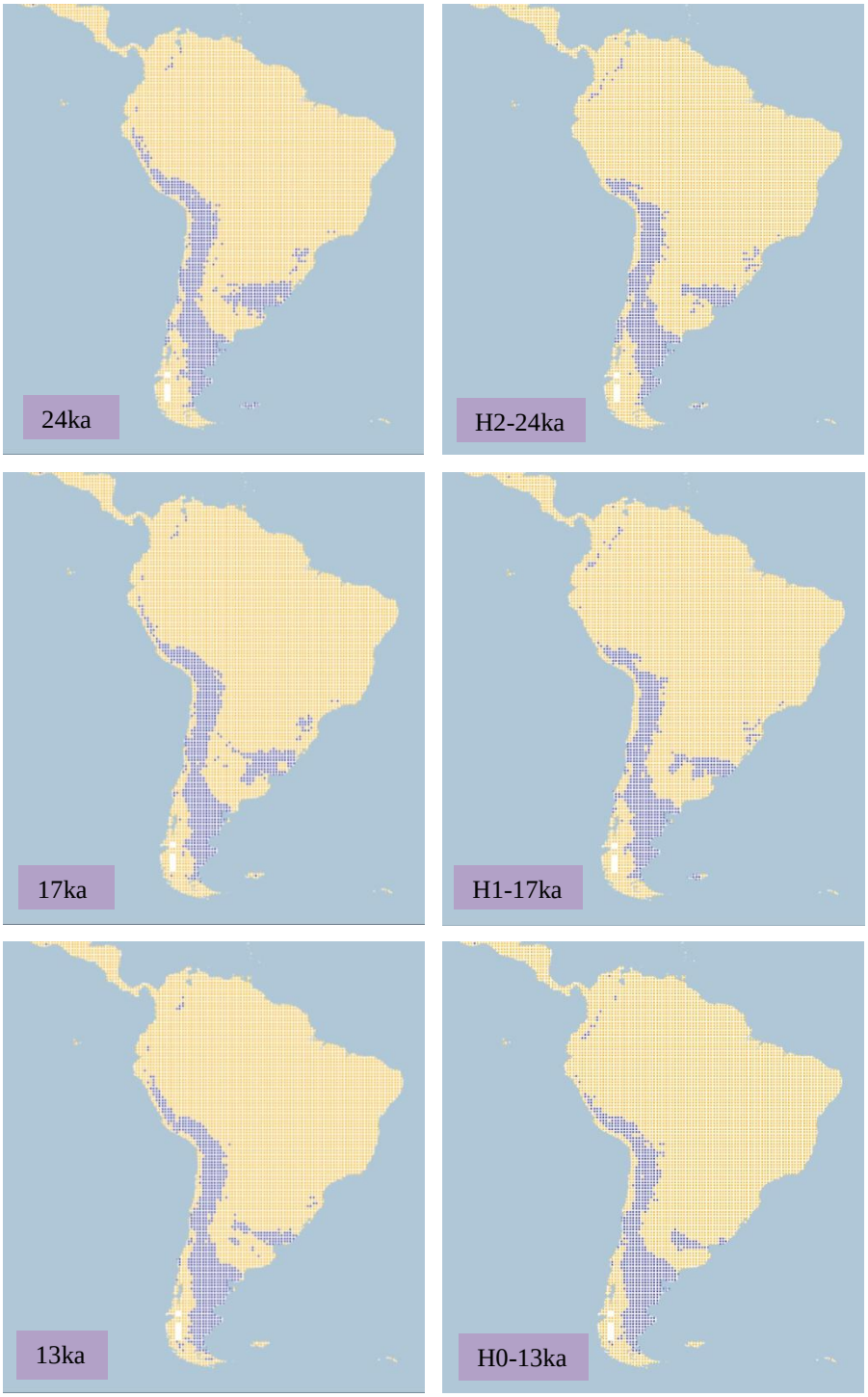

Figure 4.1.4.8.b. Simulation maps of Baird's Sandpiper non-breeding range.
Maps are shown for ten-time slices: 24ka, H2 (24ka), 17ka, H1 (17ka), 13ka, H0 (13ka), 9ka, 5ka, 3ka and present (1961–90).

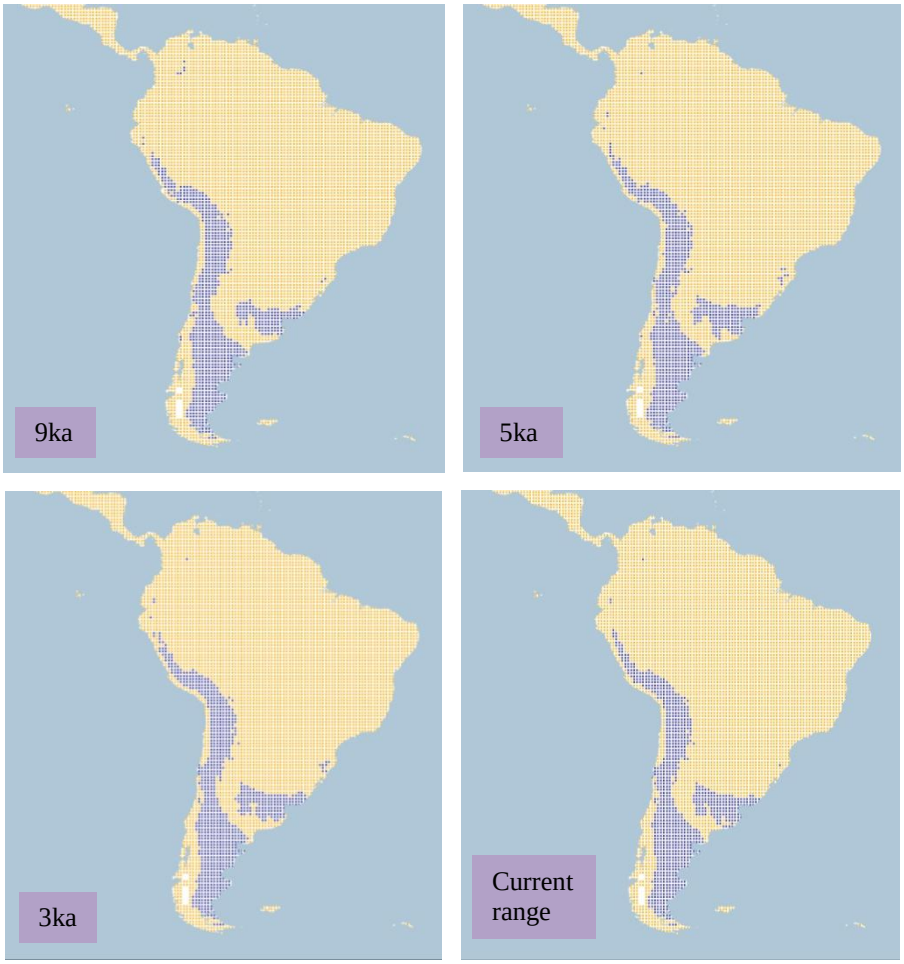

Figure 4.1.4.8.b. Simulation maps of Baird's Sandpiper non-breeding range (continued**).**

*4.1.4.9 Red Knot (*Calidris canutus *including only* C. c. roselaari, C. c. rufa *and* C. c. islandica *(breeding range only)). Conservation status: Near Threatened. Current known range Figure 4.1.4.9.*

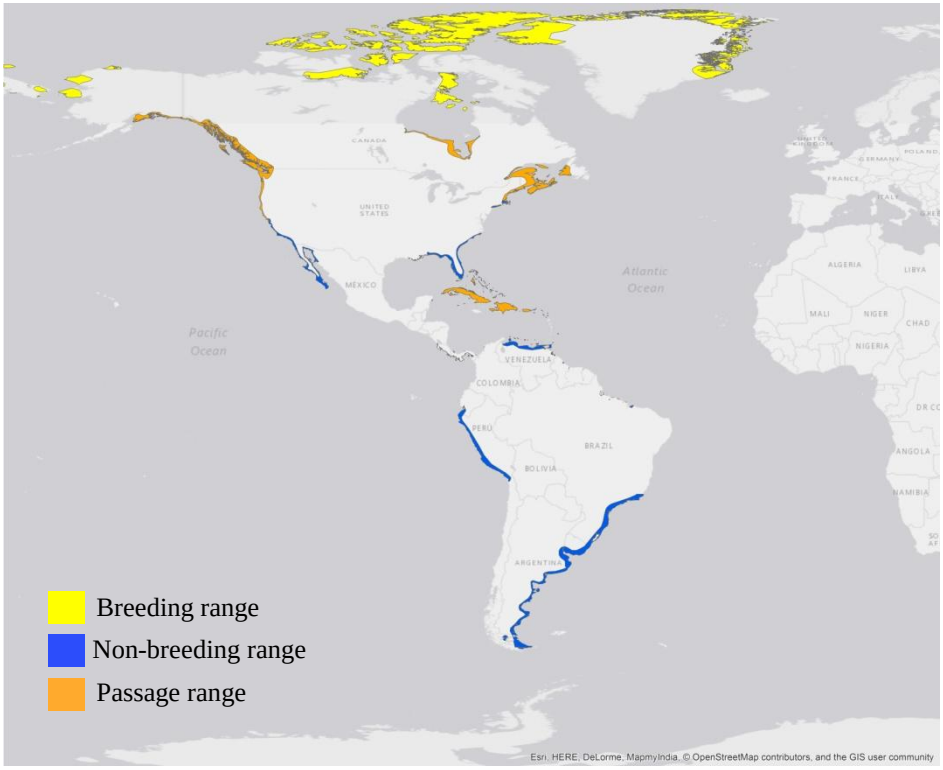

Figure 4.1.4.9. Current known range of Red Knot (sub-species *roselaari*, *rufa* and *islandica* (breeding range only)).

Breeding range (AUC: 0.971; TSS: 0.852; Kappa: 0.618): *Calidris canutus roselaari* breeds in the north-west of Alaska, *C. c. rufa* in the Canadian low Arctic and *C. c. islandica* on the islands of the Canadian high Arctic and in northern Greenland. Only for the sub-species *C. c. islandica* the breeding range was projected as it breeds in North America.

At 26 ka BP the projection shows a range in the north of Alaska, north-west of Canada and northern Greenland where the ice sheet is absent, as well as a small range in the north-central part of the USA. This pattern continues with a slow increase in the north-west range of Canada until 18 ka BP. After this at 17 ka BP and 16 ka BP there is a decrease in the northern range from Alaska and Canada which changes at 15 ka BP with the ice sheet retreat increasing inland in Canada. See Figure 4.1.4.9.a.

By 14 ka BP the northern range projected in Alaska and Canada is much reduced and only a small range is found in the Canadian Islands, but, as the ice sheet pulls back the range in the north of Canada increases again. From the beginning of the Holocene this change again and the range is concentrated to the northern parts of Canada and a small range as well in the north of Alaska. In addition, a small range is projected in easternmost Canada after 13 ka BP, initially in southern Quebec but shifting north along the Labrador coast as the ice sheet retreats.

From 9 ka BP the territory projected in Canada increases a small proportion near the ice sheet and the Alaskan range decreases to an isolated northern range. The Canadian range extends towards the high Arctic islands after 8 ka BP when a range in central-western Greenland also is projected Thereafter there are only very minor changes until 1 ka BP. This is also similar to the current breeding range projection that is focused in the Arctic regions of the Canadian islands, northern Greenland and a small range in the north-west of Alaska, although absent from central-western Greenland.

Comparing the H2 projection with that for 24 ka BP, the area predicted is similar presenting a small difference with a larger area at H2 mainly in the west of Alaska. The same characteristics are found between the H1 and 17 ka BP projections only with minimal differences. In the H0 and 13 ka BP projections the area in the north of Canada is very much alike, only with a greater extent at H0.

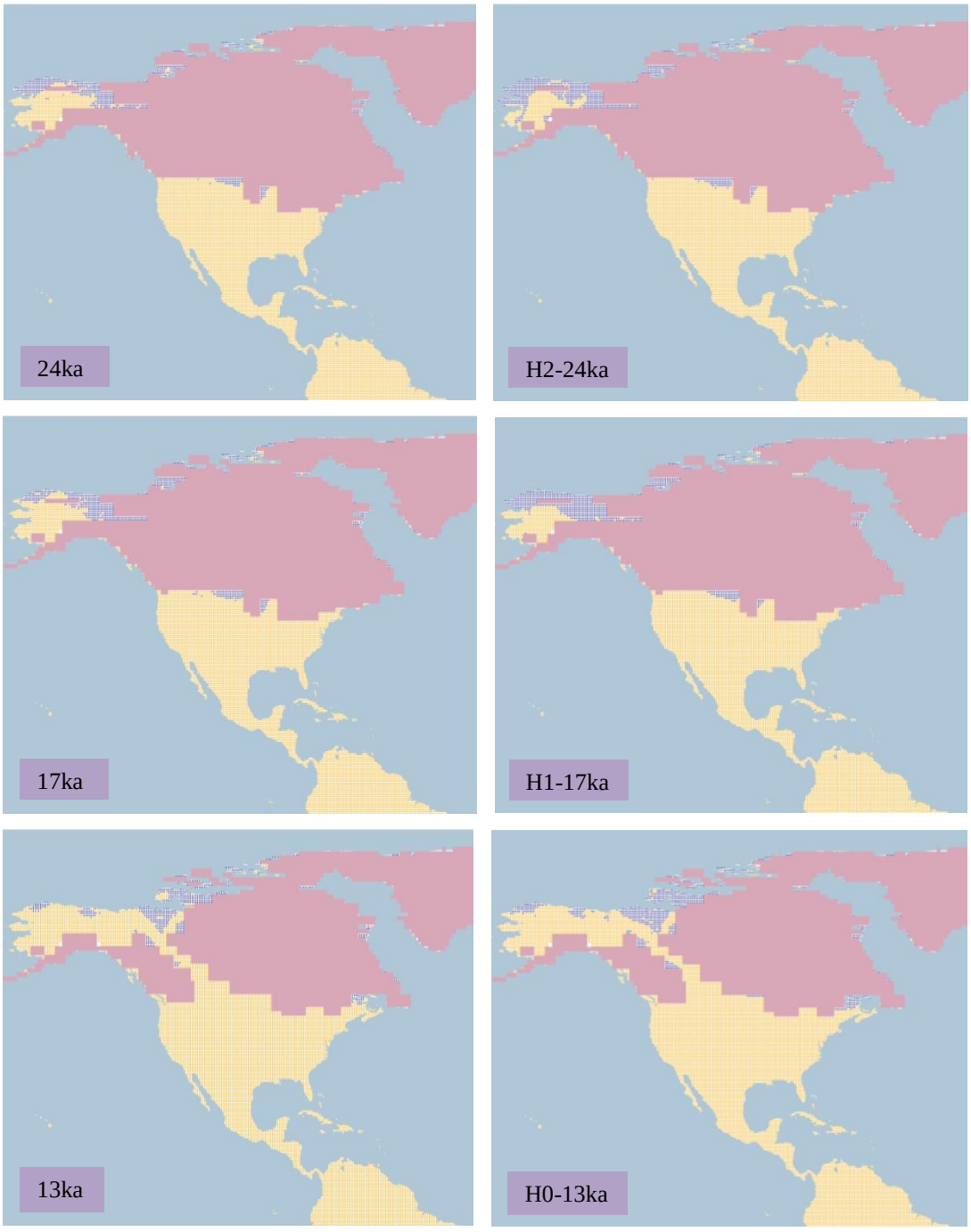

Figure 4.1.4.9.a. Simulation maps of Red Knot breeding range.
Maps are shown for ten-time slices: 24ka, H2 (24ka), 17ka, H1 (17ka), 13ka, H0 (13ka), 9ka, 5ka, 3ka and present (1961–90).

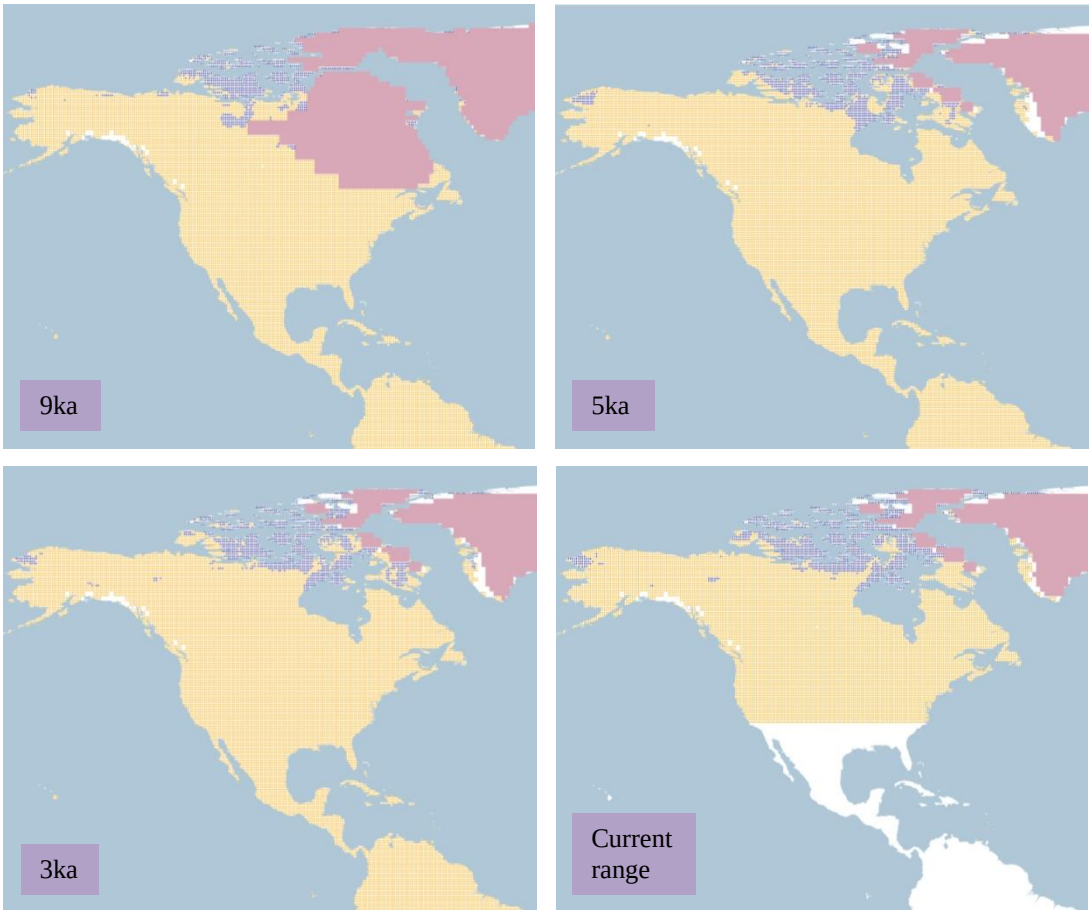

Figure 4.1.4.9.a. Simulation maps of Red Knot breeding range (continued**).**

Non-breeding range (AUC: 0.961; TSS: 0.787; Kappa: 0.583): The non-breeding ranges of *C. c. roselaari* and *C. c. rufa* are located along the coasts of the Americas from the west coast of California to Peru and on the east coast from Maine to Tierra del Fuego. *C. c. islandica*, in contrast, spends the non-breeding season on the coasts of Western Europe and is excluded here.

At 26 ka BP the range is mainly projected in South America from southern Brazil and Uruguay to northern Argentina, with a small range in southern Chile and along the western coast of Ecuador and Peru. The range in North America is projected from the western coast of California in the USA to the western coast of Jalisco in Mexico, with a small inland range in the central region of Mexico, and on the southern coast of El Salvador in Central America. This pattern continues with minimal differences in the range in southern Brazil and northern Argentina at 22 ka BP. See Figure 4.1.4.9.b.

At 18 ka BP a small range in northern Florida is projected, and by 16 ka BP the range in southern Chile increases as far as Tierra del Fuego and the eastern coast of Argentina. The range in southern Brazil is decreased at 15 ka BP, as is the range in central Mexico, with a small projected range on the north-western coast of Washington in the USA and south-western British Columbia in Canada.

By the beginning of the Holocene at 11 ka BP, the range in southern Brazil shifts to the south along the eastern coast of Argentina, with a reduction of the range in southern Chile, and with the deglaciation in North America there is an increase on the south-western coast of British Columbia in Canada. After this, at 8 ka BP, the range in central Mexico shifts to the central-northern region and there is an increase in the range projected along the western coast of Mexico.

At 3 ka BP a range is projected along the south-eastern coast of the USA from Texas to Florida that continues growing until 1 ka BP. The same pattern is observed along the south-western coast of Mexico, and in South America the range in southern Brazil shifts to the coastal region, with an extension from the south-eastern coast of Brazil as far as southern Argentina. For the current non-breeding range, a similar pattern is observed in North America, along the western coast and south-central coast of the USA and on the western coast of Mexico. In Central America a small range is projected on the southern coast of El Salvador and in South America, the range is projected along the coast of Ecuador and Peru, in southern Chile and from southern Brazil as far as southern Argentina.

A larger range is projected in North America and Central America for H2 in comparison with 24 ka BP, with an extent from eastern to southern Mexico, across Central America, and in the Greater Antilles. The range is also greater in South America, projecting suitable conditions in the northern region from Colombia to north-western Brazil, with a smaller range in southern Brazil, Bolivia and Paraguay. A small similar range is observed between H1 and 17 ka BP, in central Mexico, southern Chile and southern Brazil. The similarities continue between H0 and 13 ka BP in the range in North America and southern South America, although there is a large range projected in northern South America and across Central America and the Greater Antilles at H0.

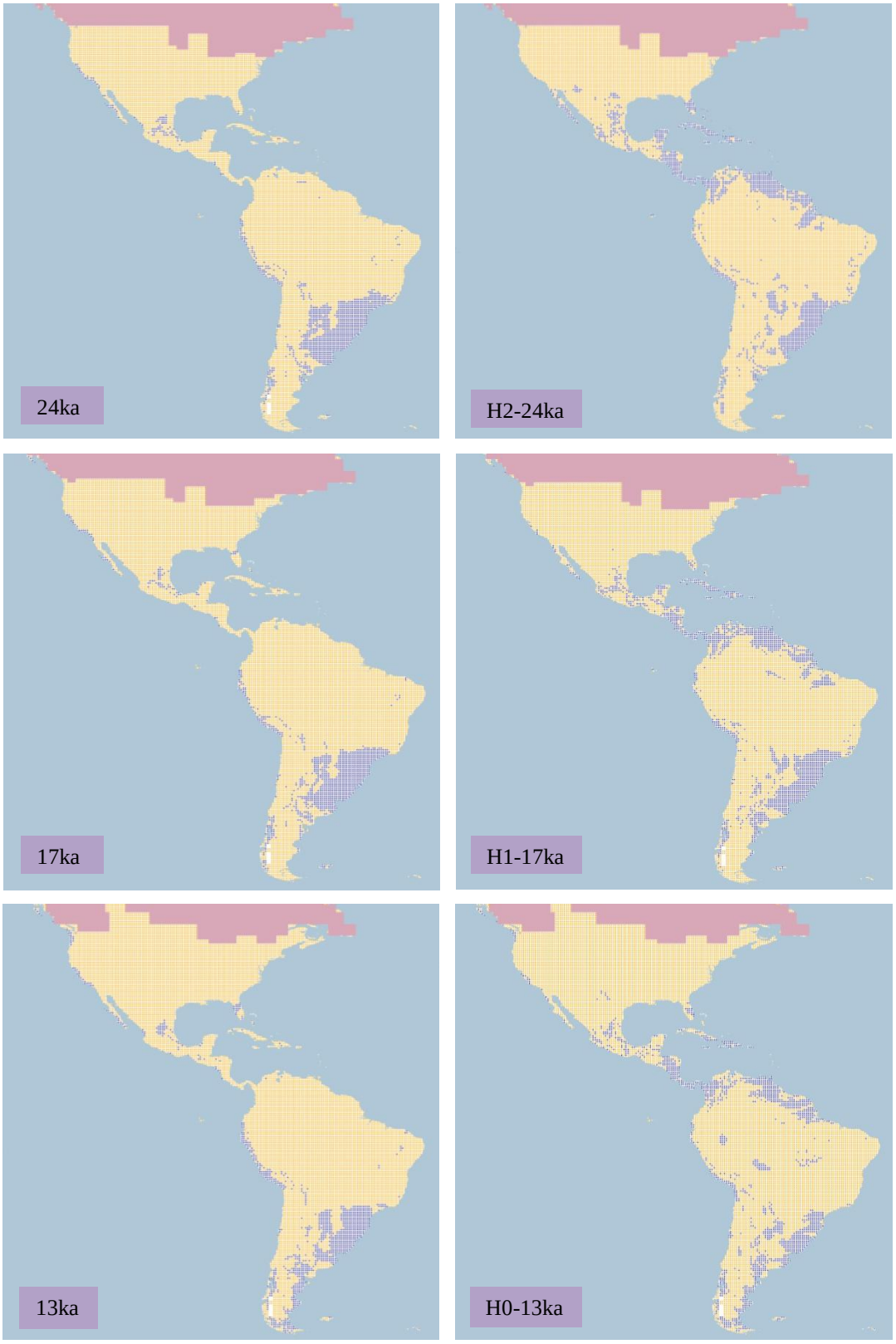

Figure 4.1.4.9.b. Simulation maps of Red Knot non-breeding range.
Maps are shown for ten-time slices: 24ka, H2 (24ka), 17ka, H1 (17ka), 13ka, H0 (13ka), 9ka, 5ka, 3ka and present (1961–90).

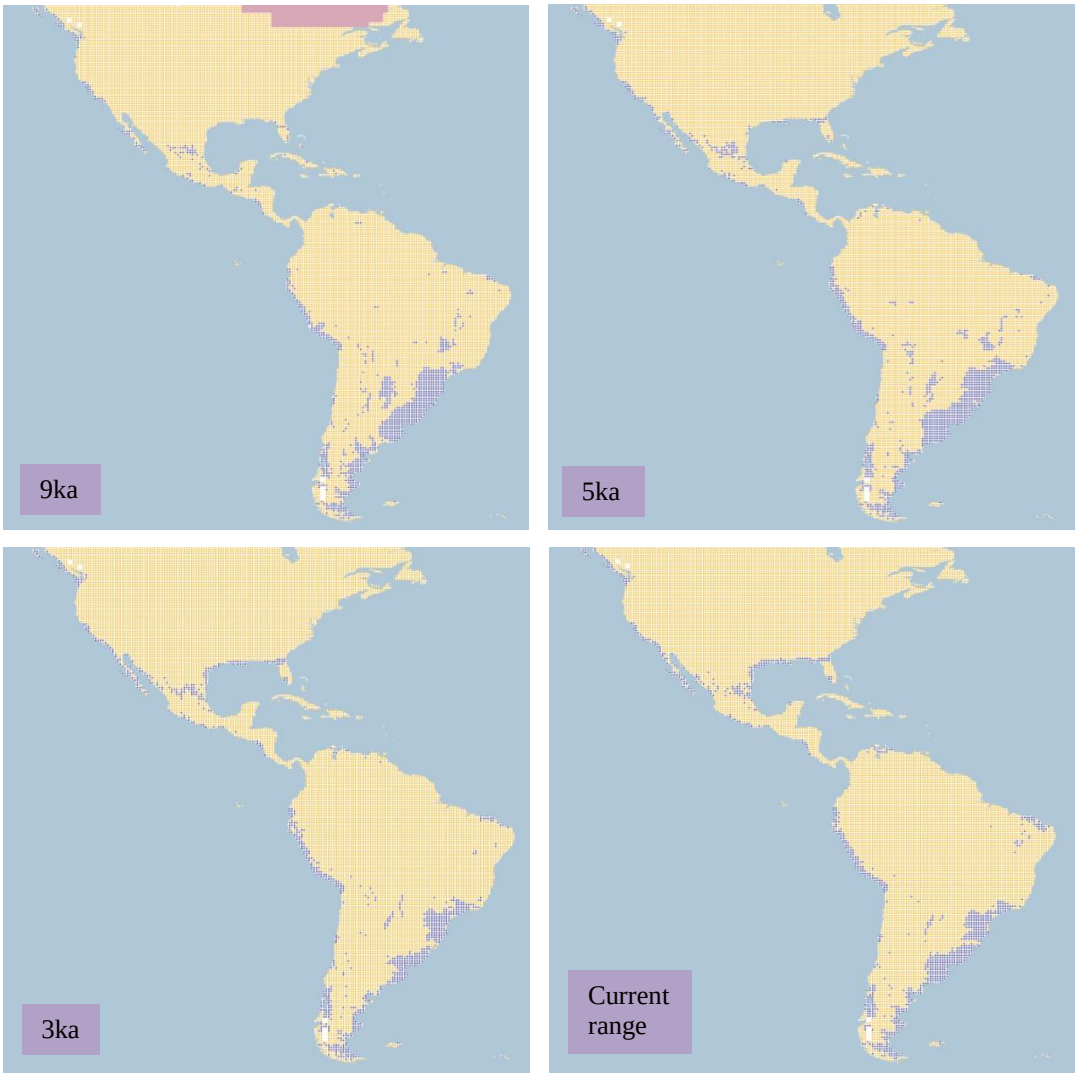

Figure 4.1.4.9.b. Simulation maps of Red Knot non-breeding range (continued**).**

*4.1.4.10 White-rumped Sandpiper (*Calidris fuscicollis*). Conservation status: Least Concern. Current known range Figure 4.1.4.10.*

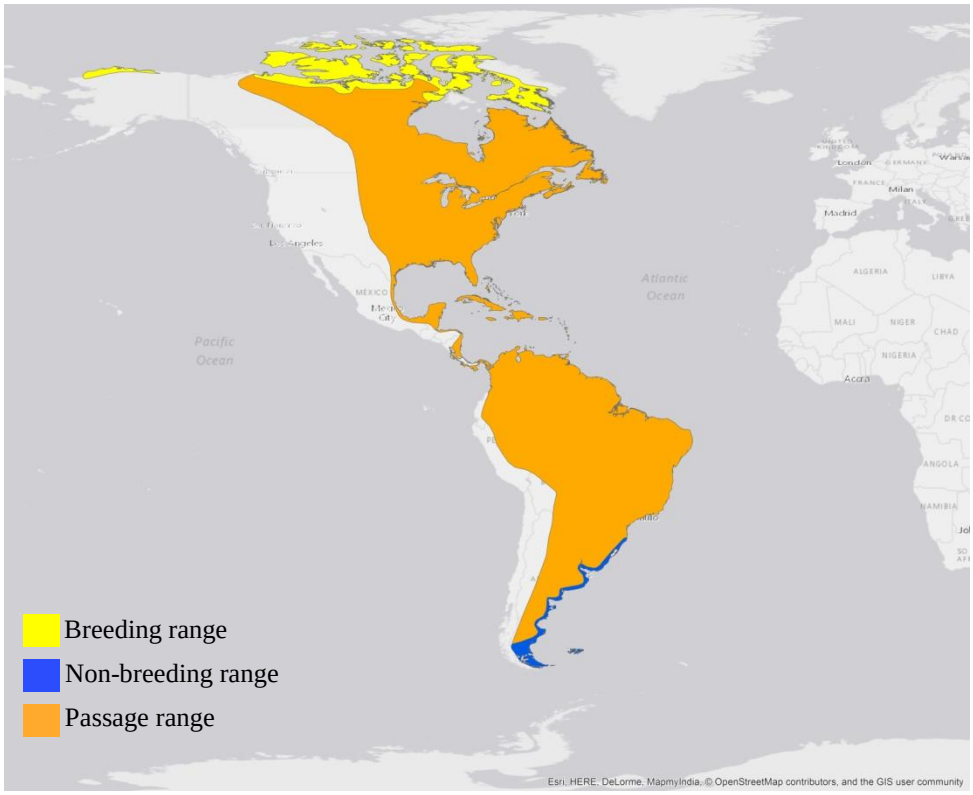

Figure 4.1.4.10. Current known range of White-rumped Sandpiper.

Breeding range (AUC: 0.972; TSS: 0.870; Kappa: 0.792): This species spends the breeding season in the north of Alaska and northern Canada, including the Canadian Arctic islands as far north as Devon Island.

The projection begins at 26 ka BP with a range in the northern part of North America from Alaska to Canada where the ice sheet is not present, and a small range in the central-north of the conterminous USA. The same pattern continues with a moderate growth until 16ka. See Figure 4.1.4.10.a.

From 15 ka BP the range changes as the ice sheet retreats, reducing the extent to the west of Alaska and in the north of Canada; particularly at 14 ka BP the range in the north of Canada reduces only covering Banks Island and a scattered range inland. This changes at 13 ka BP with an increase in the North-West Territories of Canada and at 12 ka BP the range reduces again concentrating in the northern areas.

As the Holocene begins the range decreases inland and is centred on the northern coasts between 11 ka BP and 10 ka BP. Later on, at 9 ka BP the inland range increases again in Canada, near the ice sheet as at it retreats at 8 ka BP the range moves to the east close to Hudson Bay.

The range seems to remain steady from 7 ka BP to the 5 ka BP projection and from 4 ka BP to 1 ka BP the range increases in the north-west of Canada and north of Alaska. The 1 ka BP projection shows a similar extent to the current breeding range prediction.

The H2 and 24 ka BP projections present equivalent ranges in the northern regions of North America not covered by the ice sheet with small-scale differences. At H1 the range increases in the region not covered by the ice sheet in the north-west of Canada, showing differences from the 17 ka BP projection which moves to the coastal areas instead. At H0 the range shows only diminutive differences from the 13 ka BP projection, although the range is smaller at 13 ka BP.

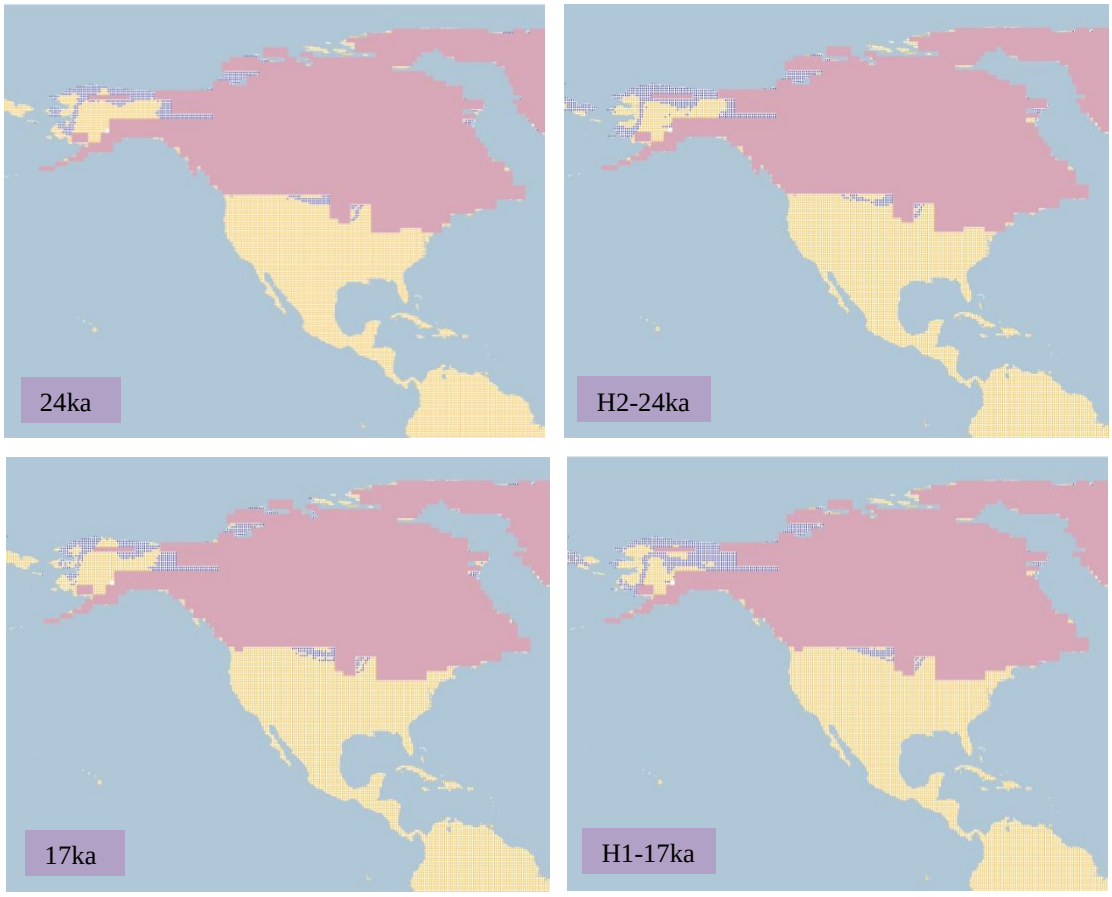

Figure 4.1.4.10.a. Simulation maps of White-rumped Sandpiper breeding range. Maps are shown for ten-time slices: 24ka, H2 (24ka), 17ka, H1 (17ka), 13ka, H0 (13ka), 9ka, 5ka, 3ka and present (1961–90).

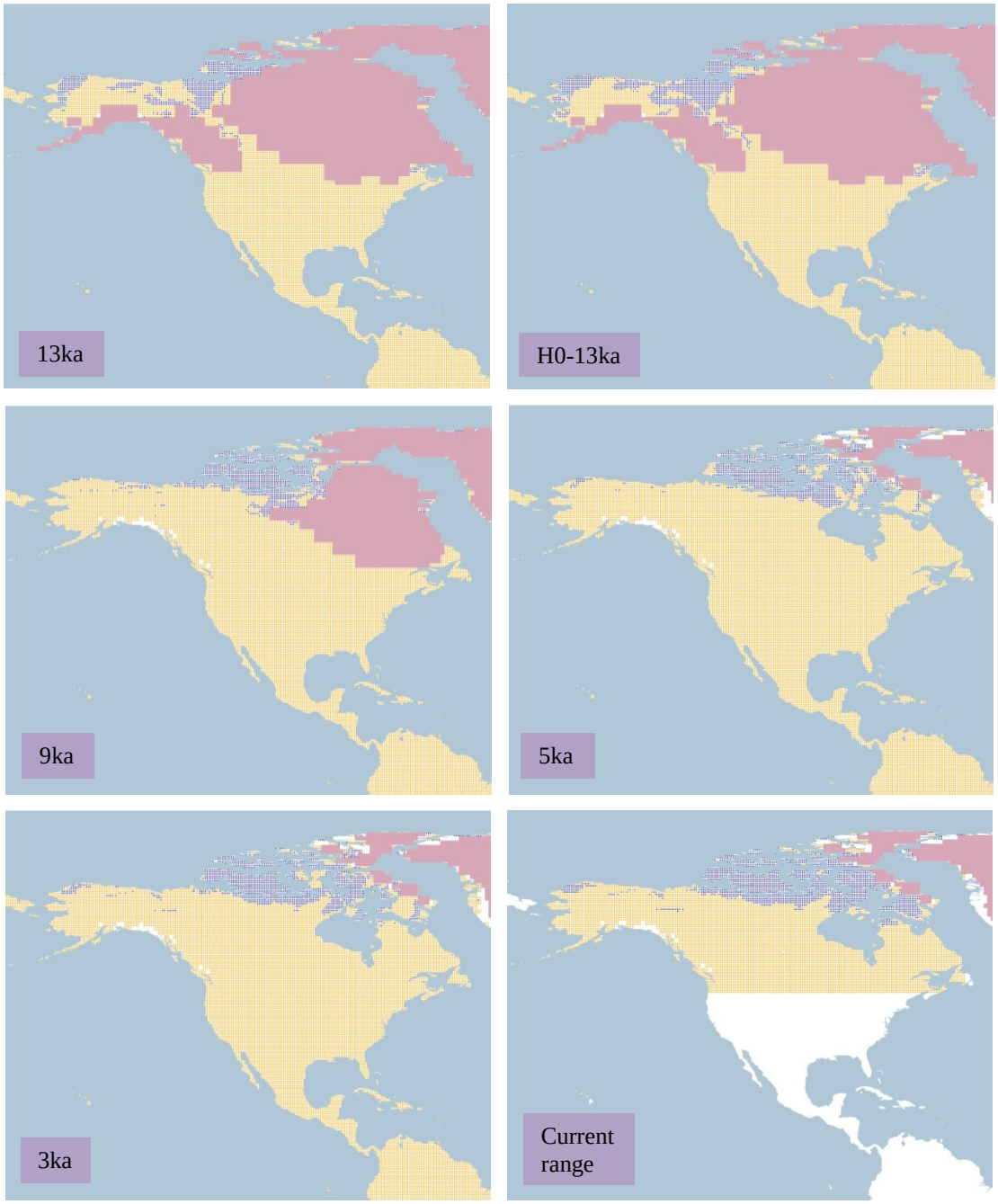

Figure 4.1.4.10.a. Simulation maps of White-rumped Sandpiper breeding range (continued**).**

Non-breeding range (AUC: 0.961; TSS: 0.796; Kappa: 0.630): This species spends the non-breeding season on the east coast of South America from the south of Brazil to Tierra del Fuego and the Falkland Islands.

At 26 ka BP the range is projected to extend from the south of Brazil to central Argentina, along the Andean Cordillera between Chile and Argentina, and extensively towards the south

in Tierra del Fuego. A similar pattern continues in South America and at 19 ka BP the range reaches the Falkland Islands, and begins fragmenting in the Andean Cordillera, focusing on the east coast of Argentina and Brazil. See Figure 4.1.4.10.b.

At 16 ka BP the range in south Brazil is dispersed to Argentina and at 15 ka BP the range in south Brazil is restricted to a few areas, the main range being located in the central-east and extending to the south-east of Argentina and the Falkland Islands. After this at 14 ka BP the range in central-east Argentina increases, as does the southern range component, although the range in the south of Brazil decreases, this pattern persisting until 12 ka BP.

At the beginning of the Holocene the central-east range of Argentina moves to the east coast and increases towards the south with a more inland range. This pattern continues with a minimal growth in the south-east of South America until 3 ka BP when there is a decrease over the central range of Argentina, retreating to the east coast and south of Argentina.

From 2 ka BP to 1 ka BP the range in the south of Brazil, Uruguay and the east of Argentina increases and the range in the south of Argentina remains abundant as well. The current non-breeding range projection shows similar range with the 1 ka BP projection, only with a smaller range over the east coast of Argentina and in the south of Brazil.

Between the H2 and the 24 ka BP projections there are different ranges simulated, particularly in the area of south Brazil, Uruguay and north-east Argentina where the range in H2 is scarce. Changes are observed at H1 and in a contrasting direction from 17 ka BP, with a decrease over Argentina and Brazil but with the south of Argentina remaining constant. The same pattern of reduction is shown at H0 with a range projected only over the east coast of Argentina and not an abundant inland range, distant from the 13 ka BP projection.

Despite the fact that the species' non-breeding range does not include North America, throughout the projections there are suitable conditions present mainly in the west of the USA from 26 ka BP to 18 ka BP and in south-west Canada, as well as from central to east between the USA and Canada in the intervals of 10 ka BP to 1 ka BP.

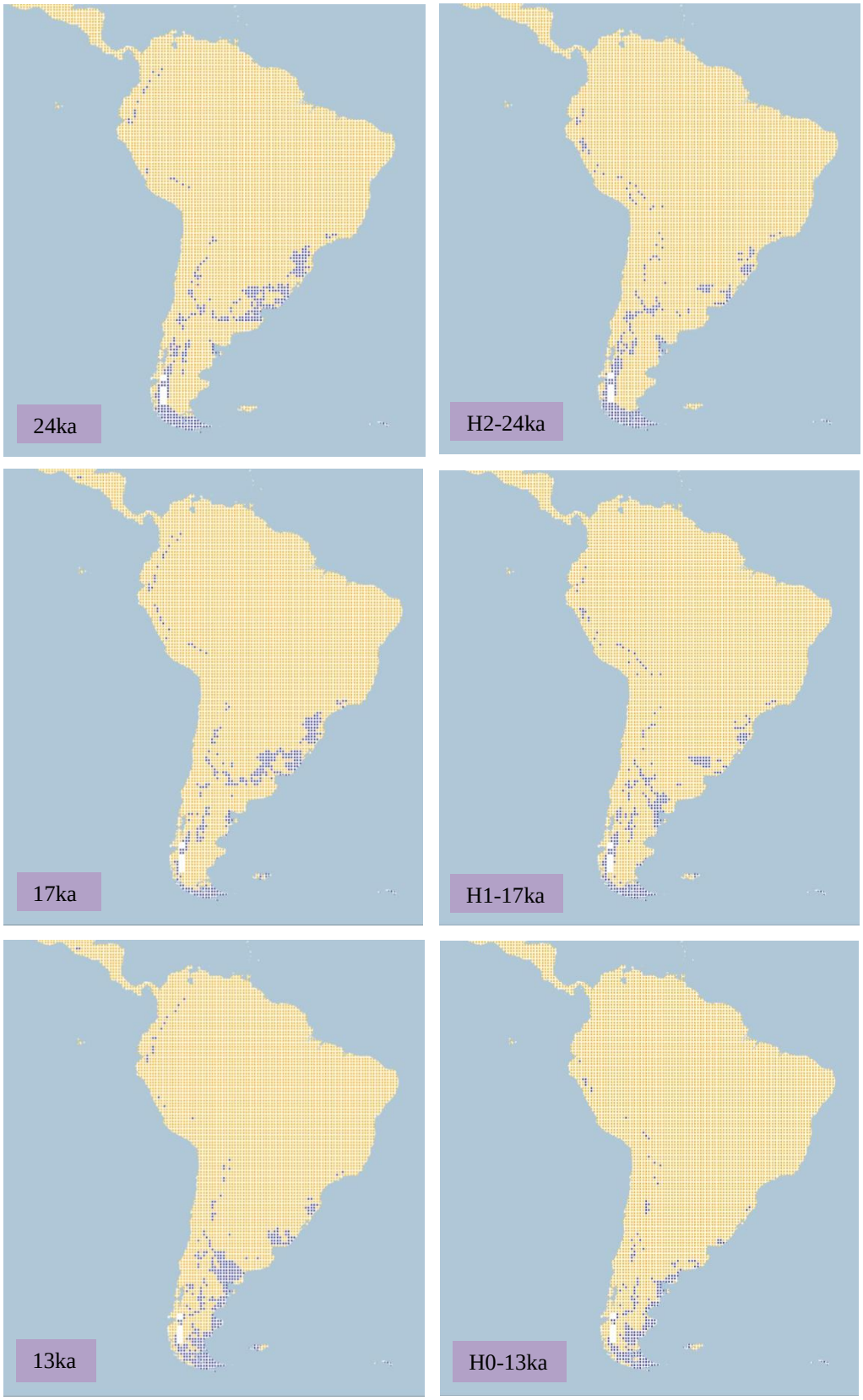

Figure 4.1.4.10.b. Simulation maps of White-rumped Sandpiper non-breeding range. Maps are shown for ten-time slices: 24ka, H2 (24ka), 17ka, H1 (17ka), 13ka, H0 (13ka), 9ka, 5ka, 3ka and present (1961–90).

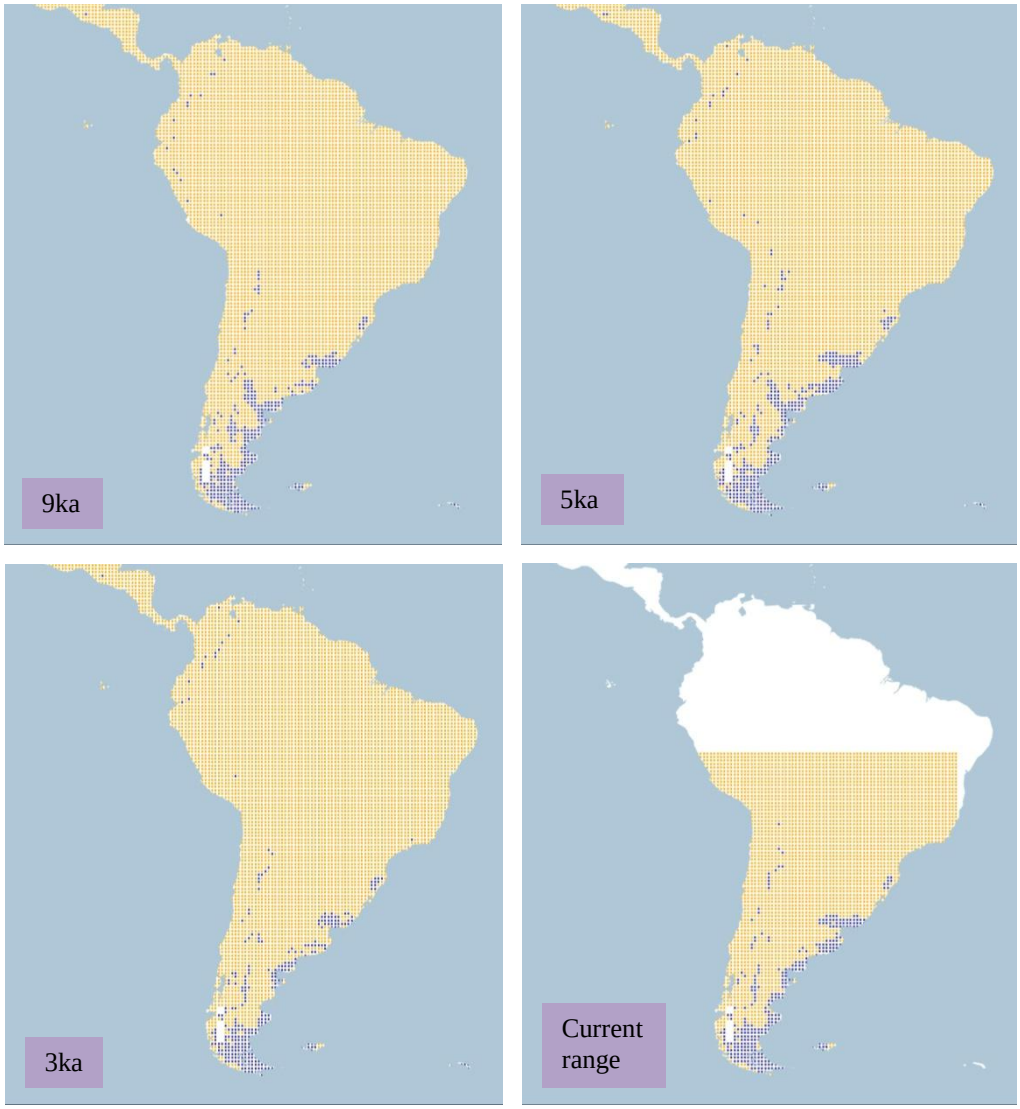

Figure 4.1.4.10.b. Simulation maps of White-rumped Sandpiper non-breeding range (continued**).**

*4.1.4.11 Stilt Sandpiper (*Calidris himantopus*). Conservation status: Least Concern. Current known range Figure 4.1.4.11.*

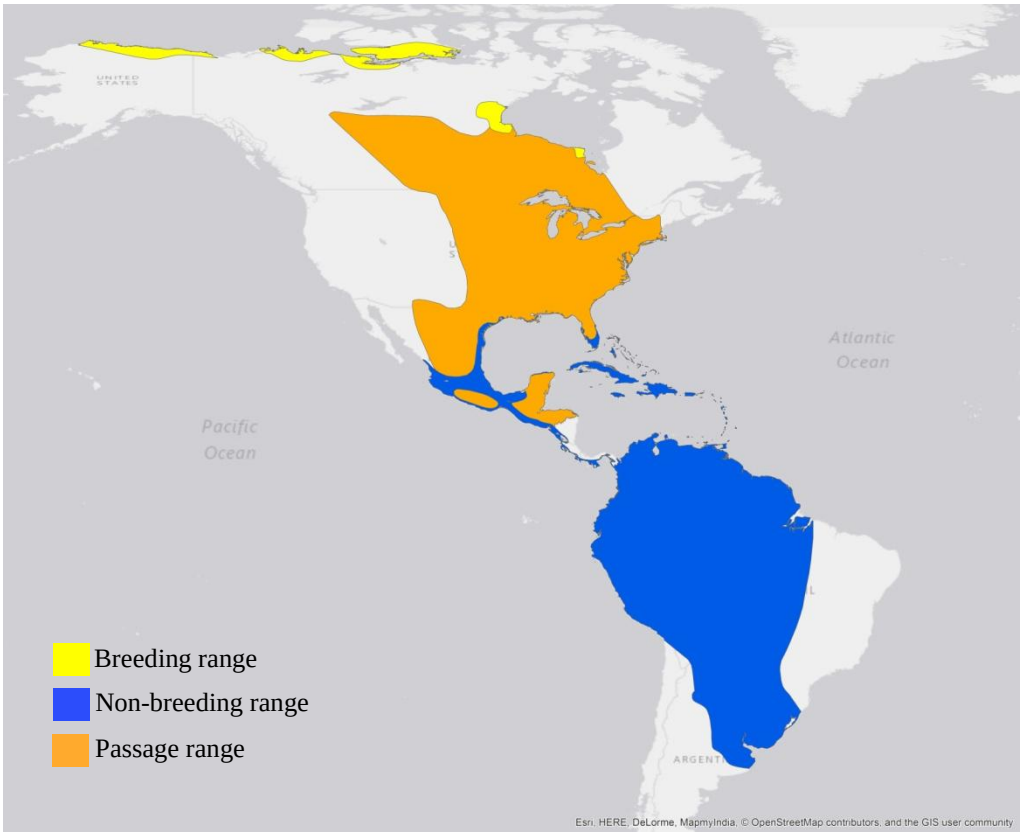

Figure 4.1.4.11. Current known range of Stilt Sandpiper.

Breeding range (AUC: 0.968; TSS: 0.855; Kappa: 0.589): This species breeds in northern Alaska, northern Canada between Yukon and Northwest Territories, south-eastern Nunavut near Hudson Bay, and a small range in northern Ontario.

At 26 ka BP the range is projected mainly in northern Alaska and north-western Yukon in Canada, with a small range in the central-northern conterminous USA. This pattern continues until 19 ka BP when there is a decrease in the range projected in northern Alaska and north-western Yukon. After this at 17 ka BP the range in the central-northern region between Montana and North Dakota in the USA is increased. See Figure 4.1.4.11.a.

At 15 ka BP, with the deglaciation of northern Canada, the range projected in Yukon is increased reaching northern parts of the Northwest Territories. After this at 13 ka BP, the range in northern Canada is reduced and a small range is projected in central Alberta. By the

beginning of the Holocene the range shifts to the northern coasts of Alaska, Yukon and the Northwest Territories. This pattern continues and at 10 ka BP the range reaches Victoria Island.

At 9ka, the range in northern Canada decreases in Yukon and the Northwest Territories, increasing in Nunavut, near the ice sheet. After this at 7 ka BP, the range increases in the Arctic Archipelago of Canada, remaining in the northern continental region as well. There is also a small range projected in the eastern part of the Northwest Territories in Canada at 6 ka BP.

From 5 ka BP onwards, the range continues with minimal variation in northern Alaska, eastern Northwest Territories and southern Nunavut until ka BP, when the range in the Norwest Territories shifts to a small range in southern Nunavut in Canada. The current breeding range projection presents a similar pattern to the 1 ka BP projection across northern North America as far as the Canadian Arctic Archipelago.

There is a similar range projected between the H2 and the 24 ka BP projections in northern Alaska and northern Yukon, with a small difference in the range projected in the central-northern region of the USA. The range in northern North America is reduced in the H1 projection, differing from the 17 ka BP projection. However, a similar range is observed between the H0 and 13 ka BP projection in northern and central Canada.

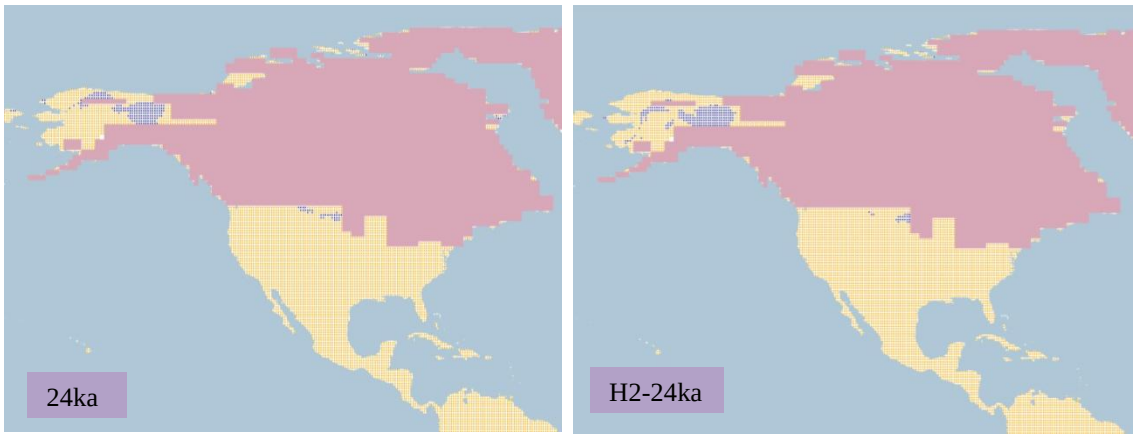

Figure 4.1.4.11.a. Simulation maps of Stilt Sandpiper breeding range.
Maps are shown for ten-time slices: 24ka, H2 (24ka), 17ka, H1 (17ka), 13ka, H0 (13ka), 9ka, 5ka, 3ka and present (1961–90).

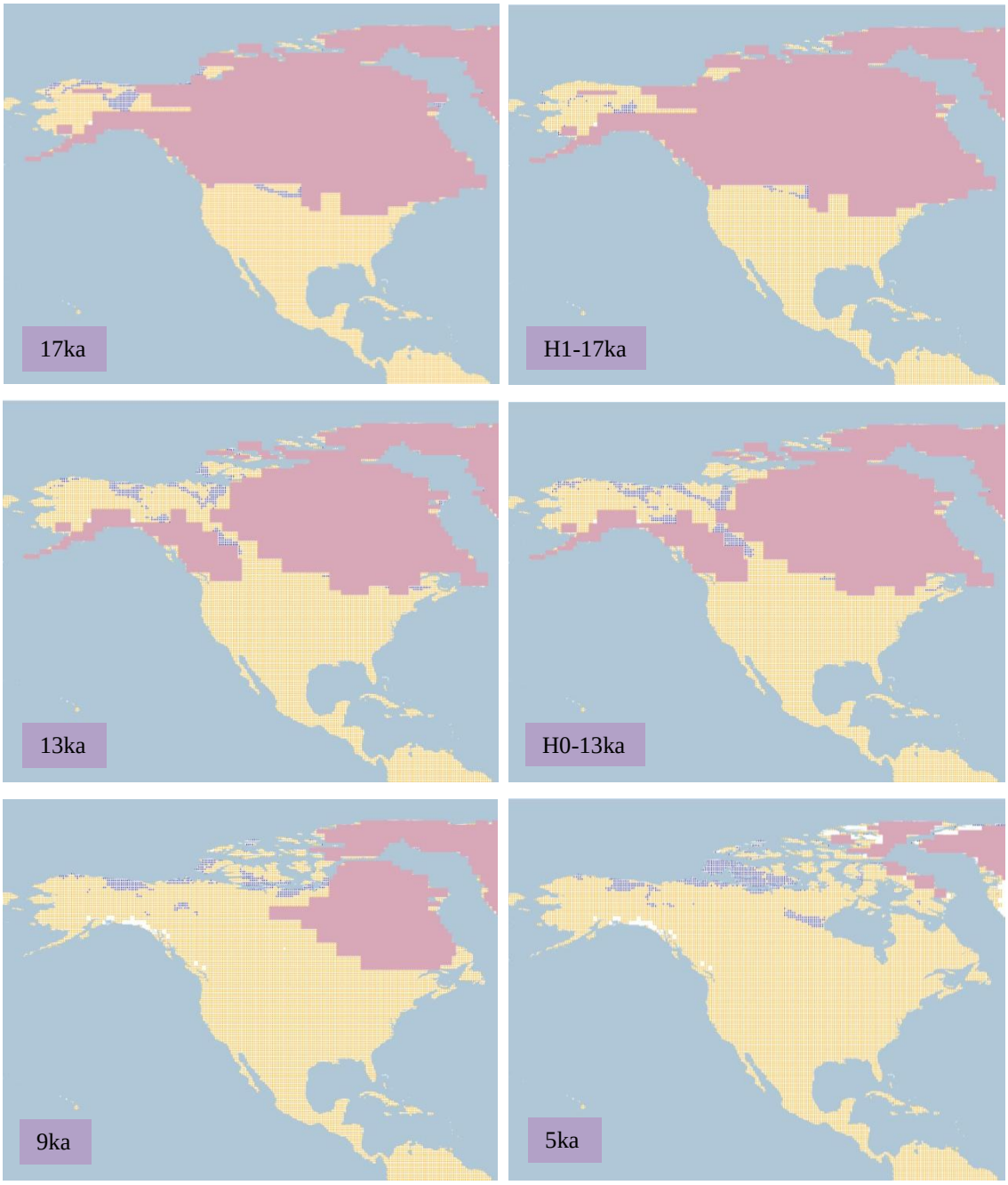

Figure 4.1.4.11.a. Simulation maps of Stilt Sandpiper breeding range (continued**).**

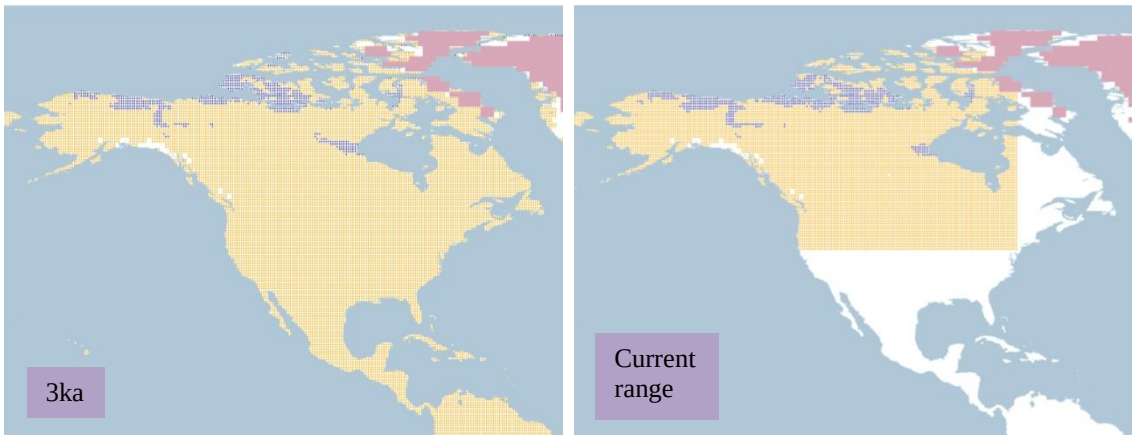

Figure 4.1.4.11.a. Simulation maps of Stilt Sandpiper breeding range (continued**).**

Non-breeding range (AUC: 0.979; TSS: 0.866; Kappa: 0.848): The non-breeding range of the species is located mainly in South America from Colombia to north-eastern Argentina and central Brazil. A smaller range is found along the southern coast of Central America, in central-southern and eastern Mexico, in the Greater Antilles and in southern Florida and Texas, USA.

At 26 ka BP a large range is projected in South America, from Colombia to northern Argentina in the south, also as far as the western coast of Ecuador and Peru and in the northern region of Brazil. There is also a small range projected in Central America, central-southern Mexico and southern Florida in the USA. This pattern continues with minimal difference until 19 ka BP, with a small range projected along the eastern coast of Brazil. See Figure 4.1.4.11.b.

By the beginning of the Holocene at 11 ka BP a range is projected from central-southern Mexico, southern Florida in the USA, along the Greater Antilles, Central America and in South America as far as northern Argentina. At 8 ka BP, there is an increase in the range projected in central Mexico, shifting towards the northern region. The pattern of increase continues and by 3 ka BP the range covers the north-western and north-eastern region of Mexico, with the remainder of the range unchanged. This pattern remains until the 1 ka BP projection and the current non-breeding range projection presents a similar range as 1 ka BP.

There are differences between the H2 and 24 ka BP projections, mainly in the range projected in central South America, with a scattered range in the Amazonian region at H2,

and with larger range projected in north-eastern Mexico than at 24 ka BP. A similar pattern continues at H1 in the Amazonian region and between Bolivia and central Brazil. The H0 projection presents a similar range in South America, although the range is extended to the north-eastern coast of Brazil, differing from the 13 ka BP projection.

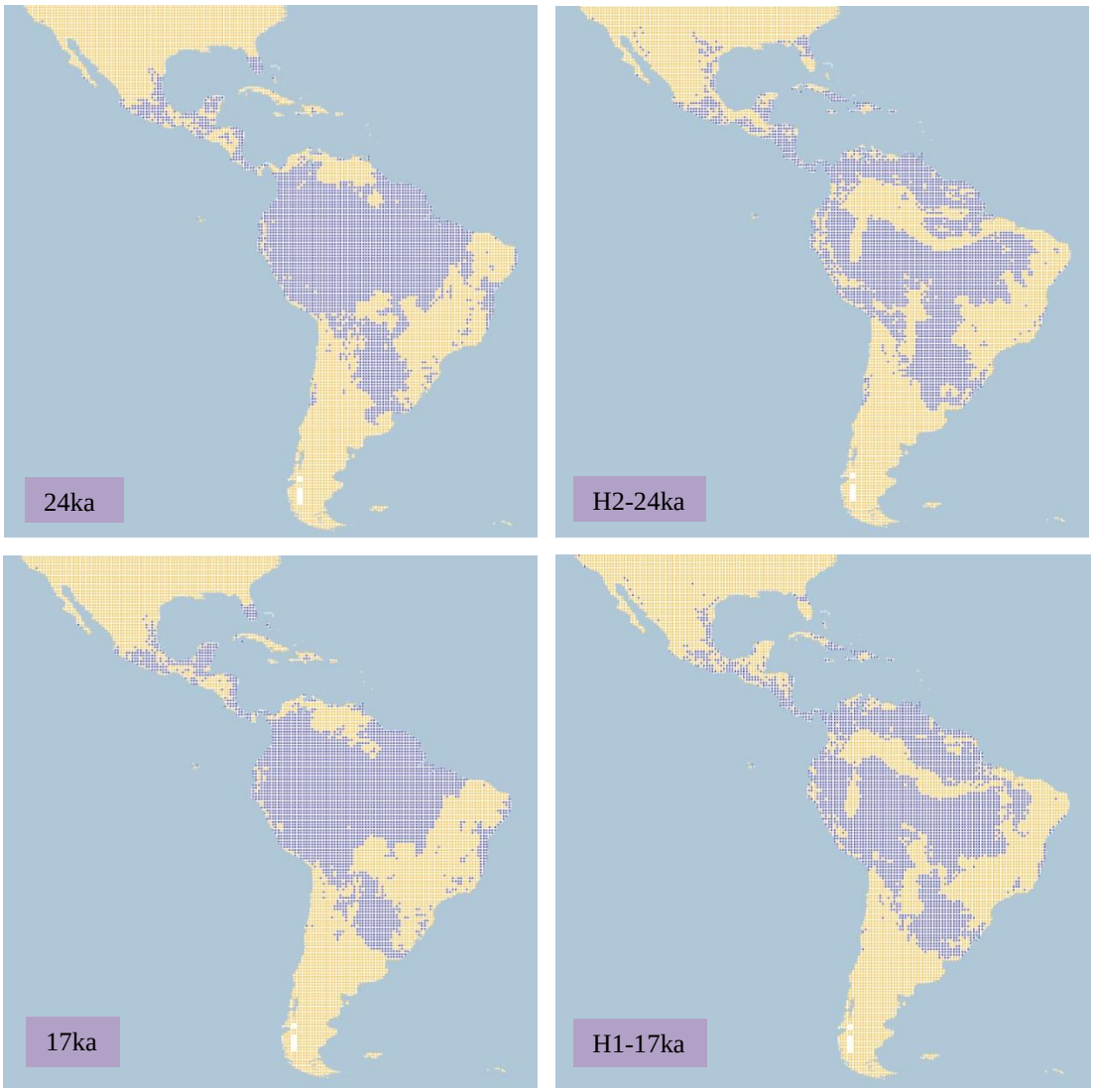

Figure 4.1.4.11.b. Simulation maps of Stilt Sandpiper non-breeding range.
Maps are shown for ten-time slices: 24ka, H2 (24ka), 17ka, H1 (17ka), 13ka, H0 (13ka), 9ka, 5ka, 3ka and present (1961–90).

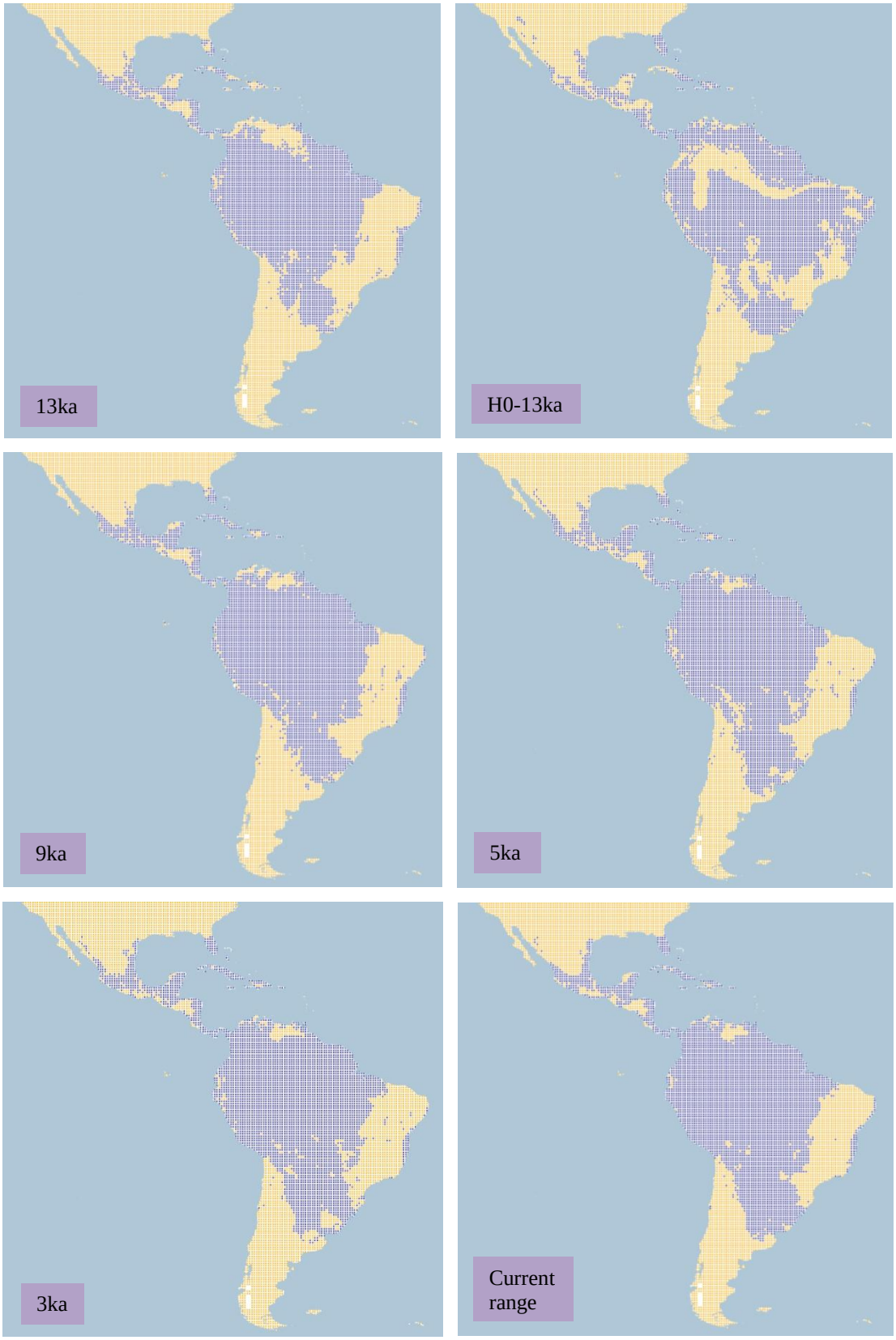

Figure 4.1.4.11.b. Simulation maps of Stilt Sandpiper non-breeding range (continued**).**

*4.1.4.12 Western Sandpiper (*Calidris mauri*). Conservation status: Least Concern. Current known range Figure 4.1.4.12.*

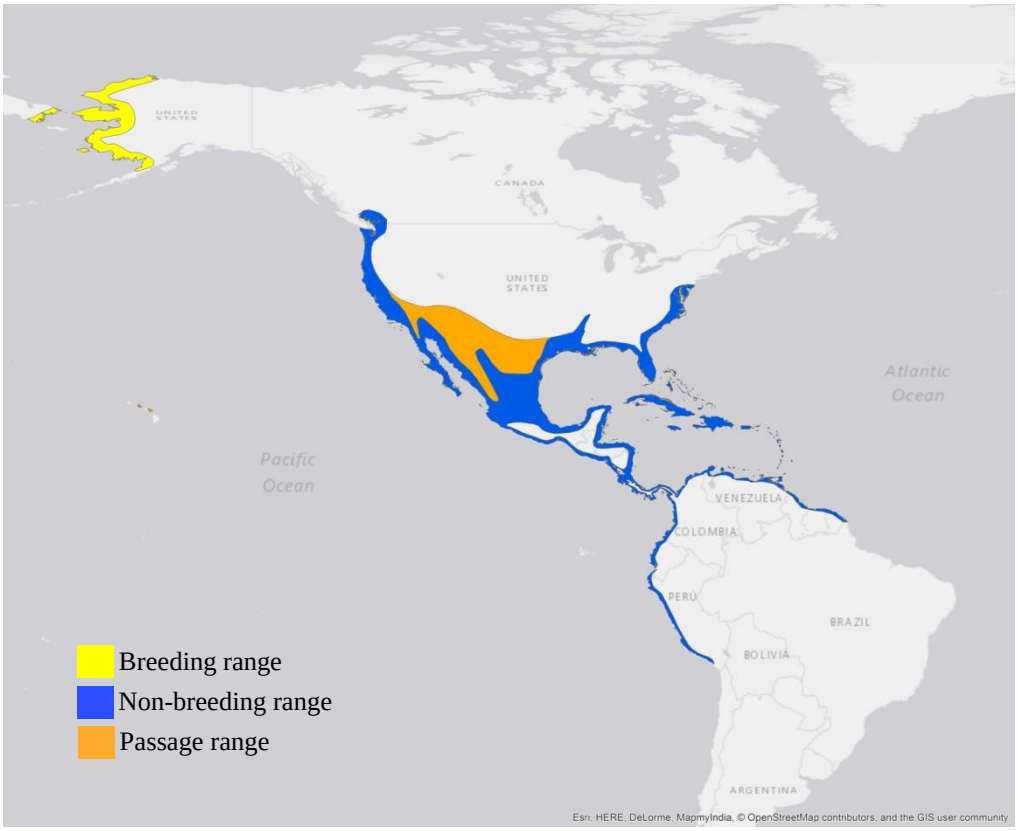

Figure 4.1.4.12. Current known range of Western Sandpiper.

Breeding range (AUC: 0.977; TSS: 0.904; Kappa: 0.575): Spends the breeding season along the western coast of Alaska from north-western North Slope Borough as far as the northern region of the Alaska Peninsula. Also, there is a small breeding range in eastern Chukotka, Russia.

At 26 ka BP a small range is projected in central Alaska and in the north-western and eastern region of the USA, in Minnesota, Wisconsin and Pennsylvania. This pattern continues until 16 ka BP when there is a decrease in the range projected in Minnesota and in southern Alaska in the USA. After this at 15 ka BP, the range in Pennsylvania disappears and a small range is projected in New Hampshire in the USA. See Figure 4.1.4.12.a.

At the deglaciation at 13 ka BP, there is a projected range in northern Canada in the Northwest Territories. By the beginning of the Holocene at 11 ka BP, a scattered range is projected in southern Alaska in the USA, northern British Columbia, and southern Albert and

in northern Northwest Territories in Canada. After this at 10 ka BP, there is an increase in the range projected in Alaska, covering the western region; there is also an increase in the range projected near the ice sheet in the Northwest Territories of Canada. At 9ka, the range in the Northwest Territories shifts near the ice sheet in southern Nunavut. With the reduction of the ice sheet at 8 ka BP, the range in central Canada shifts near Hudson Bay between Ontario and Quebec. This range near Hudson Bay is reduced at 7 ka BP.

At 6 ka BP, the range is mainly projected in western and southern Alaska, in northern British Columbia and southern Alberta with a small range in Quebec near Hudson Bay and in eastern Newfoundland and Labrador. This pattern continues with minimal differences until the 1 ka BP projection. The current breeding range projection presents a larger range in western Alaska than the 1 ka BP projection.

A similar range is seen in the H2 and 24 ka BP projections, in the north-western conterminous USA, with a larger range in the eastern region between Iowa and Wisconsin at H2. This increasing pattern continues at H1, with the range in the northern region of the USA shifting to the central region, differing from the small range projected at 17ka. This change, however, at H0, when the range in central-northern parts of the conterminous USA is reduced, and a small range is projected in northern Northwest Territories of Canada at H0, similar to the 13 ka BP projection.

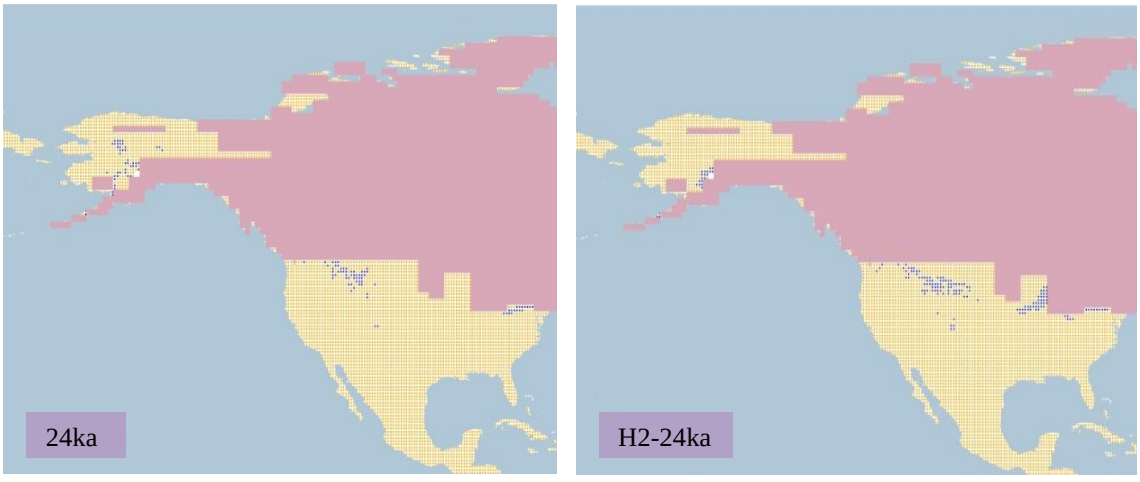

Figure 4.1.4.12.a. Simulation maps of Western Sandpiper breeding range.
Maps are shown for ten-time slices: 24ka, H2 (24ka), 17ka, H1 (17ka), 13ka, H0 (13ka), 9ka, 5ka, 3ka and present (1961–90).

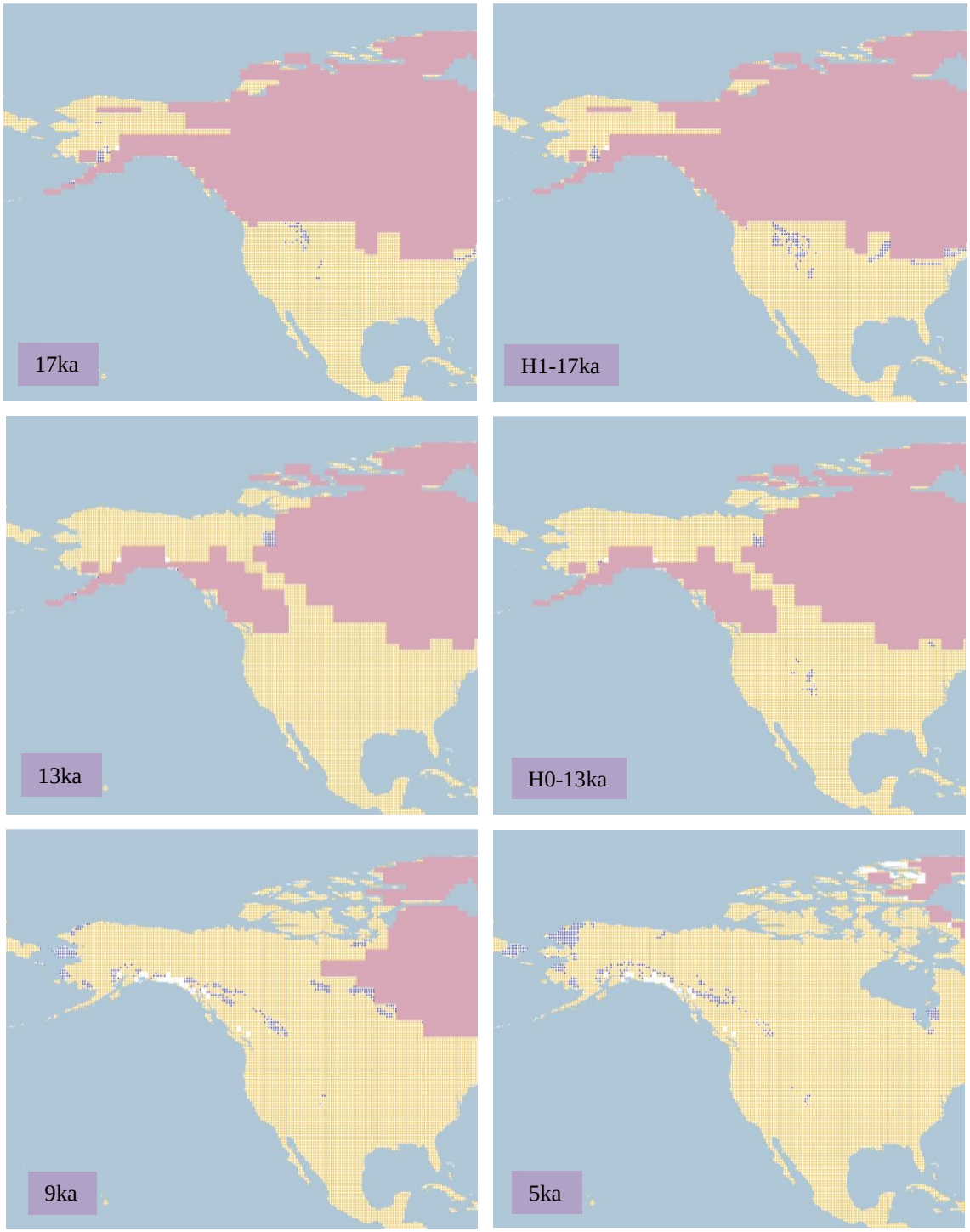

Figure 4.1.4.12.a. Simulation maps of Western Sandpiper breeding range (continued**).**

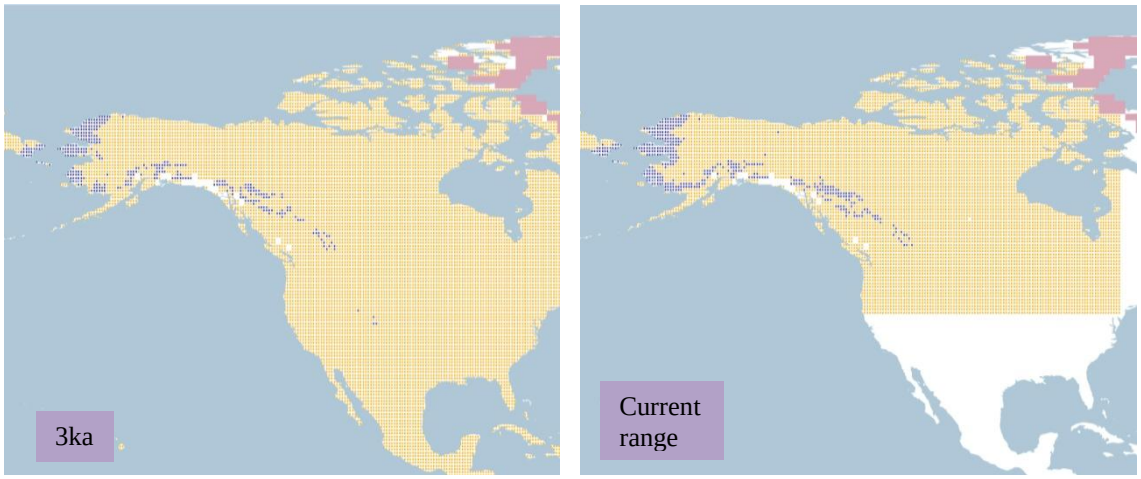

Figure 4.1.4.12.a. Simulation maps of Western Sandpiper breeding range (continued**).**

Non-breeding range (AUC: 0.963; TSS: 0.780; Kappa: 0.689): The species spends the winter season from the south-western coast of Canada along the western coast of the USA, Mexico, Central America and South America as far as southern Peru. The range also extends to the eastern coast of the USA, Mexico, Central America and South America as far as French Guiana, and along the Greater Antilles.

At 26 ka BP the range is projected along the western coast of the USA and western coast of Mexico as far as Oaxaca with an inland range covering the central and eastern region of Mexico. A small range is also projected in Florida in the USA and along the coast of Ecuador and Peru in South America, with a scattered range along the Andean cordillera and in eastern Brazil. This pattern continues until 18 ka BP when there is a decrease in the range located in the western part of the USA. See Figure 4.1.4.12.b.

At 13 ka BP, the range is projected along the western coast of the USA and Mexico with an inland range from central to northern Mexico, a small range in Florida in the USA, along the coast of Ecuador and Peru and in the Andean cordillera, with a projected range in northern Brazil. The range at 12 ka BP increase in the northern region of Brazil, in Florida and the western coast of the USA.

By the beginning of the Holocene the range is projected mainly in Mexico, the western and south-eastern coast of the USA with a small range in the Greater Antilles, northern Brazil and the Andean cordillera. After this at 10 ka BP, there is a small projected range in south-central Canada near the ice sheet.

In northern Mexico and in the central region of South America the range is increased at 6ka; however, this range in central South America is reduced at 5 ka BP. The pattern continues through Mexico, the Greater Antilles, the western and south-eastern coast of the USA, and along the western coast of Ecuador and Peru until the 1 ka BP projection. The current non-breeding range projection presents a similar range across North America and South America as 1 ka BP.

There are differences between H2 and 24 ka BP, mainly with a projected range in the southern region of the USA, in Central America and northern South America at H2, differing from the 24 ka BP projection. This pattern is continued at H1, although the range in the southern part of the USA shifts to north-western Mexico, still with a different range projected than at 17ka. Between the H0 and 13 ka BP projection a similar range is projected along the western coast of the USA and in Mexico, although with a larger range from southern Mexico as far as northern South America at H0, differing from the 13 ka BP projection.

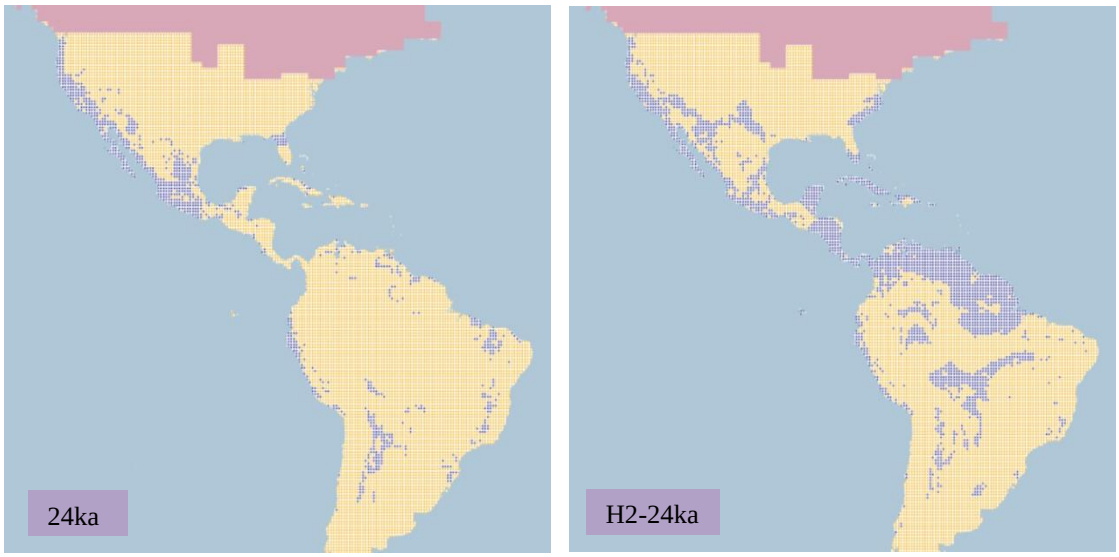

Figure 4.1.4.12.b. Simulation maps of Western Sandpiper non-breeding range.
Maps are shown for ten-time slices: 24ka, H2 (24ka), 17ka, H1 (17ka), 13ka, H0 (13ka), 9ka, 5ka, 3ka and present (1961–90).

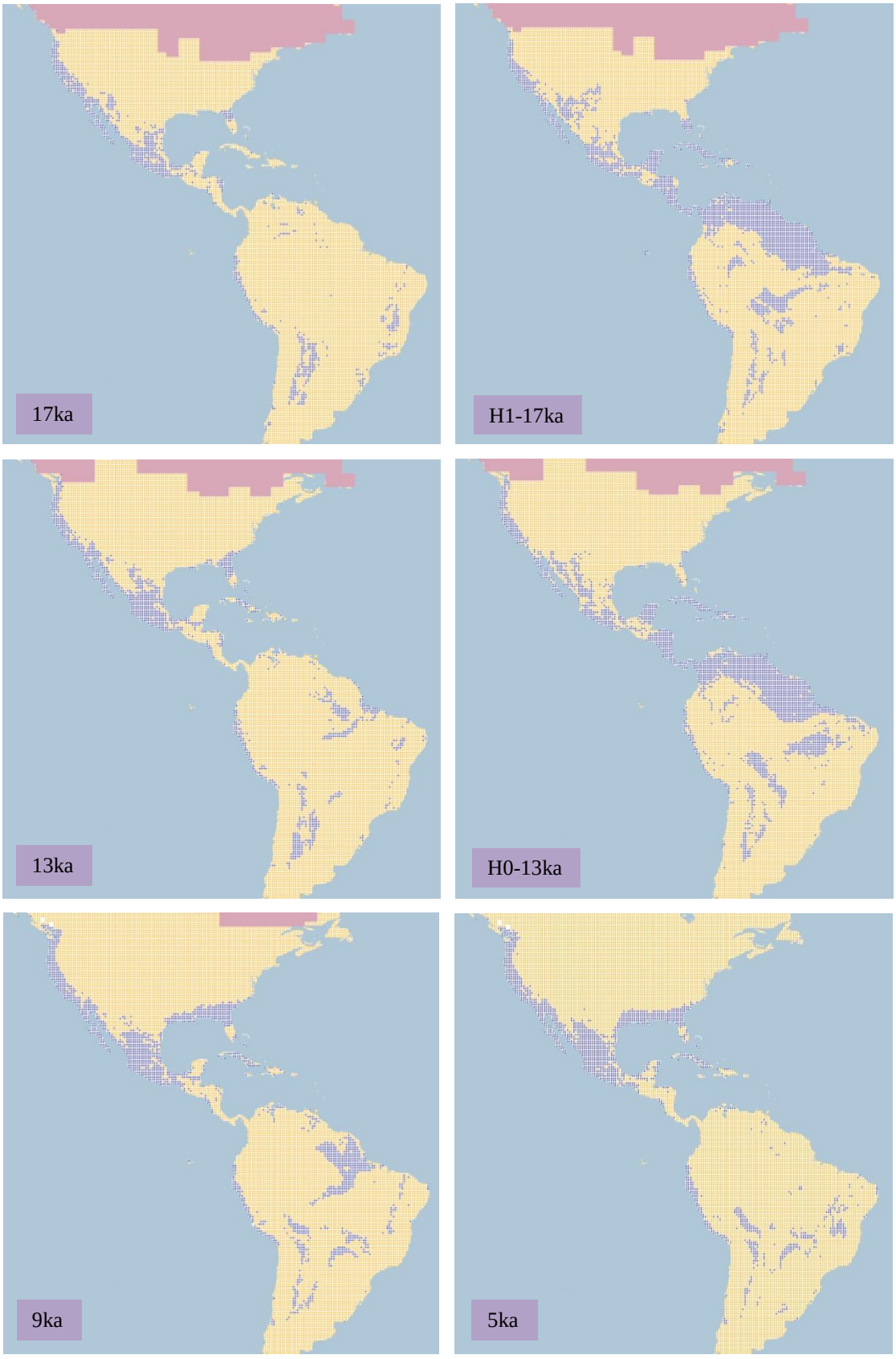

Figure 4.1.4.12.b. Simulation maps of Western Sandpiper non-breeding range (continued**).**

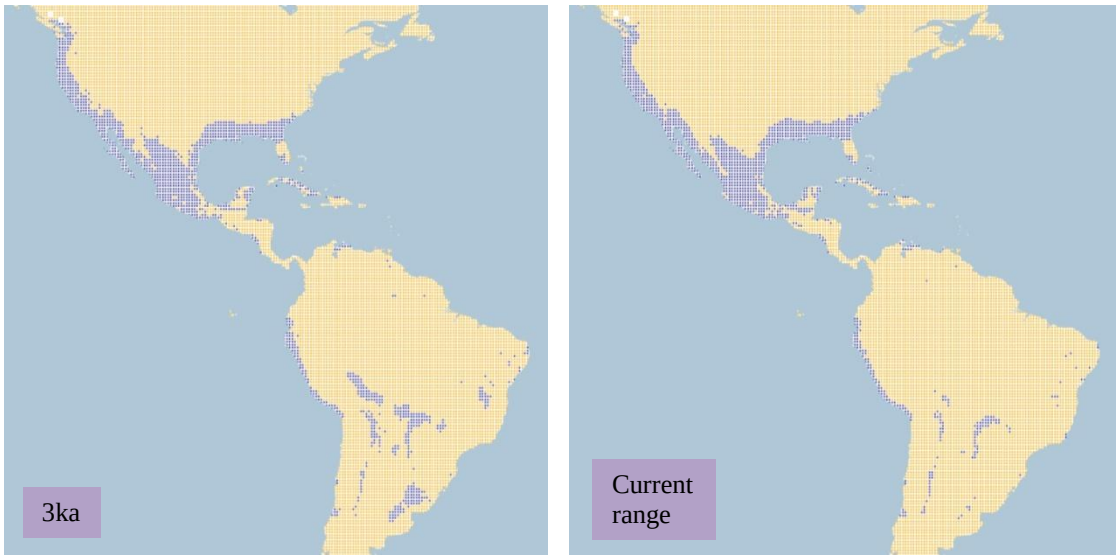

Figure 4.1.4.12.b. Simulation maps of Western Sandpiper non-breeding range (continued**).**

*4.1.4.13 Pectoral Sandpiper (*Calidris melanotos*). Conservation status: Least Concern. Current known range Figure 4.1.4.13.*

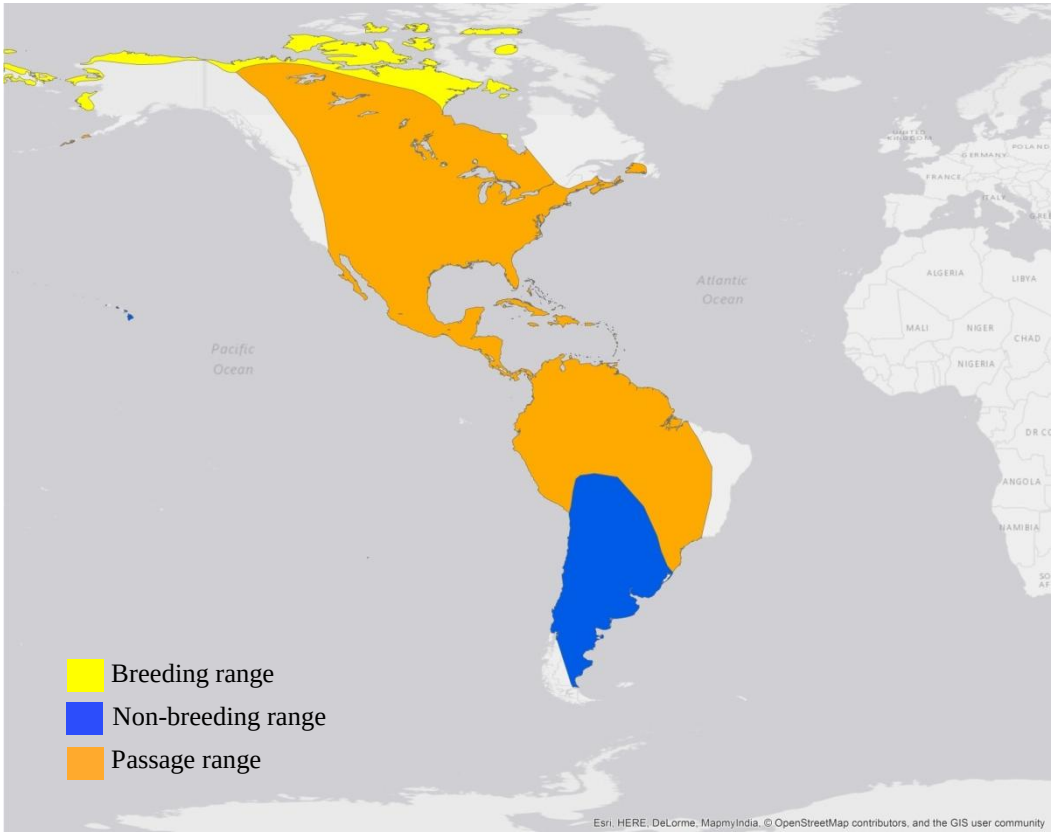

Figure 4.1.4.13. Current known range of Pectoral Sandpiper.

Breeding range (AUC: 0.940; TSS: 0.752; Kappa: 0.639): Only the North American breeding range was modelled. This extends across western and northern Alaska, and north-central Canada from Yukon as far as Hudson Bay. The species also breeds in northern Siberia, however, from the Yamal Peninsula to the Chukotskiy Peninsula, as well as on the New Siberian Islands and Wrangel Island.

At 26 ka BP the range is projected in northern Canada in areas not covered by ice, between Yukon and the Northwest Territories; there is also a projected range in northern and western parts of Alaska, and in the central-northern part of the conterminous USA between Montana and Minnesota. This pattern continues until 16 ka BP, when the range in the central-northern part of the conterminous USA shifts to the north between the boundaries of central-southern Canada near the ice sheet. See Figure 4.1.4.13.a.

At 15 ka BP, the range in southern Canada decreases, with an increase in the northern part as the ice sheet is reduced. After this at 14 ka BP, the range in northern Canada is reduced, as is that in northern Alaska in the USA. The decreasing pattern continues at 12 ka BP when the range is restricted to the northern region of Canada and the northern and western part of Alaska.

By the beginning of the Holocene at 11 ka BP the range in western Alaska disappears, with the range covering the northern part of Canada and the Arctic Archipelago. This pattern continues and at 7 ka BP with the deglaciation, a range is projected in northern Nunavut in Canada. From 4 ka BP until 1 ka BP the range is projected in the northern part of North America, from northern Alaska in the USA to northern Nunavut in Canada. This pattern is continued in the current breeding range projection.

A similar range is projected between H2 and 24 ka BP in the northern part of Canada, western Alaska and the central-northern conterminous USA. The same is observed between H1 and 17 ka BP with minimal differences in the range projected in Alaska. A larger range is projected in northern Yukon at H0 than at 13 ka BP, with the remainder of the range unchanged.

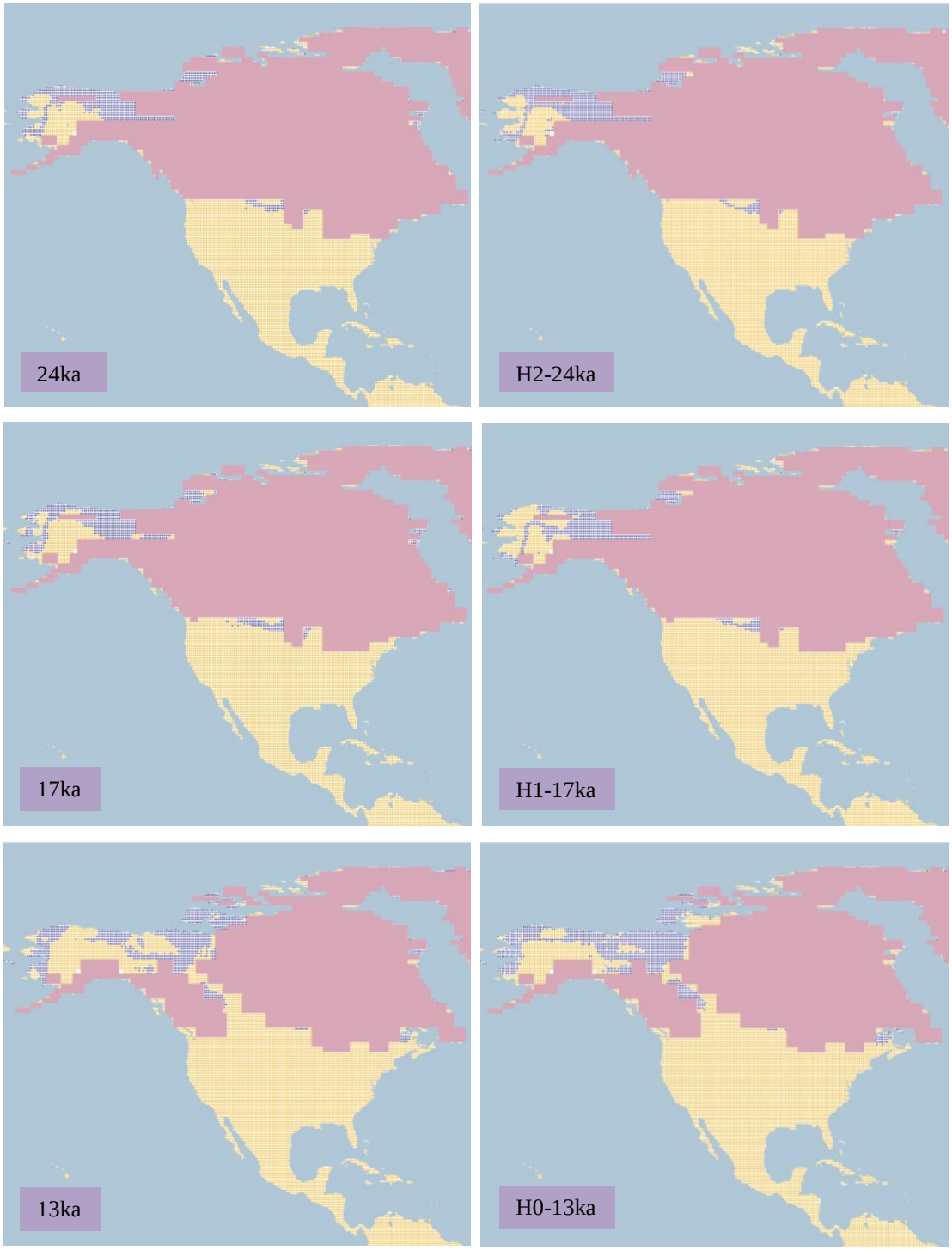

Figure 4.1.4.13.a. Simulation maps of Pectoral Sandpiper breeding range.
Maps are shown for ten-time slices: 24ka, H2 (24ka), 17ka, H1 (17ka), 13ka, H0 (13ka), 9ka, 5ka, 3ka and present (1961–90).

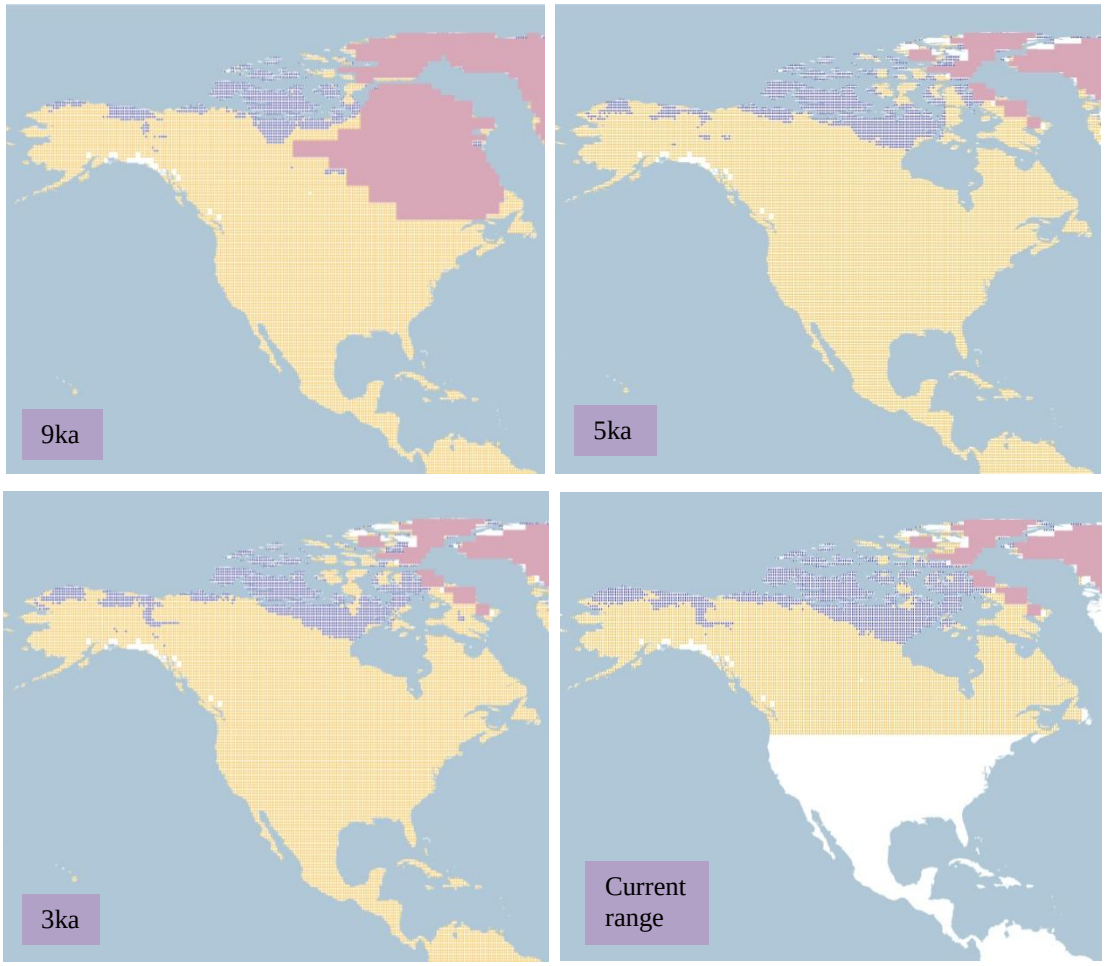

Figure 4.1.4.13.a. Simulation maps of Pectoral Sandpiper breeding range (continued**).**

Non-breeding range (AUC: 0.988; TSS: 0.887; Kappa: 0.816): The species' non-breeding range is located in central and southern South America, from Bolivia to southern Chile and Argentina.

At 26 ka BP a large range is projected in the central-southern region of South America, from southern Peru and southern Brazil as far as south-eastern Argentina. This pattern continues until there is a reduction in the range in southern Brazil at 21 ka BP. After this at 15 ka BP, the range is increased in southern Brazil. See Figure 4.1.4.13.b.

By the beginning of the Holocene the range in central-southern Brazil is increased, with the remainder of the range unchanged. After this, there is a small reduction in the range in southern Brazil, Bolivia and northern Argentina at 7 ka BP, which is increased at 6 ka BP. From 3 ka BP until ka BP, the range remains in central-southern South America, with minimal variations. The current non-breeding range projection presents a similar range from

central to southern South America as the 1 ka BP projection. There is a similar range projected between H2 and 24 ka BP in South America, with minimal variations in southern Brazil. This continues at H1, although a small range is projected in northern Brazil, differing from the 17 ka BP projection. This small range in northern Brazil is decreased at H0, with a smaller range also in southern Brazil and Bolivia than at the 13 ka BP projection.

Even though the current non-breeding range of the species is located in South America, there are suitable conditions projected for the species in the south-western part of the USA and in central-southern Mexico.

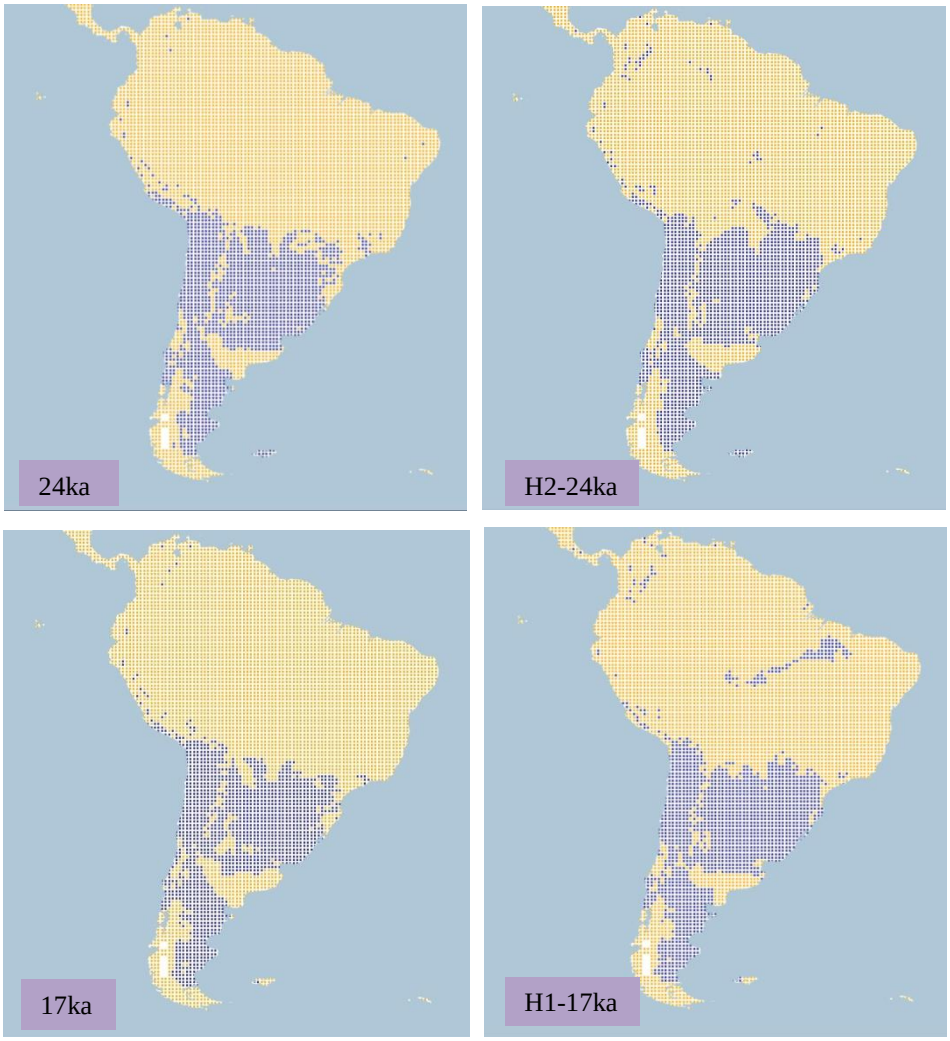

Figure 4.1.4.13.b. Simulation maps of Pectoral Sandpiper non-breeding range.
Maps are shown for ten-time slices: 24ka, H2 (24ka), 17ka, H1 (17ka), 13ka, H0 (13ka), 9ka, 5ka, 3ka and present (1961–90).

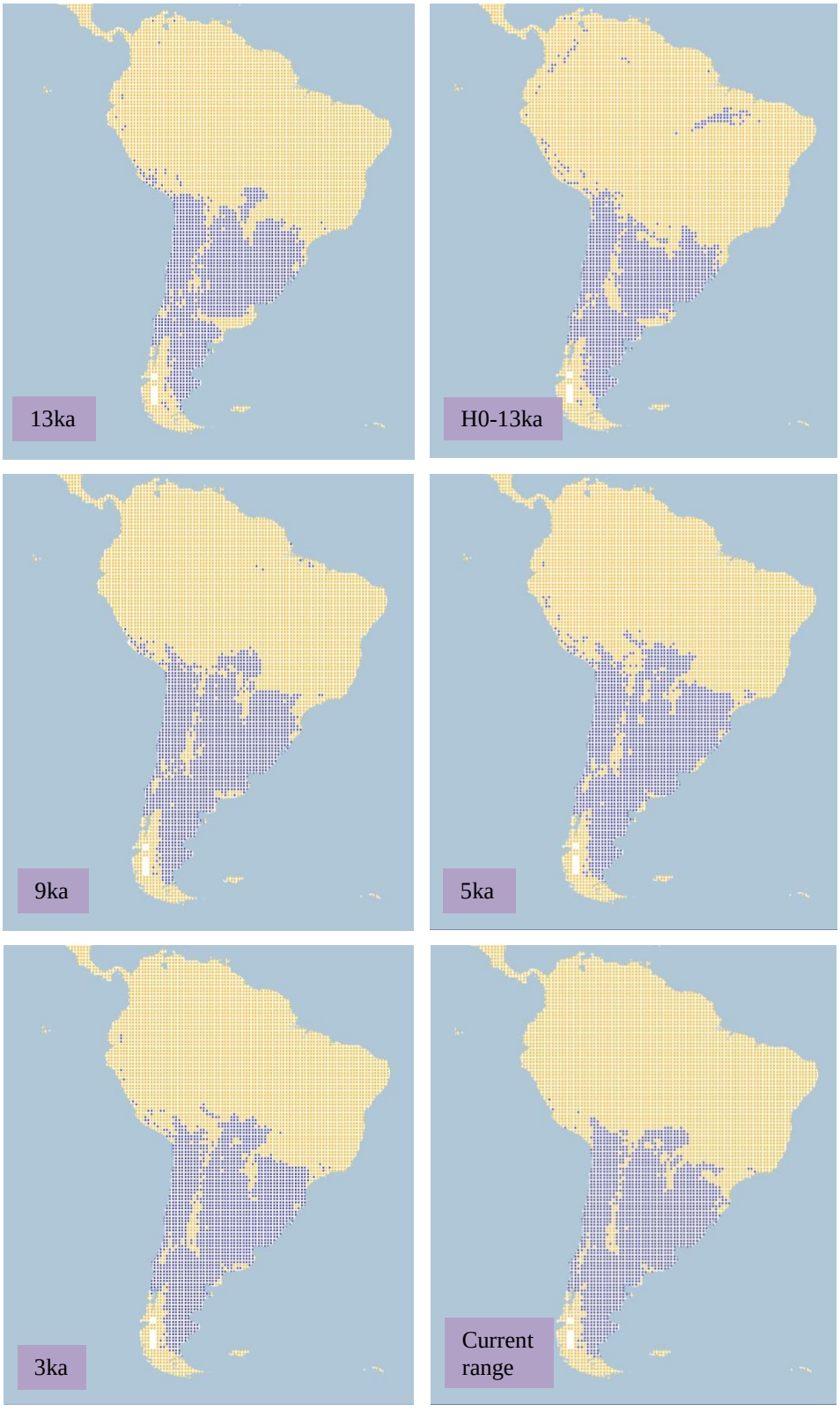

Figure 4.1.4.13.b. Simulation maps of Pectoral Sandpiper non-breeding range (continued**).**

*4.1.4.14 Least Sandpiper (*Calidris minutilla*). Conservation status: Least Concern. Current known range Figure 4.1.4.14.*

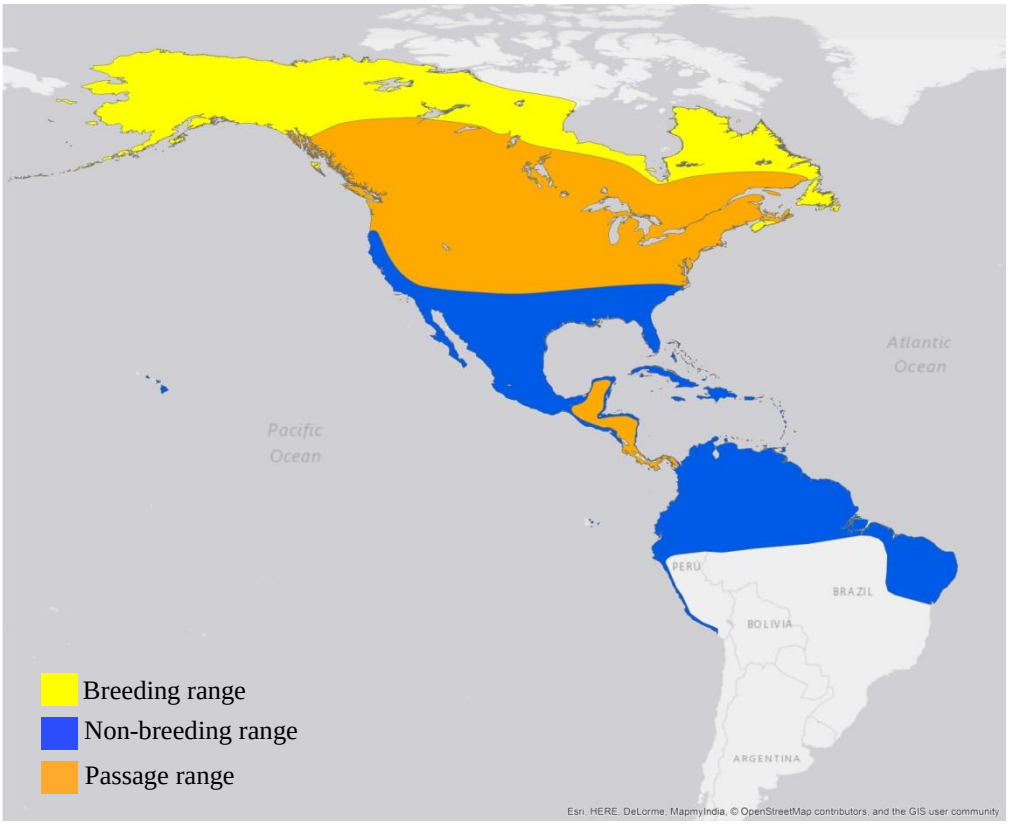

Figure 4.1.4.14. Current known range of Least Sandpiper.

Breeding range (AUC: 0.987; TSS: 0.896; Kappa: 0.847): Breeds in northern North America from Alaska in USA to north-central Yukon, north-central Northwest Territories, central Nunavut, and across northern Manitoba and Ontario near Hudson Bay to north-central Quebec, Newfoundland and Labrador.

At 26 ka BP the range is projected in the northern region of North America from central Alaska in the USA to north-western Yukon in Canada, and across the northern part of the conterminous USA. This pattern continues with minimal differences until 15 ka BP, when the range in the northern region of the conterminous USA is reduced. After this at 14 ka BP, the range in northern Canada and in Alaska is increased. With the deglaciation at 13 ka BP, the range in the north of the conterminous USA shifts to southern and central Canada, meeting the northern range from extending from Yukon to Alaska. See Figure 4.1.4.14.a.

By the beginning of the Holocene the range is projected from Alaska to the Northwest Territories, and with a small range in British Columbia and in south-eastern Quebec next to the ice sheet. The range continues growing at 10 ka BP with the deglaciation, mainly in Canada. After this at 9ka, the range in the northern part of Northwest Territories and Nunavut is reduced.

By 8 ka BP, the range in Canada reaches Hudson Bay and as far as Newfoundland and Labrador. This pattern continues from 3 ka BP until 1 ka BP. The current breeding projection also presents a similar range in northern North America to the 1 ka BP projection.

There are differences between H2 and 24 ka BP in the range projected in the conterminous USA, with a larger range projected at H2 from the central to northern part of the USA. This range is reduced at H1, although with differences persisting in the central area of the conterminous USA and with a smaller range in Alaska than at 1 ka BP. Between H0 and 13 ka BP, a similar range is projected from Alaska to southern Canada; however, for H0 there is a small range projected in the central-western conterminous USA, differing from 13 ka BP.

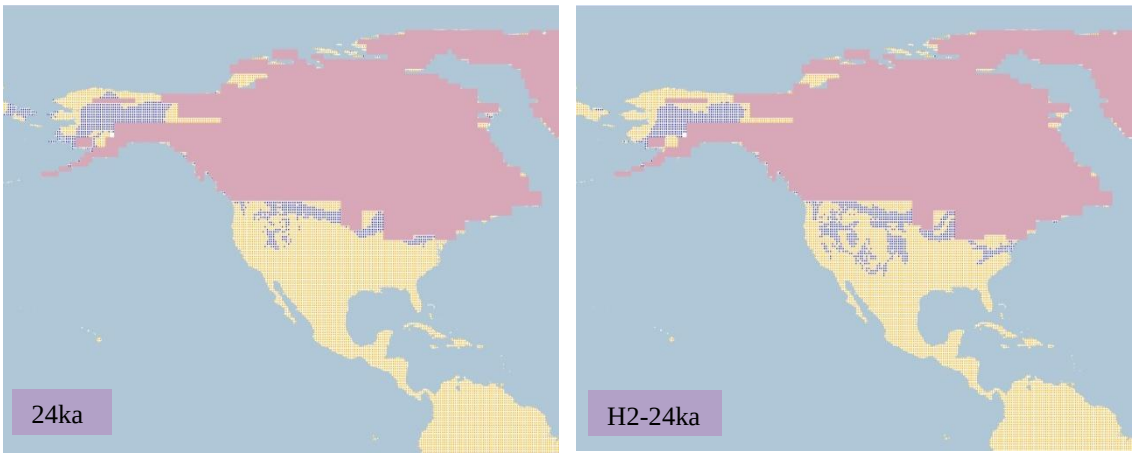

Figure 4.1.4.14.a. Simulation maps of Least Sandpiper breeding range.
Maps are shown for ten-time slices: 24ka, H2 (24ka), 17ka, H1 (17ka), 13ka, H0 (13ka), 9ka, 5ka, 3ka and present (1961–90).

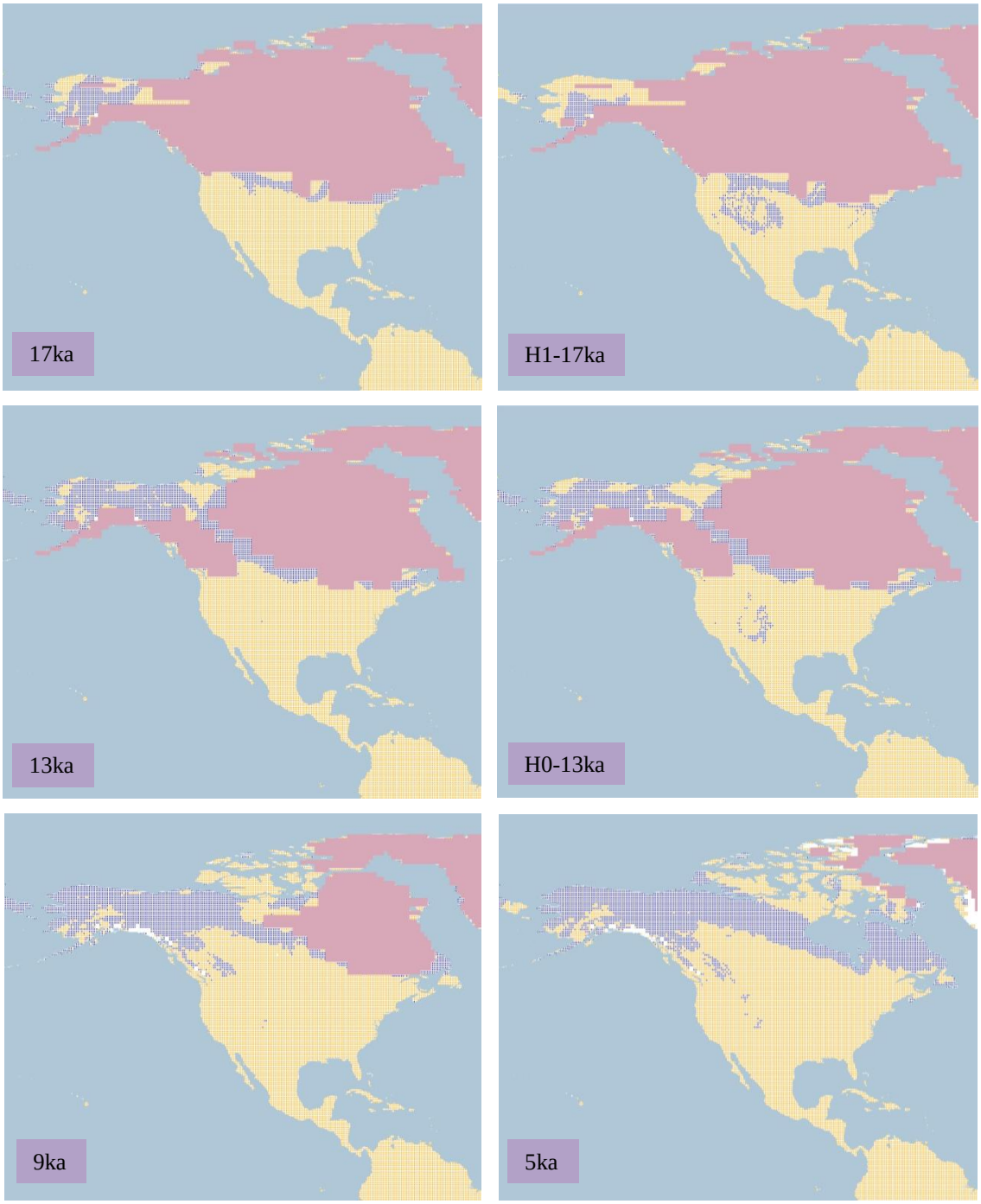

Figure 4.1.4.14.a. Simulation maps of Least Sandpiper breeding range (continued**).**

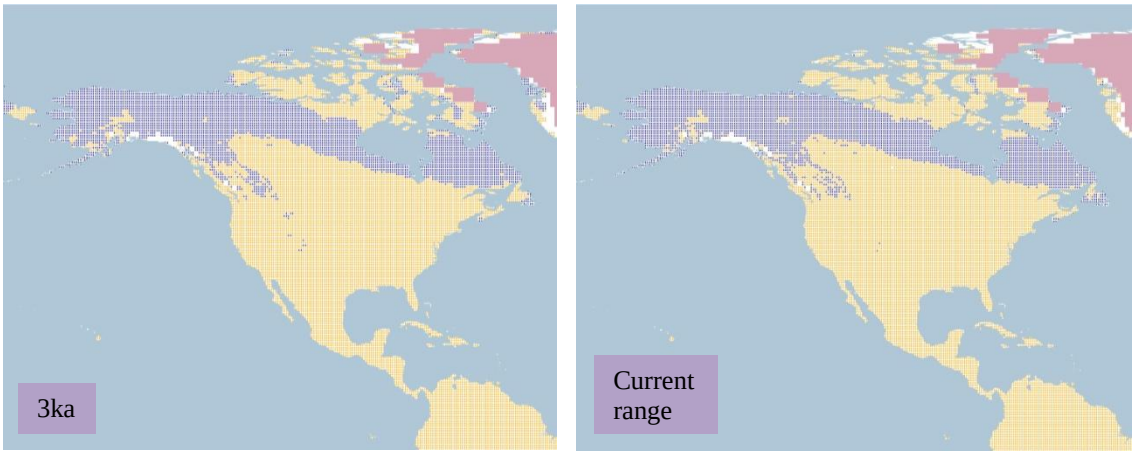

Figure 4.1.4.14.a. Simulation maps of Least Sandpiper breeding range (continued**).**

Non-breeding range (AUC: 0.979; TSS: 0.866; Kappa: 0.817): This species spends the winter season from the southern USA, through Mexico, coastal areas of Central America, the Greater Antilles and in northern South America as far as coastal Peru and north-eastern Brazil.

At 26 ka BP a range is projected from the western coast and southern region of the USA, through central and northern Mexico, the Greater Antilles, to Central America and northern South America, with a small range along the Andean cordillera. This pattern continues with minimal differences in South America and northern Mexico until 16 ka BP, when the range in the southern part of the USA is increased. See Figure 4.1.4.14.b.

By the beginning of the Holocene the range is projected from the southern region of the USA, along most of the territory in Mexico, and in northern South America. This continues until 8 ka BP, when there is a projected range in Central America and the Greater Antilles, and an increase in the range projected in north-eastern Brazil in South America.

From 5 ka BP until ka BP, the range continues with only minimal variations from the southern part of the USA, in Mexico except in the southern region, through Central America, a small range in the Greater Antilles, and in the northern part of South America. This pattern is followed in the current non-breeding range projection as well.

When comparing the Heinrich event H2 with the 24 ka BP projection, there is no range projected in the central-southern part of the USA and northern part of Mexico and there is a projected range in southern Mexico and Central America at H2, being different from 24ka.

This change at H1, with a range projected in the southern region of the USA and northern part of Mexico, although of smaller extent than for 17ka. The same is observed between H0 and 13 ka BP with a smaller range projected in the southern part of the USA and central-northern Mexico, but a larger range in northern South America.

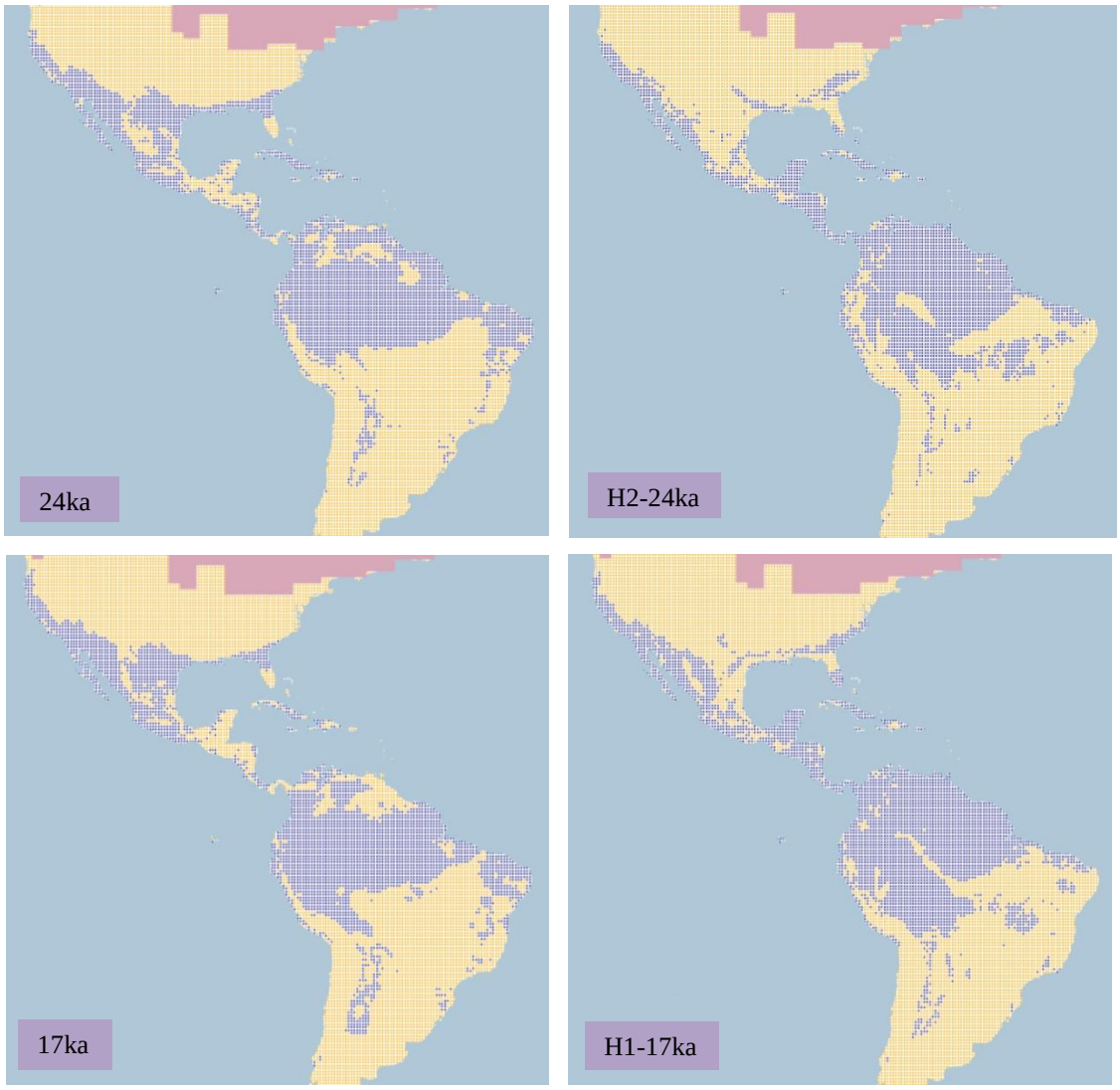

Figure 4.1.4.14.b. Simulation maps of Least Sandpiper non-breeding range.
Maps are shown for ten-time slices: 24ka, H2 (24ka), 17ka, H1 (17ka), 13ka, H0 (13ka), 9ka, 5ka, 3ka and present (1961–90).

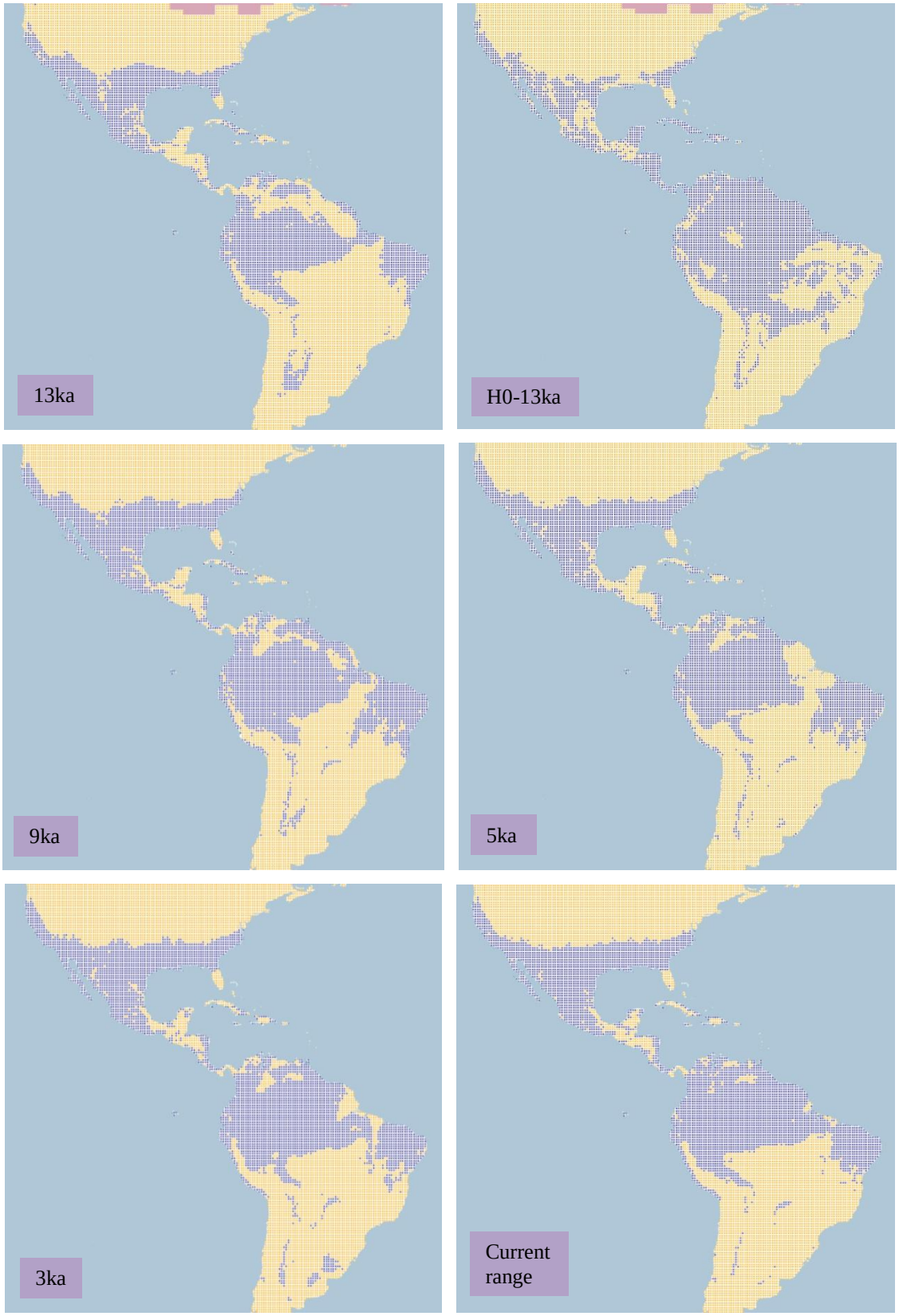

Figure 4.1.4.14.b. Simulation maps of Least Sandpiper non-breeding range (continued**).**

*4.1.4.15 Semipalmate Sandpiper (*Calidris pusilla*). Conservation status: Near Threatened. Current known range Figure 4.1.4.15.*

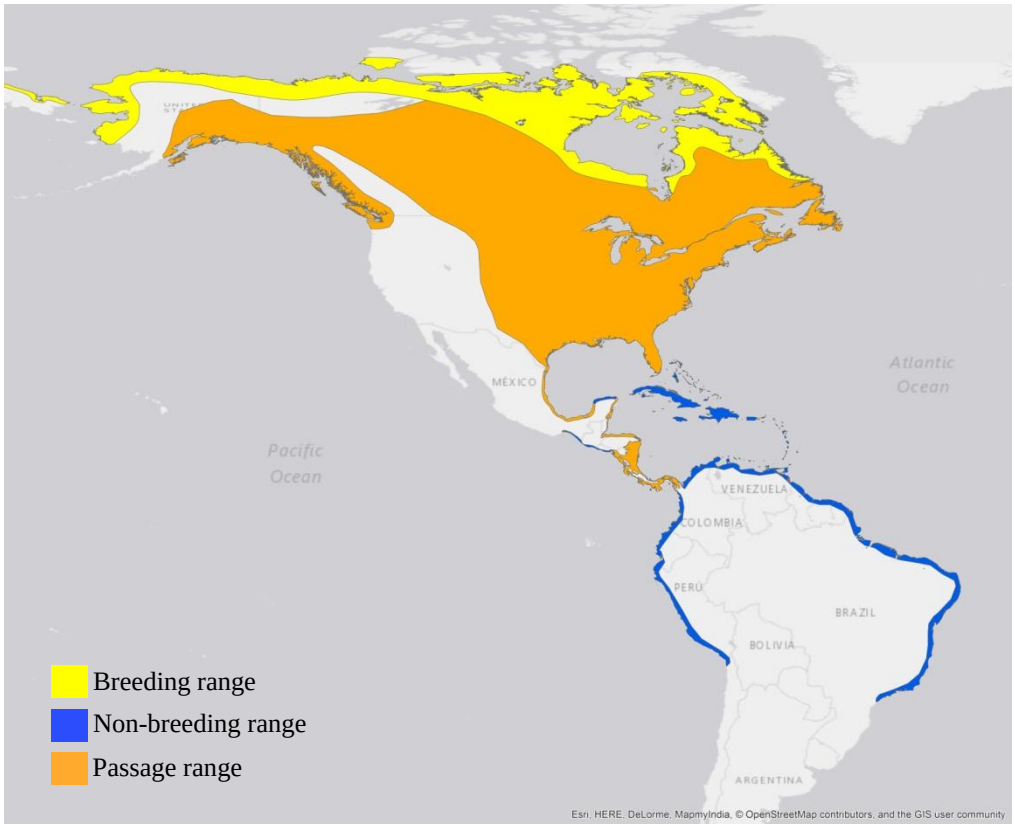

Figure 4.1.4.15. Current known range of Semipalmated Sandpiper.

Breeding range (AUC: 0.978; TSS: 0.888; Kappa: 0.581): Spends the breeding season in northern North America, from western Alaska to northern Yukon, northern Northwest Territories, central-northern Nunavut, northern Manitoba, northern Ontario near Hudson Bay, northern Quebec and Newfoundland and Labrador. There is also a small range in extreme eastern Siberia on the Chukotskiy Peninsula.

At 26 ka BP the range is projected in the northern part of conterminous USA, from Montana to Wisconsin near the ice sheet, and with a smaller range in northern Alaska. This pattern continues with minimal variations until 16 ka BP, when the range in the northern region of the conterminous USA is reduced and shifted to the southern boundary of Canada near the ice sheet. Following this, at 15 ka BP, the range in the northern part of conterminous USA disappears, increasing in the northern part of Canada not covered by ice. See Figure 4.1.4.15.a.

With the deglaciation at 13 ka BP, the range is projected in the Yukon, northern Northwest Territories and in central Alberta in Canada, with a small range in northern Alaska and southern Quebec. After this at 12 ka BP, the range shifts to the northern region of the Yukon and the Northwest Territories, disappearing from Alberta in Canada.

By the beginning of the Holocene the range is projected in the northern part of North America from Alaska in the USA to the Northwest Territories in Canada. The range is increased in the northern part of Canada at 9ka, reaching Nunavut. With the deglaciation at 8 ka BP the range is projected in Nunavut near Hudson Bay and in the northern part of Quebec and the Arctic Archipelago.

At 5 ka BP the range in central Nunavut and northern Quebec in Canada is reduced; after this, at 4 ka BP the range in the northern part of Alaska increased. This pattern continues with minimal differences until the 1 ka BP projection. The current breeding range projection also presents a similar range in the northern region of North America as 1 ka BP.

There are small differences between the H2 and 24 ka BP projections, with a smaller range in Alaska and a larger range in the northern conterminous USA for H2. The range is reduced in the H1 projection, similar to the 17 ka BP projection, although with a smaller range in southern Alaska. The H0 and 13 ka BP projections present similar ranges, only with a larger range projected in northern Yukon in Canada at H0.

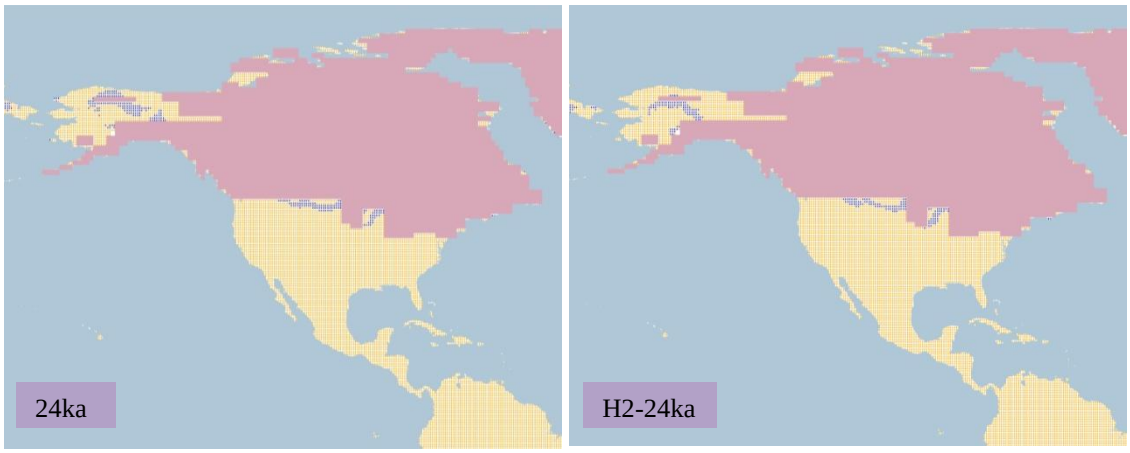

Figure 4.1.4.15.a. Simulation maps of Semipalmated Sandpiper breeding range.
Maps are shown for ten-time slices: 24ka, H2 (24ka), 17ka, H1 (17ka), 13ka, H0 (13ka), 9ka, 5ka, 3ka and present (1961–90).

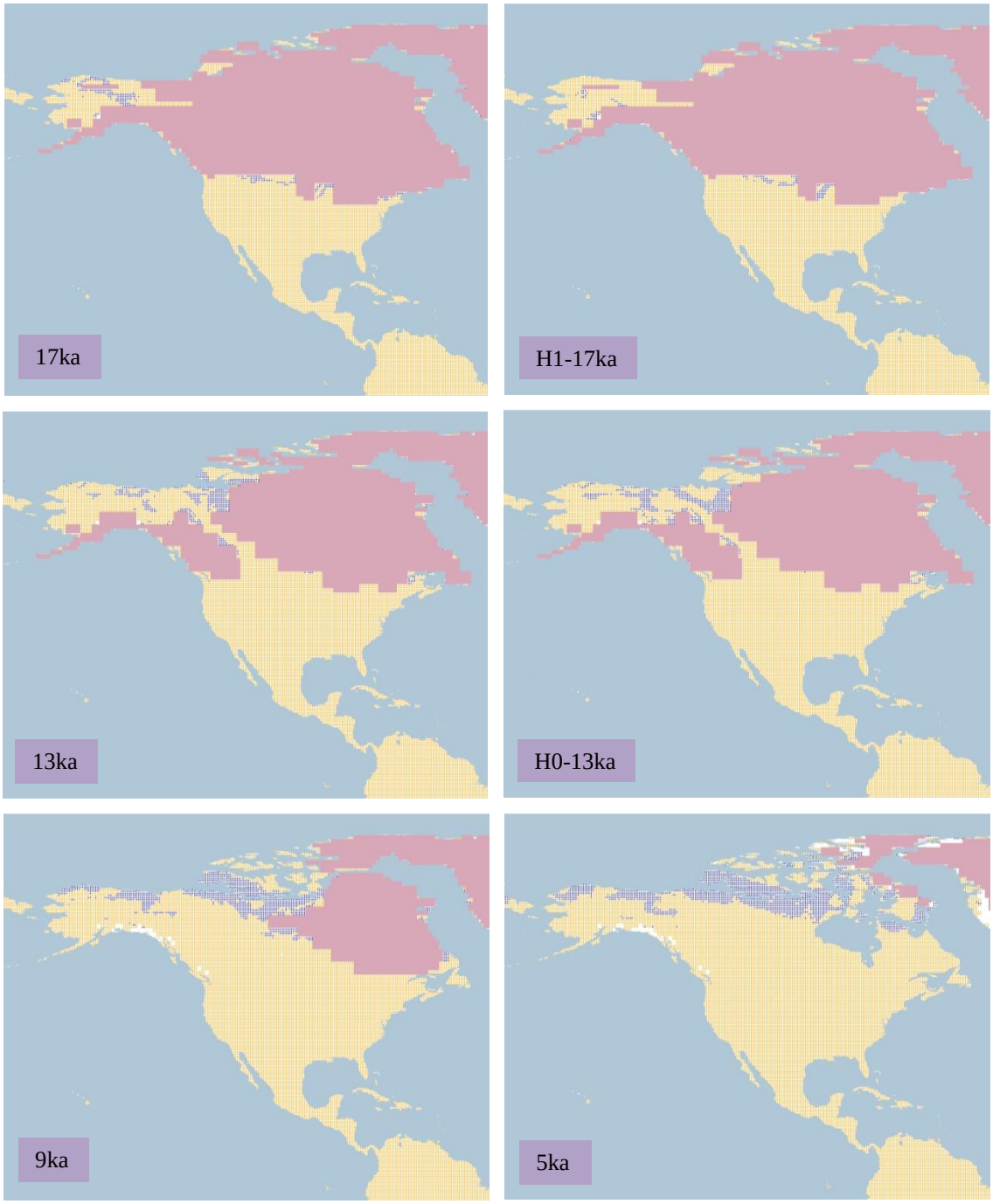

Figure 4.1.4.15.a. Simulation maps of Semipalmated Sandpiper breeding range (continued**).**

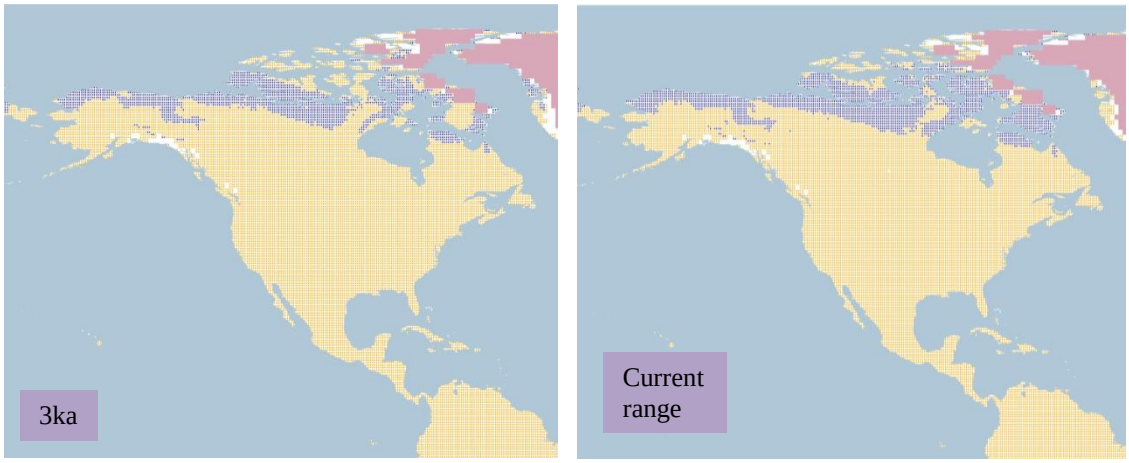

Figure 4.1.4.15.a. Simulation maps of Semipalmated Sandpiper breeding range (continued**).**

Non-breeding range (AUC: 0.977; TSS: 0.874; Kappa: 0.451): Wintering grounds are mainly located along coasts in the Greater Antilles, and in South America from the Pacific coast of Colombia as far as Peru and on the Atlantic side from northern Colombia to central-eastern Brazil. Also, a small range in northern Yucatan and southern Chiapas in Mexico and along coastal Guatemala and El Salvador in Central America.

At 26 ka BP a small range is projected along the coast of Ecuador and on the southern coast of Peru in South America. This pattern continues with minimal variation until 13 ka BP, when the range on the coast of Peru increases to the northern coast. After this, the pattern remains similar until 9ka, when the range on the northern coast of Peru is reduced, and at 8 ka BP is increased again. See Figure 4.1.4.15.b.

From 7 ka BP until 1 ka BP the range remains with a similar pattern along the western coast of Ecuador and Peru in South America. The current non-breeding range projection presents a larger range along the western coast of Ecuador and Peru, with also a range projected in southern Mexico, in Belize, along the Greater Antilles, in the northern region of Colombia, Venezuela, Guyana and Suriname, with an inland range in the north-eastern part of Brazil and as small range in central Bolivia and southern Brazil.

The Heinrich event H2 when compared with the 24 ka BP projection presents a larger range projected in the northern part of South America, between Colombia and northern Brazil, across Central America and as far as southern Mexico, with a small range in central Brazil. This range decreases at H1, mainly in northern South America and in Central America,

differing from the 17 ka BP range projected only on the western coast of Ecuador and southern Peru. At H0, the range in the northern part of South America is reduced, remaining in Central America, in central Brazil and along the coasts of Ecuador and Peru, although at a different extent than the 13 ka BP projection.

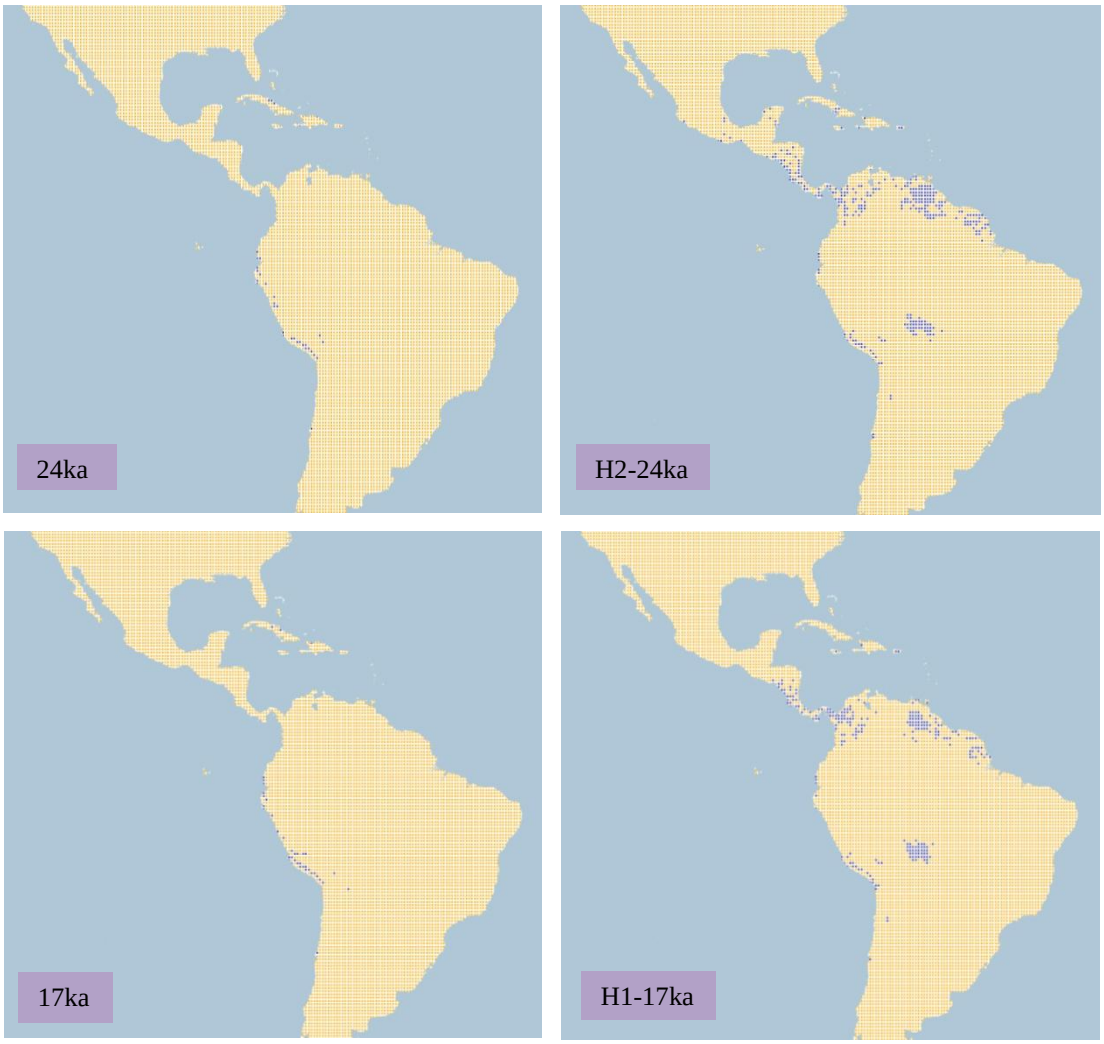

Figure 4.1.4.15.b. Simulation maps of Semipalmated Sandpiper non-breeding range. Maps are shown for ten-time slices: 24ka, H2 (24ka), 17ka, H1 (17ka), 13ka, H0 (13ka), 9ka, 5ka, 3ka and present (1961–90).

Figure 4.1.4.15.b. Simulation maps of Semipalmated Sandpiper non-breeding range (continued**).**

*4.1.4.16 Buff-breasted Sandpiper (*Calidris subruficollis*). Conservation status: Near Threatened. Current known range Figure 4.1.4.16.*

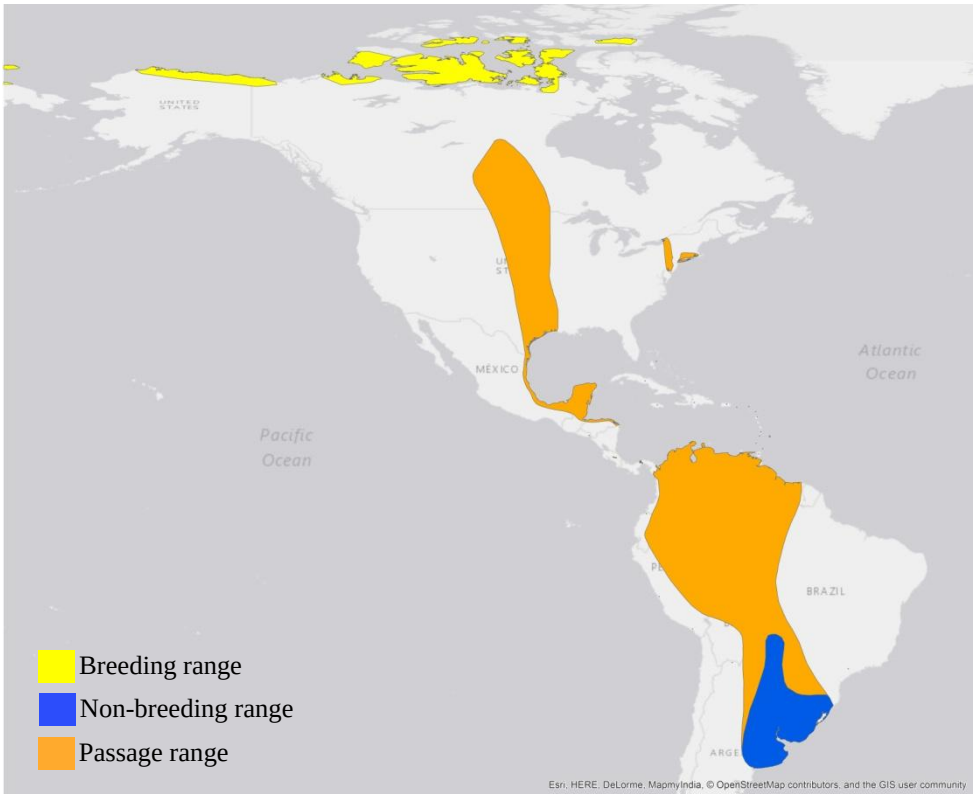

Figure 4.1.4.16. Current known range of Buff-breasted Sandpiper.

Breeding range (AUC: 0.945; TSS: 0.762; Kappa: 0.565): Spends the breeding season in northern Alaska and the Canadian low Arctic from northern Yukon as far as Devon Island in the Arctic Archipelago.

At 26 ka BP the range is projected in the northern part of Alaska and northern Canada in the areas not covered by the ice sheet. There is also a small range projected in the central-northern area of the conterminous USA. This pattern continues with minimal variation until 16 ka BP, when the range in the central-northern part of the USA shifts to the southern part of Canada, and there is also an increase in the range projected in the northern Yukon in Canada. After this at 15 ka BP, the range in southern Canada is reduced and the range in northern Yukon continues to increase. See Figure 4.1.4.16.a.

The range at 14 ka BP decreases in the northern part of Alaska and northern Yukon in Canada. This pattern continues at 13 ka BP, and by the beginning of the Holocene the range

is restricted to the northern coast of Alaska in the USA and in Yukon as far as Melville Island in Canada. With the deglaciation at 9ka, the range increases in the northern part of the Northwest Territories and Nunavut in Canada, that latter disappearing at 8 ka BP.

From 7 ka BP until 1 ka BP the range is restricted mainly to the Arctic Archipelago and the northern coast of Yukon, Northwest Territories and Nunavut in Canada and the northern coast of Alaska in the USA. This pattern continues in the current breeding range projection, although with a larger range projected in northern Alaska in the USA.

The Heinrich event H2 shares a similar range with the 24 ka BP projection in the northern part of Alaska in the USA and the northern part of Canada not covered by the ice sheet. A small difference is observed only in the northern region of the conterminous USA. This pattern continues at H1, decreasing the range in the northern part of Alaska, as with the 17 ka BP projection. H0 and 13 ka BP also present a similar range in the northern part of Canada and northern Alaska in the USA.

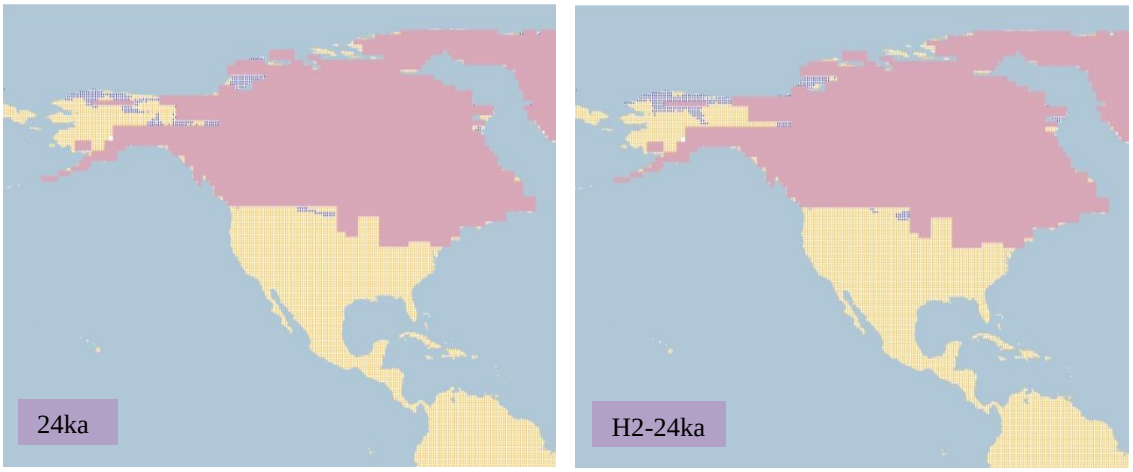

Figure 4.1.4.16.a. Simulation maps of Buff-breasted Sandpiper breeding range. Maps are shown for ten-time slices: 24ka, H2 (24ka), 17ka, H1 (17ka), 13ka, H0 (13ka), 9ka, 5ka, 3ka and present (1961–90).

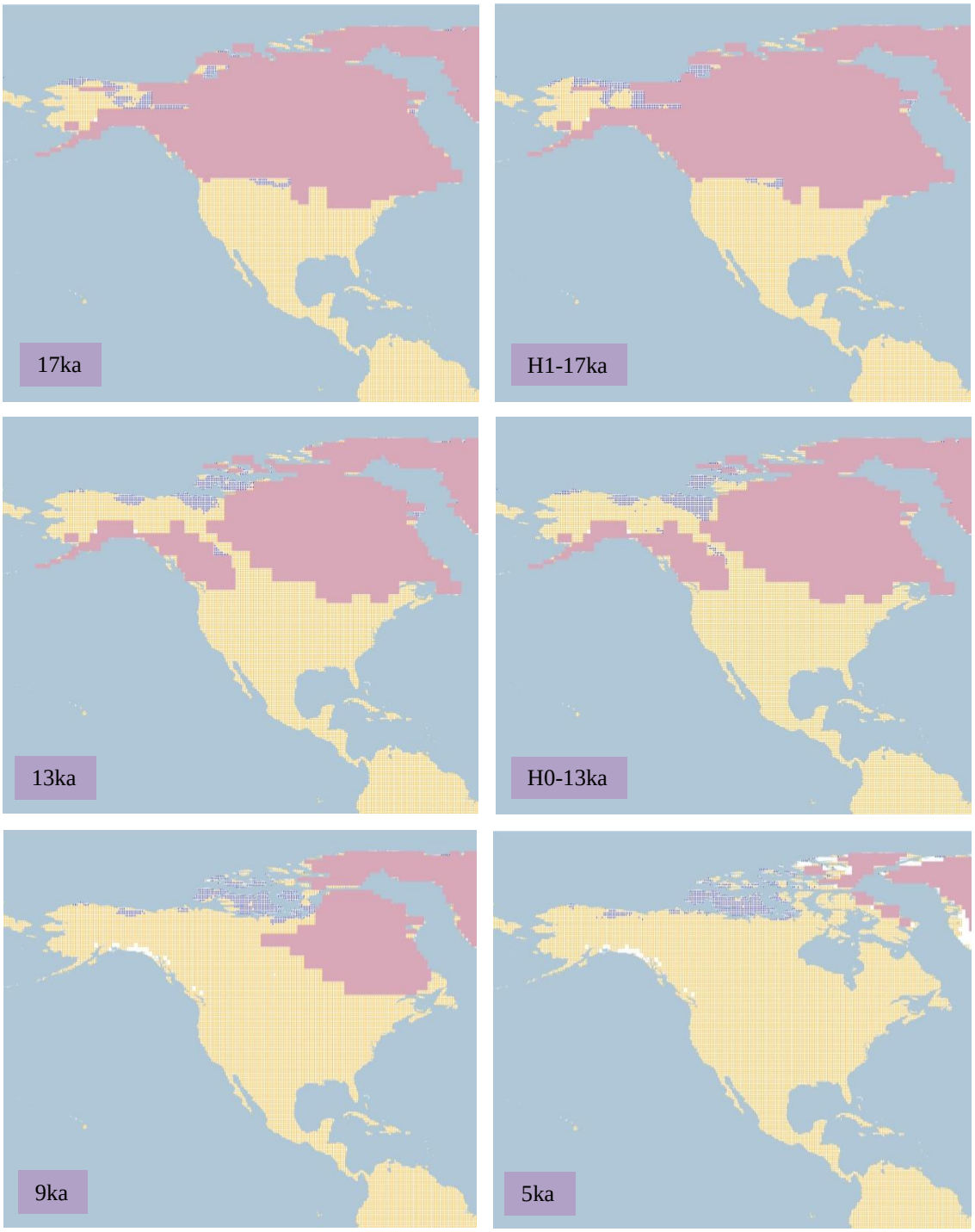

Figure 4.1.4.16.a. Simulation maps of Buff-breasted Sandpiper breeding range (continued**).**

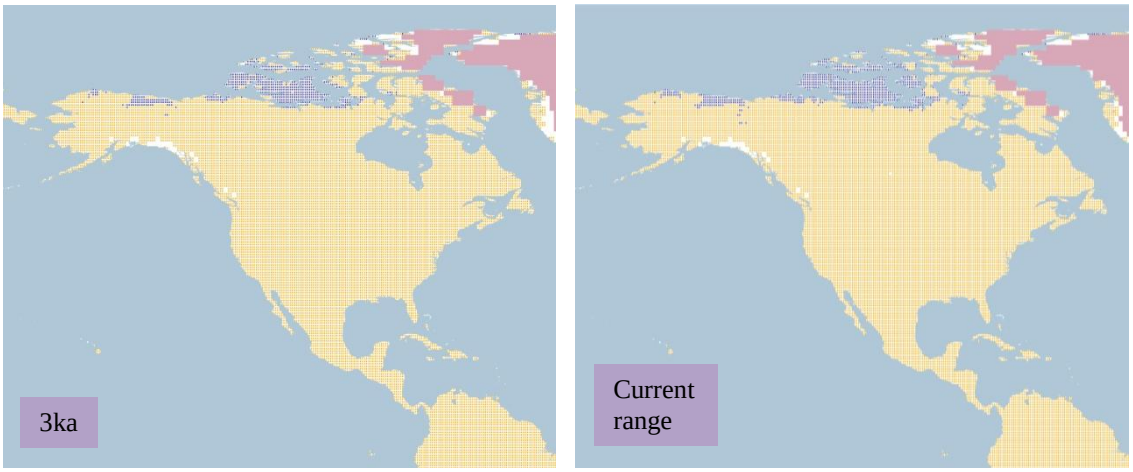

Figure 4.1.4.16.a. Simulation maps of Buff-breasted Sandpiper breeding range (continued**).**

Non-breeding range (AUC: 0.945; TSS: 0.762; Kappa: 0.565): This species spends the non-breeding season in South America from southern Brazil to Paraguay, Uruguay and as far as north-eastern Argentina.

At 26 ka BP the range is projected from southern Brazil to northern Argentina. This pattern continues until 20 ka BP when there is an increase in the central region between Bolivia and Paraguay, which decreases at 19 ka BP. After this, the range continues with a similar pattern until 14 ka BP, when the range in northern Argentina is decreased. See Figure 4.1.4.16.b.

By the beginning of the Holocene the range is projected from southern Argentina to Uruguay and in north-eastern Argentina. This range pattern continues with minimal variation, especially at 7 ka BP, when the range is reduced. From 6 ka BP until 1 ka BP the range remains with the same pattern. The current non-breeding range projection also persists with the same pattern as the 1 ka BP projection.

When comparing the Heinrich event H2 with the 24 ka BP projection, a similar range is projected in South America, only with a small projected range in north-western Argentina at H2, not projected at 24ka. The same pattern continues at H1, with minimal differences from the 17 ka BP projection. The H0 projection presents a smaller range in southern Brazil than the 13 ka BP projection.

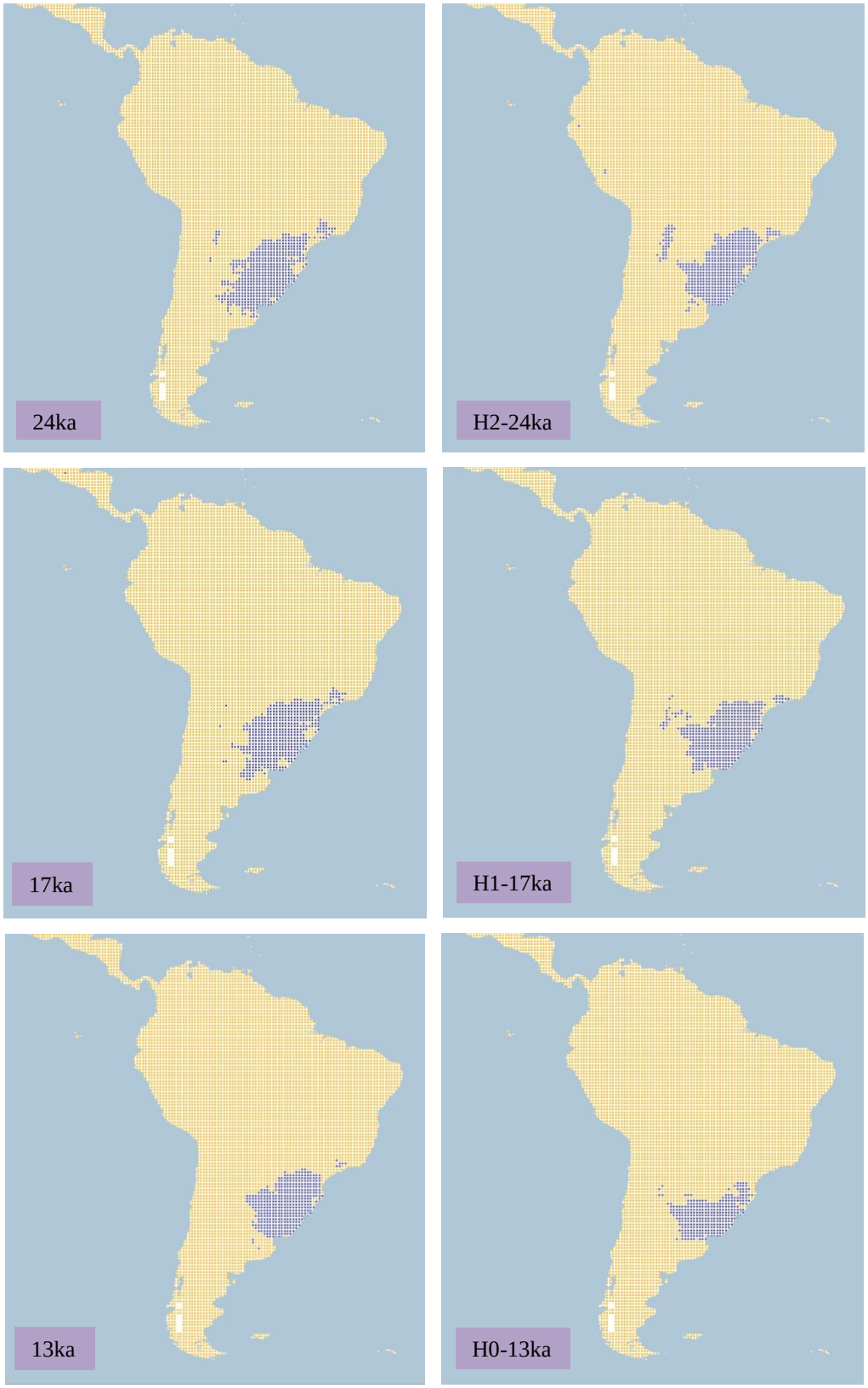

Figure 4.1.4.16.b. Simulation maps of Buff-breasted Sandpiper non-breeding range. Maps are shown for ten-time slices: 24ka, H2 (24ka), 17ka, H1 (17ka), 13ka, H0 (13ka), 9ka, 5ka, 3ka and present (1961–90).

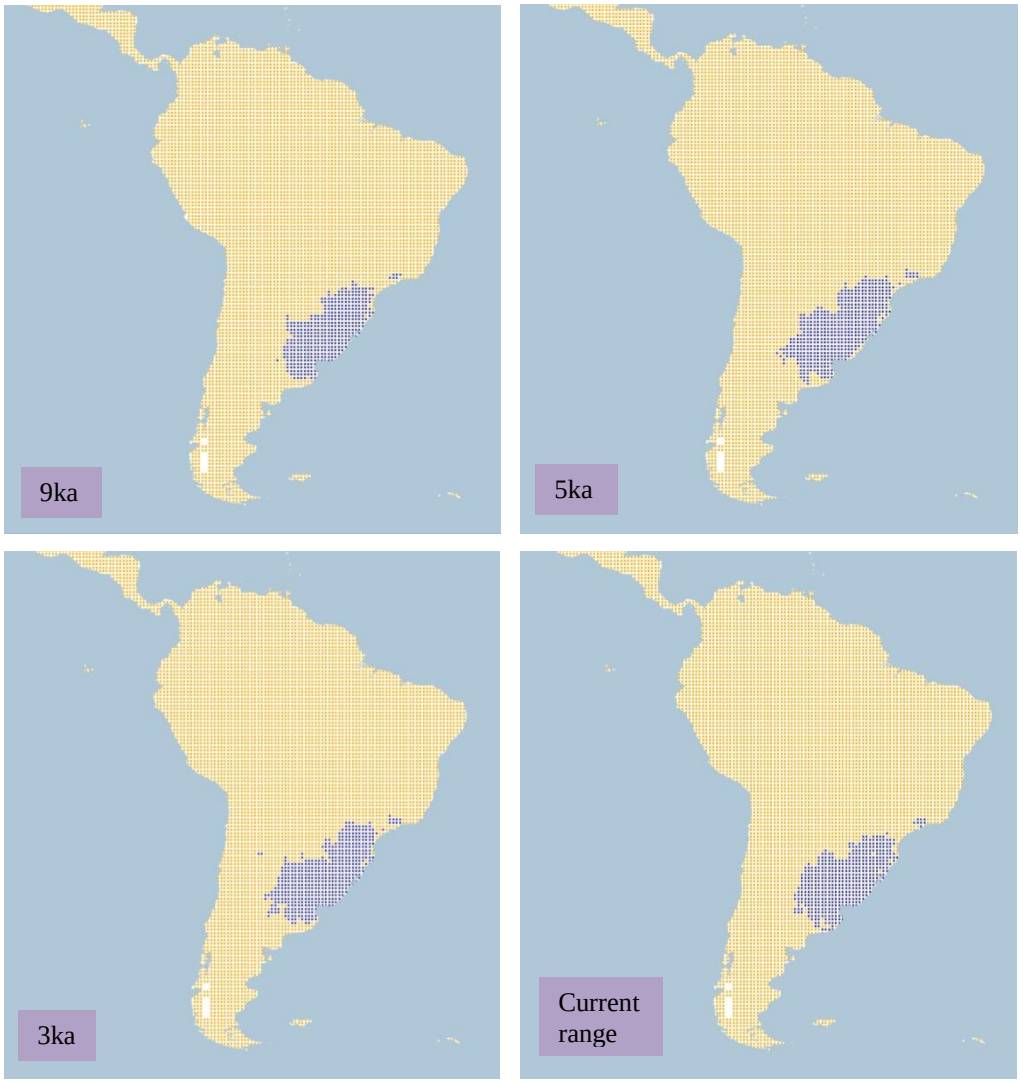

Figure 4.1.4.16.b. Simulation maps of Buff-breasted Sandpiper non-breeding range (continued**).**

*4.1.4.17 Surfbird (*Calidris virgata*). Conservation status: Least Concern. Current known range Figure 4.1.4.17.*

Figure 4.1.4.17. Current known range of Surfbird.

Breeding range (AUC: 0.889; TSS: 0.612; Kappa: 0.517): This species has a fragmented breeding range in central and southern Alaska in the USA and western Yukon in Canada.

At 26 ka BP the range is projected in central to southern Alaska and in central-northern, and north-eastern regions of the conterminous USA. This pattern continues until 17 ka BP, when the range in the central-northern part of the conterminous USA is reduced. This decreasing range pattern continues and at 15 ka BP the range in the northern region of the conterminous USA reduces to a small range near the ice sheet. See Figure 4.1.4.17.a.

With the deglaciation at 13 ka BP the range in the northern part of the conterminous USA shifts to the central and northern region of Canada, with the range in Alaska also shifting to the northern part. The range in central and northern Canada reduces at 12 ka BP and by 11 ka BP, the range increases, covering the western part of Yukon and the Northwest Territories in Canada and the south-western part of Alaska in the USA.

By 10 ka BP the range projected in the northern part of Canada decreases, covering mainly the western part of Yukon and central-southern Northwest Territories near the ice sheet. This change at 8 ka BP with the range in the central part of Canada shifting to the northern part of Manitoba and Ontario and in the south-eastern part of Quebec as far as Newfoundland and Labrador in Canada.

At the 5 ka BP projection the range in the north-eastern part of Canada increases, with a smaller range in northern Manitoba and Ontario and with the remainder of the range in western Alaska and Yukon unchanged. After this at 4 ka BP the range in the north-eastern part of Canada decreases. This pattern continues until the 1 ka BP projection. The current breeding range projection presents a similar range along central Alaska in the USA and northern Yukon in Canada as the 1 ka BP projection.

When comparing the Heinrich event H2 with the 24 ka BP projection, a similar range is observed in the central-northern region of the conterminous USA and in central Alaska. This pattern continues at H1, although differing from the 17 ka BP projection with a smaller range in the northern part of the conterminous USA. The range projected at H0 also presents a similar range to the 13 ka BP projection across northern and central Canada and in northern Alaska in the USA.

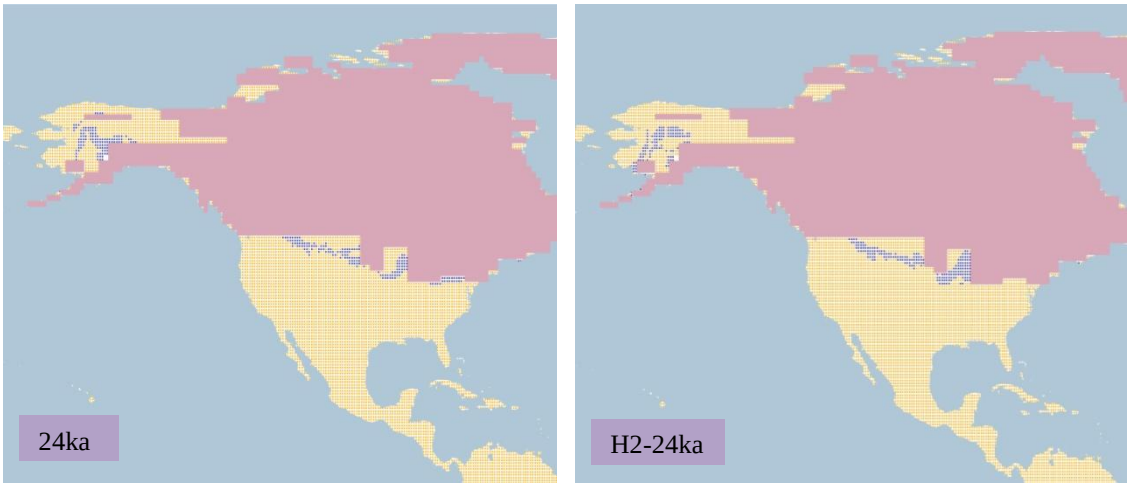

Figure 4.1.4.17.a. Simulation maps of Surfbird breeding range.
Maps are shown for ten-time slices: 24ka, H2 (24ka), 17ka, H1 (17ka), 13ka, H0 (13ka), 9ka, 5ka, 3ka and present (1961–90).

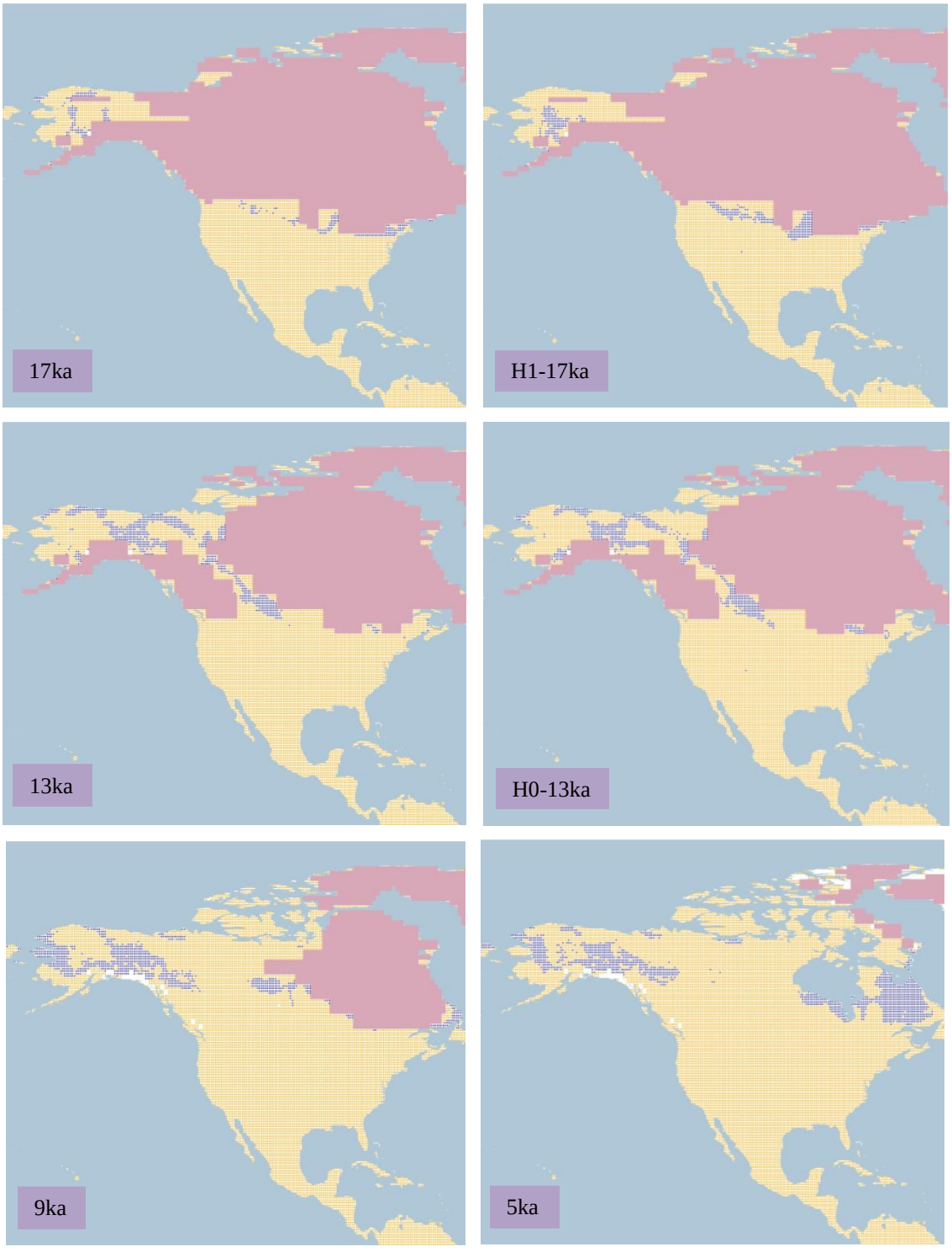

Figure 4.1.4.17.a. Simulation maps of Surfbird breeding range (continued**).**

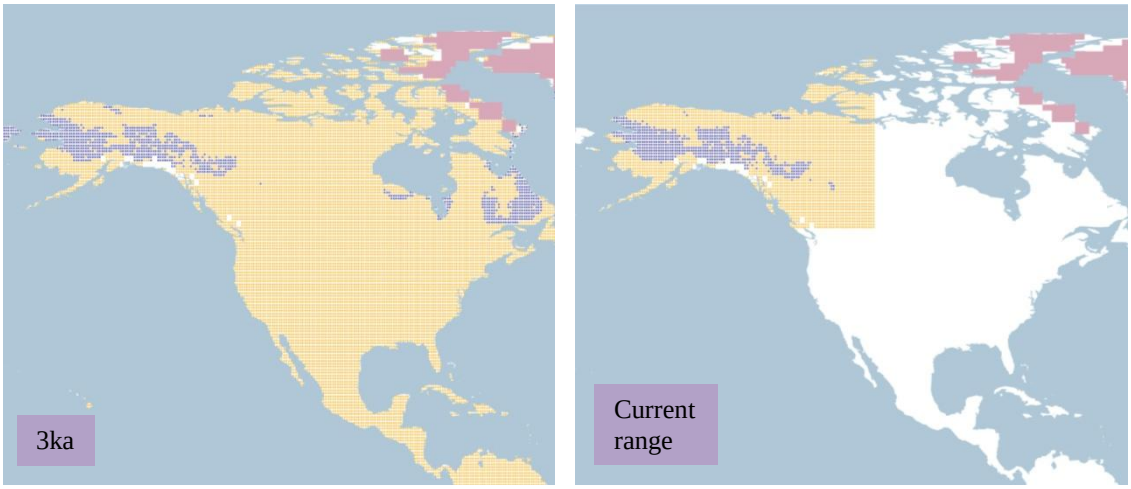

Figure 4.1.4.17.a. Simulation maps of Surfbird breeding range (continued**).**

Non-breeding range (AUC: 0.988; TSS: 0.874; Kappa: 0.827): This species spends the non-breeding season along the Pacific coast of the Americas, from southern Alaska in North America as far as southern Chile in South America.

At 26 ka BP the range is projected from the western coast of the USA as far as southern Mexico on the western coast of Oaxaca, with a small range on the western coast of Nicaragua, and along the western coast from Ecuador to southern Chile in South America. An inland range is also projected in the central-western region of the USA, a small scattered range in central Mexico and between Venezuela and Suriname and the north-eastern region of Brazil in South America. This pattern continues and at 21ka the range in the north-eastern part of Brazil is increased. See Figure 4.1.4.17.b.

At 19 ka BP, the range projected in the central-western part of the USA is reduced, with an increase in the central part of Mexico. After this at 16 ka BP, the range in the north-eastern part of Brazil increases, and the range in the USA is restricted to the western coast. This pattern of decrease continues at 15 ka BP, mainly in central Mexico, in the northern part of South America between Venezuela and Suriname, and in the north-eastern region of Brazil.

By the beginning of the Holocene the range is projected along the western coast of British Columbia in Canada as far as the western coast of Nicaragua in Central America, with a small inland range in central Mexico, and in South America along the western coast from Ecuador to southern Chile, with a large inland range in north-eastern Brazil. This pattern continues until 8 ka BP, when the range in north-eastern Brazil is reduced.

At ka BP, the range in central Mexico is increased, the remainder of the range being unchanged. The range in north-eastern Brazil increases at 4 ka BP decreasing again at 3 ka BP and remaining as with the rest of the range with minimal variations until the 1 ka BP projection. The current non-breeding range projection also projects a range along the western coast of North America and South America, although without a range in central Mexico and in the north-eastern part of Brazil.

The H2 projected range presents a larger range than the 24 ka BP projection in the central region of the USA, central and southern Mexico, and Central America as far as northern South America. The range in the central part of the USA is reduced at H1, with the remainder of the range in Central America and northern South America unchanged and differing from the 17 ka BP projection. A similar range is projected between H0 and 13 ka BP along the western coast of the USA and Mexico; however, there is still a large range projected in southern Mexico, Central America and northern South America at H0 that is not projected at 13 ka BP.

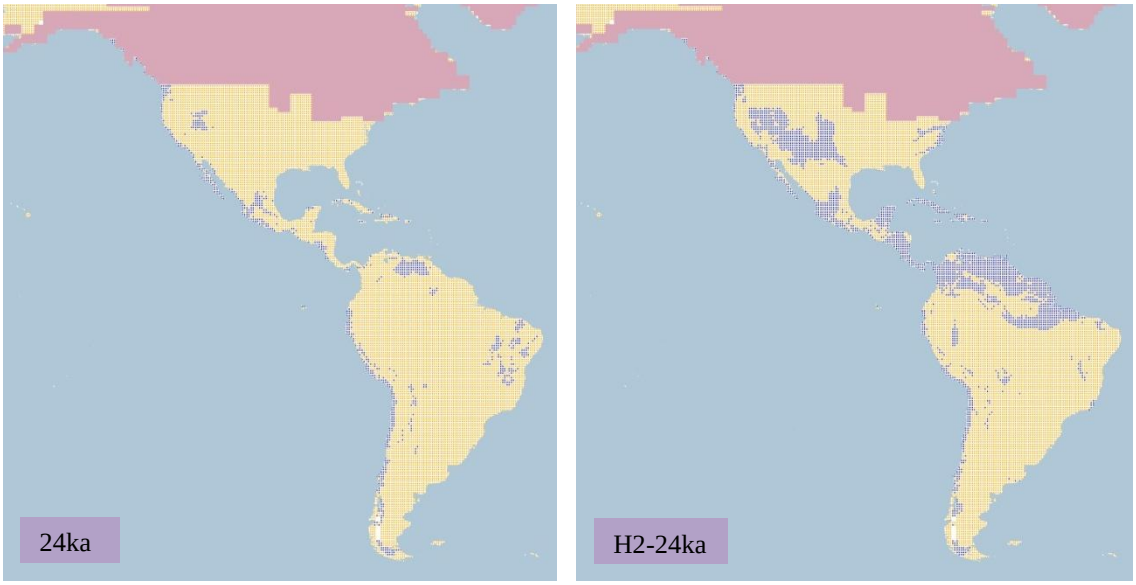

Figure 4.1.4.17.b. Simulation maps of Surfbird non-breeding range.
Maps are shown for ten-time slices: 24ka, H2 (24ka), 17ka, H1 (17ka), 13ka, H0 (13ka), 9ka, 5ka, 3ka and present (1961–90).

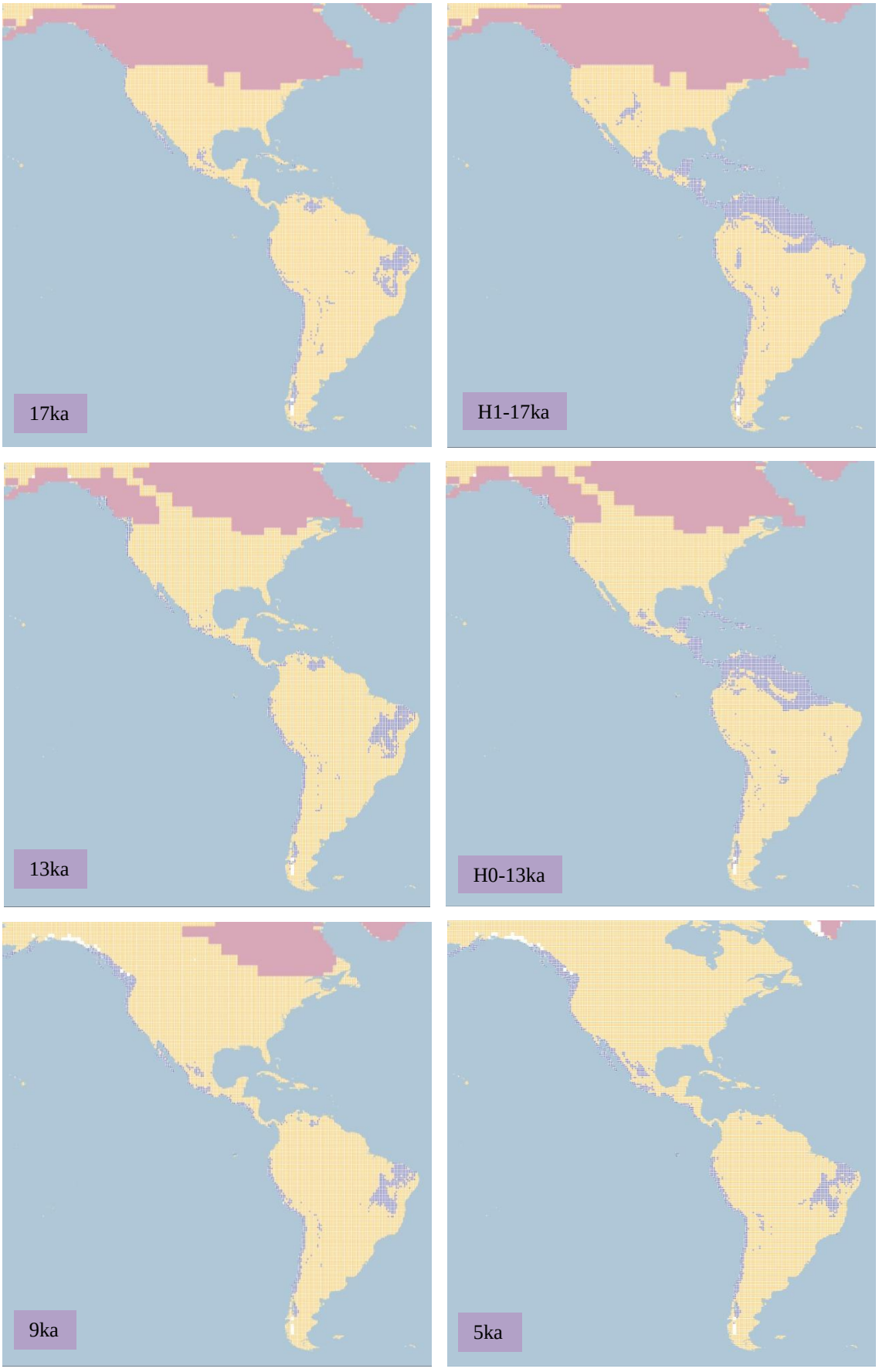
17ka
H1-17ka
13ka
H0-13ka
9ka
5ka

Figure 4.1.4.17.b. Simulation maps of Surfbird non-breeding range (continued**).**

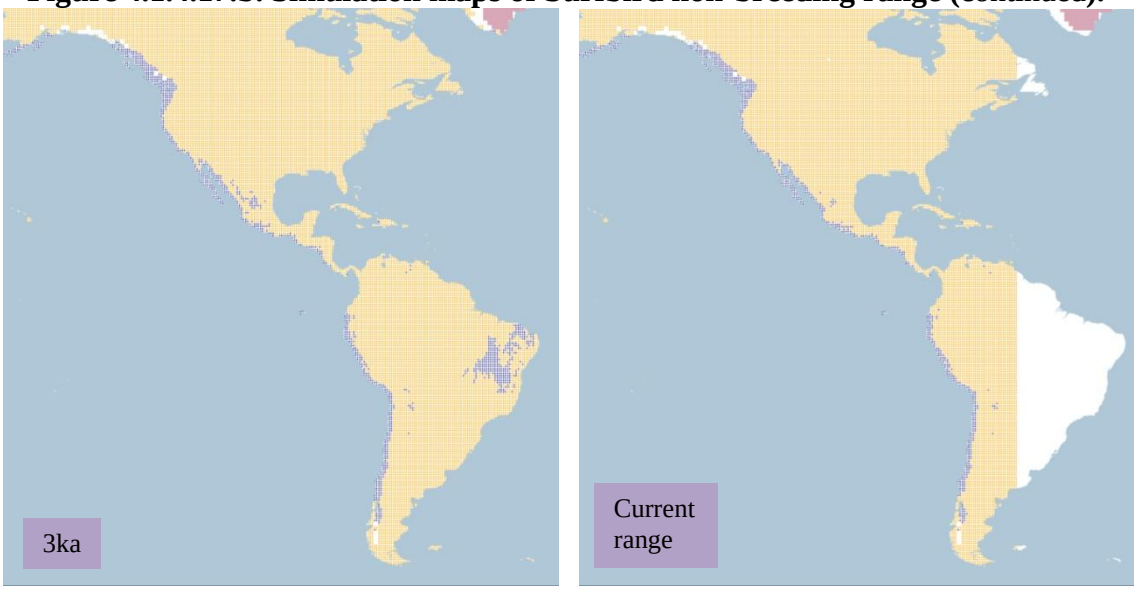

Figure 4.1.4.17.b. Simulation maps of Surfbird non-breeding range (continued**).**

*4.1.4.18 Wilson's Snipe (*Gallinago delicata*). Conservation status: Least Concern. Current known range Figure 4.1.4.18.*

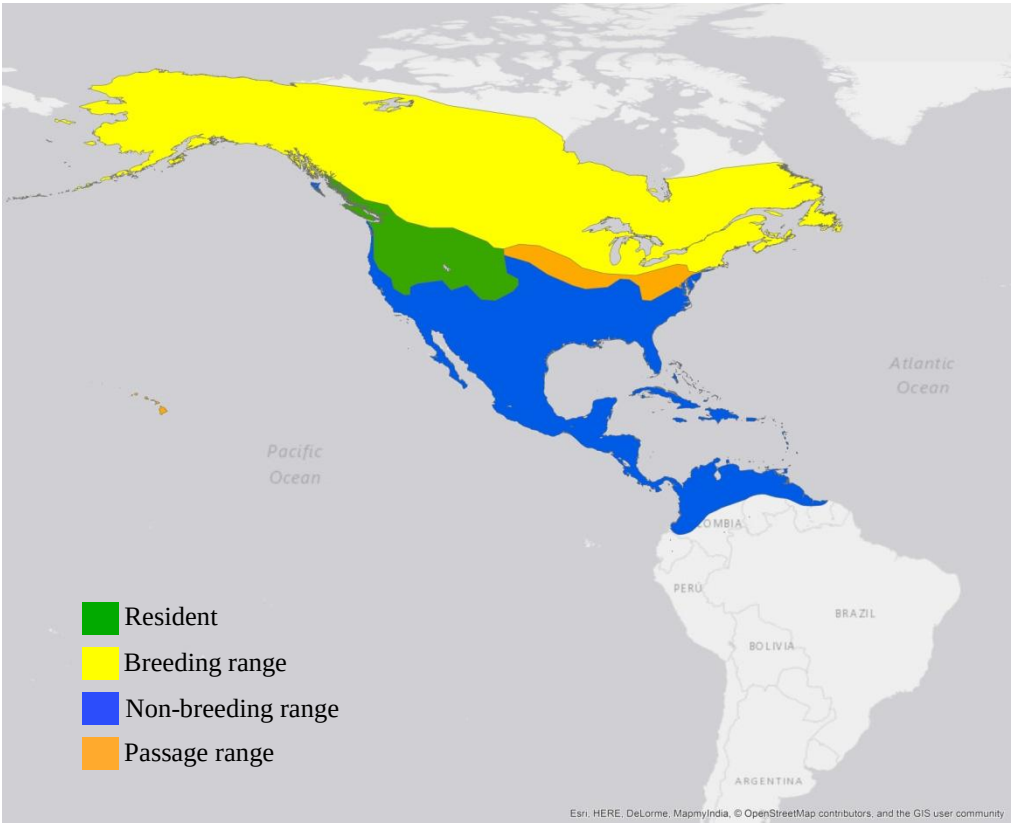

Figure 4.1.4.18. Current known range of Wilson's Snipe.

Breeding range (AUC: 0.996; TSS: 0.940; Kappa: 0.939): Spends the breeding season in Canada from Newfoundland and Labrador as far as the Yukon, except in northern Nunavut, in Alaska as far as the Aleutian Islands and St Lawrence Island, as well as in the northern conterminous USA, as far south as New Jersey, and in south-east Canada; recently discovered to breed also on the Chukotskiy Peninsula, Russia, although this is excluded from the model. In addition, the species has a year-round resident range extending from the western coast of British Columbia in Canada through the north-western USA between Washington and Nevada and as far as Nebraska, South Dakota and North Dakota.

At 26 ka BP the range is projected in Alaska in the USA and northern Yukon in Canada, with a larger range across the conterminous USA except the southern region. This pattern continues until the start of the deglaciation at 16 ka BP, with the range shifting to the southern part of Canada. After this at 13 ka BP the range extent is projected from western Alaska to the central part of Canada and in the central-northern region of the conterminous USA. See Figure 4.1.4.18.a.

By the beginning of the Holocene at 11 ka BP the range is projected from central-northern parts of the conterminous USA as far as western Alaska and across Canada. This pattern continues and by 8 ka BP the range is increased in the south-eastern part of Canada and north-eastern region of the USA. From 7 ka BP until 1 ka BP the range remains with a similar pattern only with minimal variation in the central-eastern part of the USA. The current breeding range projection presents a similar pattern to that for 1 ka BP across the USA and Canada.

The Heinrich event H2 projection is of a similar range as at 24 ka BP in Alaska and northern Canada, but with a larger range in the south-western region of the conterminous USA. This pattern continues at H1, increasing in the central region of the conterminous USA and agreeing with the 17 ka BP projection. The H0 and 13 ka BP projections only present a different extent in the northern part of the Northwest Territories in Canada, with a larger range at 13 ka BP than at H0.

Even though the species' breeding range is restricted to North America, there are suitable conditions projected in central-southern Argentina in the projections.

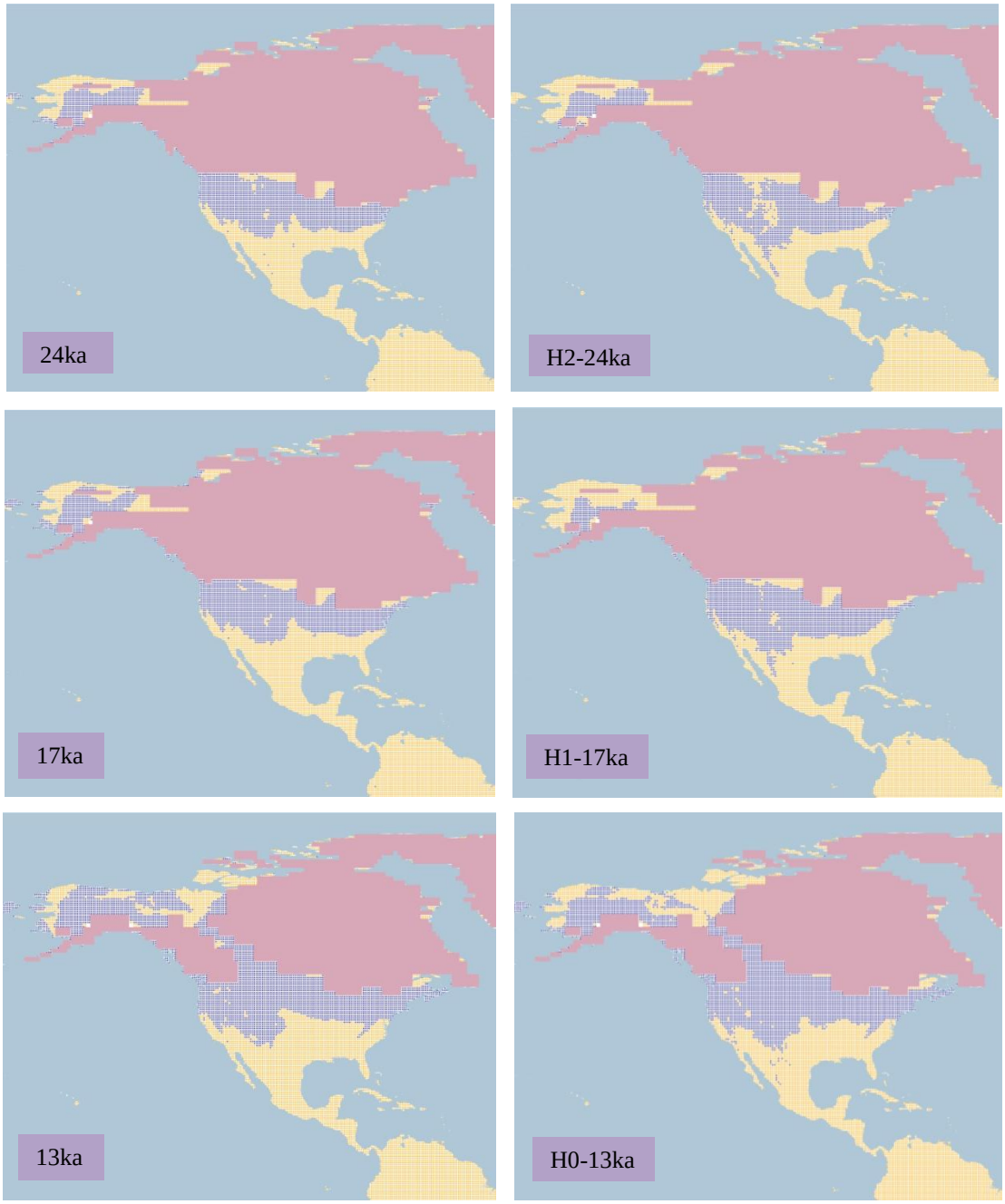

Figure 4.1.4.18.a. Simulation maps of Wilson's Snipe breeding range.
Maps are shown for ten-time slices: 24ka, H2 (24ka), 17ka, H1 (17ka), 13ka, H0 (13ka), 9ka, 5ka, 3ka and present (1961–90).

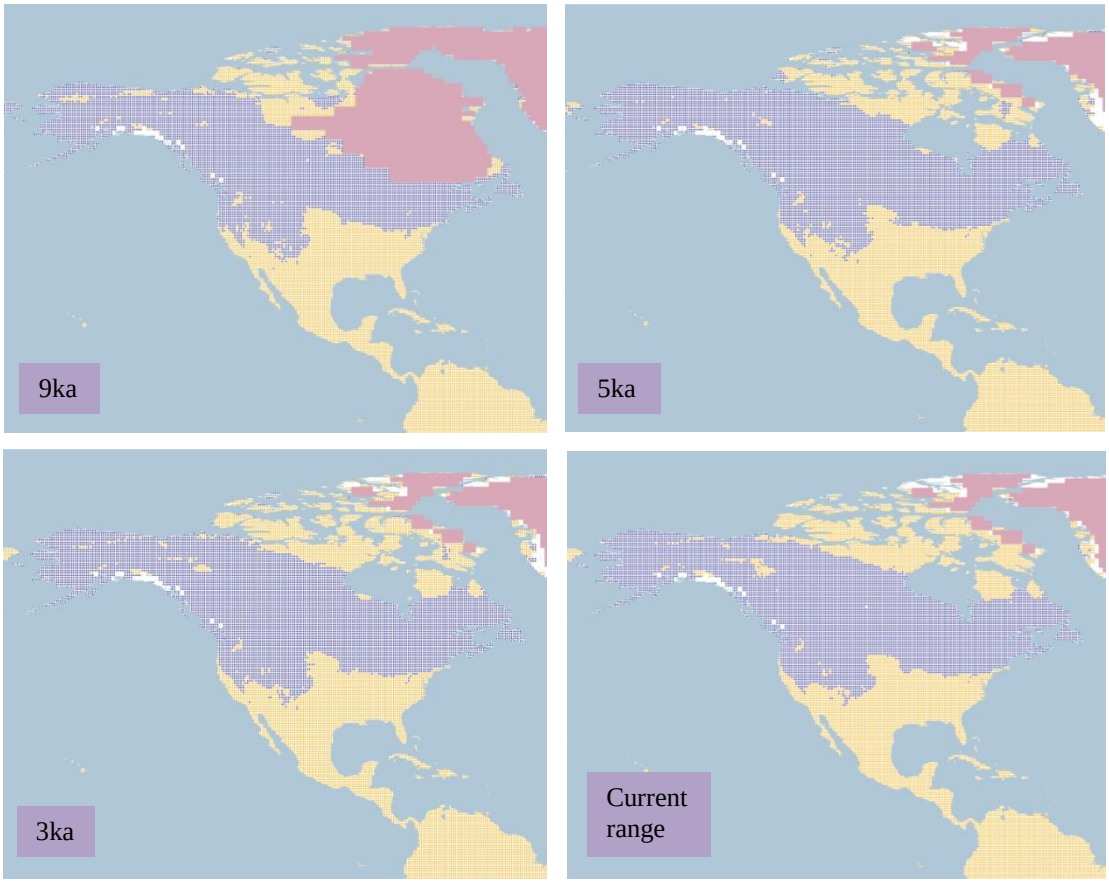

Figure 4.1.4.18.a. Simulation maps of Wilson's Snipe breeding range (continued**).**

Non-breeding range (AUC: 0.982; TSS: 0.851; Kappa: 0.841): The species has a large winter range from central USA to Mexico, the Greater Antilles, Central America and northern South America in Colombia, Venezuela, Guyana and Suriname. The species also has a year-round resident range in the north-western USA.

At 26 ka BP the range is projected in the southern, western and central regions of the conterminous USA, as well as in Mexico, Central America and along the Andean cordillera in South America. This pattern continues until 19 ka BP with the increase of the range in the western region of the USA. After this at 17 ka BP the range in the central and southern region of the USA gradually increases until 12 ka BP. See Figure 4.1.4.18.b.

By the beginning of the Holocene the range reaches the south-western region of British Columbia and a small range is projected between Manitoba and Ontario near the ice sheet in Canada, with the remainder of the range unchanged. At 10 ka BP the range in central-southern Canada increases with the deglaciation, but is decreased after this at 9 ka BP.

From 8 ka BP until the 1 ka BP projection, the range presents a minimal variation, extending from south-western Canada, across the conterminous USA, Mexico and Central America with a small range along the Andean cordillera in South America, and in the Greater Antilles. The current non-breeding range projection presents a similar pattern as 1 ka BP.

A similar pattern is projected between H2 and 24 ka BP in the southern region of the USA and in Mexico, although with a smaller extent for H2 and with no range projected in Central America. This pattern continues at H1, with a growth in the western part of the USA, although of a smaller extent than in the 17 ka BP projection. The range at H0 increases in the western and southern regions of the USA, with a small range in Central America, differing from the larger range projected in the central region of the USA at 13 ka BP.

Even though the species' non-breeding range is located in North America and northern South America, there are suitable conditions for the species from central to southern South America.

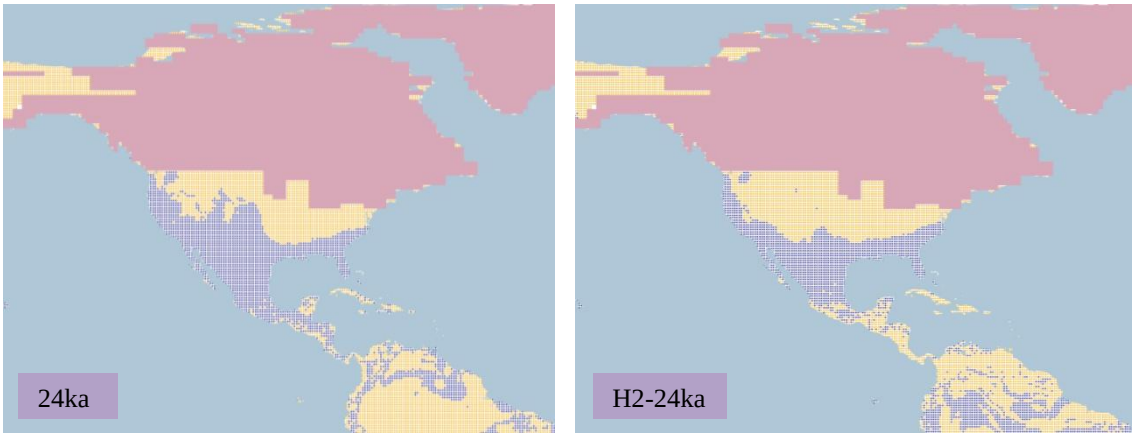

Figure 4.1.4.18.b. Simulation maps of Wilson's Snipe non-breeding range.
Maps are shown for ten-time slices: 24ka, H2 (24ka), 17ka, H1 (17ka), 13ka, H0 (13ka), 9ka, 5ka, 3ka and present (1961–90).

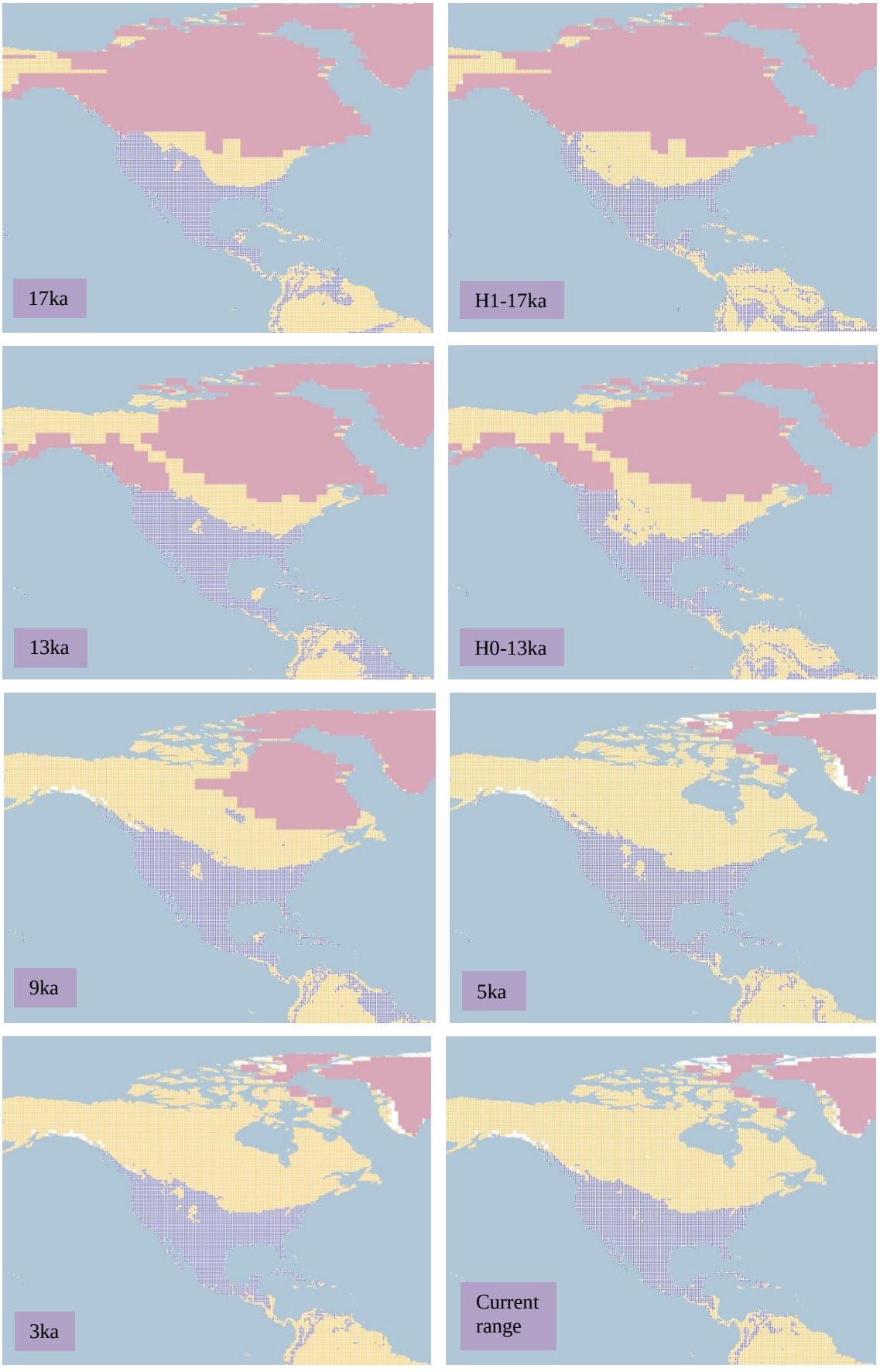
17ka
H1-17ka
13ka
H0-13ka
9ka
5ka
3ka
Current range

Figure 4.1.4.18.b. Simulation maps of Wilson's Snipe non-breeding range (continued**).**

*4.1.4.19 Short-billed Dowitcher (*Limnodromus griseus *including* L. g. caurinus, L. g. hendersoni, L. g. griseus*). Conservation status: Least Concern. Current known range Figure 4.1.4.19.*

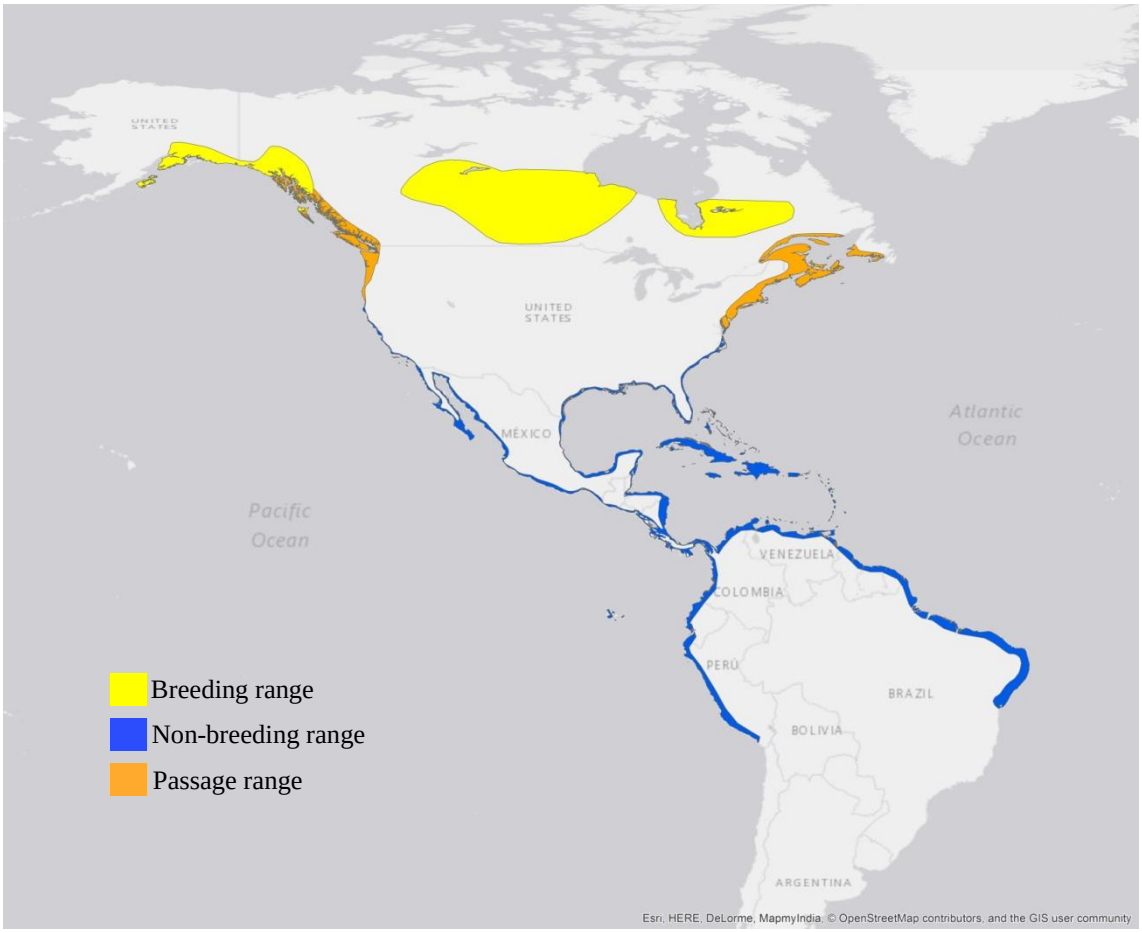

Figure 4.1.4.19. Current known range of Dowitcher.

Breeding range (AUC: 0.967; TSS: 0.814; Kappa: 0.723): Spends the breeding season in southern Alaska, southern Yukon and north-west British Columbia (*Limnodromus griseus caurinus*), from central Alberta to northern Ontario (*L. g. hendersoni*) and from James Bay to western Labrador (*L. g. griseus*).

At 26 ka BP a small range is projected in central northern parts of the conterminous USA and in central Alaska. This pattern continues with minimal variation until 18 ka BP when the range in Alaska is decreased and the range in the central-northern part of the

conterminous USA increases. This change at 15 ka BP, when the range in the northern part of the conterminous USA decreases and the range in Alaska increases. After this at 14 ka BP, the range in the northern region of the conterminous USA increases reaching the north-eastern region near the ice sheet in the USA and the southern boundaries of Canada. See Figure 4.1.4.19.a.

With the deglaciation at 12 ka BP the range from northern conterminous USA shifts to the southern and central-western region of Canada. At 10 ka BP the range increases in the south-eastern region of Canada and the north-eastern region of conterminous USA. This growing pattern continues at 9 ka BP and by 8 ka BP the range in the south-eastern region of Canada and in the north-eastern part of the USA decreases.

From 7 ka BP the range is projected in central Alaska in the USA and in western, central and south-eastern regions of Canada with minimal variations until the 1 ka BP projection. The current breeding range projection presents a similar pattern across Canada and in Alaska as 1 ka BP.

At H2 the range in the northern part of conterminous USA is smaller than at 24ka. This pattern continues at H1, with a small increase in the northern region of the USA, although of a smaller extent than for 17ka. This pattern is changed at H0, with the range projected between the boundaries of the northern conterminous USA and southern Canada, similar to the 13 ka BP projection.

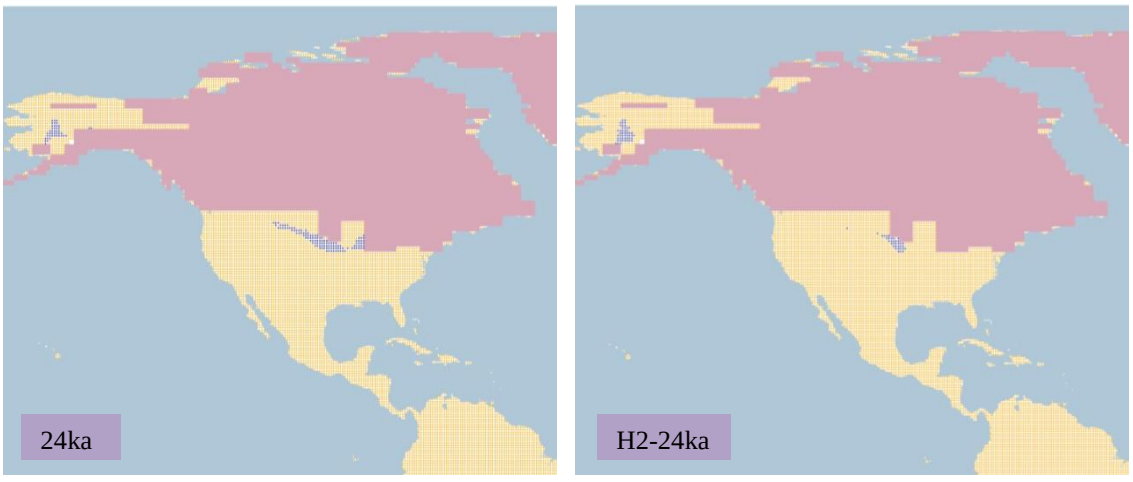

Figure 4.1.4.19.a. Simulation maps of Short-billed Dowitcher breeding range.
Maps are shown for ten-time slices: 24ka, H2 (24ka), 17ka, H1 (17ka), 13ka, H0 (13ka), 9ka, 5ka, 3ka and present (1961–90).

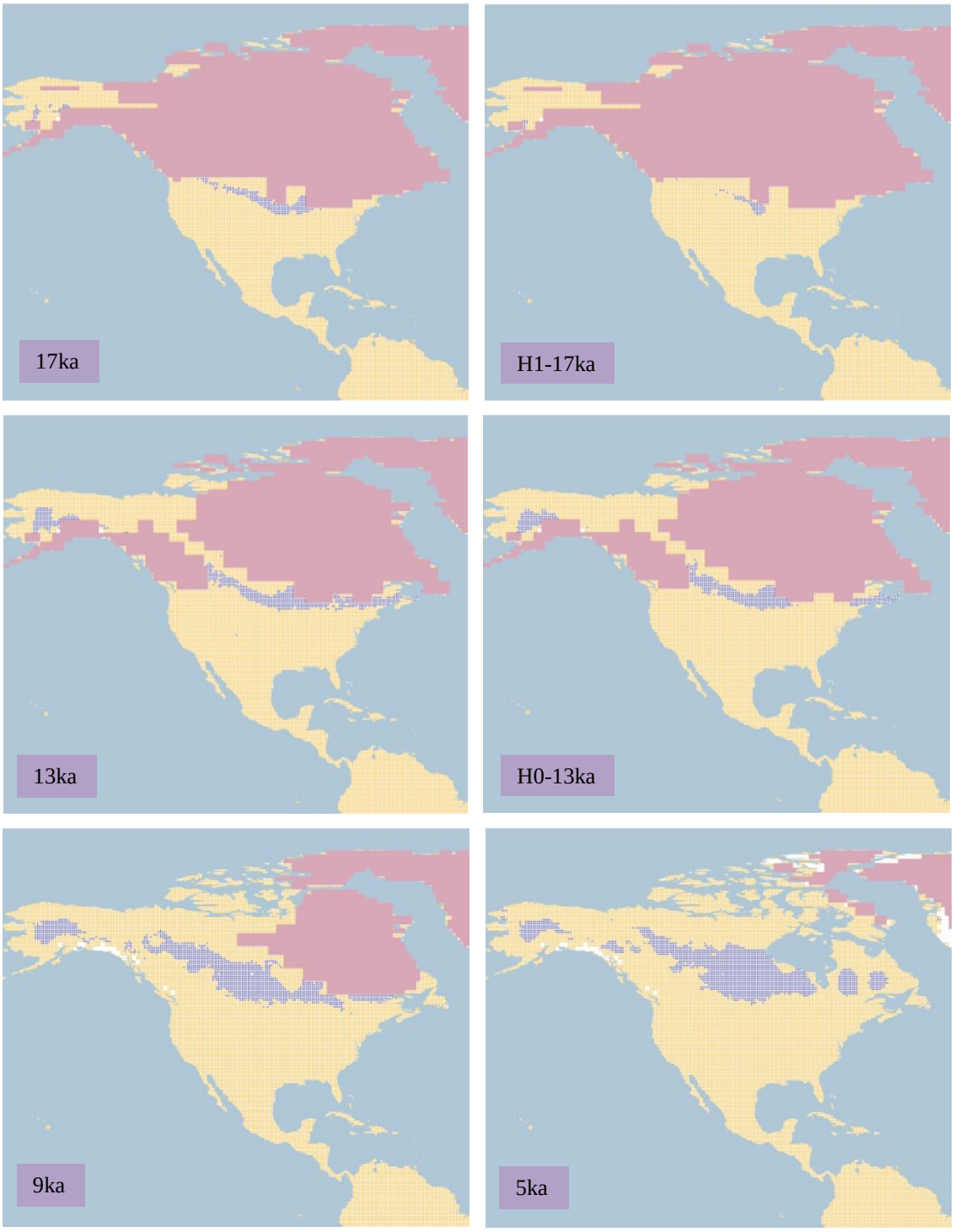

Figure 4.1.4.19.a. Simulation maps of Short-billed Dowitcher breeding range (continued**).**

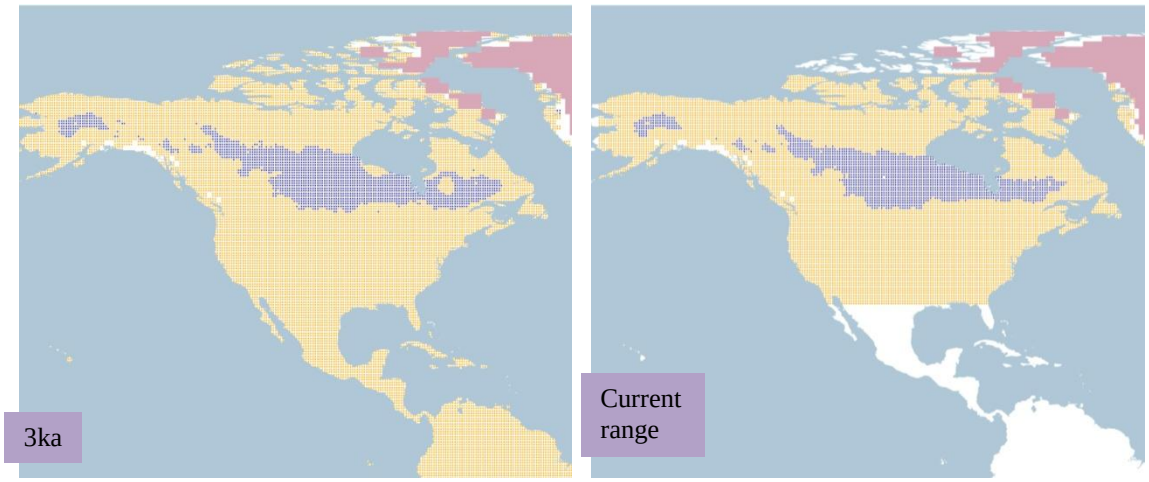

Figure 4.1.4.19.a. Simulation maps of Short-billed Dowitcher breeding range (continued**).**

Non-breeding range (AUC: 0.958; TSS: 0.782; Kappa: 0.586): Spends the winter season along the Pacific coast from California in the USA as far as southern Peru and along the Atlantic coast from Virginia in the USA as far as the north-eastern coast of Brazil, as well as in the Greater Antilles.

At 26 ka BP the range is projected along the western coast of Mexico with an inland range in central Mexico, in the Greater Antilles, and along the coasts of Central America and the coast of Ecuador and Peru. A scattered range is projected in the northern region of South America from Colombia to north-western Brazil with a smaller range in the north-eastern extreme of Brazil and in the Andean cordillera. This pattern continues until 22 ka BP when the range in northern South America decreases, increasing in the central region of Brazil. See Figure 4.1.4.19.b.

At 13 ka BP there is a larger range projected in central-northern Brazil, with the range in Mexico restricted to coastal areas. By the beginning of the Holocene the range in central Brazil is fragmented and decreases at 10 ka BP, with the range in central Mexico and in Florida in the USA increasing. This pattern continues with minimal variation mainly in the central region of Brazil until 6 ka BP, when the range in central Mexico increases to the north, and the range in Florida shifts to the south-eastern coast in the USA.

From 5 ka BP until ka BP, the range in central and northern Brazil presents a minimal variation, and the range on the south-eastern coast of the USA increases as far as the southern coast of Mexico. The current non-breeding range presents a similar pattern as ka BP, with

the range projected along the western and south-eastern coast of the USA, along the coast of Mexico in the Pacific and Gulf of Mexico, followed with a small range in Central America and in the Greater Antilles, covering the coast of Ecuador and Peru and the northern part of South America with a small range in Bolivia and central-southern Brazil.

The Heinrich event H2 projection is of a larger range in central-northern South America, across Central America and as far as southern Mexico than at 24 ka BP when it is restricted to the coastal areas of Mexico and with a small range in northern South America. This range in South America increases at H1, differing from the 17 ka BP projection. The range at H0 decreases from H1, although with a larger range projected in the central and northern part of South America, not projected in the 13 ka BP projection.

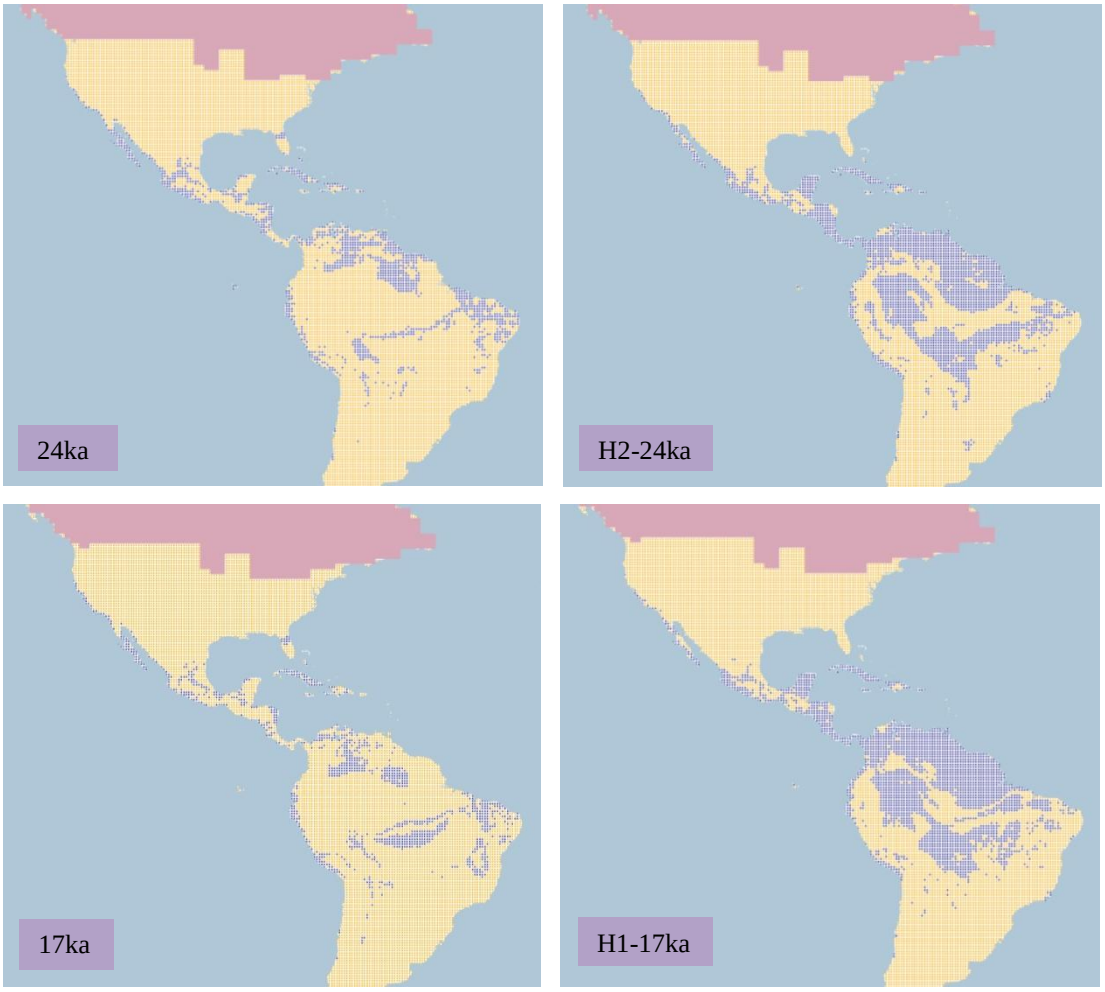

Figure 4.1.4.19.b. Simulation maps of Short-billed Dowitcher non-breeding range. Maps are shown for ten-time slices: 24ka, H2 (24ka), 17ka, H1 (17ka), 13ka, H0 (13ka), 9ka, 5ka, 3ka and present (1961–90).

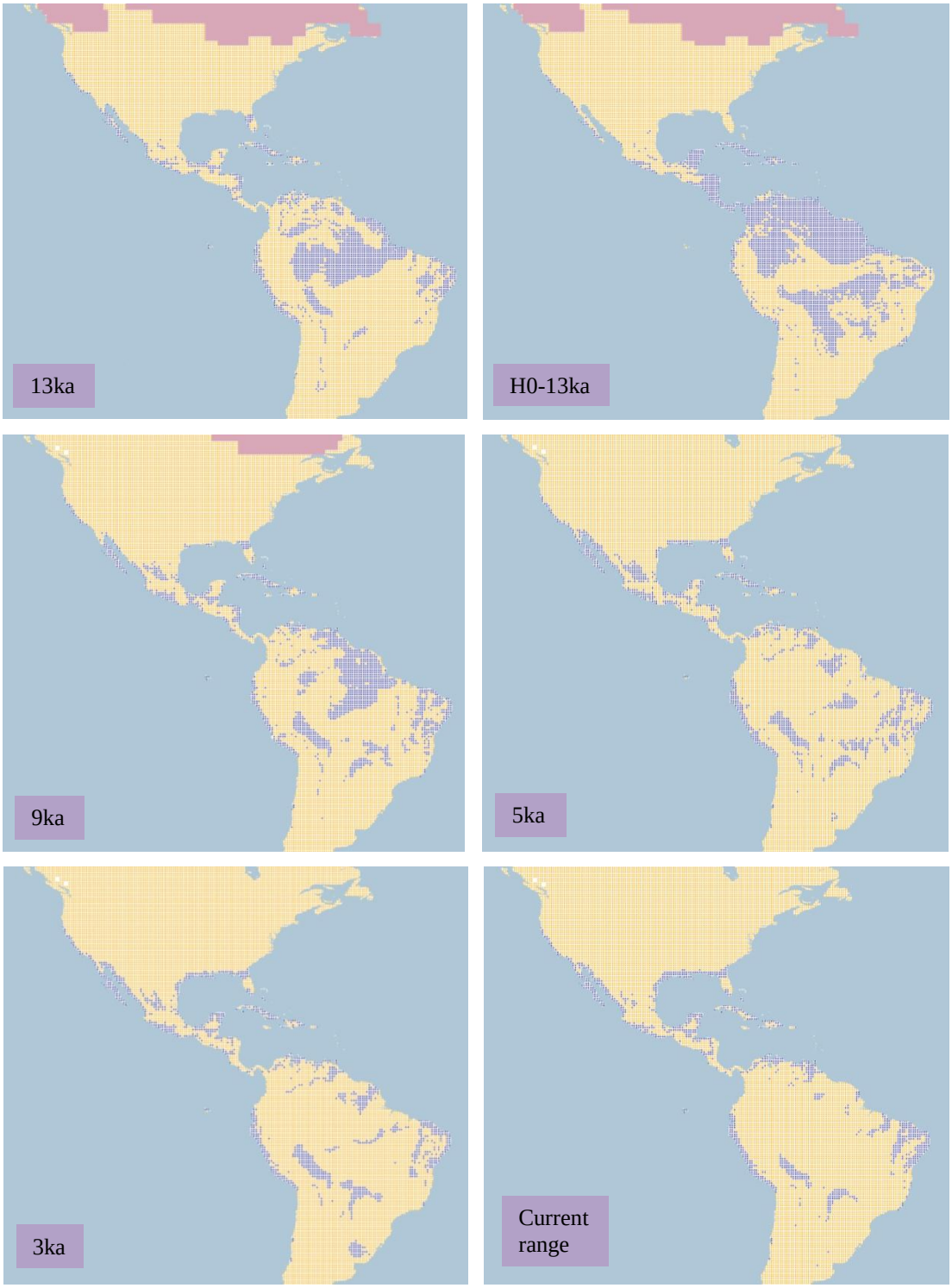

Figure 4.1.4.19.b. Simulation maps of Short-billed Dowitcher non-breeding range (continued**).**

*4.1.4.20 Long-billed Dowitcher (*Limnodromus scolopaceus*). Conservation status: Least Concern. Current known range Figure 4.1.4.20.*

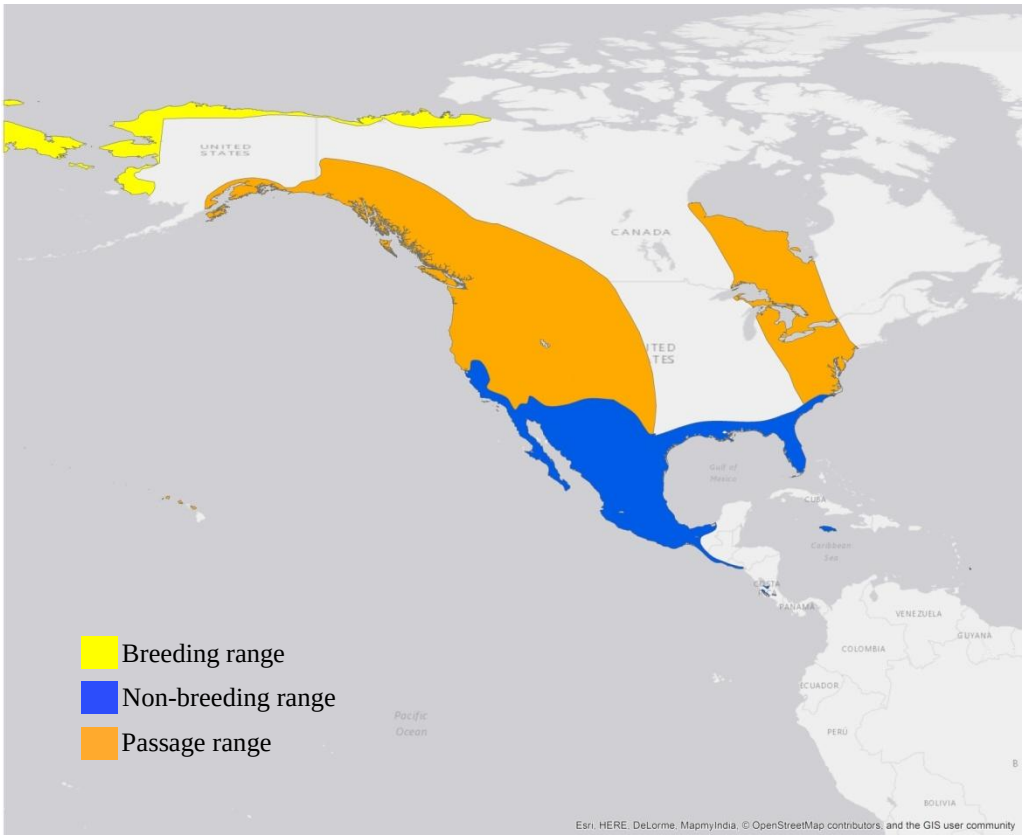

Figure 4.1.4.20. Current known range of Long-billed Dowitcher.

Breeding range (AUC: 0.980; TSS: 0.896; Kappa: 0.519): This species' North American breeding range extends from the western and northern regions of Alaska in the USA to the northern coasts of the Yukon and Northwest Territories in Canada. The species also breeds in north-east Siberia, eastwards from the Chukotskiy Peninsula to the Yana River, although this part of its range is excluded from the model.

At 26 ka BP a fragmented range is projected in northern Alaska in the USA and northern Yukon in Canada, with a small range in the northern region of the conterminous USA. This pattern continues with minimal variation until the beginning of the deglaciation at14ka, shifting the northern range in the conterminous USA to southern Canada, and with the range in northern Canada increasing. At 13 ka BP the range in southern Canada shifts to the northern part between Yukon and the Northwest Territories, reducing in northern Alaska in the USA. See Figure 4.1.4.20.a.

By the beginning of the Holocene the range is projected in the northern region of North America, between northern Alaska in the USA and Yukon and the Northwest Territories in Canada. After this at 10 ka BP a small range is projected near the ice sheet in central Canada, disappearing at 8 ka BP, and increasing in Yukon and in the Arctic Archipelago in Canada.

From 7 ka BP until 4 ka BP a similar pattern is projected in the northern region of North America, increasing from 3 ka BP until 1 ka BP in northern Alaska in the USA and northern Yukon and Northwest Territories in Canada. This same pattern continues in the current breeding range projection.

A similar pattern is observed between H2 and 24 ka BP although with a larger range in western Alaska and a smaller range in the northern conterminous USA at H2. This pattern changes at H1, shifting from western to central Alaska in the USA. The H0 and 13 ka BP projection present a similar range in the northern region of North America, only with a larger range projected at H0 than at 13 ka BP.

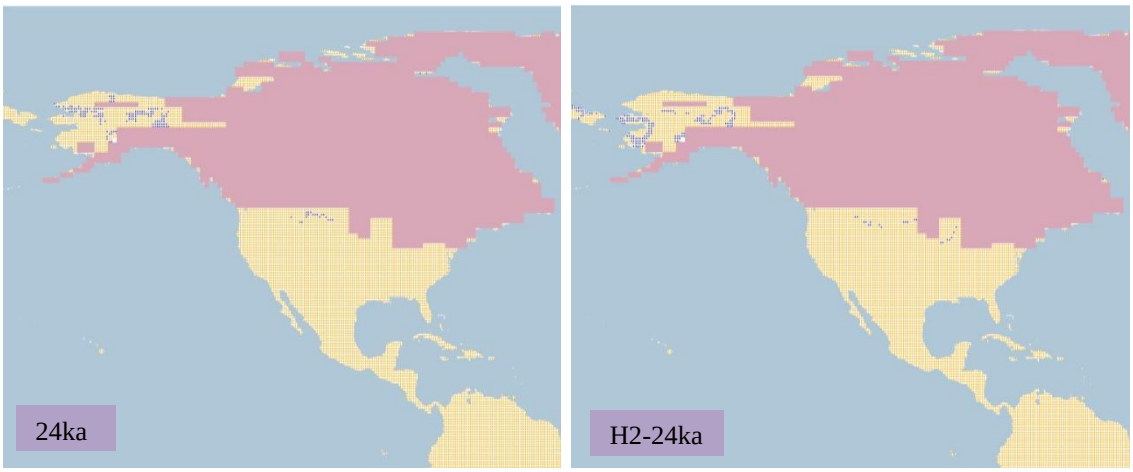

Figure 4.1.4.20.a. Simulation maps of Long-billed Dowitcher breeding range.
Maps are shown for ten-time slices: 24ka, H2 (24ka), 17ka, H1 (17ka), 13ka, H0 (13ka), 9ka, 5ka, 3ka and present (1961–90).

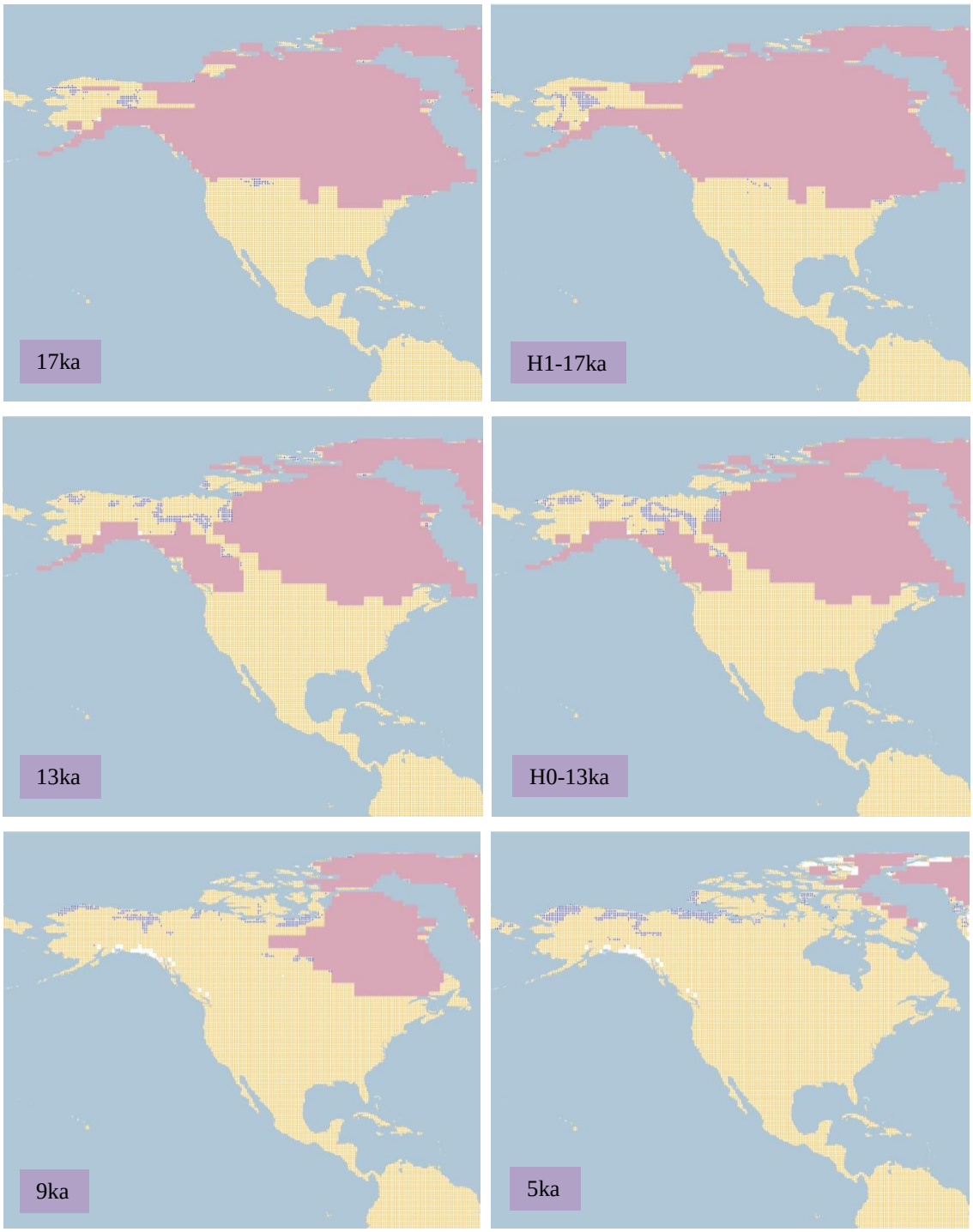

Figure 4.1.4.20.a. Simulation maps of Long-billed Dowitcher breeding range (continued**).**

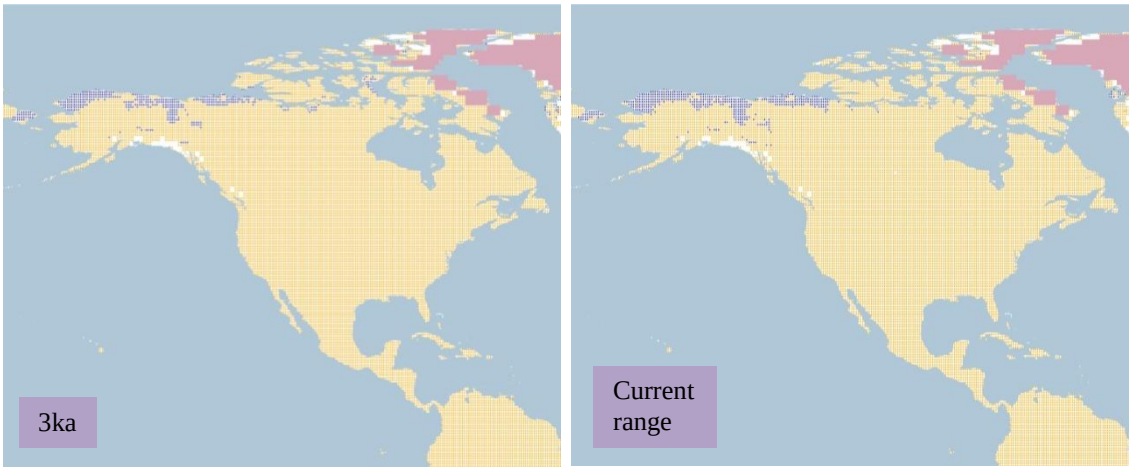

Figure 4.1.4.20.a. Simulation maps of Long-billed Dowitcher breeding range (continued**).**

Non-breeding range (AUC: 0.983; TSS: 0.873; Kappa: 0.624): Spends the winter season in the southern USA from California to the eastern coast of North Carolina, and in Mexico as far as Tabasco and Oaxaca, as well as in Jamaica and a small area in central Costa Rica.

At 26 ka BP the range is projected in the central-southern and south-western parts of the USA, and in the north-western and central-northern parts of Mexico. This pattern continues until 18 ka BP with a range projected in northern Florida in the USA. See Figure 4.1.4.20.b.

At 15 ka BP the range in the south-western USA decreases, increasing in the south-eastern part instead. This pattern continues until 12 ka BP when with the deglaciation the range in the south-eastern USA is increased. After this at 10 ka BP the range also increases in the central and northern part of Mexico.

At 7 ka BP a larger range is projected in the northern part of Mexico and the south-eastern region of the USA, with a smaller range in California in the USA and in central Mexico. This similarity continues until 1 ka BP, when the range in the southern part of the USA increases, remaining until the 1 ka BP projection with a minimal variation. The current non-breeding range projection also displays the same range as 1 ka BP, although with a larger extent in the southern USA, and in central-northern Mexico.

The Heinrich event H2 presents a different range from 24 ka BP with a scattered range projected in California in the USA and in Baja California and central-northern Mexico. This range increases at H1, agreeing with the 17 ka BP projection only with respect to the range

in central Mexico. The H0 projection is of a different range to that projected for 13 ka BP, located in central-northern Mexico with a small range in the southern part of the USA.

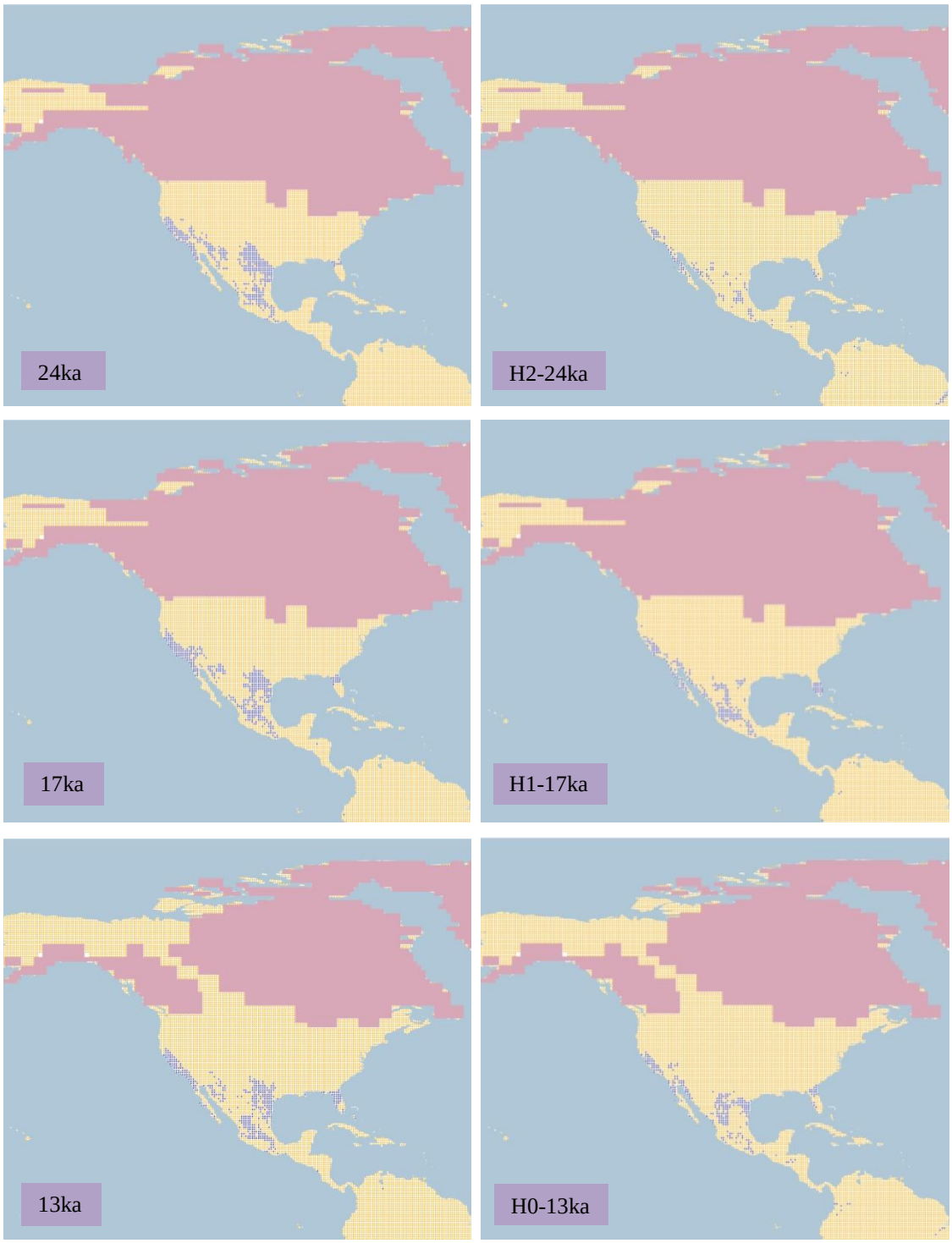

Figure 4.1.4.20.b. Simulation maps of Long-billed Dowitcher non-breeding range. Maps are shown for ten-time slices: 24ka, H2 (24ka), 17ka, H1 (17ka), 13ka, H0 (13ka), 9ka, 5ka, 3ka and present (1961–90).

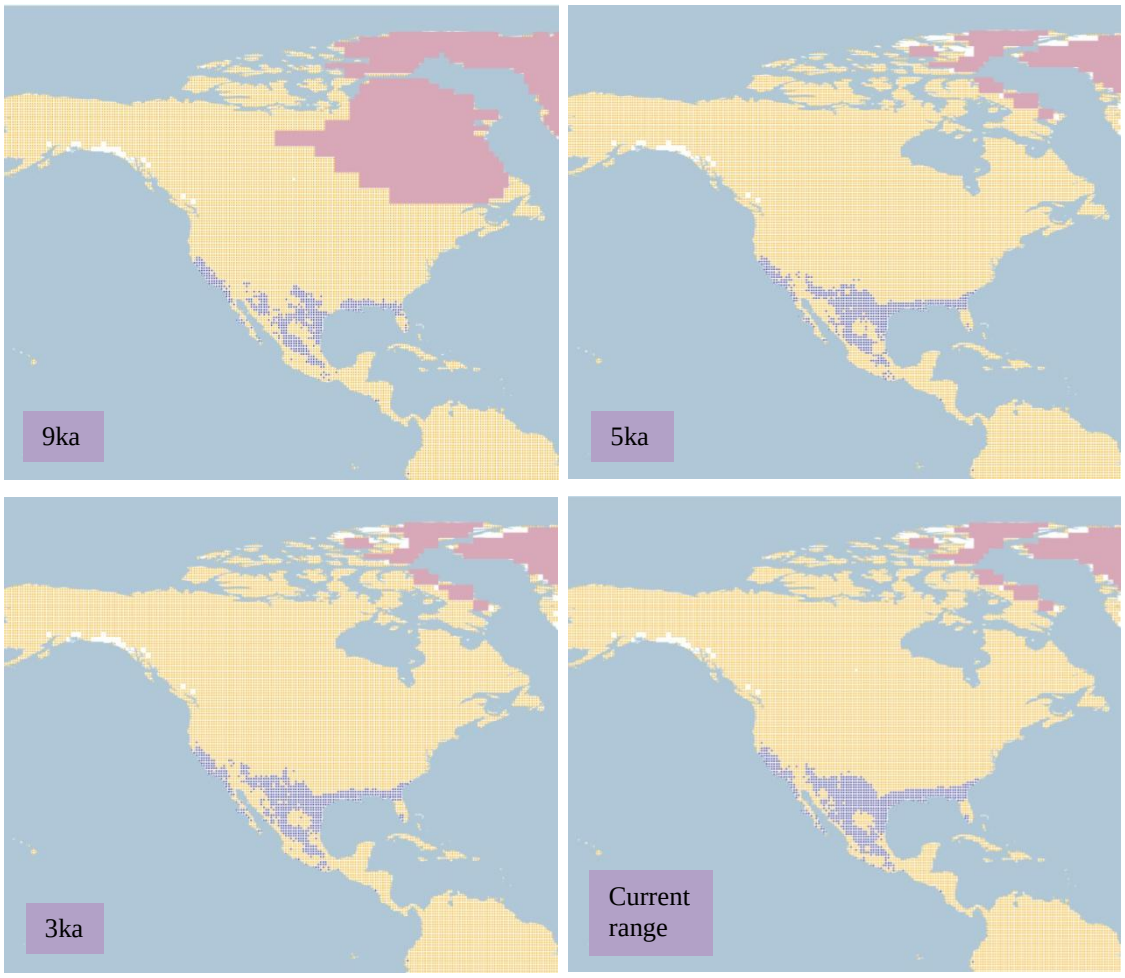

Figure 4.1.4.20.b. Simulation maps of Long-billed Dowitcher non-breeding range (continued**).**

*4.1.4.21 Marbled Godwit (*Limosa fedoa *including* L. f. beringiae *and* L. f. fedoa*). Conservation status: Least Concern. Current known range Figure 4.1.4.21.*

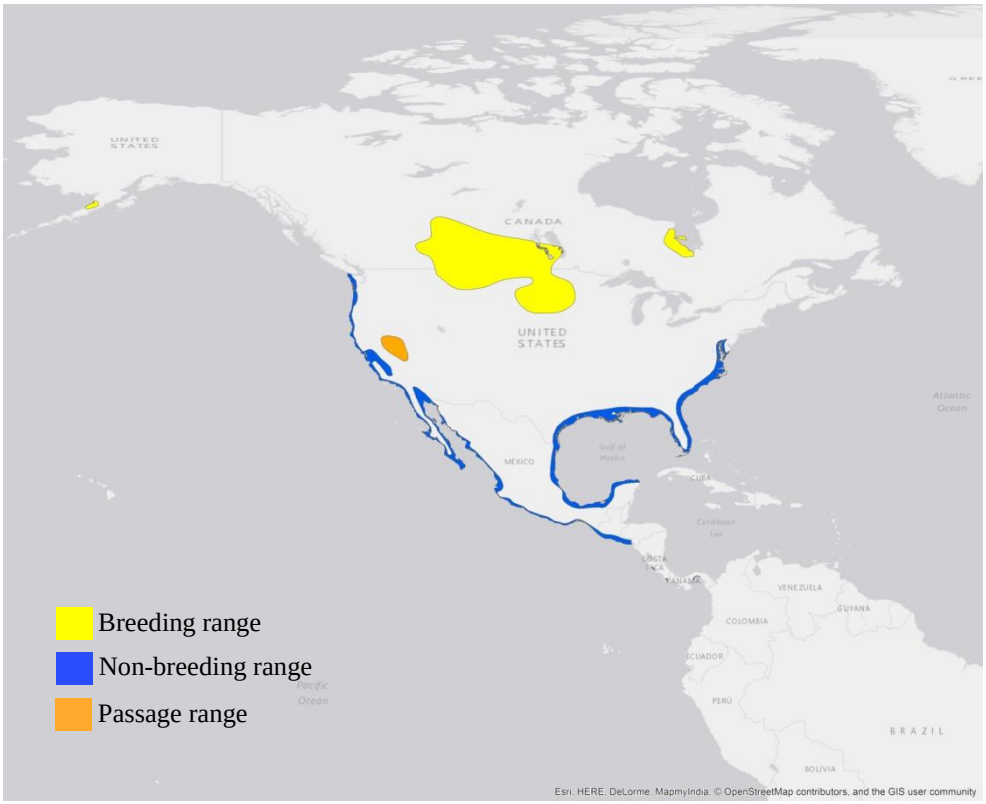

Figure 4.1.4.21. Current known range of Marble Godwit.

Breeding range (AUC: 0.988; TSS: 0.890; Kappa: 0.818): *Limosa fedoa* spends the breeding season mainly in central-southern Canada and the central-northern USA, with a separate smaller range along the eastern coast of Ontario on James Bay in Canada. *L. f. beringiae* has a very small breeding range on the north side of the Alaska Peninsula, from Ugashik Bay to Port Heiden.

At 26 ka BP a small range is projected in the central-northern region of the USA between Nebraska and South Dakota. This pattern continues until 21ka when there is a small increase to the eastern and the north-western region of the USA. After this at 16 ka BP the range shifts to the northern region of the USA and by 14 ka BP the range extent is located in the northern part of the USA and the southern boundary of Canada. See Figure 4.1.4.21.a.

At 12 ka BP the range in the northern part of the USA increases and shifts to the southern part of Canada as far as areas near the ice sheet. This change at 11 ka BP in the beginning of

the Holocene when the range reduces in the north-eastern part of the USA, and with the deglaciation at 10 ka BP the range in the north-eastern region increases, with a reduction in the central-northern part of the USA and central-southern part of Canada.

At 8 ka BP the range in the north-eastern part of the USA disappears and the range is projected in the central-northern part of the USA and central-southern part of Canada. This continues with a minimal variation until the 1 ka BP projection. The current breeding range projection also presents a similar pattern as 1 ka BP.

In the H2 projection only a small range is projected in the north-western part of the USA near the ice sheet, with no projected range in the central area as at 24ka. There is an increase at H1 in the north-western and central-northern parts of the USA, although of a smaller extent than the 17 ka BP projection. Between the H0 and the 13 ka BP projection, a similar range is observed from the central-northern part of the USA and central-southern Canada.

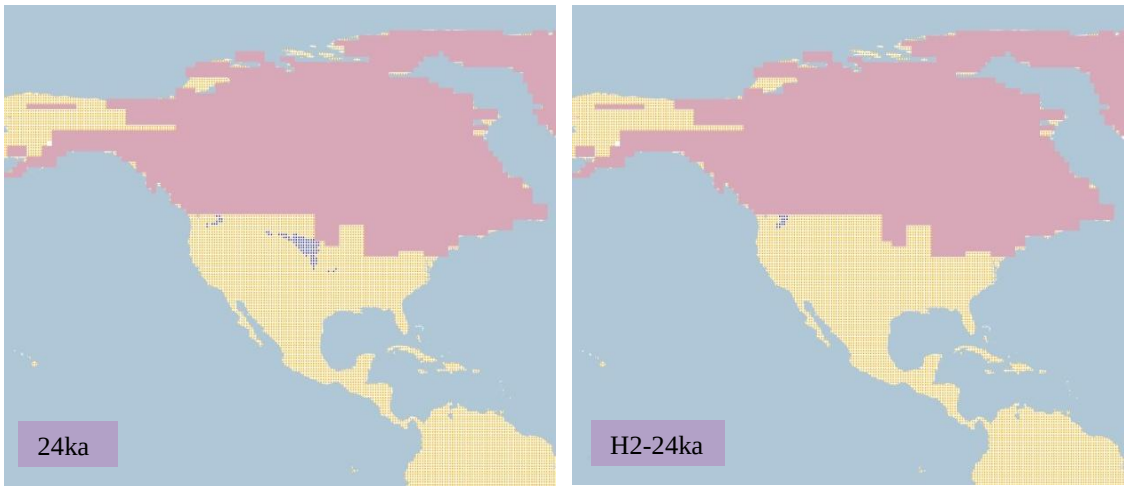

Figure 4.1.4.21.a. Simulation maps of Marbled Godwit breeding range.
Maps are shown for ten-time slices: 24ka, H2 (24ka), 17ka, H1 (17ka), 13ka, H0 (13ka), 9ka, 5ka, 3ka and present (1961–90).

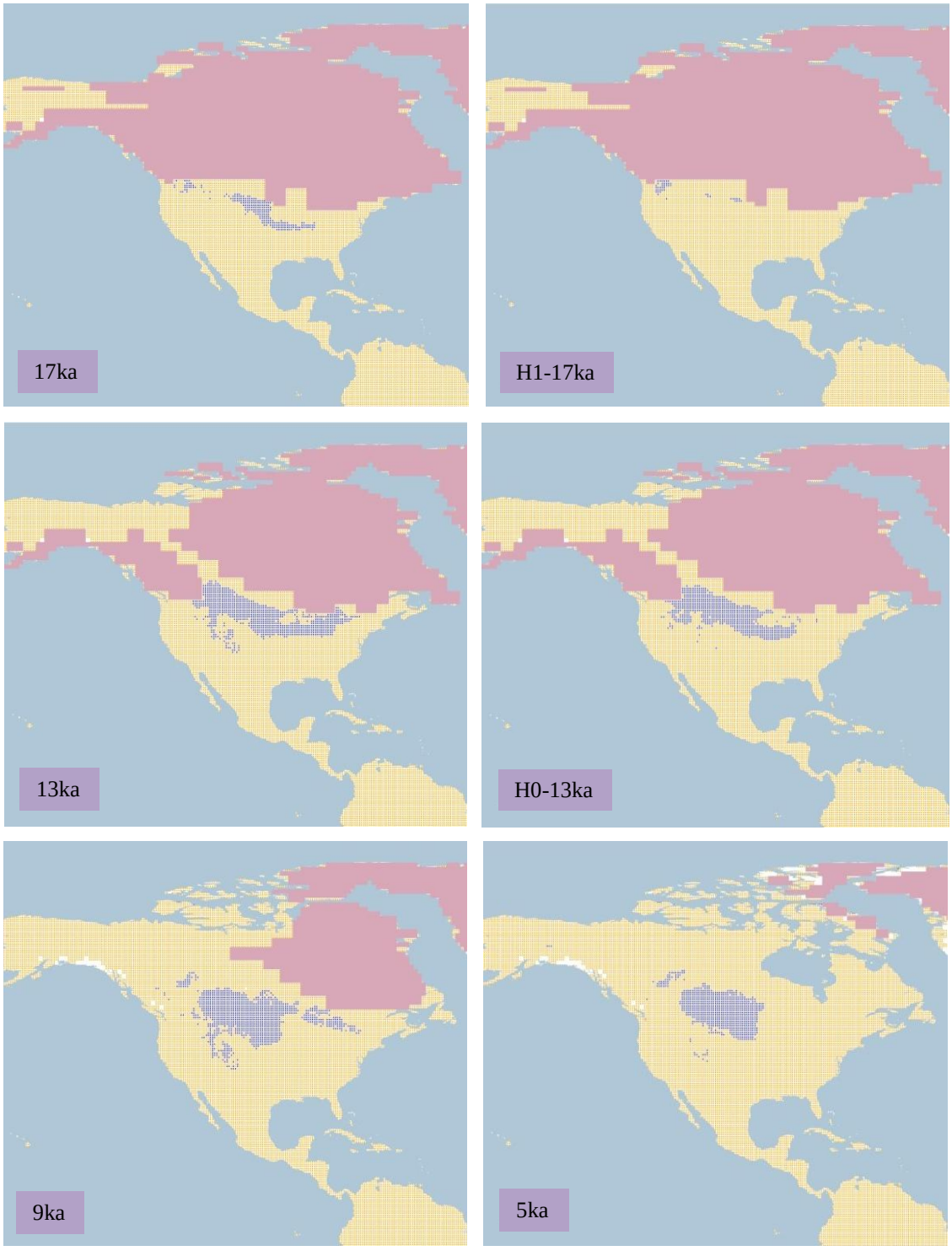

Figure 4.1.4.21.a. Simulation maps of Marbled Godwit breeding range (continued**).**

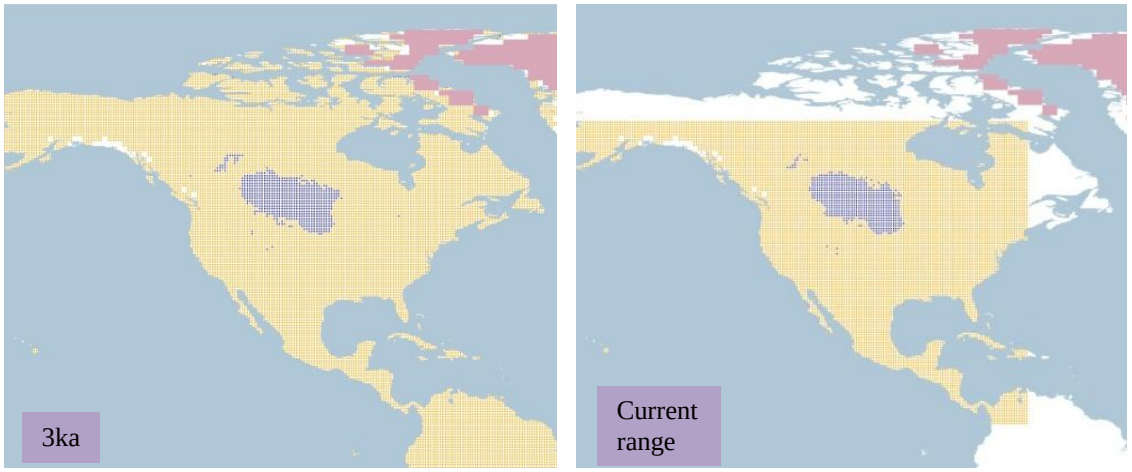

Figure 4.1.4.21.a. Simulation maps of Marbled Godwit breeding range (continued**).**

Non-breeding range (AUC: 0.981; TSS: 0.881; Kappa: 0.754): The species winters along the western and eastern coast of the USA and Mexico with a small range in inland California in the USA and along the southern coast of Guatemala and El Salvador in Central America.

At 26 ka BP the range is projected in Florida and on the western coast in the USA, extending to the western coast of Mexico and as far as Central America, with an inland range in central and southern Mexico. This pattern continues until 17 ka BP when the range on the western coast of the USA reaches Washington. See Figure 4.1.4.21.b.

At the beginning of the Holocene it continues to be projected in Florida, on the western coast of the USA, and on the western and eastern coasts of Mexico, although with a smaller range in central and southern Mexico. This continues until 7 ka BP when there is a projected range in Louisiana in the USA. After this at 1 ka BP, the range increases on the south-eastern coast of the USA as far as the eastern coast of Mexico, the remainder of the range being unchanged until the 1 ka BP projection. The current non-breeding projection continues with the same pattern as 1 ka BP along the coasts of the USA and Mexico, only with no projected range in inland Mexico as 1 ka BP.

The Heinrich event H2 projected range presents differences from 24 ka BP, with a larger range projected in central and southern Mexico and as far as Central America. This continues at H1, with a similar range as 17 ka BP only on the western coast of the USA. The range in central Mexico reduces at H0, but differs from that in the 13 ka BP projection. Even though the non-breeding range is located in North America there are suitable conditions for the species to occur in South America.

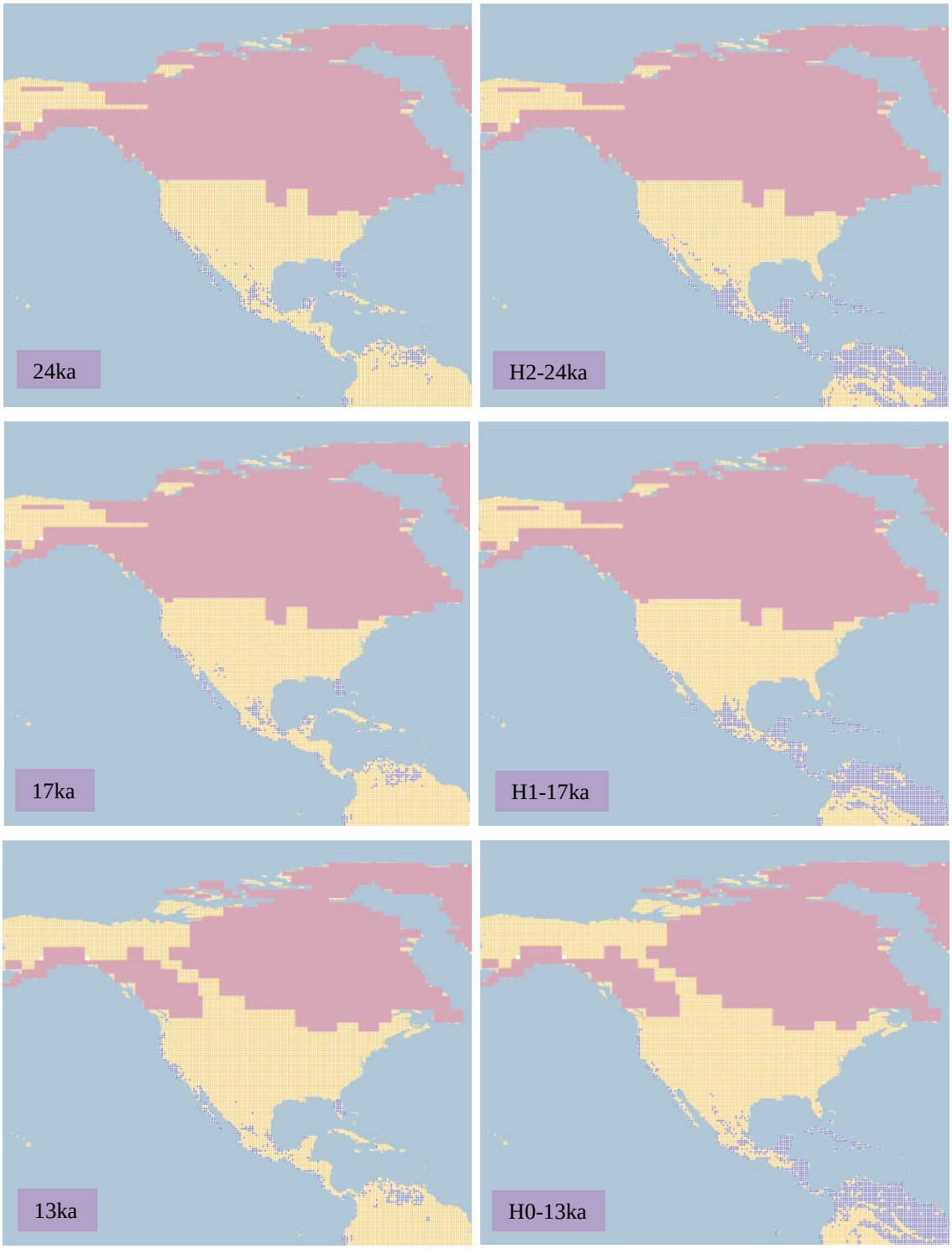

Figure 4.1.4.21.b. Simulation maps of Marbled Godwit non-breeding range.
Maps are shown for ten-time slices: 24ka, H2 (24ka), 17ka, H1 (17ka), 13ka, H0 (13ka), 9ka, 5ka, 3ka and present (1961–90).

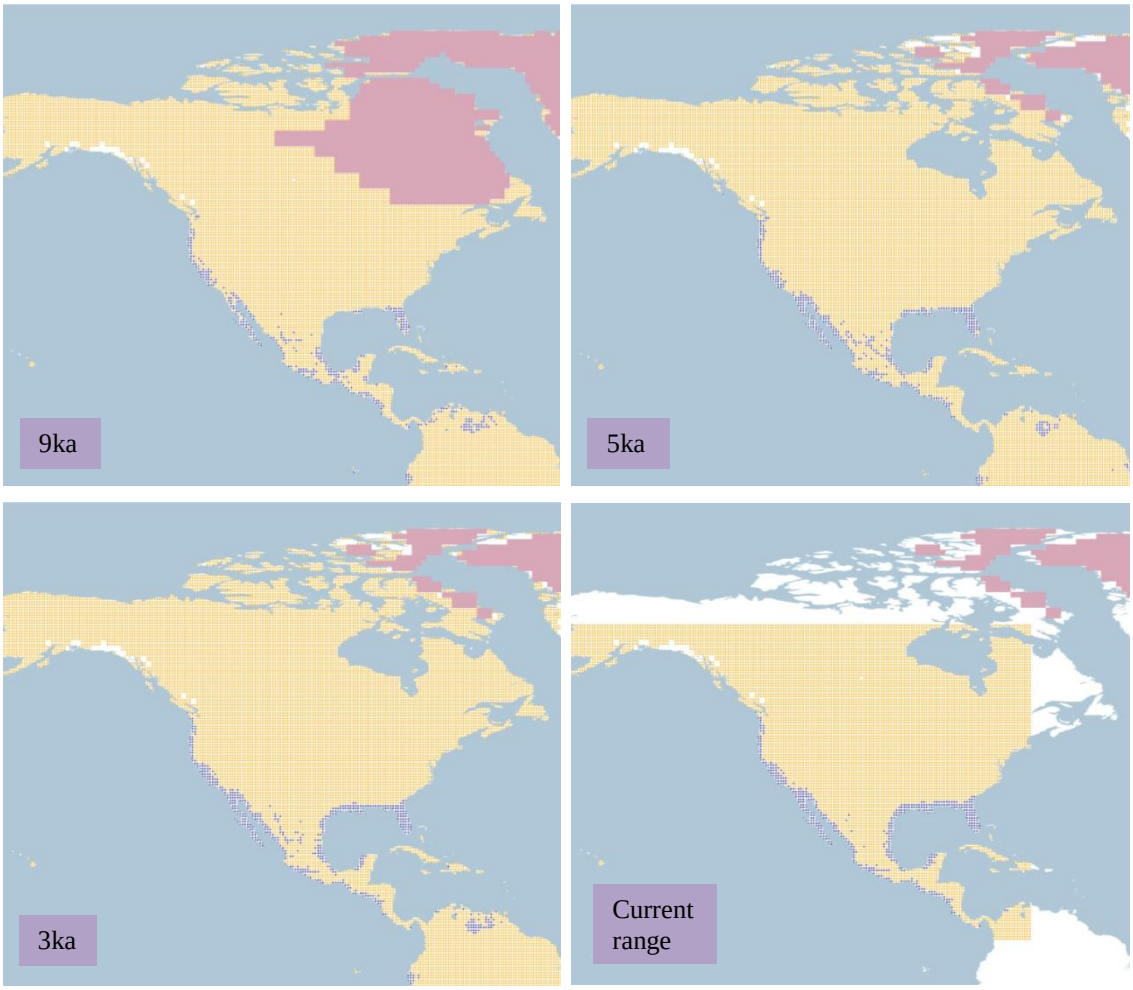

Figure 4.1.4.21.b. Simulation maps of Marbled Godwit non-breeding range (continued**).**

*4.1.4.22 Hudsonian Godwit (*Limosa haemastica*). Conservation status: Least Concern. Current known range Figure 4.1.4.22.*

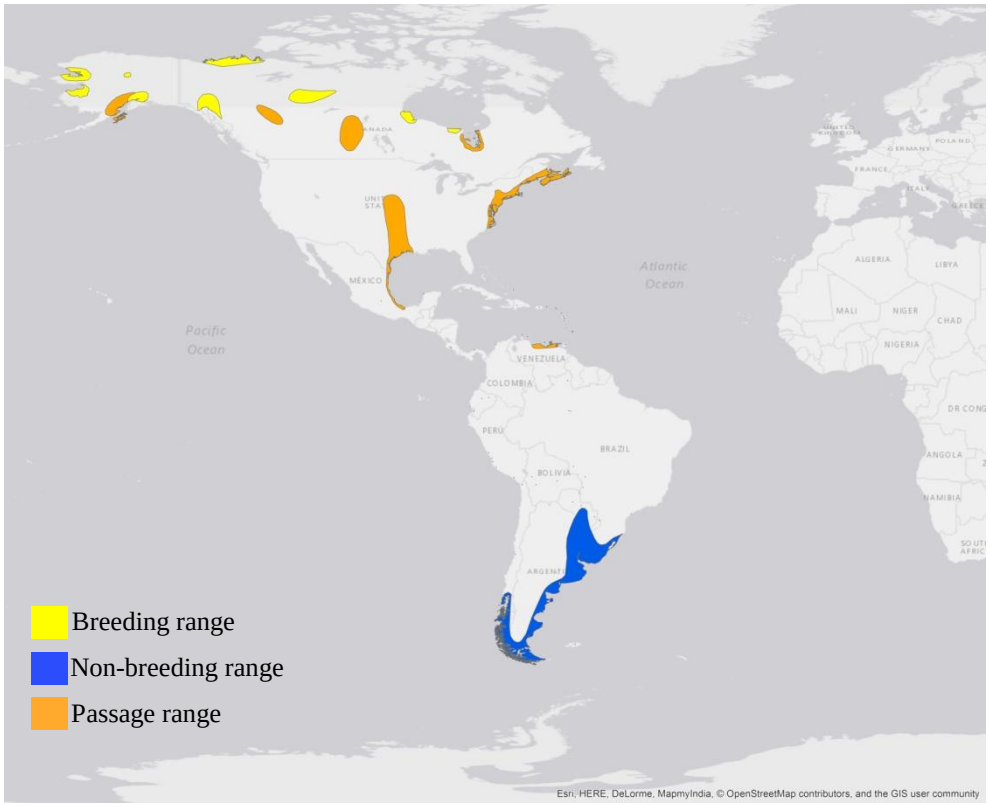

Figure 4.1.4.22. Current known range of Hudsonian Godwit.

Breeding range (AUC: 0.979; TSS: 0.880; Kappa: 0.523): This species has a small and scattered breeding range comprising a series of discrete areas in western and southern Alaska in the USA, in southern and northern Yukon, north-western British Columbia, central Northwest Territories, northern Manitoba and northern Ontario near Hudson Bay in Canada.

At 26 ka BP the range is projected in central and northern Alaska and with a smaller extent in the northern region of the conterminous USA. This pattern continues until 17 ka BP when the range in the northern conterminous part of the USA increases, and the range in Alaska reduces. After this at 14 ka BP the range shifts to southern Canada near the ice sheet, and increases in Alaska in the USA and in northern Yukon and Northwest Territories in Canada. See Figure 4.1.4.22.a.

With the deglaciation at 13 ka BP, the range increases in the central part of Canada, decreasing in Alaska in the USA. After this at 12 ka BP the range disappears from central

Canada and shifts to the central-northern region of Northwest Territories and northern part of Yukon in Canada.

By the beginning of the Holocene the range is projected mainly in northern Canada from Yukon to the Northwest Territories and in the northern coast of Alaska in the USA. This pattern increases at 10 ka BP with the deglaciation in Canada, reducing after this at 9 ka BP. Between 7 ka BP and 6 ka BP the range covers the north-western part of Canada until there is a decrease at 5 ka BP.

At 5 ka BP the projected range is fragmented in northern Canada and in Alaska in the USA, remaining with minimal variation until the 1 ka BP projection. The current breeding range projection presents a similar range as 1 ka BP.

The H2 projected range is similar to 24 ka BP in the range of Alaska, with a smaller range in the northern part of the conterminous USA than for 24ka. At H1 the range in the northern conterminous USA increases, although differing in location from that for 17 ka BP and of much smaller extent. At last the H0 and 13 ka BP projections present similar ranges across central and northern Canada.

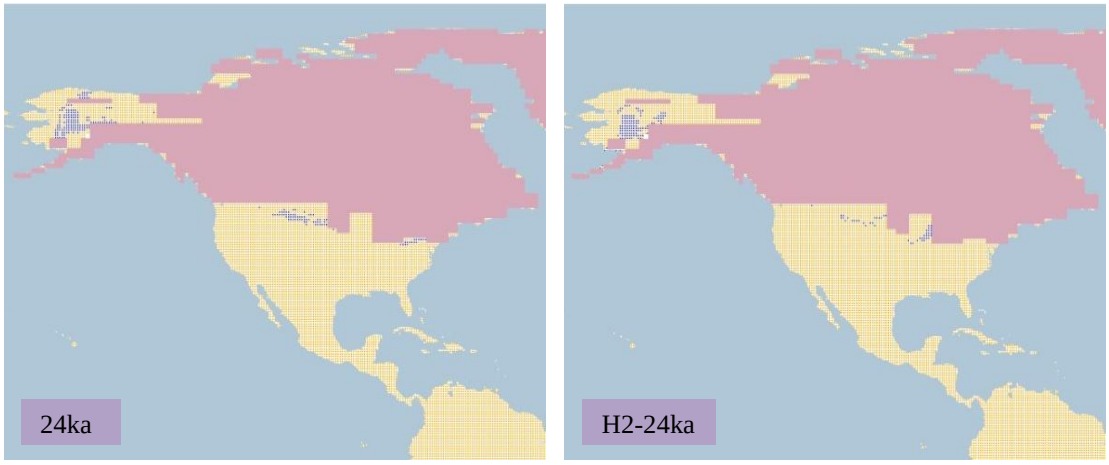

Figure 4.1.4.22.a. Simulation maps of Hudsonian Godwit breeding range.
Maps are shown for ten-time slices: 24ka, H2 (24ka), 17ka, H1 (17ka), 13ka, H0 (13ka), 9ka, 5ka, 3ka and present (1961–90).

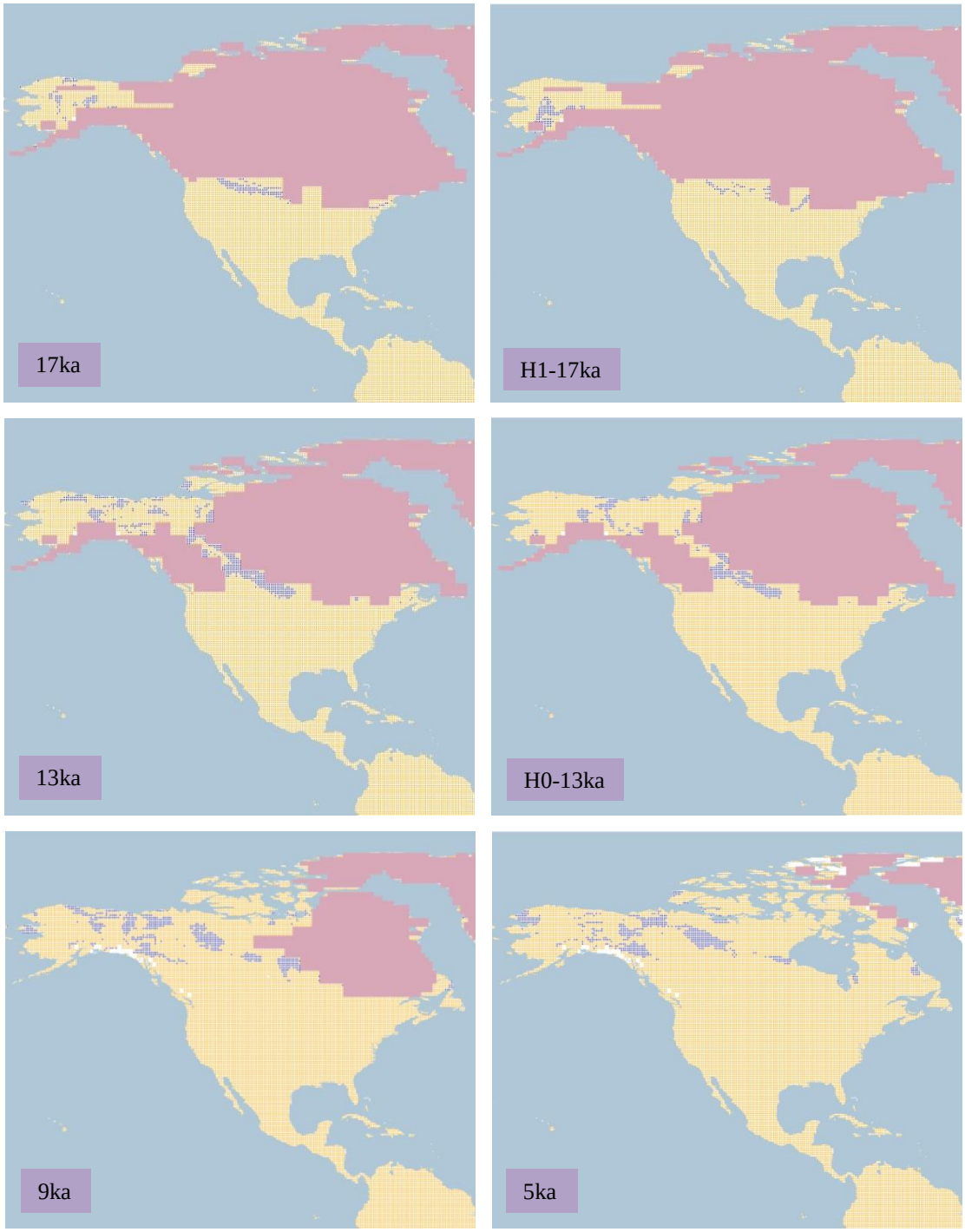

Figure 4.1.4.22.a. Simulation maps of Hudsonian Godwit breeding range (continued**).**

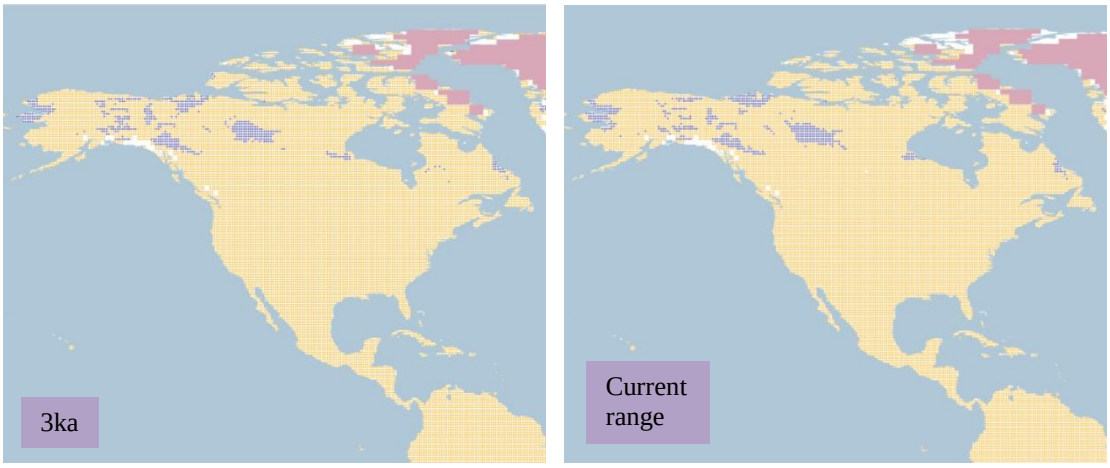

Figure 4.1.4.22.a. Simulation maps of Hudsonian Godwit breeding range (continued**).**

Non-breeding range (AUC: 0.994; TSS: 0.955; Kappa: 0.767): This species spends the non-breeding season in South America along the eastern coast and in northern Argentina to central Paraguay, Uruguay and southern Brazil, along the southern coast of Chile and south to Tierra del Fuego.

The range at 26 ka BP is projected in South America, from southern Brazil to northern Argentina with a small range in the Andean cordillera and in southern Chile. The range in southern Brazil decreases at 21 ka BP, increasing after this at 20 ka BP. At 18 ka BP the range is reduced again, shifting to Paraguay and increasing in the Andean cordillera. See Figure 4.1.4.22.b.

At 16 ka BP the range in South America increases in southern Chile, reaching southern Argentina. After this the range in northern Argentina shifts to southern Brazil and Paraguay, with a small range projected in the north-eastern part of Argentina.

By the beginning of the Holocene the range is projected in southern Brazil, Paraguay, Uruguay and northern Argentina, with a large range in southern Chile and from central to south-eastern Argentina. This continues until 8 ka BP when the ranges in southern Brazil and northern Argentina increase, decreasing again at 7 ka BP.

From 6 ka BP to 3 ka BP the range is projected from southern Brazil to northern Argentina and along the eastern coast reaching southern Chile. This range changes at 2 ka BP decreasing in southern Brazil, and increasing again at 1 ka BP. The current non-breeding projected range presents a similar pattern to 1 ka BP in South America.

There is a similar range observed between H2 and 24 ka BP from the southern region of Brazil to northern Argentina and in southern Chile, only with a larger range projected in the Andean cordillera at H2. This pattern continues at H1 with an increase in Paraguay, which differs from 17 ka BP. The differing range in southern Brazil continues between H0 and 13 ka BP, only with a similar range on the eastern coast of Argentina and in southern Chile.

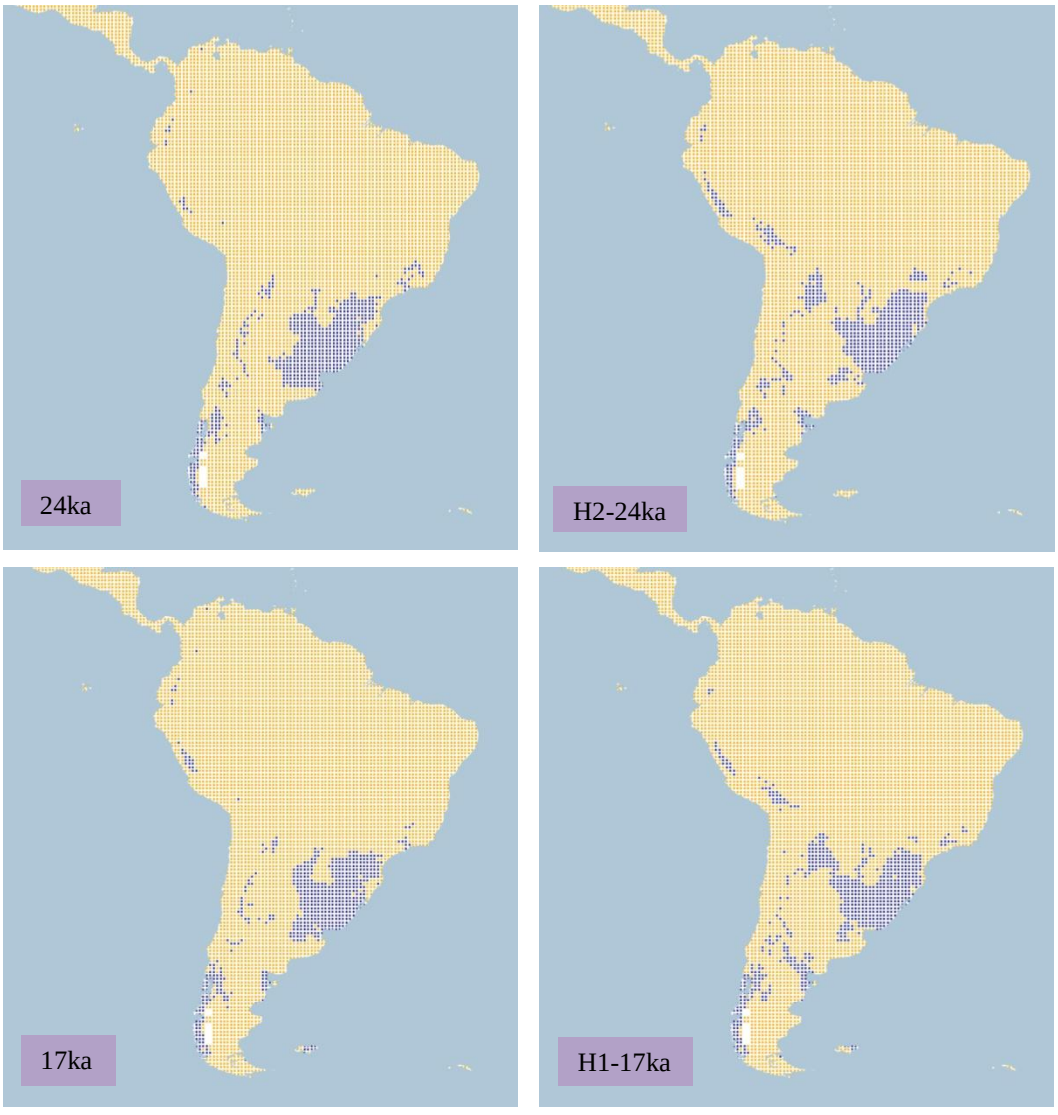

Figure 4.1.4.22.b. Simulation maps of Hudsonian Godwit non-breeding range. Maps are shown for ten-time slices: 24ka, H2 (24ka), 17ka, H1 (17ka), 13ka, H0 (13ka), 9ka, 5ka, 3ka and present (1961–90).

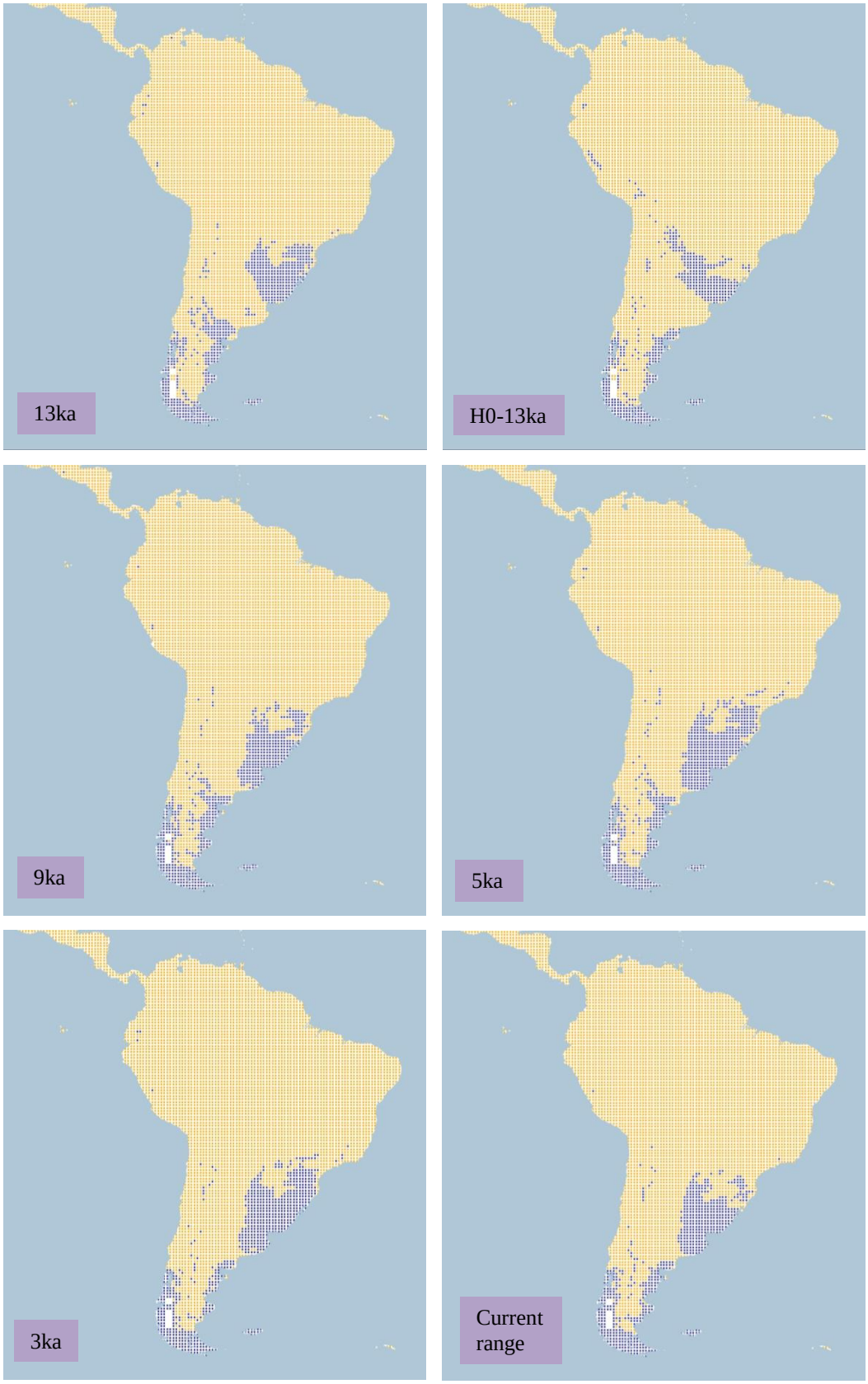

Figure 4.1.4.22.b. Simulation maps of Hudsonian Godwit non-breeding range (continued**).**

*4.1.4.23 Long-billed Curlew (*Numenius americanus *including* N. a. parvus *and* N. a. americanus*). Conservation status: Least Concern. Current known range Figure 4.1.4.23.*

Figure 4.1.4.23. Current known range of Long-billed Curlew.

Breeding range (AUC: 0.994; TSS: 0.937; Kappa: 0.870): This species breeds in the central and western conterminous USA, with a small range in south-western Canada.

At 26 ka BP the range is projected in north-western and central regions of the USA, as far as the Sierra Madre Occidental in northern Mexico. This pattern continues with minimal difference until 17 ka BP when the range in the western region of the USA is increased, with the range reducing along the Sierra Madre Occidental in Mexico. After this, with the deglaciation, the range in the USA shifts to southern Canada near the ice sheet, particularly from 16 ka BP to 14 ka BP. See Figure 4.1.4.23.a.

By the beginning of the Holocene the projected range extends from the western to central region of the USA and the south-western region of Canada, with a small range projected in central-southern Canada near the ice sheet. The range in south-eastern Canada reduces at 10 ka BP and disappears at 9 ka BP. After this, the range continues with the same pattern in

the USA and south-western Canada with a minimal difference until 1 ka BP. The current breeding range projection agrees with the breeding range at 1 ka BP.

The projected range at H2 is smaller in the western region of the USA than at 24 ka BP, with no projected range in the central region. The range increases in the western part of the USA as far as the Sierra Madre Occidental at H1, although differing from 17 ka BP with a large range projected in the USA. The range changes at H0, shifting to the north-western part of the USA and southern Canada, with no projected range in the central region of the USA as 13 ka BP.

Even though the breeding range is located in North America, suitable conditions are projected in South America from Chile to Argentina for the species to occur.

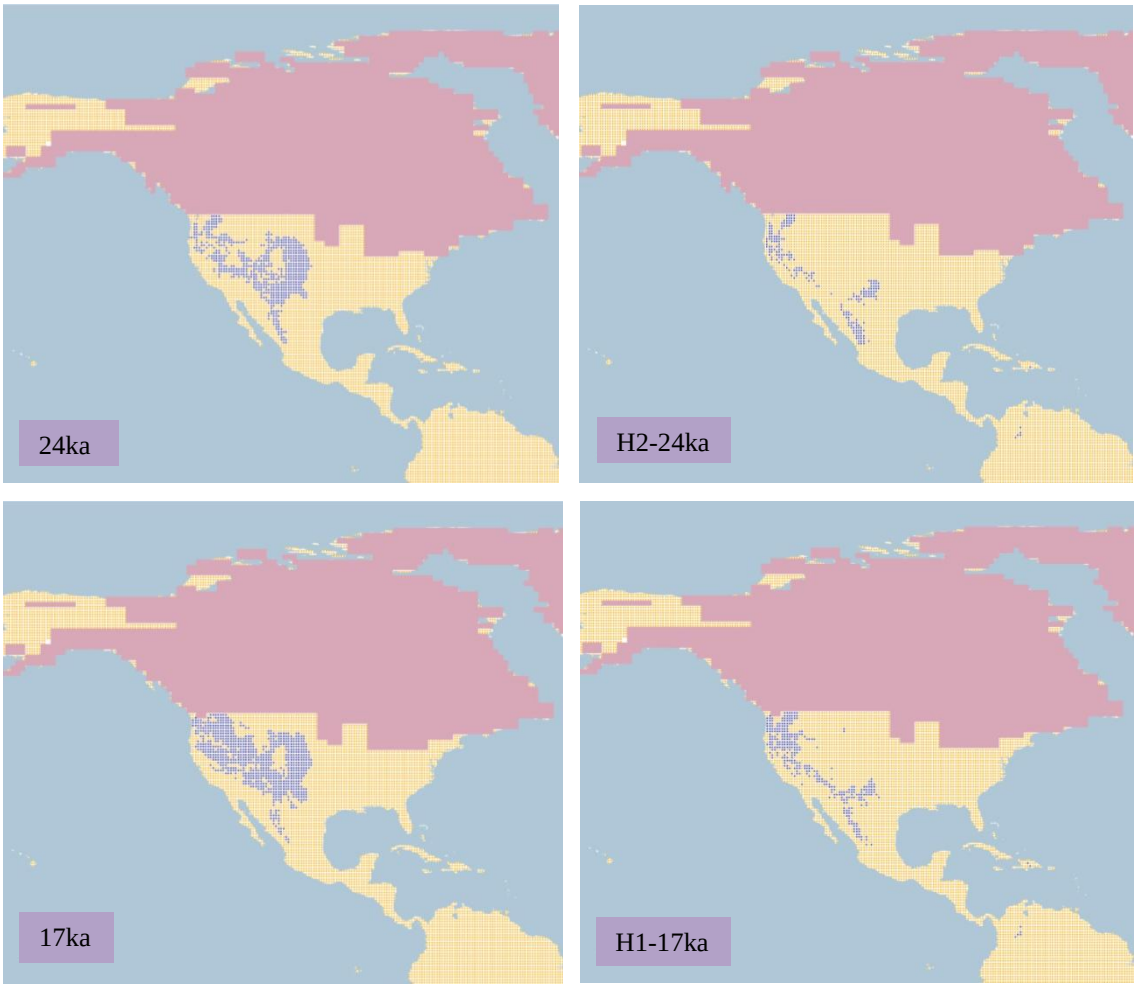

Figure 4.1.4.23.a. Simulation maps of Long-billed Curlew breeding range.
Maps are shown for ten-time slices: 24ka, H2 (24ka), 17ka, H1 (17ka), 13ka, H0 (13ka), 9ka, 5ka, 3ka and present (1961–90).

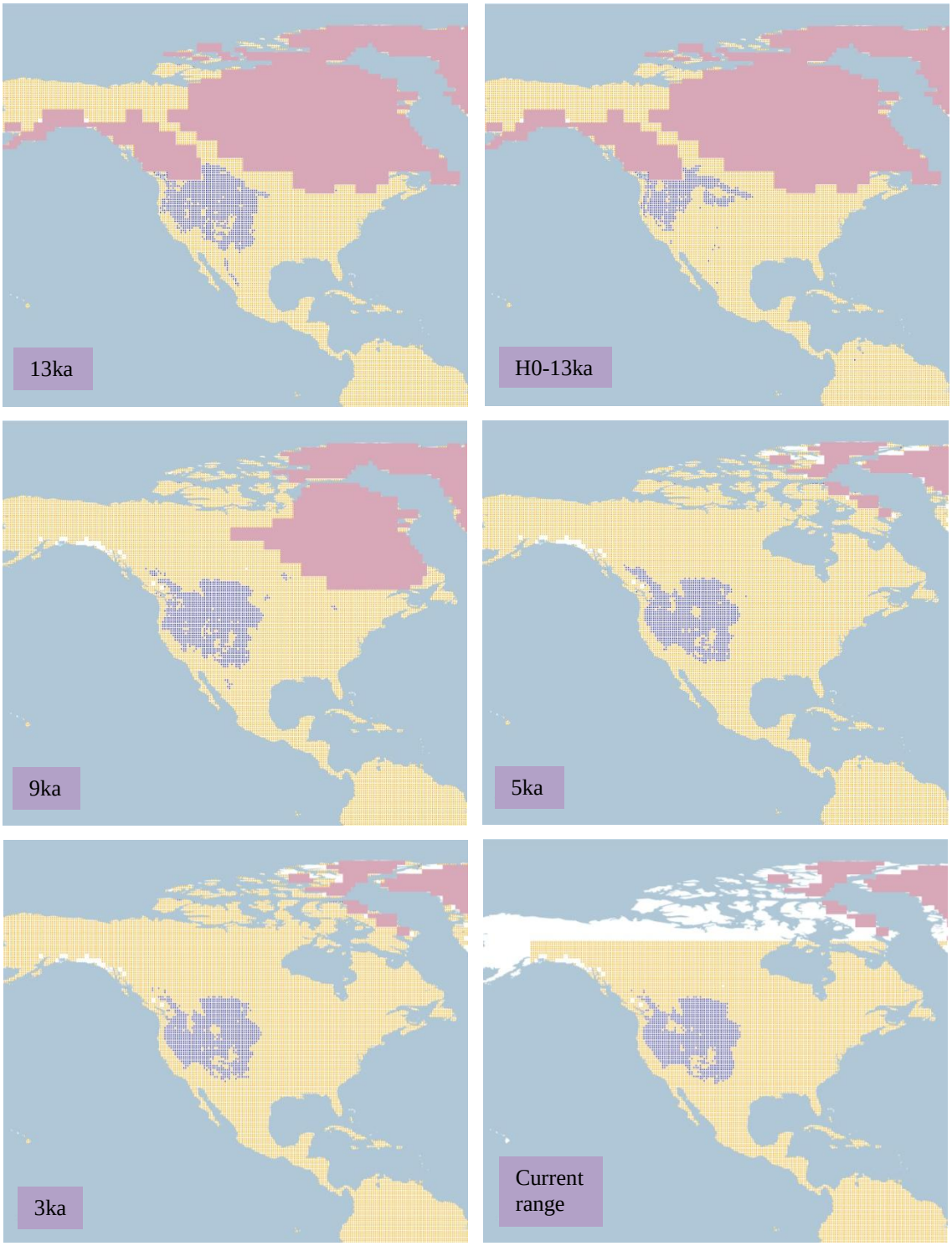

Figure 4.1.4.23.a. Simulation maps of Long-billed Curlew breeding range (continued**).**

Non-breeding range (AUC: 0.995; TSS: 0.933; Kappa: 0.883): This species spends the winter along the western coast and in the southern region of the USA, in central to northern Mexico and along the western and eastern coast from Baja California to Chiapas on the Pacific side

and from Tamaulipas to Yucatan on the Gulf of Mexico. A small range extends to the southern coast of Guatemala and El Salvador in Central America.

The projected range at 26 ka BP is located along the western coast and southern region of the USA as far as central Mexico and with a small range in the north of Yucatan and in Florida in the USA. This pattern continues until 16 ka BP, when the range is in the south-west of the USA and north-west of Mexico. The range returns to the north-west of Mexico at 14 ka BP, and with a larger range projected along the western coast of the USA. See Figure 4.1.4.23.b.

By the beginning of the Holocene the range is projected in Mexico and as far as the western coast and southern region of the USA. This is changed at 8 ka BP when the range in Florida disappears and the range in southern Mexico decreases. After this the range continues with the same pattern until 1 ka BP. The current non-breeding projection shares a similar pattern with the 1 ka BP projection.

When comparing H2 with 24 ka BP a similar range is projected in Mexico and in the western and southern region in the USA, although with a smaller range in the north-western part of Mexico and with a scattered range in Central America. A similar pattern continues between H1 and 17 ka BP, although a larger range is projected along the south-eastern coast of the USA and in southern Mexico at H1. These differences persist in the H0 and 13 ka BP projections.

Even though the species' non-breeding range is located in North America, there are suitable conditions for the species to occur in South America, mainly in the central-southern region between Argentina and Chile.

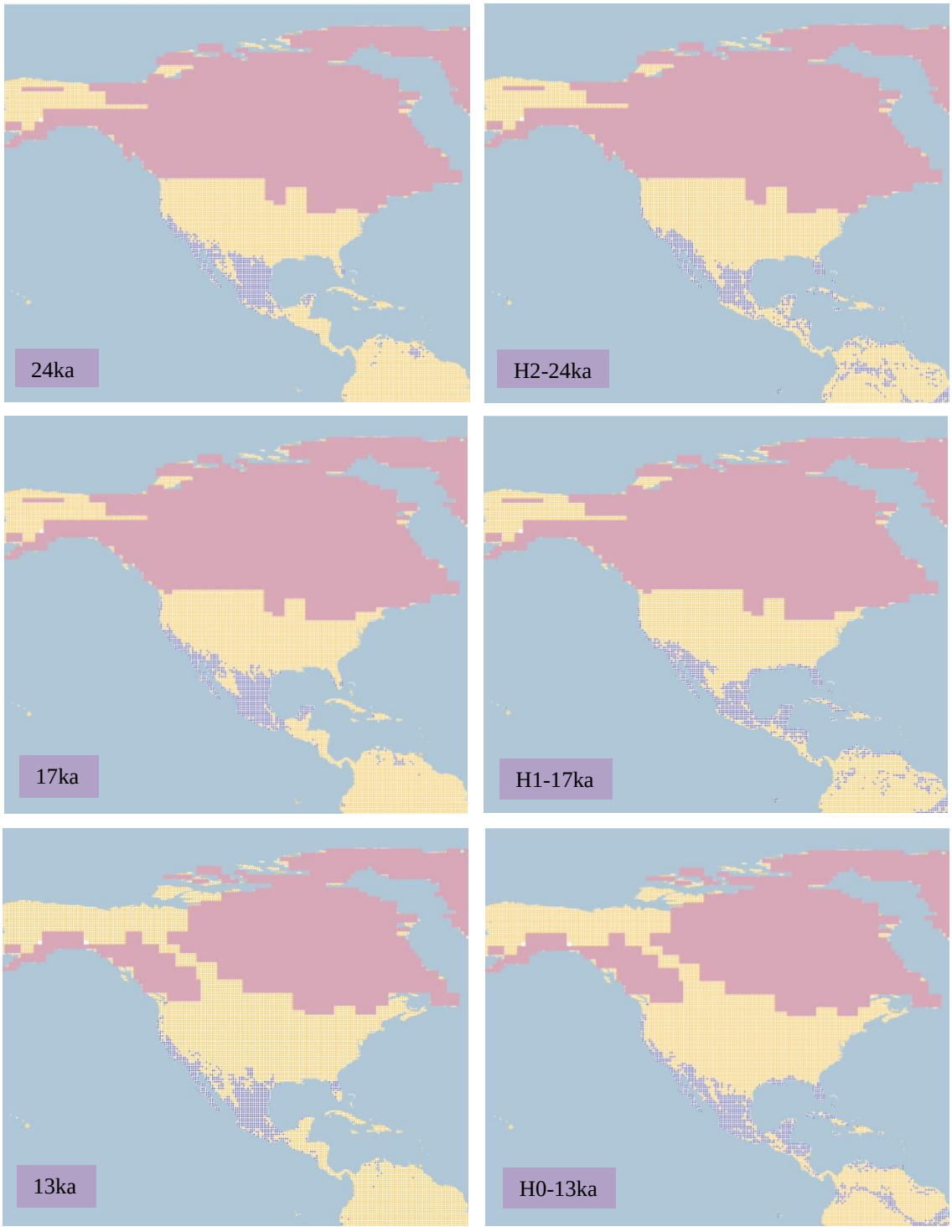

Figure 4.1.4.23.b. Simulation maps of Long-billed Curlew non-breeding range. Maps are shown for ten-time slices: 24ka, H2 (24ka), 17ka, H1 (17ka), 13ka, H0 (13ka), 9ka, 5ka, 3ka and present (1961–90).

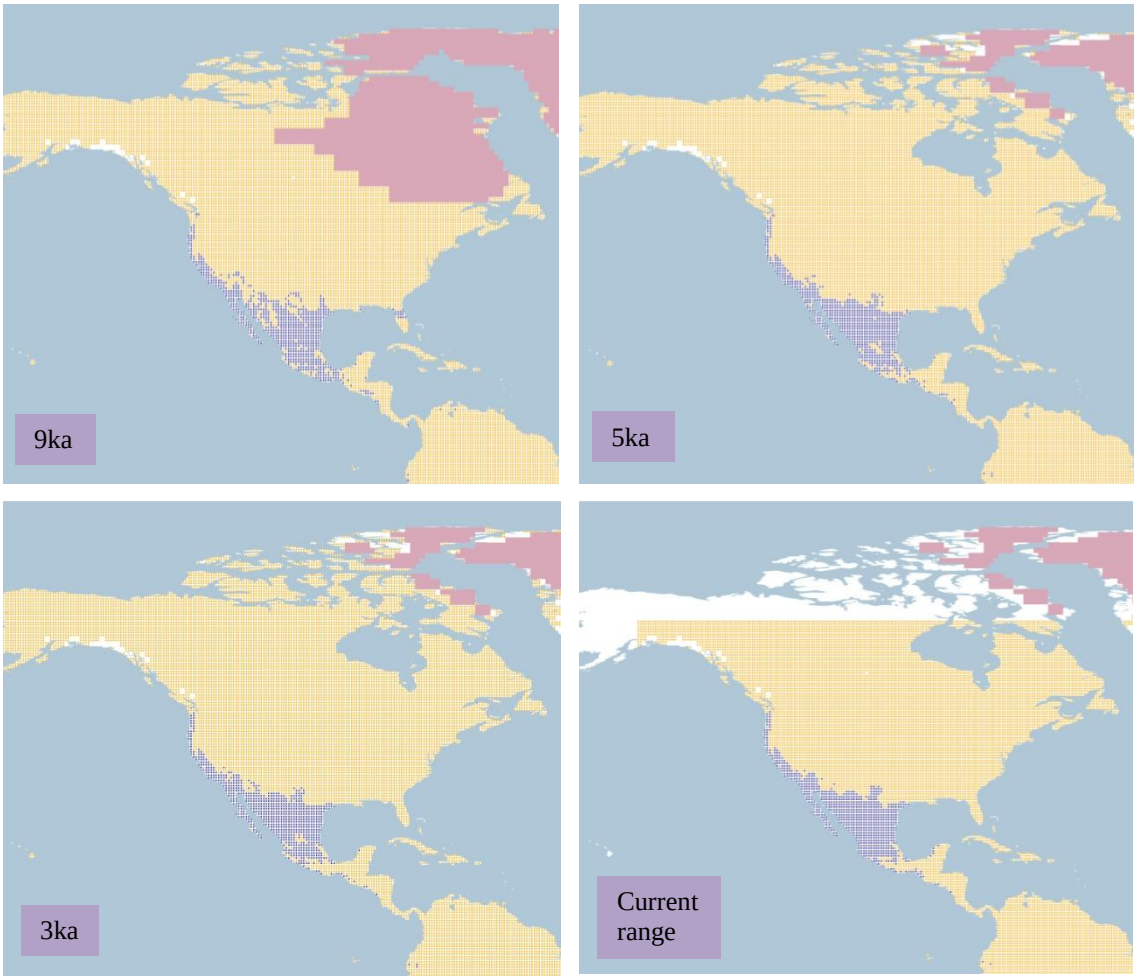

Figure 4.1.4.23.b. Simulation maps of Long-billed Curlew non-breeding range (continued**).**

*4.1.4.24 American Whimbrel (*Numenius phaeopus hudsonicus*). Conservation status: Least Concern. Current known range Figure 4.1.4.24.*

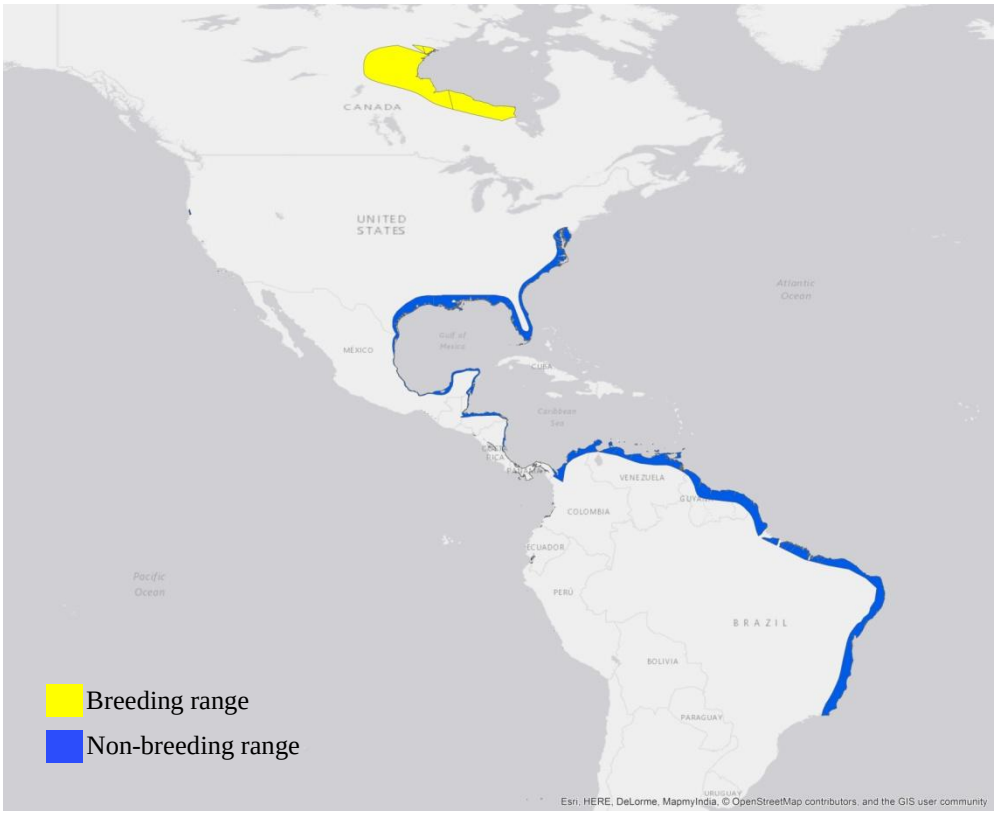

Figure 4.1.4.24. Current known range of American Whimbrel.

Breeding range (AUC: 0.980; TSS: 0.931; Kappa: 0.786): This sub-species breeding range is located in central-southern Nunavut, along northern Manitoba and northern Ontario in Canada.

The range projected at 26 ka BP is restricted to south-eastern South Dakota near the ice sheet, and with a range projected in extreme eastern Siberia. This pattern continues until 17 ka BP when a small range is projected in Alaska. After this, the range in the northern conterminous USA disappears. See Figure 4.1.4.24.a.

At 15 ka BP the range is projected from central to western Alaska in the USA. This increases with the deglaciation at 13 ka BP, with also a small range projected near the ice sheet in southern Canada and the north-eastern conterminous USA. By 12 ka BP the range increases in central Alaska and in northern Canada, as well as near the ice sheet in the north-

eastern conterminous USA. This pattern continues in the beginning of the Holocene, but with decreasing extent at 9 ka BP.

At 8 ka BP, a small range is projected in central Canada between Saskatchewan and the Northwest Territories. The range increases in the central and north-eastern region of Canada at 7 ka BP and reaches Baffin Island at 6 ka BP. After this the range continues with a similar pattern and with minimal variation until 1 ka BP. The current breeding range continues with the same pattern as 1 ka BP in the region of central-northern Canada.

When comparing the H2 projection with 24 ka BP, a similar pattern is found in the small range projected in the central-northern conterminous USA. This continues at H1, with no projected range, differing from 17ka. The H0 projection presents a range in central-western Alaska and near the ice sheet in central-southern Canada and in the north-eastern USA as in the 13 ka BP projection.

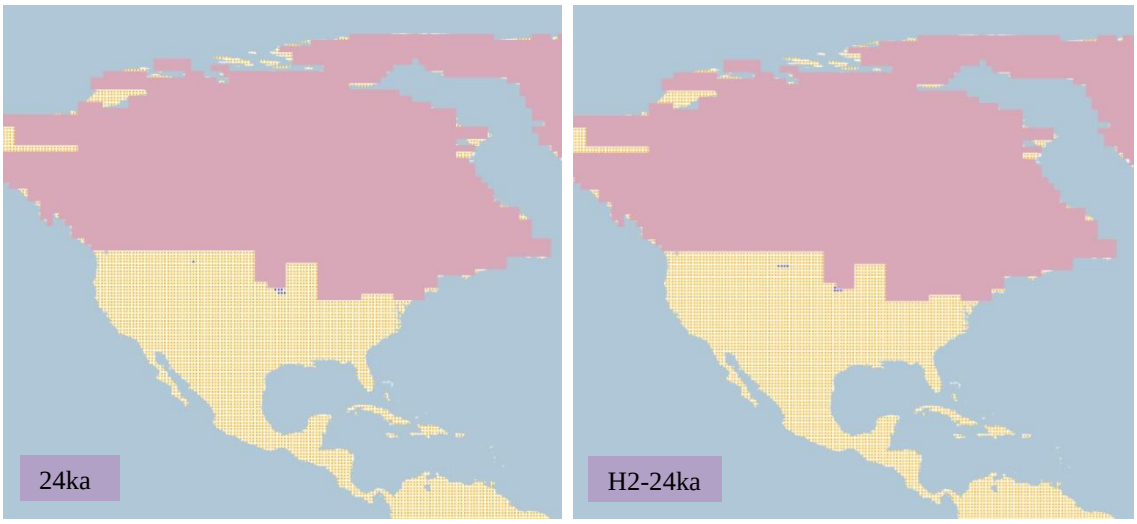

Figure 4.1.4.24.a. Simulation maps of American Whimbrel breeding range.
Maps are shown for ten-time slices: 24ka, H2 (24ka), 17ka, H1 (17ka), 13ka, H0 (13ka), 9ka, 5ka, 3ka and present (1961–90).

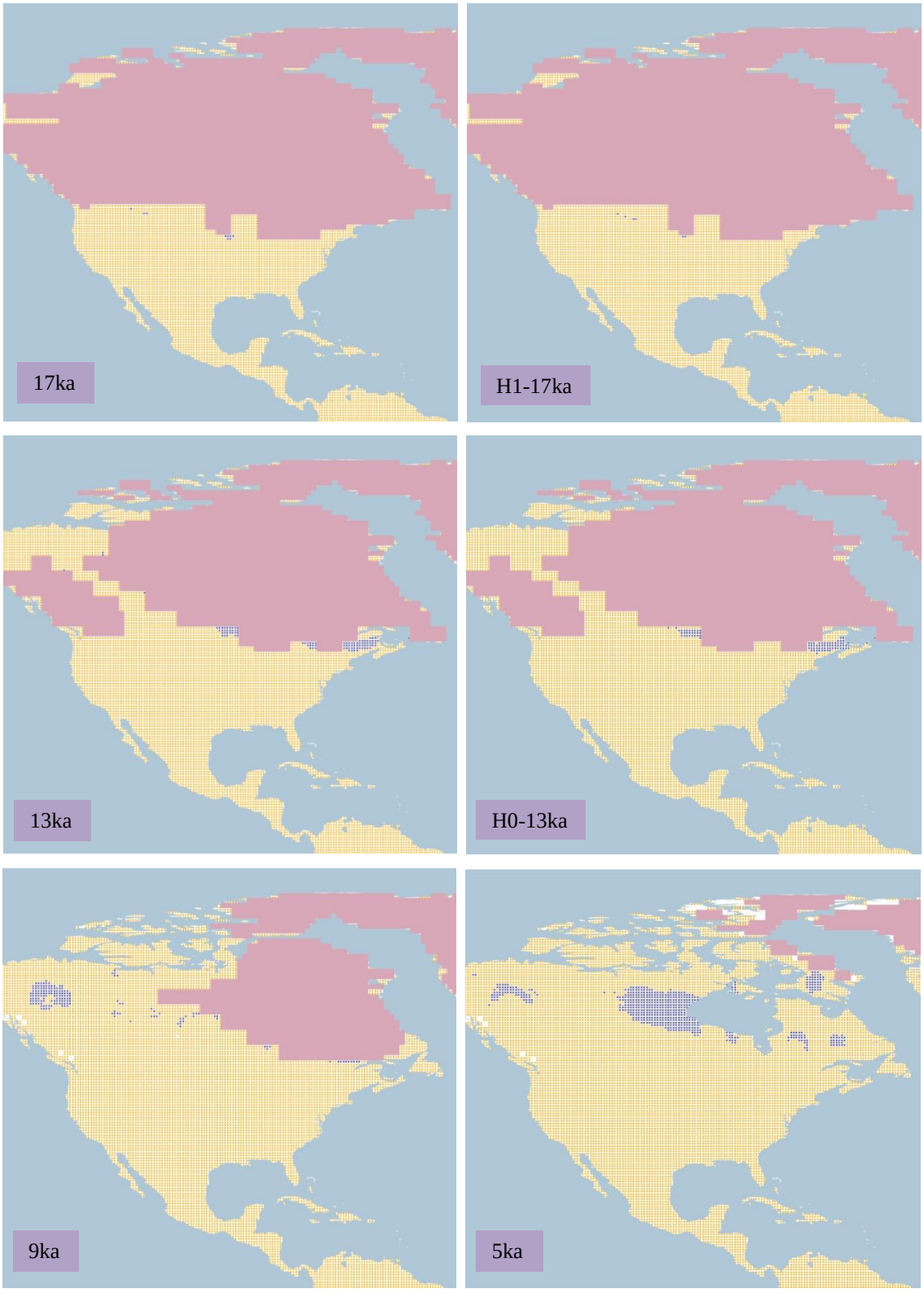

Figure 4.1.4.24.a. Simulation maps of American Whimbrel breeding range (continued**).**

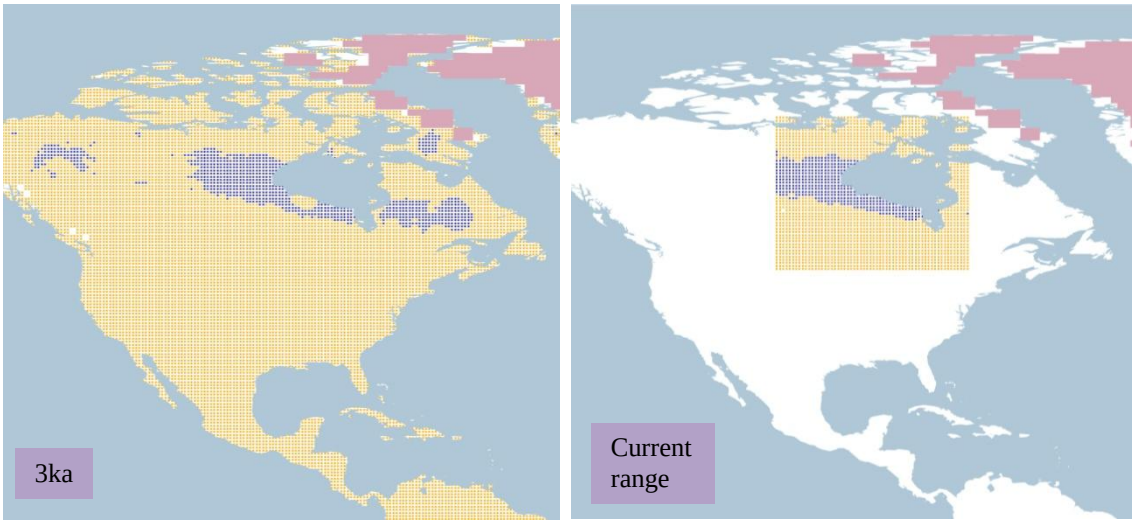

Figure 4.1.4.24.a. Simulation maps of American Whimbrel breeding range (continued**).**

Non-breeding range (AUC: 0.919; TSS: 0.664; Kappa: 0.502): This sub-species wintering ground is located along the Atlantic coast of the USA, Mexico, Central America and as far as south-eastern Brazil in South America.

At 26 ka BP the range is projected in northern Florida in the USA, in the Greater Antilles, in central Mexico with a scattered range in the southern region as far as Central America and in South America with a scattered range from the northern region, to Bolivia and southern Chile. This pattern continues until 22 ka BP, with a projected range in north-eastern Argentina and Uruguay, with a decrease in the central region of South America. After this at 21 ka BP, the range in central Mexico is reduced. See Figure 4.1.4.24.b.

With the deglaciation at 13 ka BP the range in Florida in the USA increases, as well as the range on the central-eastern coast of Mexico and along the eastern coast of Central America, with a larger range projected in the northern region of South America and in southern Chile. This continues until 11 ka BP, when the range in the northern part of South America is reduced to a fragmented range. However, there is an increase in the range projected on the south-eastern coast in the USA.

At 7 ka BP the range in central and on the eastern coast of Mexico increases, as does that on the south-eastern coast of the USA, and in the central region of South America. A similar pattern continues with minimal variation in the northern and central part of South America, increasing in north-eastern Brazil and the south-eastern USA until 1 ka BP. The current non-

breeding projection continues with a similar range as at 1 ka BP in the USA and Mexico, although with a larger range in northern South America.

The Heinrich event H2 projects a large range in the Amazonian region in South America, with a small scattered range in Mexico, differing from the 24 ka BP projection. This range increases at H1 and shifts to the north-western region at H0, both with different projections than 17 ka BP and 13 ka BP.

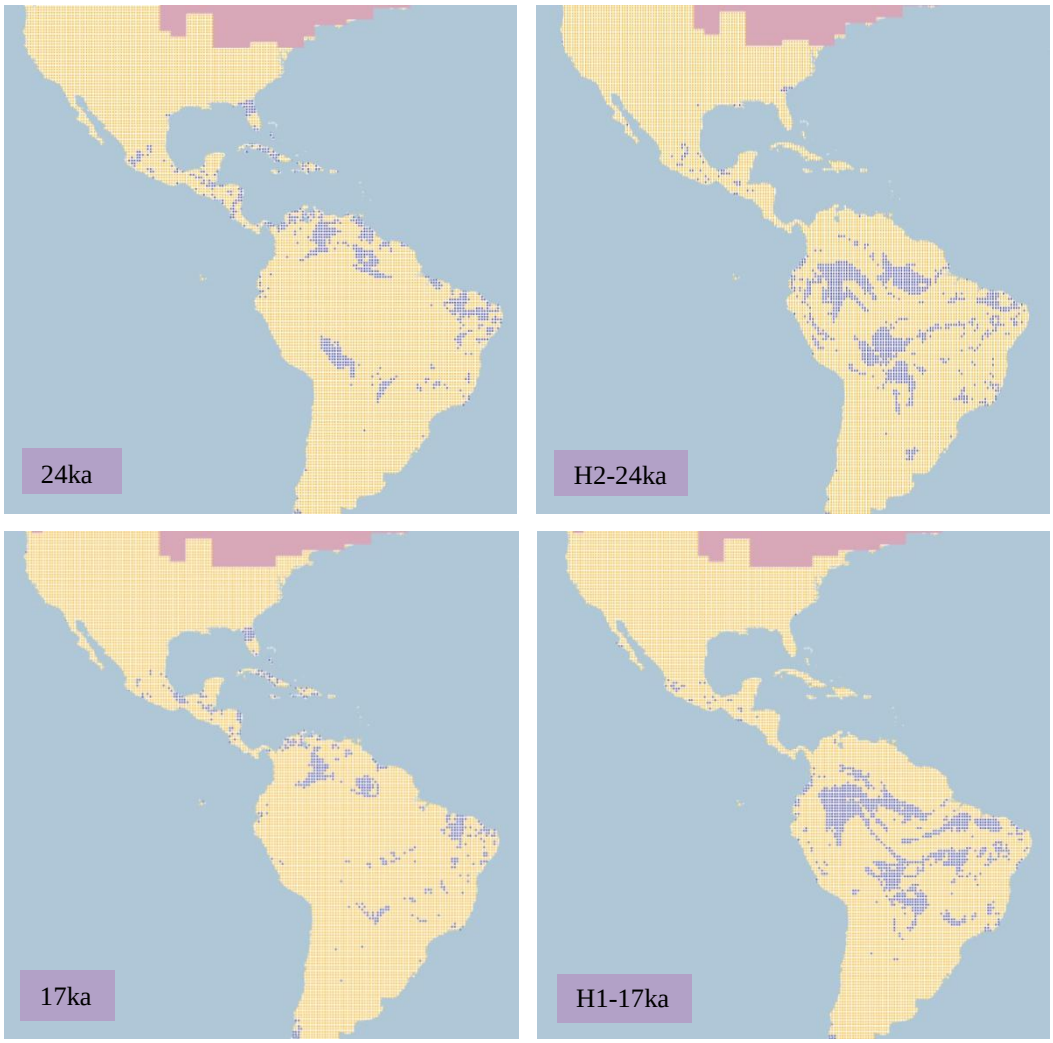

Figure 4.1.4.24.b. Simulation maps of American Whimbrel non-breeding range.
Maps are shown for ten-time slices: 24ka, H2 (24ka), 17ka, H1 (17ka), 13ka, H0 (13ka), 9ka, 5ka, 3ka and present (1961–90).

Figure 4.1.4.24.b. Simulation maps of American Whimbrel non-breeding range (continued**).**

*4.1.4.25 Red-necked Phalarope (*Phalaropus lobatus*). Conservation status: Least Concern. Current known range Figure 4.1.4.25.*

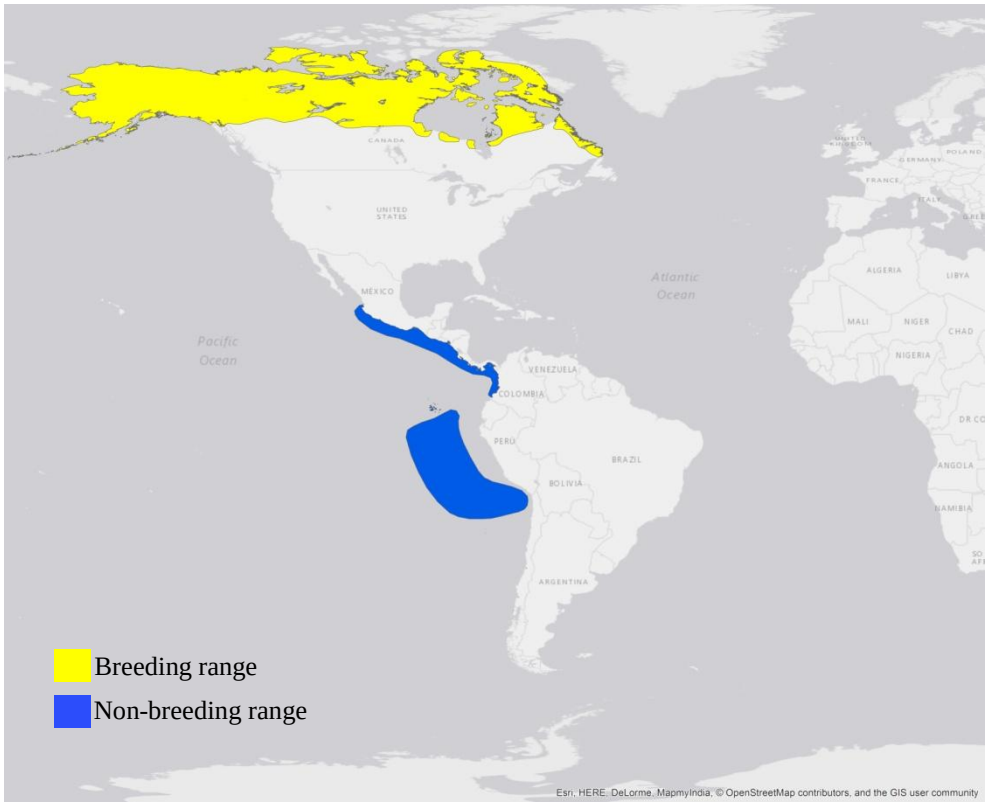

Figure 4.1.4.25. Current known American range of Red-necked Pharalope.

Breeding range (AUC: 0.948; TSS: 0.731; Kappa: 0.731): This species has a circumpolar breeding range. In the Americas it breeds in northern North America from Alaska in the USA to central-northern Canada, Newfoundland and Labrador and the islands of the southern Arctic Archipelago in Canada.

At 26 ka BP the range is projected across Alaska and in those areas of northern Canada not covered by the ice sheet. There is also a range projected in the northern part of the conterminous USA. This pattern continues until 16 ka BP when the range in the northern region of the conterminous USA shifts to the southern boundaries of Canada near the ice sheet. See Figure 4.1.4.25.a.

At 15 ka BP the range in the northern part of the conterminous USA decreases, and by 13 ka BP, with the deglaciation, the range extends from southern to central and north-western parts of Canada, with a small range projected in the south-eastern part of Quebec in Canada

and the north-eastern part of the USA. The range in the southern and central region of Canada decreases at 12 ka BP.

By the beginning of the Holocene the range is projected from western Alaska to northern Canada in the region not covered by the ice sheet. This pattern continues until 8 ka BP when the range increases near Hudson Bay and in the north-eastern part of Canada. From 6 ka BP until 1 ka BP the range continues with a similar pattern from north-western Alaska across northern Canada and in the Arctic Archipelago. This same pattern is observed in the current breeding range projection.

When comparing H2 with 24 ka BP, a similar range is projected in northern Canada, in Alaska and in the northern region of the conterminous USA, only differing in the range projected in the central-western region of the USA at H2. The range in the central-western part of the conterminous USA disappears at H1, and the range is similar range to that at 17ka. At H0, the range shifts to southern and central Canada as in the 13 ka BP projection.

Even though the species' breeding range is located in North America, a suitable range in southern Chile is projected for the species to occur.

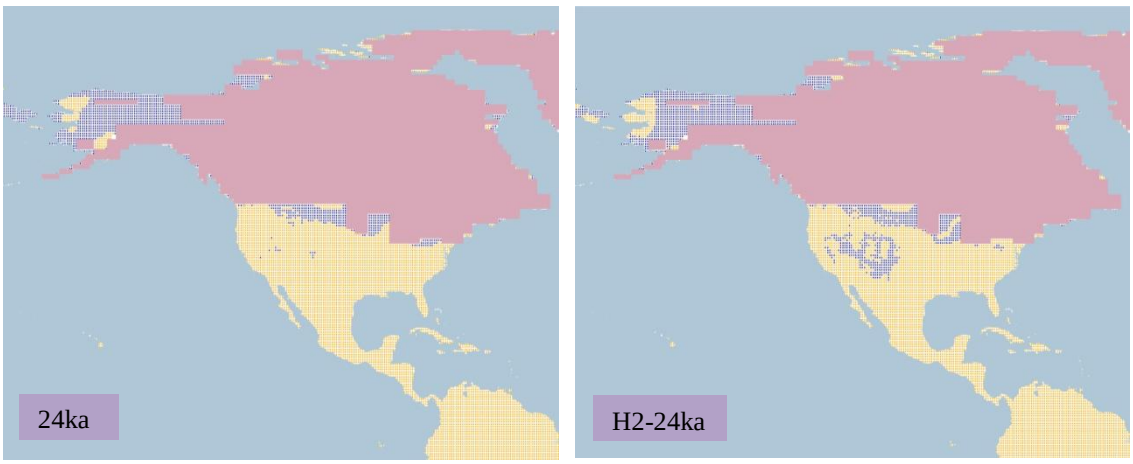

Figure 4.1.4.25.a. Simulation maps of Red-necked Phalarope breeding range.
Maps are shown for ten-time slices: 24ka, H2 (24ka), 17ka, H1 (17ka), 13ka, H0 (13ka), 9ka, 5ka, 3ka and present (1961–90).

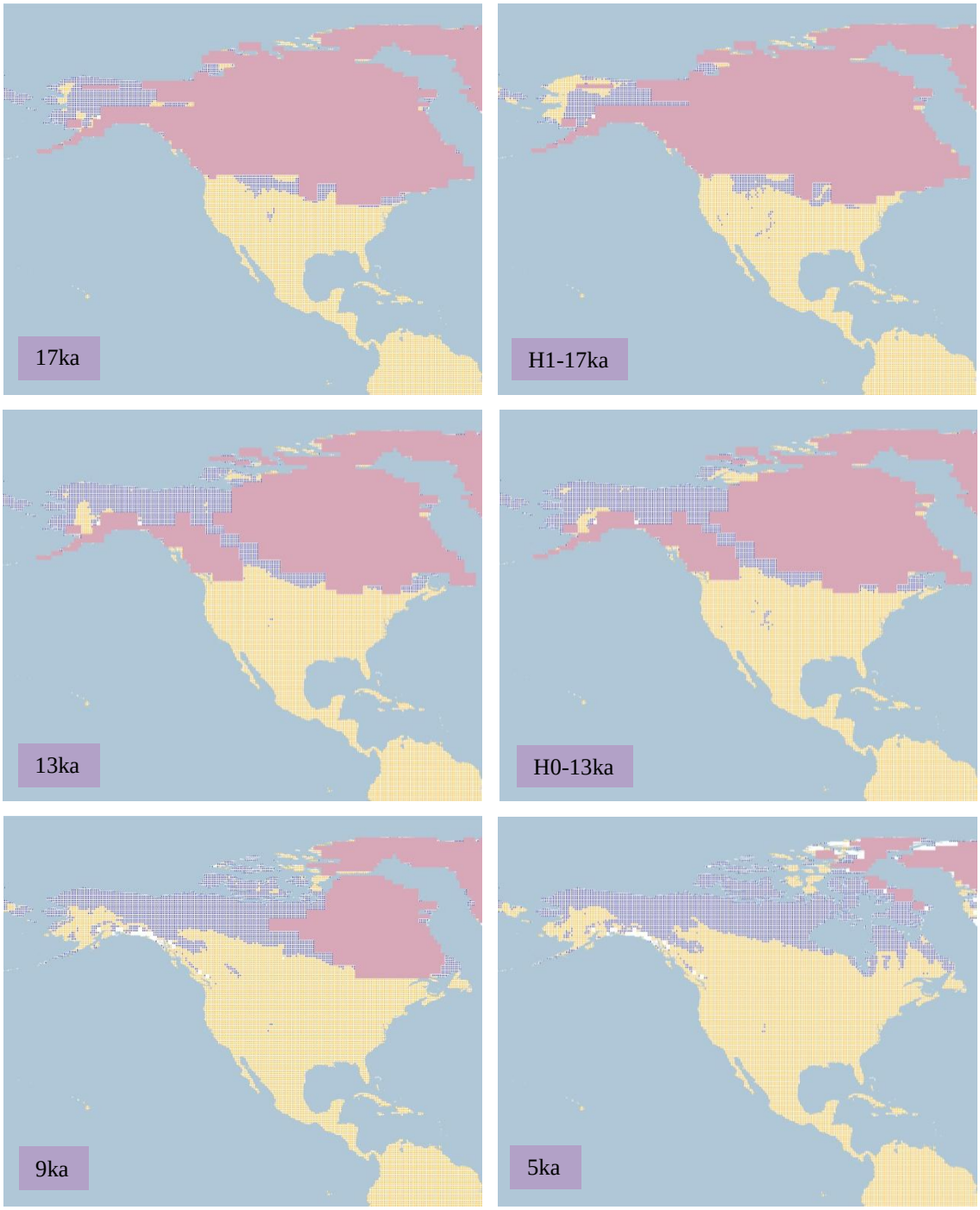

Figure 4.1.4.25.a. Simulation maps of Red-necked Phalarope breeding range (continued**).**

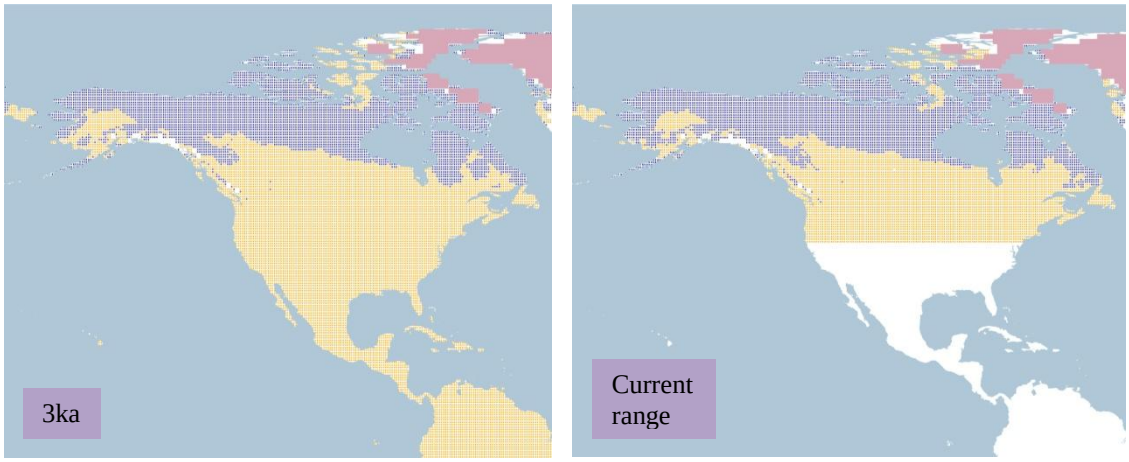

Figure 4.1.4.26.a. Simulation maps of Red-necked Phalarope breeding range (continued**).**

Non-breeding range (AUC: 0.952; TSS: 0.724; Kappa: 0.708): The population of this species that breeds in North America is believed to spend the non-breeding season in two areas of the eastern Pacific, along the coast of central-southern Mexico, Central America and the northern region of Colombia, and in a larger area west of Ecuador, Peru and Chile. Although an attempt was made to model the non-breeding range, the absence of meteorological data from the oceans limited modelling to those areas where the non-breeding range intersects the coast. As a result, the model cannot project the majority of the species' pelagic non-breeding range.

At 26 ka BP a small range is projected in the Greater Antilles, between eastern Venezuela and western Guyana, with a scattered range from central to north-eastern Brazil and a small range along the Pacific coast from central-southern Mexico as far as Central America. A similar pattern continues until 16 ka BP when the range in the north-eastern part of Brazil increases. See Figure 4.1.4.25.b.

By the beginning of the Holocene the range is projected along the central-southern coast of Mexico as far as Costa Rica in Central America, with a small range in Venezuela and a large range in the north-eastern region of Brazil. This range in Brazil increases at 9 ka BP and decreases at 8 ka BP. From 7 ka BP until 4 ka BP the range in Brazil increases, decreasing at 3 ka BP and shifting to the central-northern region at 1 ka BP. The remainder of the range continues along the central-southern coast of Mexico as far as Central America, which agrees with the current non-breeding range projection as well.

In the H2 projection a large range is projected in central-northern Brazil, differing from 24 ka BP. This range decreases at H1, increasing again at H0, with no similar pattern shared with the 17 ka BP and 13 ka BP projections.

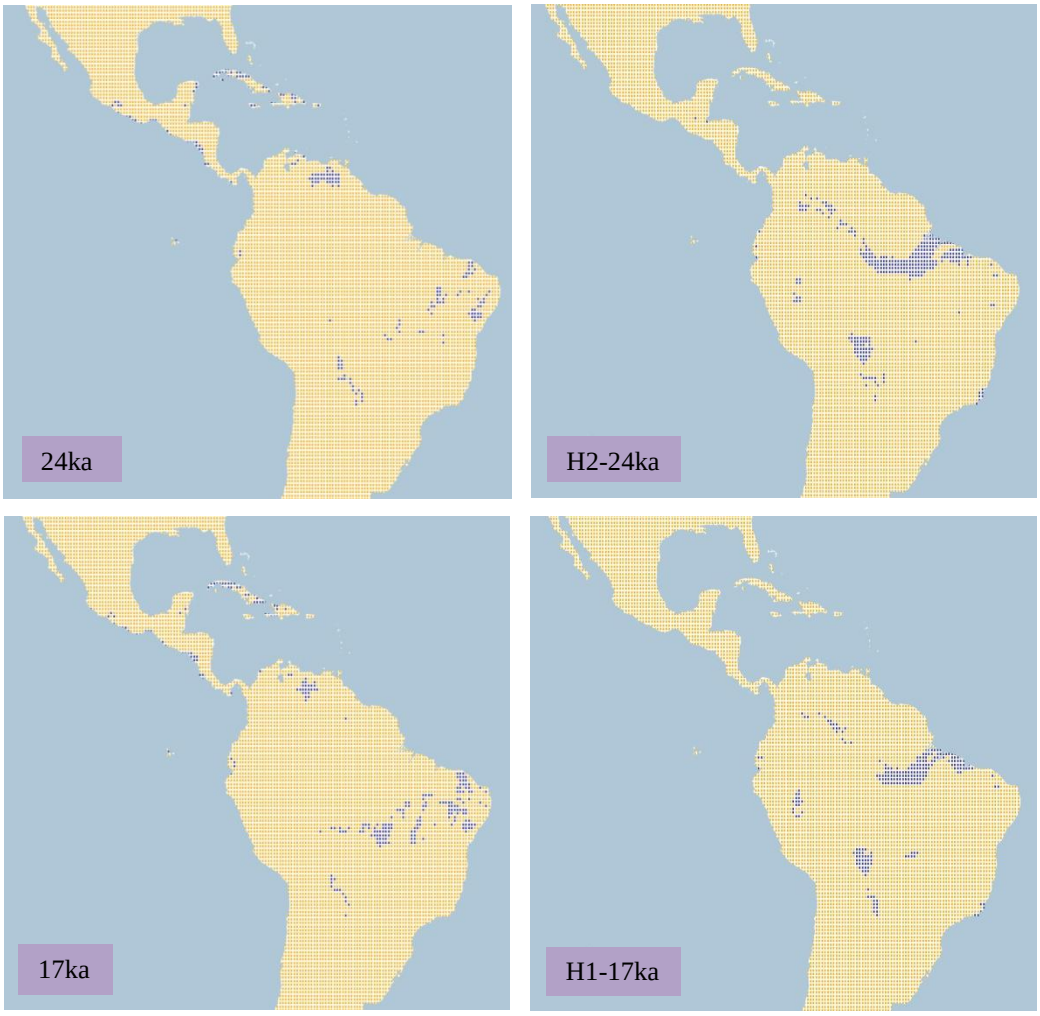

Figure 4.1.4.25.b. Simulation maps of Red-necked Phalarope non-breeding range. Maps are shown for ten-time slices: 24ka, H2 (24ka), 17ka, H1 (17ka), 13ka, H0 (13ka), 9ka, 5ka, 3ka and present (1961–90).

Figure 4.1.4.25.b. Simulation maps of Red-necked Phalarope non-breeding range (continued**).**

*4.1.4.26 American Woodcock (*Scolopax minor*). Conservation status: Least Concern. Current known range Figure 4.1.4.26.*

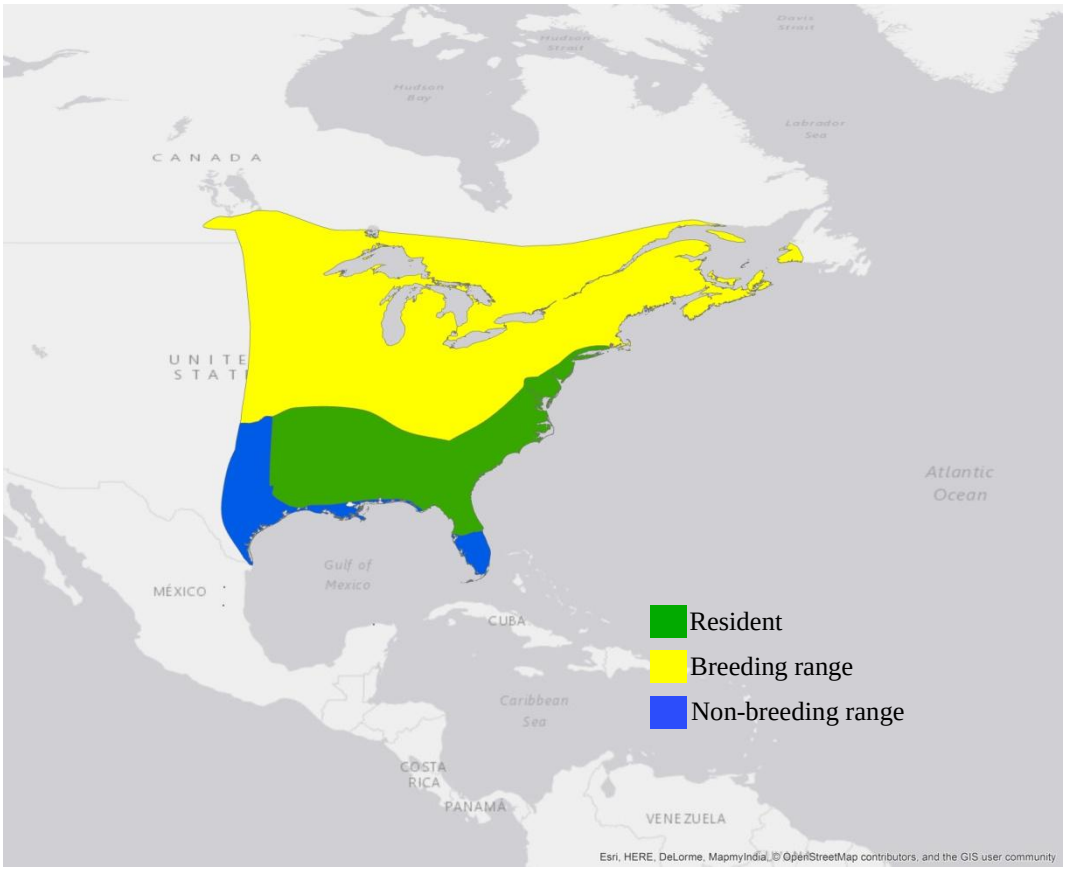

Figure 4.1.4.26. Current known range of American Woodcock.

Breeding range (AUC: 0.995; TSS: 0.943; Kappa: 0.933): This species has a breeding range extending from the central to north-eastern regions of the USA and as far as south-eastern Canada. It also has a year-round resident range in the central-eastern and southern regions of the USA.

The projected range at 26 ka BP extends across the central-eastern USA. This range remains unchanged until 15 ka BP when it shifts northward and increases in the USA. After this at 14 ka BP a small range is projected in the north-western part of Washington, and decrease is projected in the northern USA. See Figure 4.1.4.26.a.

By the beginning of the Holocene the range is mainly projected in central to north-eastern parts of the USA with a small range in north-western Washington and in central British Columbia and Alberta in Canada. This pattern continues with minimal variation until 8 ka

BP, when the range in the north-eastern region of the USA increases to the southern boundary of Canada. During this time frame there is also an increase in the range between British Columbia and Alberta in Canada.

At 5 ka BP, there is a reduction in the range projected in Newfoundland and Labrador in Canada and in the north-western part of Washington in the USA. The remainder of the range is unchanged and is maintained until the 1 ka BP projection. This similar pattern continues in the current breeding range projection.

A similar range is projected for H2 and 24 ka BP in the central to eastern region of the USA, although there is a small range projected in the southern part of the USA at H2. The range increases in the central and western region of the USA at H1, differing from 17 ka BP. This increase continues at H0, covering most of the territory in the conterminous USA, with a small range in northern Mexico and thus a different projection from that for 13 ka BP.

Even though the species' current breeding range is located in North America, there are suitable conditions projected for the species to occur in South America, from southern Chile, to the northern region of Argentina and southern Brazil.

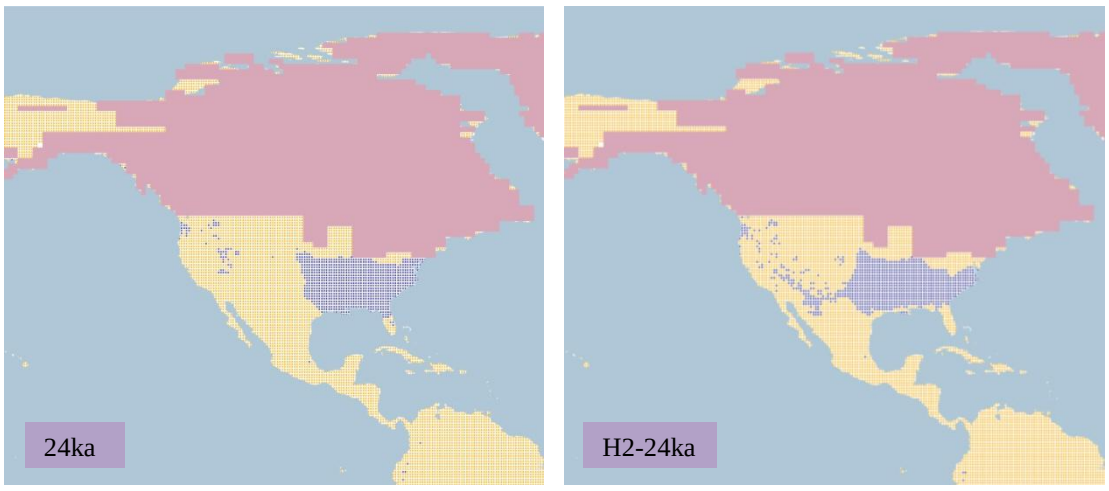

Figure 4.1.4.26.a. Simulation maps of American Woodcock breeding range.
Maps are shown for ten-time slices: 24ka, H2 (24ka), 17ka, H1 (17ka), 13ka, H0 (13ka), 9ka, 5ka, 3ka and present (1961–90).

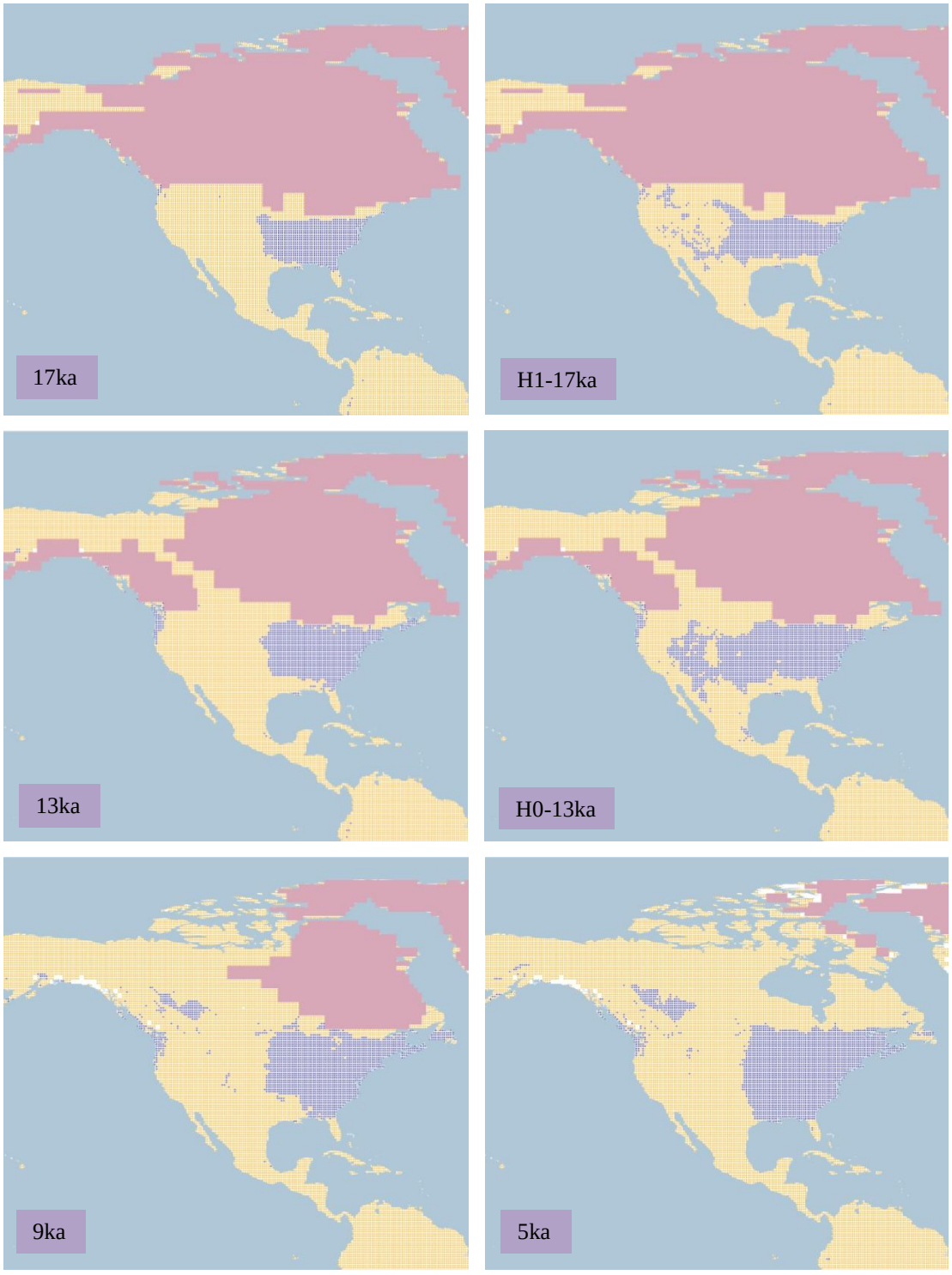

Figure 4.1.4.26.a. Simulation maps of American Woodcock breeding range (continued**).**

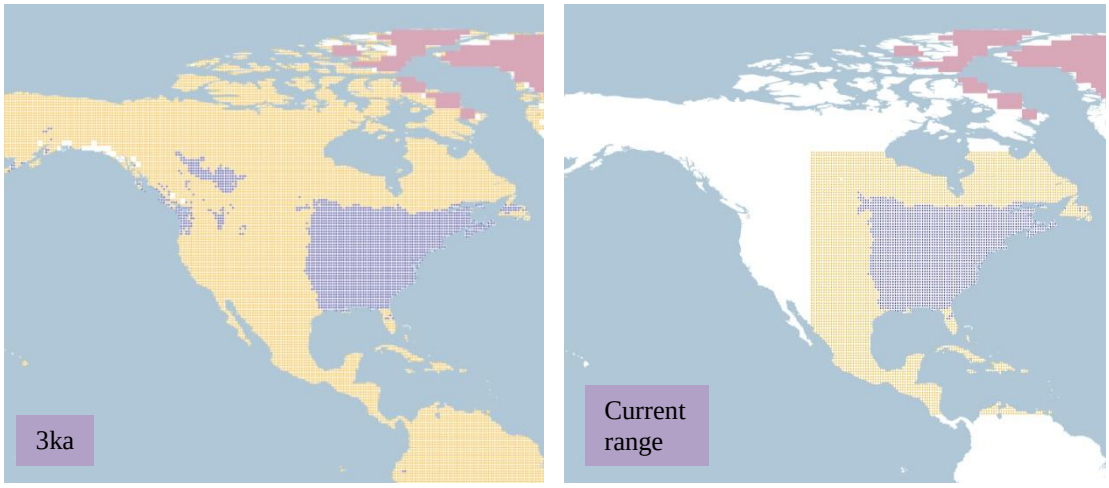

Figure 4.1.4.26.a. Simulation maps of American Woodcock breeding range (continued**).**

Non-breeding range (AUC: 0.995; TSS: 0.938; Kappa: 0.891): This species spends the winter in Texas and on the south-eastern coast of the USA, as well as in its resident range that extends from the central-south to north-eastern USA.

At 26 ka BP the range is projected in the south-eastern region of the USA, from Texas to South Carolina. Small variation is observed in the range, and at 15 ka BP the range increases, remaining unchanged until 12 ka BP. See Figure 4.1.4.26.b.

B the beginning of the Holocene the range extends from Texas and Oklahoma as far as Virginia in the eastern USA. After this there is a small variation in the range, remaining until 1 ka BP, and reaching the north-eastern region of Mexico. This same pattern continues in the current non-breeding range projection.

A similar range is projected between H2 and 24 ka BP, except in the area of Florida in the USA at H2. The range decreases at H1 in the south-eastern region of the USA, differing from 17 ka BP. At H0, the range increases in Texas in the USA and in the north-eastern and north-western region of Mexico, differing from 13 ka BP with a projected range only in the south-eastern region of the USA.

A small range in South America is projected with suitable conditions for the species to occur, even though the species' current non-breeding range is located in North America.

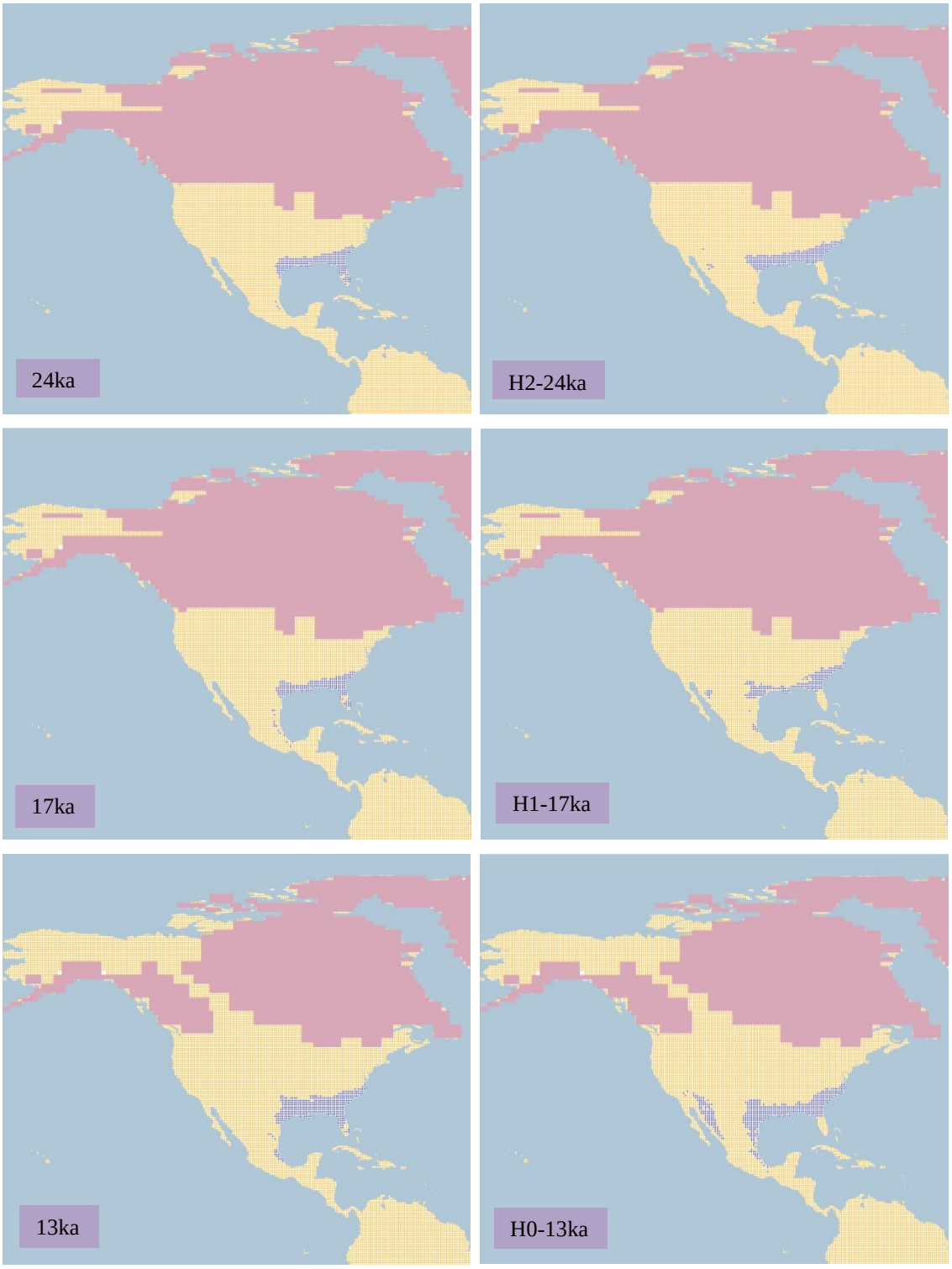

Figure 4.1.4.26.b. Simulation maps of American Woodcock non-breeding range. Maps are shown for ten-time slices: 24ka, H2 (24ka), 17ka, H1 (17ka), 13ka, H0 (13ka), 9ka, 5ka, 3ka and present (1961–90).

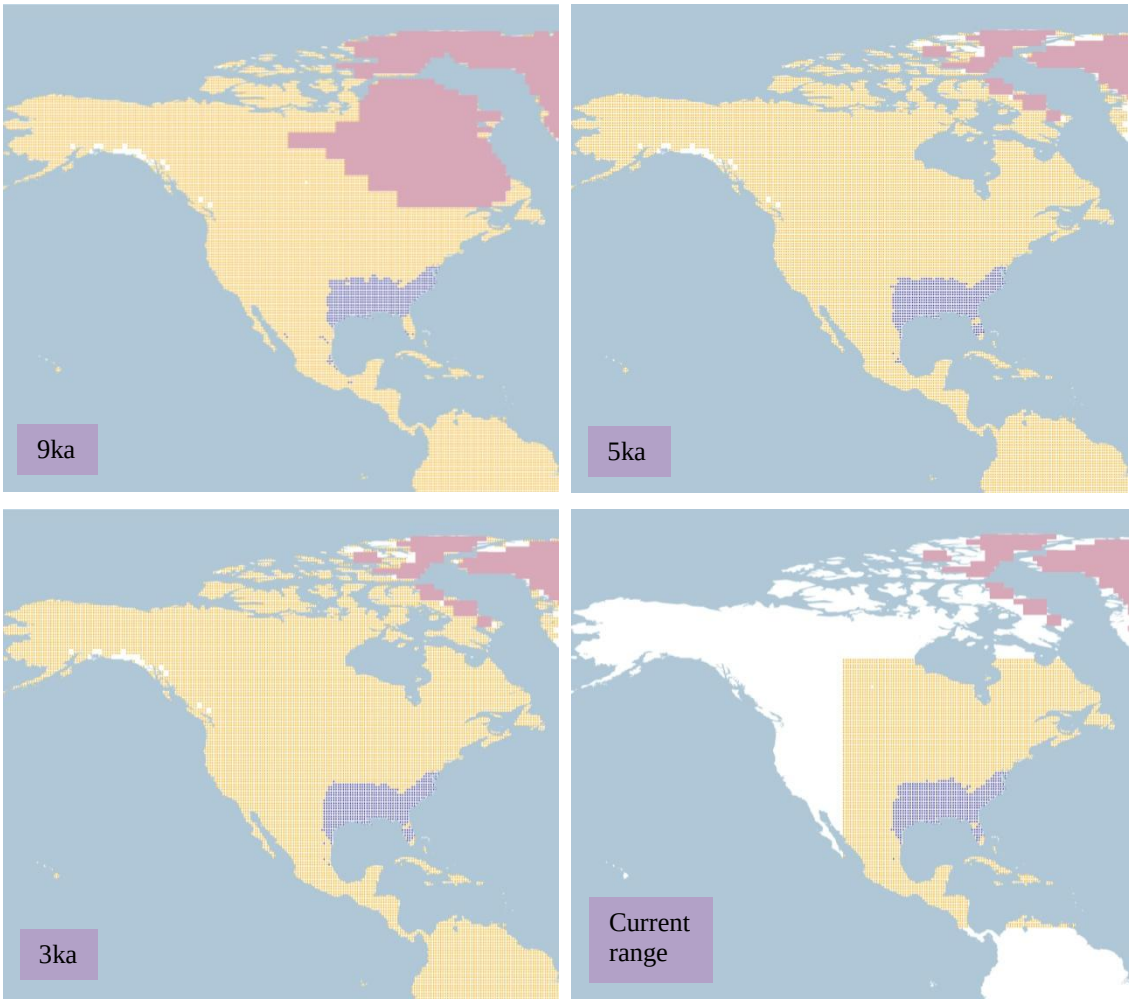

Figure 4.1.4.26.b. Simulation maps of American Woodcock non-breeding range (continued**).**

*4.1.4.27 Wilson's Phalarope (*Steganopus tricolor*). Conservation status: Least Concern. Current known range Figure 4.1.4.27.*

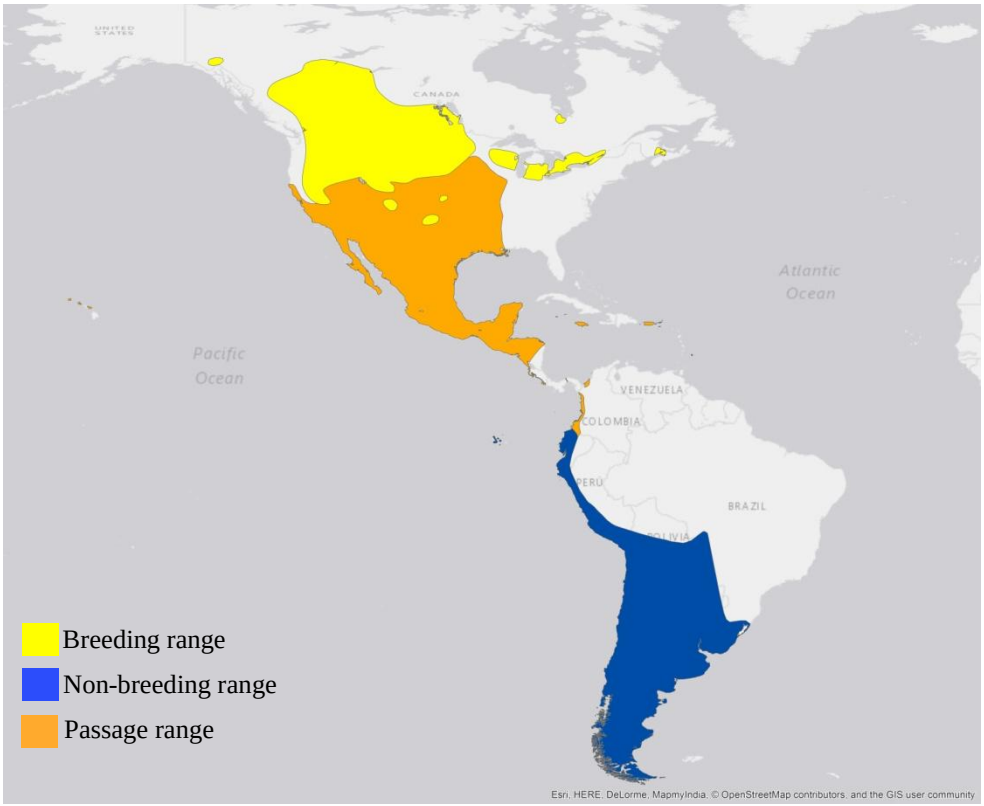

Figure 4.1.4.27. Current known range of Wilson's Pharalope.

Breeding range (AUC: 0.985; TSS: 0.876; Kappa: 0.779): This species spends the breeding season in western and central-northern parts of the USA, in central-southern to western Canada, and near the Great Lakes in the USA.

At 26 ka BP the range is projected to extend across the USA from the western to central regions but decreasing in the east. This pattern continues with minimal variation until 18 ka BP when the range in the western and central part of the USA increases. After this at 16 ka BP the range shifts to the southern part of Canada as the ice sheet retreats. See Figure 4.1.4.27.a.

With the deglaciation at 13 ka BP the range is projected in north-western, central-northern and north-eastern parts of the USA and reaching the central-southern boundaries of Canada. By the beginning of the Holocene the range shifts to the central part of Canada and decreases

in the north-eastern part of the USA. This pattern continues with an increase in the range at 9 ka BP in central Canada.

At 8 ka BP the projected range in south-eastern Canada disappears and the north-eastern range in the USA decreases. The range continues with minimal variation until 2 ka BP, and the current breeding range shares the same pattern as 1 ka BP.

The H2 projection presents a small and scattered range in the USA, differing from the 24 ka BP projection. This range increases at H1 in western and central-northern parts of the USA, although of a different extent than that for 17 ka BP. The H0 projected range increases in the USA, being similar to the 13 ka BP projection.

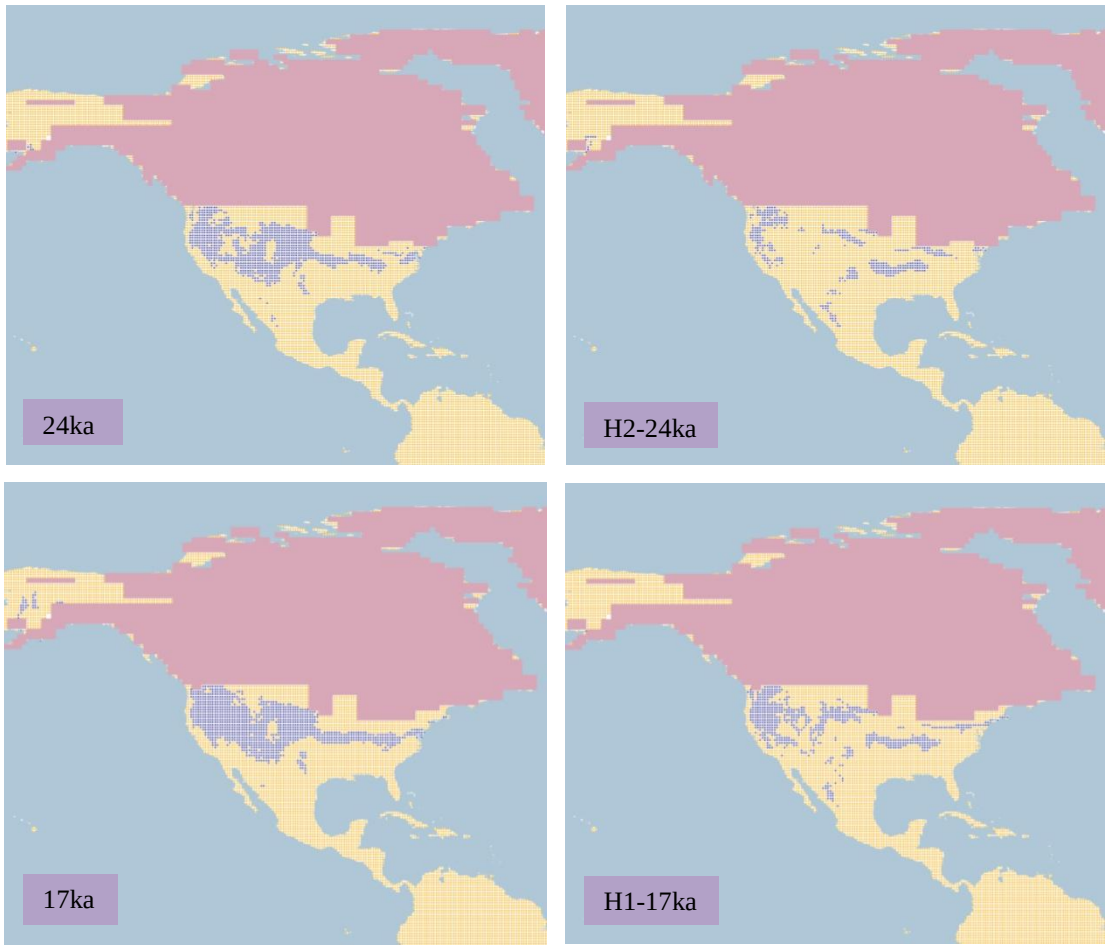

Figure 4.1.4.27.a. Simulation maps of Wilson's Phalarope breeding range.
Maps are shown for ten-time slices: 24ka, H2 (24ka), 17ka, H1 (17ka), 13ka, H0 (13ka), 9ka, 5ka, 3ka and present (1961–90).

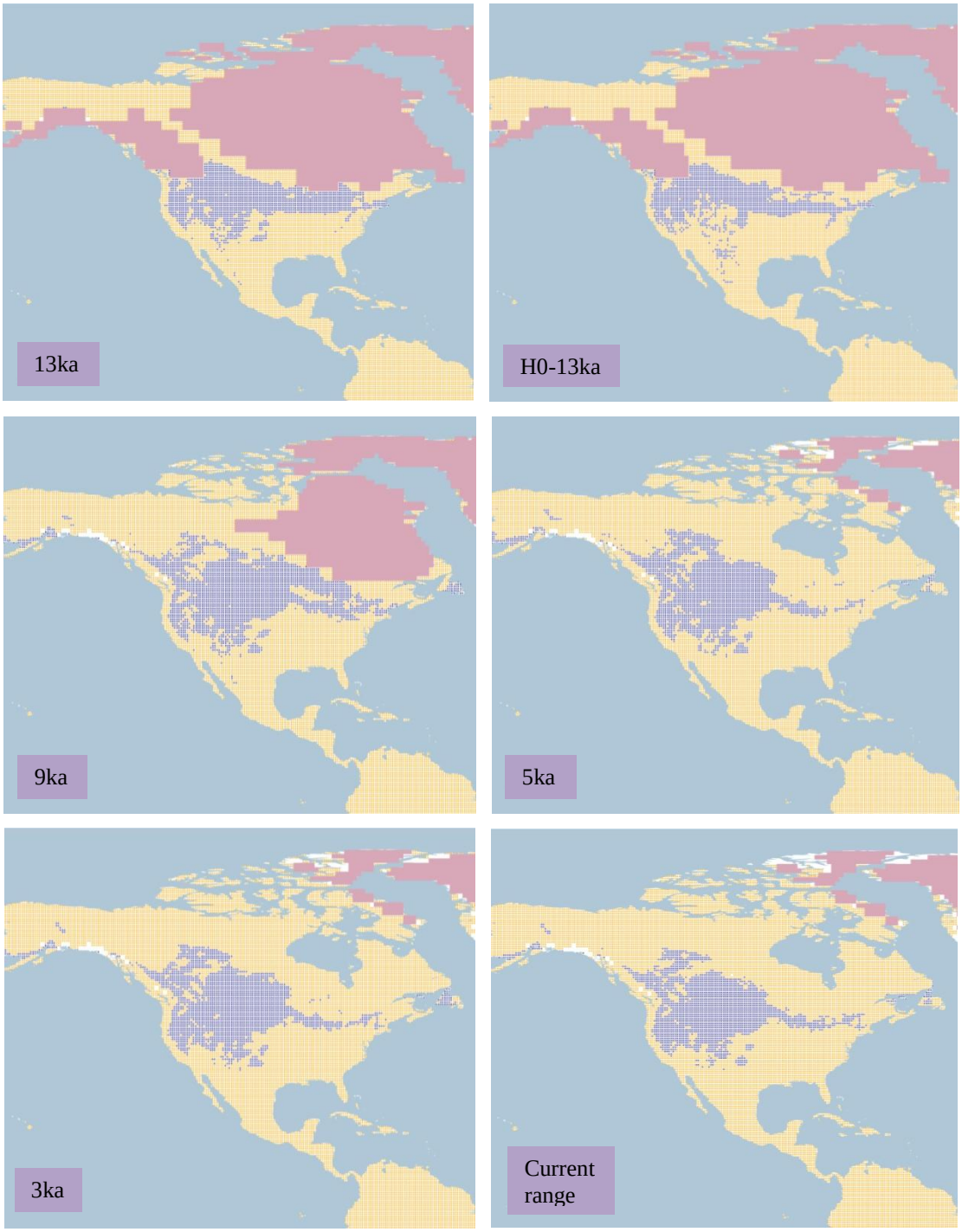

Figure 4.1.4.27.a. Simulation maps of Wilson's Phalarope breeding range (continued**).**

Non-breeding range (AUC: 0.993; TSS: 0.924; Kappa: 0.881): This species' non-breeding range is in South America, extending from the coasts of Ecuador and Peru to an inland range from southern Bolivia and southern Brazil as far as southern Argentina and Chile.

The range projected at 26 ka BP extends from the coasts of Ecuador and Peru to southern Chile and Argentina. This pattern continues with minimal differences in southern Argentina until 16 ka BP when the range is increased in southern Chile and southern Argentina. After this, the range remains unchanged until 9 ka BP when the range in Paraguay and central-southern Brazil increases. See Figure 4.1.4.27.b.

From 8 ka BP until 1 ka BP the projected range persists with the same pattern with minimal difference in southern Brazil. This pattern, is also shared in the current non-breeding range projection.

At H2 the range is similar as at 24 ka BP from Peru to southern Chile and southern Argentina, although there is a projected range in northern South America, Central America, Mexico, the southern USA and the Greater Antilles which is not projected at 24ka. The range in Mexico decreases at H1, with the remainder of the range unchanged, differing from 17ka. This pattern continues at H0, sharing a similar range with 13 ka BP only from Peru to southern Argentina and southern Chile in South America.

Even though the current non-breeding range of the species is located in South America, there are suitable conditions projected in Mexico for the species to occur.

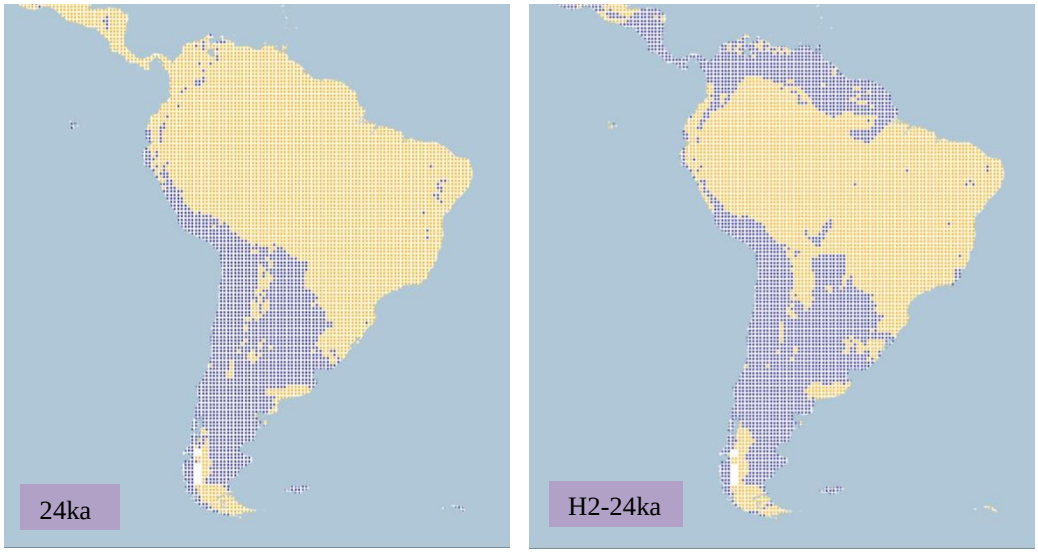

Figure 4.1.4.27.b. Simulation maps of Wilson's Phalarope non-breeding range. Maps are shown for ten-time slices: 24ka, H2 (24ka), 17ka, H1 (17ka), 13ka, H0 (13ka), 9ka, 5ka, 3ka and present (1961–90).

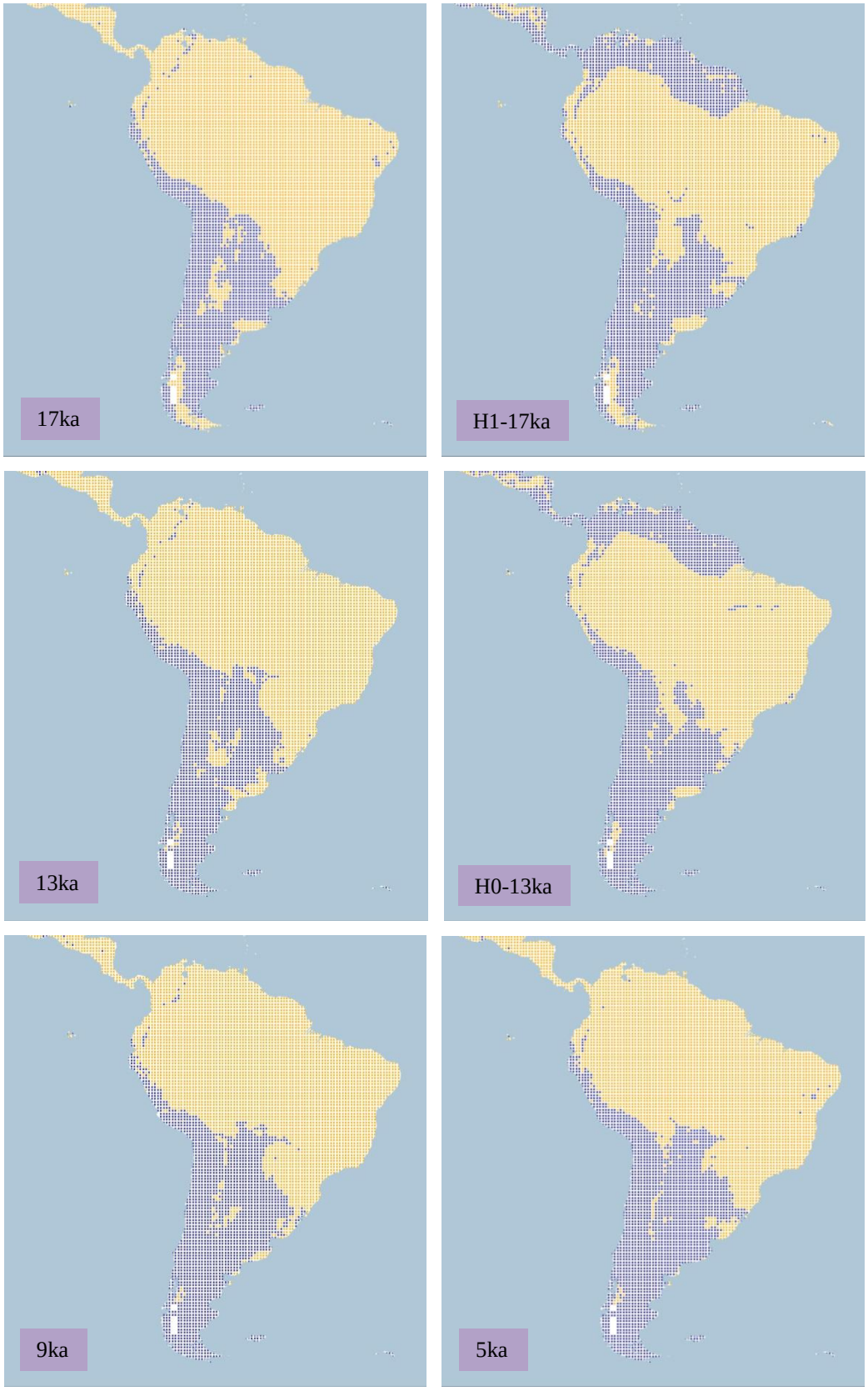

Figure 4.1.4.27.b. Simulation maps of Wilson's Phalarope non-breeding range (continued**).**

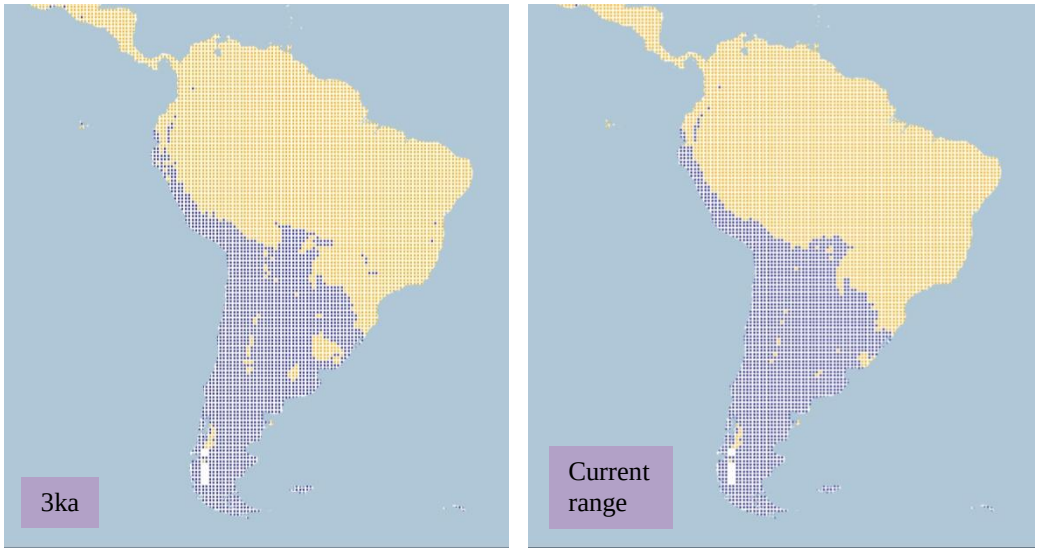

Figure 4.1.4.28.b. Simulation maps of Wilson's Phalarope non-breeding range (continued**).**

*4.1.4.28 Lesser Yellowlegs (*Tringa flavipes*). Conservation status: Least Concern. Current known range Figure 4.1.4.28.*

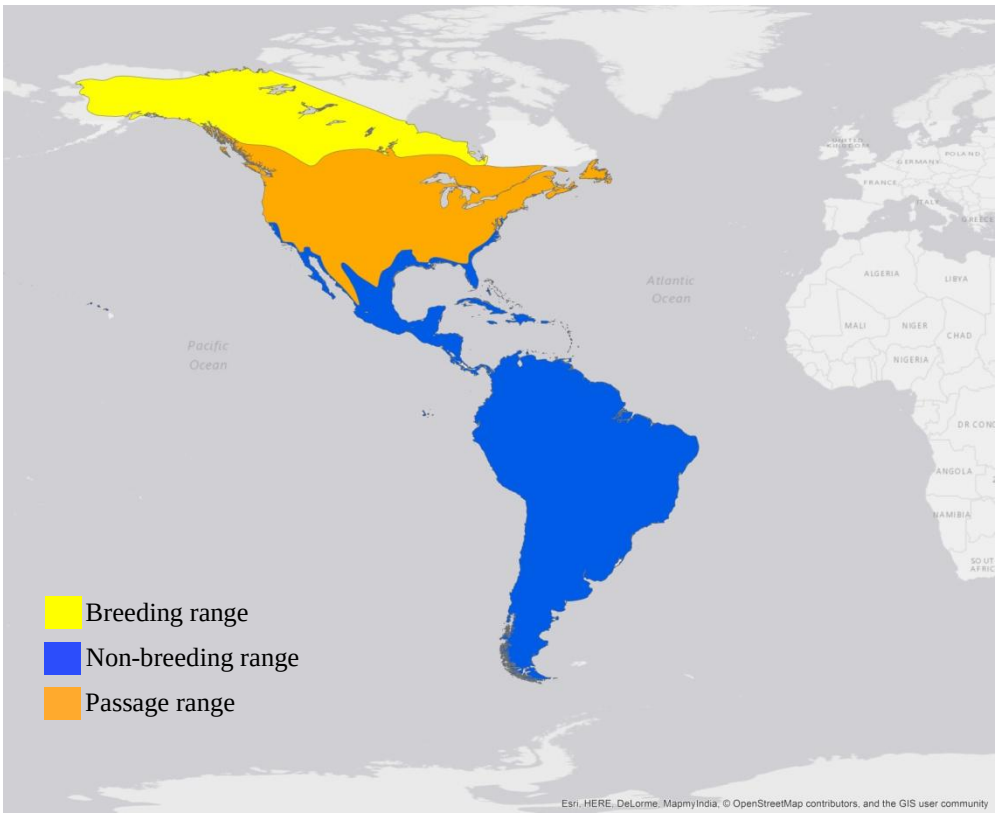

Figure 4.1.4.28. Current known range of Lesser Yellowlegs.

Breeding range (AUC: 0.985; TSS: 0.878; Kappa: 0.799): This species breeding range extends from Alaska across northern Canada, from Yukon as far as north-western Quebec near James Bay.

The projected range at 26 ka BP is located in Alaska and in the northern conterminous USA. This range persists until decreases at 16 ka BP in the northern part of the conterminous USA, with the range shifting near the ice sheet in Canada. After this at 14 ka BP the projected range extends from Alaska to northern Canada and between the boundaries of southern Canada and the northern USA, near the ice sheet. See Figure 4.1.4.28.a.

With the deglaciation at 13 ka BP the range in Canada increases in the central region and by 12 ka BP the projected range extends from western Alaska as far as south-eastern Canada and the north-eastern conterminous USA.

By the beginning of the Holocene at 10 ka BP the range in central-southern Canada decreases. However, from 8 ka BP onwards the range is projected across Alaska and central northern Canada except in Nunavut and northern Quebec. This range continues with minimal differences until 1 ka BP. The current breeding range projection presents a similar range to that at 1 ka BP.

When comparing H2 with the 24 ka BP there is a similar range projected in the north of the conterminous USA and in Alaska. The range in Alaska decreases at H1, and the range in the northern conterminous USA increases, differing from 17ka. The H0 and 13 ka BP projections present a similar projected range from Alaska to south-eastern Canada.

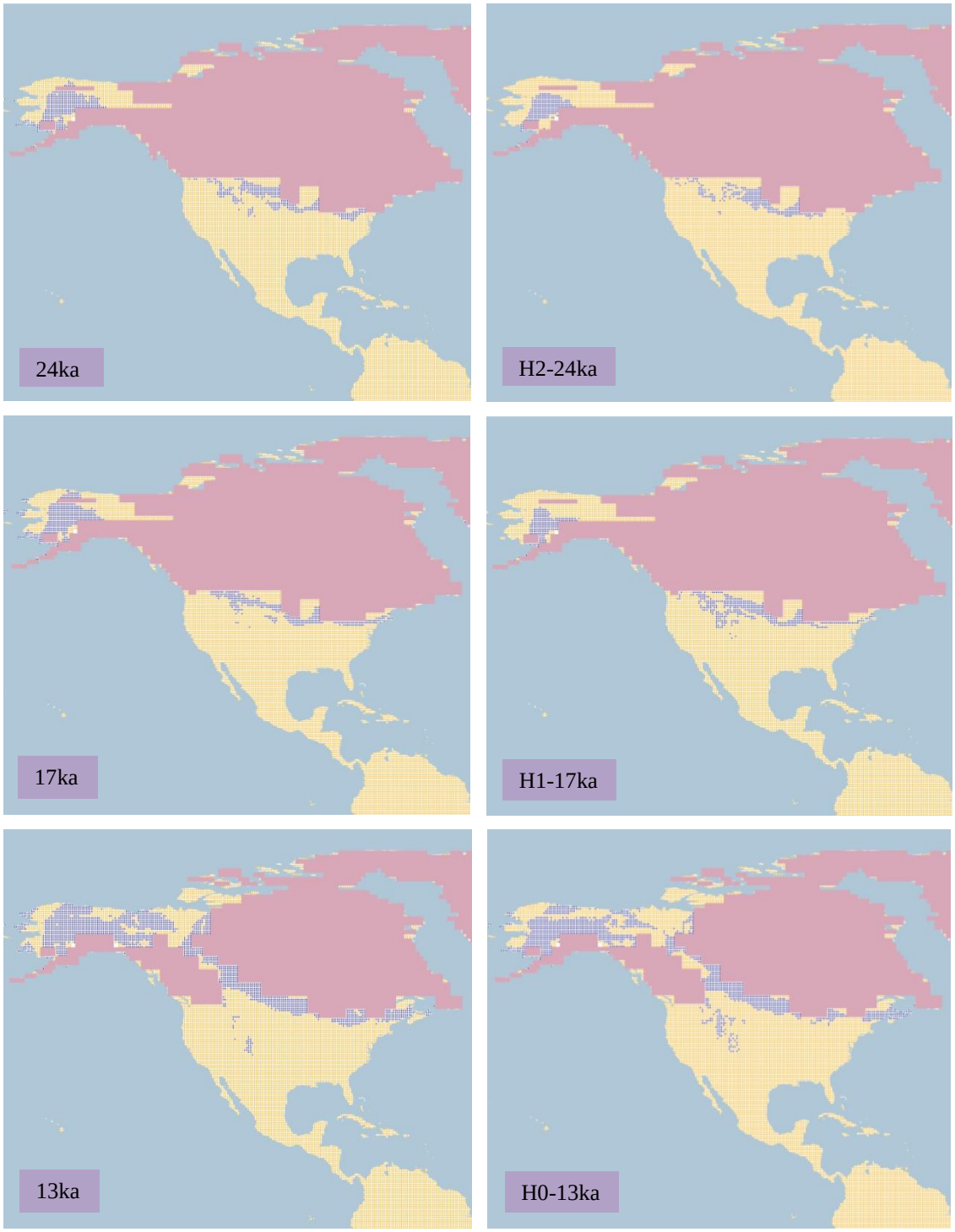

Figure 4.1.4.28.a. Simulation maps of Lesser Yellowlegs breeding range.
Maps are shown for ten-time slices: 24ka, H2 (24ka), 17ka, H1 (17ka), 13ka, H0 (13ka), 9ka, 5ka, 3ka and present (1961–90).

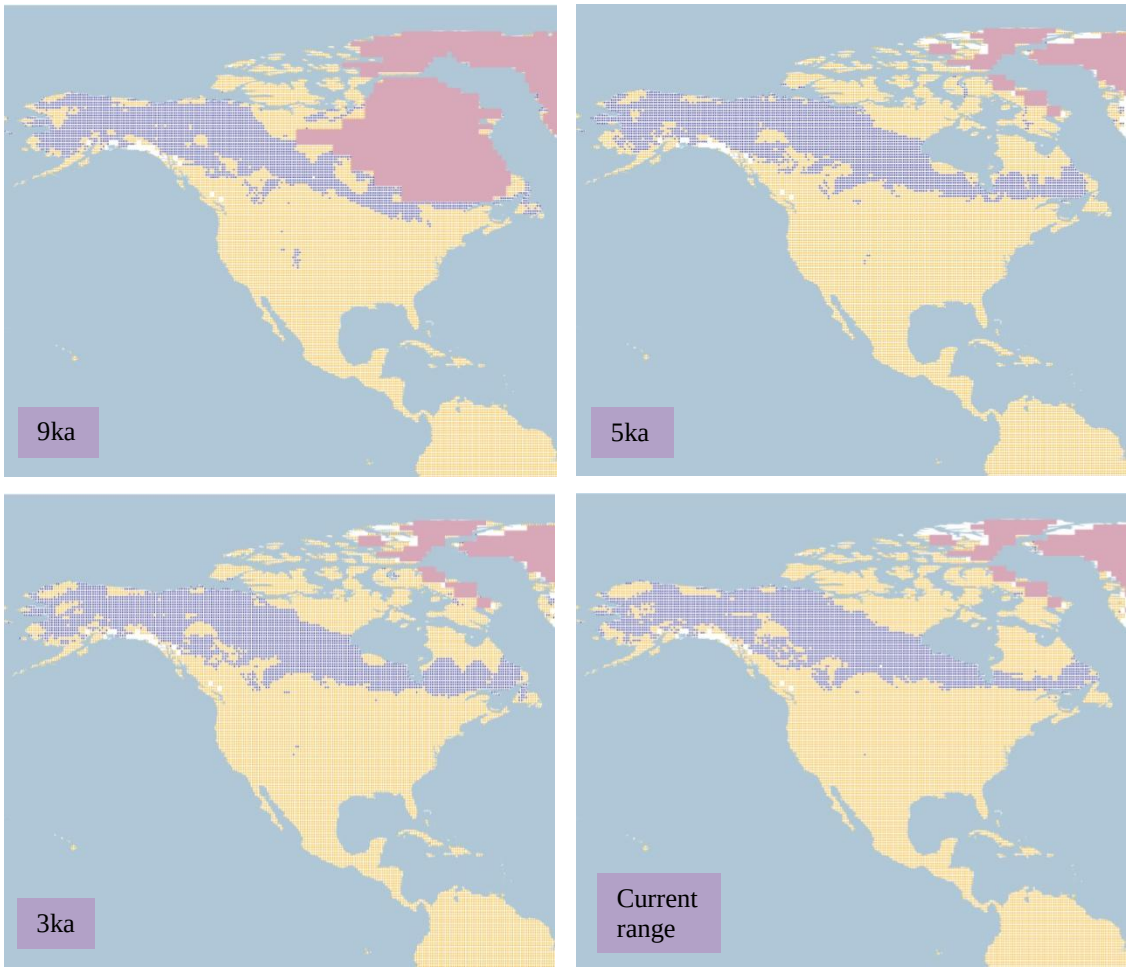

Figure 4.1.4.28.a. Simulation maps of Lesser Yellowlegs breeding range (continued**).**

Non-breeding range (AUC: 0.995; TSS: 0.947; Kappa: 0.941): This species spends the non-breeding season in South America, Central America, the Greater Antilles, Mexico except for the north-western region and on the western and eastern coasts of the USA.

At 26 ka BP the range is projected from the west coast and Florida in the USA, as far as southern South America, covering the Greater Antilles, Central America and Mexico. This projected range continues until 21ka when the range in northern Mexico decreases. After this a similar pattern continues until 12 ka BP when the range in north-eastern Mexico shifts to the south-eastern USA. See Figure 4.1.4.28.b.

By the beginning of the Holocene the range in the south-eastern part of the USA increases, with the remainder of the range unchanged. After this at 10 ka BP there is a small projected range near the ice sheet in central-southern Canada, and the range in Texas in the USA decreases. The range in Canada disappears at 9 ka BP.

At 6 ka BP the range in north-western Mexico increases, with the south-eastern range in the USA decreasing. This pattern continues until 1 ka BP and in the current non-breeding range projection.

The H2 projection presents small differences from 24 ka BP in the south-western USA and north-western Mexico. At H1 the range decreases in north-western Mexico and increases in Texas, which is not projected at 17ka. The differences in northern Mexico and the southern USA continue between H0 and 13 ka BP.

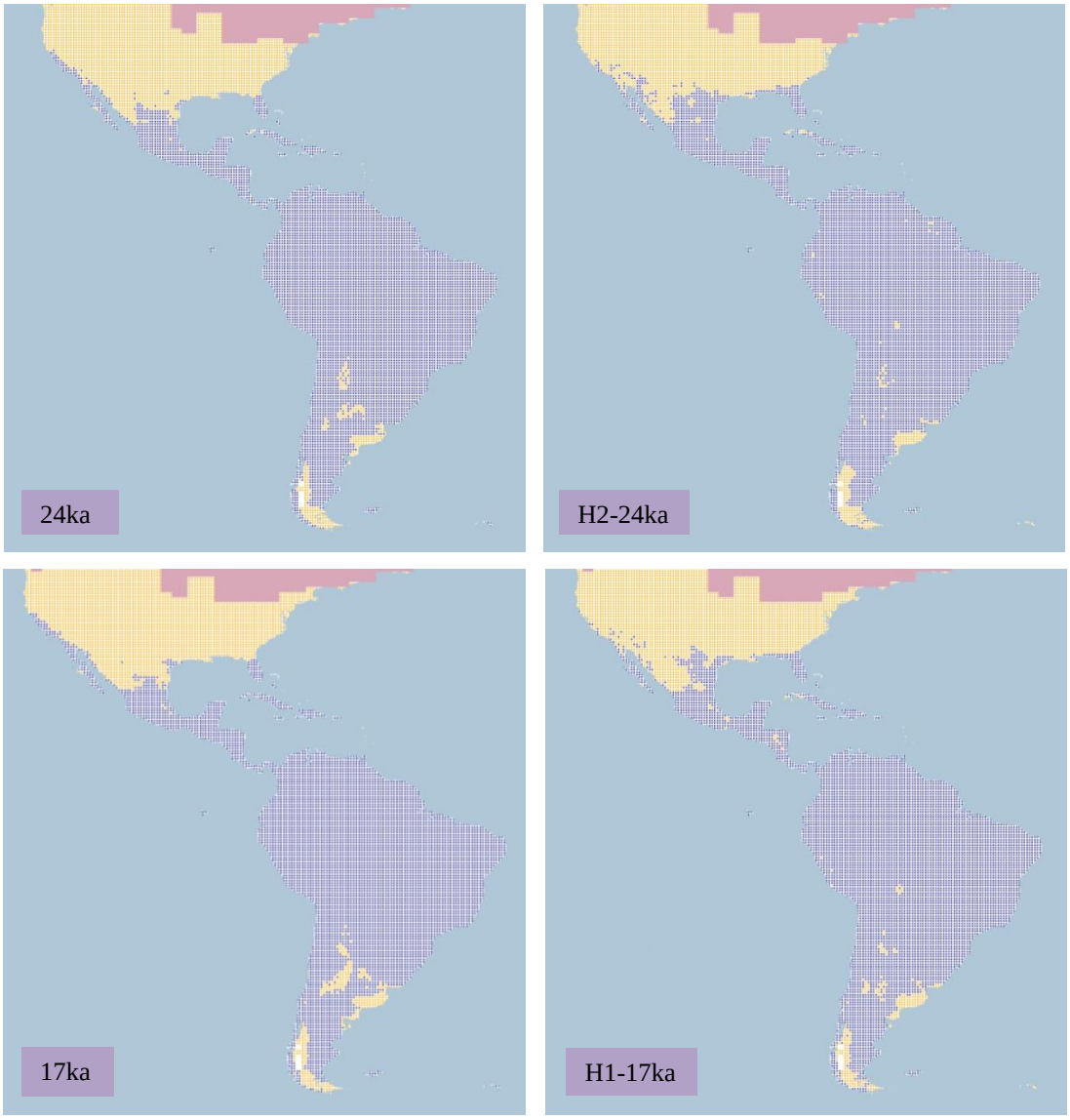

Figure 4.1.4.28.b. Simulation maps of Lesser Yellowlegs non-breeding range.
Maps are shown for ten-time slices: 24ka, H2 (24ka), 17ka, H1 (17ka), 13ka, H0 (13ka), 9ka, 5ka, 3ka and present (1961–90).

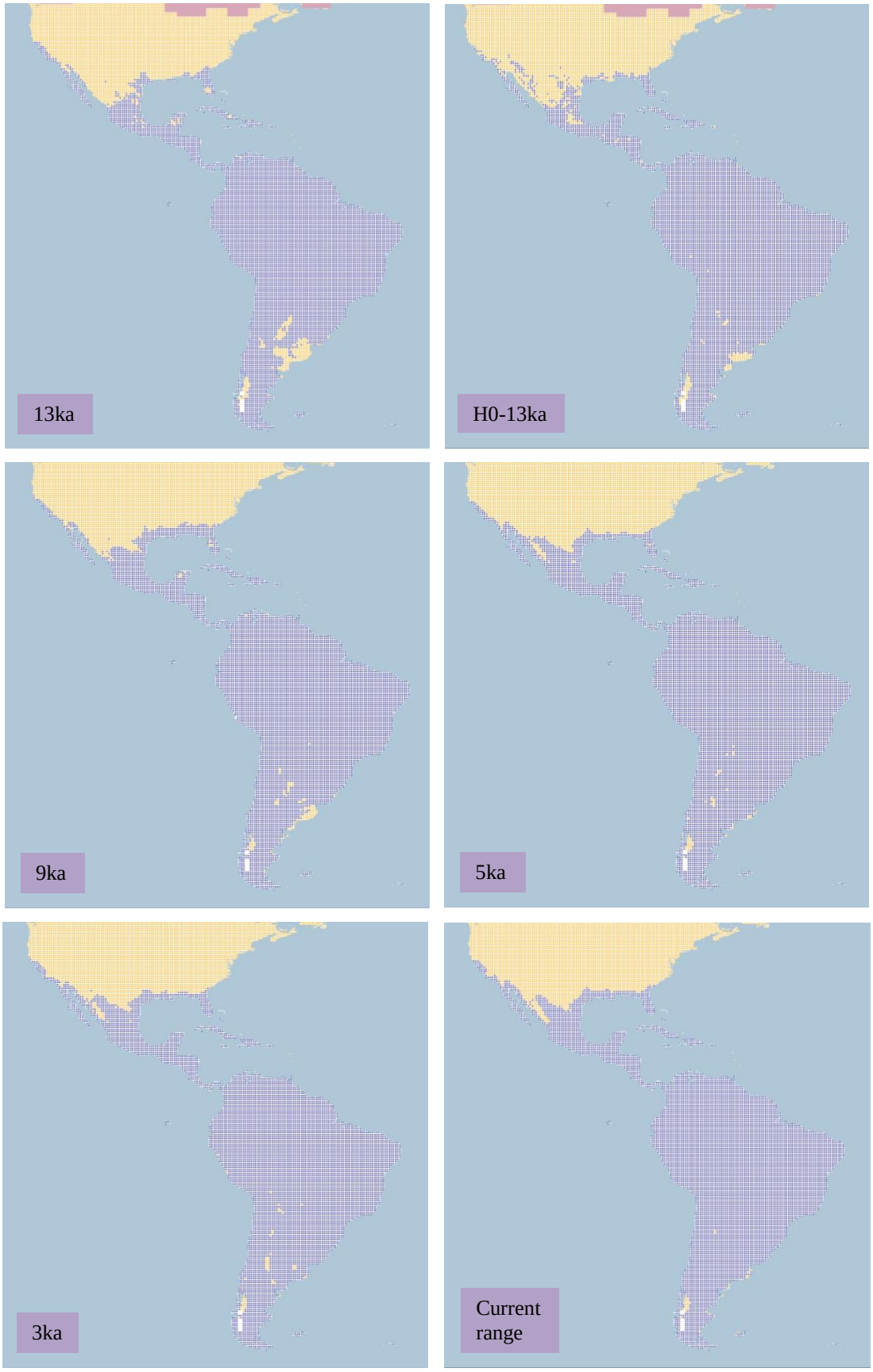

Figure 4.1.4.28.b. Simulation maps of Lesser Yellowlegs non-breeding range (continued**).**

*4.1.4.29 Wandering Tattler (*Tringa incana*). Conservation status: Least Concern. Current known range Figure 4.1.4.29.*

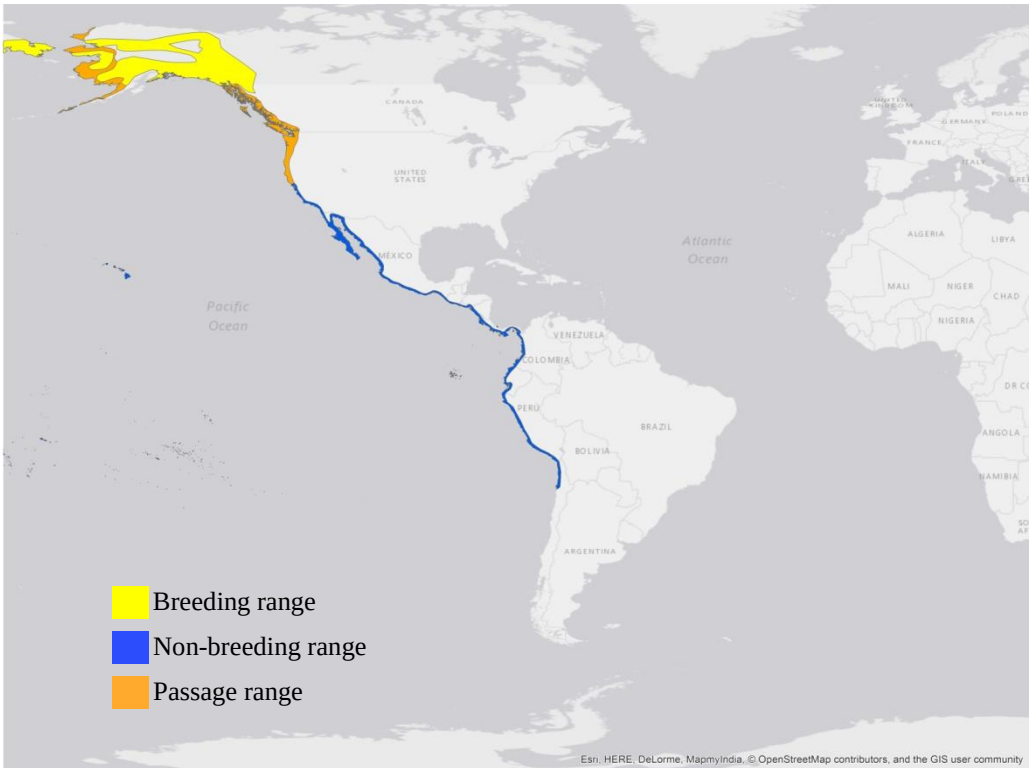

Figure 4.1.4.29. Current known range of Wandering Tattler.

Breeding range (AUC: 0.979; TSS: 0.892; Kappa: 0.469): This species' breeding range extends across central and southern Alaska in the USA, and as far as north-western Yukon in Canada, with a small range on the Chukotskiy Peninsula in north-easternmost Siberia.

At 26 ka BP the range is projected in central Alaska and in the northern conterminous USA, with a small range in north-western Yukon. This pattern continues until 19 ka BP when the range in Alaska and in the northern conterminous USA decreases. After this, the range in Alaska and the northern conterminous USA continues decreasing, especially at 15 ka BP, and disappears at 14 ka BP, the range in Alaska shifting to the north-western part of Canada. See Figure 4.1.4.29.a.

With the deglaciation at 13 ka BP the range in north-western Yukon decreases and instead shifts to the Northwest Territories near the ice sheet. This range in western Canada increases at 12 ka BP.

At 10 ka BP the range in western Canada shifts to the north-western Yukon and as far as northern Alaska in the USA. This range continues at 9ka, with a range projected in central-southern Canada, which decreases at 8 ka BP shifting to the northern part of Ontario near Hudson Bay. After this at 7 ka BP the range in Ontario disappears. From 7 ka BP until 1 ka BP the range is projected in the north-western region of Canada and in northern Alaska in the USA, with the pattern continuing in the current breeding range projection.

When comparing H2 with 24 ka BP, a similar range is projected in Alaska and in the northern conterminous USA. This pattern decreases at H1 with a similar range projected at 17 ka BP, although of a different extent. The H0 projection presents a similar range to the 13 ka BP projection.

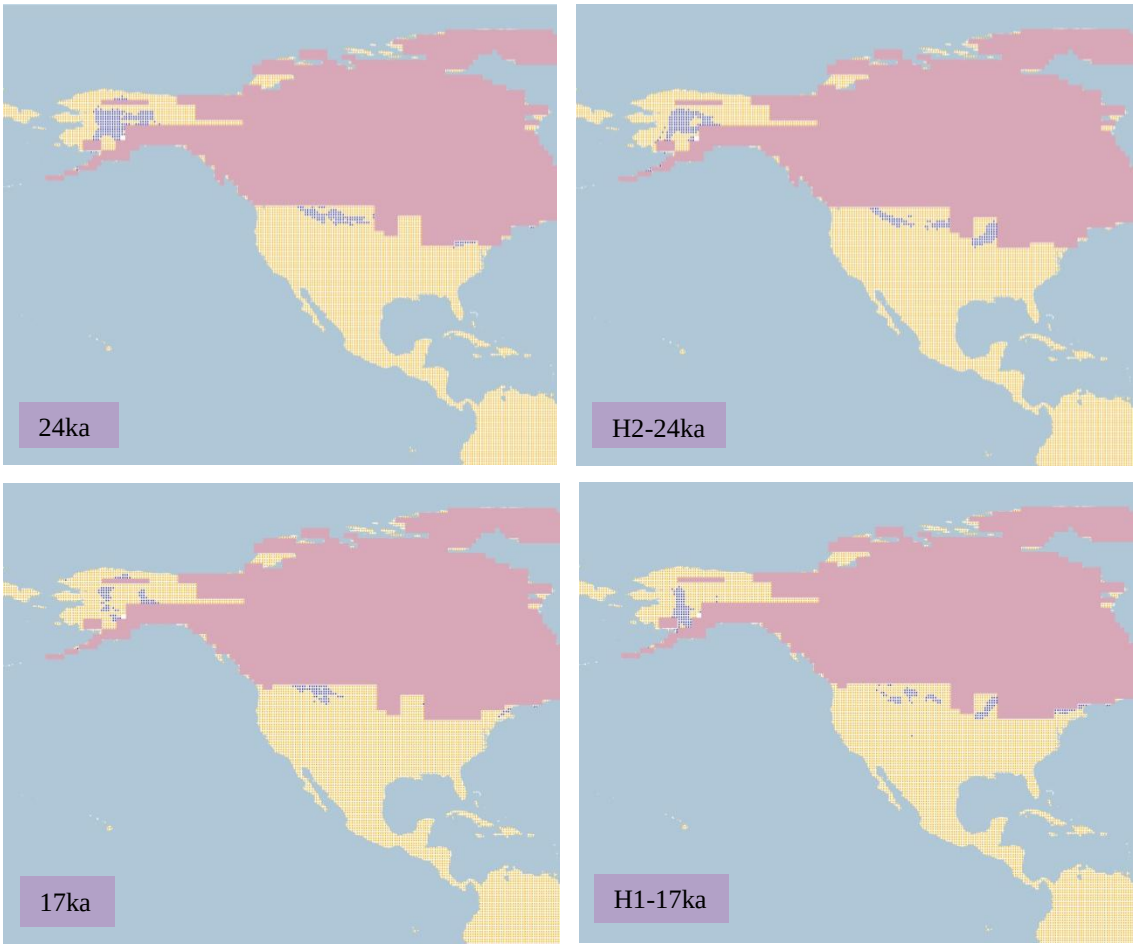

Figure 4.1.4.29.a. Simulation maps of Wandering Tattler breeding range.
Maps are shown for ten-time slices: 24ka, H2 (24ka), 17ka, H1 (17ka), 13ka, H0 (13ka), 9ka, 5ka, 3ka and present (1961–90).

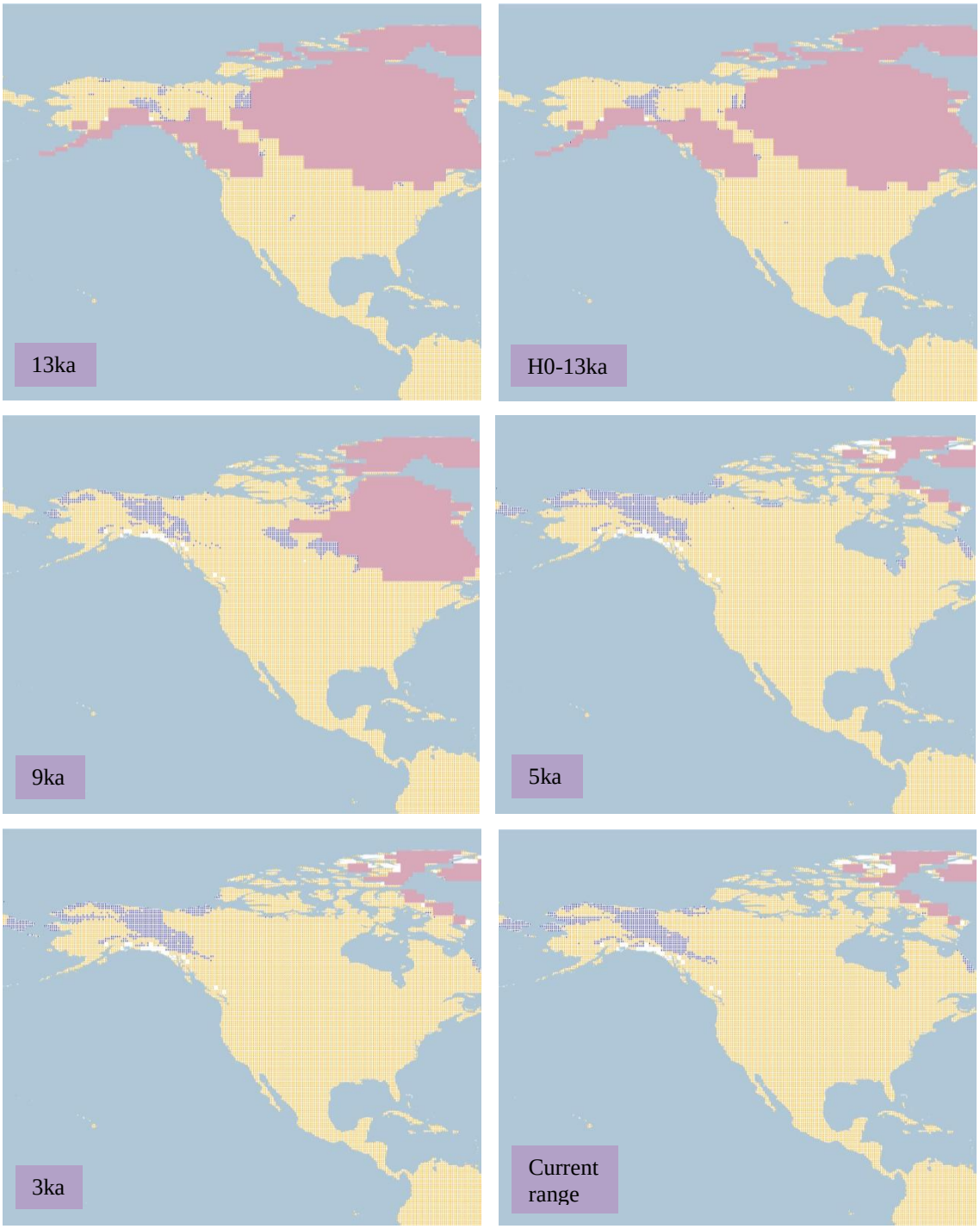

Figure 4.1.4.29.a. Simulation maps of Wandering Tattler breeding range (continued**).**

Non-breeding range (AUC: 0.972; TSS: 0.839; Kappa: 0.485): This species spends the non-breeding season mainly on the Pacific coast from California in the USA south along the coasts of Mexico and Central America to the coast of South America from Colombia to northern Chile, and the Galapagos Islands; in addition it extends inland in Baja California.

Beyond the Americas the species also occurs on the Hawaiian Islands, the islands of the central and southern Pacific, and as far west as eastern New Guinea and north-eastern Australia. Only the non-breeding range in the Americas was modelled.

The projected range at 26 ka BP extends from the south-western USA to north-western and central Mexico. In South America a range is projected on the Pacific coast from Ecuador south to central Chile, with a scattered range projected in Paraguay and Bolivia. This pattern continues until 16 ka BP when the range in north-western Mexico decreases. See Figure 4.1.4.29.b.

The range projected at 14 ka BP is mainly on the south-western coast of the USA, north-western Mexico, and in South America from Ecuador to northern Chile and in Paraguay. This projected range continues with minimal variations until 8 ka BP when there is a projected range in northern and along the central-southern coast of Mexico. After this and until 1 ka BP the range remains along the Pacific coast of the south-western USA, Mexico and in South America from Ecuador to Chile, agreeing with the current non-breeding projection.

The Heinrich event H2 projection is of a large range in northern South America, Central America, the Greater Antilles and southern Mexico, which differs from the 24 ka BP projection. At H1, the range in southern Mexico shifts to the central region, with a smaller range projected in northern South America. This pattern range continues at H0, decreasing in central Mexico, and projecting a range in Central America and northern South America that is not projected at 13 ka BP.

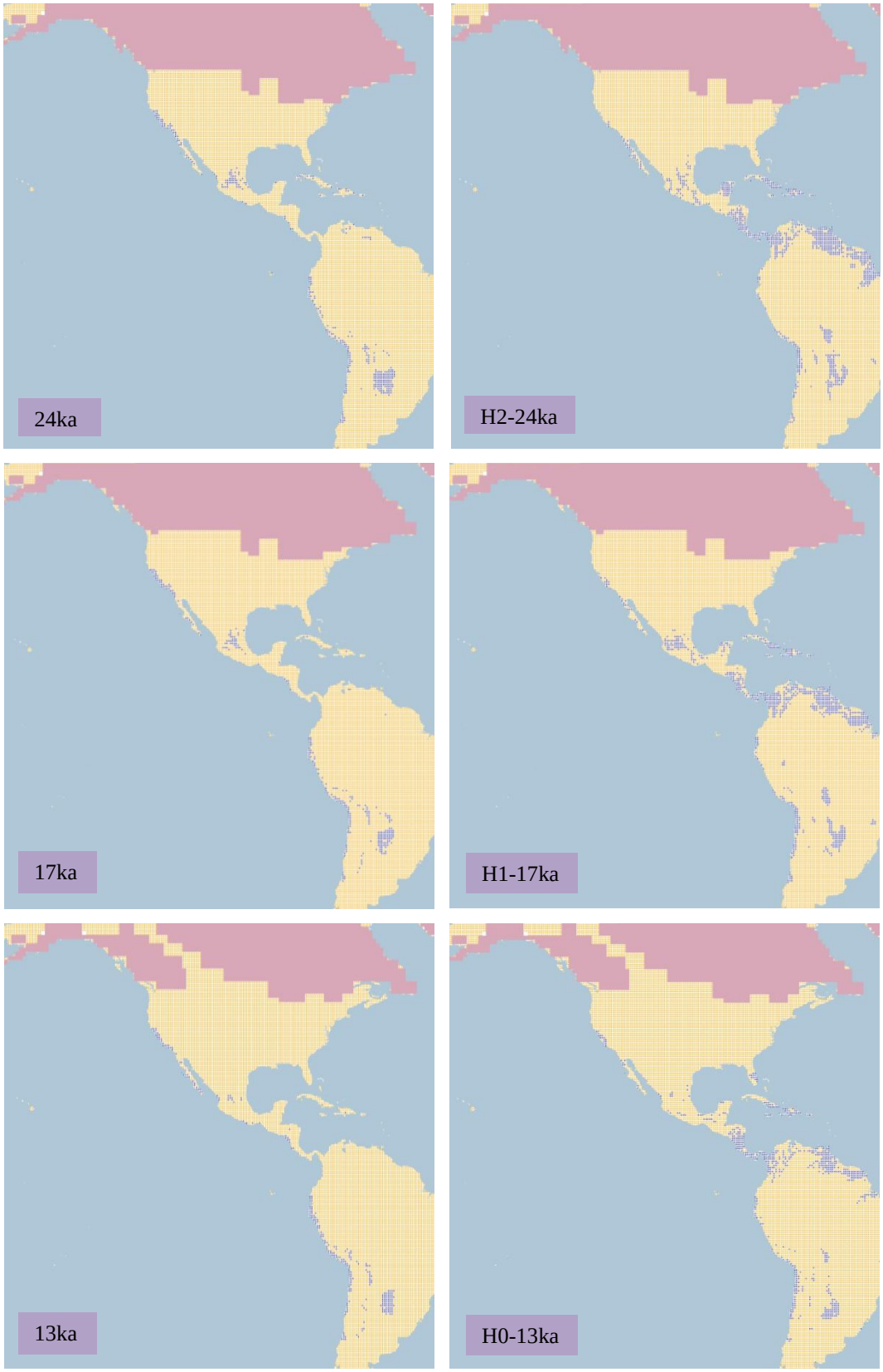

Figure 4.1.4.29.b. Simulation maps of Wandering Tattler non-breeding range. Maps are shown for ten-time slices: 24ka, H2 (24ka), 17ka, H1 (17ka), 13ka, H0 (13ka), 9ka, 5ka, 3ka and present (1961–90).

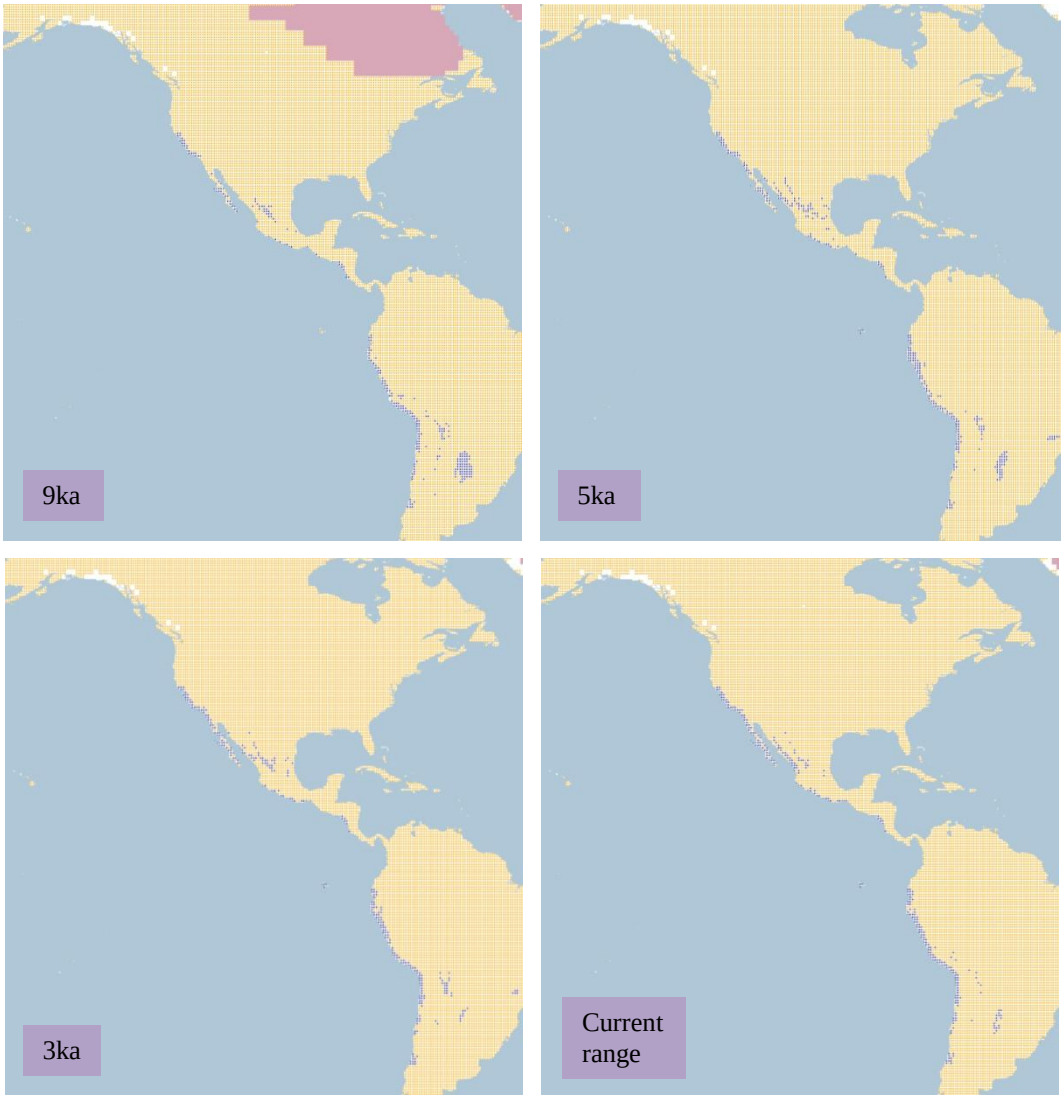

Figure 4.1.4.29.b. Simulation maps of Wandering Tattler non-breeding range (continued**).**

*4.1.4.30 Greater Yellowlegs (*Tringa melanoleuca*). Conservation status: Least Concern. Current known range Figure 4.1.4.30.*

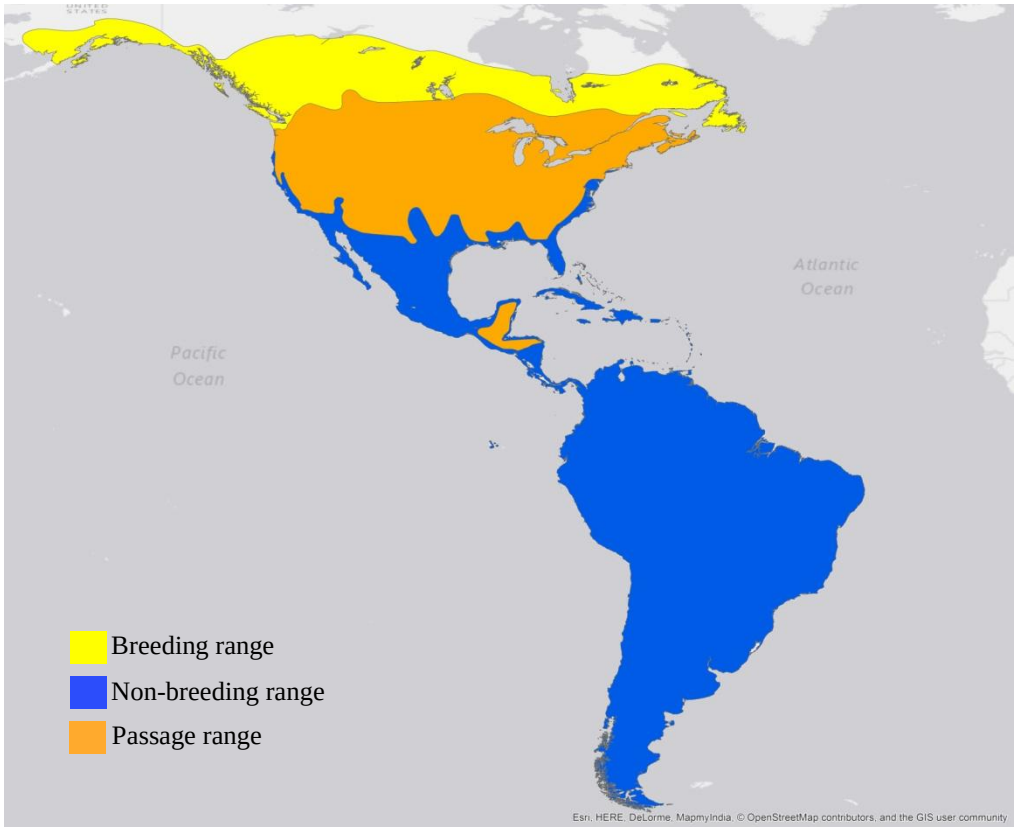

Figure 4.1.4.30. Current known range of Greater Yellowlegs.

Breeding range (AUC: 0.977; TSS: 0.871; Kappa: 0.814): This species breeds from southern Alaska east across central and southern Canada, from British Columbia to Newfoundland and Labrador.

At 26 ka BP the range is projected in the central-northern conterminous USA with a small range in southern Alaska near the ice sheet. This pattern continues until 18 ka BP when there is a decrease in the north-western part of the USA. After this at 17 ka BP the range projected in the rest of the northern conterminous USA also decreases, whereas that in southern Alaska increases. See Figure 4.1.4.30.a.

At 14 ka BP the range in Alaska persists and there is an increased extent in the northern conterminous USA, reaching the north-western coast in Washington and as far as the coast of British Columbia in Canada where it is not covered by the ice sheet. After this at 13 ka BP the range in the northern conterminous USA shifts to the southern boundary of Canada.

The range at 12 ka BP is projected in central to southern Canada, reaching the northern part of the conterminous USA and with a small range in central-southern Alaska. By the beginning of the Holocene the range in Canada persists with an increase in Alaska where the range now reaches as far as the Aleutian Islands. This pattern continues and by 8 ka BP the range in Canada reaches the south-eastern region.

From 7 ka BP until 1 ka BP the range is projected across central Canada and in central Alaska as far as the Aleutian Islands. This pattern also continues in the current breeding range projection.

When comparing H2 with 24 ka BP, there is a larger range projected in the central-western region in the USA for H2 than at 24ka. This range decreases in the western part of the USA at H1, although differing from the small range projected in the northern region of the conterminous USA at 17ka. The decreasing pattern continues at H0, sharing a similar range as 13 ka BP in the northern conterminous USA and in Alaska, and differing in the central-western region with a larger range projected at H0.

Even though the current breeding range of the species is located in North America, there are suitable conditions projected for the species to occur in southern Chile and southern Argentina in South America.

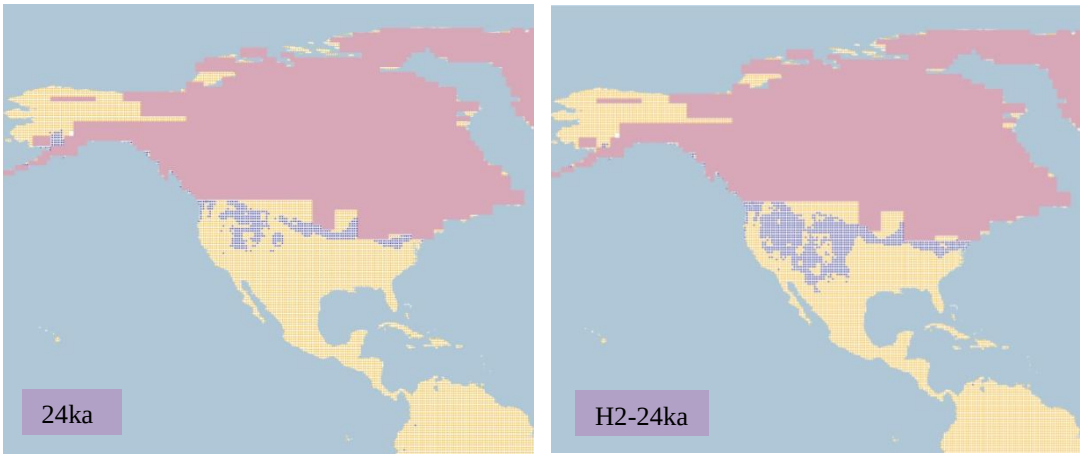

Figure 4.1.4.30.a. Simulation maps of Greater Yellowlegs breeding range.
Maps are shown for ten-time slices: 24ka, H2 (24ka), 17ka, H1 (17ka), 13ka, H0 (13ka), 9ka, 5ka, 3ka and present (1961–90).

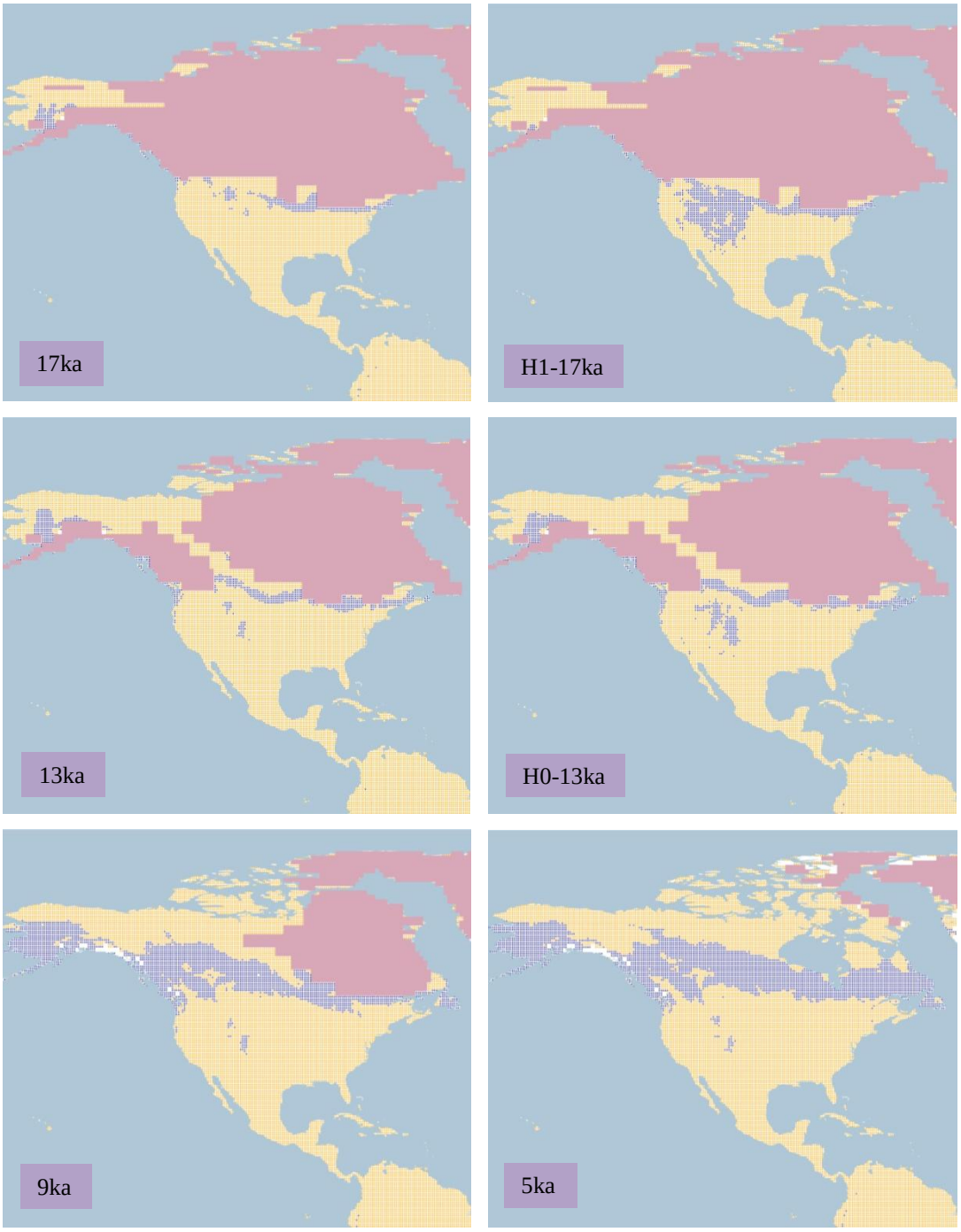

Figure 4.1.4.30.a. Simulation maps of Greater Yellowlegs breeding range (continued**).**

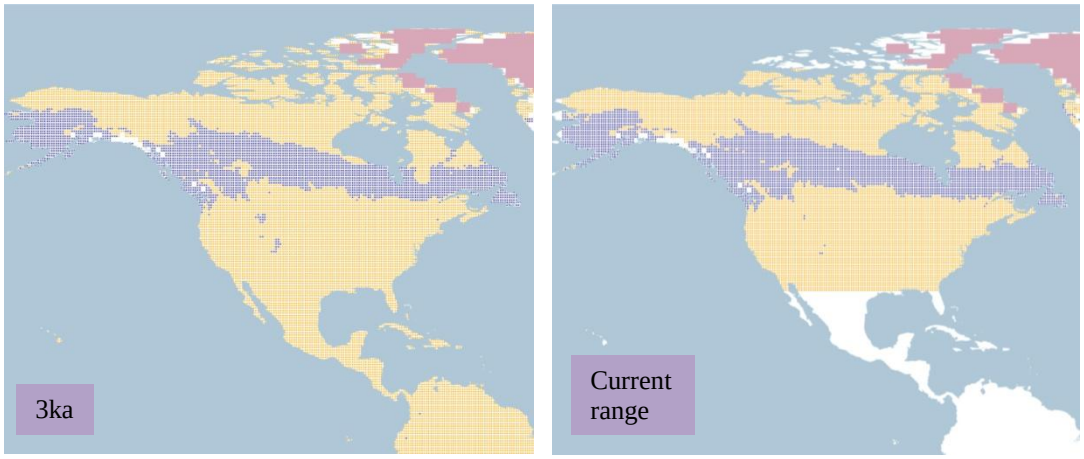

Figure 4.1.4.30.a. Simulation maps of Greater Yellowlegs breeding range (continued**).**

Non-breeding range (AUC: 0.993; TSS: 0.933; Kappa: 0.929): This species spends the non-breeding season in the southern USA, Mexico, the Greater Antilles and South America.

The projected range at 26 ka BP extends from the southern USA as far as southern Argentina in South America, with a projected range also in the Greater Antilles. This pattern continues until 19 ka BP when the range in north-western Mexico and the south-western USA decreases. The range in these areas increases again at 15 ka BP. See Figure 4.1.4.30.b.

With the deglaciation at 13 ka BP the range in the south-eastern USA increases, especially at the beginning of the Holocene, extending from Texas to South Carolina. At 10 ka BP a small range is projected in central-southern Canada near the ice sheet, which disappears at 9 ka BP. After this at 8 ka BP the range in the south-eastern USA shifts to the central-southern region.

From 7 ka BP until 1 ka BP the range extends from the southern USA as far as southern South America, including also the Greater Antilles. This same projected range continues in the current non-breeding projection.

A similar projected range is observed between H2 and 24 ka BP, with minimal variation in the southern USA. After this at H1 the range in northern Mexico decreases as in the 17 ka BP projection, and the H0 projected range increases in northern Mexico and in the southern USA as in the 13 ka BP projection.

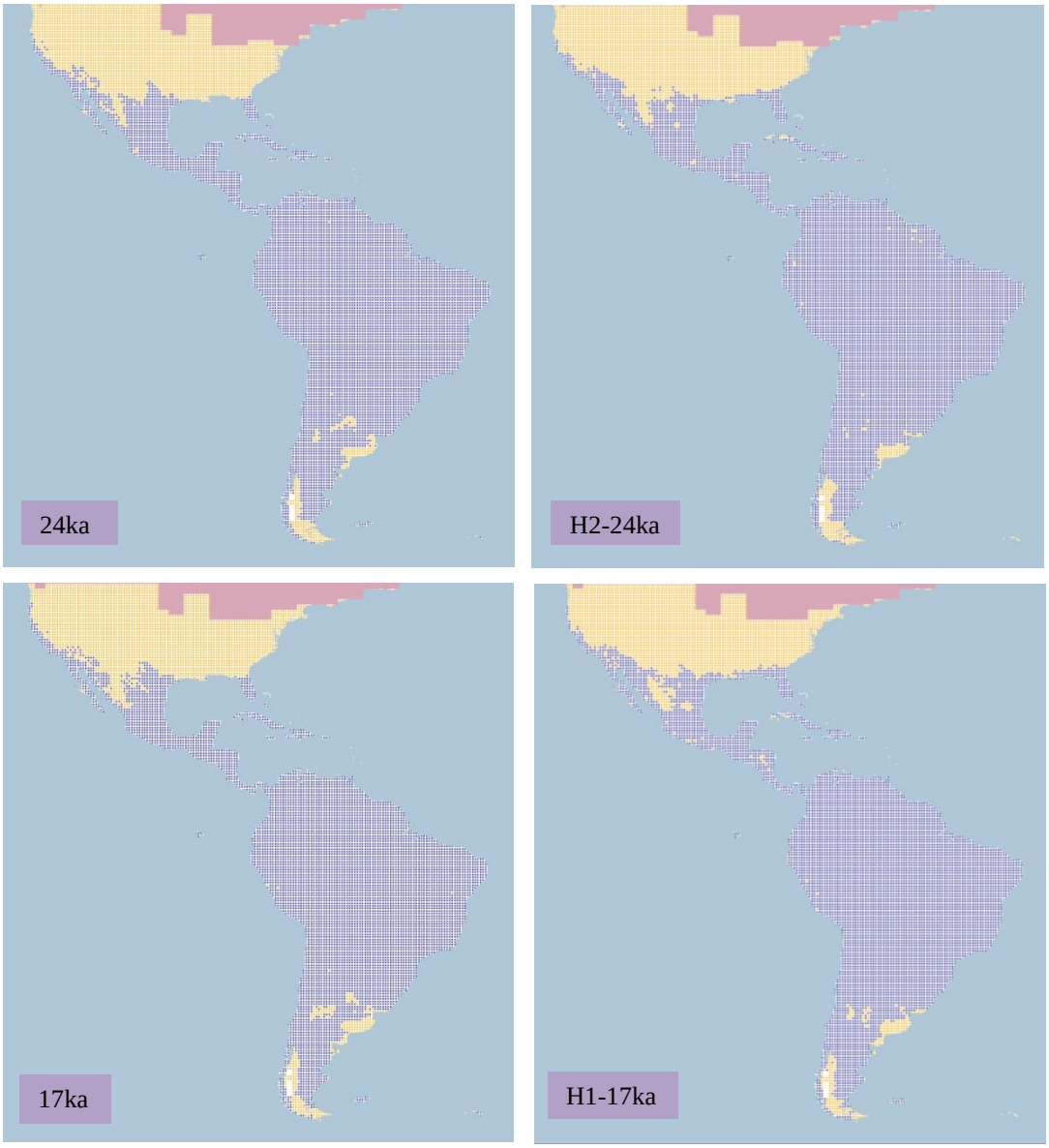

Figure 4.1.4.30.b. Simulation maps of Greater Yellowlegs non-breeding range. Maps are shown for ten-time slices: 24ka, H2 (24ka), 17ka, H1 (17ka), 13ka, H0 (13ka), 9ka, 5ka, 3ka and present (1961–90).

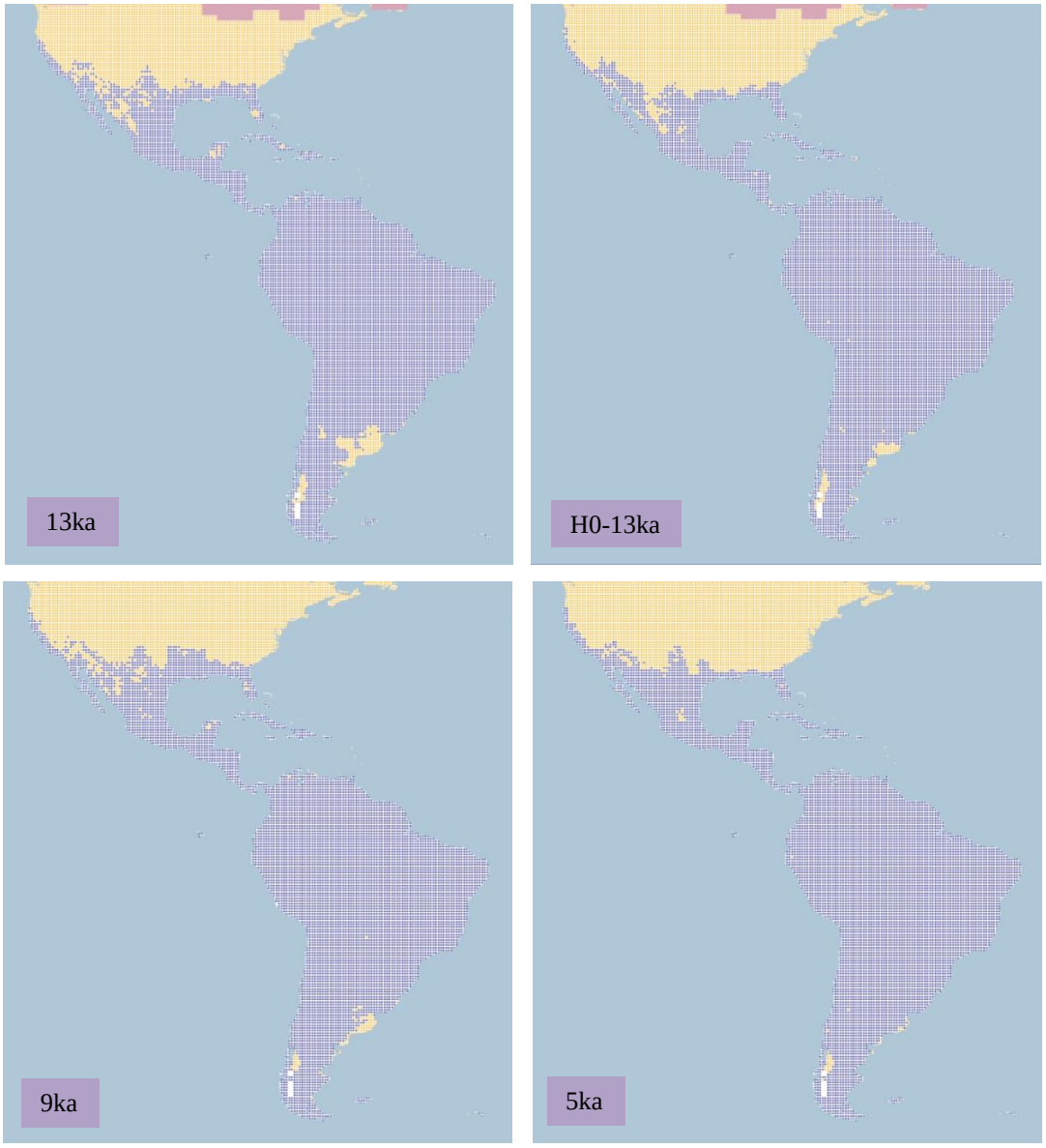

Figure 4.1.4.30.b. Simulation maps of Greater Yellowlegs non-breeding range (continued**).**

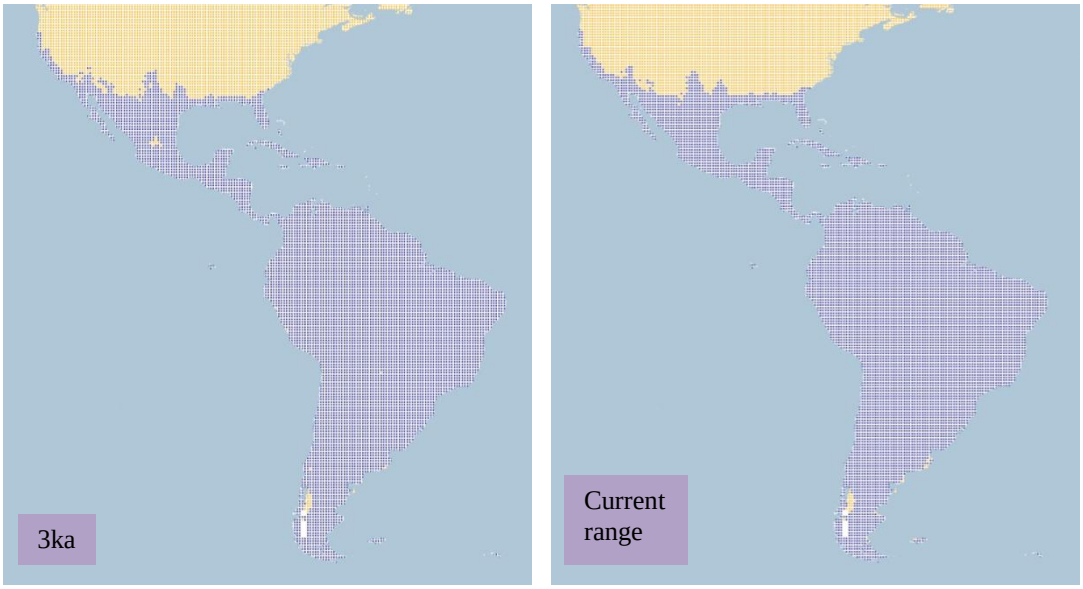

Figure 4.1.4.30.b. Simulation maps of Greater Yellowlegs non-breeding range (continued**).**

*4.1.4.31 Willet (*Tringa semipalmata *including* T. s. inornata *and* T. s. semipalmata*). Conservation status: Least Concern. Current known range Figure 4.1.4.31.*

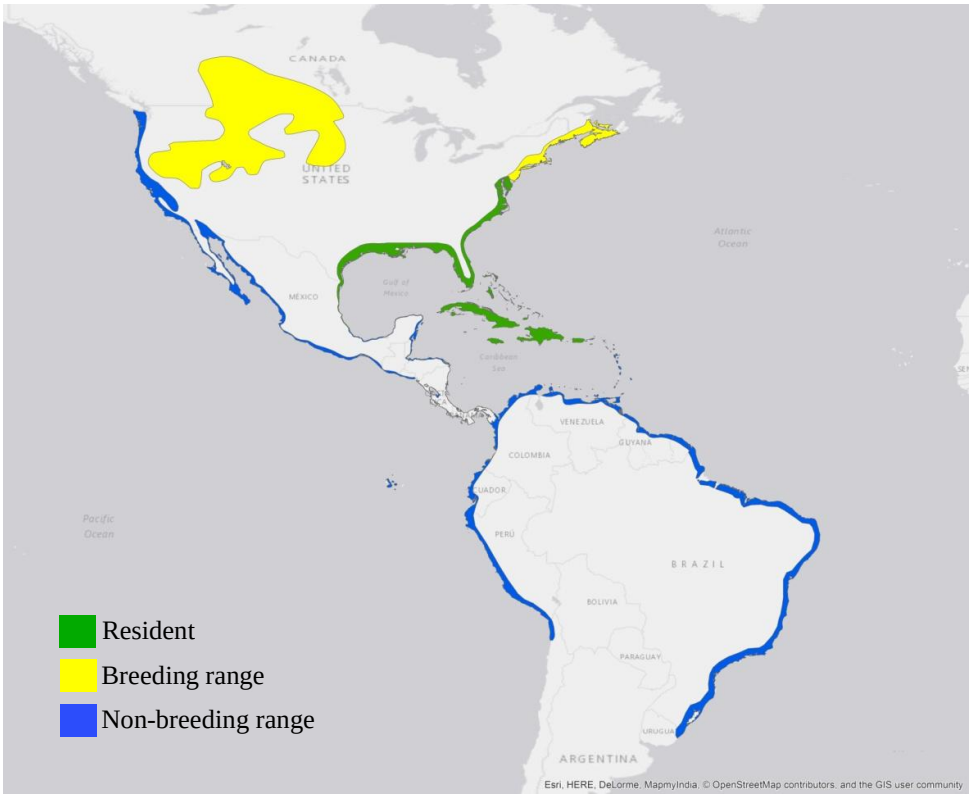

Figure 4.1.4.31. Current known range of Willet.

Breeding range (AUC: 0.979; TSS: 0.851; Kappa: 0.720): *Tringa semipalmata inornata* breeds in the western and central-northern USA and in central-southern Canada, whereas *T. s. semipalmata* breeds in south-east Canada and the north-eastern USA as well as having a year-round resident range along the east coasts of the USA and Mexico, and in the Greater Antilles.

At 26 ka BP the range is projected mainly in the central USA with a small range in the western region. This pattern continues until 17 ka BP when the range in the central and western regions of the USA increases. After this at 14 ka BP the range shifts to the northern USA near the ice sheet. See Figure 4.1.4.31.a.

With the deglaciation at 13 ka BP a small range is projected in the north-eastern USA near the ice sheet, and the range in the central-northern USA extends to southern Canada. After this at 11 ka BP the range in the central and western USA decreases, the range shifting to central-southern Canada, and a small range is projected in the south-eastern USA. This pattern persists until 9 ka BP when the range in south-eastern Canada decreases.

At 7 ka BP the range is projected in central-western and south-eastern parts of the USA with a small range in central-southern Canada. This projected range continues with minimal differences until 1 ka BP, and agrees with the current breeding range projection.

When comparing H2 with 24 ka BP, a different range is observed at H2, with a small and scattered range in the eastern and central USA. The range in the north-western USA increases at H1, although differing from 17 ka BP. The H0 projected range increases in the central and north-western USA, with a similar range as at 13 ka BP.

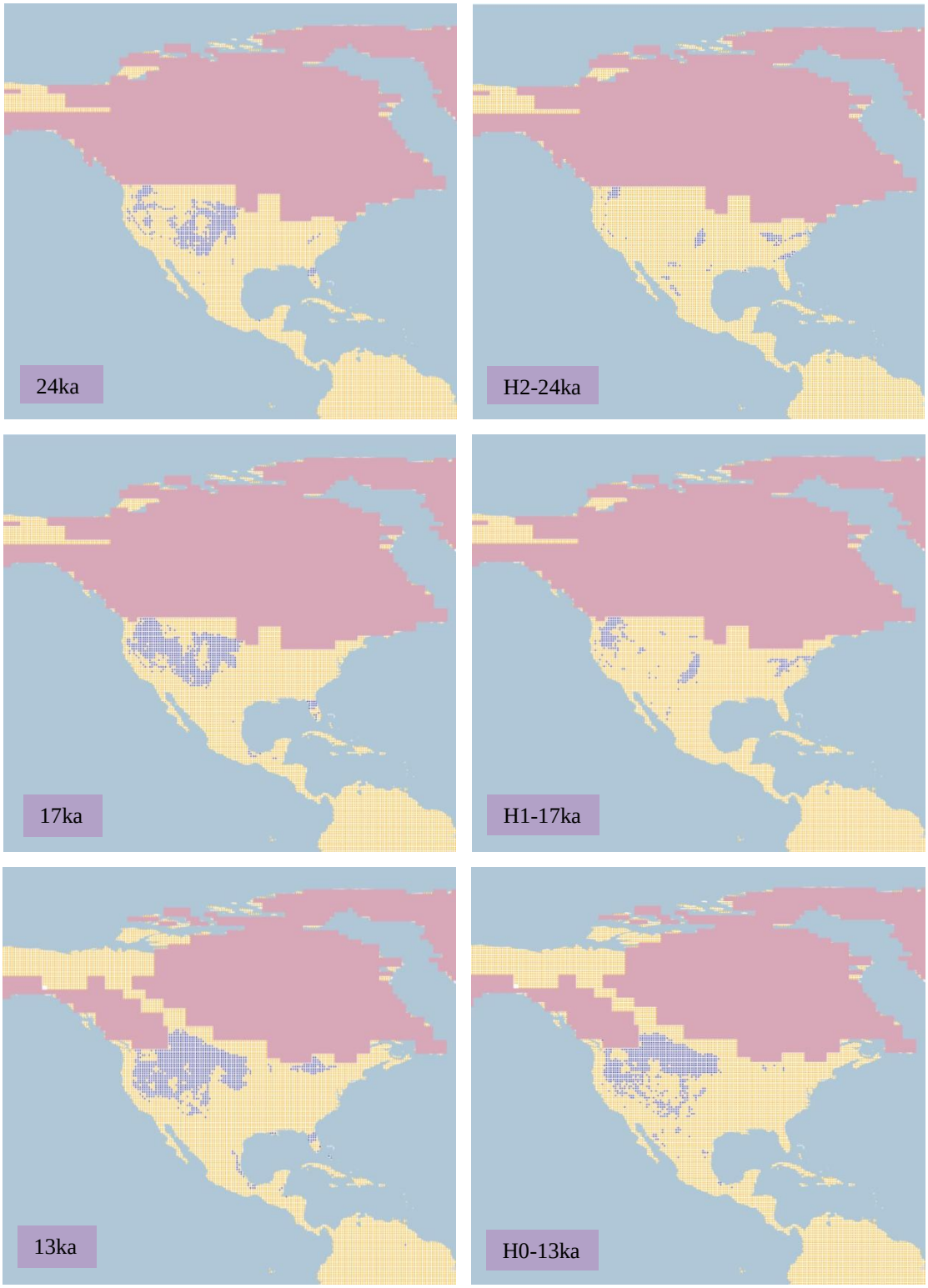

Figure 4.1.4.31.a. Simulation maps of Willet breeding range.
Maps are shown for ten-time slices: 24ka, H2 (24ka), 17ka, H1 (17ka), 13ka, H0 (13ka), 9ka, 5ka, 3ka and present (1961–90).

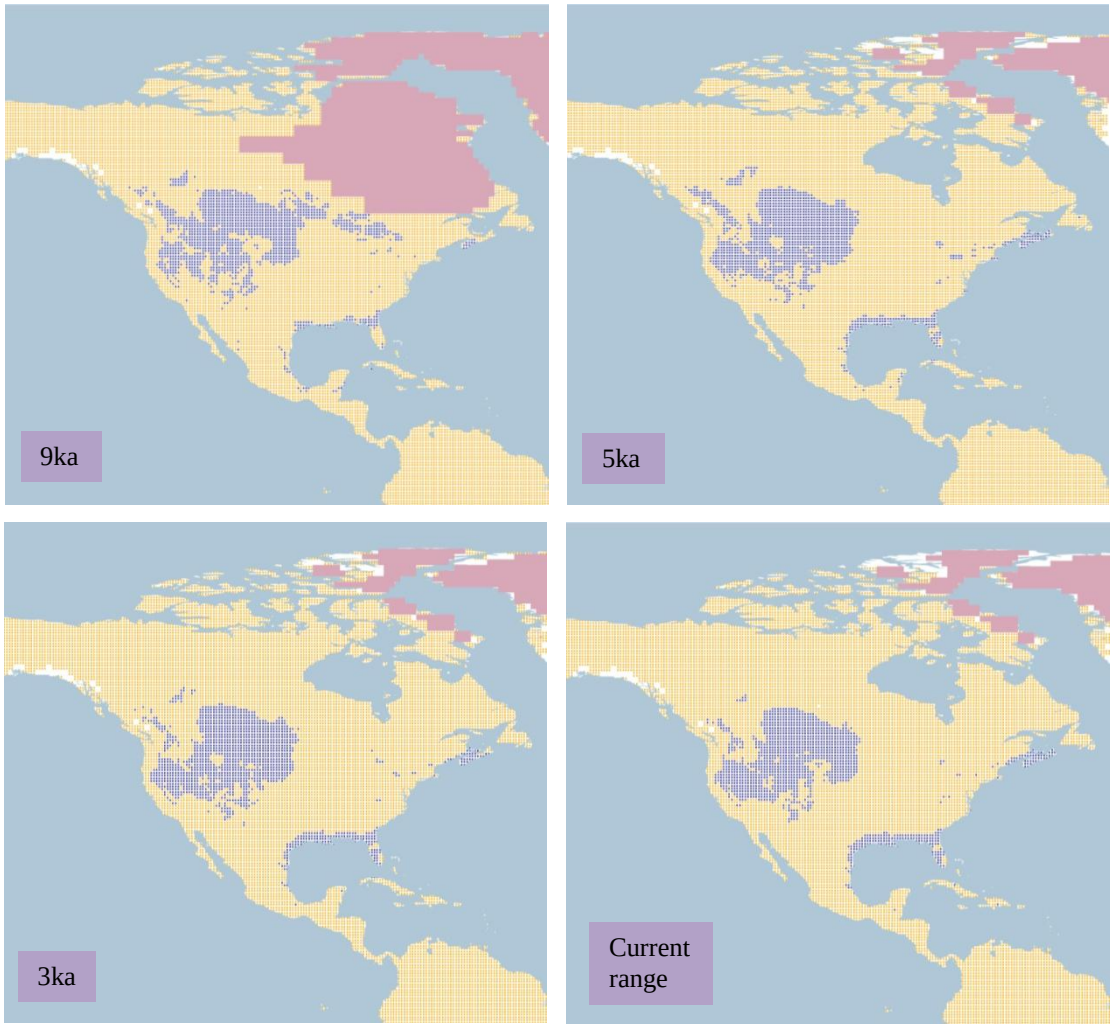

Figure 4.1.4.31.a. Simulation maps of Willet breeding range (continued**).**

Non-breeding range (AUC: 0.954; TSS: 0.758; Kappa: 0.596): This species spends the winter on the west coast of the USA, the west and south-eastern coasts of Mexico, along the coasts of Central America and on the coasts of South America from western Colombia to Peru on the Pacific side and from northern Colombia to Uruguay on the Atlantic side. It is also resident along the eastern coasts of the USA and Mexico, and in the Greater Antilles.

At 26 ka BP the range is projected along the west coasts of the USA, Mexico, El Salvador, Nicaragua, Ecuador and Peru with a scattered range in inland Mexico, the Greater Antilles and in northern South America, and a small range in southern Brazil. This pattern continues with minimal differences until 19 ka BP when the range increases in northern Mexico along the Sierra Madre Occidental. This range decreases at 15 ka BP as does that on the north-western coast of Mexico. See Figure 4.1.4.31.b.

With the deglaciation at 13 ka BP the range in northern Brazil, northern Honduras and Nicaragua, and in the north-western USA increases. After this at 10 ka BP the range in northern Brazil decreases. At 8 ka BP a range is projected in the south-eastern USA and the remainder of the range increases.

From 7 ka BP until 2 ka BP a similar pattern persists until the range in central and southern Brazil decreases. At 1 ka BP the range in the south-eastern USA and in northern Mexico increases. This pattern continues in the current non-breeding range projection.

When comparing H2 with 24 ka BP, there is a different range projected from southern Mexico through Central America and as far as northern and central South America. This pattern continues at H1, and increases in South America, differing from the 17 ka BP projection that is restricted to coastal areas. In the H0 projection the range in South America decreases, with a smaller range projected in north-western Mexico, different from that at 13 ka BP.

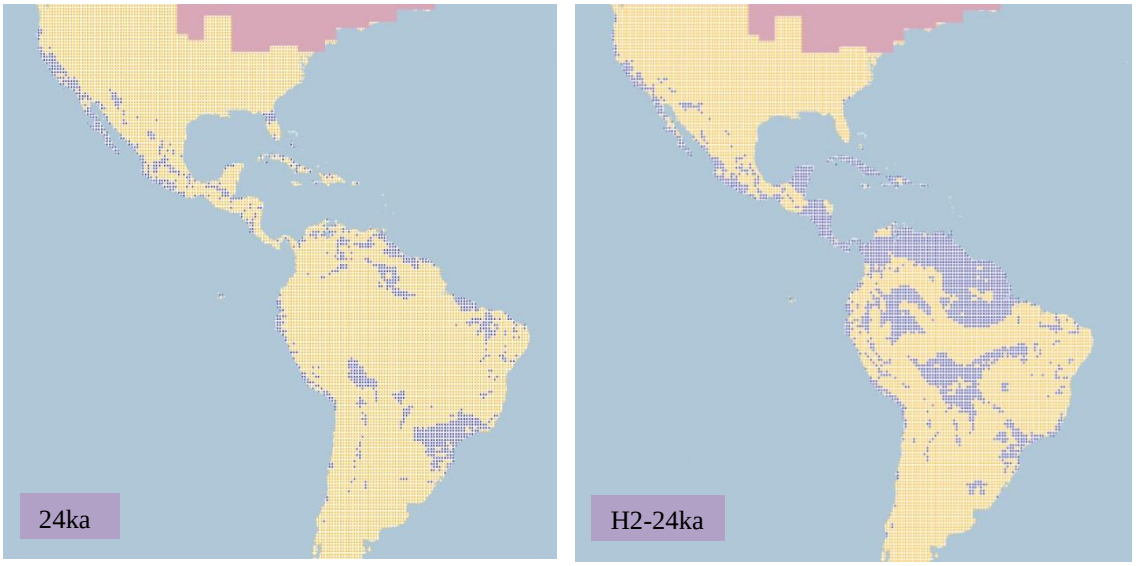

Figure 4.1.4.31.b. Simulation maps of Willet non-breeding range.
Maps are shown for ten-time slices: 24ka, H2 (24ka), 17ka, H1 (17ka), 13ka, H0 (13ka), 9ka, 5ka, 3ka and present (1961–90).

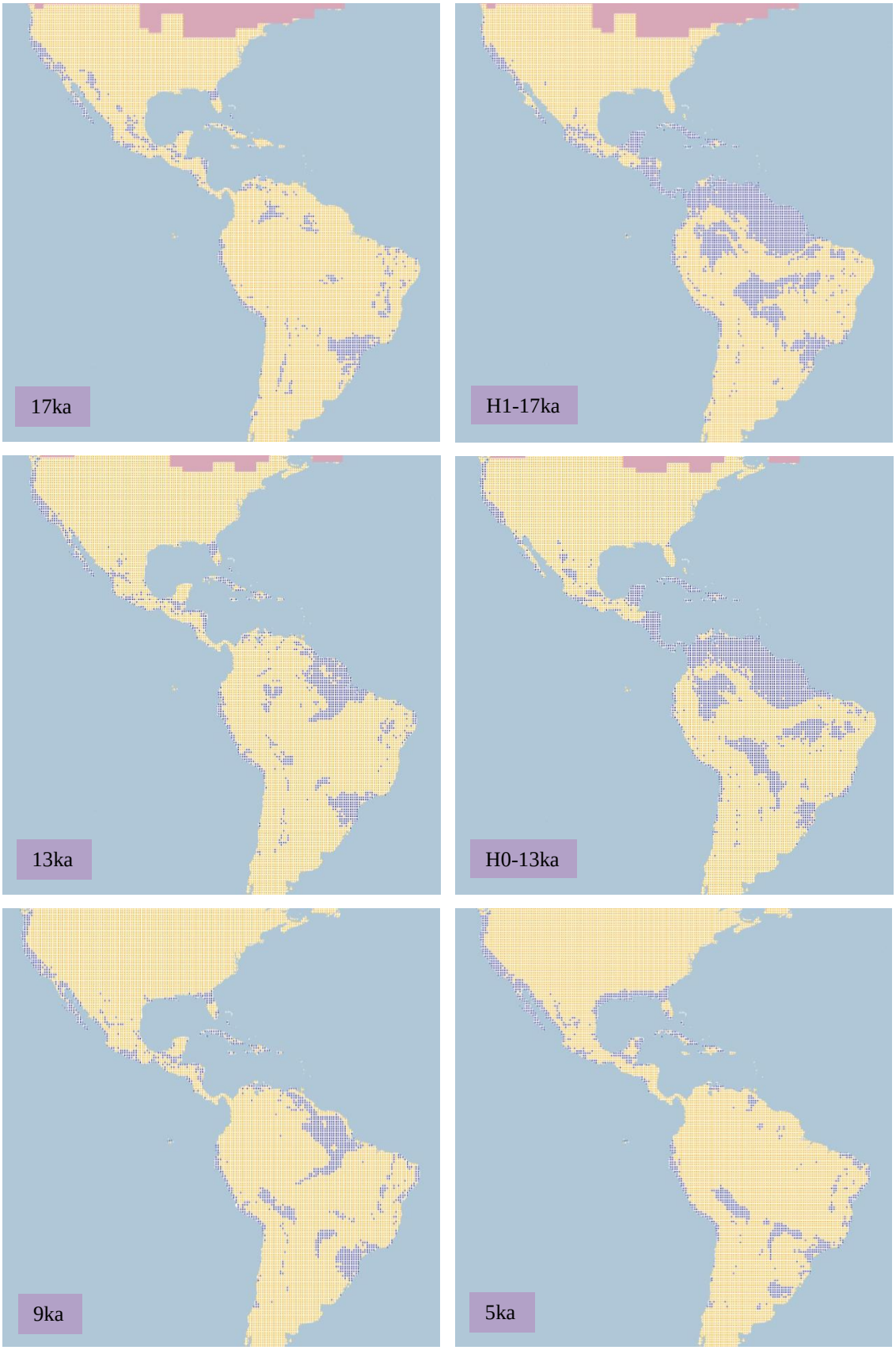

Figure 4.1.4.31.b. Simulation maps of Willet non-breeding range (continued**).**

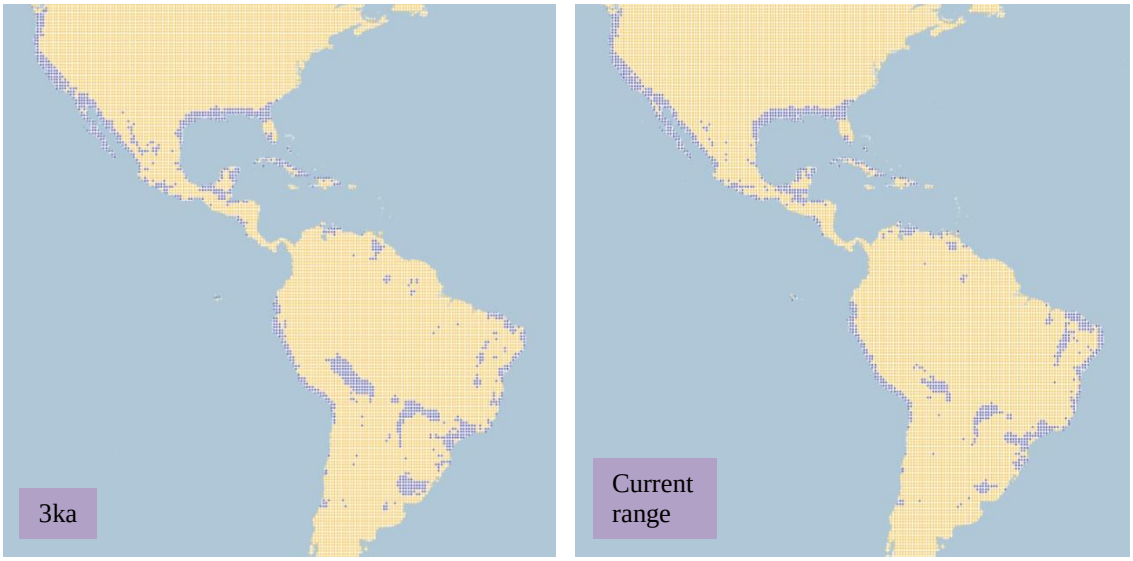

Figure 4.1.4.31.b. Simulation maps of Willet non-breeding range (continued**).**

*4.1.4.32 Solitary Sandpiper (*Tringa solitaria *including* T. s. cinnamomea *and* T. s. solitaria*).*

Conservation status: Least Concern. Current known Figure 4.1.4.32.

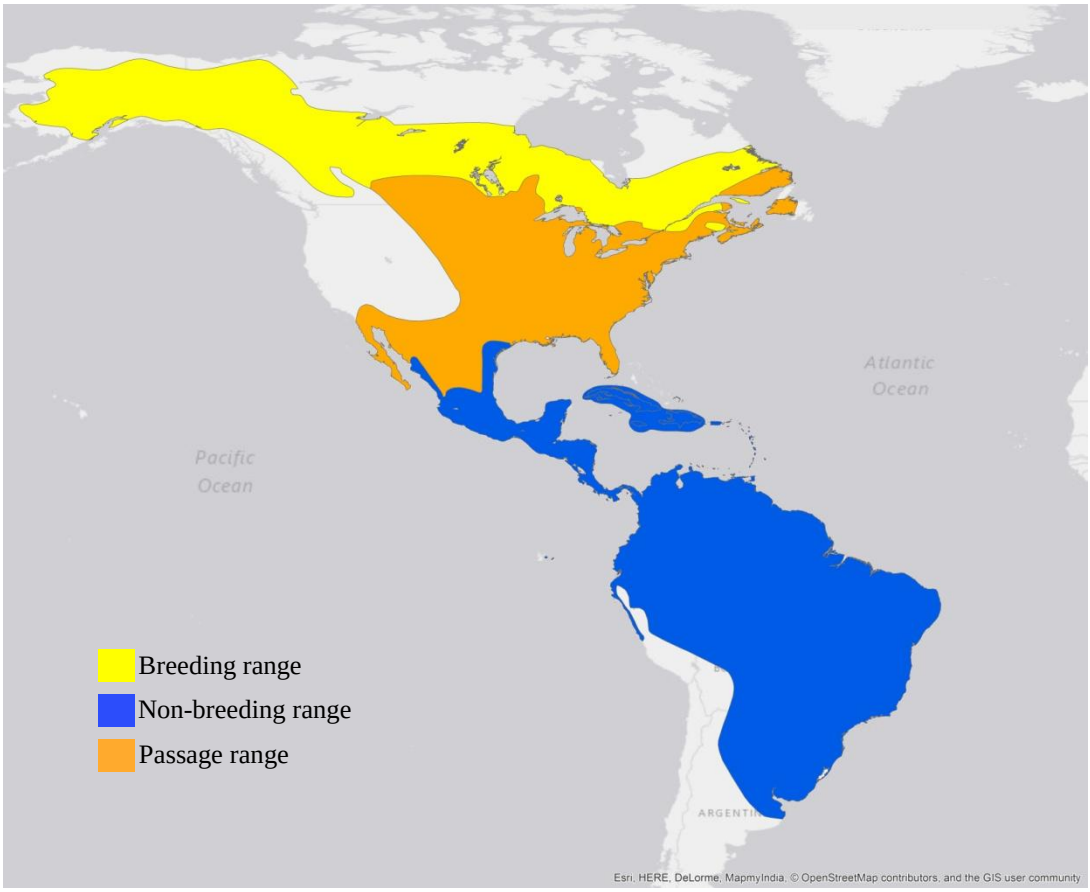

Figure 4.1.4.32. Current known range of Solitary Sandpiper.

Breeding range (AUC: 0.970; TSS: 0.807; Kappa: 0.792): This species breeds in northern North America, from Alaska to north-eastern Canada, except in Northwest Territories and Nunavut.

The projected range at 26 ka BP is located in the northern conterminous USA and in central Alaska. This pattern continues until 15 ka BP when the range in the northern conterminous USA decreases and shifts to the southern boundary of Canada near the ice sheet. After this at 14 ka BP the range in northern Canada increases, extending as far as central Alaska in the USA. With the deglaciation the range in the northern conterminous USA shifts to southern and central Canada. See Figure 4.1.4.32.a.

At 12 ka BP the range extends from central Alaska to Canada and as far as the north-eastern conterminous USA. The range in Alaska increases at 10 ka BP and the range in the northern conterminous USA disappears, restricting the range to Canada and Alaska. After this the range increases in south-eastern Canada.

From 7 ka BP until 1 ka BP the range is projected to extend from western Alaska to eastern Canada, except for the northern regions of Northwest Territories and Nunavut, and with minimal variation. This pattern continues in the current breeding range projection.

There are small differences observed between the H2 and 24 ka BP projections. At H1 the range in the northern conterminous USA increases, which differs from 17ka. At H0 the range extends from Alaska to southern Canada near the northern boundary of the USA and with a small range projected in the central conterminous USA, which differs from the 13 ka BP projection.

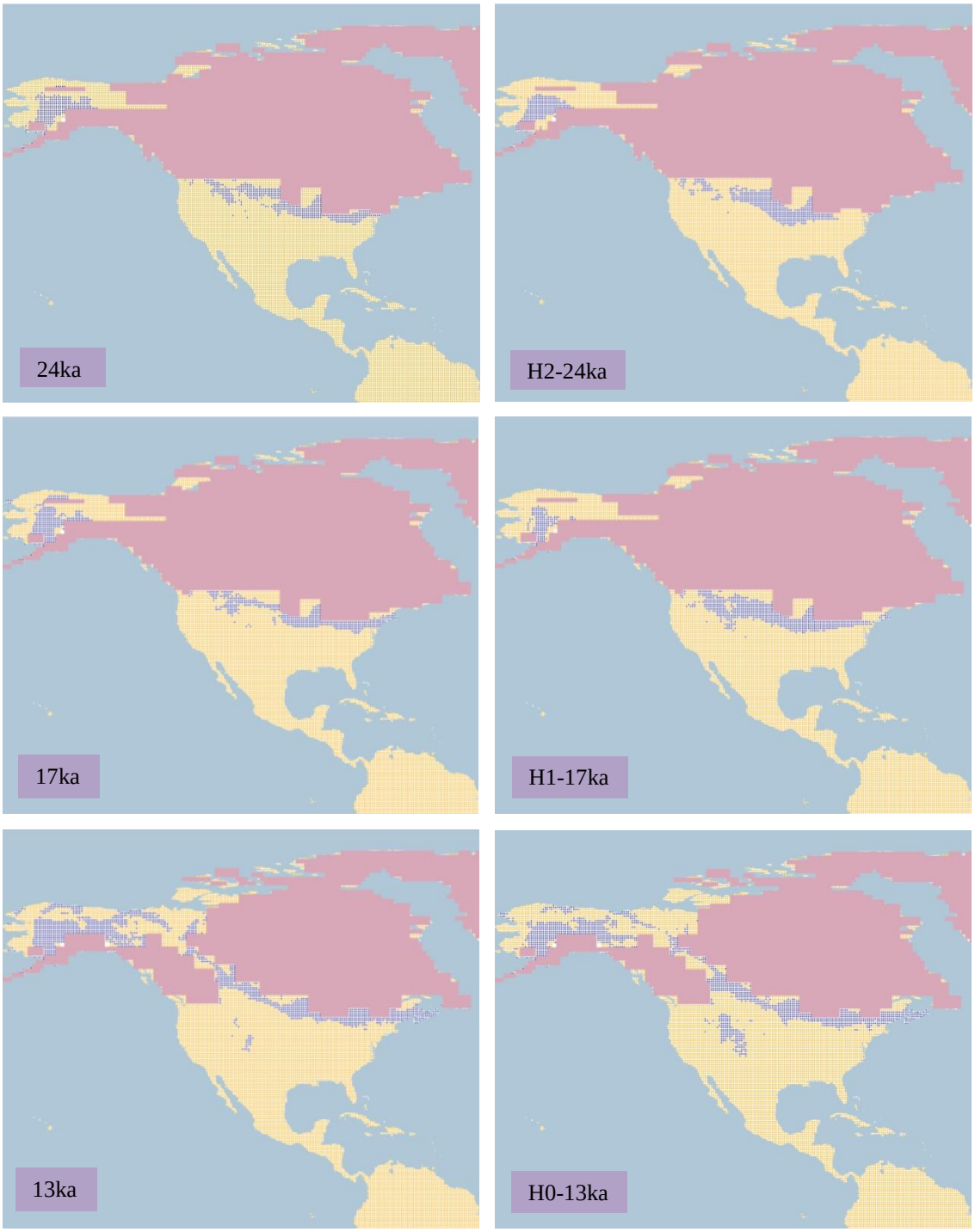

Figure 4.1.4.32.a. Simulation maps of Solitary Sandpiper breeding range.
Maps are shown for ten-time slices: 24ka, H2 (24ka), 17ka, H1 (17ka), 13ka, H0 (13ka), 9ka, 5ka, 3ka and present (1961–90).

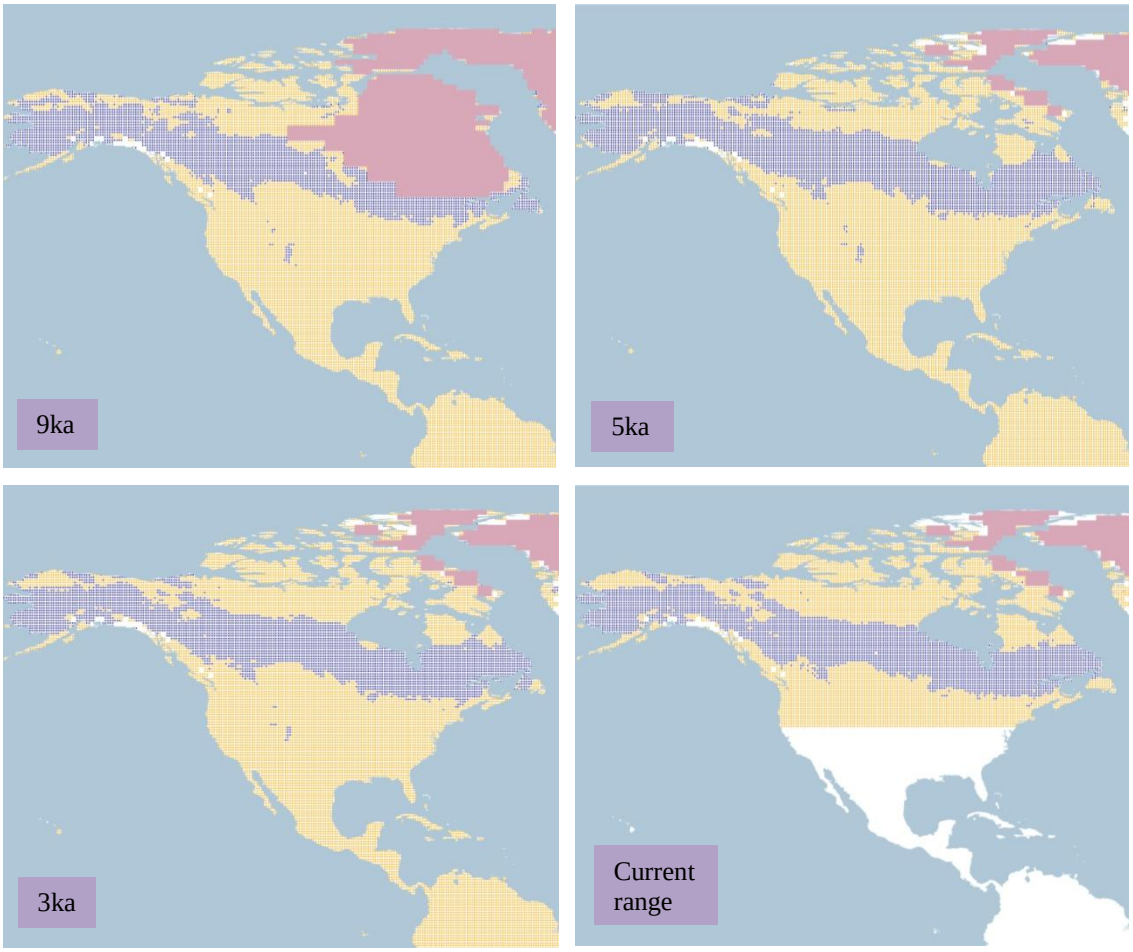

Figure 4.1.4.32.a. Simulation maps of Solitary Sandpiper breeding range (continued**).**

Non-breeding range (AUC: 0.994; TSS: 0.940; Kappa: 0.938): This species spends the non-breeding season from central Mexico as far as central-southern South America in northern Argentina, including Central America and the Greater Antilles, with a small range on the south-eastern coast of Texas in the USA.

At 26 ka BP the range is projected from eastern and central Mexico as far as northern Argentina in South America, covering also the Greater Antilles and southern Florida in the USA. This pattern continues until 18 ka BP when a small range is projected also in southern Texas. See Figure 4.1.4.32.b.

By the beginning of the Holocene the range is projected to include Texas and southern Florida in the USA, eastern and central Mexico, the Greater Antilles, and Central America and as far as northern Argentina in South America. The range in Texas decreases at 10 ka BP. After this at 8 ka BP there is an increase in north-western Mexico. A similar pattern

persists until 1 ka BP, with minimal variations, and agreeing with the current non-breeding range projection.

At H2 a scattered range is projected in eastern and central-southern parts of Mexico, in Central America as far as the northern part of South America, different from 24 ka BP. The range in north-western Mexico increases at H1, that in southern Mexico decreasing. The range in Mexico increases at H0 although at a smaller scale than the 13 ka BP projection.

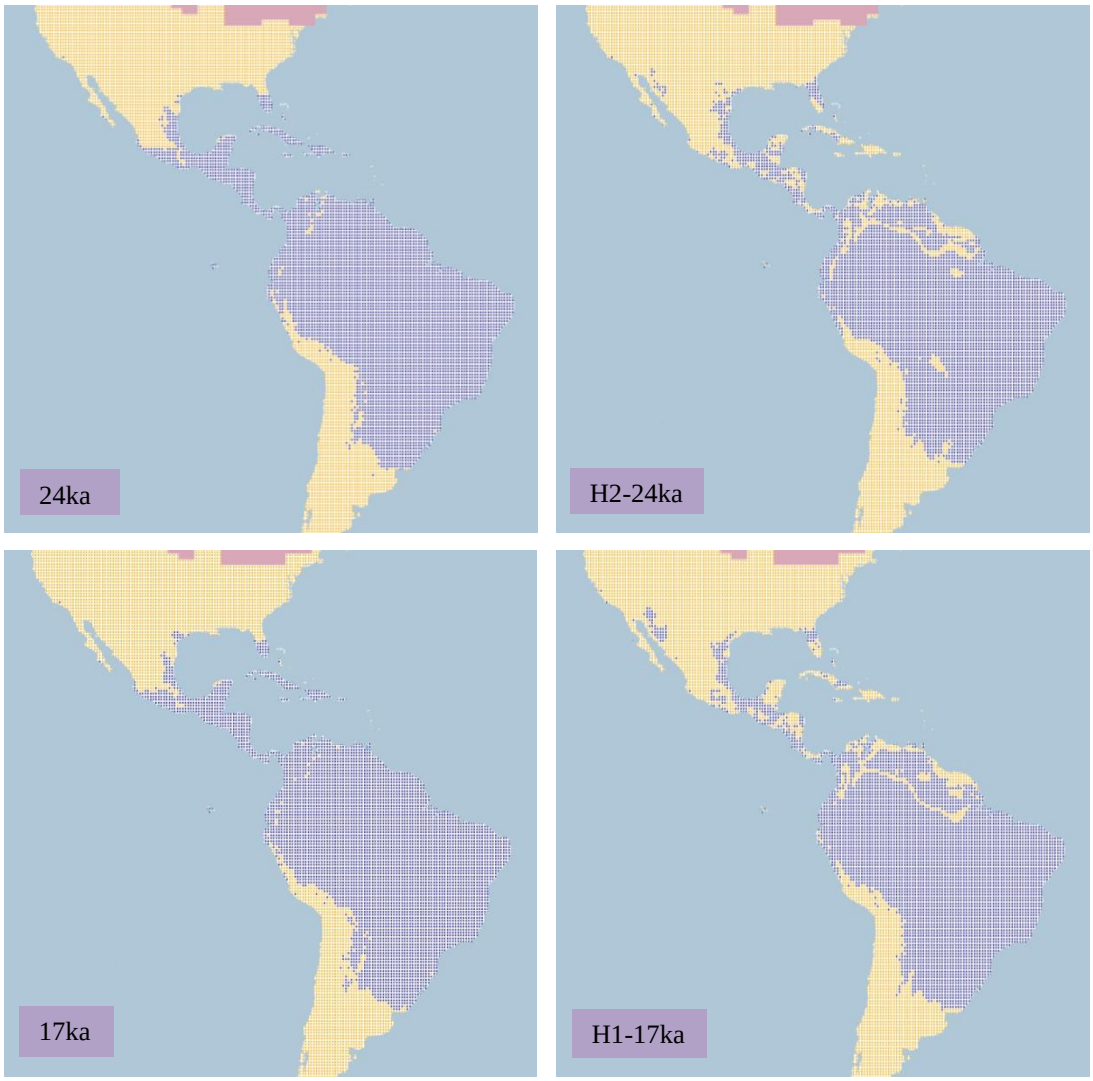

Figure 4.1.4.32.b. Simulation maps of Solitary Sandpiper non-breeding range. Maps are shown for ten-time slices: 24ka, H2 (24ka), 17ka, H1 (17ka), 13ka, H0 (13ka), 9ka, 5ka, 3ka and present (1961–90).

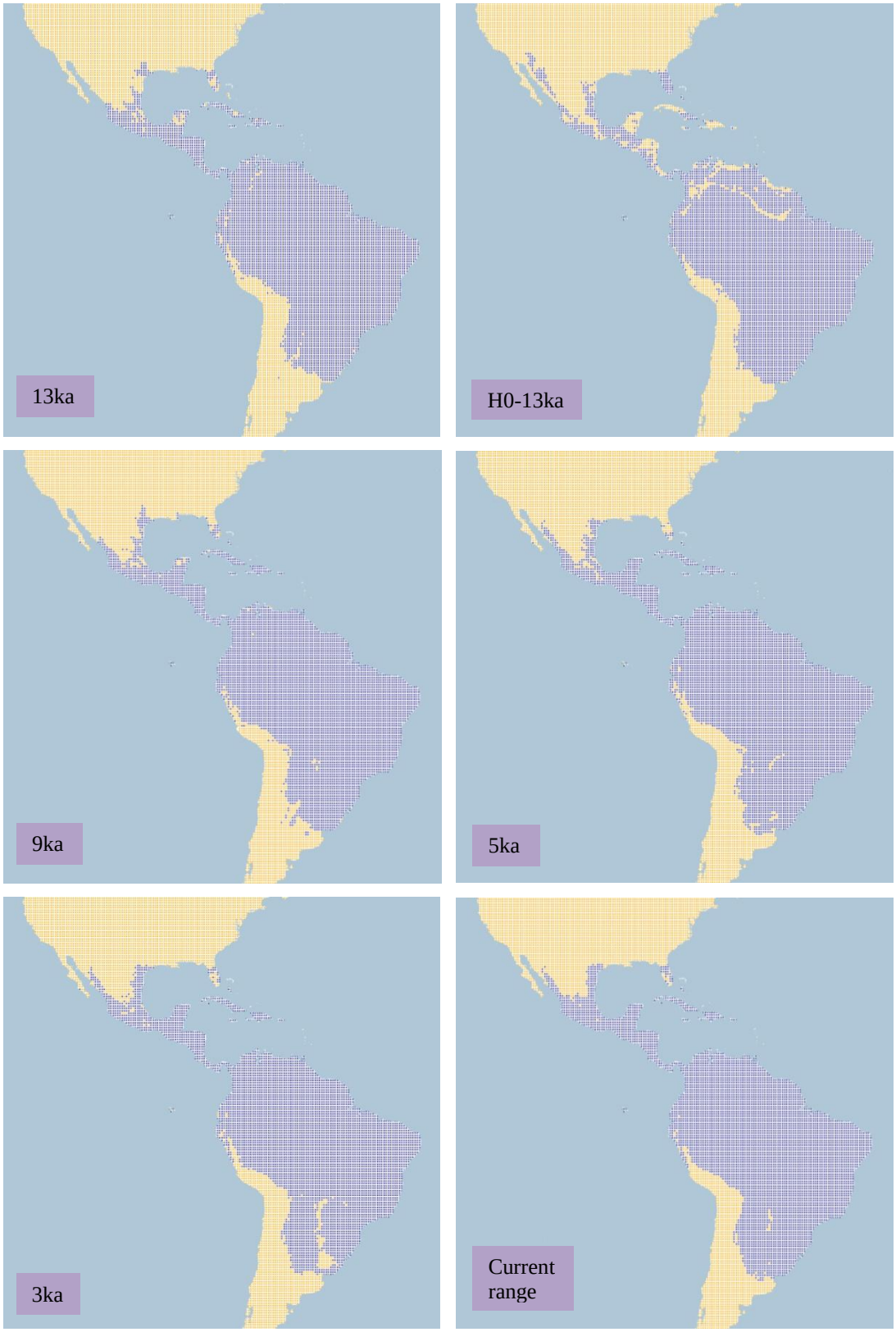

Figure 4.1.4.32.b. Simulation maps of Solitary Sandpiper non-breeding range (continued**).**

4.1.4.33 AUC, TSS and Kappa values

The CRS model performance values of AUC, TSS and Kappa for the family Scolopacidae are shown below, starting with the breeding season and then the non-breeding season as well as with graphs for a better comparison of the values.

The results of the breeding range model values show a better performance for AUC with a median of 0.978, followed by TSS with 0.882 and Kappa with 0.721. AUC values were mainly between 0.951 and 0.996, with the highest values by species Wilson's Snipe (*G. delicata*) with 0.996, followed by American Woodcock (*S. minor*) with 0.995 and Spotted Sandpiper (*A. macularius*) with 0.9949. The lowest AUC values correspond to Surfbird (*C. virgata*) with 0.889, followed by Pectoral Sandpiper (*C. melanotos*) with 0.940 and Red-necked Phalarope (*P. lobatus*) with 0.948. Although these species breed in the Arctic regions of North America they have markedly different ranges and other species of Arctic breeding Shorebirds achieve higher AUC values.

For TSS Buff-breasted Sandpiper (*C. subruficollis*) has the highest value with 0.952, followed by Sanderling (*C. alba*) with 0.943 and American Woodcock (*S. minor*) with 0.943. The lowest values are presented by Surfbird (*C. virgata*) with 0.612, next to Red-necked Phalarope (*P. lobatus*) with 0.731 and Pectoral Sandpiper (*C. melanotos*) with 0.752.

For Kappa the species Wilson's Snipe (*G. delicata*) has the highest value with 0.939, followed by American Woodcock (*S. minor*) with 0.933 and Spotted Sandpiper (*A. macularius*) with 0.930. The lowest Kappa values correspond to species Black Turnstone (*A. melanocephala*) with 0.437, followed by Wandering Tattler (*T. incana*) with 0.469 and Surfbird (*C. virgata*) with 0.517. See Figure 4.1.4.a.

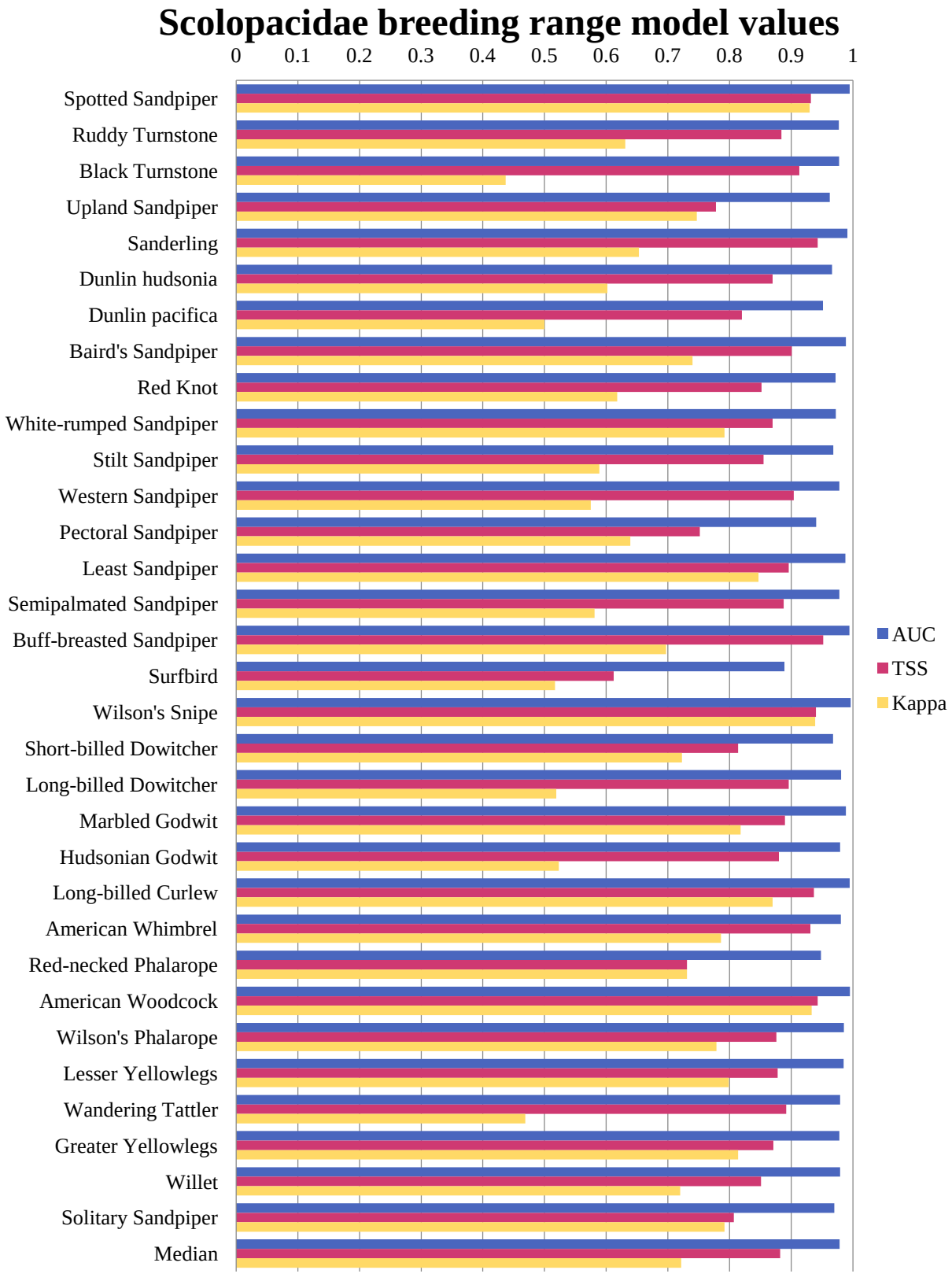

Figure 4.1.4.a. Model performance values of the family Scolopacidae breeding range. The graph shows values for each species of AUC, TSS and Kappa values from the CRS model as well as the median for each statistical measurement.

For the non-breeding range AUC showed the highest values with a median 0.982, followed by TSS with a median of 0.874 and Kappa with a median of 0.760.

For AUC the non-breeding range highest values are from the Spotted Sandpiper (*A. macularius*) with 0.996, followed by Long-billed Curlew (*N. americanus*) with 0.9952 and Lesser Yellowlegs (*T. flavipes*) with 0.9951. The lowest AUC values are presented by species American Whimbrel (*N. p. hudsonicus*) with 0.919, next to Sanderling (*C. alba*) with 0.949, both species have ranges restricted to coastal areas, and Ruddy Turnstone (*A. interpres*) with 0.950.

For TSS the Buff-breasted Sandpiper (*C. subruficollis*) showed the highest value with 0.963, followed by Spotted Sandpiper (*A. macularius*) with 0.955 and Hudsonian Godwit (*L. haemastica*) with 0.955. The lowest TSS values correspond to species American Whimbrel (*N. p. hudsonicus*) with 0.664, followed by Red-necked Phalarope (*P. lobatus*) with 0.724 and Willet (*T. semipalmata*) with 0.758. Once again this probably reflects the restriction of these species' non-breeding ranges to coastal regions, or in the case of the Red-necked Phalarope (*P. lobatus*) to ocean areas that only have a limited intersection with the coast.

The highest values of Kappa for the non-breeding range correspond to species Spotted Sandpiper (*A. macularius*) with 0.947, next to species Lesser Yellowlegs (*T. flavipes*) with 0.941 and species Solitary Sandpiper (*T. solitaria*) with 0.938. The lowest Kappa values are presented by Semipalmated Sandpiper (*C. pusilla*) with 0.451 followed by species Wandering Tattler (*T. incana*) with 0.485 and American Whimbrel (*N. p. hudsonicus*) with 0.502. See Figure 4.1.4.b.

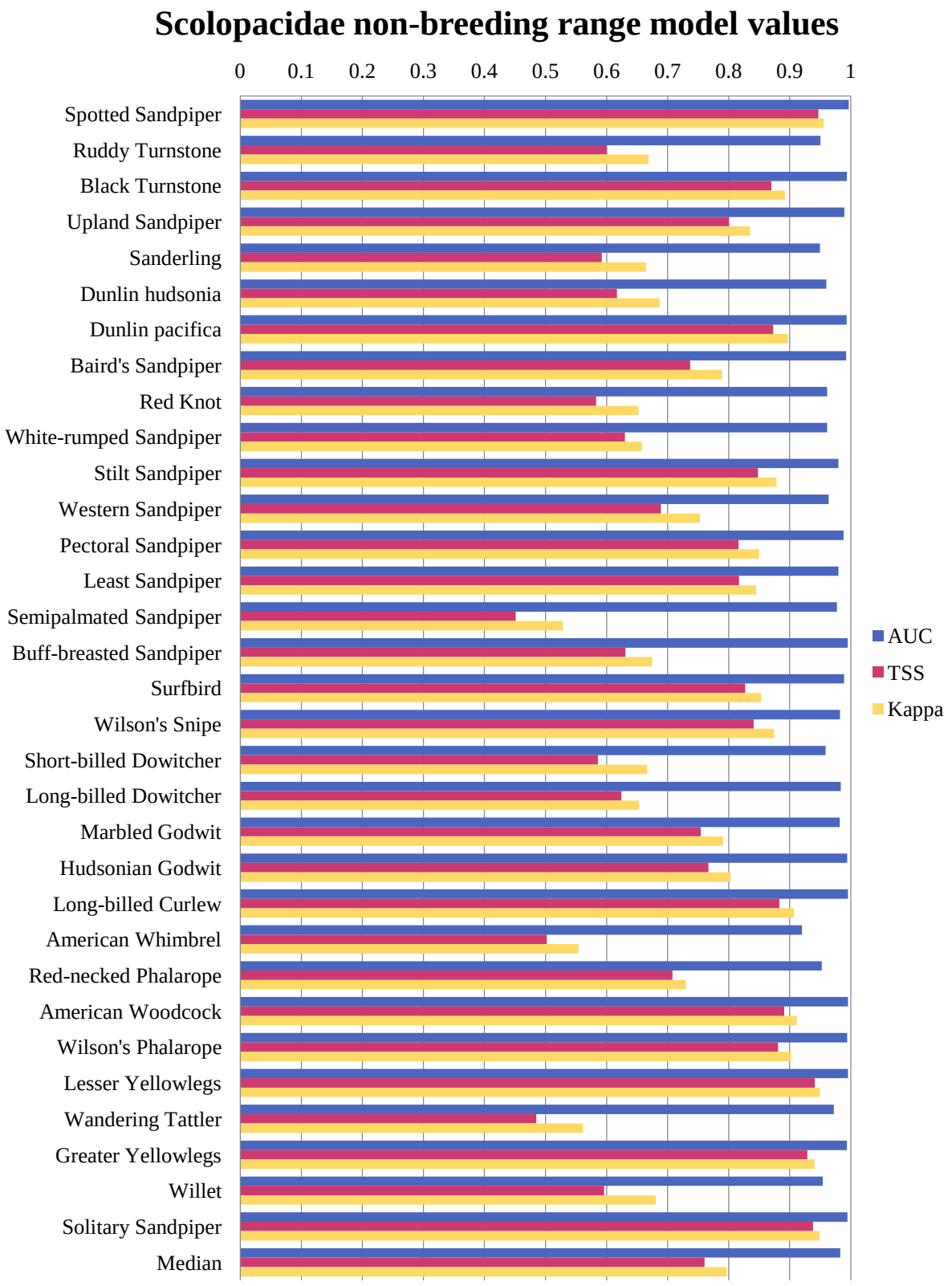

Figure 4.1.4.b. **Model performance values of the family Scolopacidae non-breeding range.**
The graph shows values for each species of AUC, TSS and Kappa values from the CRS model as well as the median for each statistical measurement.

4.1.5 Family Trochilidae

*4.1.5.1 Violet-crowned Hummingbird (*Amazilia violiceps *including* A. v. ellioti *and* A. v. violiceps*). Conservation status: Least Concern. Current known range Figure 4.1.5.1.*

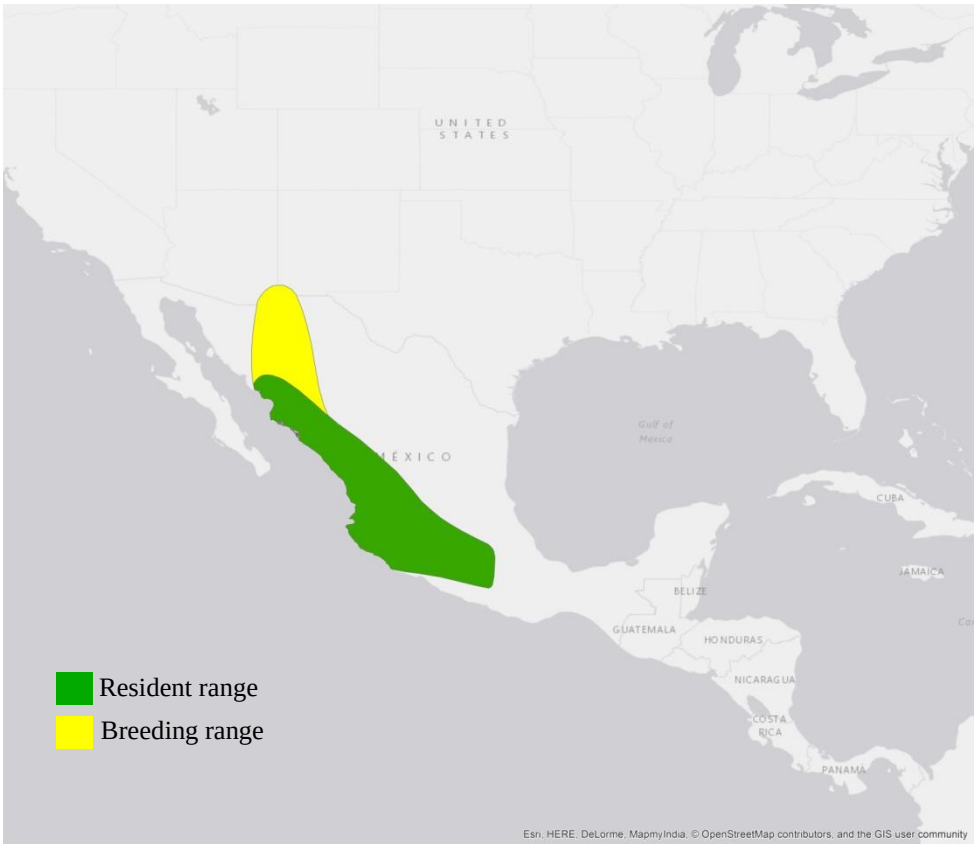

Figure 4.1.5.1. Current range of Violet-crowned Hummingbird.

Breeding range (AUC: 0.996; TSS: 0.951; Kappa: 0.909): The species has a small breeding range in the north-west of Mexico, between Sonora and Chihuahua in the Sierra Madre Occidental and in the south-west of USA between Arizona and New Mexico; the species is also a year-round resident along the west of Mexico from the south of Sonora as far as central Puebla and Oaxaca.

The projection at 26 ka BP shows a range on the west coast of USA and moving to the south between California, Arizona and the border with Mexico, also at a smaller scale in the north-east of Sonora. A larger range is projected in the north-east of Mexico in Tamaulipas and in the central-south part of Mexico, reaching the Pacific coast of Guerrero. The range on the west coast of USA decreases at 24 ka BP and then increases at 22 ka BP. After this the

range projected remains constant with minimal differences especially on the west coast of USA and at 15 ka BP the range increases inland, also in central Mexico reaching as far as Jalisco. See Figure 4.1.5.1.a.

At 14 ka BP the range projected in the central part of Mexico starts increasing towards the west in Sinaloa and in the north of Sonora, on the contrary the range in the north-east of Mexico decreases until 12 ka BP. By 11 ka BP the range increases again in the north-east of Mexico and remains similar along central Mexico and the west coast of USA, only with minimal variation.

The projection at 10 ka BP shows an increase in the range of central Mexico, reaching almost the north of Sinaloa and growing inland as well. At 8 ka BP the range reaches the north of Mexico in Sonora, increasing inland as far as Oaxaca, but disappearing from the north-east in Tamaulipas.

By 7 ka BP the range on the west coast of USA increases inland and as far as the border with Canada. Also, the range in the east of Mexico returns, from the north of Veracruz to central Tamaulipas. After this, the projections show similar conditions until 1 ka BP, only with minimal variations in the territory of the north-east of Mexico, and consistent with the current projected range.

Comparison between the Heinrich event H2 and the 24 ka BP projection illustrate differences particularly in the south-west and west coast of USA and the north-west of Mexico, where the range at H2 is present, unlike 24 ka BP, where the range is restricted to the east and central Mexico. The same behaviour remains at H1 with an increase in the range projected in the north-west of Mexico and with a range reaching the south-east of USA as far as Florida. At H0 the range reduces on the south-east coast of USA, and increases along the west coast, also, extending in almost all Mexico, from Baja California to Chiapas, differing from 13 ka BP with a concentrated range in central Mexico.

There are suitable conditions presented in South America along the projections, along the Andean cordillera and in the north of Brazil, even though the range is restricted to Mexico.

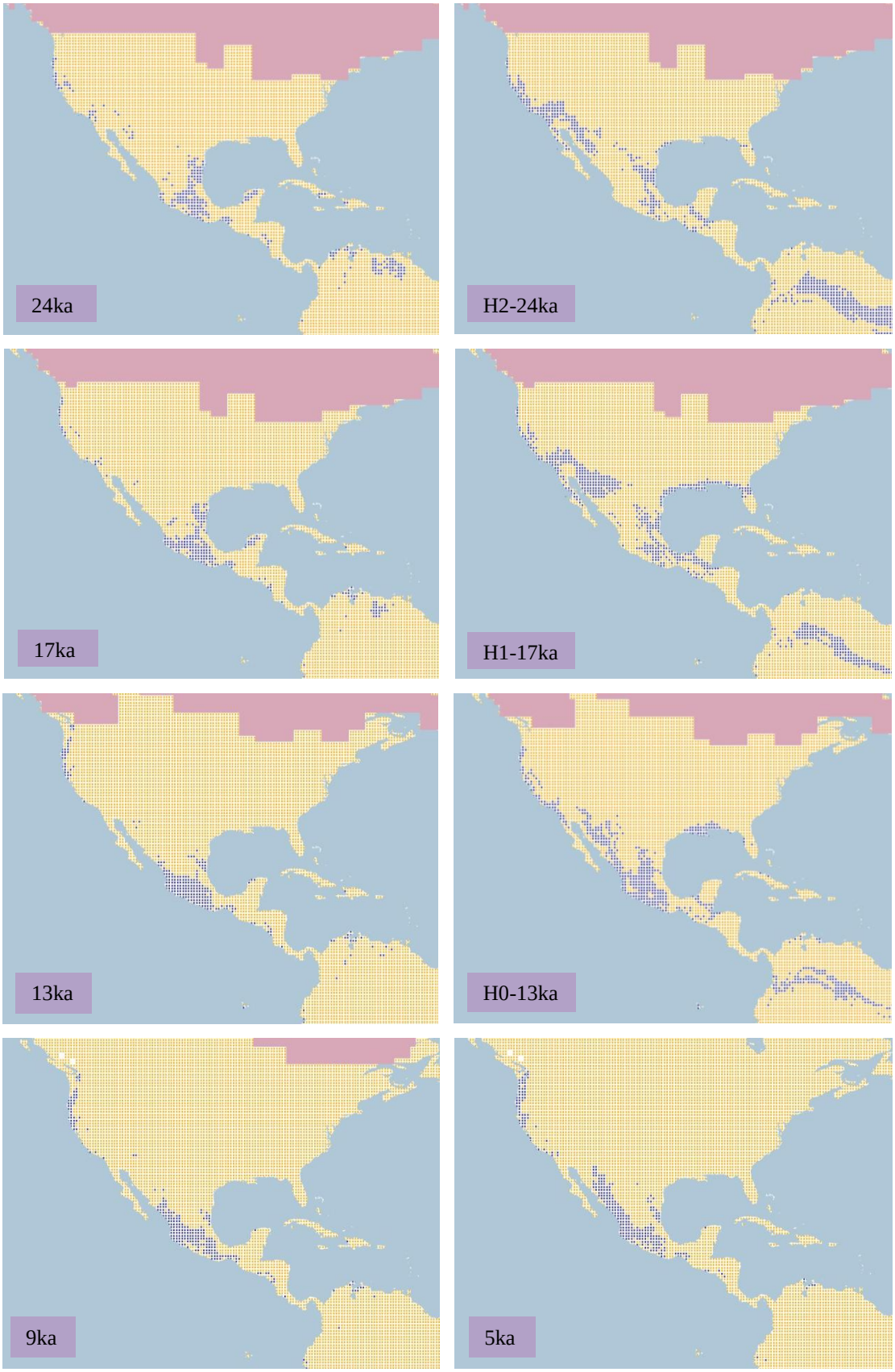

Figure 4.1.5.1.a. Simulation maps of Violet-crowned Hummingbird breeding range. Maps are shown for ten-time slices: 24ka, H2 (24ka), 17ka, H1 (17ka), 13ka, H0 (13ka), 9ka, 5ka, 3ka and present (1961–90).

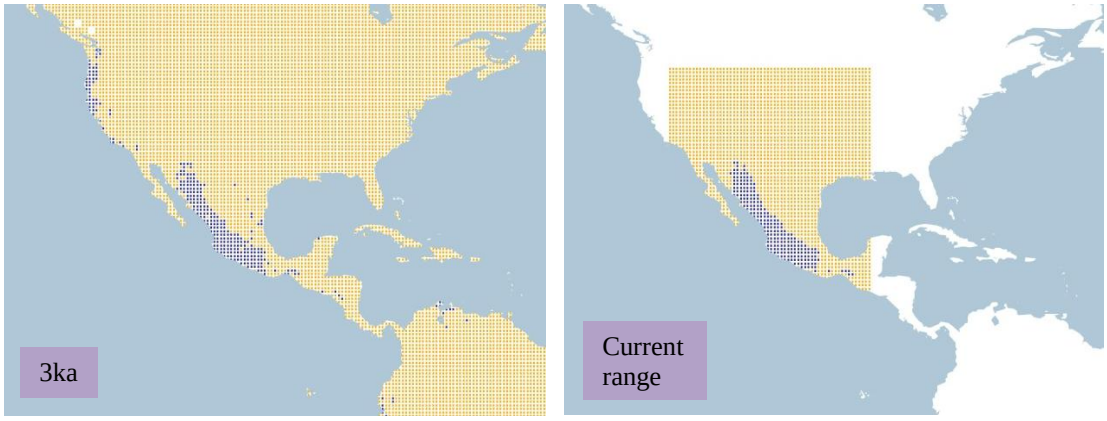

Figure 4.1.5.1.a. Simulation maps of Violet-crowned Hummingbird breeding range (continued**).**

Non-breeding range (AUC: 0.998; TSS: 0.976, Kappa: 0.931): This species is a year-round resident of Mexico on the Pacific coast and moving inland from the south of Sonora as far as Puebla and the north of Oaxaca.

At 26 ka BP the range is projected in central Mexico, from Estado de Mexico to Guerrero and Oaxaca and to the north-east to Tamaulipas. Similar projection is shown at 24 ka BP with presence also in the south of Chiapas and the north of Yucatan. At 21ka there is a growth across Jalisco as far as the Pacific coast. This pattern continues with minimal variation until 14 ka BP when the range increases towards the south of Sinaloa and establishing across the Pacific coast and the Sierra Madre del Sur as far as Chiapas. See Figure 4.1.5.1.b.

At 12 ka BP the range remains from Sinaloa to the south of Chiapas and decreases in the north-east of Mexico, which changes at 11 ka BP increasing in Tamaulipas again. By 10 ka BP the range growths to the north of Sinaloa, and to the south of Mexico reaching the south of Guatemala. This increases at 8 ka BP reaching central Sonora, following the Sierra Madre Occidental and the Sierra Madre del Sur in Mexico. This continues until 6 ka BP with a decrease in Guerrero, returning at 5 ka BP to that area and also to Tamaulipas, which remains with minimal differences until 1 ka BP, and showing the same pattern in the current non-breeding projection.

H2 and 24 ka BP show different projections in Mexico, especially as H2 projects suitable conditions in the north of Sonora as far as the south of Arizona and a scattered range in the east of Mexico from Tamaulipas to Hidalgo and Puebla, and also in the south of Campeche

and Guatemala. The H1 projection grows in the north of Mexico and along the Pacific coast of Baja California and California, and on the south-east coast of USA and a scattered range in the east of Mexico as far as Guatemala and Belize. H0 presents similar range to 13 ka BP in the central part of Mexico except the range at H0 is also projected in the north of Mexico in Sonora and in the south of Campeche and a minimal range on the south-east and west coast of USA.

Along the projections there are suitable conditions shown in the Andean cordillera, the north of Brazil and in Venezuela and Colombia in South America, and on the north-west coast of USA, although the species is resident of Mexico.

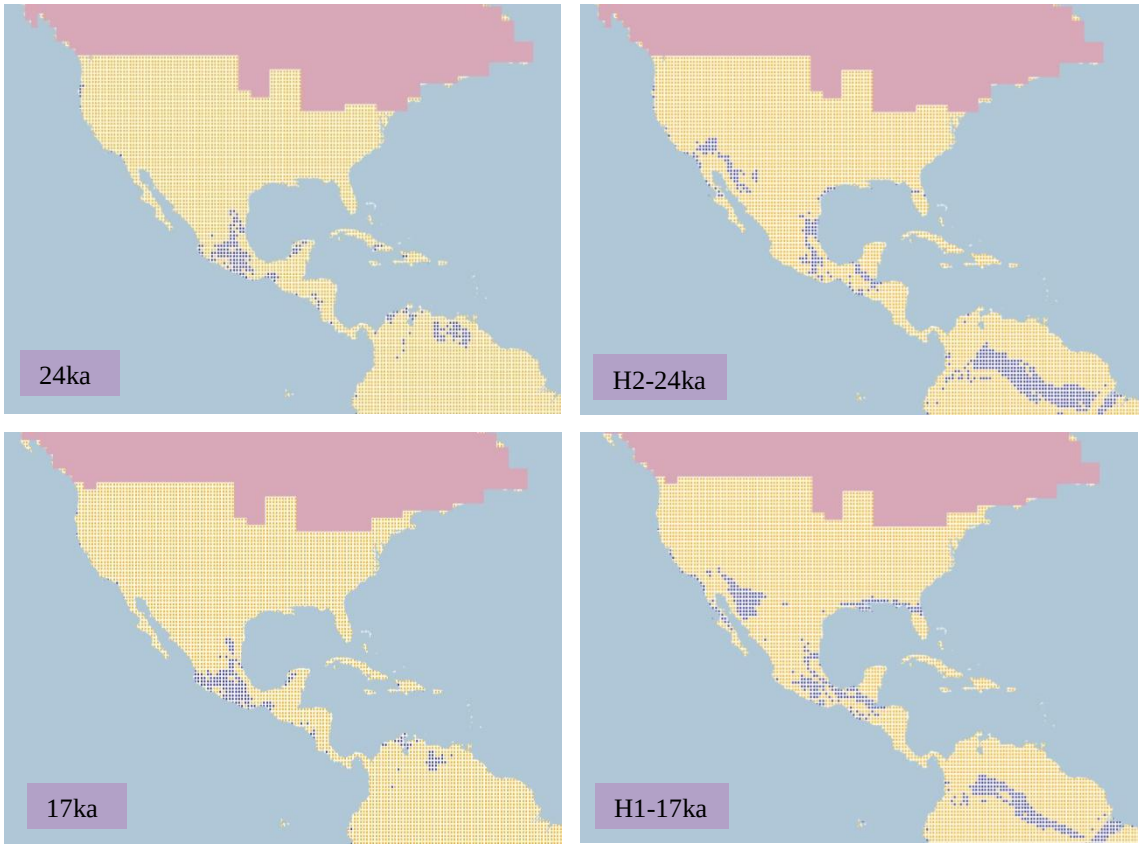

Figure 4.1.5.1.b. Simulation maps of Violet-crowned Hummingbird non-breeding range. Maps are shown for ten-time slices: 24ka, H2 (24ka), 17ka, H1 (17ka), 13ka, H0 (13ka), 9ka, 5ka, 3ka and present (1961–90).

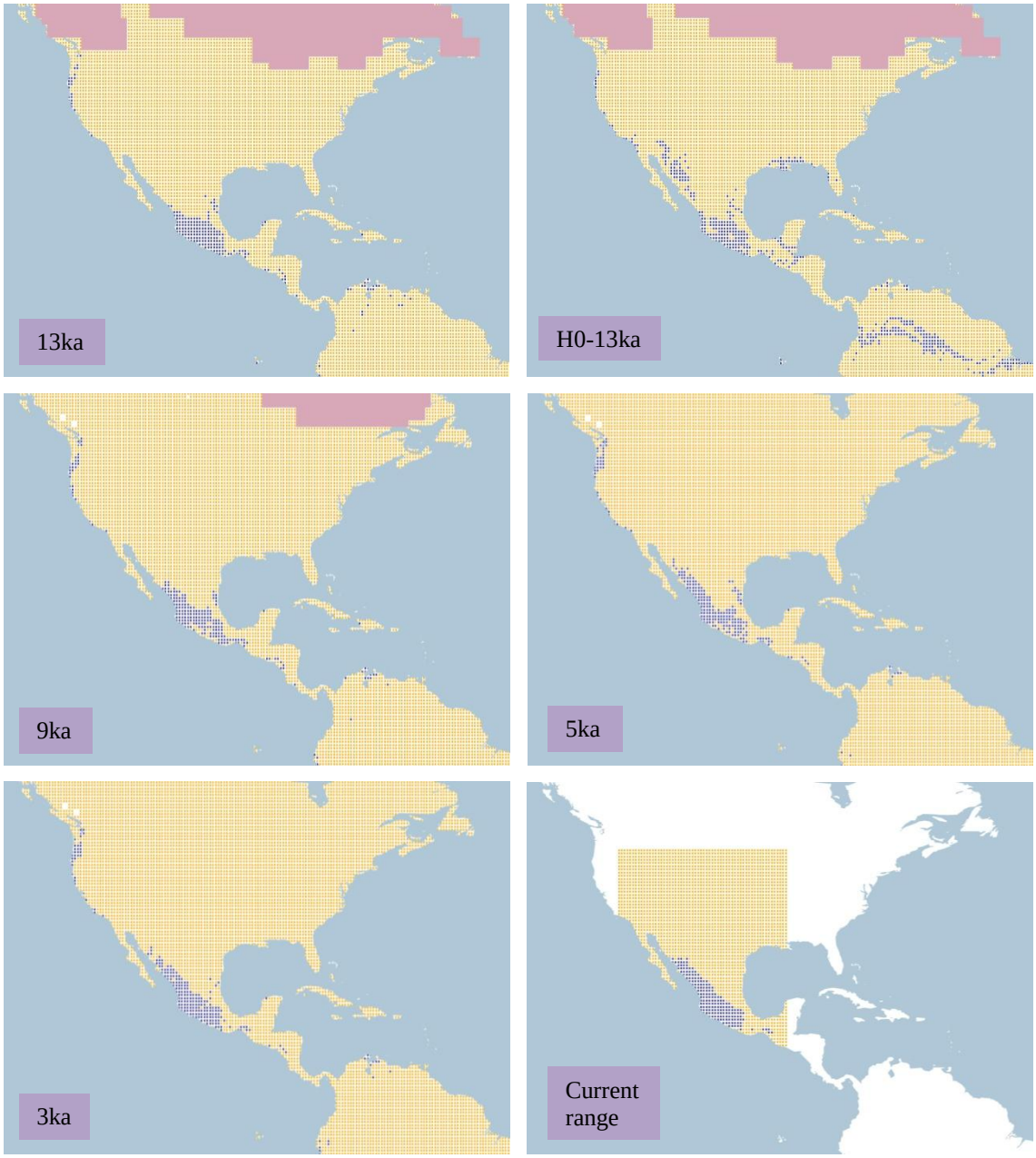

Figure 4.1.5.1.b. Simulation maps of Violet-crowned Hummingbird non-breeding range (continued**).**

*4.1.5.2 Buff-bellied Hummingbird (*A. yucatanensis *including* A. y. chalconota, A. y. cerviniventris *and* A. y. yucatanensis*). Conservation status: Least Concern. Current known range Figure 4.1.5.2.*

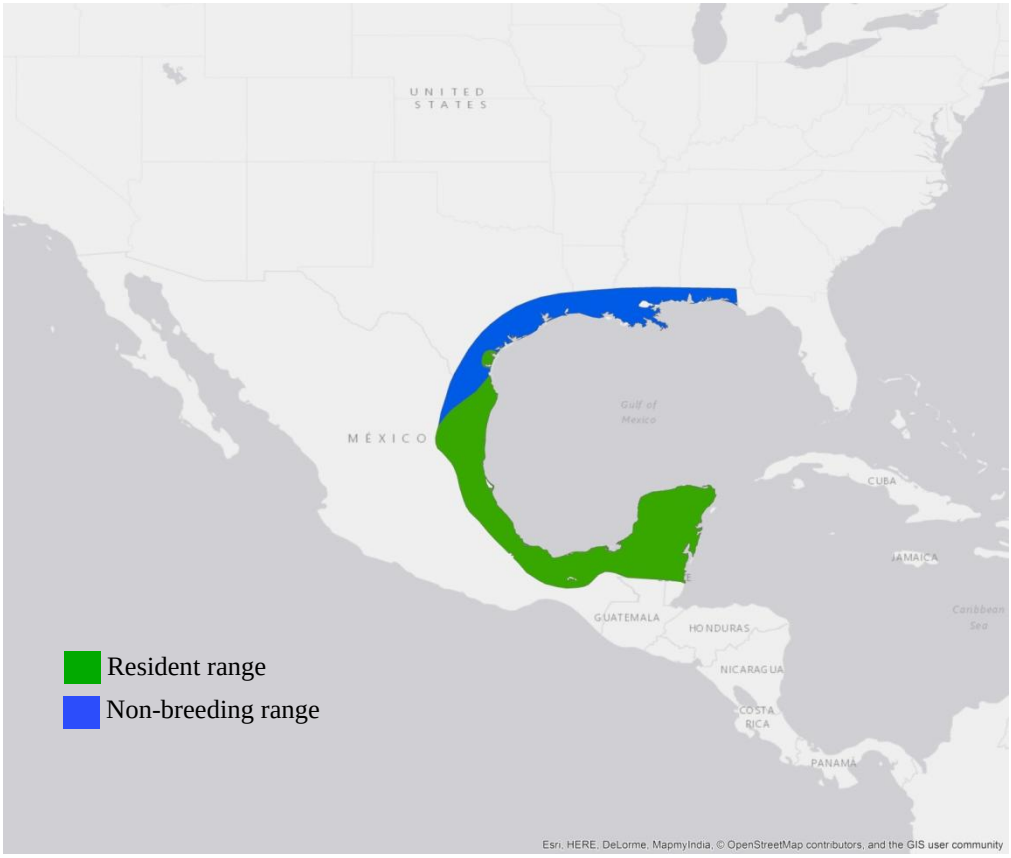

Figure 4.1.5.2. Current range of Buff-bellied Hummingbird.

Breeding range (AUC: 0.985; TSS: 0.905; Kappa: 0.745): The species has year-round grounds along the east coast of Mexico, covering a small part from the south of Texas, to Tamaulipas, Veracruz, Tabasco, Campeche, Yucatan and the north of Guatemala and Belize.

The range at 26 ka BP is projected in Mexico from Veracruz to the coast of Tabasco, the south of Campeche and across Yucatan; at a smaller scale there is range projected in the south of Florida and scattered range in Cuba, Haiti and Dominic Republic. The similar projections continue until 18 ka BP with a rise in the range projected in Campeche and Yucatan, reaching also the north of Belize, Honduras and Nicaragua. See Figure 4.1.5.2.a.

By 16 ka BP the range in the south of Florida decreases as well as the one in Cuba, Haiti and Dominican Republic, increasing on the Caribbean coast of Honduras and Nicaragua. This

continues until 14 ka BP when the range projected in Central America decreases and moves inland, also the range in the south of Mexico decreases and in Florida the range is not present.

By the beginning of the Holocene the range is projected from Tamaulipas to Campeche and the south of Yucatan with a scattered and minimal range in Florida, Haiti and Dominican Republic. This pattern continues until 8 ka BP when the range projected in Yucatan increases, and until 3 ka BP the range along the east coast of Mexico increases inland as well. After this, the range remains with the same pattern which is shown also in the current breeding range.

The Heinrich event H2 when compared with the 24 ka BP projection shows similarities in the territory projected on the east of Mexico, especially in Veracruz, although the range at 24 ka BP extends as far as Yucatan, and the range at H2 increases at the north-east in Tamaulipas. Similar patterns are shown in H1 and 17 ka BP, only that 17 ka BP projects a wider territory in the south of Mexico and in Central America. Finally, H0 and 13 ka BP also display similarities in the projections, only with minimal differences in the south of Mexico.

Although the breeding range of this species is restricted to Mexico, there are suitable conditions shown across the projections in South America, mainly in the Andean cordillera, Chile, Bolivia, Paraguay, Uruguay, the south of Brazil and north of Argentina. In North America there are suitable conditions shown in Florida and in Cuba, Jamaica, Haiti and Dominican Republic.

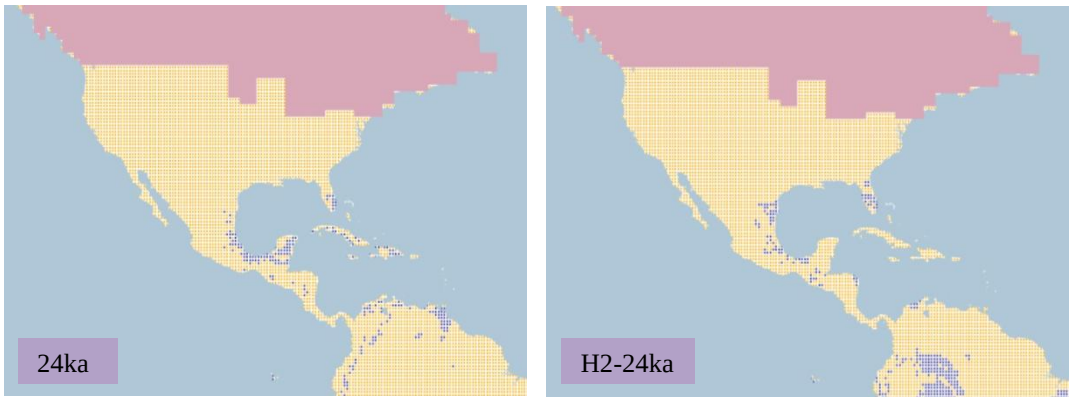

Figure 4.1.5.2.a. Simulation maps of Buff-bellied Hummingbird breeding range.
Maps are shown for ten-time slices: 24ka, H2 (24ka), 17ka, H1 (17ka), 13ka, H0 (13ka), 9ka, 5ka, 3ka and present (1961–90).

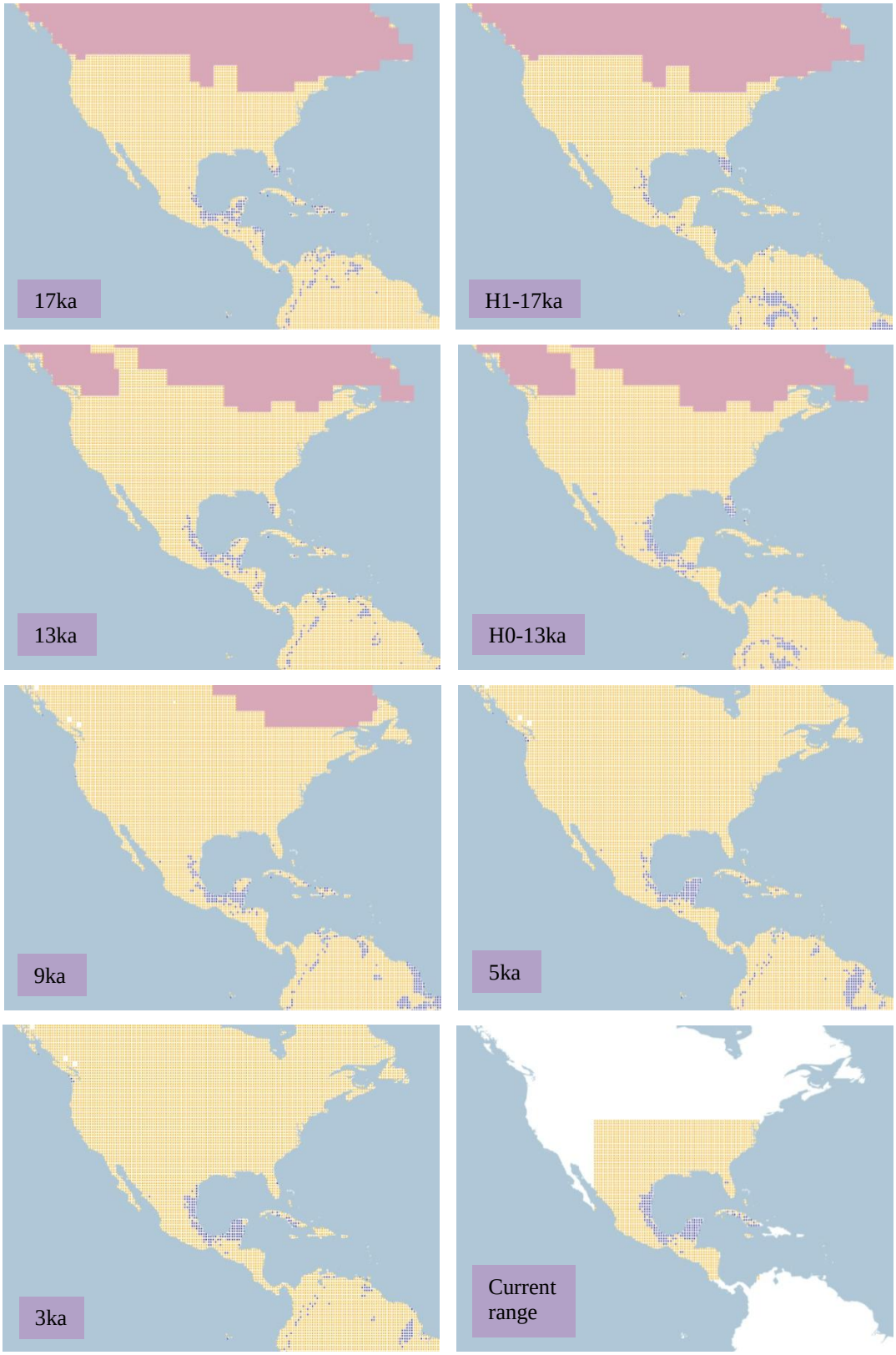

Figure 4.1.5.2.a. Simulation maps of Buff-bellied Hummingbird breeding range (continued**).**

Non-breeding range (AUC: 0.969; TSS: 0.853; Kappa: 0.690): The non-breeding range of this species is found from the north-east of Mexico in Nuevo Leon and along the south-east coast of USA, from Texas to the north of Florida. There is also a resident range along the east coast of Mexico from Tamaulipas to Yucatan and reaching the north of Guatemala and Belize.

The range is projected in the south-east of Mexico from Veracruz to Campeche and Yucatan at 26 ka BP. There is also range projected in the south of Florida. This pattern remains similar with minimal variations along the projections until 18 ka BP when the range in the south of Mexico extends towards Central America increasing even more at 16 ka BP and 15 ka BP. After this at 14 ka BP the range in Central America decreases and by the beginning of the Holocene the range is shown dispersive along the east coast of Mexico, moving inland. See Figure 4.1.5.2.b.

By 8 ka BP the range in Mexico increases along the east coast from Tamaulipas to Yucatan, and also moves inland. In the USA the range increases in the south of Louisiana and Texas. This pattern continues and until 5 ka BP the range on the south-east coast of USA from Texas to Louisiana increases. After this, the same pattern continues and increases on the south-east coast of USA until 1 ka BP and a similar range is shown in the current non-breeding range projection.

As with the breeding range, the Heinrich event projections are similar with the 24 ka BP, 17 ka BP and 13 ka BP projections. H2 and 24 ka BP project range along the east coast of Mexico and in the south of Florida. H1 projects a decrease of the range on the east coast of Mexico and in comparison, with 17 ka BP which shows a range from Veracruz to Yucatan and reaching the north of Guatemala and Belize. H0 and 13 ka BP have similar ranges along the east coast of Mexico and in the south of Florida, only that H0 projects a range in Guatemala and Belize and 13 ka BP projects to the south of Mexico in Campeche and Yucatan.

Once more, the projections display suitable conditions in South America as with the breeding range, mainly in the Andean cordillera and the south of Brazil, Bolivia, Paraguay, north of Argentina and Uruguay.

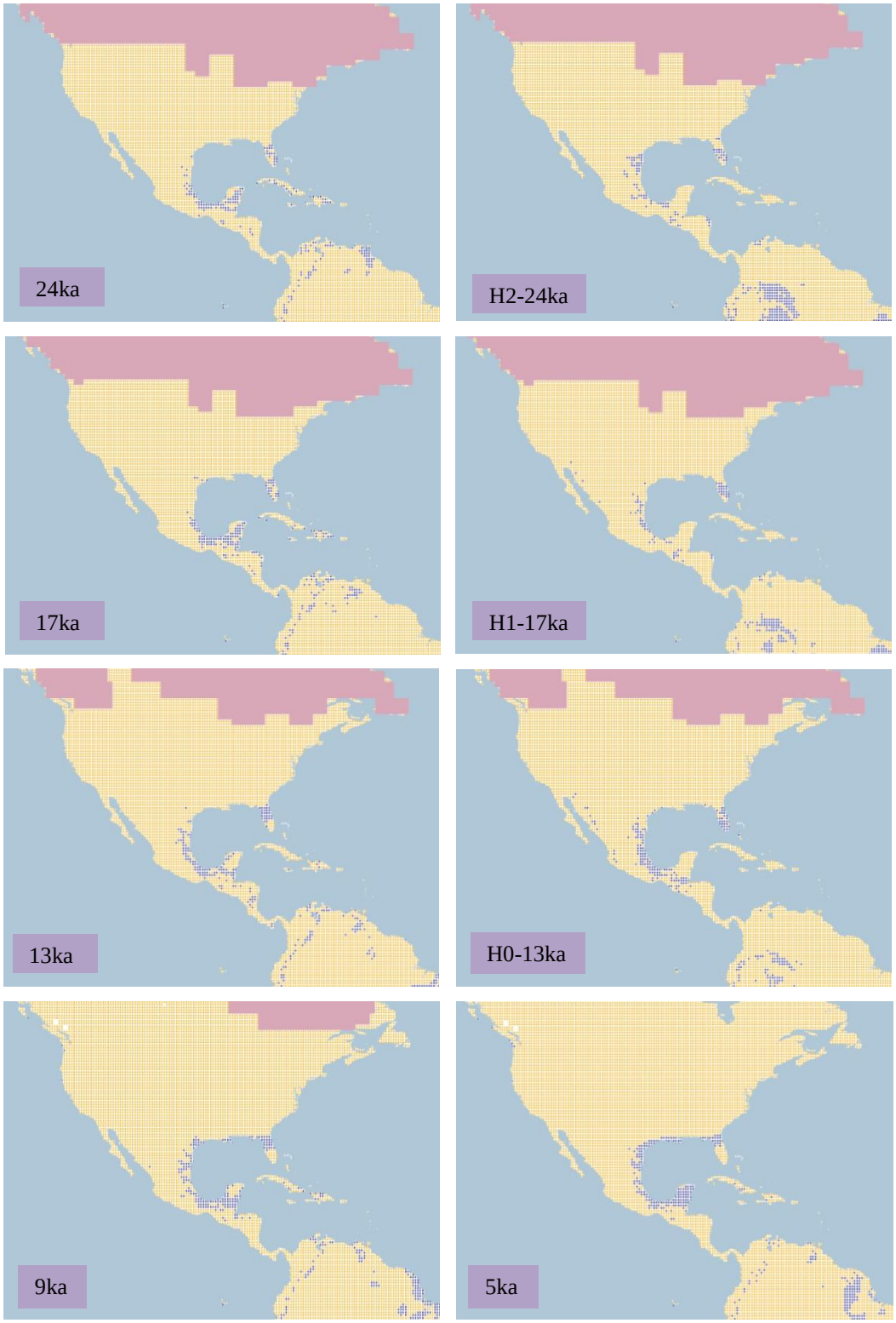

Figure 4.1.5.2.b. Simulation maps of Buff-bellied Hummingbird non-breeding range. Maps are shown for ten-time slices: 24ka, H2 (24ka), 17ka, H1 (17ka), 13ka, H0 (13ka), 9ka, 5ka, 3ka and present (1961–90).

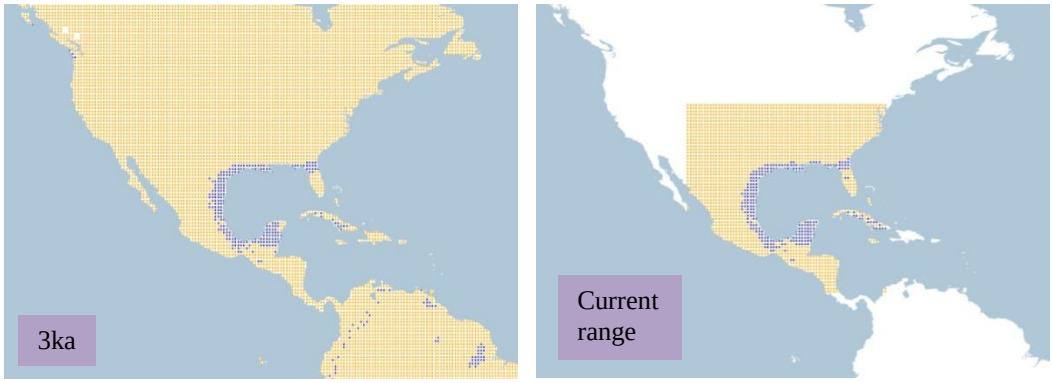

Figure 4.1.5.2.b. Simulation maps of Buff-bellied Hummingbird non-breeding range (continued**).**

*4.1.5.3 Black-chinned Hummingbird (*Archilochus alexandri*). Conservation status: Least Concern. Current known range Figure 4.1.5.3.*

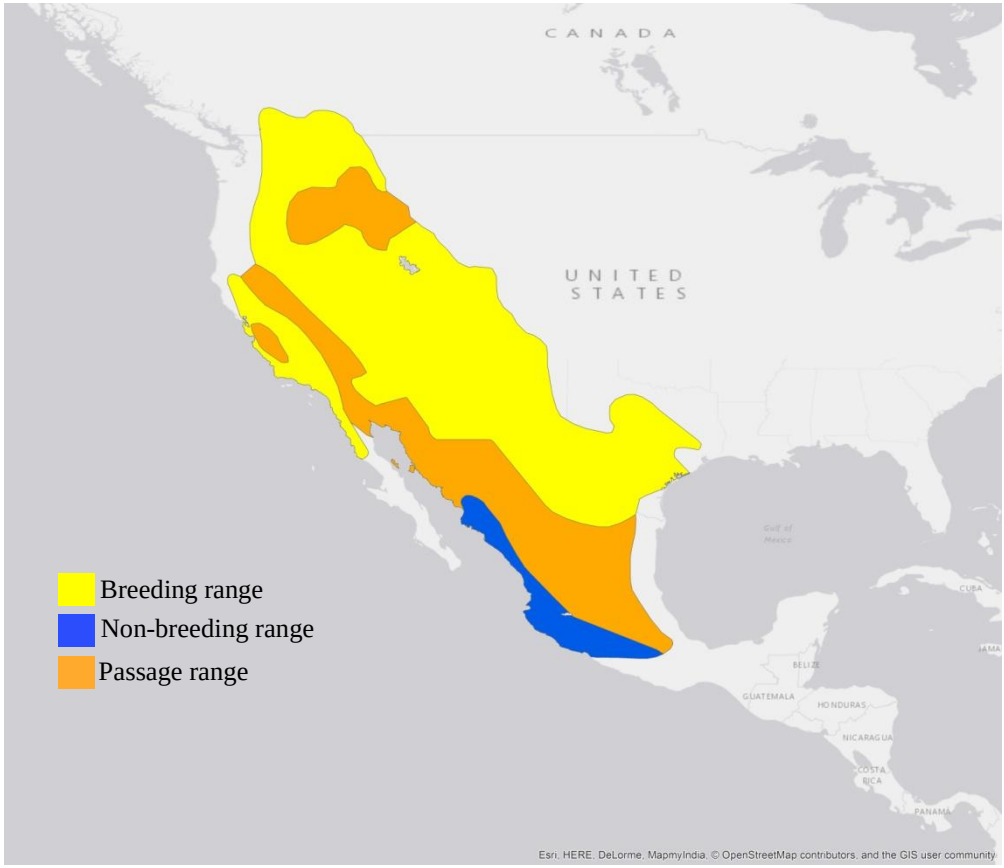

Figure 4.1.5.3. Current range of Black-chinned Hummingbird.

Breeding range (AUC: 0.988; TSS: 0.897; Kappa: 0.861): The species breeds in North America from the south-west of Canada in British Columbia through the Rocky Mountains,

the coastal area of California and along central Texas in USA. Also in the north of Mexico, in Sonora, Chihuahua and extending inland in Coahuila and Nuevo Leon.

The range at 26 ka BP is projected along the Rocky Mountains of USA, from Nebraska and as far as Texas in the central region, and on the west coast of California. The range follows in Mexico from the north-west in Baja California to Nuevo Leon, and down to central Mexico. The pattern continues at 24 ka BP with minimal variation until 15 ka BP, when the range in Texas extends to the south of Louisiana and by 13 ka BP the range reaches central Florida. Se e Figure 4.1.5.3.a.

As the ice sheet retreats in North America the range at 12 ka BP is focused from central to northern Mexico and along the west of USA in the Rocky Mountains and to the south-east in Texas, Louisiana, Mississippi, Alabama and Florida. Also, a small range is projected in Ontario, Canada near the ice sheet. This pattern continues at the beginning of the Holocene and increases in Ontario at 10 ka BP. However, at 9 ka BP the range in Ontario is reduced and by 8 ka BP disappears. Also at 8 ka BP the range on the south-east of USA decreases to the south of Texas. After this, the projected range continues with the same pattern until 1 ka BP and in the current breeding range projection.

The Heinrich event H2 projection shows a different range from 24 ka BP, with the range focused in Mexico from the north in Sinaloa and Chihuahua towards central Mexico, along Baja California at a smaller scale and a scattered range in the USA. The same patterns are projected in H1 with a growing range from west to central USA, which is different from the 17 ka BP range projection. Finally, at H0 the range in Mexico moves from central to the north of Mexico and across the USA to the south-east coast as far as Florida and the range in the western USA remains similar.

Throughout the projections there are suitable conditions projected in South America, from Peru to the south of Argentina, following the Andean cordillera, even though the current breeding range of the species is focused in North America and no populations are known to breed in that area.

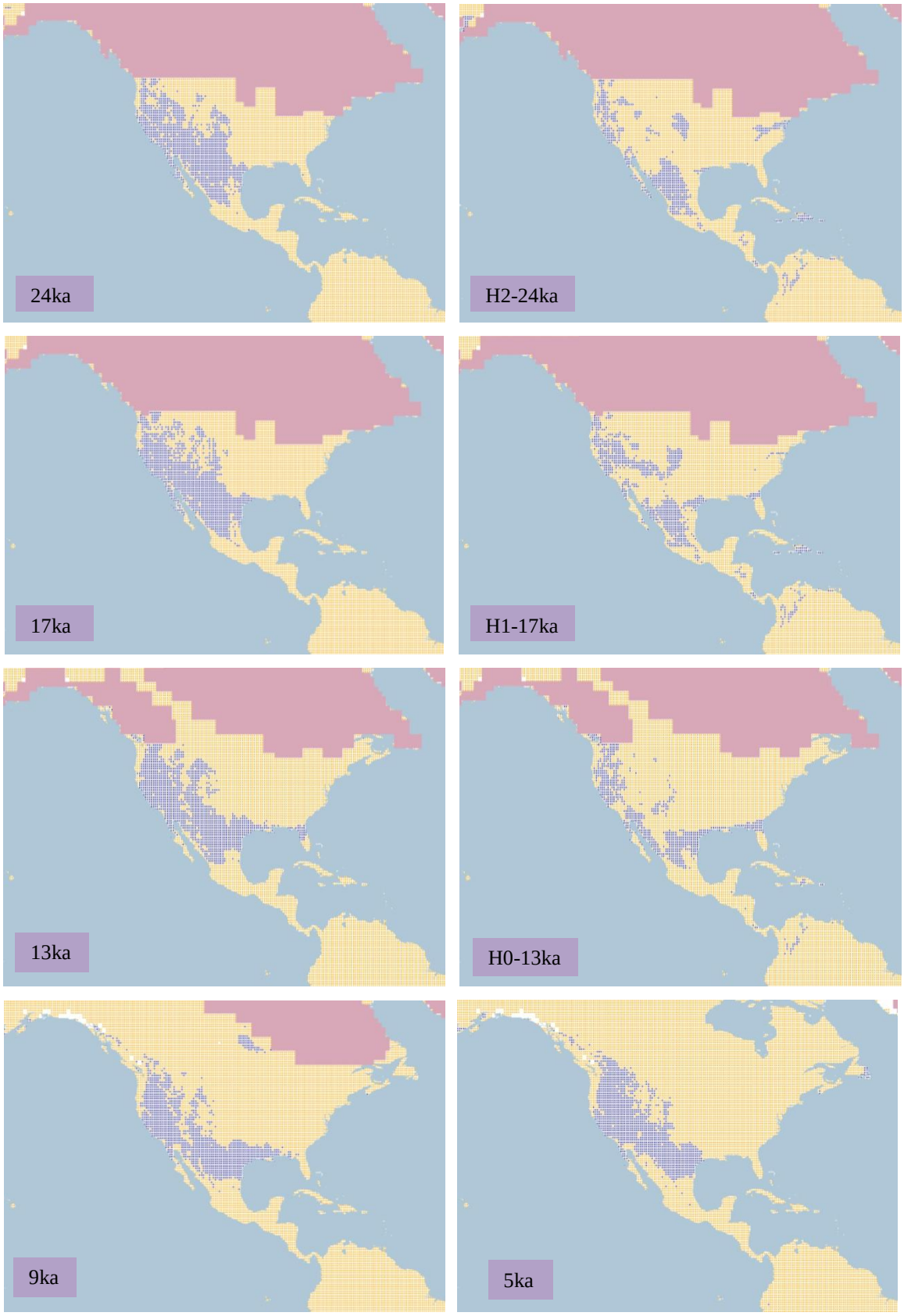

Figure 4.1.5.3.a. Simulation maps of Black-chinned Hummingbird breeding range. Maps are shown for ten-time slices: 24ka, H2 (24ka), 17ka, H1 (17ka), 13ka, H0 (13ka), 9ka, 5ka, 3ka and present (1961–90).

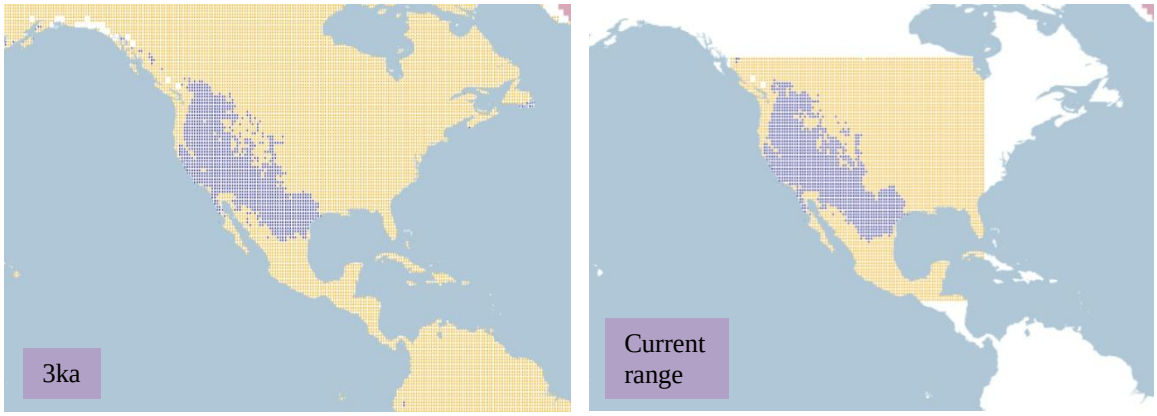

Figure 4.1.5.3.a. Simulation maps of Black-chinned Hummingbird breeding range (continued**).**

Non-breeding range (AUC: 0.999; TSS: 0.995; Kappa: 0.909): The non-breeding range of the species is located in Mexico, from the north-west to south-central, beginning in the south of Sonora down to Puebla and Veracruz.

The projection at 26 ka BP shows a small range in central Mexico, between Tamaulipas and Veracruz in the east and in Jalisco and Guerrero in south-central Mexico. This pattern continues and at 20 ka BP a small range is projected in the south of Texas in USA, and along the coast of Jalisco in Mexico. At 19 ka BP the pattern continues and is also projected in the south of Chiapas. After this, the range continues growing, especially at 15 ka BP when the range in Jalisco converges with the one in Guerrero establishing a range in south-central Mexico. See Figure 4.1.5.3b.

At 13 ka BP the projected range continues in south-central Mexico and the range in the east of Mexico decreases. By the beginning of the Holocene the range expands towards northern territories reaching central Sinaloa and at 8 ka BP the range covers a substantial area of the north-west of Mexico in the sierra of Sonora down to south-central Mexico in Oaxaca. However, there is a decline in the range projected in south-central Mexico, particularly in Jalisco, Guerrero and Oaxaca at 6 ka BP which continues until 3 ka BP with the return of the range in those areas remaining there until 1 ka BP and projected as well in the current non-breeding range.

The H2 projection predicts a different range from 24 ka BP, being located in several areas of Mexico, in the east of Sonora, in the south-east of Tamaulipas and in the south of Campeche. Also, in the south of Texas in the USA and between Guatemala, Belize and Honduras in

Central America; differing from the 24 ka BP projected range in south-central Mexico. This range increases at H1, particularly in Sonora, the south of Campeche moving towards Tabasco, and in the north of Central America. There is also a small range projected in Florida. H0 shows similarities with the 13 ka BP projection in south-central Mexico, covering the area from Jalisco to Oaxaca, although H0 projects a range along Sonora in the north of Mexico.

There are suitable conditions predicted by the projections in South America especially in the central part, between Bolivia, Paraguay and the north of Argentina and, at a smaller scale in the north of Brazil, despite the non-breeding range is known to occur in Mexico.

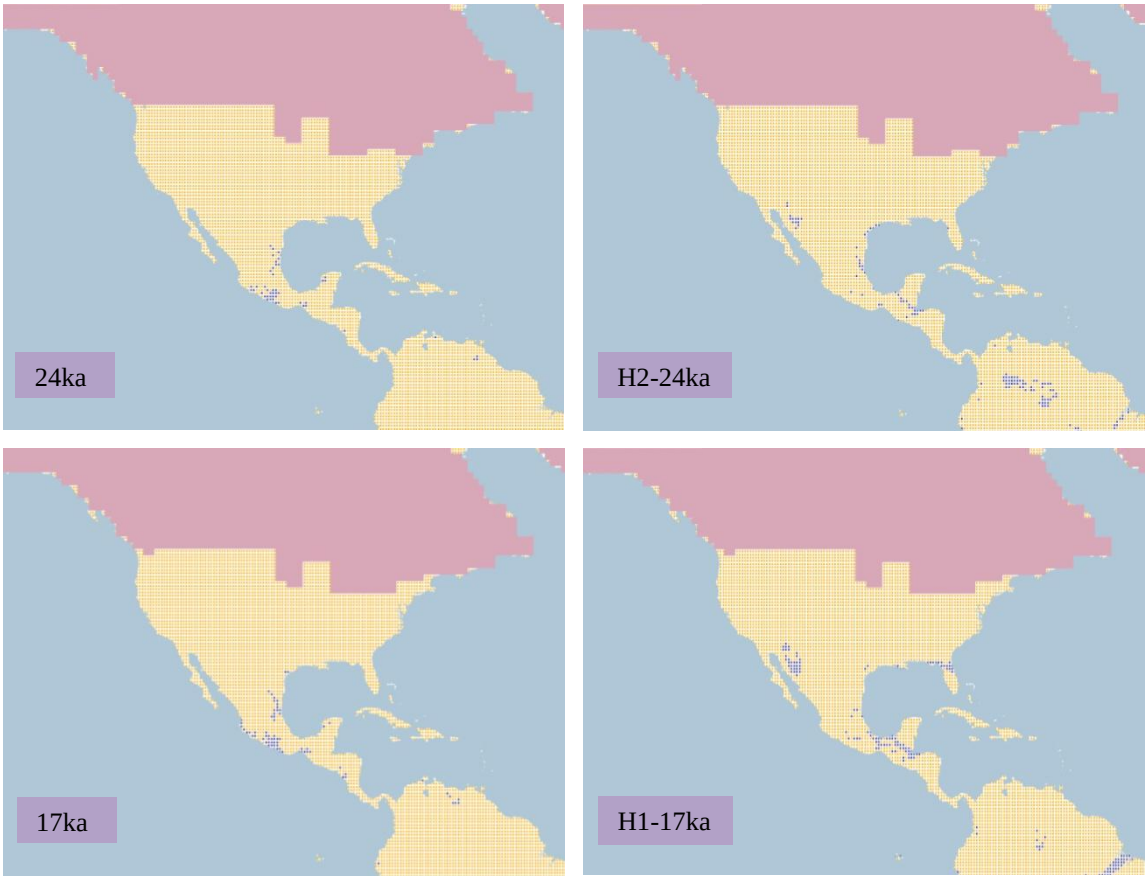

Figure 4.1.5.3.b. Simulation maps of Black-chinned Hummingbird non-breeding range. Maps are shown for ten-time slices: 24ka, H2 (24ka), 17ka, H1 (17ka), 13ka, H0 (13ka), 9ka, 5ka, 3ka and present (1961–90).

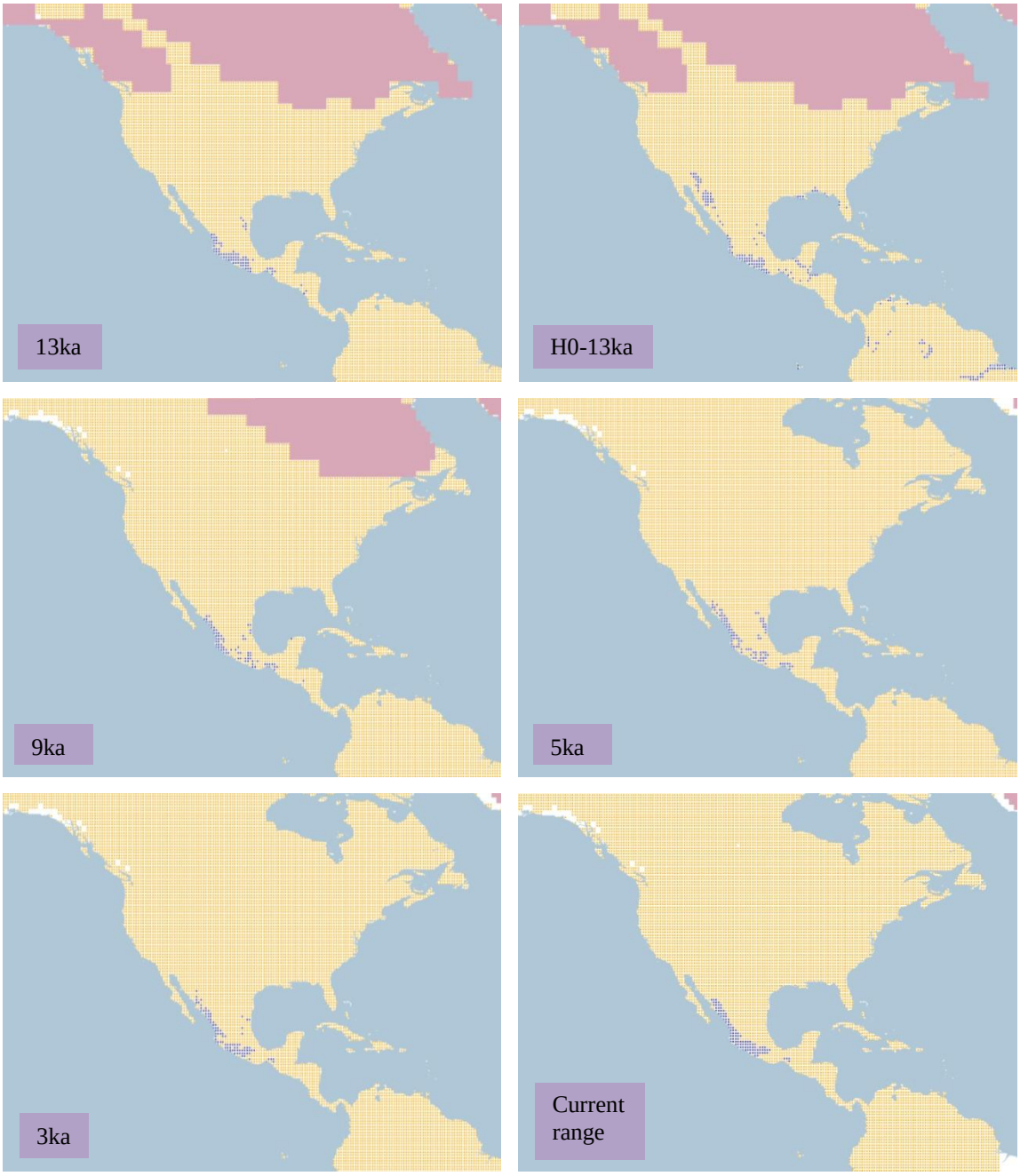

Figure 4.1.5.3.b. Simulation maps of Black-chinned Hummingbird non-breeding range (continued**).**

*4.1.5.4 Ruby-throated Hummingbird (*Archilochus colubris*). Conservation status: Least Concern. Current known range Figure 4.1.5.4.*

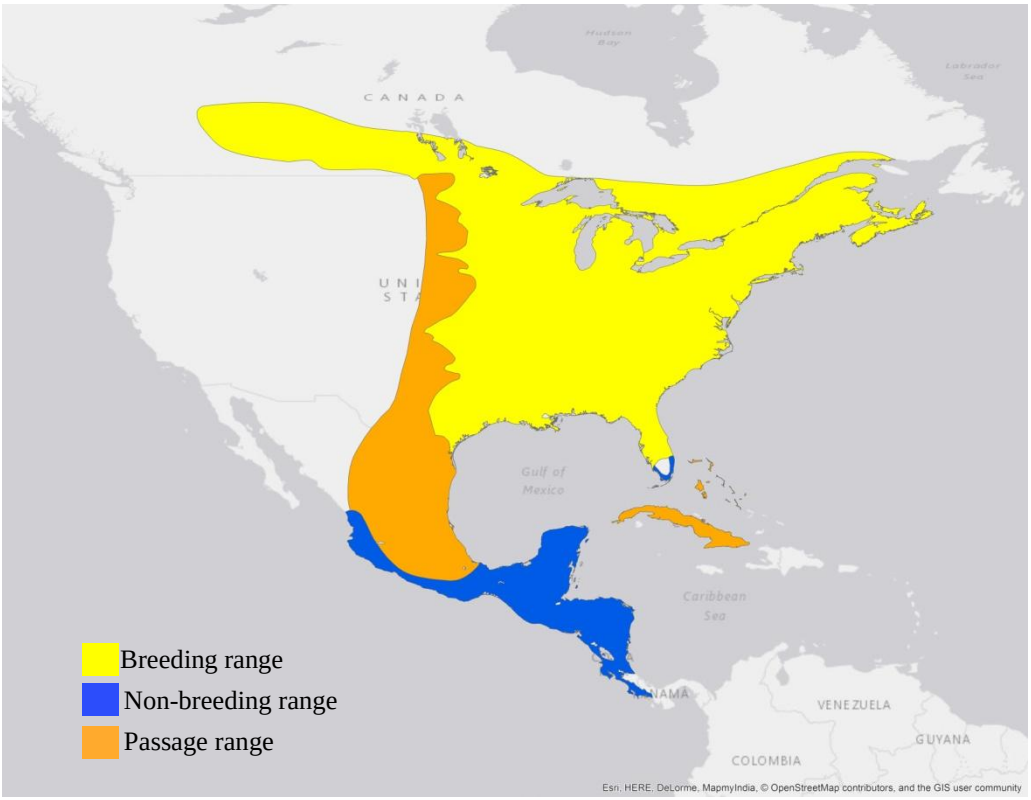

Figure 4.1.5.4. Current range of Ruby-throated Hummingbird.

Breeding range (AUC: 0.993; TSS: 0.924; Kappa: 0.913): The breeding range of the species is located from central to east of USA, and in the south of Canada from central Alberta to Nova Scotia.

At 26 ka BP the range is projected in North America, mainly from central to the east of USA and a small range in the north of Alaska and as far as north Canada in the areas not covered by the ice sheet in the Yukon and the Northern Territories. The pattern continues after this, extending on the north coast of Alaska at 20 ka BP, and decreasing in the north of Canada at18ka, also, the range in central USA increases to the north as far as Montana. See Figure 4.1.5.4.a.

By 16 ka BP and with the reduction of the ice sheet the range projected in the north of USA moves to south-central Canada and particularly in 14 ka BP the range in Alberta increases and in the north of Canada reduces, as well as on the northern coast of Alaska. After this at

12 ka BP, the range in north Canada is restricted to small areas on the northern islands of the Northern Territories, and in the north of Yukon, disappearing as well in Alaska.

At the beginning of the Holocene the range in Yukon increases and in the east of USA, reaching the south-east of Canada as far as Newfoundland. This pattern continues with minimal differences and at 6 ka BP the range on the northern coast of Alaska returns and in Yukon the range increases until 1 ka BP. The current breeding range projection presents a similar pattern to 1 ka BP in the area of south-central Canada and from central to the east of USA, except 1 ka BP predicts suitable conditions in the north of Canada, particularly across Yukon.

Comparison between the Heinrich event H2 and 24 ka BP shows similarities in the areas from central to east USA although with a more restricted range than at 24 ka BP and not moving to south-central Canada. Also, at H2 the range in the north of Canada extends to central Alaska as well. This change at H1 which when compared with 17 ka BP present similar range in the north of Canada except in the territory from central USA that extends towards central-west at H1. H0 does shows a similar range with 13 ka BP across Canada and from central to east of USA, except in predicts a range to the west from Wyoming to Arizona and New Mexico, extending to Sonora in Mexico.

There are suitable conditions predicted throughout the projections in the south of Brazil, even though the breeding grounds of the species are located in North America.

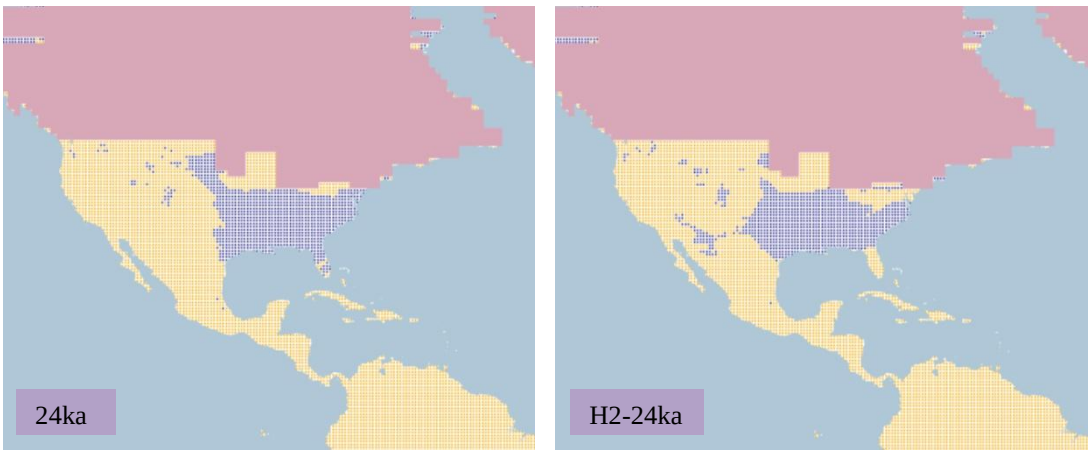

Figure 4.1.5.4.a. Simulation maps of Ruby-throated Hummingbird breeding range. Maps are shown for ten-time slices: 24ka, H2 (24ka), 17ka, H1 (17ka), 13ka, H0 (13ka), 9ka, 5ka, 3ka and present (1961–90).

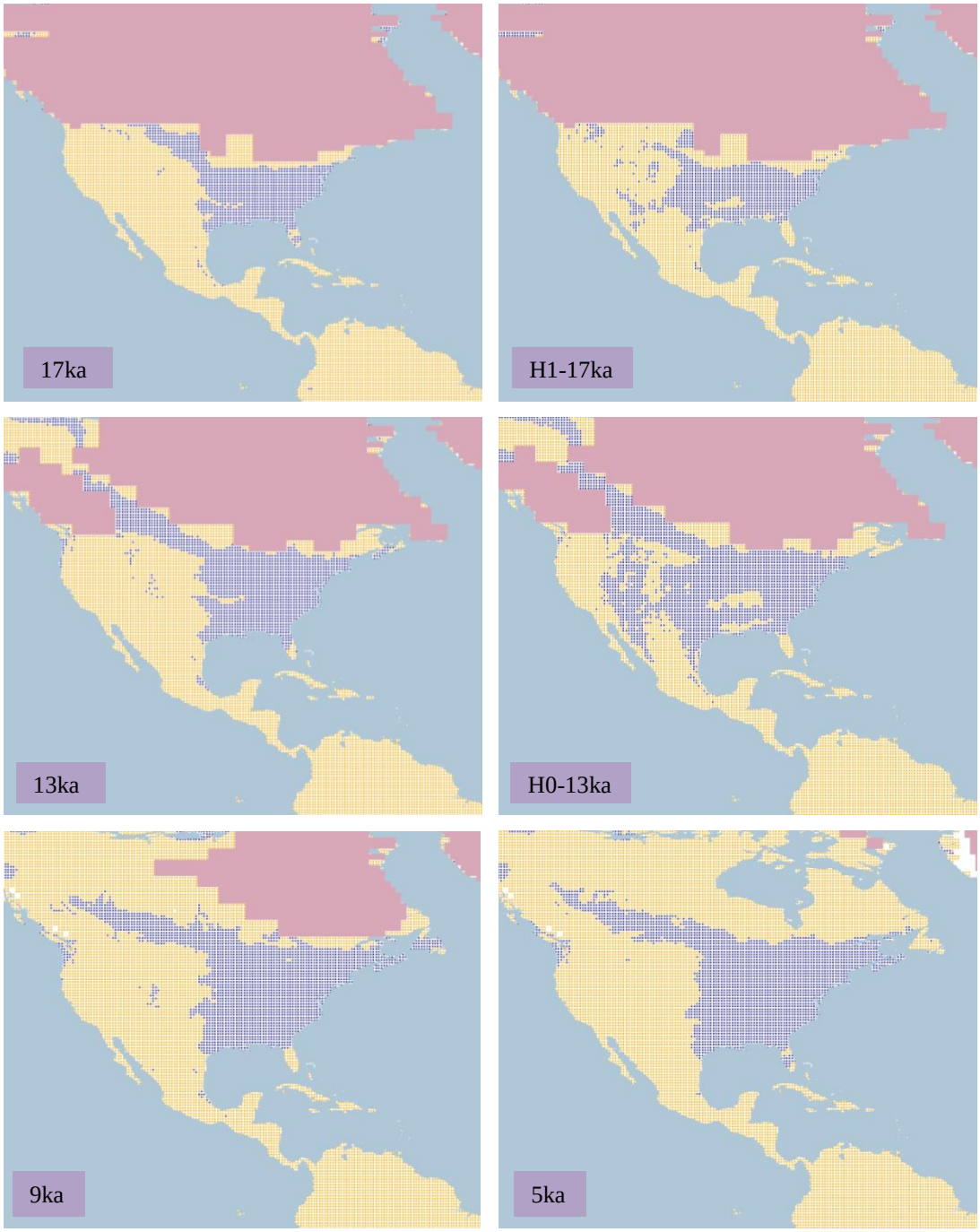

Figure 4.1.5.4.a. Simulation maps of Ruby-throated Hummingbird breeding range (continued**).**

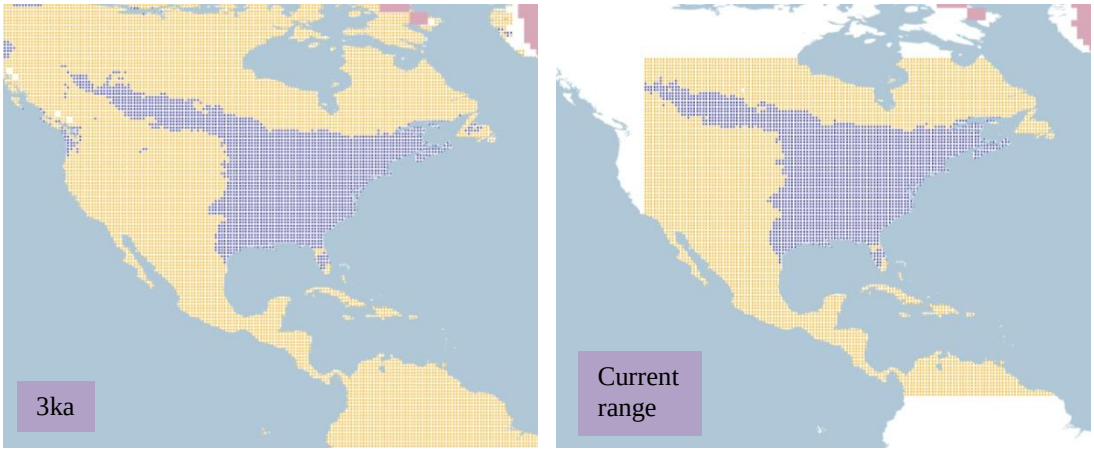

Figure 4.1.5.4.a. Simulation maps of Ruby-throated Hummingbird breeding range (continued**).**

Non-breeding range (AUC: 0.988; TSS: 0.919; Kappa: 0.749): The species spends the non-breeding season in central to south Mexico from the south of Sinaloa, the Sierra Madre del Sur down to Chiapas, Campeche and Yucatan, also in Central America as far as central Panama and a small range along the coast of Florida.

At 26 ka BP the range is projected from south-central Mexico in the Sierra Madre del Sur, and from south Veracruz to Campeche down to Central America in central Nicaragua. The range in Central America increases at 21ka reaching the south of Panama and extending to the north of South America in Colombia and Venezuela. This pattern continues with minimum differences and a small range is projected at 14 ka BP in the south of Florida. See Figure 4.1.5.4.b.

At 10 ka BP the range is projected from central Sinaloa to south-central Oaxaca and from the south of Veracruz to Tabasco, Campeche and in Central America as far as the south of Nicaragua. The pattern continues and there is a minimal variation in the south of Florida from 8 ka BP onwards. The range increases in the central-south Mexico and Central America as far as Nicaragua at 5 ka BP and remains without drastic changes until 1 ka BP which continues in the current non-breeding range projection.

The Heinrich event H2 projection predicts suitable conditions in the south-east of Mexico from Veracruz to Tabasco and in central Guatemala and Belize, there is also a small range in Florida, this contrasts the projection of 24 ka BP in central-south Mexico and Central America. At H1 the range in south-east Mexico decreases to a small range from Chiapas to

Guatemala and Belize, which is different from the 17 ka BP with a large range from central-south Mexico to Central America. At last, the H0 projection increases the range in south-central Mexico although at a smaller scale than the 13 ka BP projection.

From 24 ka BP to 7 ka BP the projections display suitable conditions in South America in Venezuela, and across Brazil with a small range to the west of South America in the Andean cordillera. After this, the range in South America is projected mostly in Brazil and at a smaller scale in Bolivia and Paraguay. Nevertheless, the range is currently known to occur only in Mexico, Central America and along the south coast of Florida in USA.

Figure 4.1.5.4.b. Simulation maps of Ruby-throated Hummingbird non-breeding range. Maps are shown for ten-time slices: 24ka, H2 (24ka), 17ka, H1 (17ka), 13ka, H0 (13ka), 9ka, 5ka, 3ka and present (1961–90).

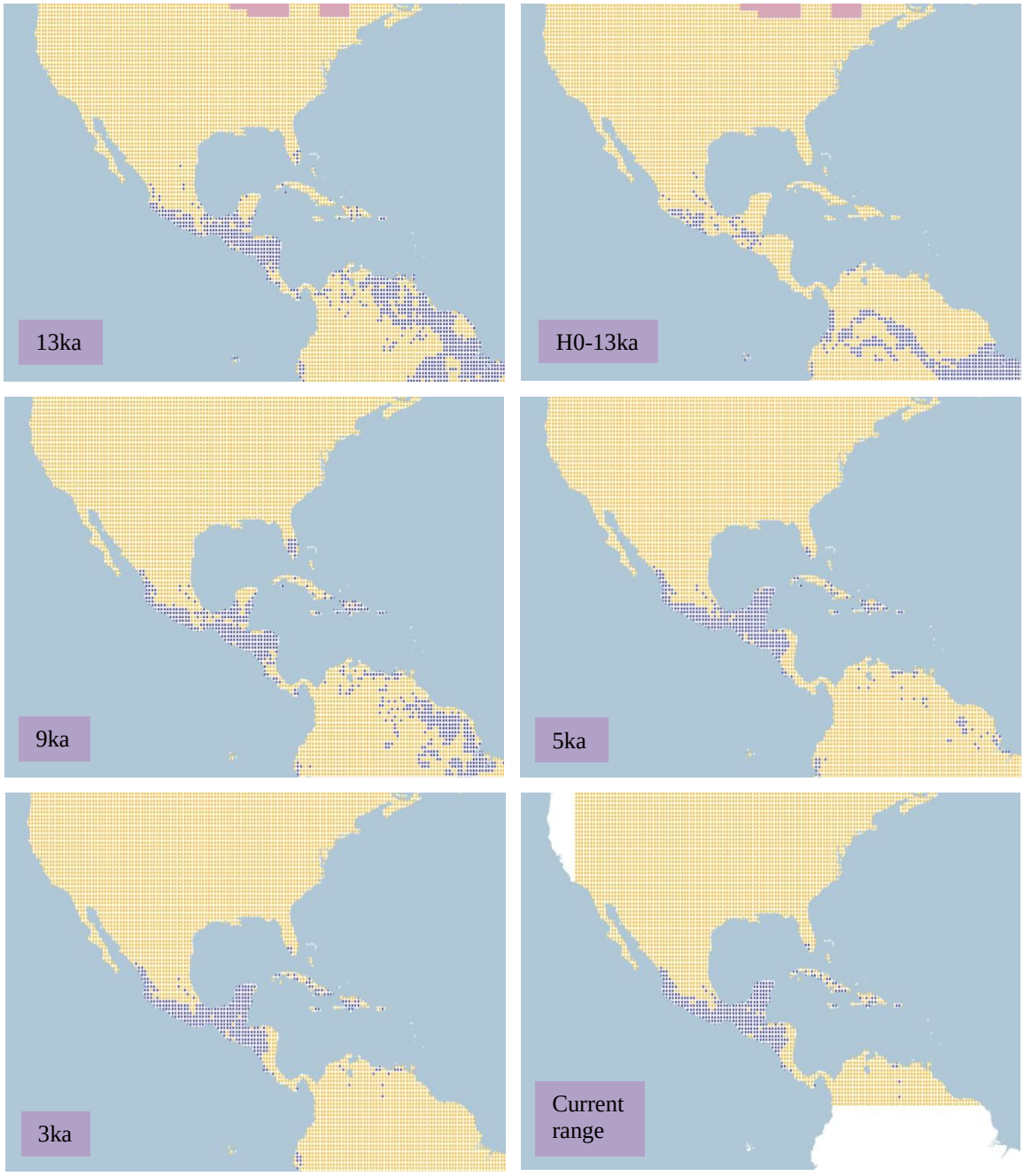

Figure 4.1.5.4.b. Simulation maps of Ruby-throated Hummingbird non-breeding range (continued**).**

*4.1.5.5 Lucifer Hummingbird (*Calothorax lucifer*). Conservation status: Least Concern. Current known range Figure 4.1.5.5.*

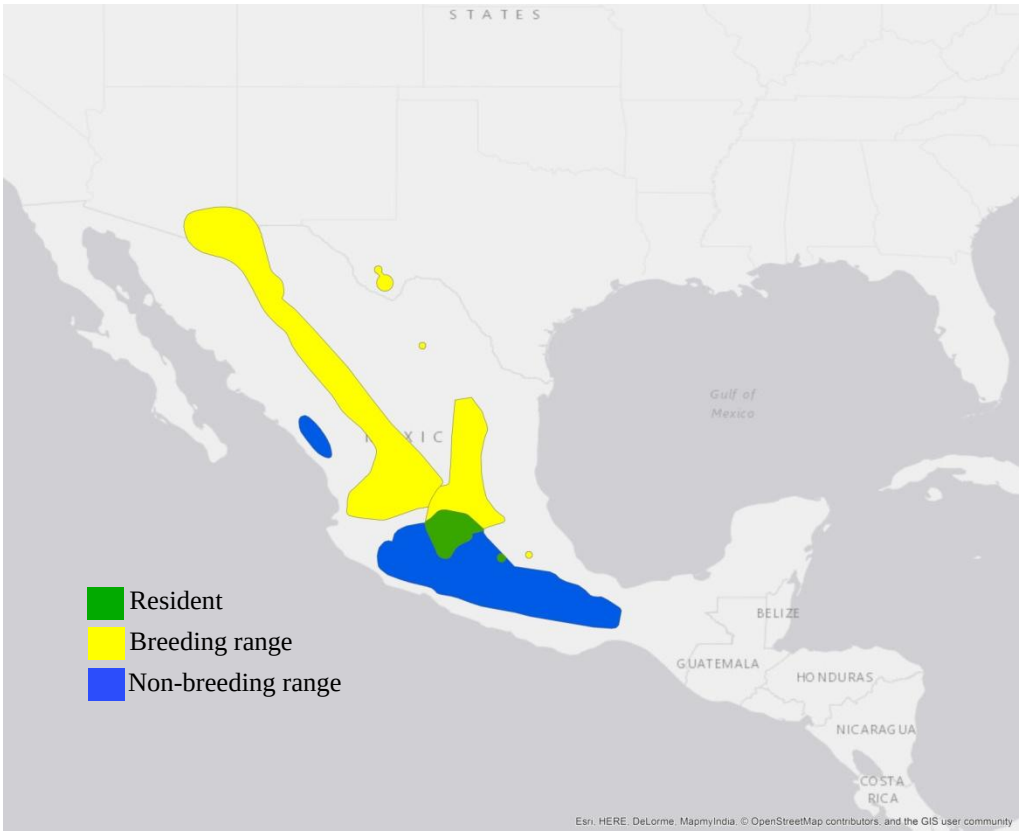

Figure 4.1.5.5. Current known range of Lucifer Hummingbird.

Breeding range (AUC: 0.994; TSS: 0.948; Kappa: 0.861): breeding ranges from the south of Arizona and New Mexico, south-west of Texas, and in Mexico in the Sierra Madre Occidental between Sonora and Chihuahua as far as Michoacán and Puebla and in the Sierra Madre Oriental to the north of Mexico between San Luis Potosi and Nuevo Leon.

At 26 ka BP the range is projected along the west coast of the USA, in the south-west of Arizona, a small range in the south-west of Texas and in Mexico in Baja California, the north-east of Sonora, the north of Nuevo Leon, and in the central part from San Luis Potosi to Jalisco and Oaxaca. This pattern continues and by 21ka the range in the south of Texas disappears and the range in the north of Sonora decreases. See Figure 4.1.5.5.a.

At 17 ka BP the range on the west coast of the USA decreases inland, and by 16 ka BP the range in the north of Sonora increases. After this, at the beginning of the Holocene at 11 ka BP there is a decline of the range on the west coast of the USA and in the north of Sonora.

This change at 10 ka BP with an increase of the range on the west coast of the USA and the growing range from central Mexico to the north of Durango. This projection persists at 9 ka BP and at 8 ka BP the range in Mexico reaches the north of Sonora and Chihuahua in Mexico and the south-west of Arizona in the USA.

There is a slight decrease of the range in the north of Mexico at 7 ka BP, returning at 6 ka BP and remaining with a minimal variation until 1 ka BP, covering the Sierra Madre Oriental and the Sierra Madre Occidental, correlating with the current breeding range projection.

The H2 projection compared with the 24 ka BP projection exhibit similar ranges in central to east Mexico, except from Jalisco to Guanajuato in H2, and the range along the west coast of the USA is larger inland at H2 than at 24 ka BP. The projected range in Mexico at H1 increases in the north and central region, although at a different scale than the 17 ka BP projection. Similarities are shown between H0 and 13 ka BP, in the central region of Mexico and along the west coast of the USA.

Even though the current known breeding range is located in Mexico, there are suitable conditions projected in the time frames along the Andean cordillera from Ecuador to Chile and Argentina as well as on the east coast between Brazil and Argentina in South America.

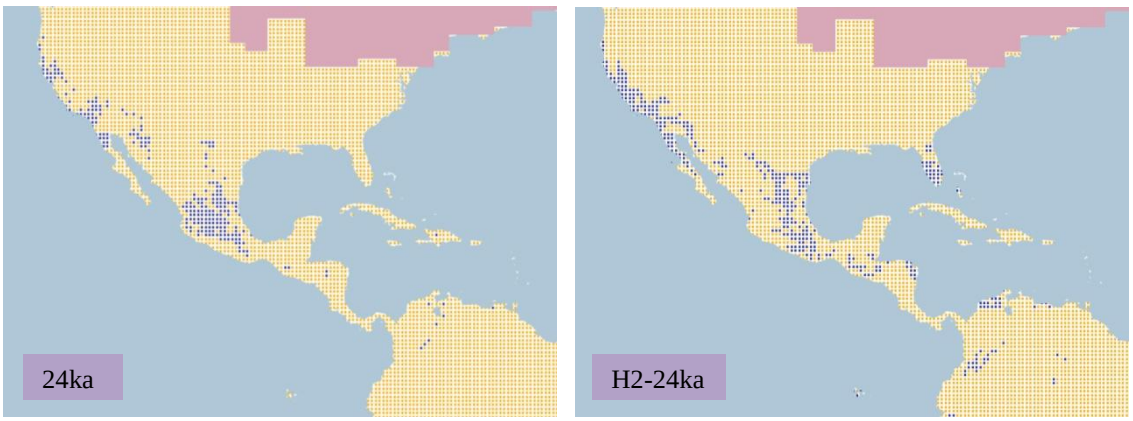

Figure 4.1.5.5.a. Simulation maps of Lucifer Hummingbird breeding range.
Maps are shown for ten-time slices: 24ka, H2 (24ka), 17ka, H1 (17ka), 13ka, H0 (13ka), 9ka, 5ka, 3ka and present (1961–90).

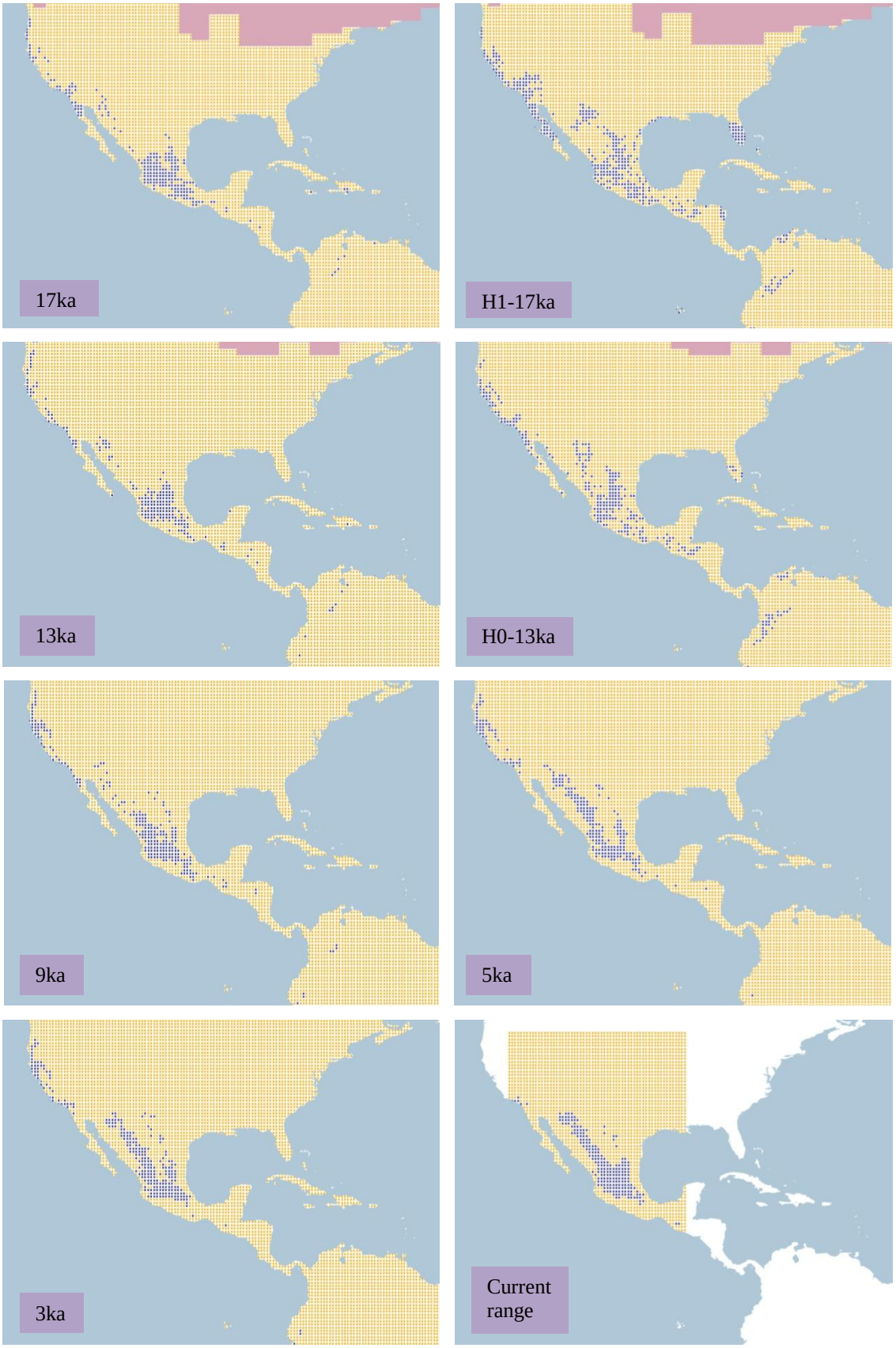

Figure 4.1.5.5.a. Simulation maps of Lucifer Hummingbird breeding range (continued**).**

Non-breeding range (AUC: 0.995; TSS: 0.954; Kappa: 0.839): The wintering grounds of the species are located in central-southern Mexico, from Jalisco to Oaxaca and a small range in central Sinaloa.

At 26 ka BP the range is projected in central-southern Mexico, from Jalisco to Oaxaca and a small range expanding to the north in San Luis Potosi. The pattern continues with minimal differences and by 19 ka BP the range in central Mexico moves to the southern coast mainly from Michoacán to Oaxaca. See Figure 4.1.5.5.b.

With the deglaciation in North America, the range in central Mexico is increased between 14 ka BP and 12 ka BP. After this, at the beginning of the Holocene the range is projected from central Sinaloa to southern Chiapas, with a smaller range on the east coast of Yucatan and northern Guatemala. The increasing trend continues between 8 ka BP and 7 ka BP from central Sinaloa to southern Chiapas, with a decrease at 6 ka BP in Michoacán, Guerrero and Puebla in Mexico.

By 5 ka BP, the extent of the range is projected from central-northern Sinaloa to southern Chiapas in Mexico, remaining until de 1 ka BP projection. The current non-breeding range projection is projected in central to southern Mexico as the 1 ka BP projection, only with a smaller range projected in Sinaloa.

In the Heinrich event projection of H2, there is a different range projected than 24 ka BP, located at a smaller scale in Tamaulipas and in southern Mexico as far as the north of Honduras. The pattern remains at H1, with the increasing range in southern Mexico and northern Central America. At H0 a small range is projected in central-southern Mexico from Jalisco to Chiapas and in Central America between southern Guatemala and northern El Salvador and Honduras.

Even though the range is restricted to Mexico, there are suitable conditions projected in the time frames in South America, mainly in eastern Brazil, northern Venezuela and along the Andean cordillera.

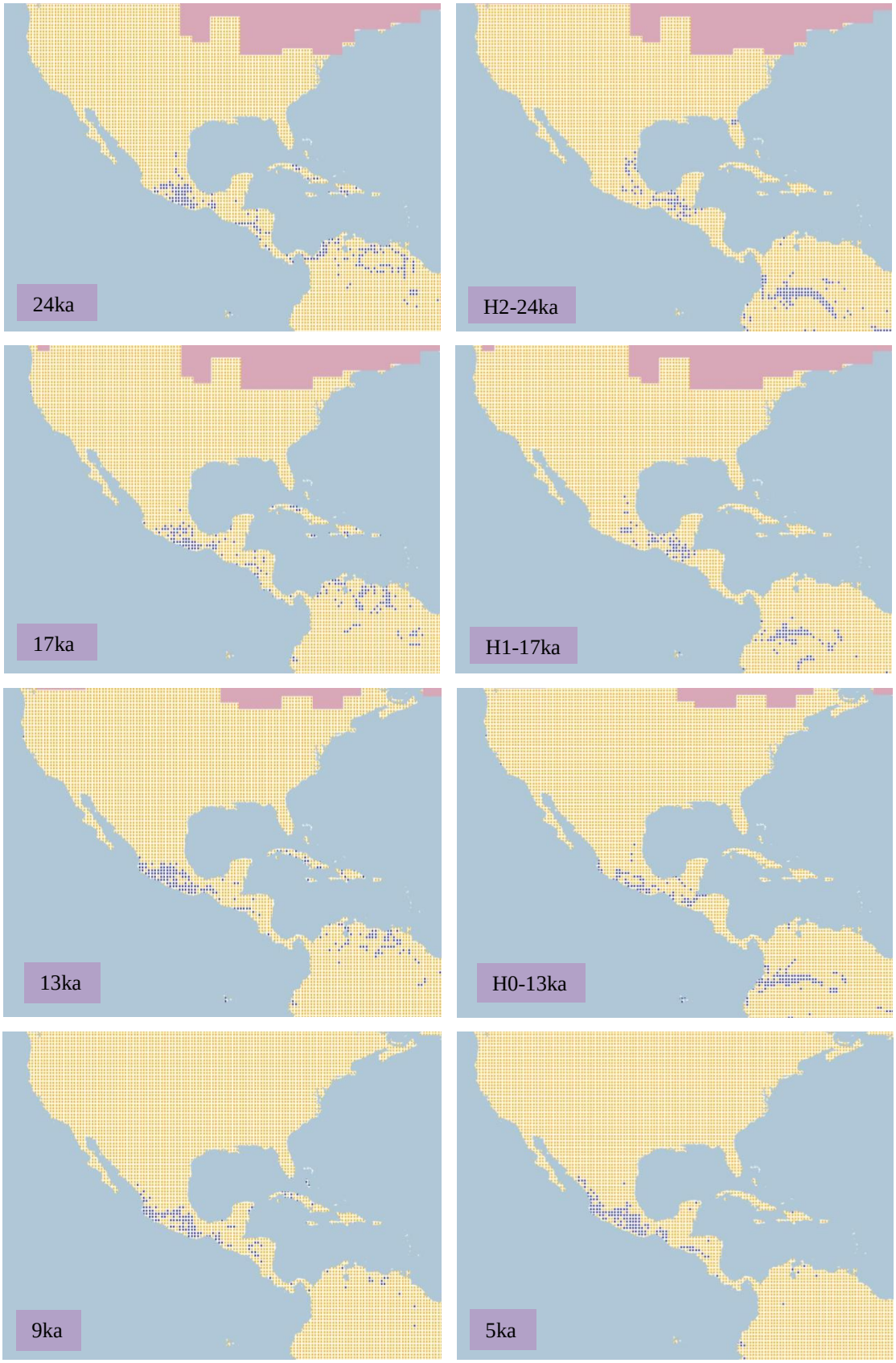

Figure 4.1.5.5.b. Simulation maps of Lucifer Hummingbird non-breeding range. Maps are shown for ten-time slices: 24ka, H2 (24ka), 17ka, H1 (17ka), 13ka, H0 (13ka), 9ka, 5ka, 3ka and present (1961–90).

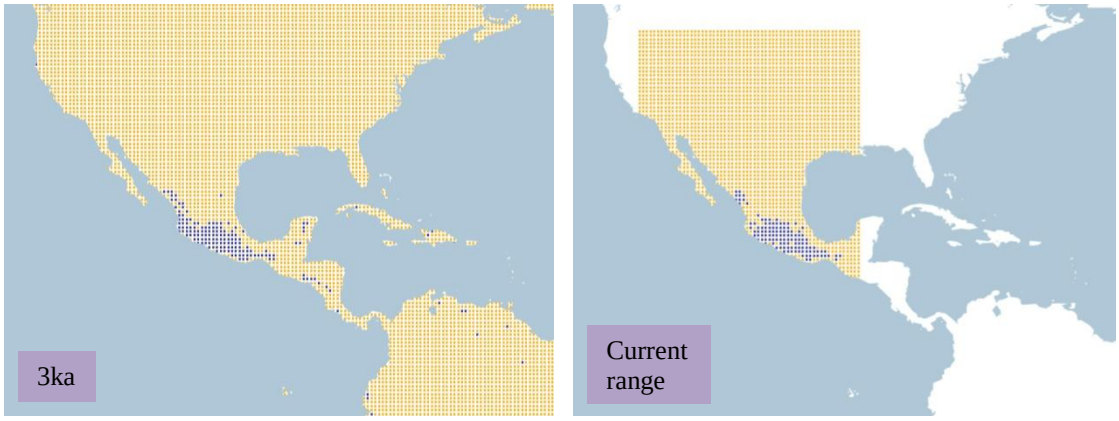

Figure 4.1.5.5.b. Simulation maps of Lucifer Hummingbird non-breeding range (continued**).**

*4.1.5.6 Anna's Hummingbird (*Calypte anna*). Conservation status: Least Concern. Current known range Figure 4.1.5.6.*

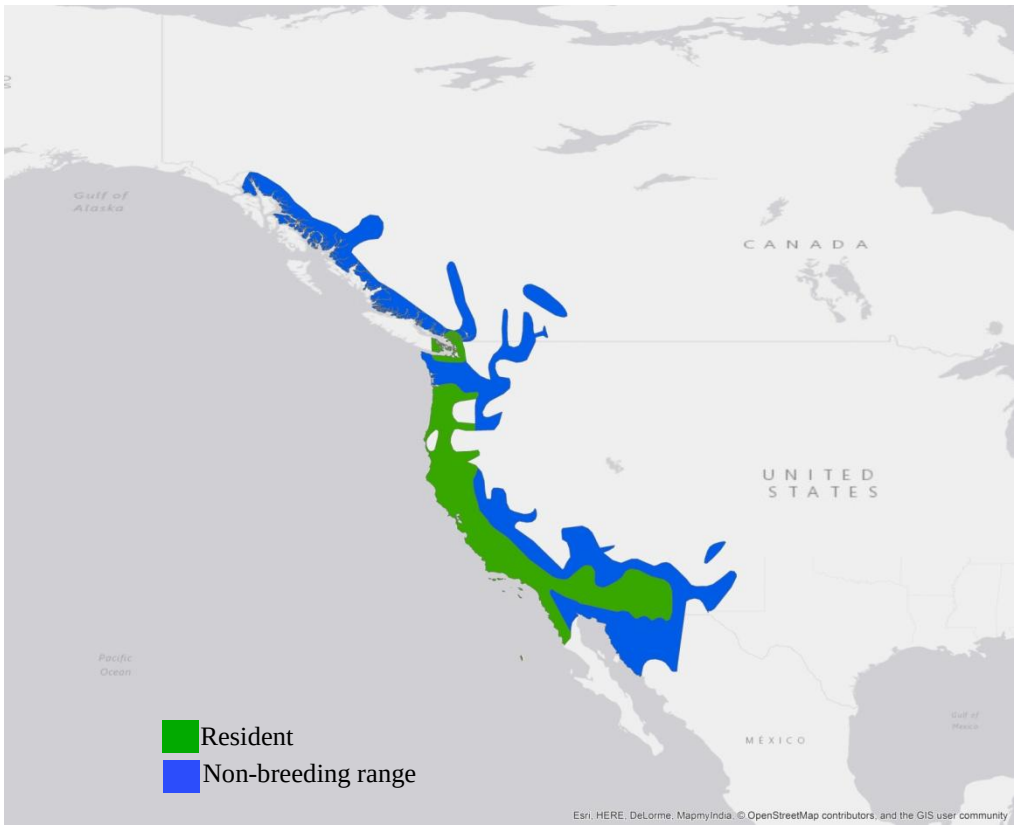

Figure 4.1.5.6. Current known range of Anna's Hummingbird.

Breeding range (AUC: 0.992; TSS: 0.914; Kappa: 0.827): The species has a year-round resident range along the western coast of USA as far as northern Mexico in Baja California,

and extending to southern Arizona, with a small range in southern British Columbia in Canada.

At 26 ka BP the range is projected along the western coast and south-east of the USA, in southern Nevada, Arizona and from Texas to North Carolina. The range continues to north-western Mexico, from Baja California to Sonora and Sinaloa, with a central range projected from Zacatecas to northern Coahuila. The pattern continues until 21ka with the decrease of the range in the eastern USA. See Figure 4.1.5.6.a.

Between 19 ka BP and 17 ka BP the range in the south-eastern USA decreases, mainly in Texas, and, there is an increase in the range projected in central Mexico. The pattern of decrease in the eastern USA continues from 16 ka BP onwards, with also a decrease of the range in central Mexico and southern Arizona at 14 ka BP. By 13 ka BP the range in the eastern USA is projected from Tennessee to North Carolina.

By the beginning of the Holocene the range in the western USA increases to the south-west of Canada whilst decreasing in the north-west of Mexico. Also, the range in the eastern USA shifts to the north, extending from Missouri to Virginia. After this, at 10 ka BP, the range in northern Mexico decreases to a northern range in Baja California and Sonora.

The increasing pattern in the eastern USA continues at 8 ka BP, remaining with minimal differences until 1 ka BP. In addition, the range in the western USA persists unchanged until 1 ka BP, with only the range in north-western Mexico and the south-western USA increasing from 5 ka BP to 2 ka BP, reducing a small proportion at 1 ka BP. Furthermore, the current breeding range projection presents a similar range in the western USA and north-western Mexico as 1 ka BP.

The Heinrich event H2 and the 24 ka BP projections present a similar range in the western and south-eastern USA, only with a different range in central and northern Mexico, having a larger range projected at H2 than at 24 ka BP. The pattern continues at H1, increasing in the south-central USA and northern Mexico, which differs from the 17 ka BP projection. However, between the H0 and 13 ka BP projection, similar ranges are observed, from the western and eastern USA, only differing with the range projected in the south-central USA and northern Mexico.

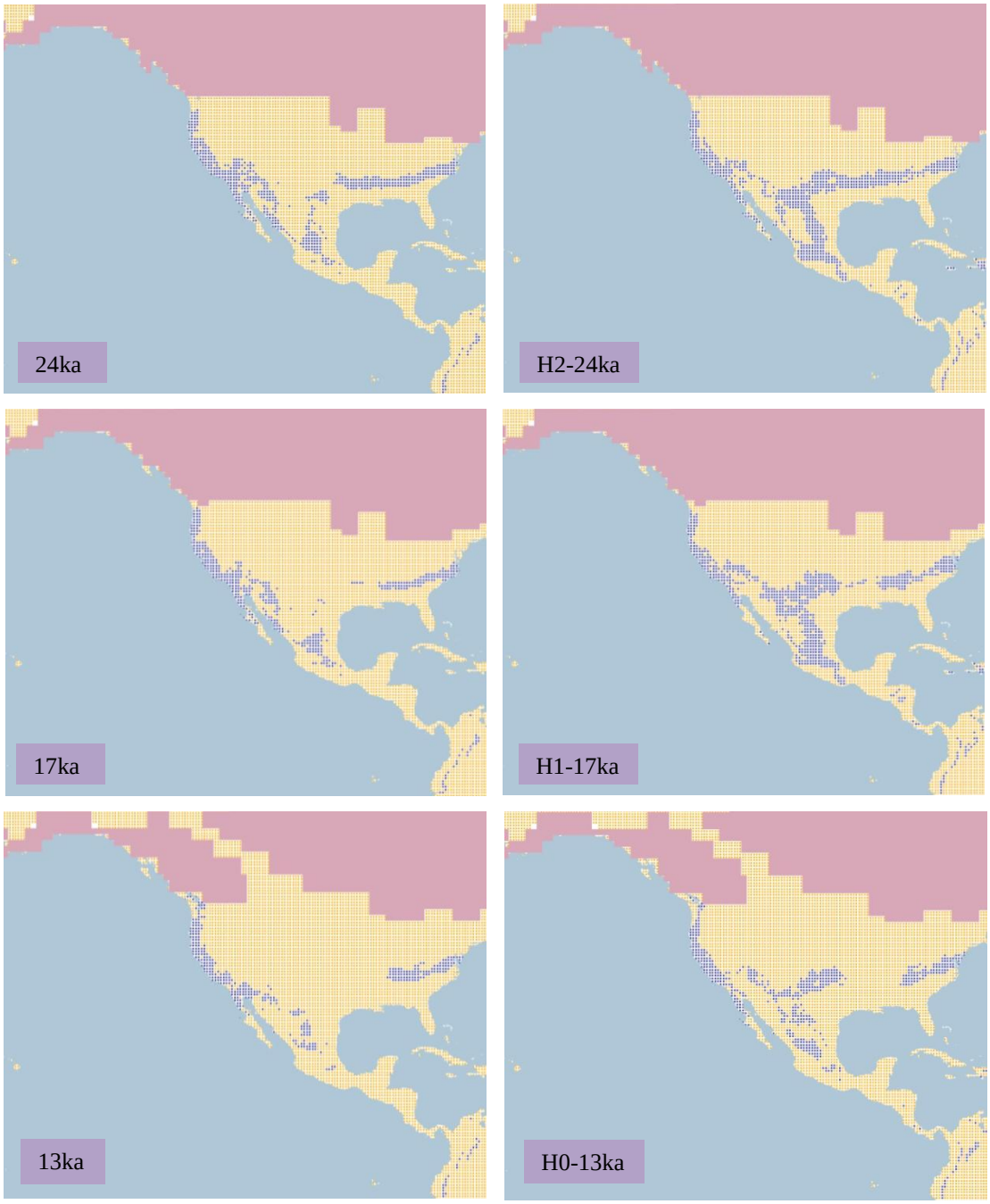

Figure 4.1.5.6.a. Simulation maps of Anna's Hummingbird breeding range.
Maps are shown for ten-time slices: 24ka, H2 (24ka), 17ka, H1 (17ka), 13ka, H0 (13ka), 9ka, 5ka, 3ka and present (1961–90).

Figure 4.1.5.6.a. Simulation maps of Anna's Hummingbird breeding range (continued**).**

Non-breeding range (AUC: 0.974; TSS: 0.832; Kappa: 0.758): The wintering grounds are located from western British Columbia and a small range in Alberta Canada. Also in the north-western, west and south-western USA, between Oregon, Washington, Idaho, Montana and Nevada, Arizona, New Mexico and Texas. A small range is also present in north-western Mexico between Baja California and Sonora. In addition, there is a year-round resident range along western USA, and the north-west coast of Mexico.

A large range is projected at 26 ka BP from western, south-central USA as far as central Mexico, with a small range in the south-east USA. This trend continues until 17 ka BP, with the decreasing range in the south-central and eastern USA as well as north-eastern Mexico. Particularly at 15 ka BP onwards, there is a decline of the range in eastern USA and north-eastern Mexico, restricting the range to the western region of the USA, and north-western and central Mexico. See Figure 4.1.5.6.b.

By the beginning of the Holocene the range in the eastern USA moves to the north, with a range projected in south-central Canada in Manitoba, and along the western region of British Columbia and in the Alaskan Peninsula of the USA. The range in Manitoba disappears at 9ka, and the range in northern and central Mexico is decreased.

Between 8 ka BP and 7 ka BP the range in the north-west of Mexico increases, as well as that in the eastern USA. This trend continues and at 6 ka BP the range in the south-central USA is increased, with the rest of the range remaining with minimal differences until 1 ka BP. The current non-breeding projection shares a similar range as 1 ka BP, from western Canada to north-western Mexico.

Similar ranges are observed between H2 and 24 ka BP, from central to northern Mexico, in the western and eastern USA, only with a larger range projected in the central USA at H2. The range is decreased in the USA at H1, mainly in the western and eastern region. At H0, the range continues decreasing in the eastern and central USA, with a smaller range projected in Mexico, and with a western range in the USA remaining unchanged.

Although the current known non-breeding range is in North America, there are suitable conditions projected in South America, mainly along the Andean cordillera and on the western coast of Chile.

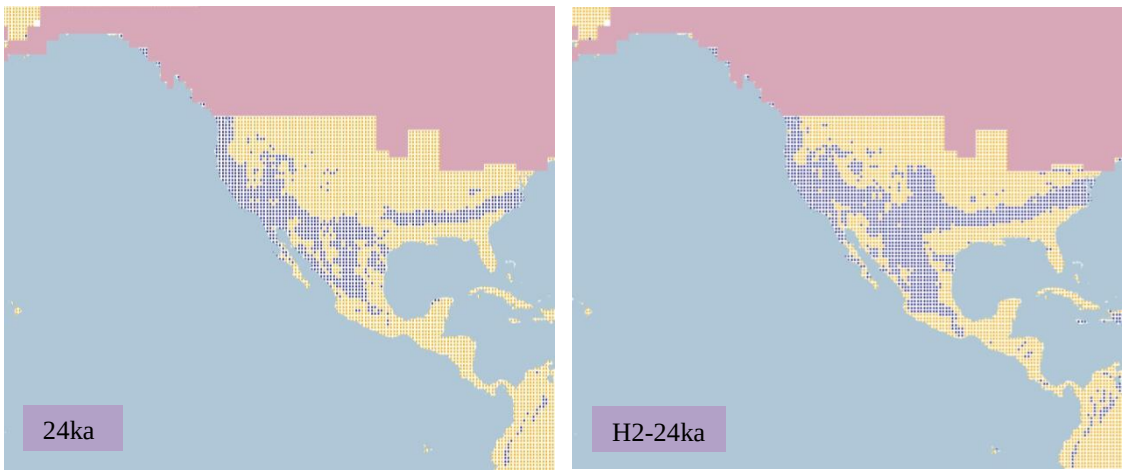

Figure 4.1.5.6.b. Simulation maps of Anna's Hummingbird non-breeding range.
Maps are shown for ten-time slices: 24ka, H2 (24ka), 17ka, H1 (17ka), 13ka, H0 (13ka), 9ka, 5ka, 3ka and present (1961–90).

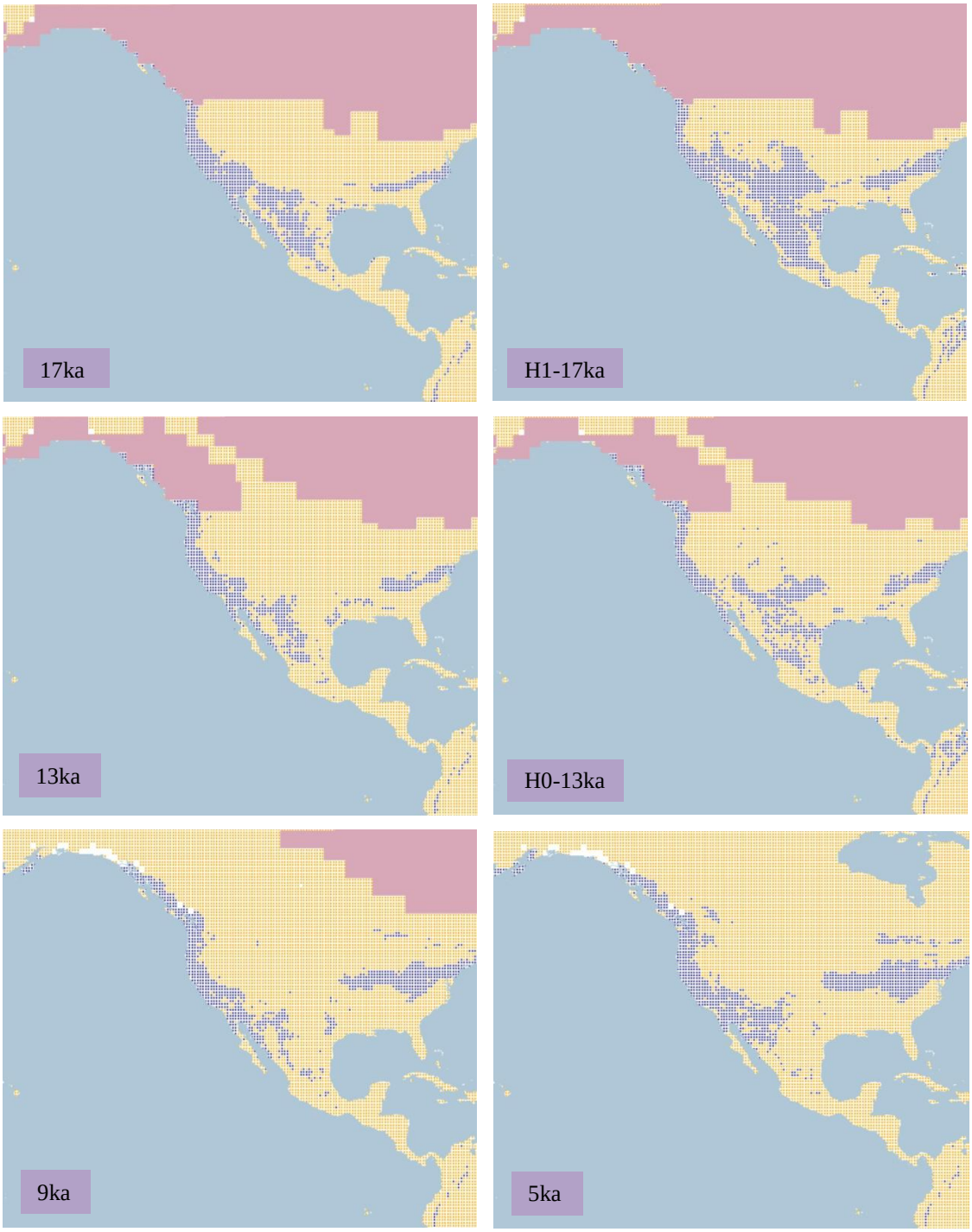

Figure 4.1.5.6.b. Simulation maps of Anna's Hummingbird non-breeding range (continued**).**

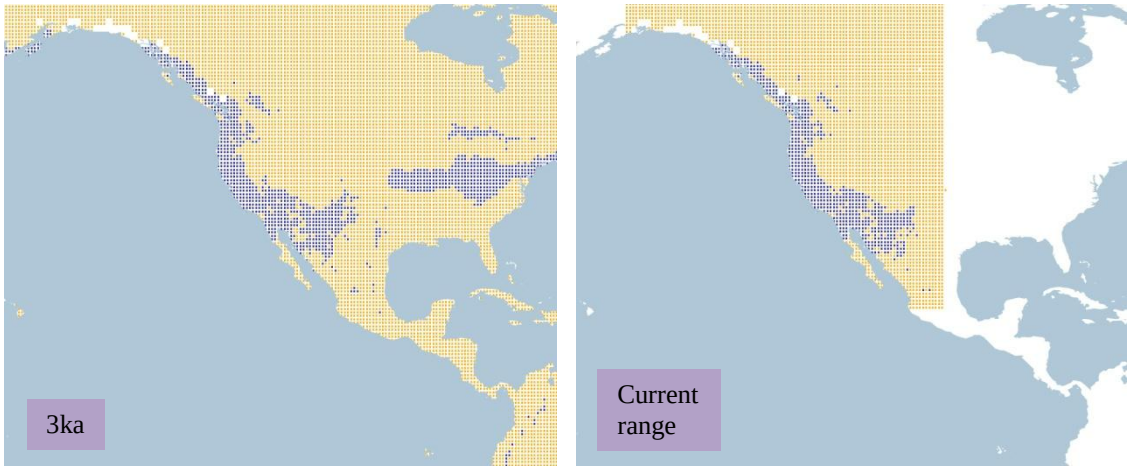

Figure 4.1.5.6.b. Simulation maps of Anna's Hummingbird non-breeding range (continued**).**

*4.1.5.7 Costa's Hummingbird (*Calypte costae*). Conservation status: Least Concern. Current known range Figure 4.1.5.7.*

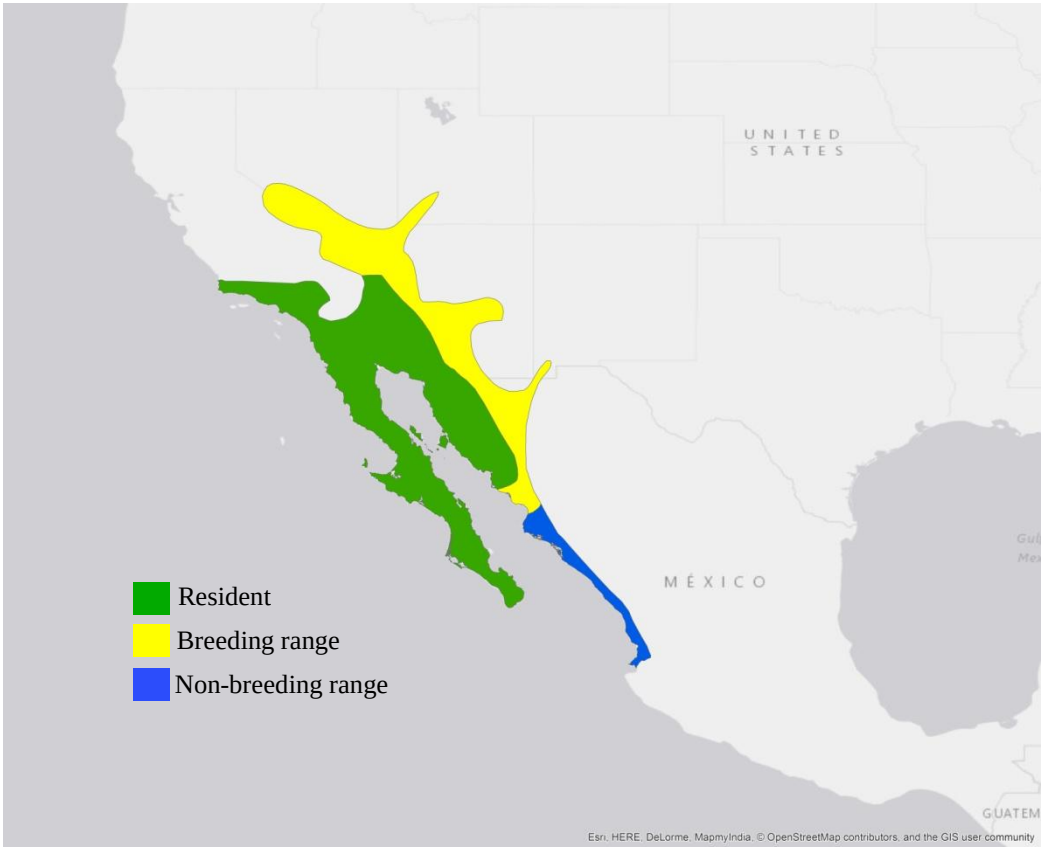

Figure 4.1.5.7. Current known range of Costa's Hummingbird.

Breeding range (AUC: 0.997; TSS: 0.950; Kappa: 0.892): The breeding range of the species is located from southern Nevada to western Arizona in the USA, and along Sonora in northern Mexico. The species also has a year-round resident range from southern California to south-western Arizona in the USA and in north-western Mexico, from Baja California to Sonora.

At 26 ka BP the range is projected in northern Mexico, from Baja California to Tamaulipas, and at a smaller scale in northern Yucatan in Mexico and eastern California in the USA. This trend continues and by 21ka the range in north-central Mexico is decreased. After this, the range continues with minimal differences and at 17 ka BP the range in north-central Mexico and the south-central USA is increased, also with a declining range in California, USA. See Figure 4.1.5.7.a.

As the ice sheet melts at 13 ka BP, the range in the south-western USA increases, with the range in the north-east of Mexico decreasing. By the beginning of the Holocene at 11 ka BP, the range is projected in south-western USA and northern Mexico; this changed at 10 ka BP with the decreasing of the range in northern Mexico and with a range projected in south-central Canada in Manitoba.

The range at 8 ka BP in north-central Mexico disappears, with the range being projected in north-western Mexico from Baja California and Sonora towards western Arizona in the USA. The projected range continues with a similar pattern until 1 ka BP. In addition, there is a similar range predicted for the current breeding range projection.

The Heinrich event H2 presents a similar range as 24 ka BP in the north-west of Mexico, although with a smaller extent, and, with a larger range projected in south-central Mexico, differing from the 24 ka BP projection. At H1 the range is mainly projected along the western and eastern coasts of Mexico, with a larger range in Yucatan. The same pattern is observed at H0 in the range projected in Mexico, being dissimilar from the 13 ka BP projection.

Throughout the projections there are suitable conditions present in South America from the coast of Ecuador to Chile and along Bolivia and Argentina, even though the current breeding range of the species is located in North America.

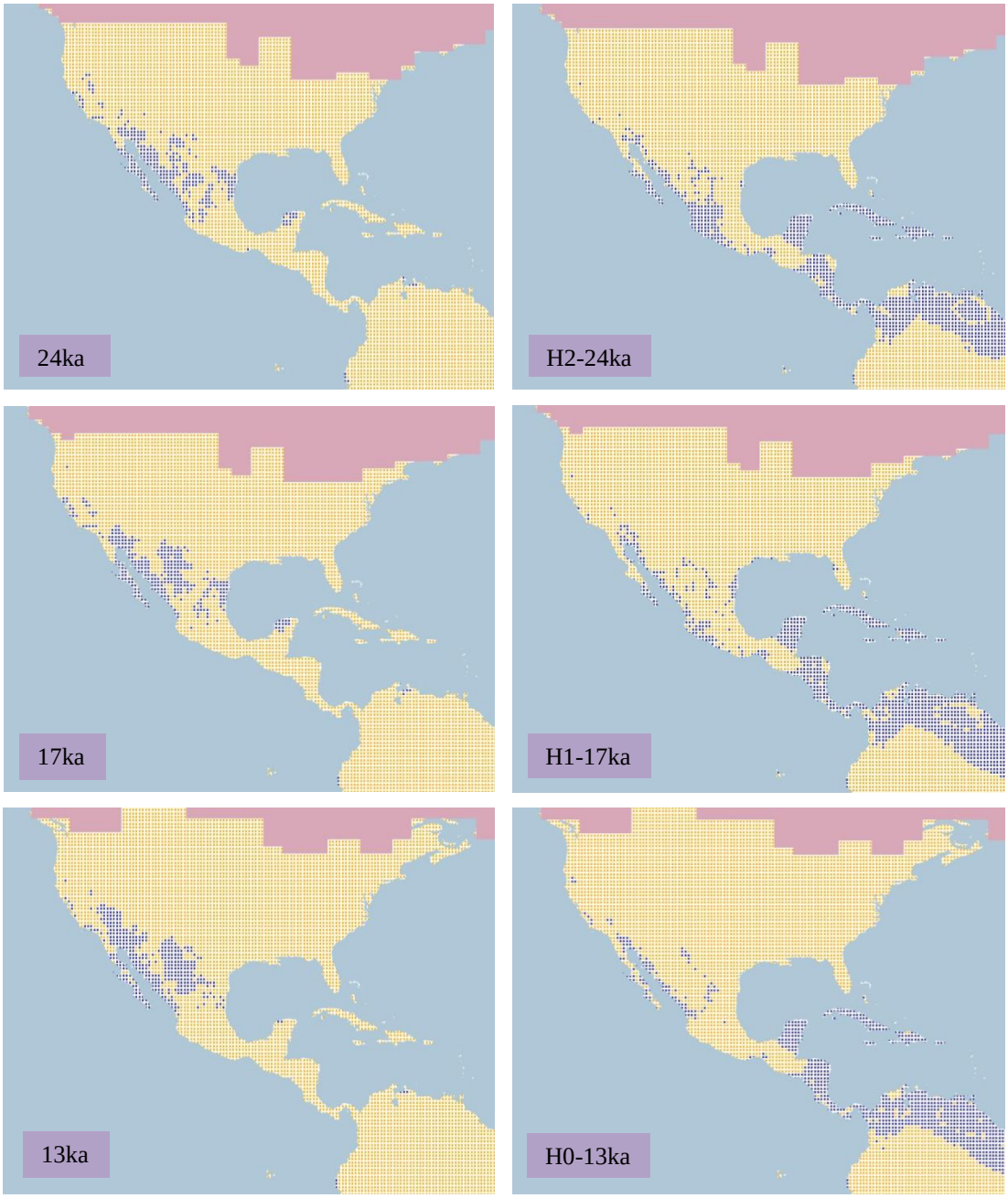

Figure 4.1.5.7.a. Simulation maps of Costa's Hummingbird breeding range.
Maps are shown for ten-time slices: 24ka, H2 (24ka), 17ka, H1 (17ka), 13ka, H0 (13ka), 9ka, 5ka, 3ka and present (1961–90).

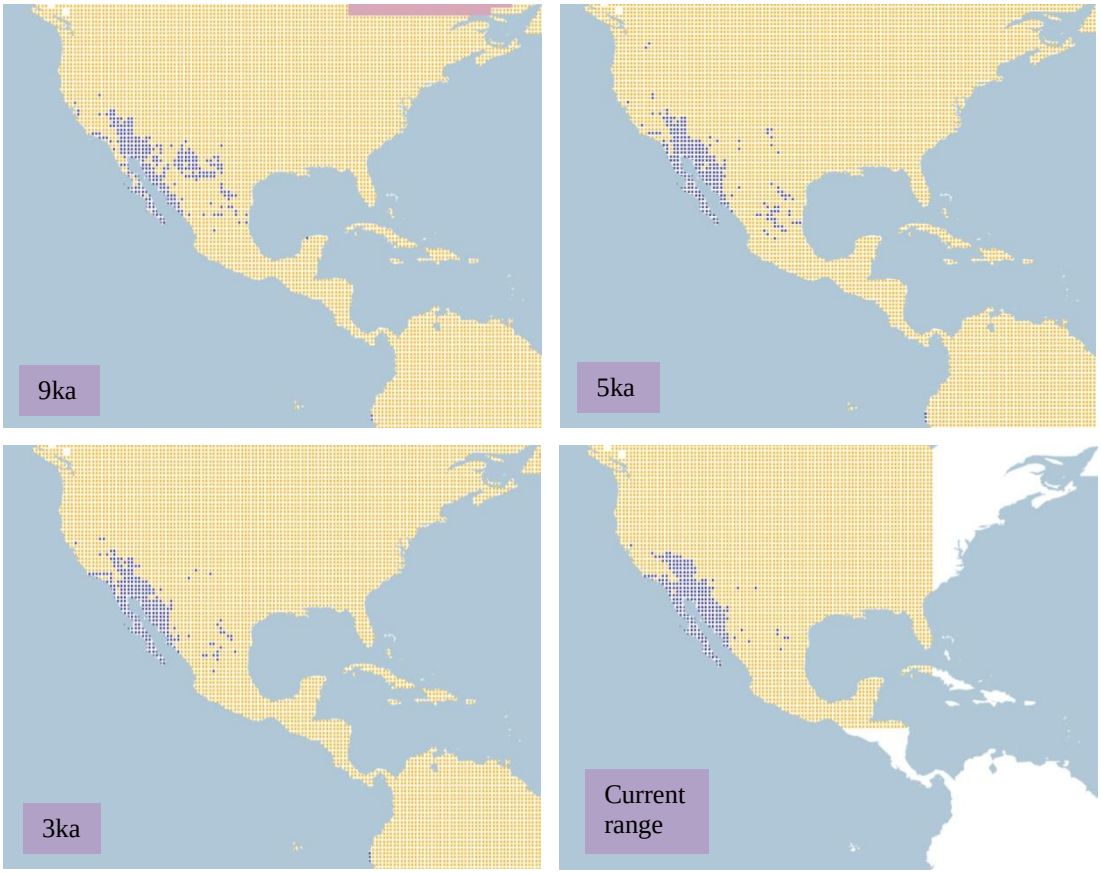

Figure 4.1.5.7.a. Simulation maps of Costa's Hummingbird breeding range (continued**).**

Non-breeding range (AUC: 0.998; TSS: 0.979; Kappa: 0.924): The non-breeding range for the species is located along Sinaloa in Mexico. Furthermore, the species has a year-round resident range from southern California and Arizona in the USA and in north-western Mexico, between Baja California and Sonora.

At 26 ka BP the range is projected in northern and north-central Mexico, from Baja California to Jalisco, and in Coahuila, Durango and Tamaulipas. There is also a small range in the north of Yucatan in Mexico and in California, USA. This trend continues until 21 ka BP, with a decrease in the range projected in northern Mexico. See Figure 4.1.5.7.b.

At 20 ka BP the range in north-central Mexico is increased, this pattern continuing until 13 ka BP, when the range in Tamaulipas disappears and the central range in Mexico moves to the northern region. There is also an increase in the range projected in south-western Arizona in the USA.

By the beginning of the Holocene the range is projected along north-western Mexico and in south-western Arizona in the USA. The range in north-central Mexico disappears after 10 ka BP. From 8 ka BP onwards the range remains in north-western Mexico and in the south-west of Arizona in the USA, with a small range projected in central Mexico from 6 ka BP to 1 ka BP. The current non-breeding projection also presents a similar range as the 1 ka BP projection.

The H2 projection presents a range in central and southern Mexico, along Central America, the Greater Antilles and the northern and south-western region of South America, with a small range along the north-west in Baja California and Sonora. The range in central Mexico is reduced at H1, with the main range being projected in southern Mexico, Central America, the Greater Antilles and northern and south-western South America. The same pattern as H1 is observed at H0 with a range along the western coast and in southern Mexico, and from Central America to northern and south-western South America.

Even though the species current non-breeding range is located in North America, there are suitable conditions observed among the projections in South America, mainly along the west coast from Ecuador to Chile and in Argentina.

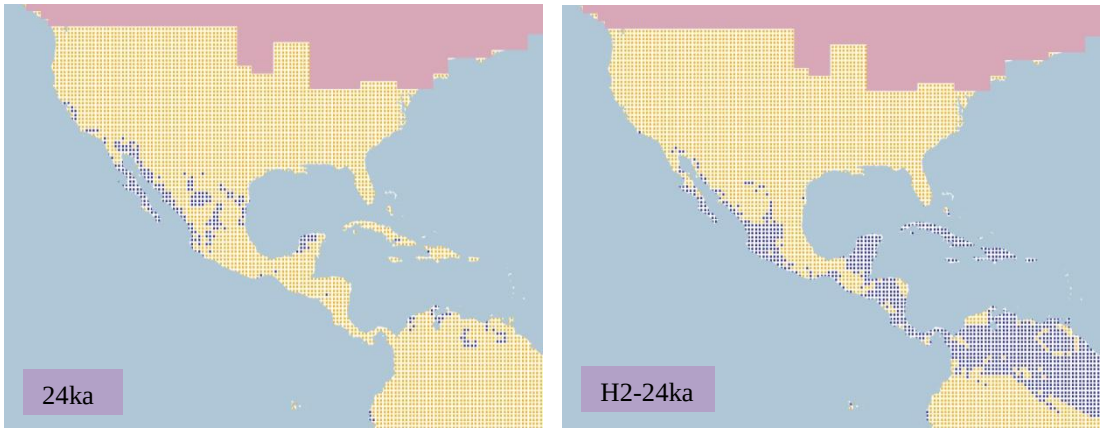

Figure 4.1.5.7.b. Simulation maps of Costa's Hummingbird non-breeding range.
Maps are shown for ten-time slices: 24ka, H2 (24ka), 17ka, H1 (17ka), 13ka, H0 (13ka), 9ka, 5ka, 3ka and present (1961–90).

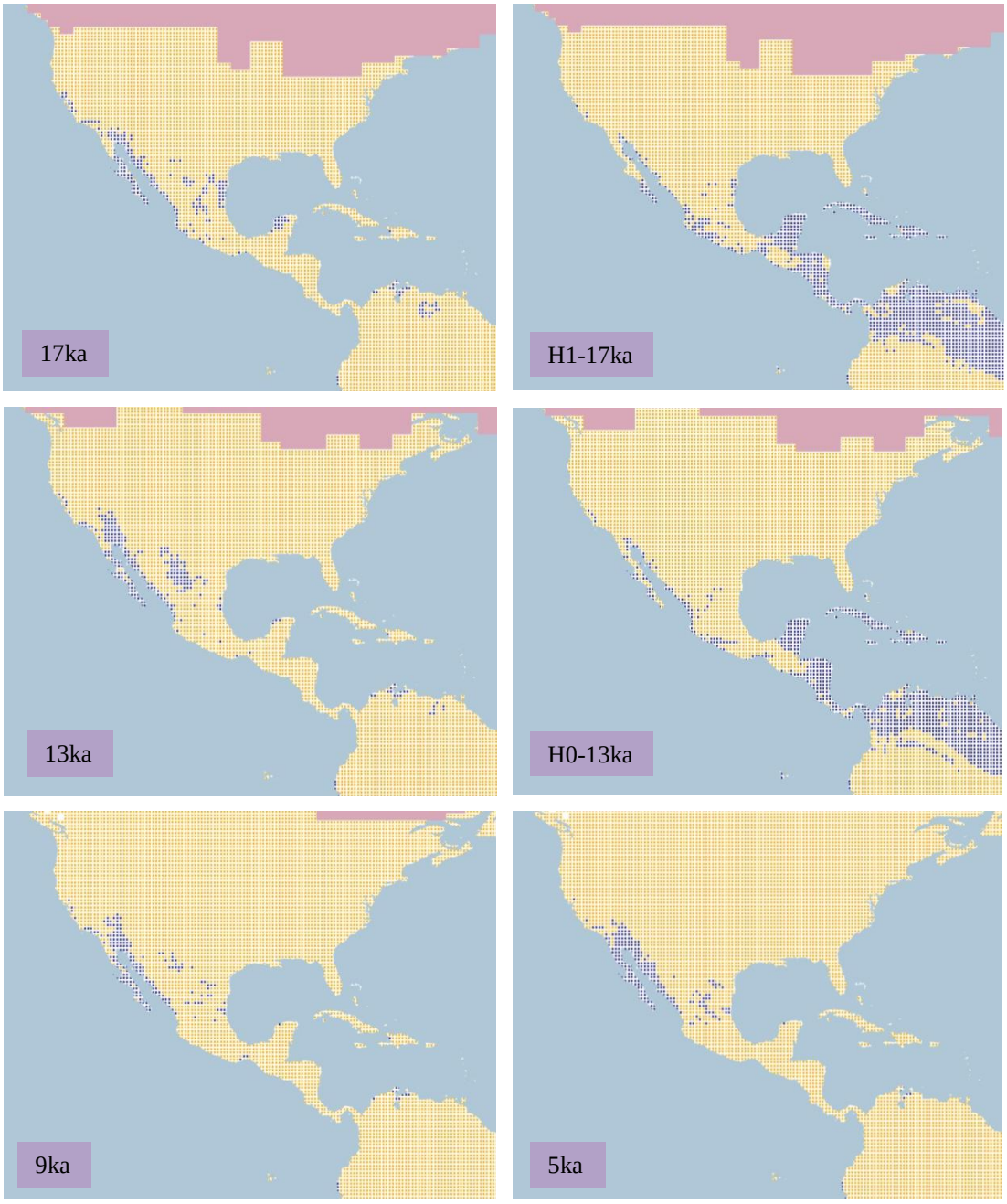

Figure 4.1.5.7.b. Simulation maps of Costa's Hummingbird non-breeding range (continued**).**

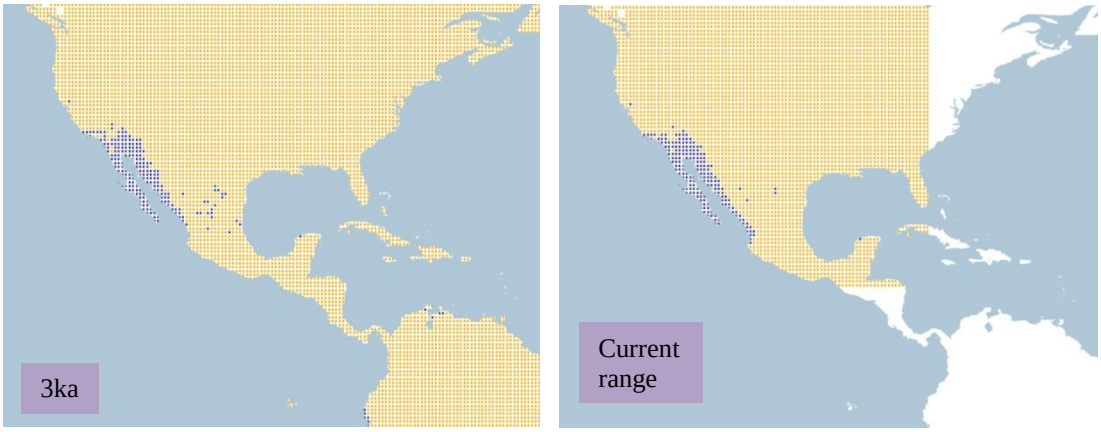

Figure 4.1.5.7.b. Simulation maps of Costa's Hummingbird non-breeding range (continued**).**

*4.1.5.8 Broad-billed Hummingbird (*Cynanthus latirostris *including* C. l. magicus, C. l. latirostris *and* C. l. propinquus*). Conservation status: Least Concern. Current known range Figure 4.1.5.8.*

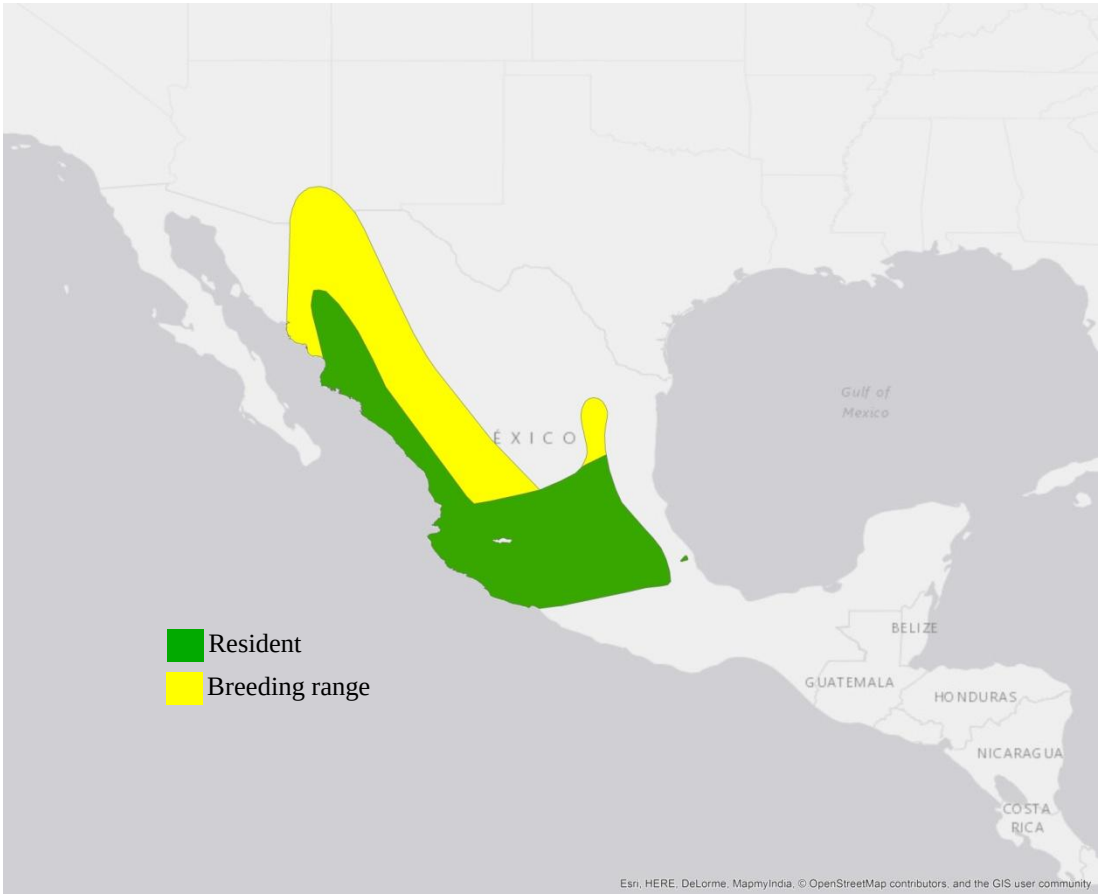

Figure 4.1.5.8. Current known range of Broad-billed Hummingbird.

Breeding range (AUC: 0.996; TSS: 0.944; Kappa: 0.915): The breeding grounds of the species are located mainly along the Sierra Madre Occidental, and at a smaller scale in eastern Sonora and in southern Nuevo Leon in Mexico. The species has a year-round resident range from south-western Chihuahua to the central region in Mexico.

The range at 26 ka BP is projected in central-eastern Mexico with a smaller range in the western USA and north-western Mexico. This pattern continues until 20 ka BP with a decreasing range in Sonora in north-western Mexico, and a rise in the range in central-south region of Mexico. See Figure 4.1.5.8.a.

At 15 ka BP, the range in north-central Mexico and the western USA is reduced. This trend continues at the beginning of the Holocene with the reduction of the range in northern Mexico. At 10 ka BP, the range in eastern Mexico shifts to the western region, and by 8 ka BP the range is extended in north-western Mexico as far as Sonora. The range in eastern Mexico returns again from 5 ka BP unti1 l ka BP, the rest of the range in the western USA and in north-western and central Mexico remains unchanged as well. Furthermore, the current breeding range projection presents similarities with the 1 ka BP projection in the Mexican range, from north-western to the central region.

When comparing H2 with the 24 ka BP projection, there are similar ranges observed in central and north-eastern Mexico, with a larger extent in the western USA and north-western Mexico, projecting a range in Central America, and in Florida also. The range is increased in the western and south-eastern USA, and north-western Mexico at the H1 projection, differing from the 17 ka BP projection. This range in the western and south-eastern USA is reduced at H0, presenting a similar range as 13 ka BP in Mexico, although with a larger extent in the north-west.

There are suitable conditions projected in central South America and along the Andean cordillera, even though the species' current range is located in Mexico.

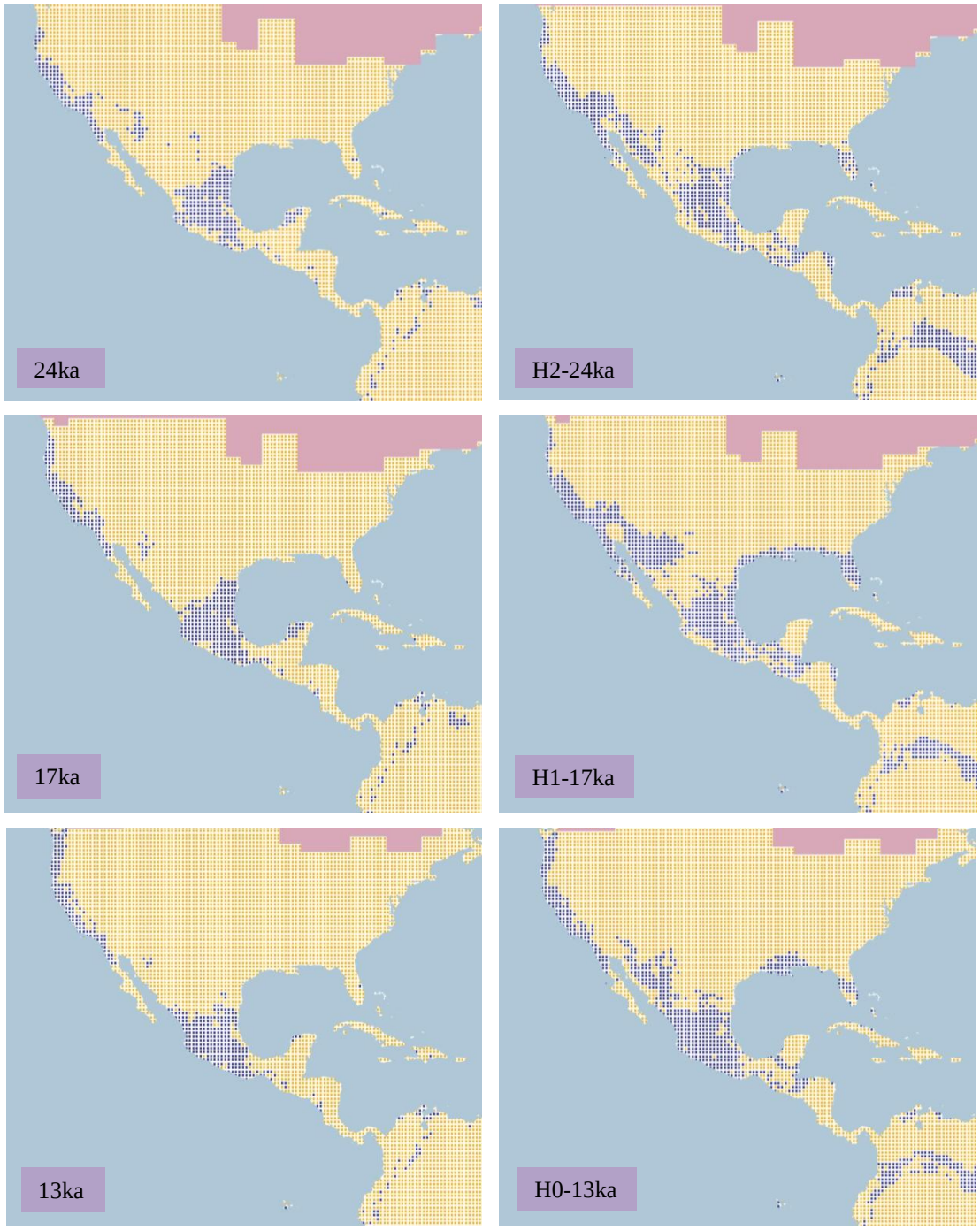

Figure 4.1.5.8.a. Simulation maps of Broad-billed Hummingbird breeding range. Maps are shown for ten-time slices: 24ka, H2 (24ka), 17ka, H1 (17ka), 13ka, H0 (13ka), 9ka, 5ka, 3ka and present (1961–90).

Figure 4.1.5.8.a. Simulation maps of Broad-billed Hummingbird breeding range (continued**).**

Non-breeding range (AUC: 0.997; TSS: 0.956; Kappa: 0.912): The species has a year-round resident range in western and central Mexico, from Sonora to Puebla.

The range at 26 ka BP is projected in eastern and central Mexico with a smaller range in the north of Yucatan. This pattern continues until 18 ka BP when there is a decreased in the central range in Mexico, migrating to the southern region. The range in south-central Mexico reaches Jalisco at 16 ka BP, and reduces in the eastern region. By the end of the Pleistocene at 12 ka BP the extent of the range is located in central Mexico. This changed at 11 ka BP, with a decrease in the central region, migrating to the north-east of Mexico in Tamaulipas. See Figure 4.1.5.8.b.

At 8 ka BP the range in Mexico is extending as far as north-western region in Sonora, decreasing in Tamaulipas and south-central Michoacán and Guerrero. At 5 ka BP the range in central Mexico is fragmented, extending in the western and eastern region. The pattern

changes at 5 ka BP, with the increased range in central Mexico, remaining unchanged until the 1 ka BP projection. This predicted range is also followed in the current non-breeding projection, from north-western to central Mexico.

The Heinrich event H2 presents a similar range as 24 ka BP in the eastern region of Mexico, although of a smaller extent, and projects a range in the north-west and south of Mexico, extending to Central America. This range is increased at H1, to the south-eastern USA and in western Arizona, with a smaller range in central Mexico than 17 ka BP. The range at H0 is increased in the western and eastern region of Mexico, with a smaller scale in central Mexico and larger range in the north than the range projected in the 13 ka BP projection.

Even though the species' current range is located in Mexico, there are suitable conditions projected for the species along the Andean cordillera in South America.

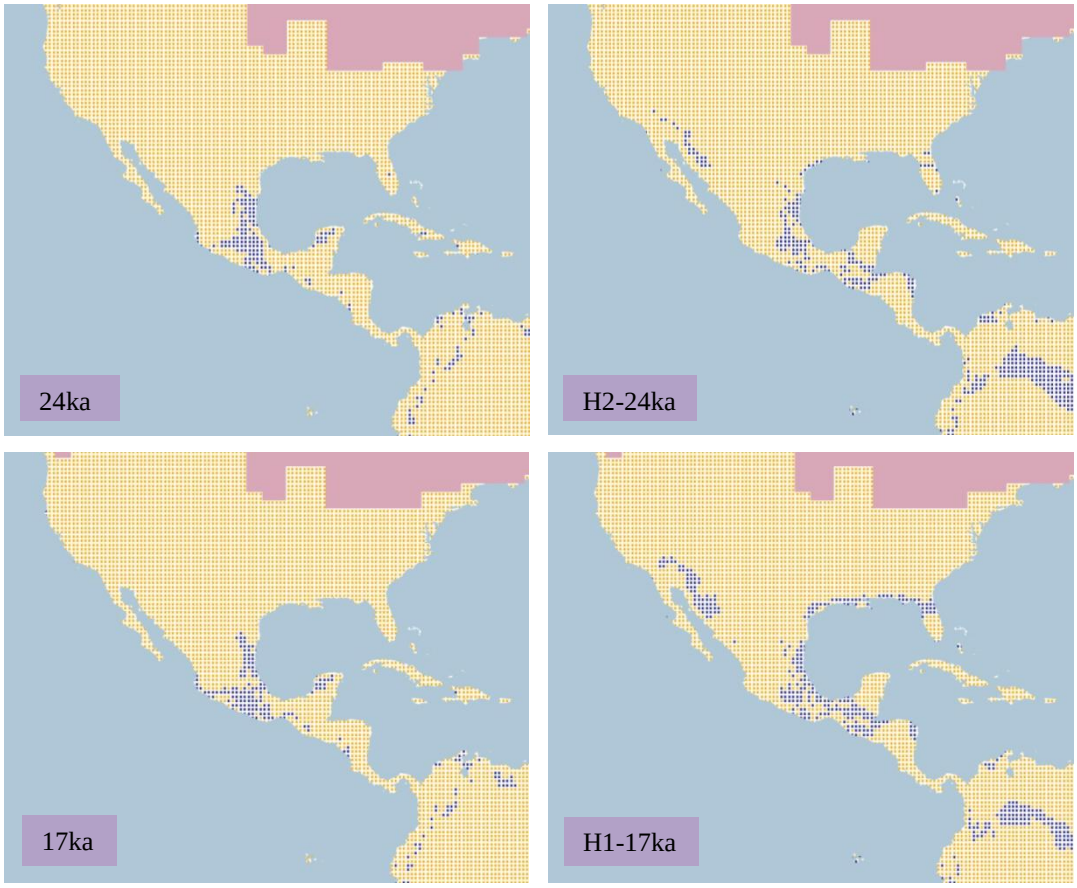

Figure 4.1.5.8.b. Simulation maps of Broad-billed Hummingbird non-breeding range. Maps are shown for ten-time slices: 24ka, H2 (24ka), 17ka, H1 (17ka), 13ka, H0 (13ka), 9ka, 5ka, 3ka and present (1961–90).

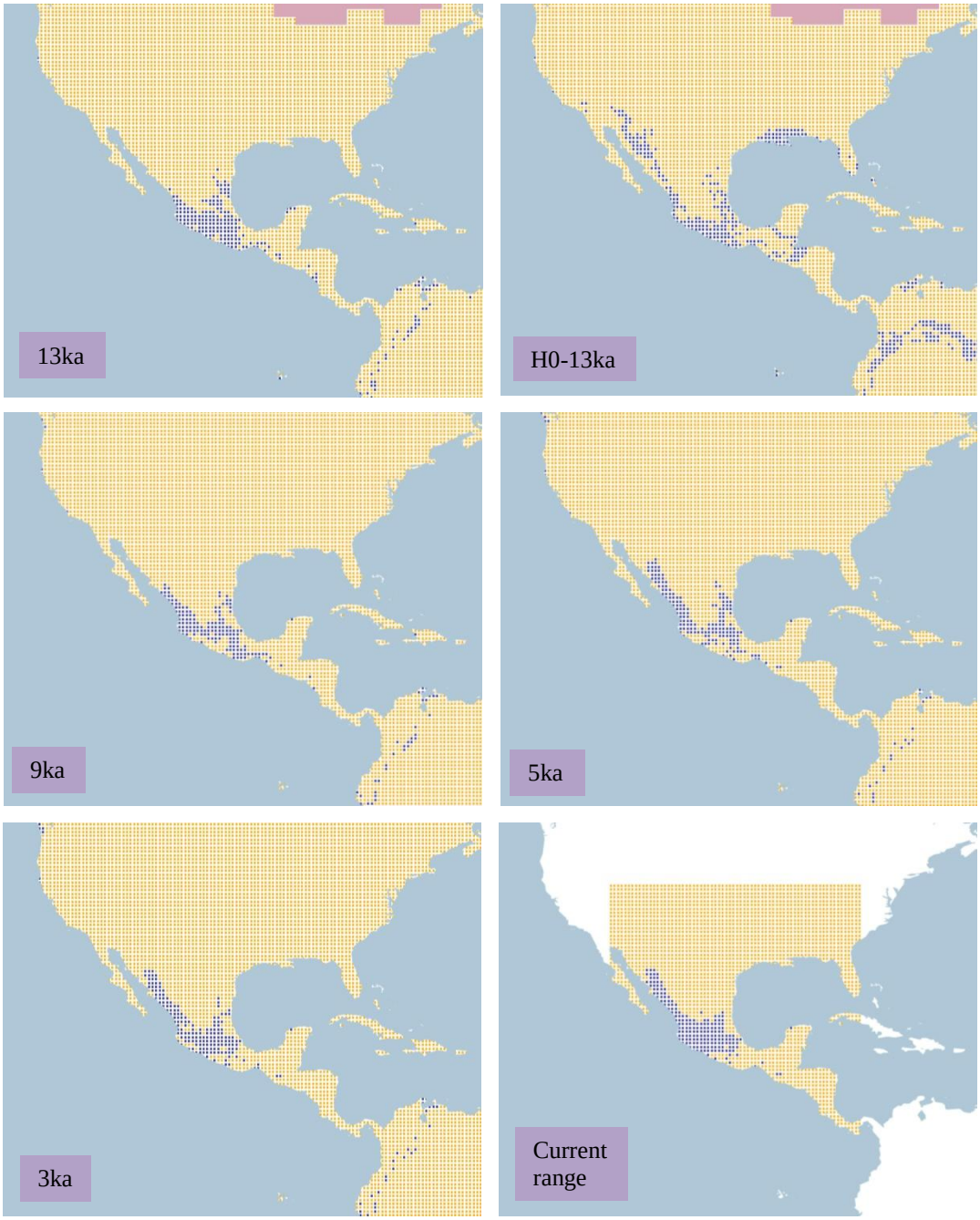

Figure 4.1.5.8.b. Simulation maps of Broad-billed Hummingbird non-breeding range (continued**).**

*4.1.5.9 Magnificent Hummingbird (*Eugenes fulgens *including* E. f. fulgens *and* E. f. spectabilis*). Conservation status: Least Concern. Current known range Figure 4.1.5.9.*

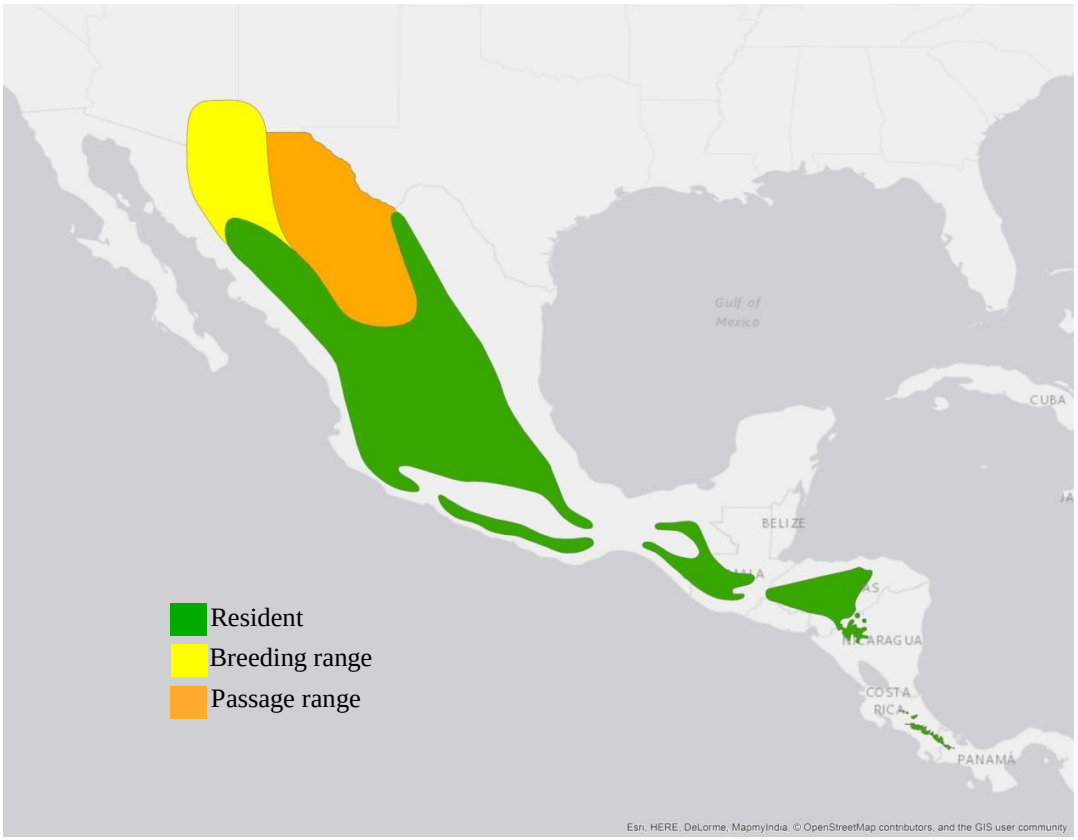

Figure 4.1.5.9. Current known range of Magnificent Hummingbird.

Breeding range (AUC: 0.994; TSS: 0.927; Kappa: 0.896): the species breeding range is located in northern Mexico, between Sonora and Sinaloa and as far as southern Arizona and New Mexico in the USA. There is also a year-round resident range along northern and central Mexico, with a smaller range in the south, extending to Central America in Guatemala, Honduras, northern Nicaragua and central Costa Rica.

At 26 ka BP the range is mainly projected in central to eastern and southern Mexico, and along Central America, with a smaller range in the western and southern USA. The trend continues with minimal variation until 16 ka BP when the range in the south-western USA is reduced. With the deglaciation at 13 ka BP the range in north-eastern Mexico begins to decrease, and especially at 12 ka BP, there is no projected range in the eastern region of Mexico. See Figure 4.1.5.9.a.

By the beginning of the Holocene the range is projected in the western USA, and in central, eastern and southern Mexico, and along Central America. The range changes at 10 ka BP with the increase of the range in central-northern Mexico, reaching from Sinaloa to central Tamaulipas. The trend continues and by 8 ka BP the range extends from the north of Sonora in Mexico as far as Central America.

From 3 ka BP until 1 ka BP the range remains with a similar pattern in Mexico and Central America, only with an increase in the range of the north of Sonora. This pattern is also similar to the current breeding range projection in Mexico and Central America.

Similar ranges are predicted in central, eastern and southern Mexico by the H2 and 24 ka BP projections; although the H2 projection presents a larger range along north-western Mexico and the western USA, with a smaller range in Central America. The range in north-western Mexico and the south-western USA is increased at H1, extending also on the south-eastern coast of the USA, which differs from the 17 ka BP projection. A more similar range is observed between H0 and 13 ka BP from central to eastern and southern Mexico and along Central America, although the H0 projection presents a larger range in the north of Mexico than the 13 ka BP projection.

In the projections there are suitable conditions for the species in the central and eastern region and along the Andean cordillera in South America, even though the species has a year-round resident range in Mexico.

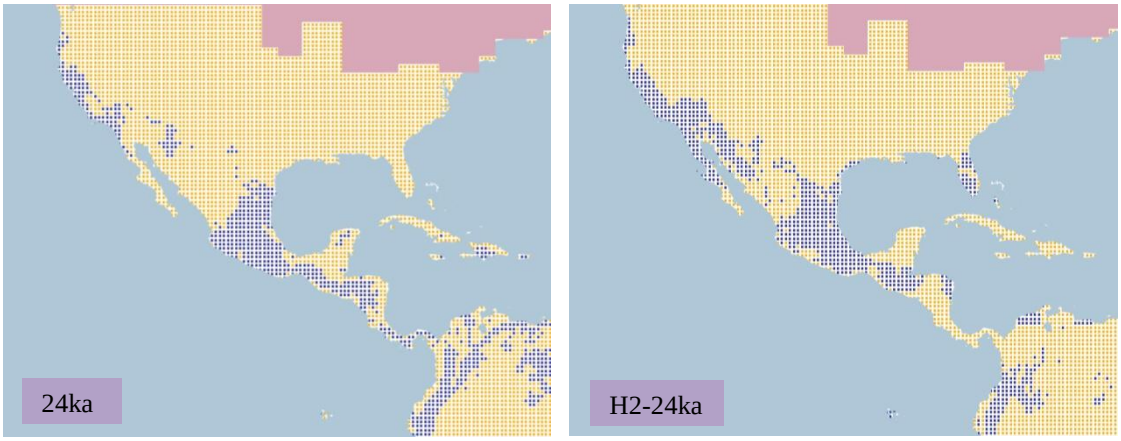

Figure 4.1.5.9.a. Simulation maps of Magnificent Hummingbird breeding range. Maps are shown for ten-time slices: 24ka, H2 (24ka), 17ka, H1 (17ka), 13ka, H0 (13ka), 9ka, 5ka, 3ka and present (1961–90).

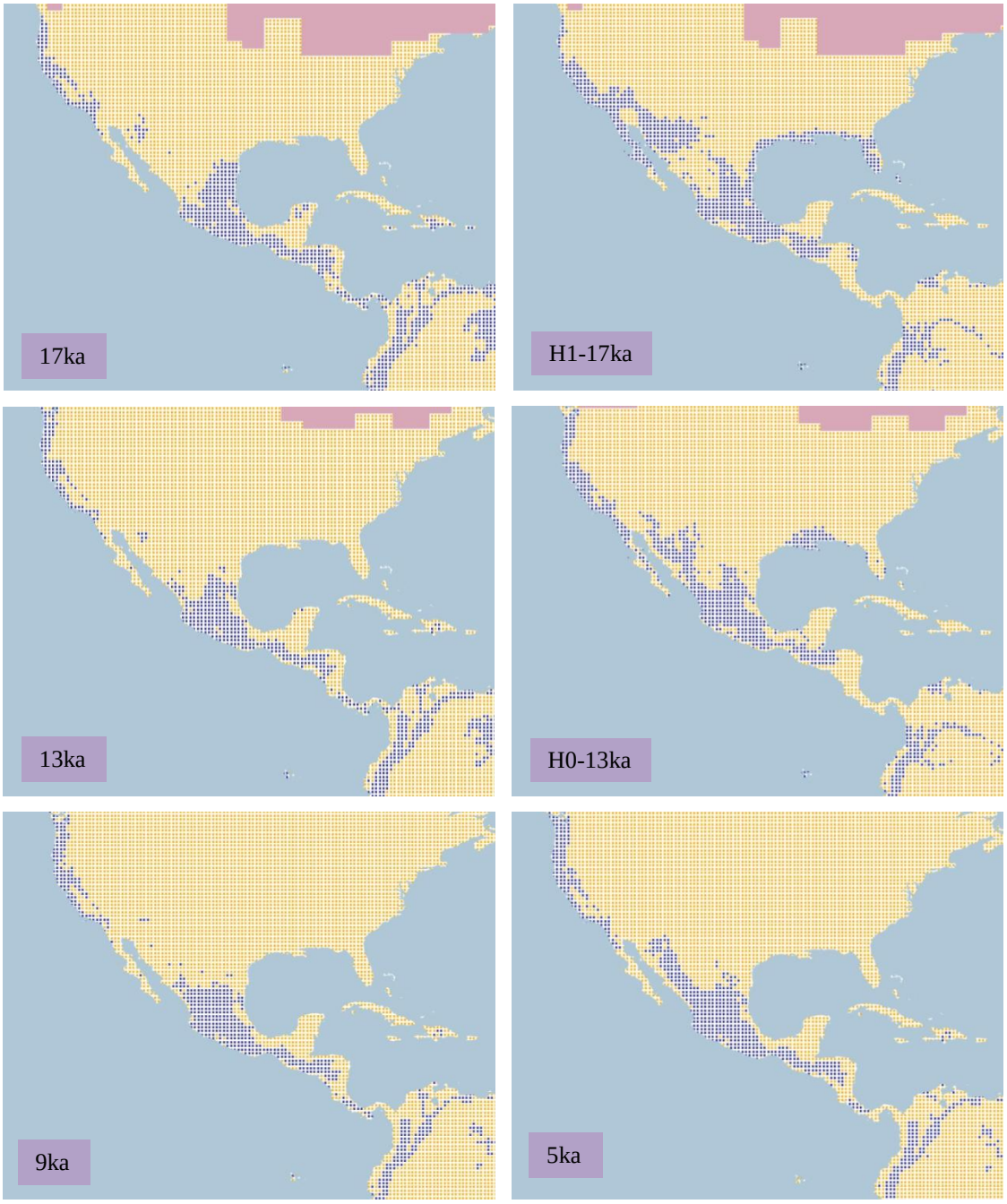

Figure 4.1.5.9.a. Simulation maps of Magnificent Hummingbird breeding range (continued**).**

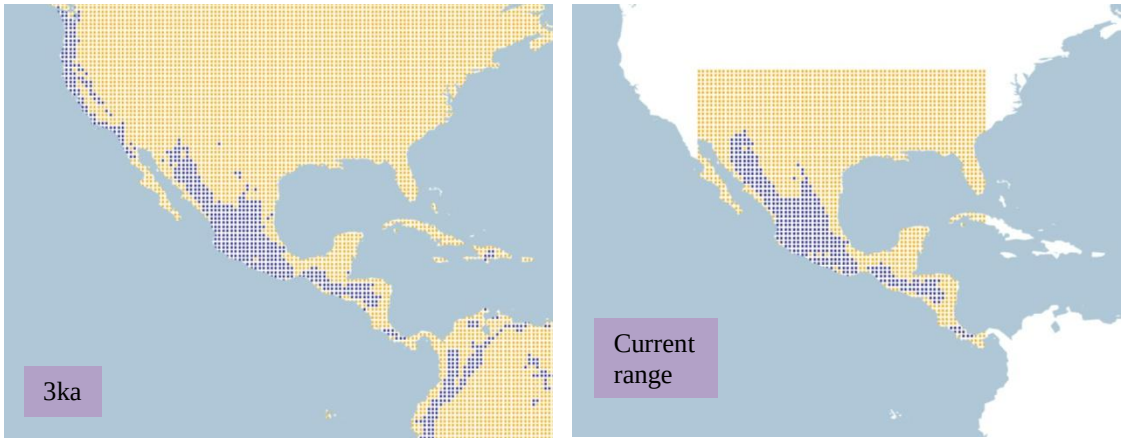

Figure 4.1.5.9.a. Simulation maps of Magnificent Hummingbird breeding range (continued**).**

Non-breeding range (AUC: 0.995; TSS: 0.937; Kappa: 0.903): The species has a year-round resident range along Mexico, from the northern to the south-central region with a smaller scale in Guatemala, Honduras, and Costa Rica in Central America.

A range in central, eastern and southern Mexico is projected at 26 ka BP, with a smaller range along Central America and the western coast of the USA. The trend continues with minimal variations in eastern Mexico at 17 ka BP and at 12 ka BP, with the remaining range unchanged. See Figure 4.1.5.9.b.

By the beginning of the Holocene at 10 ka BP, the range in eastern Mexico is extended to the western region reaching Sinaloa, and, additionally, at 8 ka BP the range in western Mexico increases in the north as far as Sonora and Chihuahua. This range pattern continues unchanged until the 1 ka BP projection, and agreeing with the current non-breeding range projection.

When comparing the Heinrich event H2 with the 24 ka BP projections, there are similar ranges in Mexico, with a smaller range in Central America and larger range in the western USA with a range projected in Florida at H2. The increasing pattern continues at H1, on the south-eastern coast of the USA and in the north of Mexico, differing from the 17 ka BP projection. At H0 the range decreases in the western and south-eastern USA as well as in central, eastern and southern Mexico, projecting a range in the western region of Mexico.

Even though the species' current non-breeding range is located in Mexico, there are suitable conditions projected in the Andean cordillera and eastern Brazil in South America in most of the projections.

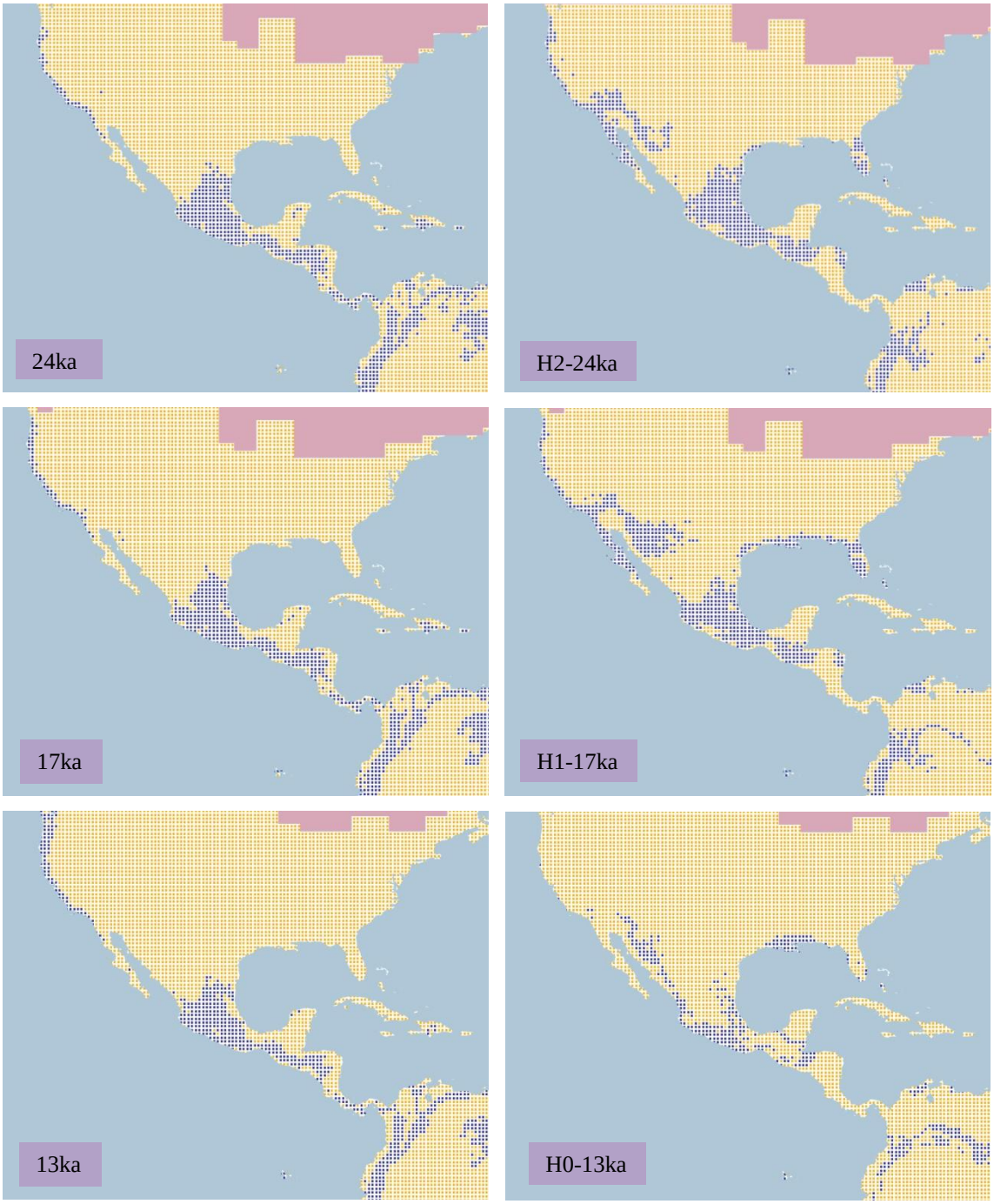

Figure 4.1.5.9.b. Simulation maps of Magnificent Hummingbird non-breeding range. Maps are shown for ten-time slices: 24ka, H2 (24ka), 17ka, H1 (17ka), 13ka, H0 (13ka), 9ka, 5ka, 3ka and present (1961–90).

Figure 4.1.5.9.b. Simulation maps of Magnificent Hummingbird non-breeding range (continued**).**

*4.1.5.10 Blue-throated Hummingbird (*Lampornis clemenciae *including* L. c. bessophilus, L. c. phasmorus, *and* L. c. clemenciae*). Conservation status: Least Concern. Current known range Figure 4.1.5.10.*

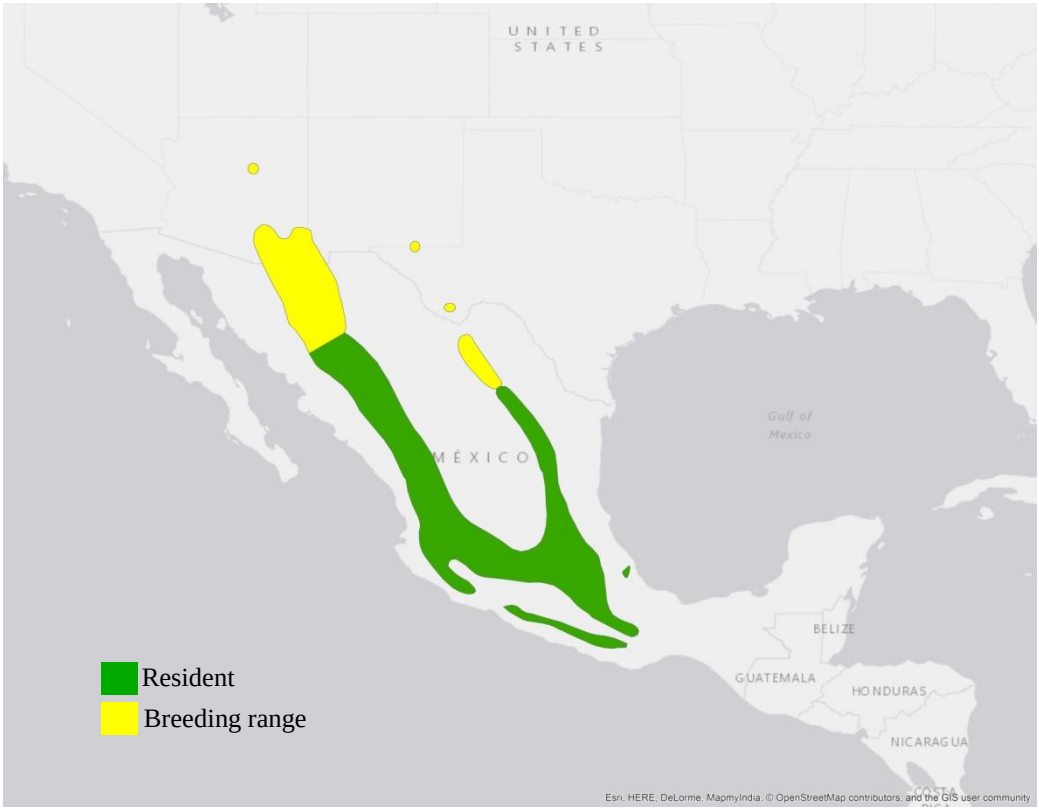

Figure 4.1.5.10. Current known range of Blue-throated Hummingbird.

Breeding range (AUC: 0.993; TSS: 0.934; Kappa: 0.871): This species spends the breeding season in the northern region of the Sierra Madre Occidental and Sierra Madre Oriental in Mexico, between Sonora and Chihuahua, with a smaller range in Coahuila, and extending to the southern USA between Arizona and New Mexico. The species also has a year-round resident range along the Sierra Madre Occidental, Sierra Madre Oriental and the Transverse Neovolcanic Belt in Mexico, with a smaller range in the Sierra Madre del Sur.

At 26 ka BP the range is projected in eastern and southern Mexico with a smaller extent in the western and southern USA. This pattern continues with minimal differences until 17 ka BP when the range in the western USA is decreased, and the central-southern range in Mexico increased as far as Jalisco. After this, at 15 ka BP, the range in north-eastern Mexico is reduced. See Figure 4.1.5.10.a.

By the beginning of the Holocene at 11 ka BP the range is projected in central and eastern Mexico, with a fragmented range in the northern region. The range is also fragmented along the western USA. At 10 ka BP, the range in western and eastern Mexico is increased, and particularly at 8 ka BP reaching as far as northern Sonora.

At 6 ka BP there is a decrease in the range projected in the Sierra Madre Occidental and Sierra Madre Oriental in Mexico, which increases again at 5 ka BP. After this, the range remains unchanged in Mexico until 1 ka BP, from the Sierra Madre Occidental, Sierra Madre Oriental and Sierra Madre del Sur.

When comparing the Heinrich event H2 with the 24 ka BP projection, there are a few similarities between the ranges. H2 projects a range in north-western and eastern Mexico, and along the south-eastern coast and west coast of the USA. The H1 projected range is increased on the south-eastern coast of the USA and the north-western region of Mexico, differing from the 17 ka BP projection. At H0, the range in the southern USA is decreased and instead the range in Mexico increases, from the northern to southern region.

Even though the current breeding range is located in Mexico, there are suitable conditions projected in South America, along the Andean cordillera, eastern Brazil and northern Argentina.

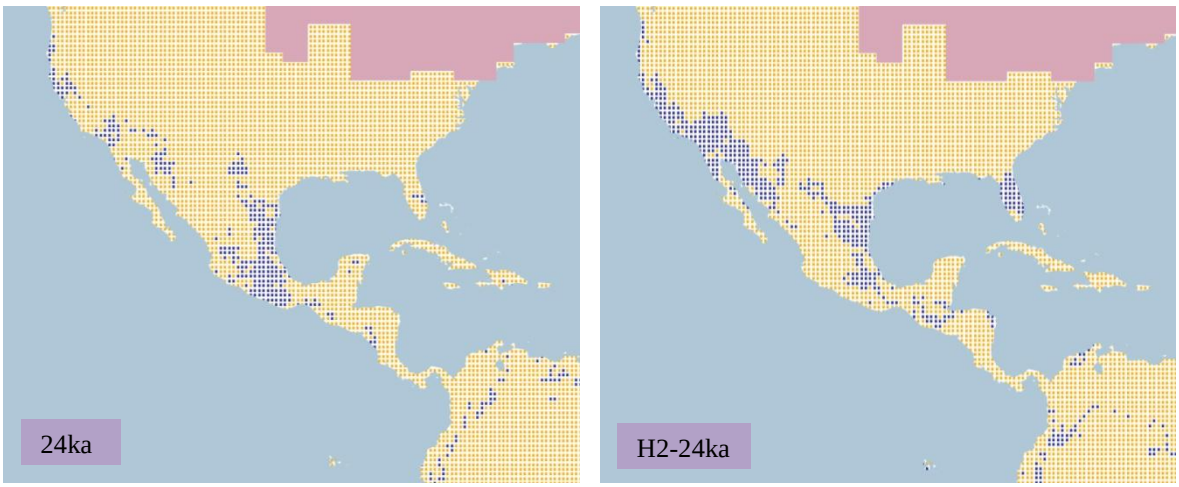

Figure 4.1.5.10.a. Simulation maps of Blue-throated Hummingbird breeding range. Maps are shown for ten-time slices: 24ka, H2 (24ka), 17ka, H1 (17ka), 13ka, H0 (13ka), 9ka, 5ka, 3ka and present (1961–90).

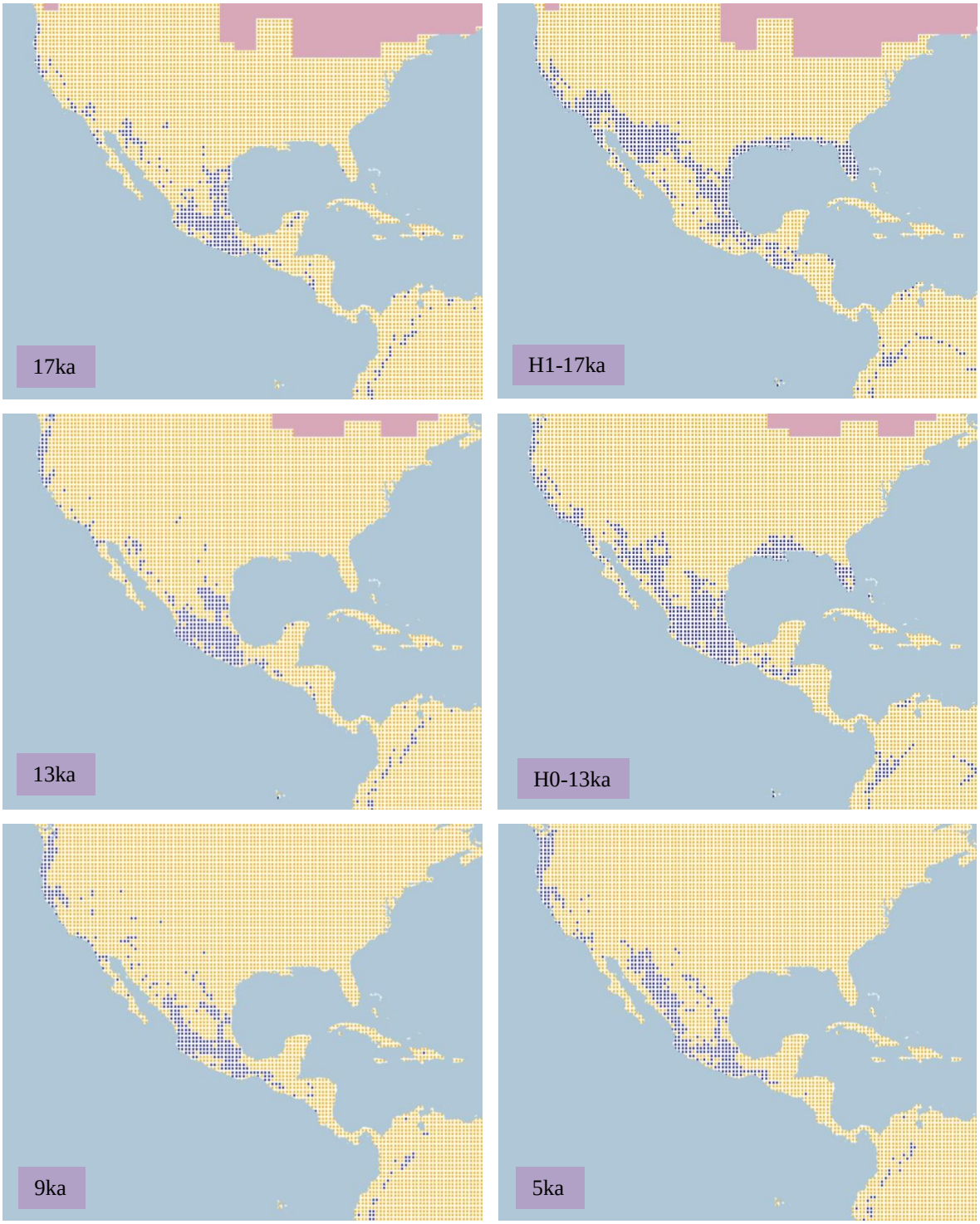

Figure 4.1.5.10.a. Simulation maps of Blue-throated Hummingbird breeding range (continued**).**

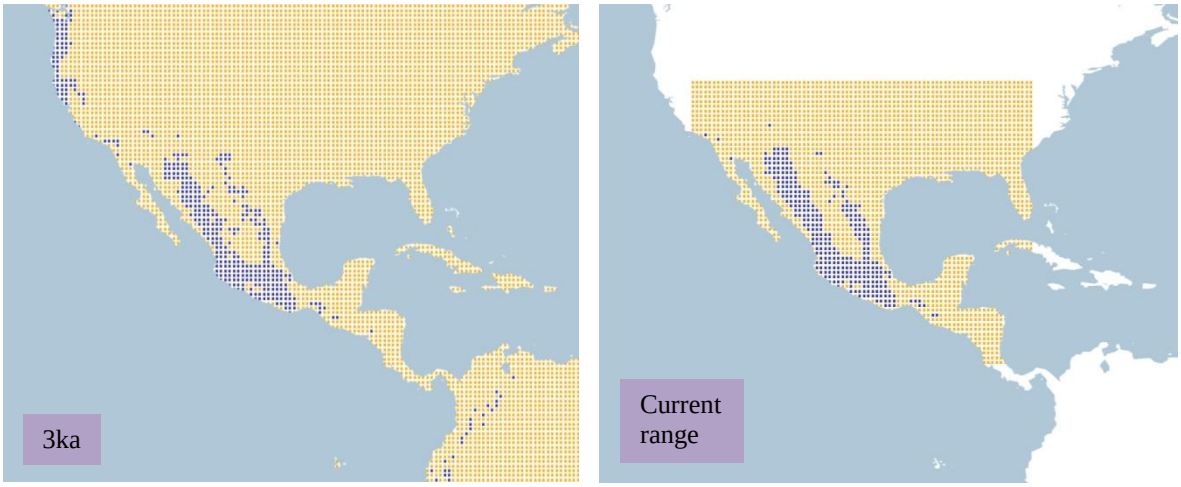

Figure 4.1.5.10.a. Simulation maps of Blue-throated Hummingbird breeding range (continued**).**

Non-breeding range (AUC: 0.996; TSS: 0.962; Kappa: 0.892): The species has a year-round resident ground in the Sierra Madre Occidental, Sierra Madre Oriental and the Transverse Neovolcanic Belt in Mexico.

At 26 ka BP the range is projected in central-eastern Mexico, with a smaller range on the western coast of the USA. The pattern continues until 17 ka BP when there is an increase to the western region as far as Jalisco in Mexico. See Figure 4.1.5.10.b.

At 10 ka BP, the range in central Mexico extends to the north in Sinaloa, and in the south of Mexico as far as Chiapas and a small range in Guatemala. The trend continues until 8 ka BP, with the increase in northern Mexico along the Sierra Madre Occidental. After this, the range remains with minimal changes until 1 ka BP. The current non-breeding projection also follows the pattern as 1 ka BP, with a similar range projected in the mountain ranges of Mexico.

The Heinrich event H2 projects a range in eastern Mexico and in the western to southern USA, differing from the 24 ka BP range, projected in central Mexico. At the H1 projection, the range in the western USA and eastern Mexico is increased, and a south-eastern coastal range is projected in the USA. The H0 projection shares a similar range in central Mexico with the 13 ka BP projection, although at H0 a range in the north-west of Mexico and the south-eastern USA is projected.

Although the non-breeding range of the species is located in Mexico, there are suitable conditions projected in the Andean cordillera and central South America.

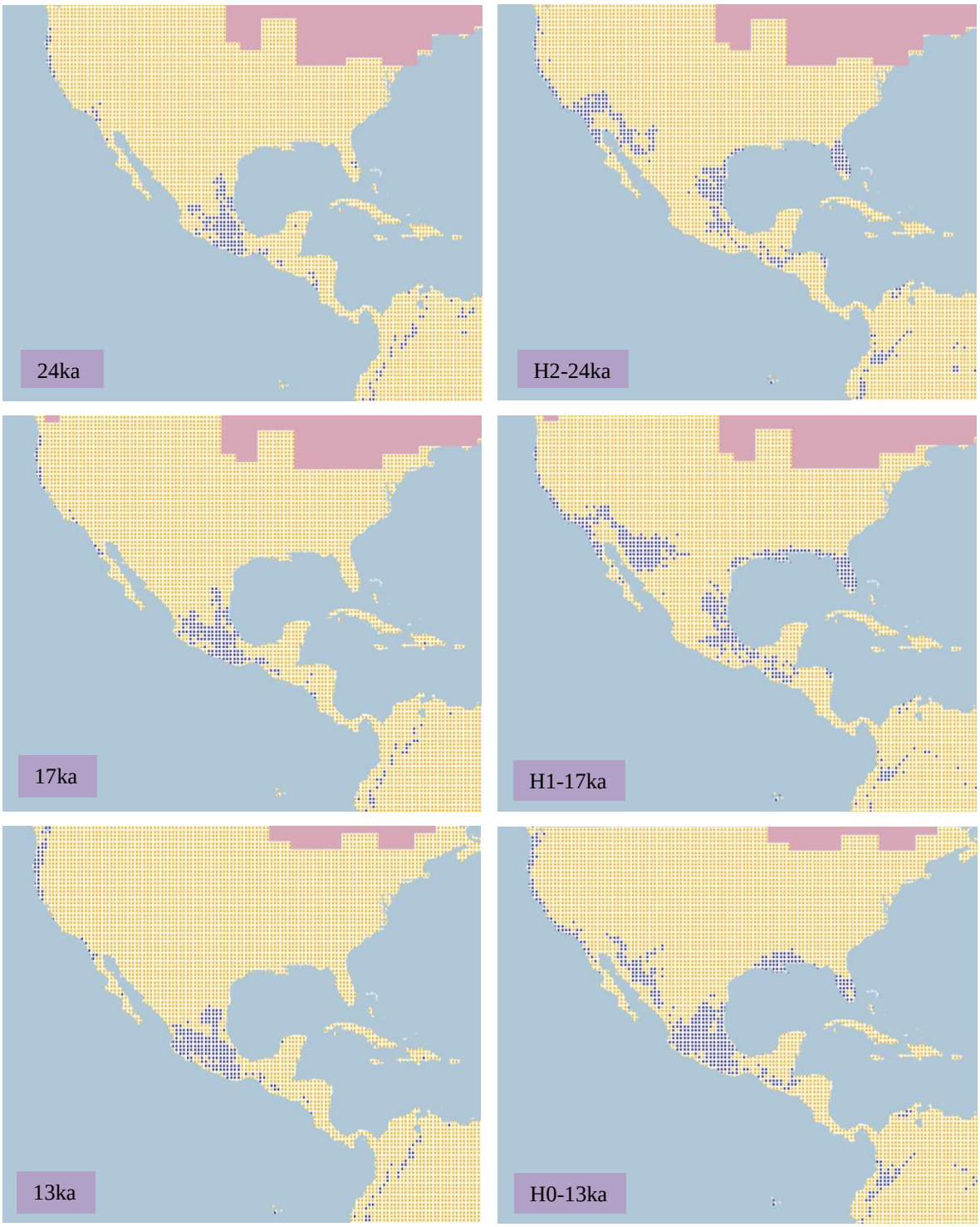

Figure 4.1.5.10.b. Simulation maps of Blue-throated Hummingbird non-breeding range. Maps are shown for ten-time slices: 24ka, H2 (24ka), 17ka, H1 (17ka), 13ka, H0 (13ka), 9ka, 5ka, 3ka and present (1961–90).

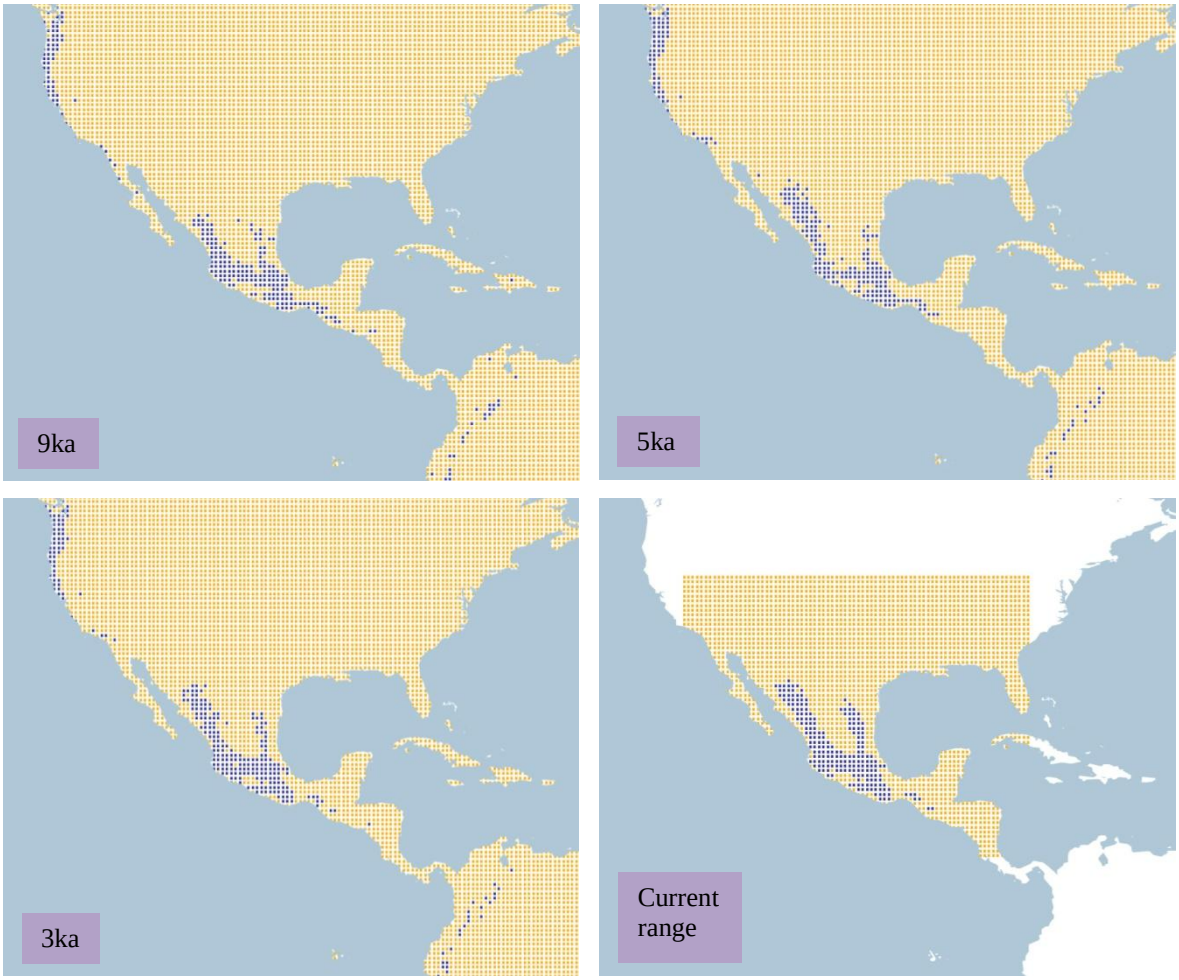

Figure 4.1.5.10.b. Simulation maps of Blue-throated Hummingbird non-breeding range (continued**).**

*4.1.5.11 Calliope Hummingbird (*Selasphorus calliope*). Conservation status: Least Concern. Current known range Figure 4.1.5.11.*

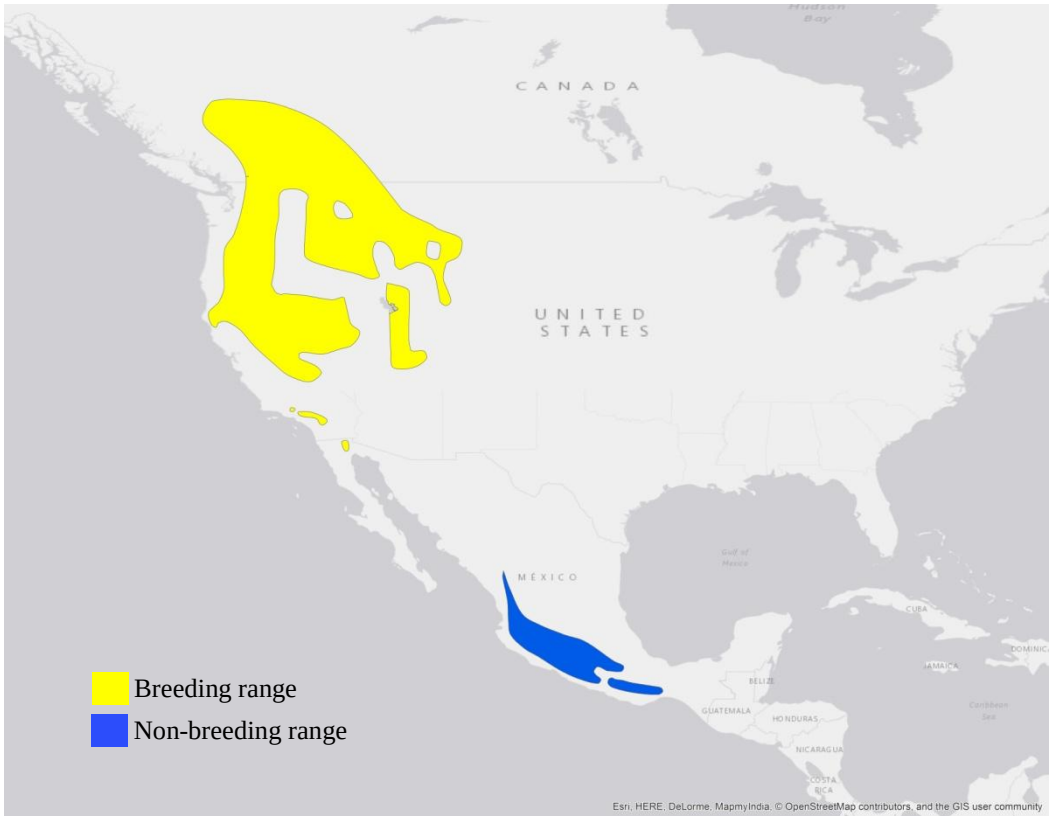

Figure 4.1.5.11. Current known range of Calliope Hummingbird.

Breeding range (AUC: 0.979; TSS: 0.863; Kappa: 0.791): This species spends the breeding season in the western USA, from California to Wyoming and Washington. The range also extends to south-western Canada in British Columbia and Alberta.

At 26 ka BP the range is projected in the central and western USA, with a smaller range in the south-eastern USA, and in the Sierra Madre Occidental as far as Sinaloa in Mexico. The range continues and at 21 ka BP, the range in northern Mexico is decreased. The pattern continues until 17 ka BP, with a decrease in the central and western USA. At 14 ka BP, the range in the western and central USA continues decreasing, with the range in the south-eastern USA shifting to the central-eastern region. With the ice sheet decline at 13 ka BP, the range in the central USA disappears, projecting the range in the western and central-eastern USA. See Figure 4.1.5.11.a.

By the beginning of the Holocene at 11 ka BP, the range in the western USA decreases inland and shifts to the south-west of British Columbia in Canada. The range in the eastern USA increases to the north, with a small range projected in south-central Canada in Manitoba as well. After this, at 9 ka BP the range in south-central Canada disappears.

At 8 ka BP the range in the western USA and south-western Canada is increased, with the eastern range in the USA reaching the north-east of Canada in Nova Scotia. This pattern continues with minimal differences until 1 ka BP. The current breeding range projection presents a similar range in the western USA and south-western Canada.

The range at H2 is projected in the USA at a smaller extent than the 24 ka BP projection with a larger range in the western and central region. At the H1 projection the range in the western USA is increased, presenting a similar range as 17 ka BP except in the central region of the USA. The H0 range is projected at a larger scale in the central region of the USA than at the 13 ka BP, agreeing only in the western and eastern regions of the USA.

Although the current breeding range is located in North America, there are suitable conditions projected along the Andean cordillera and Argentina in South America.

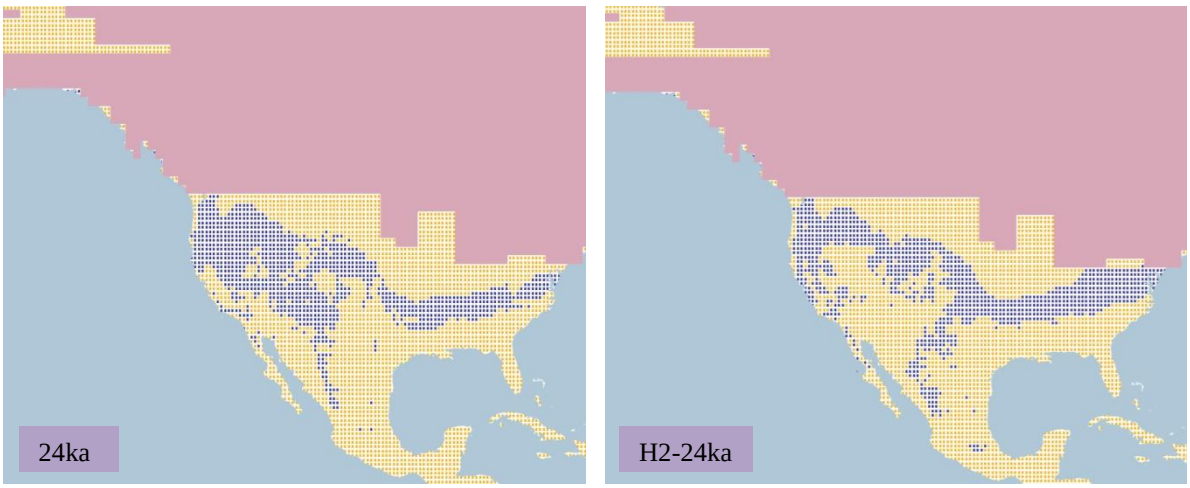

Figure 4.1.5.11.a. Simulation maps of Calliope Hummingbird breeding range.
Maps are shown for ten-time slices: 24ka, H2 (24ka), 17ka, H1 (17ka), 13ka, H0 (13ka), 9ka, 5ka, 3ka and present (1961–90).

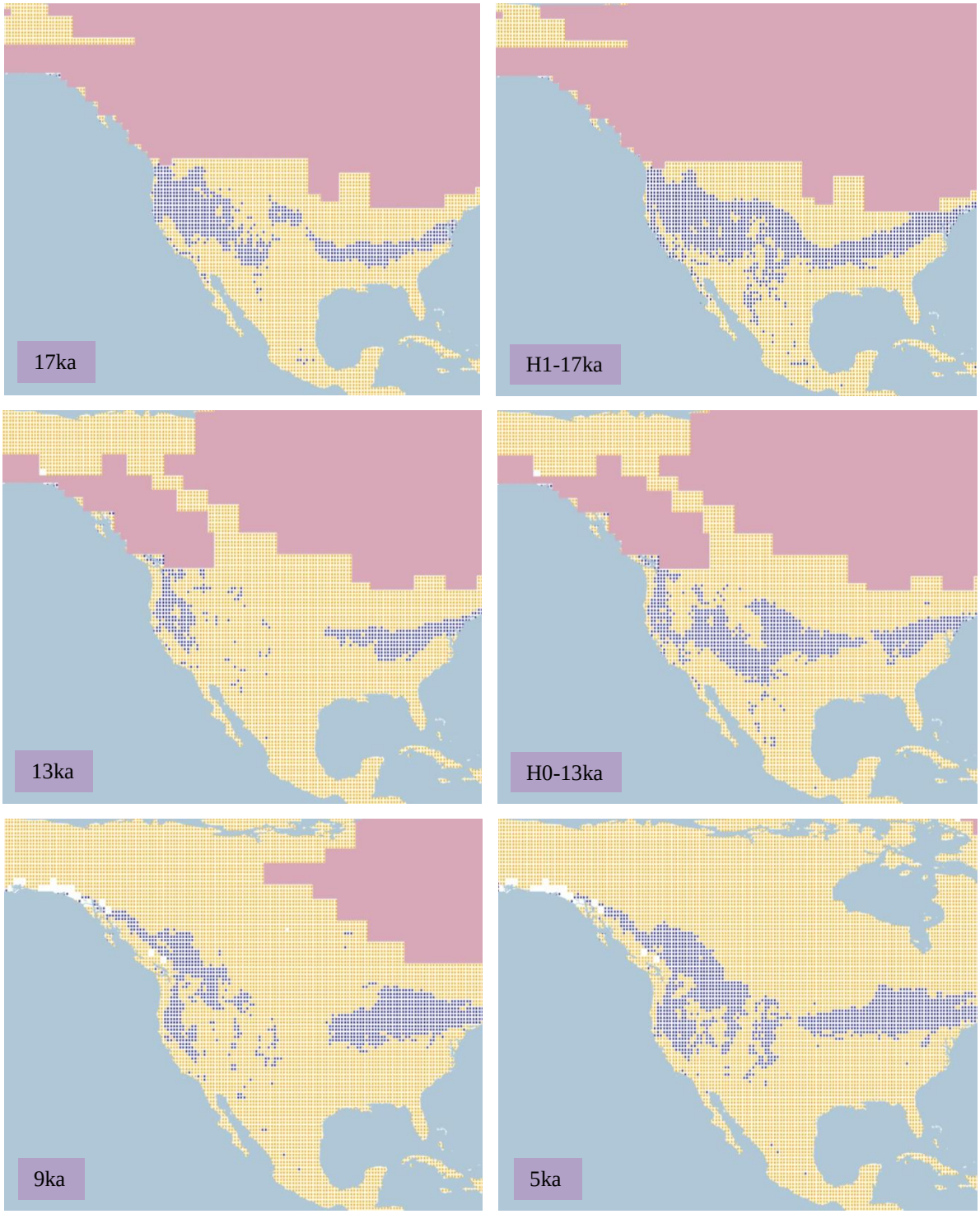

Figure 4.1.5.11.a. Simulation maps of Calliope Hummingbird breeding range (continued**).**

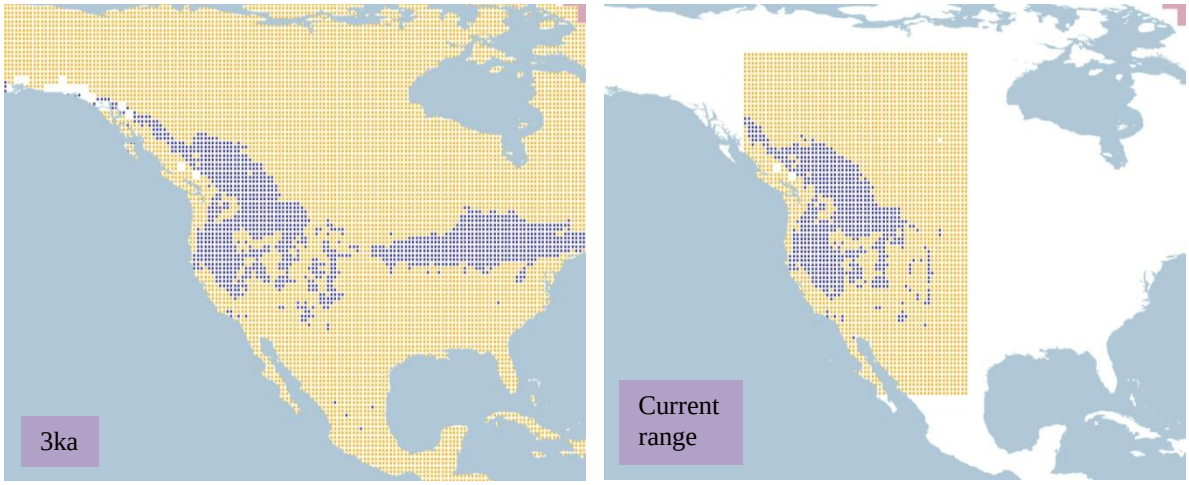

Figure 4.1.5.11.a. Simulation maps of Calliope Hummingbird breeding range (continued**).**

Non-breeding range (AUC: 0.993; TSS: 0.940; Kappa: 0.897): The wintering ground of the species is located along the Sierra Madre del Sur in Mexico.

At 26 ka BP the range is projected along the Sierra Madre del Sur in Mexico, with a scattered range in Central America. The trend continues with minimal variations until 13 ka BP, when the range is increased in Jalisco, Mexico. See Figure 4.1.5.11.b.

By the beginning of the Holocene at 10 ka BP, the range increases to the north of Jalisco as far as central Sinaloa. This range pattern continues unchanged until the 1 ka BP projection. The current non-breeding projection continues with a similar range in central Mexico along the Sierra Madre del Sur as the 1 ka BP projection.

The Heinrich event H2 projects a small and scattered range in south-eastern Mexico, differing from the range projected at 24 ka BP along the Sierra Madre del Sur in Mexico. A similar pattern as H2 continues at H1, with a scattered range in south-eastern Mexico. At H0, the range presents a similar range as the 13 ka BP projection, along the Sierra Madre del Sur in Mexico, although of a smaller extent.

Even though the non-breeding range is located in central Mexico, there are suitable conditions projected in the Andean cordillera and north-eastern Brazil in South America.

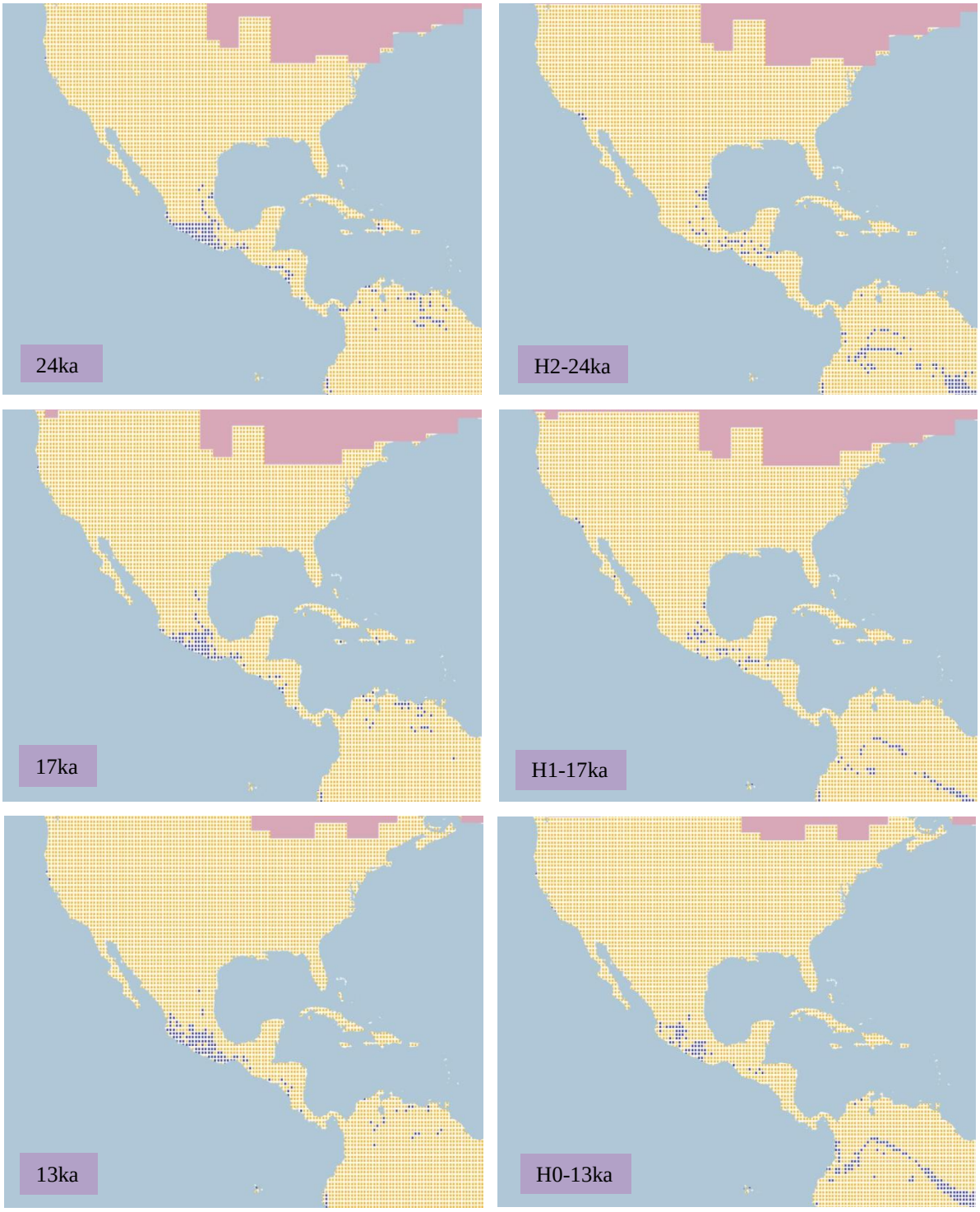

Figure 4.1.5.11.b. Simulation maps of Calliope Hummingbird non-breeding range. Maps are shown for ten-time slices: 24ka, H2 (24ka), 17ka, H1 (17ka), 13ka, H0 (13ka), 9ka, 5ka, 3ka and present (1961–90).

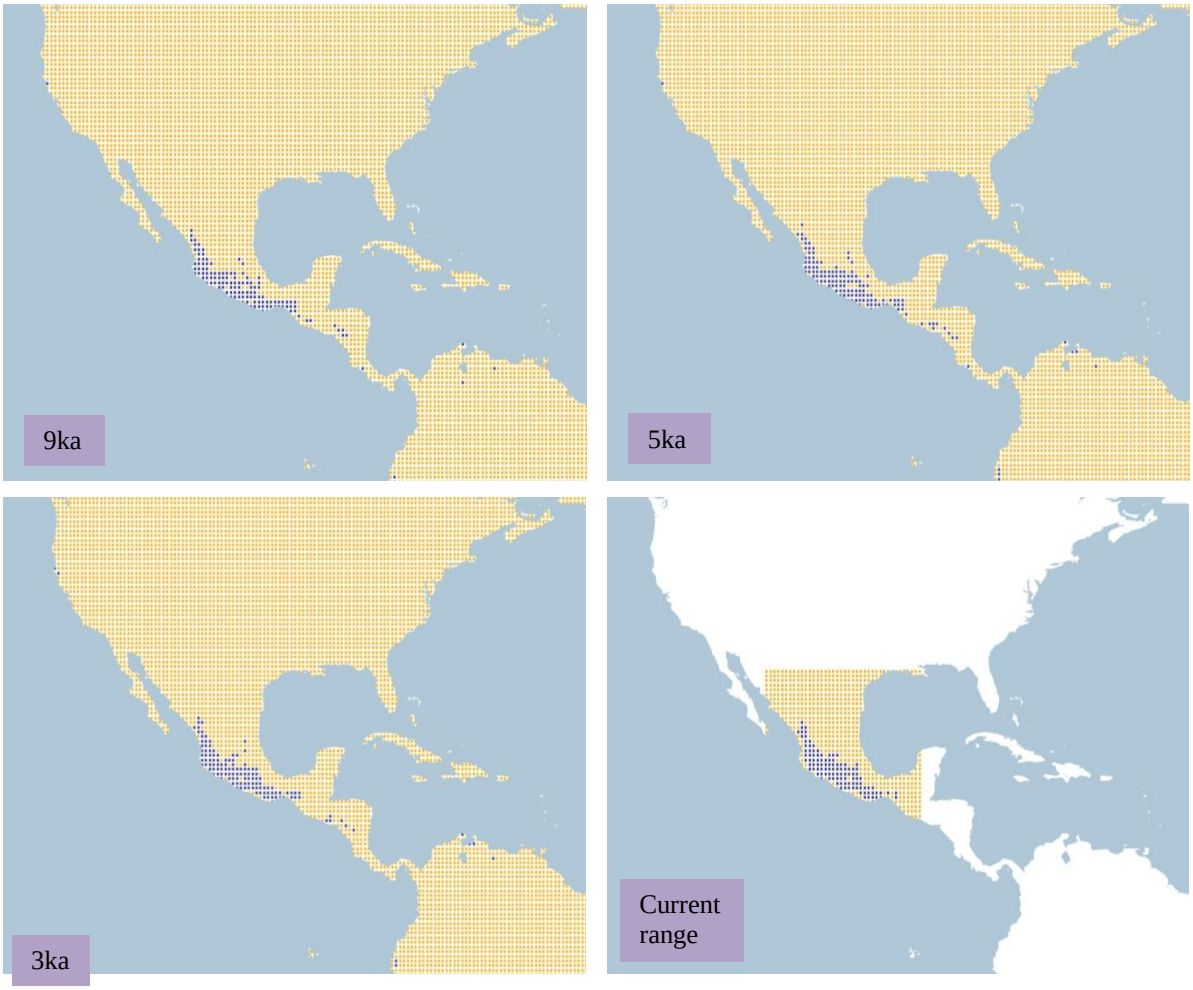

Figure 4.1.5.11.b. Simulation maps of Calliope Hummingbird non-breeding range (continued**).**

*4.1.5.12 Broad-tailed Hummingbird (*Selasphorus platycercus*). Conservation status: Least Concern. Current known range Figure 4.1.5.12.*

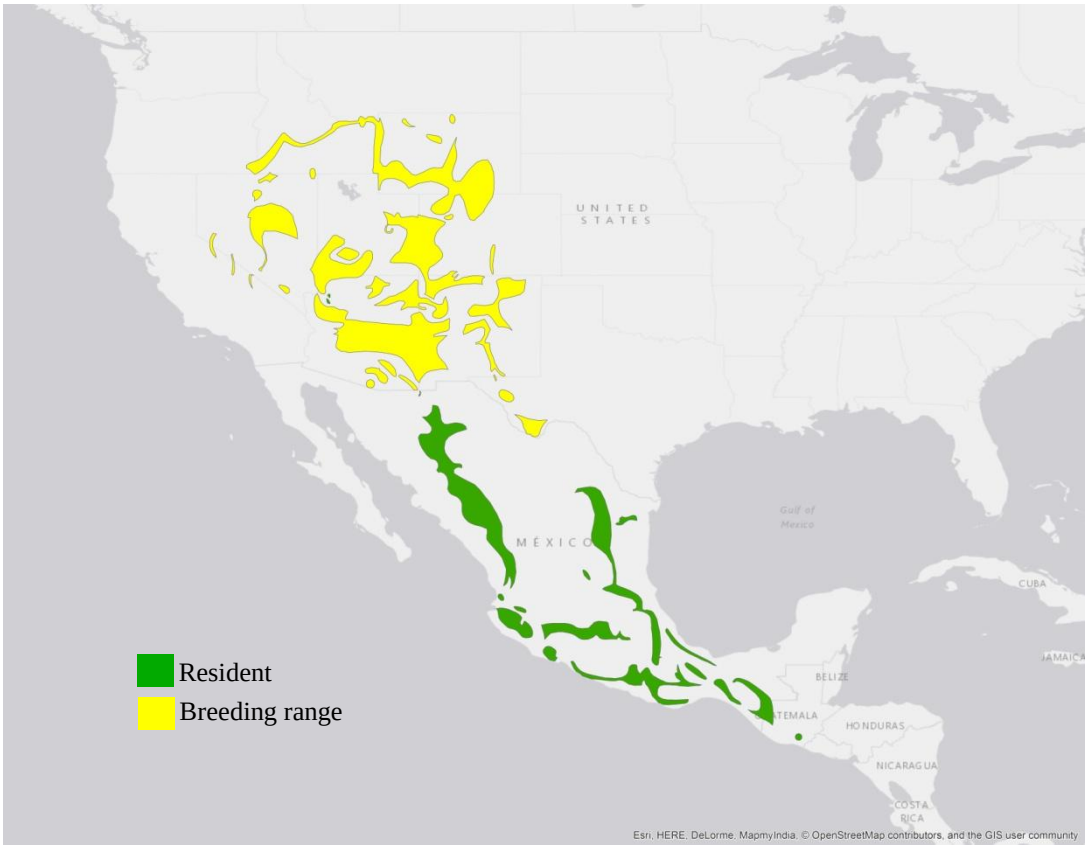

Figure 4.1.5.12. Current known range of Broad-tailed Hummingbird.

Breeding range (AUC: 0.971; TSS: 0.837; Kappa: 0.696): The breeding grounds of the species are located in a scattered range in the central USA. Also, the species has a year-round resident range along the Sierra Madre Occidental, Sierra Madre Oriental and southern Mexico, with a small range in Guatemala.

At 26 ka BP an intermittent range is projected in the central USA, south-central and northern Mexico, with a smaller range along Central America. The scattered pattern continues and at 19 ka BP the range in the central and south-western USA and northern Mexico is increased. At 14 ka BP the range in the central USA shifts to the western region, with a decrease in the range projected in northern Mexico. See Figure 4.1.5.12.a.

By the beginning of the Holocene the range is projected in the western USA, and along the Sierra Madre Occidental, Sierra Madre Oriental and south-central region of Mexico. Also, a

small range is projected in south-central Canada near the ice sheet. The range in the western USA is decreased at 9 ka BP, as well as in the northern parts of the Sierra Madre Occidental and Sierra Madre Oriental in Mexico. After this, there is an increased in the northern range of the Sierra Madre Occidental and in south-central Mexico at 8 ka BP.

At 6 ka BP the range in the USA is extending from central to western regions, with the remainder of the range projected in Mexico persisting with minimal variations. The range trend in the central-western USA and in the Sierra Madre Occidental and Sierra Madre Oriental and south-central Mexico continues with small variations until 1 ka BP. In addition, the current breeding range projection, continues with the trend in the central-western USA and in the Sierras and the south-central region of Mexico.

The Heinrich event H2 projects a different range from the 24 ka BP projection, along northern Mexico mainly in Tamaulipas, and in the south-western USA with a small range in the south of Texas and Florida, and an intermittent range in southern Mexico. The pattern continues at H1, increasing in the northern and southern region of Mexico, and in the south-western USA, differing from the 17 ka BP projection. At H0 the pattern changes, extending from south-central to northern Mexico along the Sierra Madre Oriental and with a scattered range in the western USA.

Even though the species' breeding grounds are located in North America, there are suitable conditions projected from the Andean cordillera in Peru as far as south-central Argentina in South America.

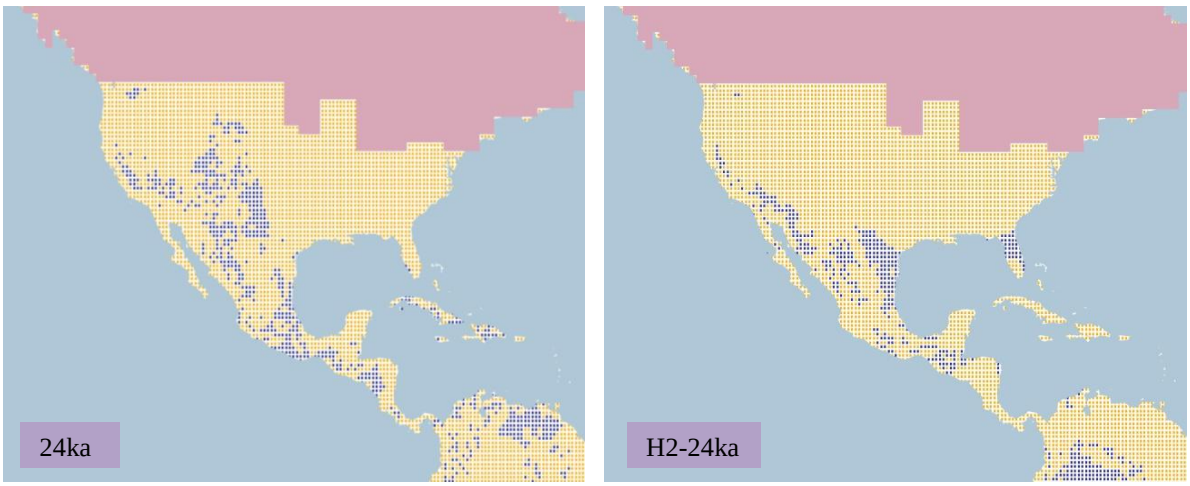

Figure 4.1.5.12.a. Simulation maps of Broad-tailed Hummingbird breeding range. Maps are shown for ten-time slices: 24ka, H2 (24ka), 17ka, H1 (17ka), 13ka, H0 (13ka), 9ka, 5ka, 3ka and present (1961–90).

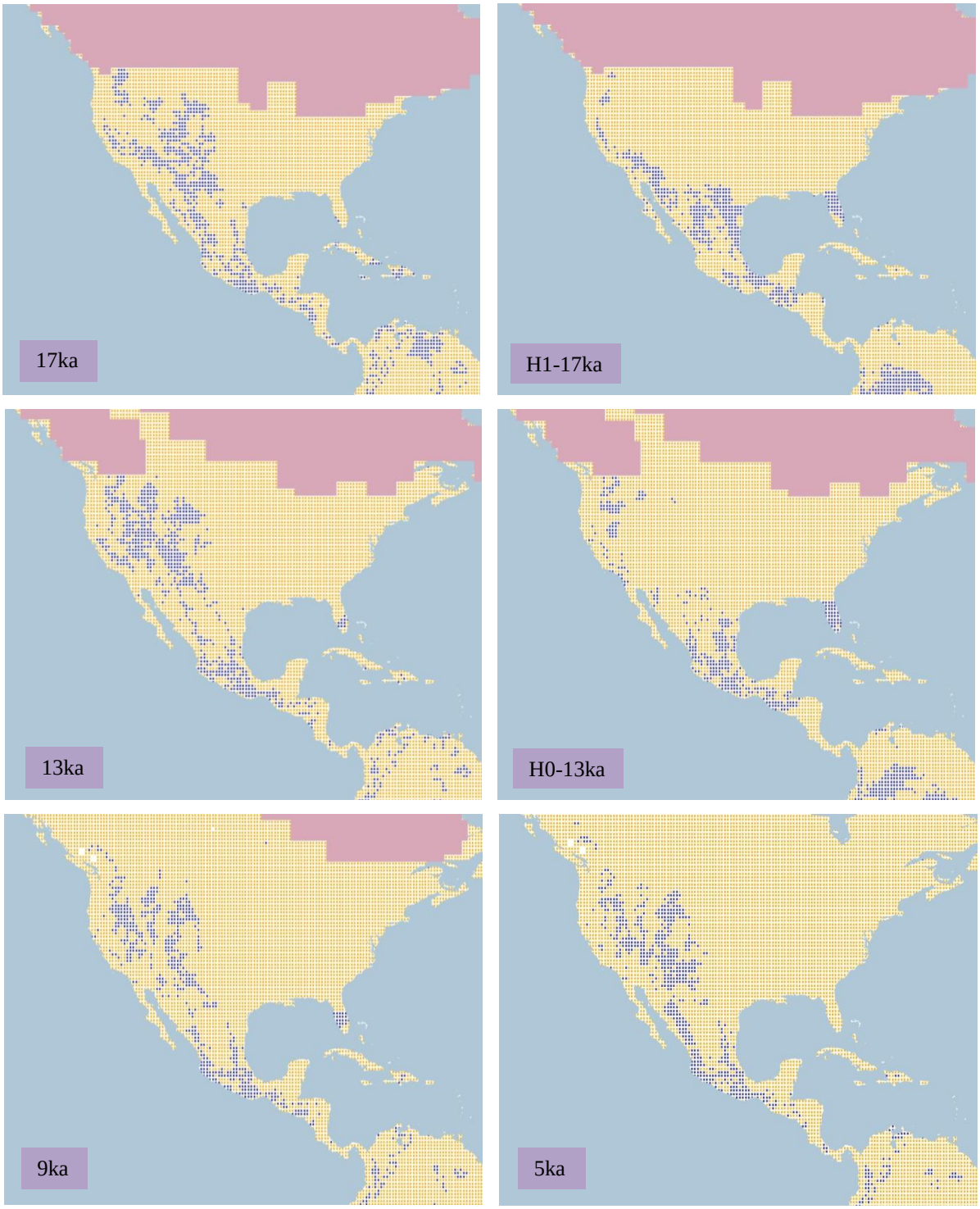

Figure 4.1.5.12.a. Simulation maps of Broad-tailed Hummingbird breeding range (continued**).**

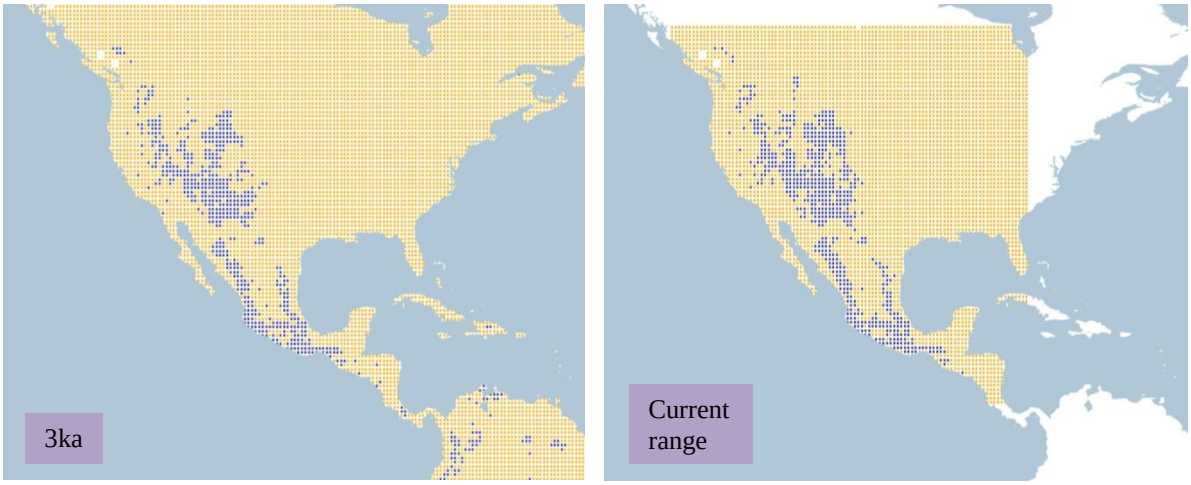

Figure 4.1.5.12.a. Simulation maps of Broad-tailed Hummingbird breeding range (continued**).**

Non-breeding range (AUC: 0.995; TSS: 0.948; Kappa: 0.824): There is only a year-round resident range recognized for the species, along the Sierra Madre Occidental, Sierra Madre Oriental and southern Mexico, with a small range in Guatemala.

At 26 ka BP a small range is projected from north-eastern to south-central Mexico, and a smaller range in Guatemala, El Salvador and Costa Rica. The trend continues with minimal variations in north-eastern Mexico until the beginning of the Holocene at 11 ka BP, when the range in north-eastern and central Mexico is reduced. After this at 10 ka BP, the range is increased along the Sierra Madre Occidental and Sierra Madre Oriental in Mexico. See Figure 4.1.5.12.b.

At 8 ka BP, there is an increased in the range projected in the Sierra Madre Occidental and the Sierra Madre Oriental in Mexico, this trend continues until 6 ka BP, when the range in central and north-eastern Mexico is decreased. However, from 4 ka BP until 1 ka BP, the range in the Sierra Madre Oriental is increased, with the remainder of the range in south-central Mexico and in the Sierra Madre Occidental persisting unchanged. This trend is continued in the non-breeding range projection, covering the Sierras and the south-central region of Mexico, with a small range in Guatemala.

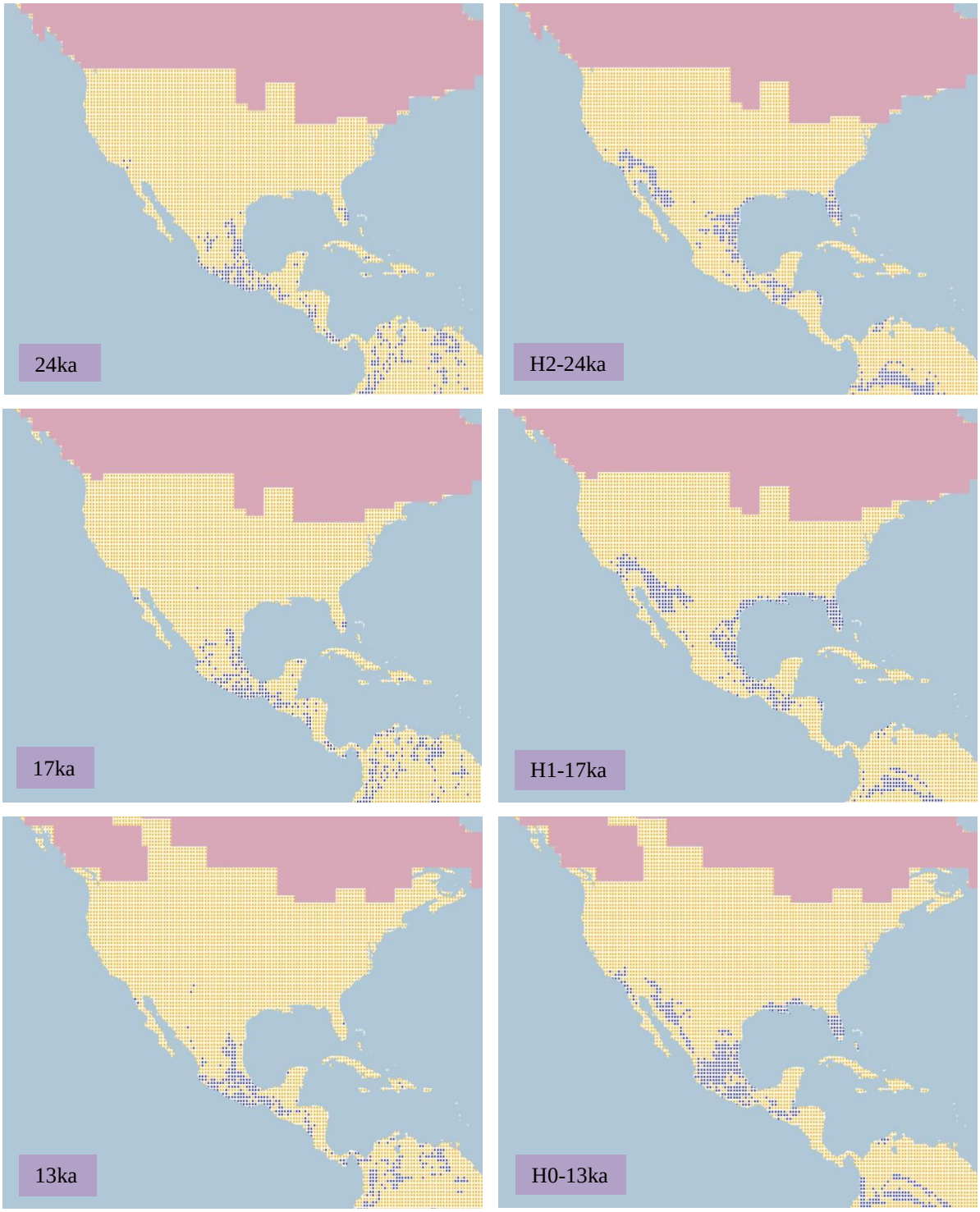

Figure 4.1.5.12.b. Simulation maps of Broad-tailed Hummingbird non-breeding range. Maps are shown for ten-time slices: 24ka, H2 (24ka), 17ka, H1 (17ka), 13ka, H0 (13ka), 9ka, 5ka, 3ka and present (1961–90).

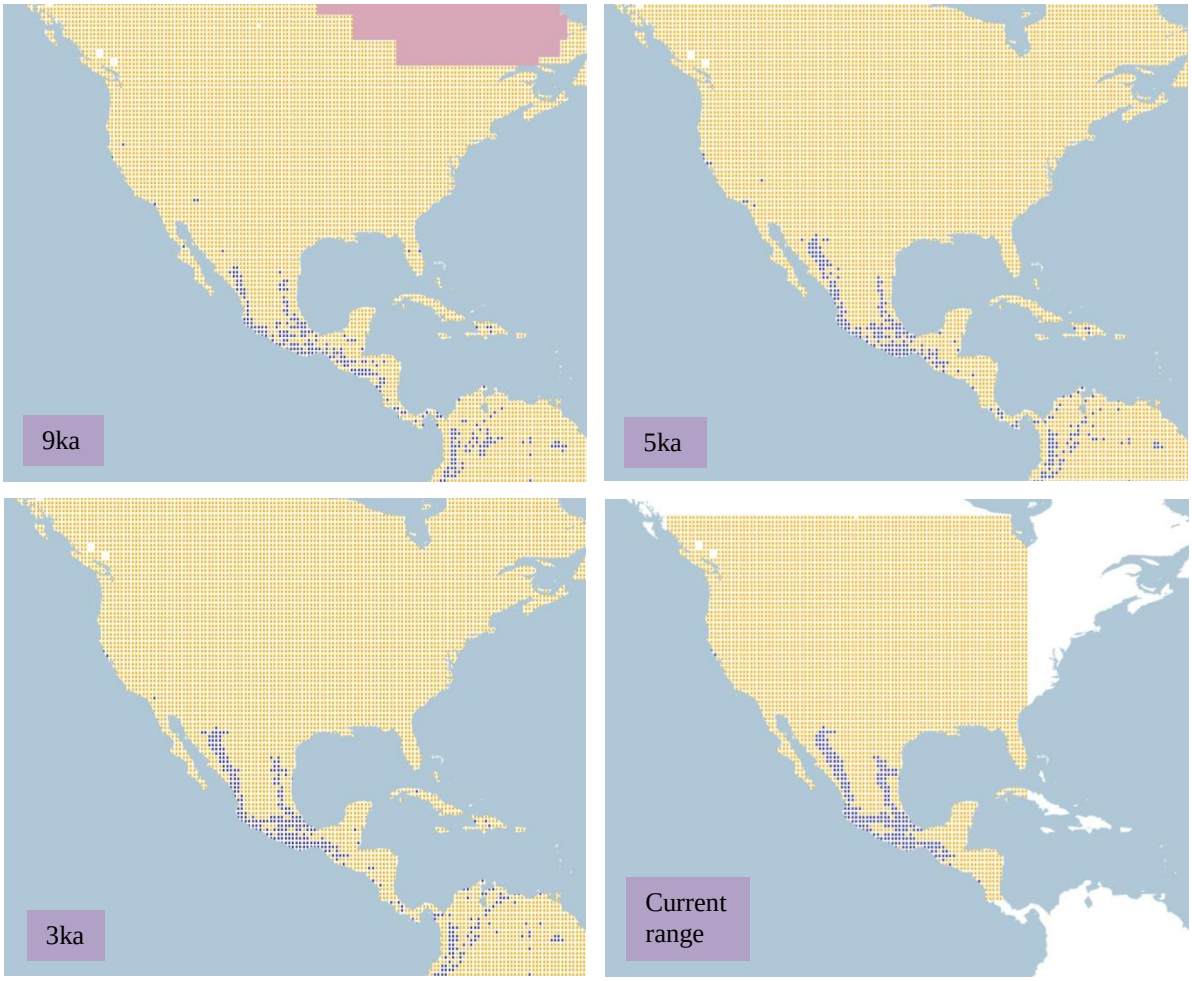

Figure 4.1.5.12.b. Simulation maps of Broad-tailed Hummingbird non-breeding range (continued**).**

*4.1.5.13 Rufous Hummingbird (*Selasphorus rufus*). Conservation status: Least Concern. Current known range Figure 4.1.5.13.*

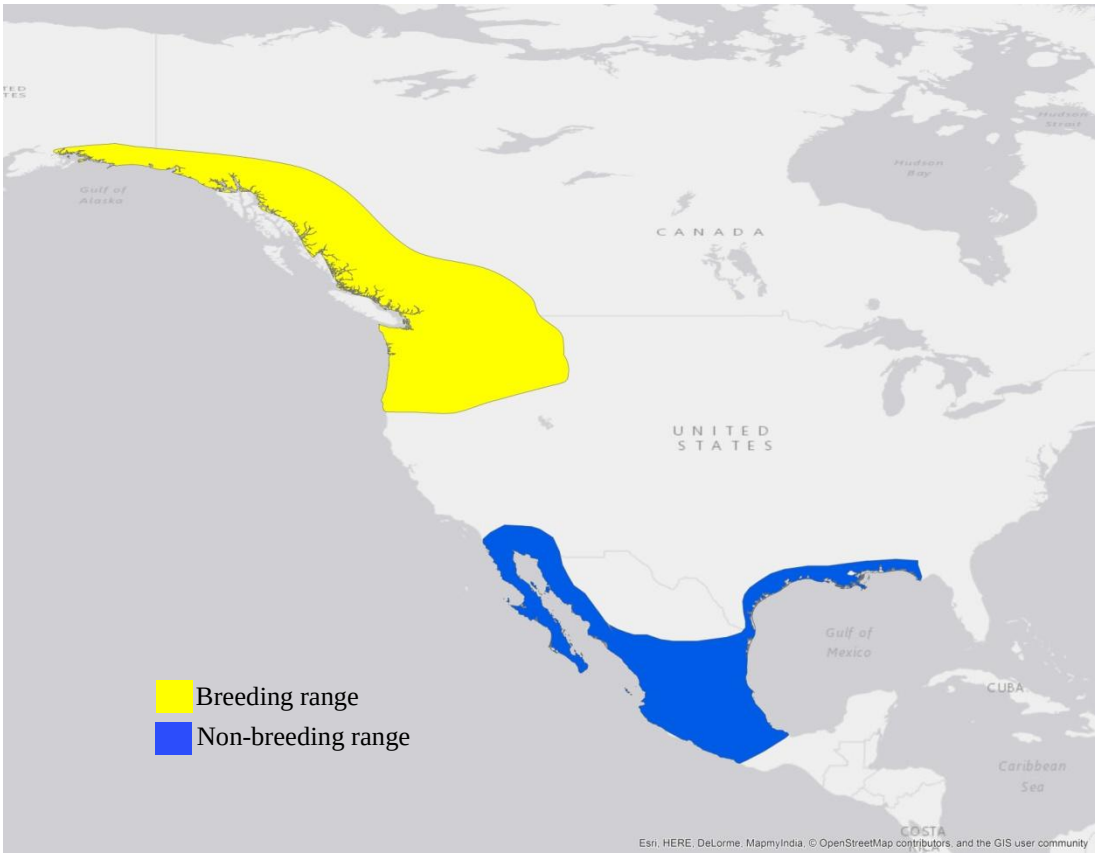

Figure 4.1.5.13. Current known range of Rufous Hummingbird.

Breeding range (AUC: 0.976; TSS: 0.840; Kappa: 0.786): This species spends the breeding season along the Western Cordillera in Canada, extending to north-western Canada and the south-eastern coast of Alaska.

At 26 ka BP the range is projected mostly in the western and central regions of the conterminous USA with a smaller extent in the south-eastern region of the conterminous USA, and in south-central Alaska near the ice sheet. This trend continues and at 19 ka BP the range in the central USA is decreased. See Figure 4.1.5.13.a.

At 17 ka BP, the range in the central USA decreases, as well as in the western region of the conterminous USA, but at a smaller scale. The decreasing pattern continues and at 14 ka BP the range is reduced to the north-western and eastern regions of the conterminous USA, with

a smaller range in south-central Alaska as well. At 13 ka BP with the reduction of the ice sheet the range in the central USA is intermittent.

At the end of the Pleistocene at 12 ka BP the range in the eastern USA is increased, as well as the range in south-western Canada with a smaller range in central Northwest Territories and south-central Manitoba in Canada. As the ice sheet is reduced at 10 ka BP, the range in Manitoba Canada is increased, as well as the eastern and western ranges in the conterminous USA and in western Alaska. The range in central Canada is decreased by 9ka; however, at 8 ka BP the range in Canada shifts to Ontario and Quebec near Hudson Bay, with an increase in the north-eastern and north-western regions of the USA.

The range in Ontario and Quebec is reduced at 7ka; instead there is an increase in western Canada between British Columbia and Alberta. The range in the central USA begins increasing as well. After this at5 ka BP, there is a projected range in north-eastern Canada from Newfoundland and Labrador to Nova Scotia.

At 4 ka BP the range in northern Canada and the central USA is reduced, suitable conditions persisting in the western region of Alaska, British Columbia, Alberta and the north-western conterminous USA, and on the central-east side from Nebraska as far as Maine. This pattern continues until the 1 ka BP projection. The projected range in western Canada and the USA remains in the current breeding range projection.

Similar ranges are projected at H2 and 24 ka BP in the USA, although of a larger extent in the western and central regions at H2. This pattern continues at H1 and the range is increased in the south-central region of the USA, reaching the northern part of Mexico, differing from the 17 ka BP projection with a smaller range in western and central regions of the USA. The range at H0 in the western and eastern USA is reduced, remaining in the central area, contrasting with the 13 ka BP projection with no range projected in the central region of the USA.

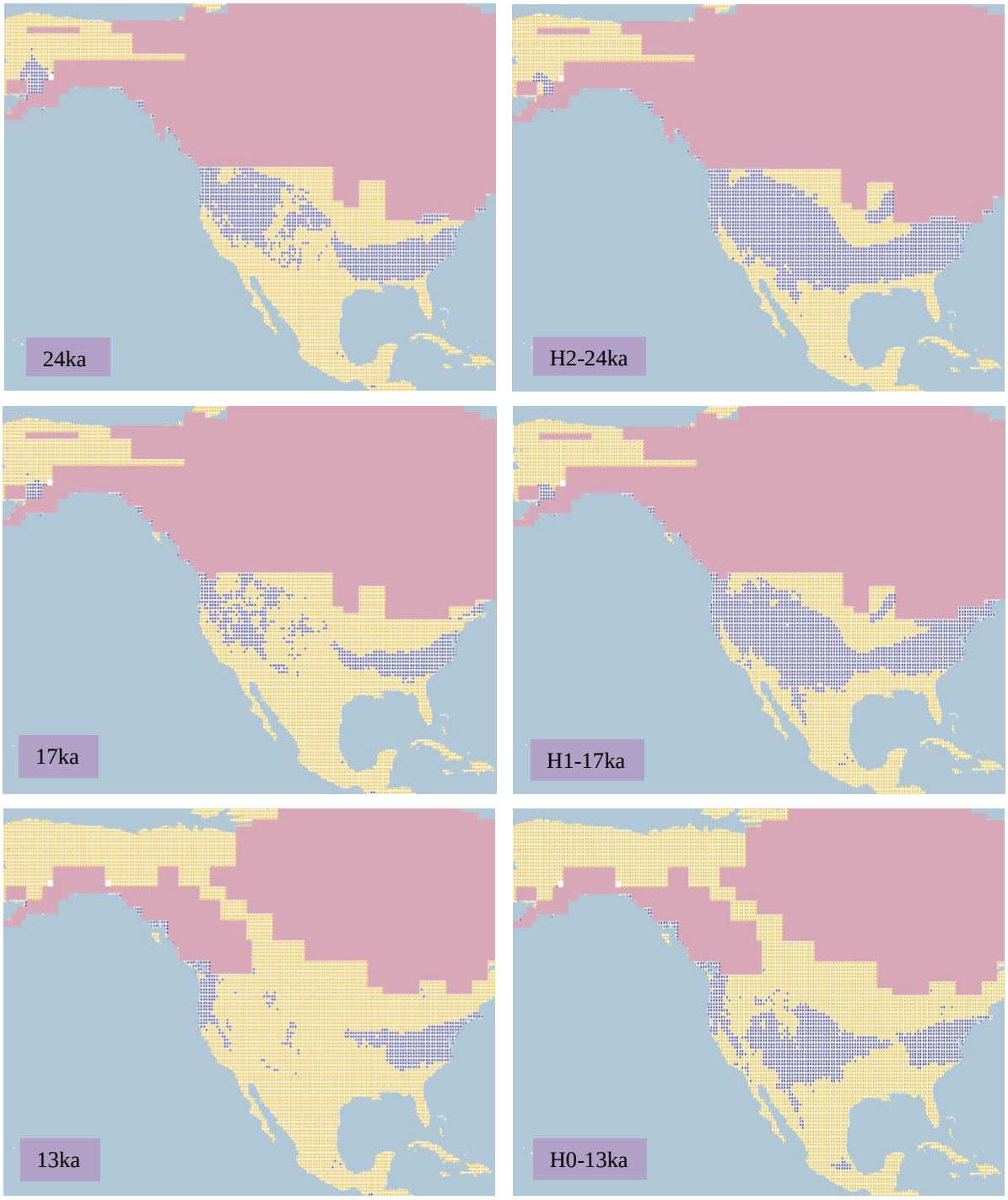

Figure 4.1.5.13.a. Simulation maps of Rufous Hummingbird breeding range.
Maps are shown for ten-time slices: 24ka, H2 (24ka), 17ka, H1 (17ka), 13ka, H0 (13ka), 9ka, 5ka, 3ka and present (1961–90).

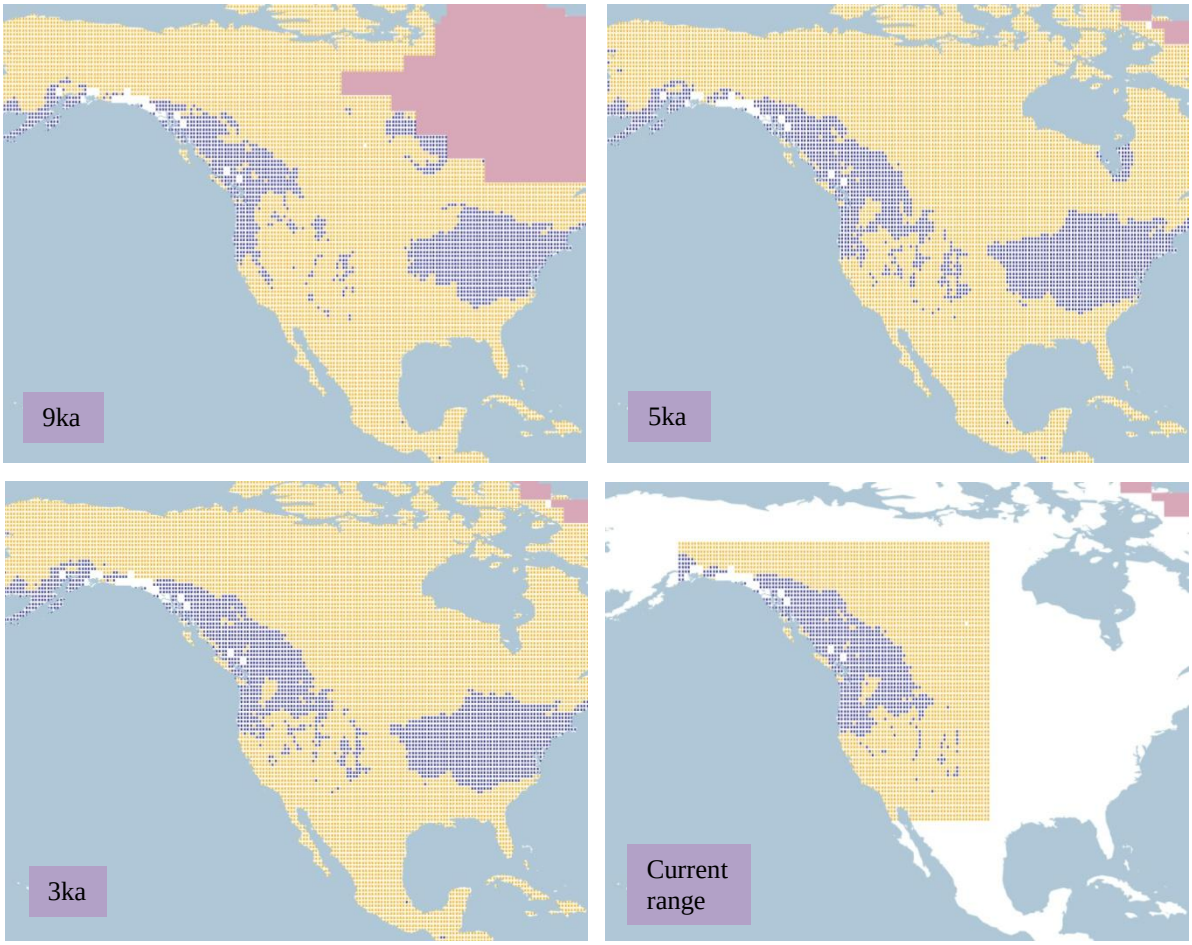

Figure 4.1.5.13.a. Simulation maps of Rufous Hummingbird breeding range (continued**).**

Non-breeding range (AUC: 0.989; TSS: 0.897; Kappa: 0.856): The wintering grounds of the species are located in Mexico from the western to the southern region, except in northern Mexico between Chihuahua, Coahuila and Nuevo Leon. The range is also located along the south-eastern coast of the USA from Texas to western Florida.

At 26 ka BP the range is projected along the western coast of Mexico and as far as the eastern and south-central regions in Mexico, with a smaller range in Yucatan and in Florida, USA. This pattern continues with minimal variation in central Mexico and at 15 ka BP the range between Baja California and Sonora is increased. See Figure 4.1.5.13.b.

By the beginning of the Holocene at 11 ka BP the range in the northern region of Mexico is increased; a small range is also projected along the western coast of the USA, with the decrease of the range in Yucatan, Mexico and Florida, USA. The range in northern Mexico is reduced at 10 ka BP, extending mainly from the western coast to central and south-central

Mexico. This pattern continues until 8 ka BP when the range in north-western Mexico is increased.

At 5 ka BP, the range in eastern Mexico increases as far as the south-eastern coast of the USA. After this the range continues with a similar pattern along western, central and eastern Mexico and along the south-eastern coast of the USA until the 1 ka BP projection. The current non-breeding projection continues with the same pattern as ka BP, in Mexico and on the south-central coast of the USA.

A similar range is projected between H2 and 24 ka BP in western and central Mexico, although the range at H2 is extended in southern Mexico, the Greater Antilles, and along Central America as far as north-eastern South America. At H1 the range in eastern Mexico is reduced and instead increases in the north of Sonora, differing from the 17 ka BP projection. In the H0 projection there is a similar range projected in Mexico as 13 ka BP, although at H0 the range continues in southern Mexico, Central America and northern South America.

Even though the current non-breeding range of the species is located in Mexico and the south-eastern coast of the USA, there are suitable conditions for the species to occur along the Andean cordillera and central-eastern South America.

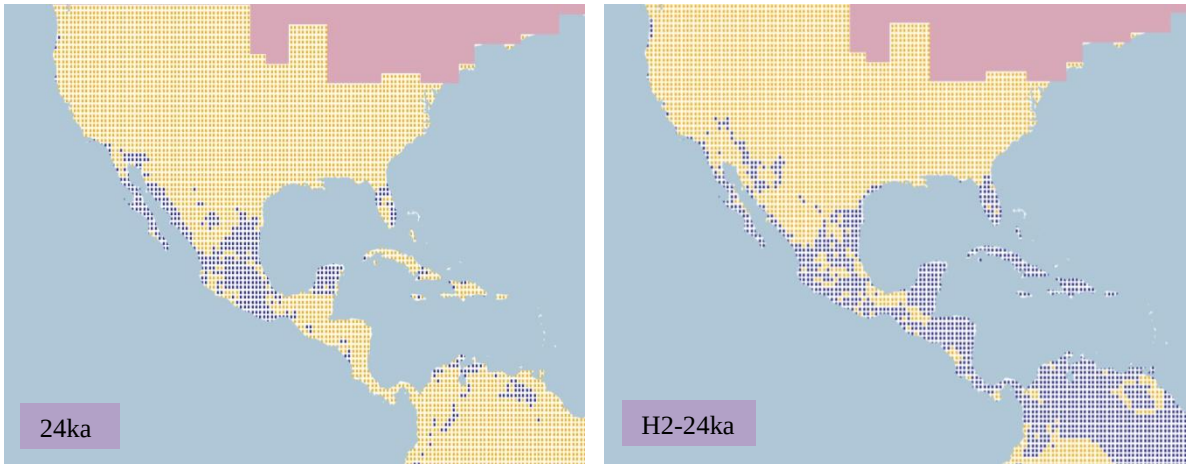

Figure 4.1.5.13.b. Simulation maps of Rufous Hummingbird non-breeding range. Maps are shown for ten-time slices: 24ka, H2 (24ka), 17ka, H1 (17ka), 13ka, H0 (13ka), 9ka, 5ka, 3ka and present (1961–90).

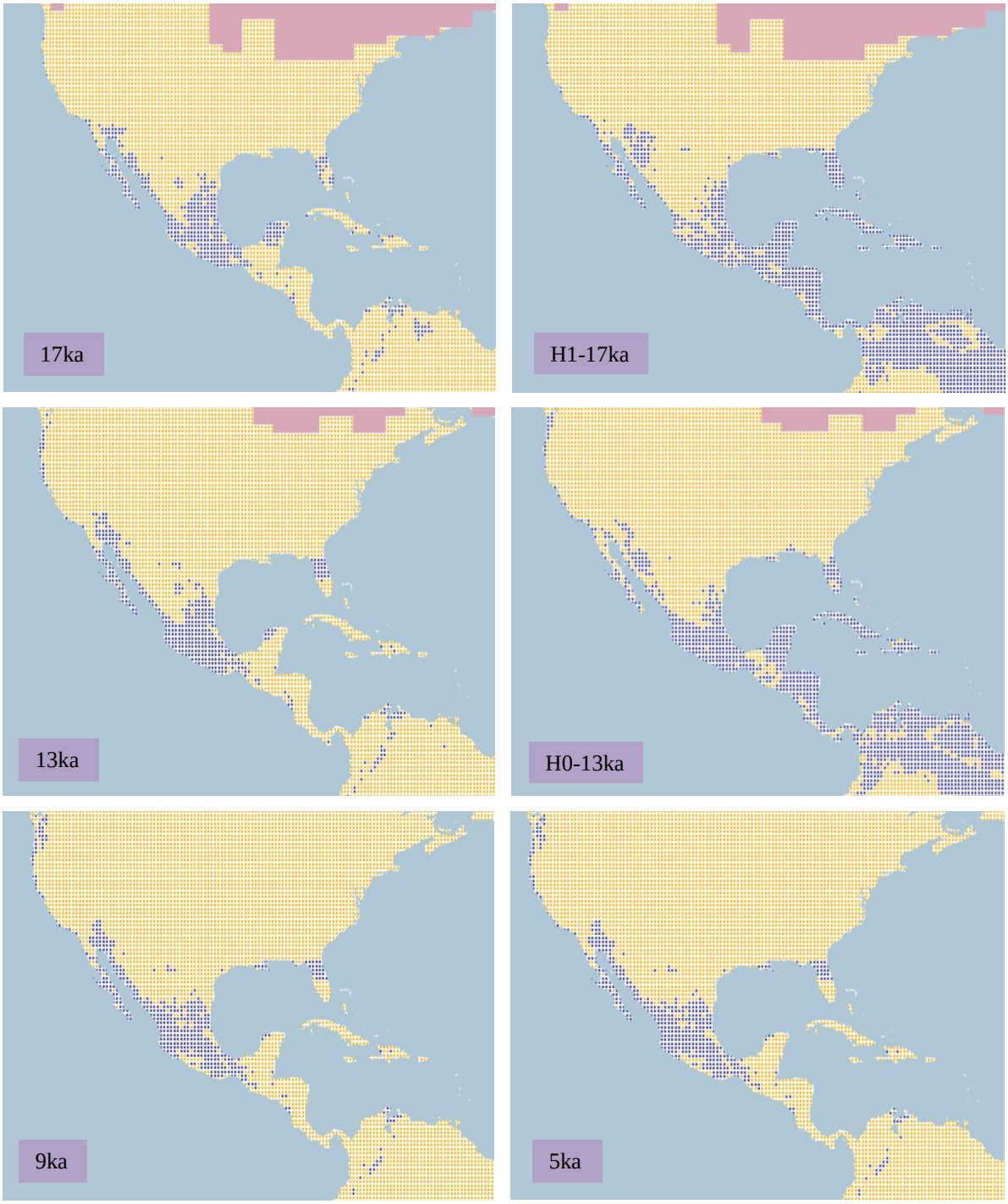

Figure 4.1.5.13.b. Simulation maps of Rufous Hummingbird non-breeding range (continued**).**

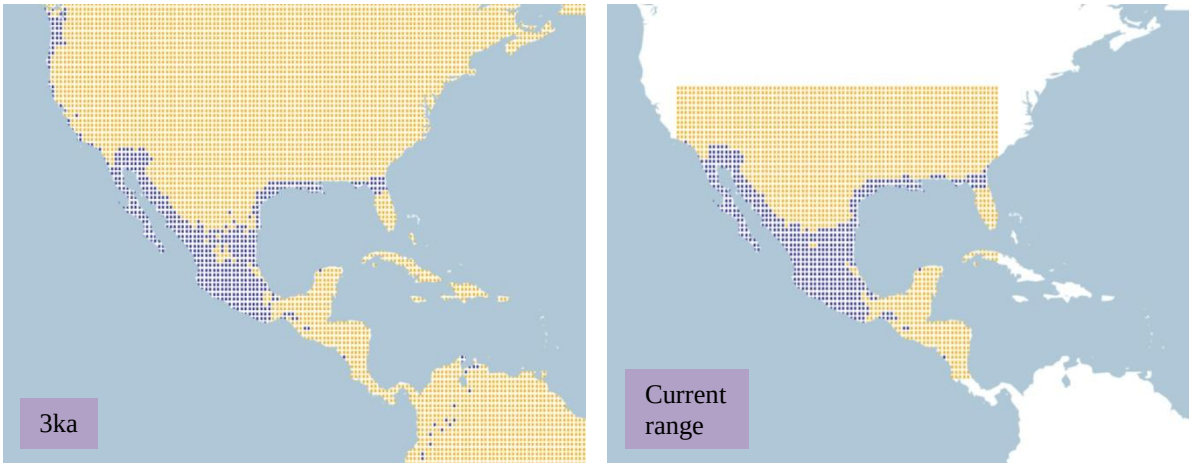

Figure 4.1.5.13.b. Simulation maps of Rufous Hummingbird non-breeding range (continued**).**

*4.1.5.14 Allen's Hummingbird (*Selasphorus sasin *including* S. s. sasin *and* S. s. sedentarius*).*

Conservation status: Least Concern. Current known range Figure 4.1.5.14.

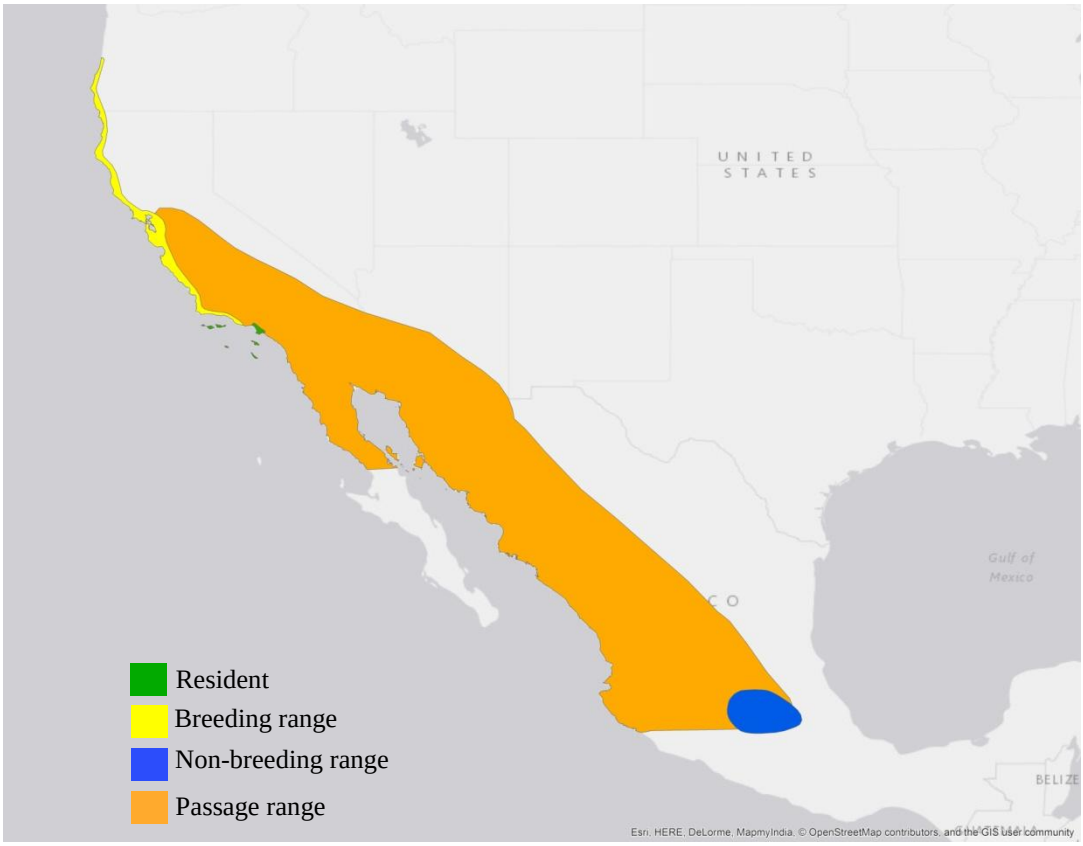

Figure 4.1.5.14. Current known range of Allen's Hummingbird.

Breeding range (AUC: 0.999; TSS: 0.984; Kappa: 0.925): A small breeding range along the western coast of the USA from southern Oregon to California and as far as Baja California in Mexico. A year-round resident range is recognized on the Channel Islands of California in USA.

A small range is projected at 26 ka BP on the south-western coast of the USA and extending to the north-western coast of Baja California in Mexico. There is also a small range projected in central Mexico from the Mexico City to the central-north in Guanajuato and San Luis Potosi. The same pattern continues and at 19 ka BP the range in central Mexico increases in Puebla and the range along the south-western coast of the USA and north-western Mexico increases as well. See Figure 4.1.5.14.a.

At 15 ka BP the range in central Mexico is intermittent, with the remainder of the range along the western coast of the USA and north-western Mexico unchanged. This pattern continues and at the beginning of the Holocene the range on the south-western coast of the USA is decreased, with a small range projected in northern Tennessee, USA. The range continues with minimal differences on the south-western coast of the USA and projecting a small range in the Sierra Madre Occidental from 8 ka BP until 1 ka BP.

The range at 1 ka BP is projected mainly along the western coast of the USA, with a small range in southern Missouri, USA and in the Sierra Madre Occidental in Mexico. The current breeding range projection presents a similar range as 1 ka BP along the western coast of the USA.

At the Heinrich event H2, there is a larger range projected in central Mexico from San Luis Potosi to Oaxaca, with a small range on the western coast of the USA and north-western Mexico. The pattern in central Mexico continues and increases at H1, with a small range projected in the southern USA. At the H0 projection there is a similar range projected along the western coast of the USA as the 13 ka BP projection, although with a large range projected in central Mexico, not present at 13 ka BP.

Even though the species' breeding range is located in North America, there are suitable conditions for the species to occur along the Andean cordillera and southern Chile in South America.

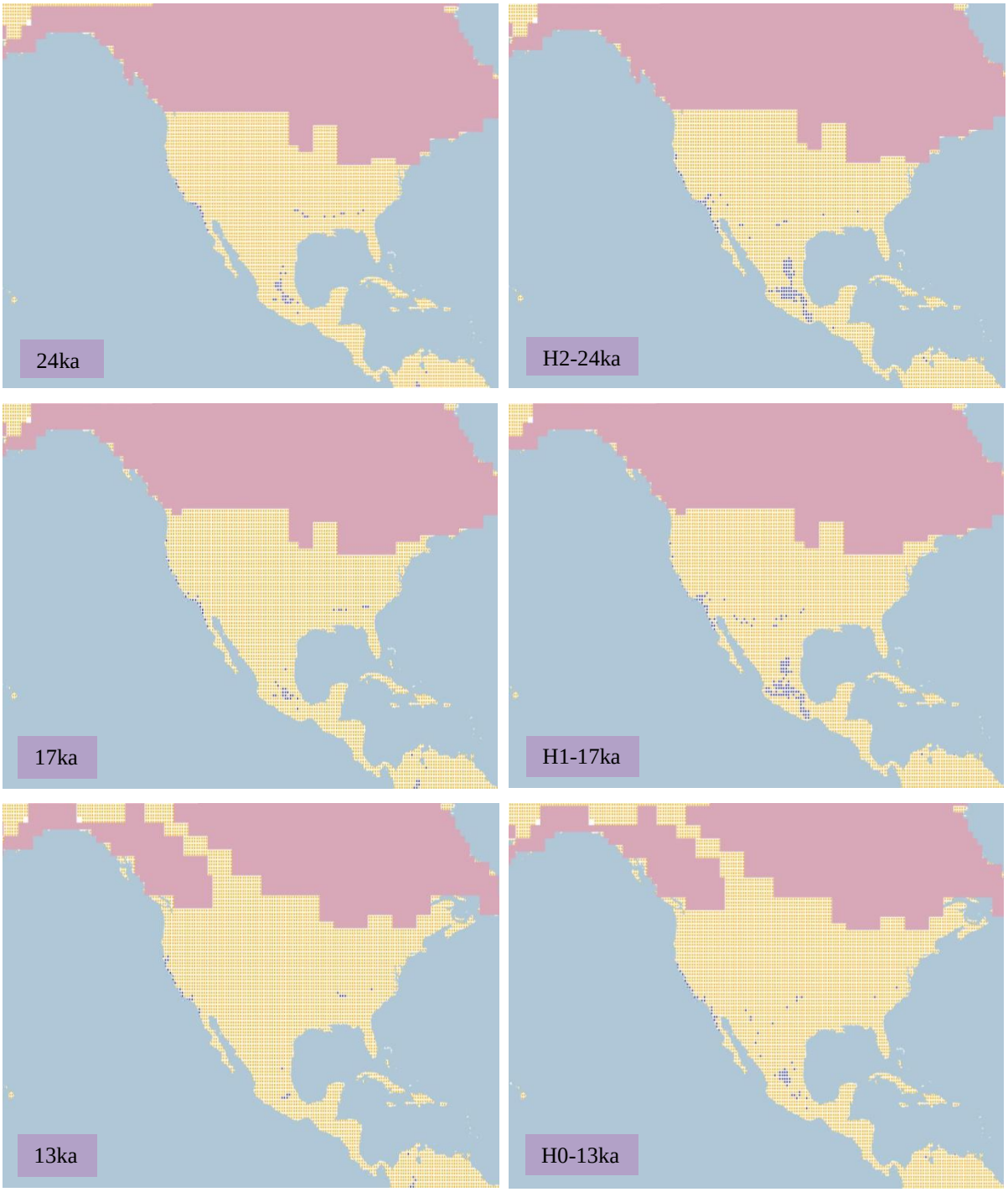

Figure 4.1.5.14.a. Simulation maps of Allen's Hummingbird breeding range.
Maps are shown for ten-time slices: 24ka, H2 (24ka), 17ka, H1 (17ka), 13ka, H0 (13ka), 9ka, 5ka, 3ka and present (1961–90).

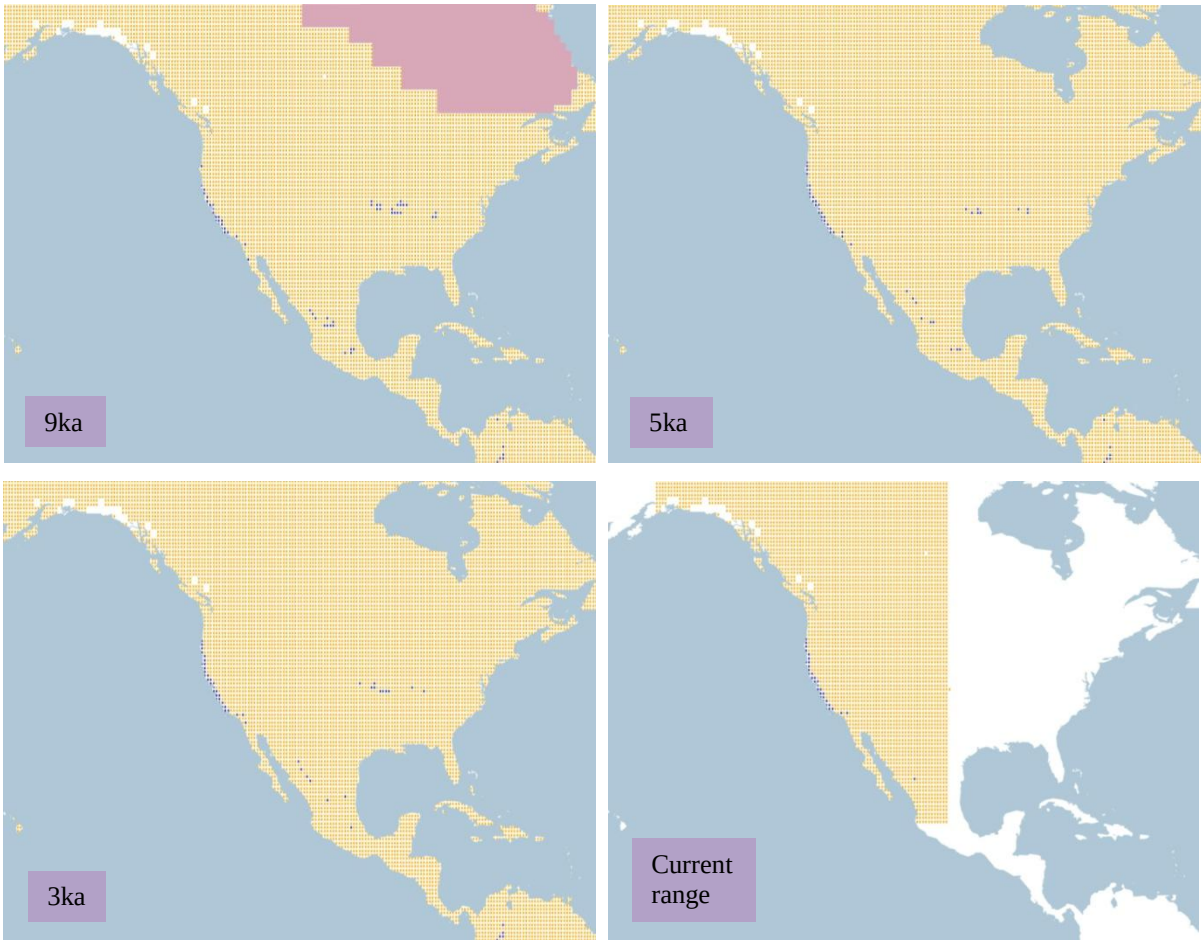

Figure 4.1.5.14.a. Simulation maps of Allen's Hummingbird breeding range (continued**).**

Non-breeding range (AUC: 0.998; TSS: 0.986; Kappa: 0.829): The wintering ground of the species is of small extent and located in central Mexico, between Guanajuato, Estado de Mexico and Hidalgo.

At 26 ka BP a small range is projected in central Mexico from San Luis Potosi to southern Oaxaca. The pattern continues and at 22 ka BP the range in central Mexico is increased. After this, there is a decline in the range of San Luis Potosi at 19 ka BP, increasing in southern Oaxaca. See Figure 4.1.5.14.b.

The range in southern Oaxaca declines at 15 ka BP, with the range remaining in the central region of Estado de Mexico. The range in central Mexico increases at 14 ka BP, and by the beginning of the Holocene the range shifts to San Luis Potosi in the north of Estado de Mexico. After this there is a small decline in the central region of Mexico at 9 ka BP.

At 7 ka BP the range in central Mexico is increased remaining with minimal differences until ka BP, when the range is decreased in the central region of Mexico. The current non-breeding range presents a different range than ka BP, concentrated in central Mexico, mainly along Estado de Mexico.

A larger range is projected in central Mexico at H2 than at 24ka. This range decreases at the H1 projection, covering mainly Jalisco, and differing from 17 ka BP with the range projected in Puebla and Oaxaca. A similar pattern as H1 continues at H0, although with a smaller extent and located in the Sierra Madre del Sur rather than the central region as the 13 ka BP projection.

Even though the current non-breeding range is restricted to central Mexico, there are suitable conditions for the species to occur along the Andean cordillera in South America.

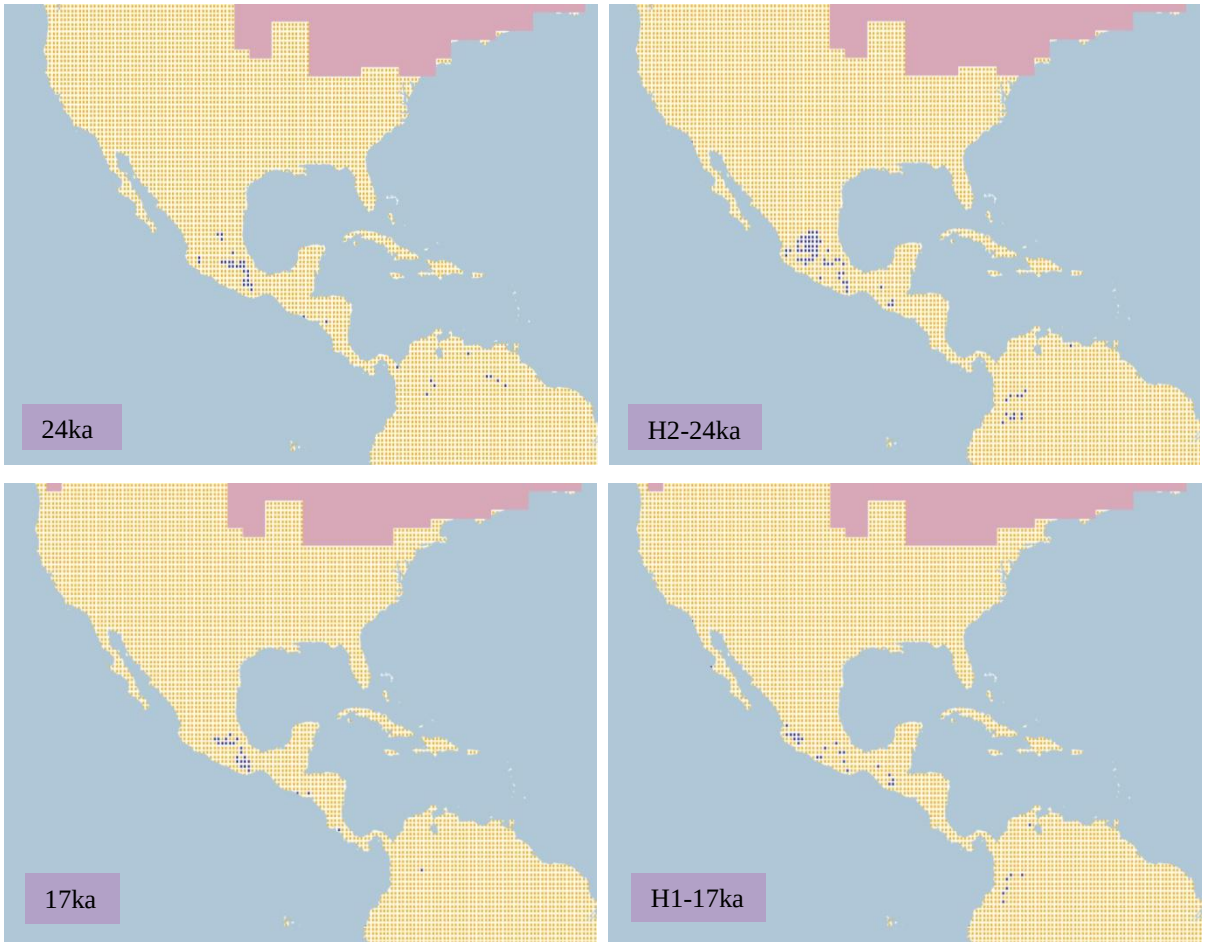

Figure 4.1.5.14.b. Simulation maps of Allen's Hummingbird non-breeding range. Maps are shown for ten-time slices: 24ka, H2 (24ka), 17ka, H1 (17ka), 13ka, H0 (13ka), 9ka, 5ka, 3ka and present (1961–90).

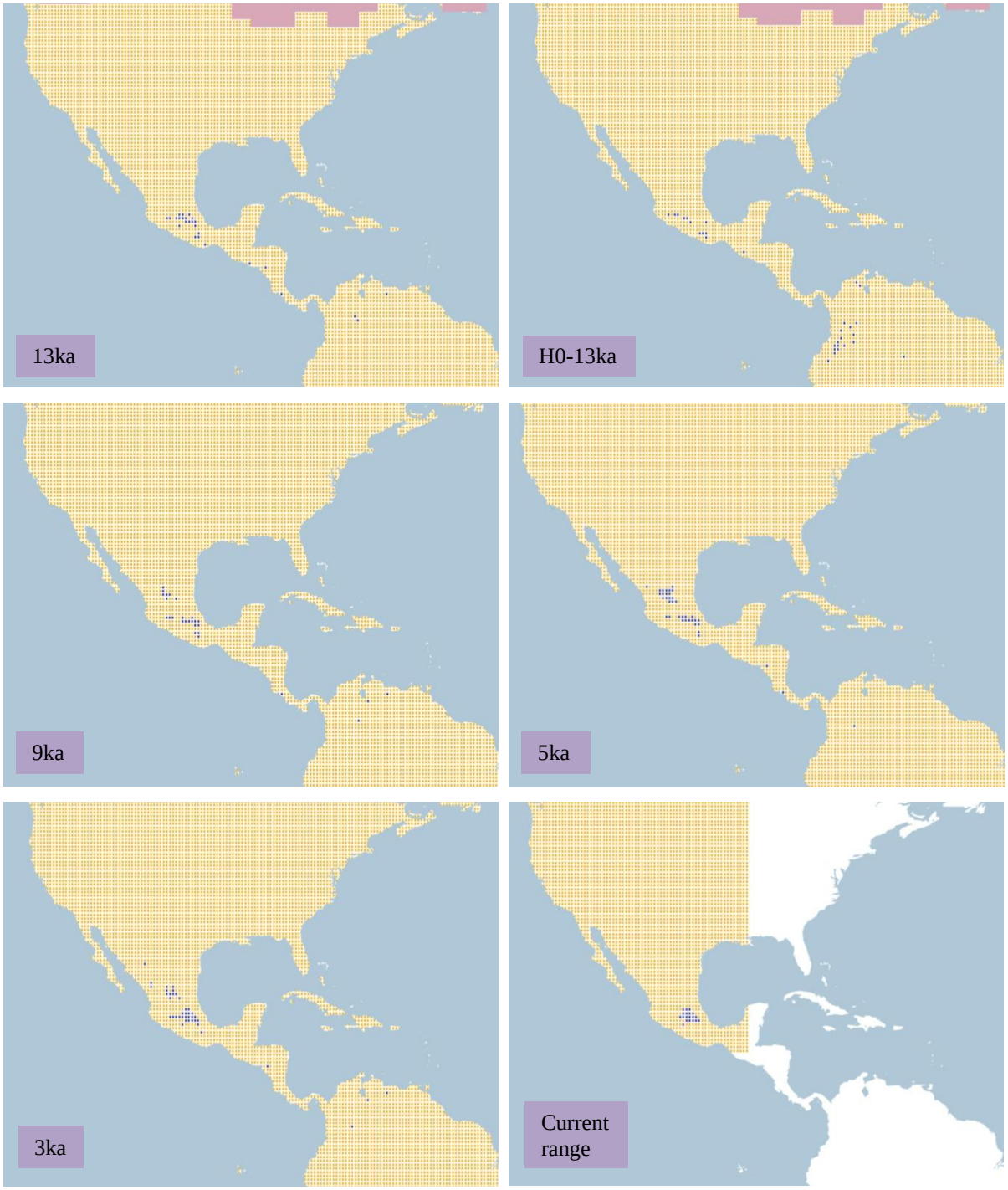

Figure 4.1.5.14.b. Simulation maps of Allen's Hummingbird non-breeding range (continued**).**

4.1.5.15 AUC, TSS and Kappa values

The resulted AUC, TSS and Kappa values for each species of the family Trochilidae are shown in here. These are divided in breeding and non-breeding ranges.

For the breeding range AUC displays mostly values > 0.950 differing from TSS and Kappa, with median for AUC of 0.993, TSS of 0.925 and Kappa of 0.866.

AUC values for individual species show the highest for Allen's Hummingbird (*S. sasin*) with 0.999, followed by Costa's Hummingbird (*C. costae*) with 0.997 and Violet-crowned Hummingbird (*A. violiceps*) with 0.996. The poorest performance for AUC is presented by Broad-tailed Hummingbird (*S. platycercus*) with 0.971, followed by Rufous Hummingbird (*S. rufus*) with 0.976 and Calliope Hummingbird (*S. calliope*) with 0.979.

For TSS the highest value is for Allen's Hummingbird (*S. sasin*) with 0.984, then Costa's Hummingbird (*C. costae*) with 0.950 and Violet-crowned Hummingbird (*A. violiceps*) with 0.951, as before. For TSS the lower values are shown again by Broad-tailed Hummingbird (*S. platycercus*) with 0.837, next to Rufous Hummingbird (*S. rufus*) with 0.840 and Calliope Hummingbird (*S. calliope*) with 0.863.

Finally, for Kappa the best performance is presented again by Allen's Hummingbird with 0.925, followed by Broad-billed Hummingbird with 0.915 and Violet-crowned with 0.909. The lower values for Kappa correspond to Broad-tailed Hummingbird (*S. platycercus*) with 0.696, followed by Buff-bellied Hummingbird (*A. yucatanensis*) with 0.745 and Rufous Hummingbird (*S. rufus*) with 0.786. See Figure 4.1.5.a.

The lower values were obtained for species with current breeding ranges that are relatively less extensive; even the lowest values obtained, however, indicate model with a good performance.

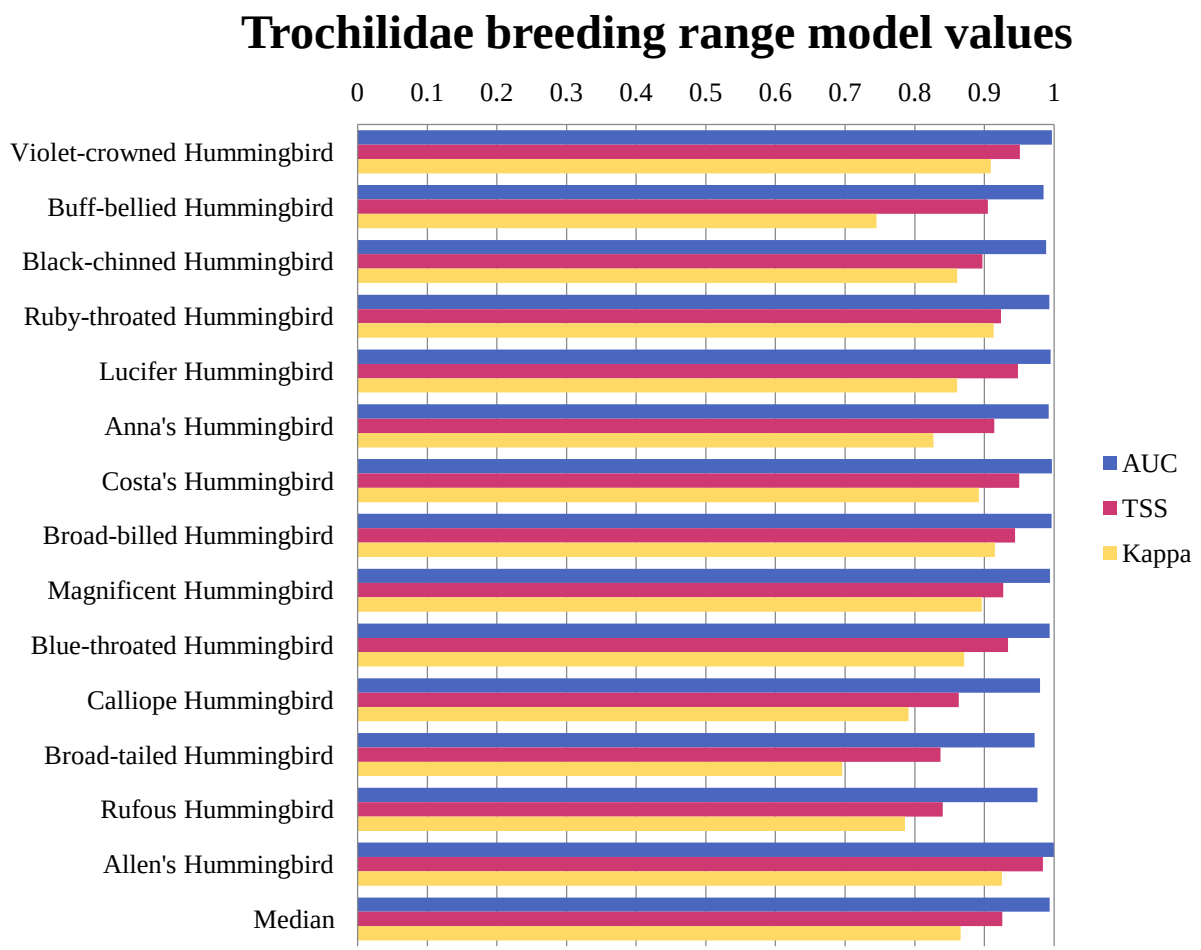

Figure 4.1.5.a. Model performance values of the family Trochilidae breeding range. The graph shows values for each species of AUC, TSS and Kappa values from the CRS model as well as the median for each statistical measurement.

For the non-breeding season modelling the median value of AUC was 0.995, TSS 0.951 and Kappa 0.874. It appears that the non-breeding season presents better performance values. For individual species the best performance for AUC is for Black-chinned Hummingbird (*A. alexandri*) with 0.999 followed by Costa's Hummingbird (*C. costae*) with 0.9989 and Allen's Hummingbird (*S. sasin*) with 0.9984. The lower values for the model performance of AUC are displayed by Buff-bellied Hummingbird (*A. yucatanensis*) with 0.969, followed by Anna's Hummingbird (*C. anna*) with 0.974 and Ruby-throated Hummingbird (*A. colubris*) with 0.988.

For TSS the best performance is shown again for Black-chinned Hummingbird (*A. alexandri*) with 0.995, followed by Allen's Hummingbird (*S. sasin*) with 0.986 and Costa's Hummingbird (*C. costae*) with 0.979. The lower values of TSS are presented by Anna's

Hummingbird (*C. anna*) with 0.832, followed by Buff-bellied Hummingbird (*A. yucatanensis*) with 0.853 and Rufous Hummingbird (*S. sasin*) with 0.897.

For Kappa the best performance corresponds to species Violet-crowned Hummingbird (*A. violiceps*) with 0.931, followed by Costa's Hummingbird (*C. costae*) with 0.924 and Broad-billed Hummingbird (*C. latirostris*) with 0.912. The lower values of Kappa are shown by Buff-bellied Hummingbird (*A. yucatanensis*) with 0.690, followed by Ruby-throated Hummingbird (*A. colubris*) with 0.749 and Anna's Hummingbird (*C. anna*) with 0.758.

Once again, the majority of the projections of the model displayed a good performance according to the AUC, TSS and Kappa values; considering the lower values as well it is possible to assume that the model had a good performance. See Figure 4.1.5.b.

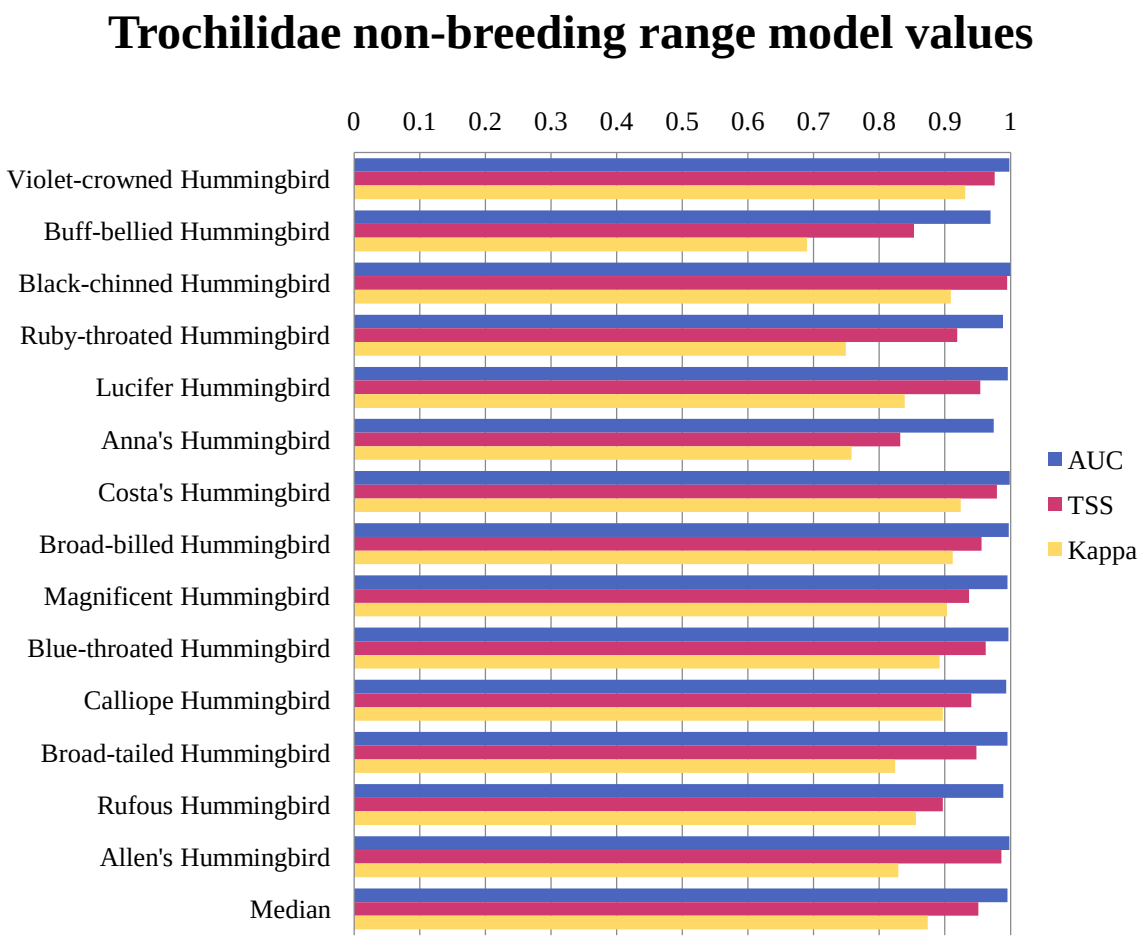

Figure 4.1.5.b. Model performance values of the family Trochilidae non-breeding range. The graph shows values for each species of AUC, TSS and Kappa values from the CRS model as well as the median for each statistical measurement.

CHAPTER 5 DISCUSSION

In this chapter I begin by reviewing the performance of the CRS model, by discussing AUC, TSS and Kappa's values. Furthermore, the past projected ranges are discussed, divided into the families Charadriidae, Haematopodidae, Recurvirostridae, Scolopacidae and Trochilidae, with a deeper discussion on several key species. There is also an analysis of the species richness of each family, and a comparison with similar studies.

5.1 Climate Response Surface model performance

The results of the CRS model used previously showed the effectiveness when fitting the species to suitable areas. To evaluate the performance of the model the Area Under the Curve (AUC), the True Skill Statistics value (TSS), and Cohen's Kappa were used.

As discussed before, the AUC value describes the overall accuracy of the model and the TSS is a value that combines specificity and sensitivity to jointly express errors of commission and omission; it is based on the four values in the confusion matrix (Allouche et al. 2006). For AUC and TSS the accuracy of the models is valued from >0.9 as a good performance, 0.7 to 0.9 as a useful model, 0.5 to 0.7 low performance and <0.5 as worse than random performance.

As the results shown in this project the AUC and TSS values for every family from Charadriidae, Haematopodidae, Recurvirostridae, Scolopacidae and Trochilidae show a good performance on the modelling approach. This is useful for interpreting the simulations made by the model that permit a more robust and supported research.

Cohen's Kappa maximization approach also describes the accuracy of the model using presence-absence data, although it is taken into account that the use of this indicator has been criticized given a tendency to bias in its measure of the accuracy of a model (Liu et al. 2005, Allouche et al. 2006). An excellent performance of the model is valued at >0.9, with 0.7 to 0.85 as very good, 0.55 to 0.7 as good performance, 0.4 to 0.55 as fair and <0.4 as a poor or very poor performance. Even though Kappa's values within each family were lower than AUC and TSS, still can be considered with a good performance when simulating species response to different climate, and this as well, would support the interpretation and discussion of the results.

Following the literature of previous studies, it was possible to try and avoid 'over-fitting' the models given small sets of bio-variables used that resulted in considerably good levels of AUC for the CRS model (Huntley et al. 2007). It is important to mention that the limitations of the model itself are well known and that there was no use of more contemporary methods such as data-splitting or a jack-knife approach (Bagchi et al. 2013). This would be considered for future improvement on this work, with the implementation use of a different modelling approach that would enable a comparison between models.

5.2 Past Projected Ranges

The simulated past suitable ranges show similar patterns between the Shorebird's breeding range projections, especially in the Arctic regions of North America which can be interpreted as an indicator of a population bottleneck for the species during the glacial periods. However, it appears that species with breeding range southern to the ice sheet did not display the same impact as the ones breeding in the Arctic region; this could be because of the climate affinity that the species could present with no radical climatic conditions.

The Shorebirds with non-breeding range restricted to coastal areas most of the projections show suitable climatic conditions inland; however, this can be interpreted as a limitation of the same model that is based only on the climate and does not consider the food resources and/or habitat requirements of the species. One possible approach to overcoming this limitation could be by incorporating the same method as a previous study on European breeding birds that fitted the CRS model for coastal species using only data from coastal grid squares, and making the projections for the species only on such squares (Huntley et al. 2007).

For the Hummingbirds, it appears that they present a different pattern during the LGM and the Alti-thermal in both breeding and non-breeding projections, with continuous ranges and minimal changes. This can be possibly to the settled populations that could withstand unfavourable conditions, or that maybe those climatic fluctuations did not represent a dramatic change that did not enable the species to adapt. This will be further discussed below.

It is also important to mention the Heinrich events projections that show different patterns of impacts upon many species' ranges between North and South America, projecting similar or smaller ranges to the 'normal' projections in North America, but projecting much larger

extents of suitable conditions in South America. Where these more extensive ranges are in southern South America, this may be an indicator that the climatic conditions simulated for Heinrich events had warmer conditions in southern South America because of the bi-polar see-saw phenomenon. In the case of the more extensive ranges simulated for some species in areas of northern South America north of the equator, however, it is more likely that this reflects extension southwards of glacial cooling when the Atlantic Meridional Overturning Circulation is slowed or even halted during Heinrich Event stadials.

5.2.1 Charadriidae

The current breeding ranges of the species located in the Americas are restricted mainly to the Arctic region, the projections of the species presented a similar pattern during the LGM and stadial phases, with a restricted range near the Laurentide Ice sheet in the north of the conterminous USA, in north-western Canada and in Alaska, likely causing a glacial population bottleneck; i.e. the ice sheet restricted the breeding ranges of the species in the Arctic whilst there was limited scope for their ranges to shift to more southern regions. With deglaciation the breeding ranges shifted solely to Arctic regions, but retreat of the ice sheet allowed an increase in range extent. After this during the Holocene and the Alti-thermal the species' breeding range was mainly restricted to the Arctic regions, with a small increase during the Little Ice Age at 1 ka BP.

For the species with breeding range in the central region of the USA and northern Mexico the projections show a rather different pattern to that for the Arctic breeding species. Although their projected breeding ranges decrease during the LGM and stadial phases, this decrease is of a smaller extent than for the Arctic breeding species. Also, during the Holocene and Alti-thermal their projected breeding ranges increase. This may indicate that species breeding in central regions of the USA and northern Mexico are less susceptible to glacial–interglacial climatic variability than are Arctic species, and therefore less likely to suffer a glacial population bottleneck, as discussed above.

The ranges of the year-round resident species in North America are maintained throughout the projections. Similarly, the breeding ranges of species in South America are maintained with minimal differences. Although this might be interpreted as evidence that these species were able to adapt to the changing climatic conditions *in situ*, rather than shifting their

geographical ranges, a more parsimonious interpretation is that the climatic conditions simulated for southern North America and much of South America showed only relatively limited changes during the Late Pleistocene and Holocene.

For the non-breeding ranges of some species with current ranges limited to coasts the projections indicated suitable climatic conditions for the species to occur inland. However, current evidence of these species' resource and habitat requirements does not support such inland occurrences. As stated above, this reflects the use only of climatic variables in the models that thus project climate suitability rather than overall niche suitability, as the species' food resources are obtained from coastal areas or wetlands. This can be observed especially in the projections for Heinrich events, with large inland non-breeding ranges projected for many of these species mainly in northern South America, where they are extremely unlikely to have occurred given that there would be no food resources available there for these species.

Two sub-species of the Piping Plover (*Charadrius melodus*) have been recognized, based on genetic studies. However, the projected breeding range for the species does not include the coastal breeding range of *C. m. melodus*, with only an inland range in the central USA, but with suitable conditions projected also in north-western Canada. This most likely reflects the restriction of *C. m. melodus* to coastal areas that are not climatically distinctive, resulting in an overall low suitability of these conditions for the species.

The Snowy Plover (*C. nivosus*) also has two sub-species with differentiated ranges; *C. n. nivosus* has a breeding range in North America and *C. n. occidentalis* has a year-round resident range along the west coast of South America. In the projections distinct ranges are maintained for the two sub-species with no projected overlap of their breeding ranges during the past 26,000 years. However, suitable conditions for the species are projected in northern South America during Heinrich events. Given the species' current limitation to coastal areas, even though climatic conditions were suitable it is extremely unlikely that this area was occupied because it does not offer a suitable habitat for the species.

For Killdeer (*C. vociferus*) there are three sub-species recognized, *C. v. vociferus, C. v. ternominatus* and *C. v. peruvianus*, the latter two being year-round residents of the Bahamas and Greater Antilles, and of coastal areas from Ecuador to Peru, respectively. This differentiation is partially represented in the projections, with the distinctive ranges of *C. v.*

vociferus and *C. v. peruvianus* clearly seen in the projections. However, the limited range of *C. v. ternominatus* in the Greater Antilles and Bahamas is not projected.

Wilson's Plover (*C. wilsonia*) has four sub-species, *C. w. wilsonia, C. w. beldingi, C. w. cinnamominus* and *C. w. crassirostris*, each with a separate current breeding range on the coasts of North and South America. If projections of suitable conditions inland are ignored than the sub-species' differentiated coastal ranges are maintained without overlap in the projections throughout the last 26,000 years.

Even though two sub-species are recognized for the Tawny-throated Dotterel (*Oreopholus ruficollis*), because there is overlap in their current ranges an interpretation for each sub-species cannot be made.

5.2.2 Haematopodidae

The species of the family Haematopodidae are mostly year-round residents with ranges restricted to coastal areas. Hence, throughout the projections for the breeding and non-breeding ranges a similar pattern is observed.

As discussed above with respect to the Charadriidae, species with ranges restricted to coastal areas frequently have suitable conditions projected inland, although the food resources and/or habitat that they require will not be found in those areas. This is an inevitable result of using only climatic variables in the models.

As an example of this, the American Oystercatcher (*Haematopus palliatus)* in the Heinrich events projections has climatically suitable areas projected inland in northern South America, but these areas would not offer the habitat and food resources required for the species to occur.

Similar projections are seen for the Magellanic Oystercatcher (*H. leucopodus*) that is restricted to the coasts of southern South America. Inland areas are projected as offering suitable climatic conditions for the species to occur, although there is little likelihood of this happening given the species' food resource requirements.

5.2.3 Recurvirostridae

Breeding ranges of members of the Recurvirostridae are projected to be of limited extent during the LGM, increasing during the deglaciation and of greater extent during the Holocene, when there is only limited variation. This suggests that these species may be another group that experienced a glacial population bottleneck in Arctic North America.

For the Black-winged Stilt (*Himantopus himantopus*) two sub-species are recognized in the Americas, *H. h. melanurus* and *H. h. mexicanus*. The breeding ranges of the two sub-species are today separated largely by Amazonia, although with their minimum separation in Peru. During the latter part of the last glacial and the early Holocene, however, especially between 16 ka BP and 9 ka BP, as well as during Heinrich events, their projected ranges meet in northern South America, with a continuous range projected from Venezuela to Argentina in the east and during Heinrich events also from Venezuela to northern Chile in the west. This suggests some scope for mixing and potential inter-breeding of the two sub-species during stadials of the last glacial, as well as during the period of transition from the last glacial to the Holocene. Alternatively, the sub-species may only have become differentiated during the later Holocene, although the parallels in plumage patterning between *H. h. melanurus* and *H. h. leucocephalus*, the latter breeding from the East Indies to New Zealand and wintering on numerous Pacific islands, on the one hand, and between *H. h. mexicanus* and *H. h. knudseni* of Hawaii, on the other, may suggest an earlier differentiation underlies such hemisphere-specific parallels.

For the American Avocet (*Recurvirostra americana*) the projections show the breeding range increasing in extent as deglaciation permits the species to expand its range to the northern USA and southern Canada. During the Holocene the range shows minimal variation. Suitable climatic conditions are consistently projected also in South America where this species is absent; interestingly, however, the area projected consistently includes the current range of the congeneric Andean Avocet (*R. andina*).

5.2.4 Scolopacidae

For the many members of the Scolopacidae that breed today in Arctic or northern Boreal regions of North America, their breeding ranges during the last glacial are projected to have

been in Alaska, north-western Canada and near the ice sheet in the northern conterminous USA, the latter shifting northwards into Canada and increasing in extent during the deglaciation. This may indicate an important influence of glacial conditions on the extent of the breeding range of these species, with the restricted glacial range extent leading to a population bottleneck during that period.

During the Holocene and the Alti-thermal some species' ranges once again decreased in extent, becoming restricted to northern areas of Canada, and in some cases disappearing from the conterminous USA. For such species the period of deglaciation apparently offered the greatest extent of suitable climatic conditions.

For those species that currently breed in central or southern regions of the conterminous USA and northern Mexico, the glacial period did not have the same impact as it did upon Arctic breeding species. Although their projected breeding range is generally of smaller extent during the LGM, probably indicating some degree of glacial population reduction, this is of a much smaller degree than is likely for the Arctic breeding species. These more southern species are projected to increase in range during deglaciation and the Holocene Alti-thermal rapidly occupying a similar range to their current breeding range.

The non-breeding range simulations present a similar pattern to that seen in the other shorebird families for species with ranges restricted to coastal areas. The range on the coastal areas is maintained with minimal variation throughout the projections but with suitable conditions also inland, although there is no evidence that the species occur inland or can find the necessary resources there to do so. As with the other shorebird families, this reflects a limitation of models fitted using only climatic variables.

A similar pattern to that seen in the other Shorebird families is also observed in the projections for the Heinrich events, with extensive ranges projected inland in northern South America. This probably reflects an extension of the area of markedly colder conditions to this region because of the slowing down or cessation of the Atlantic Meridional Overturning Circulation during Heinrich events.

It is important once again to consider how the history of species' ranges during the late Pleistocene and Holocene may relate to any recognised sub-species. The Short-billed Dowitcher (*Limnodromus griseus*), for example, has three recognised sub-species, *L. g. caurinus, L. g. hendersoni* and *L. g. griseus* with current breeding ranges that are distinct and

non-overlapping. The species' projected range also has three recognisably separate components for most time slices, although this is especially clear during the deglaciation. The westernmost range component, occupied today by *L. g. caurinus*, is the most consistently distinct, whereas particularly since 3 ka BP the central and eastern range components are projected to coalesce. Although the tendency towards three distinct range components for most of the past 26,000 years is no more than circumstantial evidence of the maintenance of the discrete breeding ranges of the three sub-species through that time, it provides the basis for a hypothesis that might be tested using genetic evidence.

The non-breeding ranges of the three sub-species are also today geographically separate, they are purely coastal and are much less clearly differentiated than the breeding range, especially for the two sub-species (*L. g. griseus* and *L. g. hendersonii*) that use the Atlantic coasts that today overlap at least on the coasts of the southern USA. The non-breeding range projections show this pattern consistently since 26 ka BP, with no clearly differentiated range sub-divisions that might correspond to the ranges of the sub-species, although it is likely that the consistent projection of suitable conditions on the Pacific coasts corresponds to a continuity of occupation of this coast by *L. g. caurinus* during the non-breeding season.

For the species American Whimbrel (*Numenius phaeopus hudsonicus*) a restricted breeding range was simulated, as the sub-species *N. p. rufiventris*, not considered in this study, breeds in western North America reaching Siberia, however, they do not present a stacked breeding range.

The Red-necked Phalarope (*Phalaropus lobatus*) currently spends the wintering season in the Pacific Ocean in Central and South America, which unfortunately was not projected in the model as it is restricted to inland conditions. However, there was a rather fragmented and poor simulated area inland in South America that indicates a potential suitable climate for the species, although it does not take into account other factors as barriers and competition.

The Willet (*Tringa semipalmata*) is another example of a species with recognised sub-species that have geographically distinct ranges. Two sub-species are recognized, *T. s. inornata* and *T. s. semipalmata*, and have distinct breeding and non-breeding ranges. In the projections there are distinct breeding ranges, the first in the north-western conterminous USA and, once the area is ice-free during deglaciation, also in south-central Canada, and the second along the southern and eastern coasts of the USA. These two areas correspond to the current breeding

ranges of the two sub-species, *T. s. inornata* in the north-western conterminous USA and south-central Canada and *T. s. semipalmata* on the southern and eastern coasts of the USA. Although the inland range extends progressively into Canada with deglaciation, thereafter there are only minimal variations during the Holocene. The range along the coasts also persists with some increases during the Holocene.

These projections suggest that the two sub-species breeding ranges have been differentiated since at least 26,000 years ago, and that the LGM and the subsequent deglaciation did not fundamentally alter these ranges. During the non-breeding season, the range currently is restricted to coastal areas of North, Central and South America, with *T. s. inornata* mainly on the Pacific coasts and *T. s. semipalmata* on the Atlantic coasts. These coastal areas are in general projected as suitable in the non-breeding season throughout the past 26,000 years, although inland areas are also projected to offer suitable climatic conditions during glacial time slices. As previously discussed, the absence of the required habitat and/or food resources in inland areas means that it is very unlikely that such areas were occupied.

Finally, it is important to mention the species *Phalaropus lobatus*, the non-breeding range of which is mainly oceanic. The projections for the non-breeding range were, however, limited to coastal areas of Mexico and north-western South America because the climatic variables used for modelling are available only for continental regions, most of the meteorological stations from which these data ultimately are derived being in these regions.

5.2.5 Trochilidae

The breeding ranges of the Hummingbird species examined are mainly located in the conterminous USA and Mexico. The projections for the LGM and for stadial intervals generally show breeding ranges of reduced extent compared to the present. This likely resulted in smaller populations under glacial conditions, although it is unlikely for most species that this was a sufficient reduction to result in a genetic bottleneck. The projected ranges of most species then increased in extent with deglaciation and during the Holocene Alti-thermal, then remaining similar until 1 ka BP and the present.

For a minority of species, however, the projected breeding range is more extensive than today between 26 ka BP and the deglaciation, the projected range decreasing during the Holocene Examples of species showing this pattern include Black-chinned Hummingbird (*Archilochus*

alexandri), Calliope Hummingbird (*Selasphorus calliope*) and Rufous Hummingbird (*S. rufus*). This may be because these species breed in northern regions of North America.

A more extensive range is projected during the LGM and stadial periods also for Anna's Hummingbird (*Calypte anna*), Costa's Hummingbird (*C. costae*) and Allen's Hummingbird (*S. sasin*), all of which have breeding ranges restricted to areas relatively close to the Pacific coast in the western or south-western USA or Mexico, Given that the projected increases in extent are largely to areas further inland, they might be interpreted as the result of the models being fitted only to climatic variables. However, of the three species, only *S. sasin* is limited to coastal or near coastal habitats during the breeding season, and even it does not depend upon food resources that are available only in coastal habitats, unlike many of the Shorebirds. In contrast to many of the Shorebirds, therefore, the greater inland extent of the projected breeding ranges of these species under glacial conditions is likely to have been realised.

The non-breeding ranges of the Hummingbirds examined are also mainly projected to have been of smaller extent than nowadays during the LGM and stadial intervals of the last glacial. Once again, this likely also indicates reduced populations during the glacial, although probably not sufficiently to result in a genetic bottleneck. The projected non-breeding ranges then increase during the Holocene Alti-thermal, often increasing in extent towards northern regions, and are largely similar thereafter.

For most species the non-breeding range projections indicate climatic suitability in South America, where the species do not currently occur. The absence of the species from these areas may reflect the persistent presence of biogeographical and/or ecological barriers that have prevented them colonising these areas, one of the barriers could be due to competition with other species. Alternatively, it might reflect that birds do not require moving long distances to encounter a suitable habitat and resources to successfully meet their requirements.

Both during the glacial and the early Holocene, i.e. between 26 ka BP and 9ka, the non-breeding range of the Ruby-throated Hummingbird (*A. colubris*) is, for example, projected to extend with only limited gaps from Mexico through Central America and northern South America to southern Brazil. The projections for more recent millennia, however, have a large gap between areas of suitable climatic conditions in central latitudes of South America and those in Mexico and northern Central America. The species' current non-breeding range

extends south only as far as Panama. It is thus likely that the species' later Holocene range has been similar to that today, and that the climatically suitable areas projected in central latitudes of South America may not have been occupied at any time. However, the possibility must be entertained that the non-breeding range of this species, and of others with similar patterns of projected range history, may have extended to northern South America during the glacial and/or early Holocene.

Most of the Hummingbirds examined have relatively extensive ranges projected in South America for the Heinrich events, although none currently occurs in that continent. As discussed above, areas of suitable climate simulated in northern South America may reflect regional cooling because of the slowing or cessation of the Atlantic Meridional Overturning Circulation, whilst those simulated in southern South America tend to reflect regional warming associated with the bi-polar see-saw pattern of warming in higher latitudes of the Southern Hemisphere corresponding to episodes of cooling in the Northern Hemisphere, such as the Heinrich event stadials.

For several of the Hummingbirds examined their breeding range in North America is also projected to be more extensive during the Heinrich events, contrasting with the projections for the 'normal' glacial climates that are of ranges of smaller extent. In general, such range extensions are principally northwards, through the western USA and in some cases as far as Alaska, and/or eastwards, across the southern USA, often as far as Florida. It is unclear to what extent such extended areas of climatic suitability would also have offered the habitats and resources required by these species, although the reconstruction from palaeoecological evidence of higher tree densities in north-western North America during Heinrich stadials, compared to interstadial conditions (Williams, 2003), offers support for the possibility that at least the northward range expansions might have been realised.

5.3 Range extents and species richness

The extent of each species' breeding and non-breeding ranges for each time slice was assessed by counting half-degree grid cells predicted by the relevant model to have a suitability value greater than the threshold value that optimised the True Skill Statistic for that model, and that had some land area available to be occupied at that time. Whether or not land was available in each grid cell at a given time was determined using a binary mask (B. Huntley, unpublished) in which grid cells were considered to have available land area if their maximum elevation was above the eustatically-adjusted sea-level for that time and their fractional ice cover for that time was <100%. Species richness of each individual half-degree grid cell with land available was then assessed for any given time slice by counting the number of species for which that grid cell was predicted to be suitable at that time. Counts were made separately for each family (Charadriidae, Haematopodidae, Recurvirostridae, Scolopacidae and Trochilidae).

5.3.1 Family Charadriidae

Species' breeding ranges are generally projected to have been of reduced extent during the peak of the last glacial stage, increasing steadily in extent after *ca*. 17 ka BP to reach more or less their present extent by the early Holocene (*ca*. 9 ka BP); Figure 5.1(a) shows the results for Semipalmated Plover (*Charadrius semipalmatus*) as an example of this pattern which is probably a consequence of the breeding range of most species being located in Boreal and Arctic regions that were largely covered by ice during the late Pleistocene. Ice-free areas in these latitudes also may have experienced more severe climatic changes than areas at lower latitudes (Anisimov et al. 2007).

In contrast, the models project generally greater extents of species' non-breeding ranges in the past, especially for species of the genus *Charadrius*. Range extents peak during the late-Pleistocene and early Holocene (*ca*. 16 – 6 ka BP); Figure 5.1(b) shows the results for Semipalmated Plover as an example of this pattern. This species non-breeding range is also of greater extent than today during interstadials, but of reduced extent during the extreme stadials associated with Heinrich Events H1 and H2. The non-breeding ranges were located mostly at lower latitudes, including equatorial regions, and in coastal areas. Pleistocene

climatic changes were generally of smaller magnitude in tropical regions than at higher latitudes of North America (Farrera et al. 1999).

Overall, projected ranges for species of the Charadriidae did not show dramatic variations between 26 ka BP and 1 ka BP. The general projected increase in breeding range during the late Pleistocene and early Holocene can be related to the deglaciation of the Laurentide ice sheet that progressively increased the land area available in Boreal and Arctic regions of North America. Given the natural history of the Charadriidae, such relatively limited variation in projected range extents may be a result of their adaptation to harsh environments (Piersma and Bonan 2018).

The impact of the extreme stadial climates associated with Heinrich Events varies, most *Charadrius* spp. being projected to have reduced extents of both breeding and non-breeding ranges; although Semipalmated Plover is an exception, its breeding range being projected to increase marginally in extent during Heinrich events. On the other hand, species such as Tawny-throated Dotterel (*Oreopholus ruficollis*), American Golden Plover (*Pluvialis dominica*) and Grey Plover (*P. squatarola*) are projected to have increased breeding range extents during Heinrich events. This may indicate *Charadrius* spp. are more susceptible to the extreme cold and dry conditions associated with Heinrich Event stadials than are other species in the family.

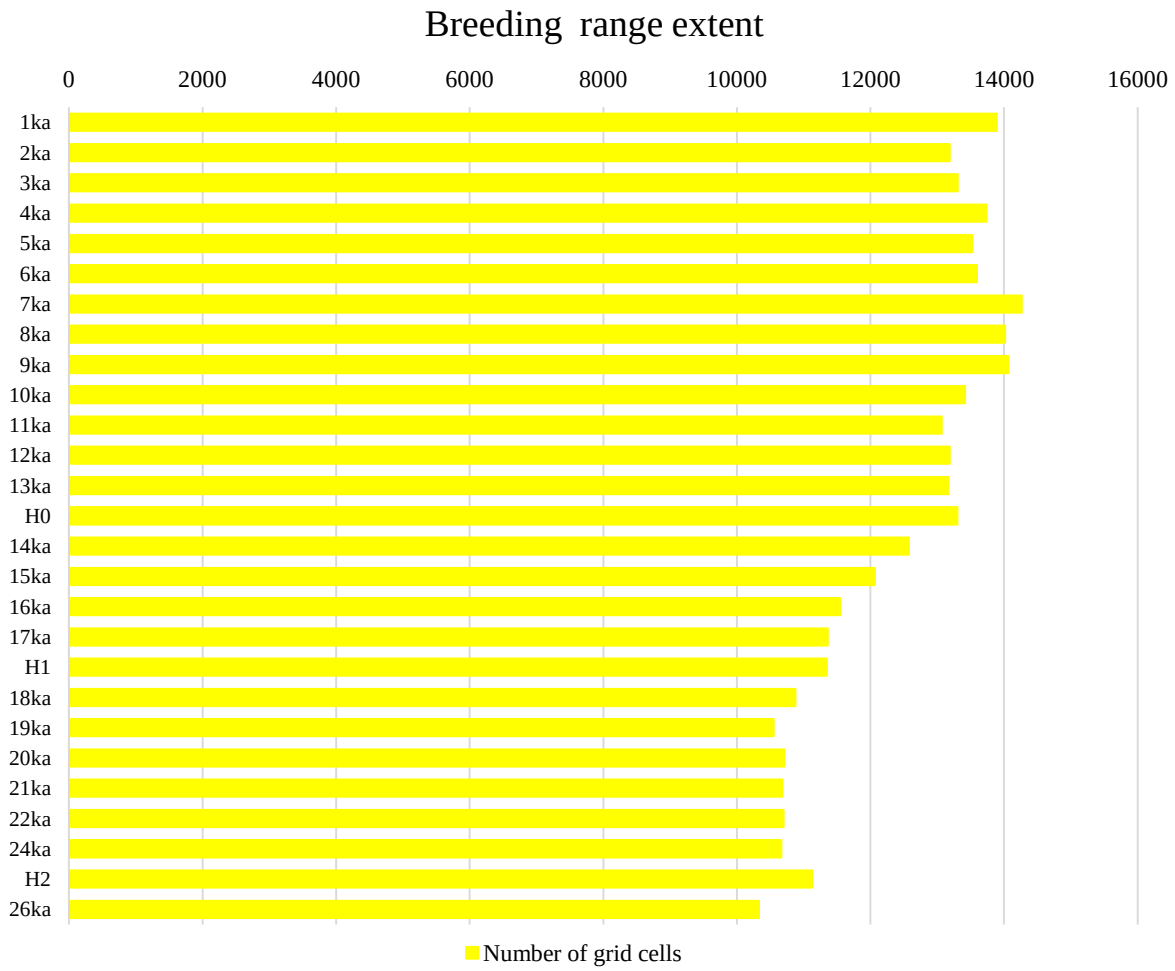

Figure 5.1(a). Changing extent of the breeding range of Semipalmated Plover (*Charadrius semipalmatus*) during the late-Pleistocene and Holocene.

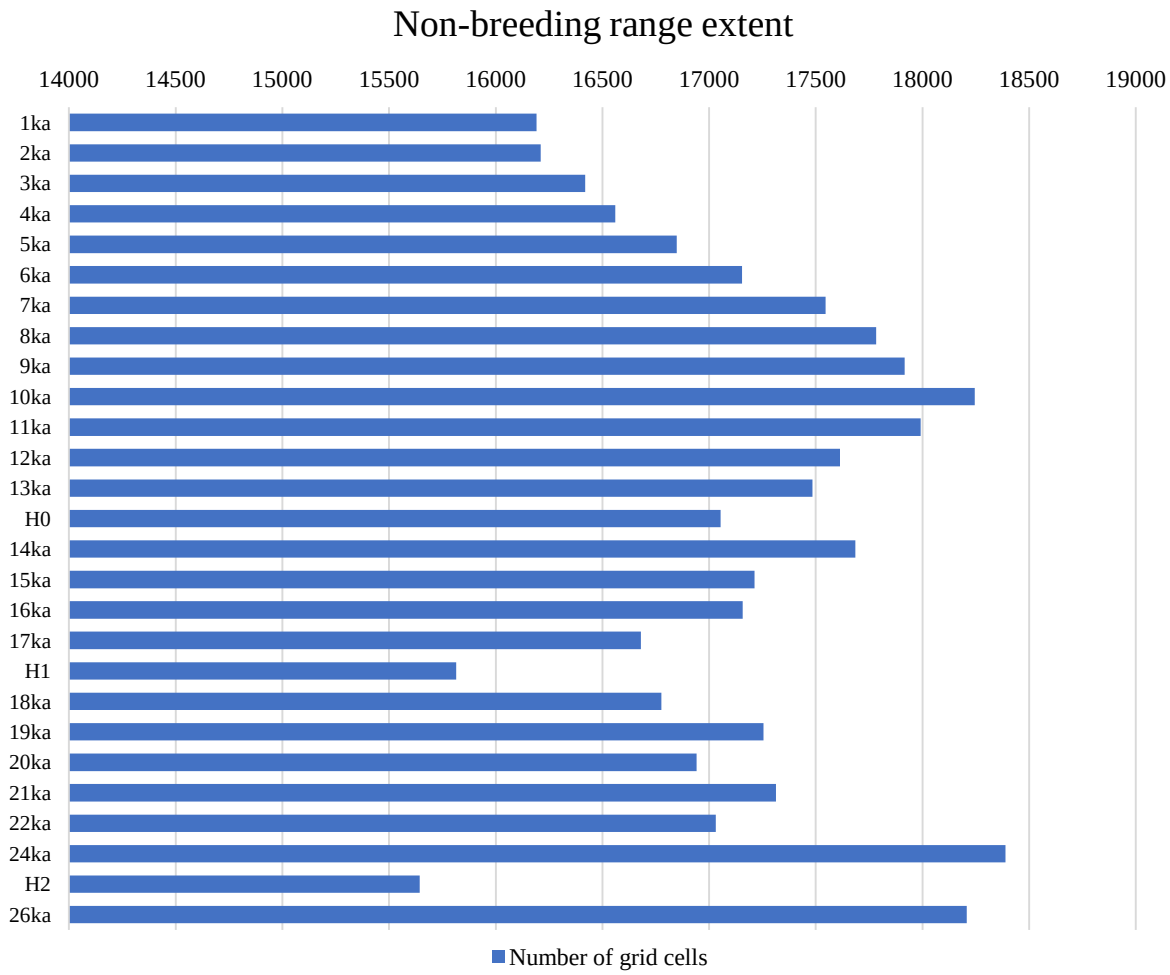

Figure 5.1(b). Changing extent of the non-breeding range of Semipalmated Plover (*C. semipalmatus*) during the late-Pleistocene and Holocene.

The projections with the higher species richness values were 8 ka BP and 26 ka BP, shown in Figure 5.1.1. Although this study has focused on the distributions of species of the Charadriidae family in the Americas, projections were made for the entire globe so as to explore the potential for the species to occur in areas outside the Americas, where in fact other species of the Charadriidae family occur (Piersma and Bonan 2018). For the purpose of illustration the mapped projection results have been clipped to focus upon the Americas.

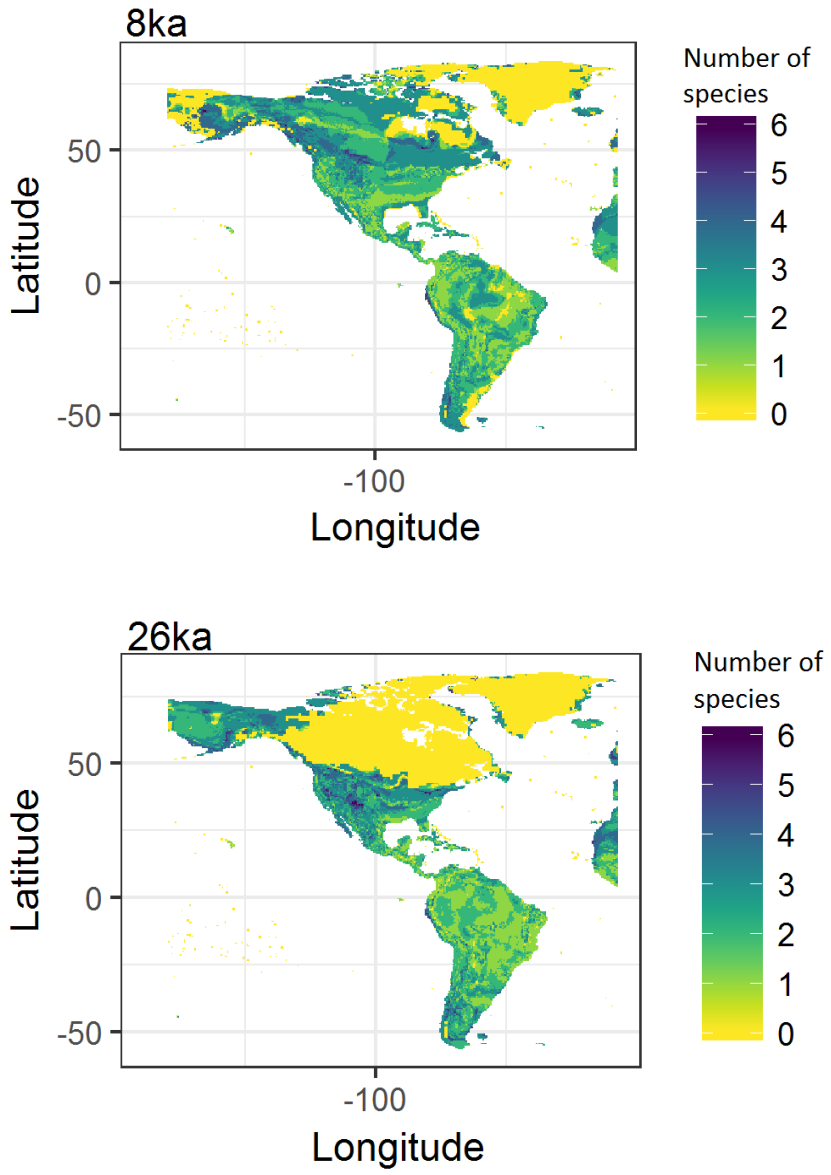

Figure 5.1.1. Projections of breeding-season species richness of Charadriidae for 8 ka BP (above) and 26 ka BP (below), two times when projected species richness was generally high. Areas with no species projected to occur are predominantly ice-covered areas.

The lower species richness values are illustrated on the 5 ka BP and H2 projections as seen on Figure 5.1.2. It could be due to the Altithermal that species richness was low for the 5 ka BP projection, given that climatic conditions were stable and allowed the spreading of species across North America. As for the H2 projection, it is no surprise that species richness was lower due to the extreme cold event.

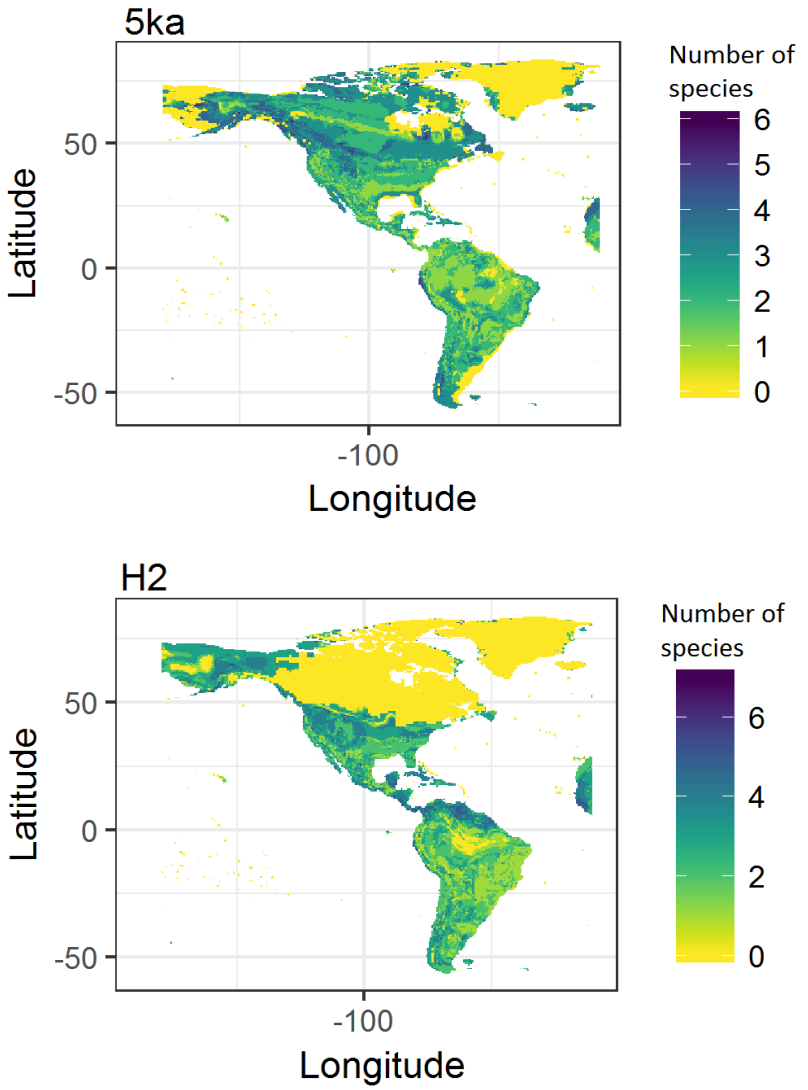

Figure 5.1.2. Projections of breeding-season species richness of Charadriidae for 5 ka BP (above) and Heinrich Event 2 (24 ka BP, below), two times when projected species richness was generally low.

For the non-breeding range the higher species richness is shown on the 10 ka BP projection (see Figure 5.1.3), which could be related to the deglaciation leading to changes in the inland vegetation that rendered it suitable for more species to be present.

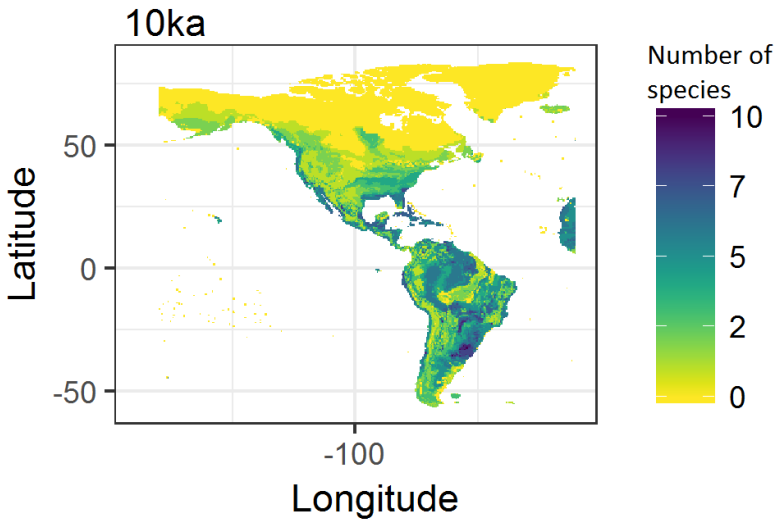

Figure 5.1.3. Projection of non-breeding-season species richness of Charadriidae for 10 ka BP, a time when projected species richness was generally high.

The lower species richness for the non-breeding range are presented on the H1 and H2 projections (see Figure 5.1.4) which again shows a possible vulnerability of Charadriidae species to colder climate events, especially during the Heinrich events.

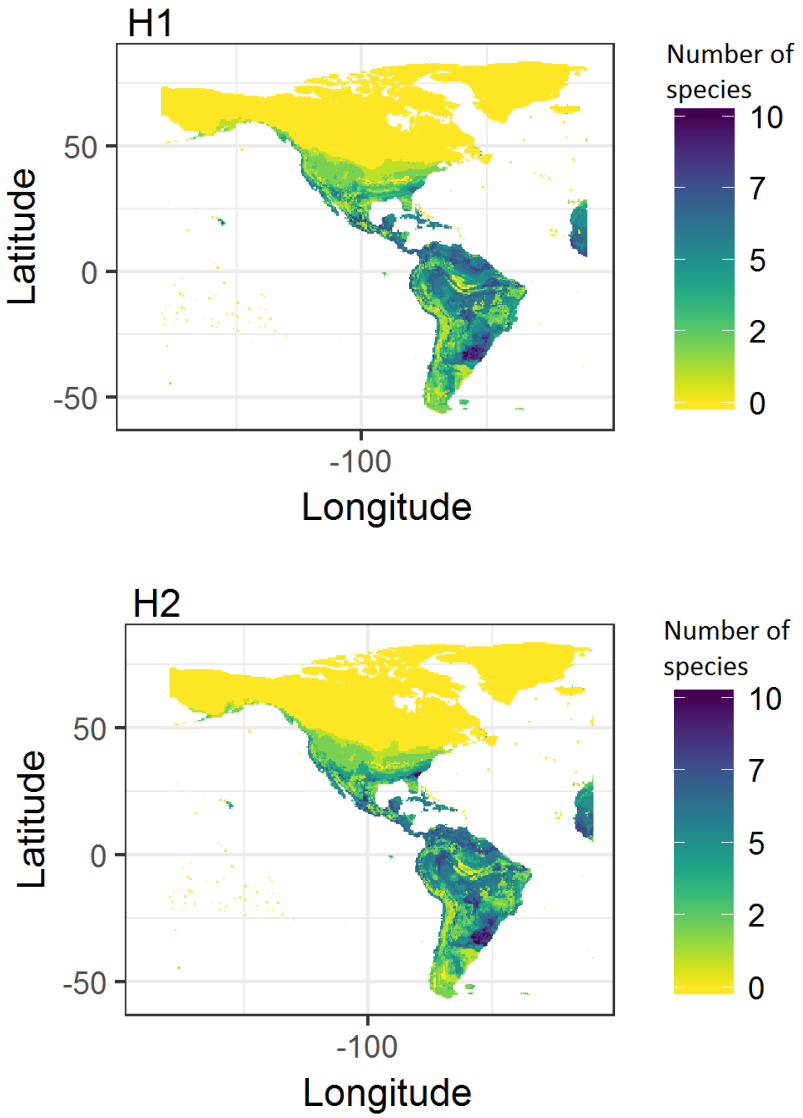

Figure 5.1.4. Projections of non-breeding-season species richness of Charadriidae for Heinrich Events H1 (17 ka BP, above) and H2 (24 ka BP, below), two times when projected species richness was generally low.

Overall, areas offering climatic conditions for members of the Charadriidae have not changed dramatically in extent over the last 26,000 years, and the spatial pattern and magnitude of species richness for the family changed little between the late Pleistocene (around 13 ka BP) and mid-Holocene (the Altithermal, around 7 ka BP). In addition, species that breed in the Arctic increased the extent of their breeding range after the LGM (e.g. Semipalmated Plover, Figure 6(a)).

Non-breeding range extents are generally larger than breeding range extents for the whole family, although this is in large part a result of projections of suitable climatic conditions in many inland areas for species that are currently restricted to coastal areas in the non-breeding season even if several inland areas might offer suitable habitat associated with areas of fresh water. The failure of these species to use such areas at present may reflect a lack of suitable prey, competition or predation excluding them from inland but climatically-suitable areas; whether such interactions would have similarly excluded them in the past is not readily predicted.

5.3.2 Family Haematopodidae

Potential presence values were analysed for the time-series of simulations for the breeding and non-breeding ranges of species of Haematopodidae. The three species studied display different patterns of change in range extents, probably reflecting the geographical and habitat differences between their present ranges. The breeding ranges of the coastal species, Blackish Oystercatcher (*H ater*) and American Oystercatcher (*H. palliatus*), show no dramatic fluctuations before or during the LGM (26 ka BP to 18 ka BP). Both species' range extents decrease from *ca.* 17 ka BP to 10 ka BP; this could be associated with the deglaciation process.

For the Magellanic Oystercatcher (*H. leucopodus*), a South-American species, the projections tell a different story as the range extent is reduced during the late Pleistocene (from 26 ka BP to 12 ka BP), and increases during the early Holocene, especially at 8 ka BP (see Figure 5.2(a)). It is also important to mention that the Heinrich events did not have any marked impact upon the breeding or non-breeding ranges of these three species.

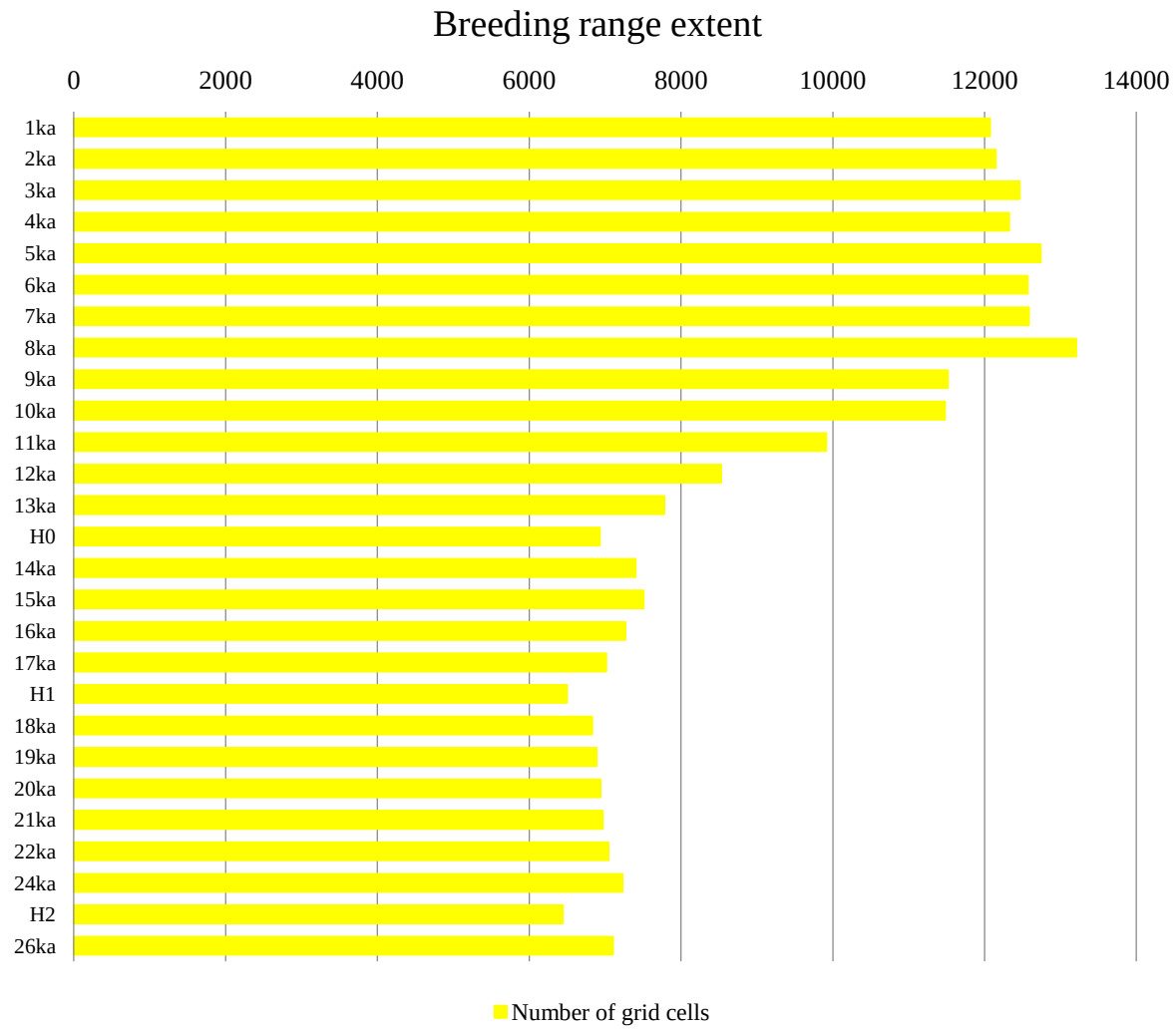

Figure 5.2(a). Changing extent of the Magellanic Oystercatcher (*H. leucopodus*) breeding range during the late-Pleistocene and Holocene.

The projected changes in non-breeding range extents show a similar pattern to those for the breeding range for both the Blackish Oystercatcher (*H. ater*) and American Oystercatcher (*H. palliatus*). Range extent was somewhat greater before and during the LGM (26 ka BP to 19 ka BP) than subsequently at *ca.* 18 ka BP and 17 ka BP, increasing during the early Holocene only to decrease again somewhat after the Altithermal, especially in the case of the American Oystercatcher. For the Magellanic Oystercatcher (*H. leucopodus*) the trends in non-breeding range extent largely mirrored those for the breeding range, with smaller extents from 26 ka BP to 12 ka BP followed by an increase in extent during the early Holocene. As with the breeding ranges, the Heinrich events did not seem markedly to affect the species' range extents. See Figure 5.2(b) as an example of this.

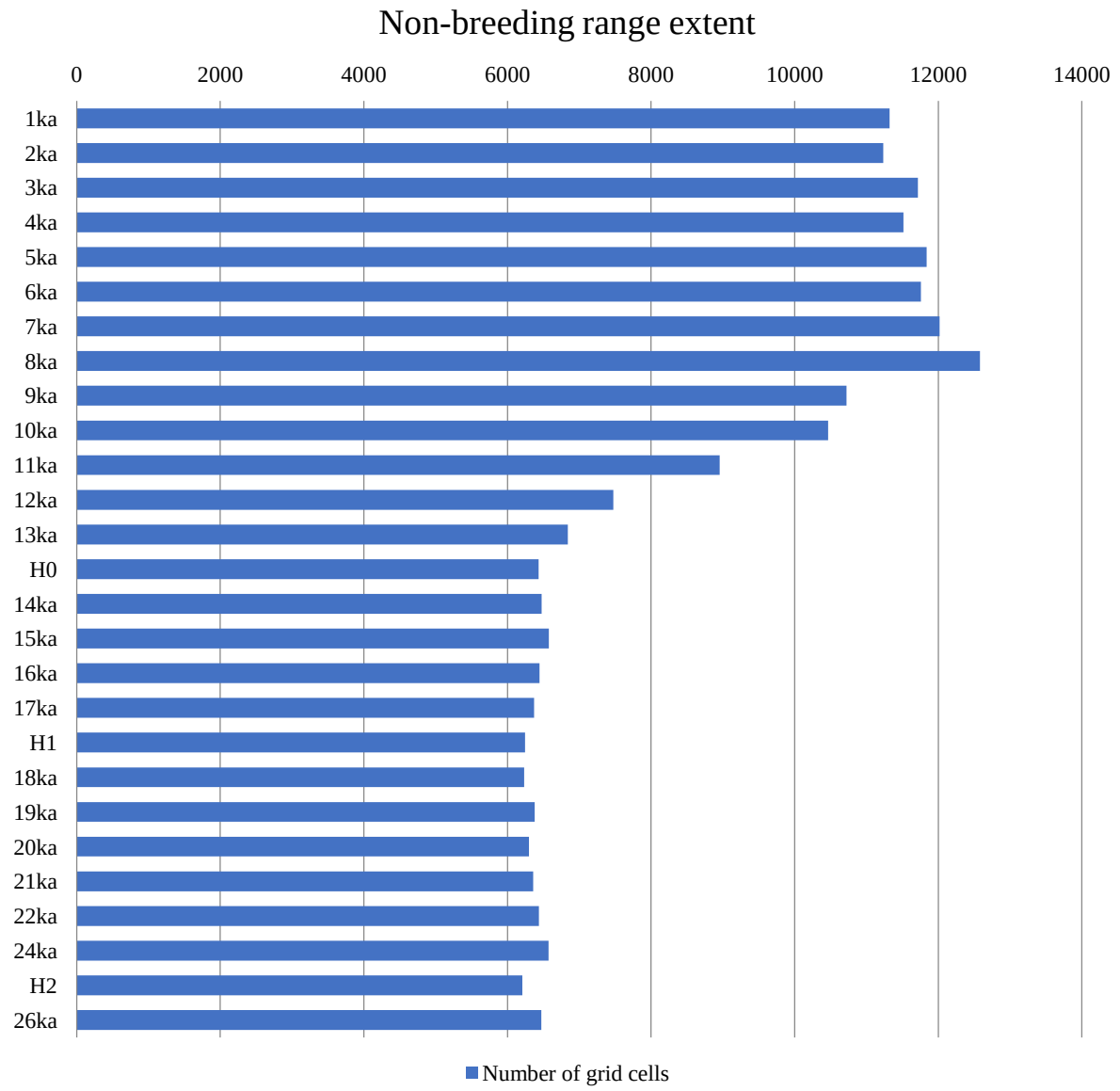

Figure 5.2(b). Changing extent of the Magellanic Oystercatcher (*H. leucopodus*) non-breeding range during the late-Pleistocene and Holocene.

The higher breeding-season species-richness values for the Haematopodidae are seen in the 26 ka BP projection (see Figure 5.2.1), reflecting the greater extent of suitable climate for the coastal species during the LGM; after the LGM their range extent declines, possibly as a result of deglaciation during the late Pleistocene that raised sea level and also of changes in ocean currents. As with the Charadriidae the projections were made globally, although the species modelled are restricted to the Americas. Interestingly, examination of the literature for other species of Haematopodidae distributed outside the Americas (Hockey et al. 2018)

showed the models predict suitable areas for the current climate corresponding generally to areas currently occupied by other members of the family.

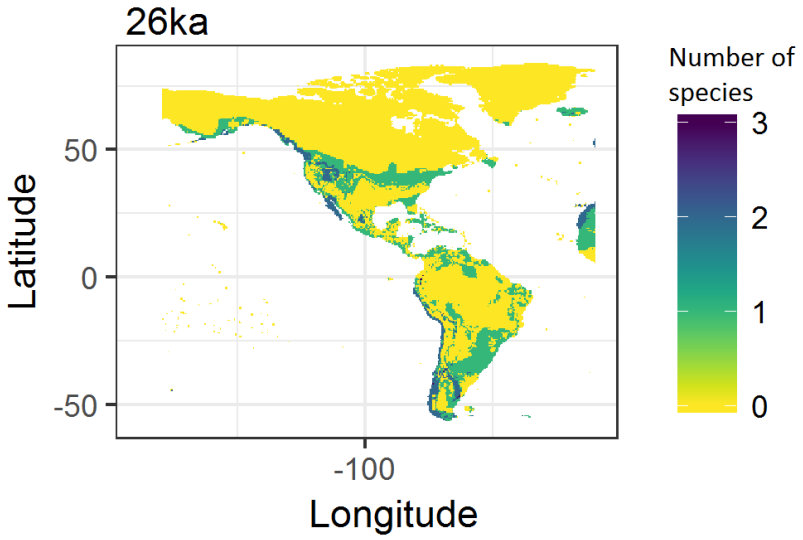

Figure 5.2.1. Projection of breeding-season species richness of Haematopodidae for 26 ka BP, when projected species richness was generally high.

The lower species richness of the breeding range is observed at H0, probably reflecting a response to the Younger Dryas cold phase (Adams et al. 1999), especially since the species of this family are primarily restricted to coastal areas. See Figure 5.2.2.

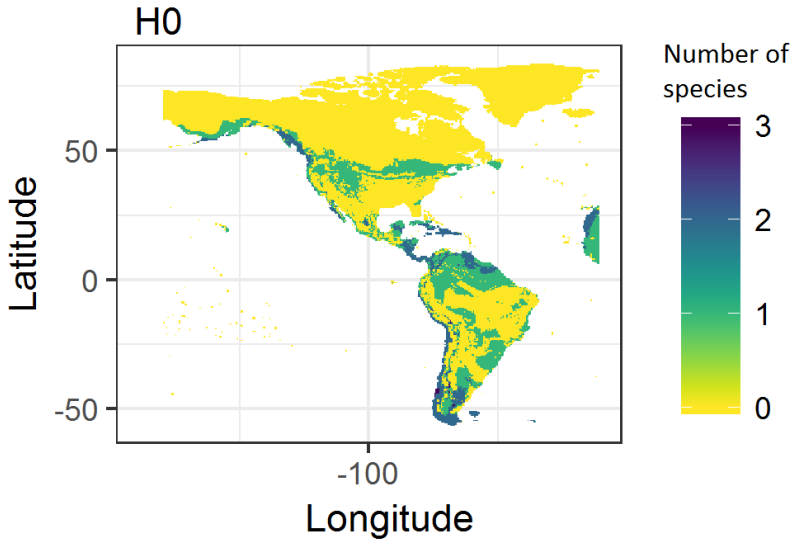

Figure 5.2.2. Projection of breeding-season species richness of Haematopodidae for H0 (13 ka BP), when projected species richness was generally low.

Higher species richness during the non-breeding season is seen in the projection for 8 ka BP (Figure 5.2.3), reflecting the Altithermal maximum in breeding range extents.

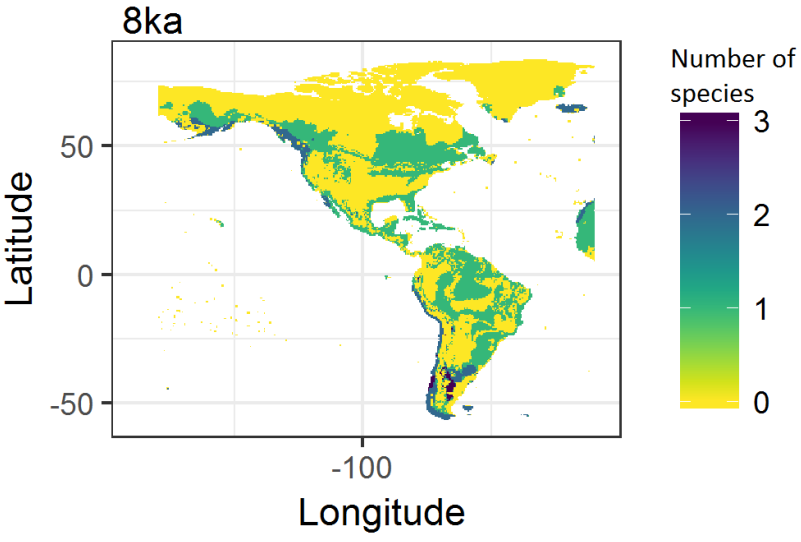

Figure 5.2.3. Projection of non-breeding-season species richness of Haematopodidae for 8 ka BP, when projected species richness was generally high.

Even though there are no dramatic differences between each time-slice, the lower non-breeding season species richness of the Haematopodidae is in the H0 projection, corresponding to the Younger Dryas cold phase of extreme cold and aridity (Adams et al. 1999). See Figure 5.2.4.

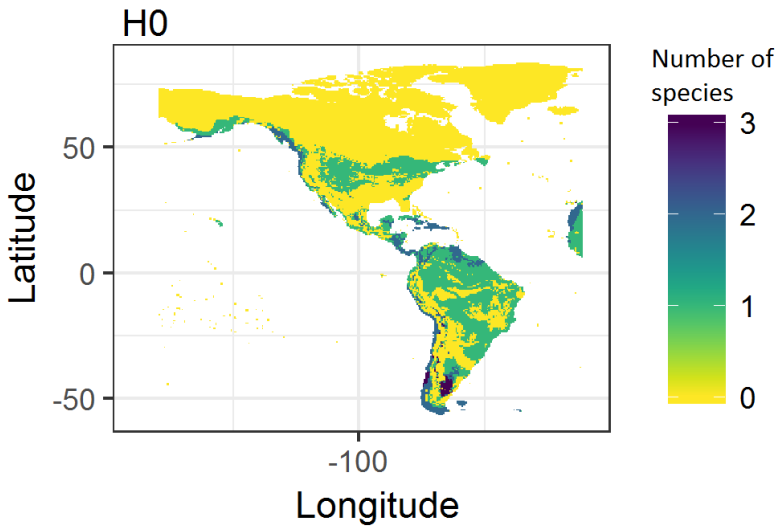

Figure 5.2.4. Projection of non-breeding-season species richness of Haematopodidae for H0 (13 ka BP), when projected species richness was generally low.

Overall for the Haematopodidae the differences in the patterns of change of their range extents could be due to their different habitats as both Blackish Oystercatcher and American Oystercatcher current ranges are along coastlines, whereas the Magellanic Oystercatcher, that is limited to southern South America, has a more inland range. For both breeding and non-breeding range there were no dramatic fluctuations, even during the Heinrich events, which may indicate that the species' range extents are not primarily determined by climatic conditions, although the success of the models in predicting suitable areas globally that correspond well to areas supporting other members of the family contradicts this. More probably, members of this family just happen to occupy climatic conditions that continued to be available over a similar extent of land during the climatic fluctuations of the late-Pleistocene and Holocene.

5.3.3 Family Recurvirostridae

Potential presence values for the two species of the Recurvirostridae were analyzed for both breeding and non-breeding projections. For both species, the Black-winged Stilt (*Himantopus himantopus*) and the American Avocet (*Recurvirostra americana*), the greatest breeding range extent was simulated in projections between 13 ka BP and 9 ka BP; this could reflect particularly suitable conditions for the species during the late-glacial interstadial and the beginning of the Holocene, the latter including the warming temperature trend towards the 'Altithermal' (Borzenkova et al. 2015). Both species' breeding range extents then follow a similar pattern of decrease from 5 ka BP to 1 ka BP, especially at 1 ka BP, perhaps reflecting the aridity at this time (Hodell et al. 1995, Fritz et al. 2001, Wang et al. 2016), given that the species favour habitats such as wetlands, shallow lagoons and flooded lowlands (Sibley 2014). See Figure 5.3(a) as an example of this.

Breeding range extents during Heinrich events are greater for both species, reflecting larger suitable areas mostly in northern South America; only the H1 projection for the American Avocet (*R. americana*) had a reduced extent.

For the non-breeding season, the range extent of the Black-winged Stilt (*H. himantopus*) is similar throughout the simulations from 26 ka BP to 1 ka BP, whereas for the American Avocet (*R. americana*) the simulations display a pattern similar to that for the breeding range extent, although of a greater magnitude, particularly during the beginning of the Holocene, when suitable conditions are simulated to have been markedly more extensive during the warm period of the Altithermal. Anomalously, the simulations for Heinrich events also are of markedly greater non-breeding range extent of both species than in the equivalent glacial time slices, See Figure 5.3(b) as an example of this.

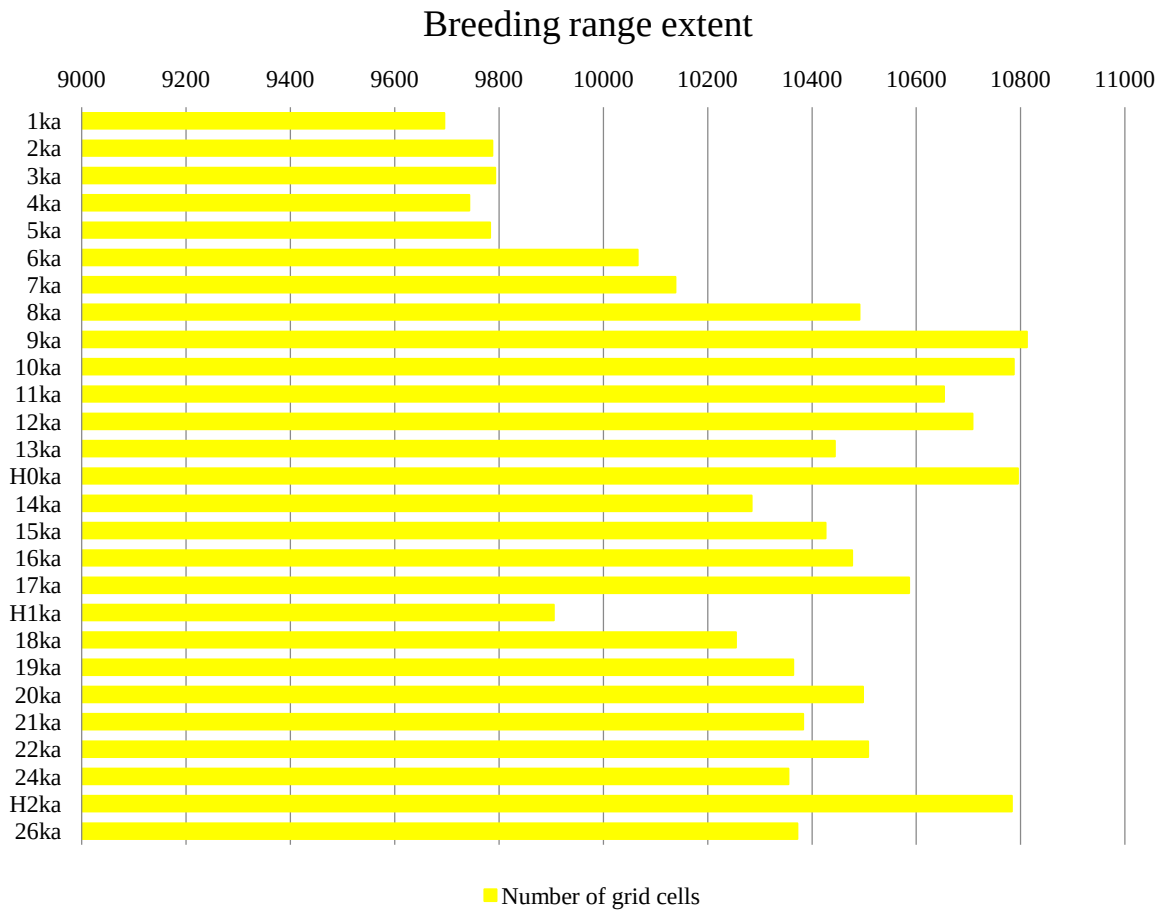

Figure 5.3.(a). Changing extent of the American Avocet (*R. americana*) breeding range during the late-Pleistocene and Holocene.

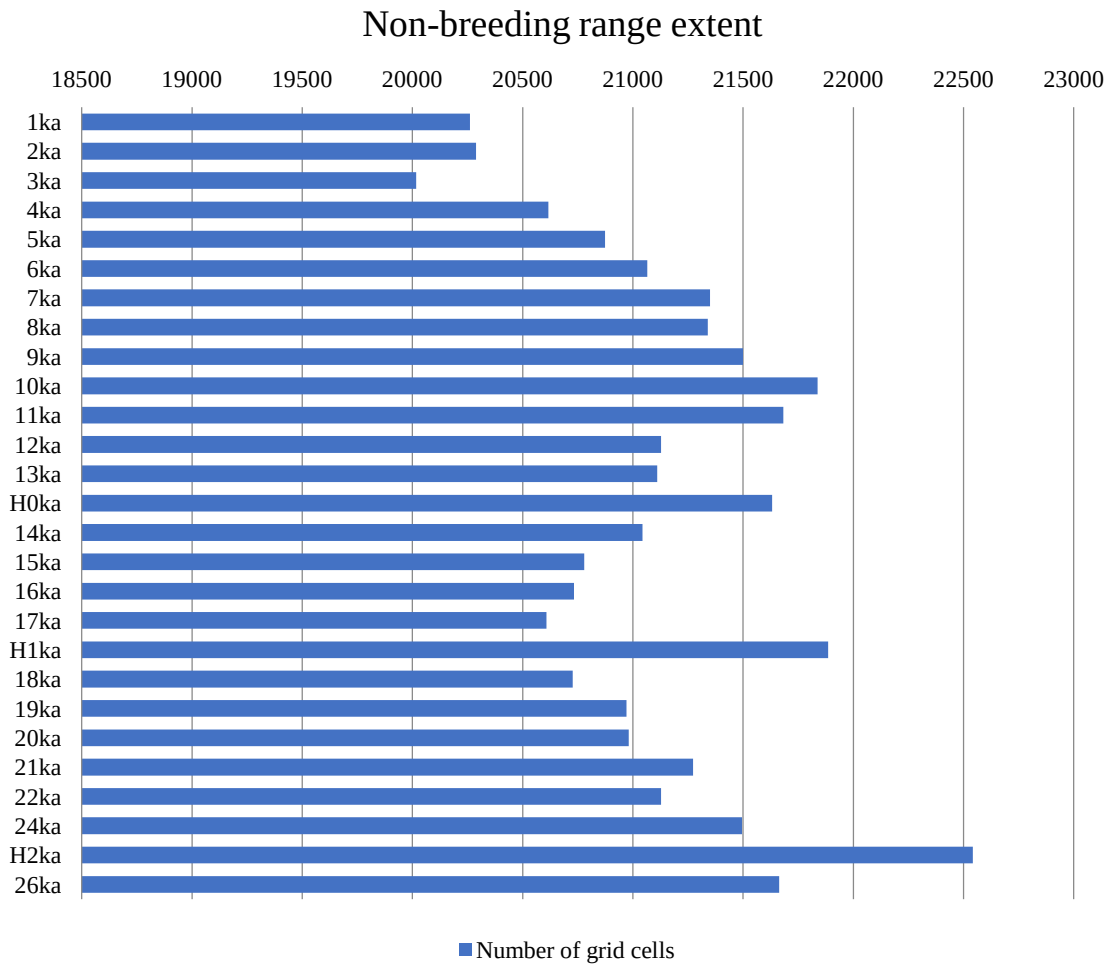

Figure 5.3(b). Changing extent of the American Avocet (*R. americana*) non-breeding range during the late-Pleistocene and Holocene.

For the breeding season, species richness of the Recurvirostridae is higher at the beginning of the Holocene, particularly in the 10 ka BP projection, indicating beneficial conditions from the deglaciation and the more stable climatic conditions of the early Holocene (Borzenkova et al. 2015). See Figure 5.3.1.

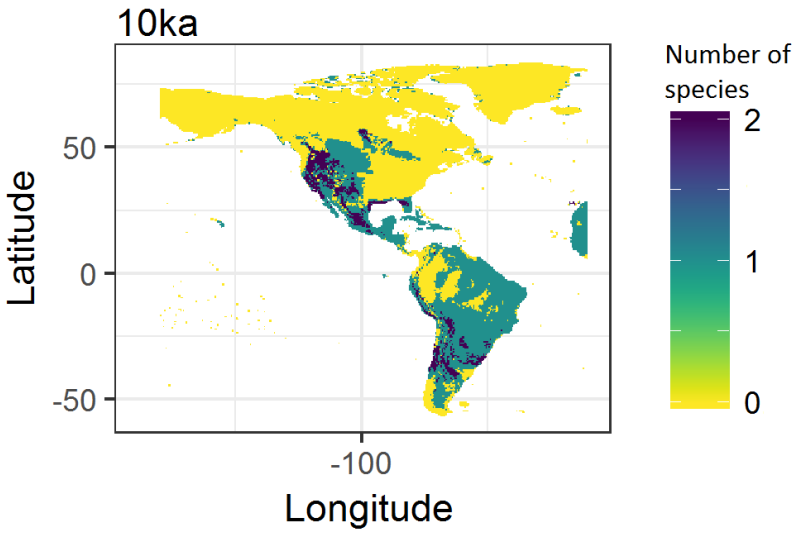

Figure 5.3.1. Projection of breeding-season species richness of Recurvirostridae for 10 ka BP, when projected species richness was generally higher.

The lowest species richness for the breeding season is seen in the 1 ka BP projection. This corresponds to a period of arid conditions (Hodell et al. 1995, Fritz et al. 2001, Wang et al. 2016) that could have affected the availability of the freshwater sites preferred by the species of this family. See Figure 5.3.2.

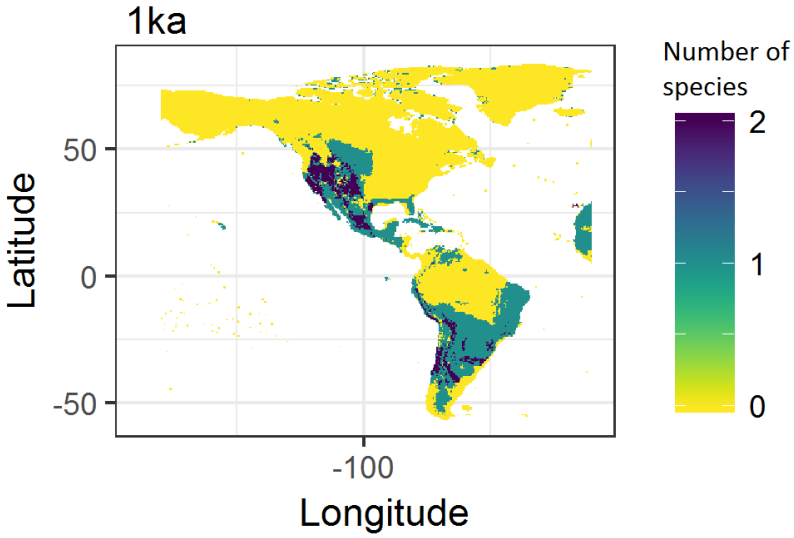

Figure 5.3.2. Projection of breeding-season species richness of Recurvirostridae for 1 ka BP, when projected species richness was generally lower.

For the non-breeding season, species richness was higher for the H2 projection, where freshwater input from the melting icebergs, and associated marked cooling of the North Atlantic region, might have positively influenced the availability of suitable conditions in more southern latitudes of the Northern Hemisphere, resulting in an overall increase in the extent of both species non-breeding ranges. See Figure 5.3.3.

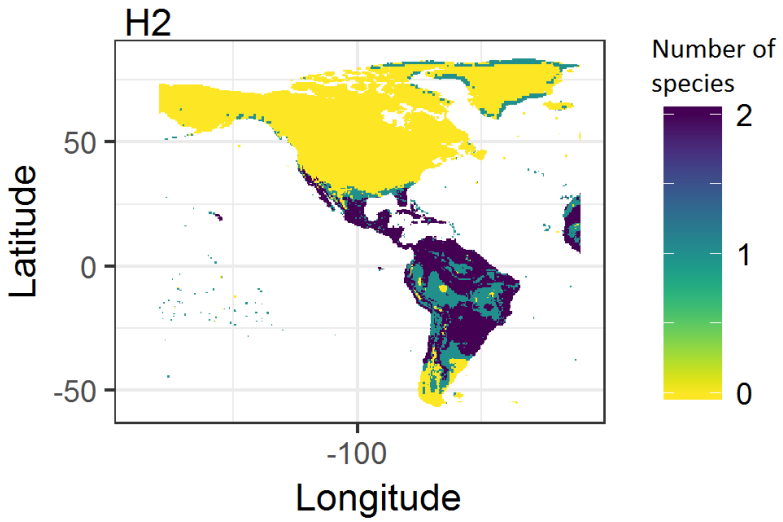

Figure 5.3.3. Projection of non-breeding-season species richness of Recurvirostridae for H2 (24 ka BP), when projected species richness was generally higher.

As with the breeding season, the lowest species richness for the non-breeding season is simulated for 1 ka BP. This may again reflect the aridity of this period (Hodell et al. 1995, Fritz et al. 2001, Wang et al. 2016). See Figure 5.3.4.

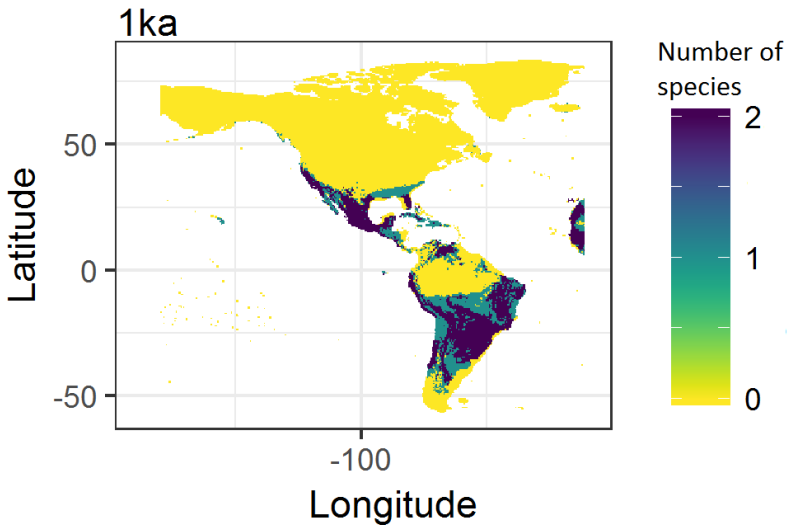

Figure 5.3.4. Projection of non-breeding-season species richness of Recurvirostridae for 1 ka BP, when projected species richness was generally lower.

Overall the simulations for the Recurvirostridae displayed similar patterns, especially for the early Holocene projections (*ca.* 10 ka BP to 8 ka BP) when higher species richness could reflect the deglaciation, and also the lower species richness between 5 ka BP and 1 ka BP that may indicate susceptibility of this family to arid conditions, corresponding to the family's current strong association with wetland habitats.

5.3.4 Family Scolopacidae

The projections of breeding and non-breeding range extents for the 32 species of Scolopacidae studied were analyzed. For the breeding range, most of the species show greater range extents during the Holocene and particularly at 8 ka BP. It seems that most species of this family benefited from the deglaciation of the Laurentide ice sheet as well as from the 'Altithermal' with its more stable climate, allowing them to expand their breeding grounds. See Figure 5.4(a) as an example of this.

Only three species, Sanderling (*Calidris alba*), Baird's Sandpiper (*C. bairdii*) and Red Knot (*C. canutus*), show reduced range extents during the Holocene. Although deglaciation increased the land area available at high northern latitudes during the Holocene, compared to during the last glacial stage, potentially benefitting these high Arctic breeders, their projected glacial ranges are extensive in Beringia and also include areas south of the Laurentide ice sheet, both regions from which their ranges retreat with the onset of the Holocene.

More than half of the members of the Scolopacidae showed increases in breeding range extent during Heinrich events; only 11 species showed reduced extent of their breeding range during these events: Spotted Sandpiper (*Actitis macularius*); Least Sandpiper (*C. minutilla*); Wilson's Snipe (*Gallinago delicata*); Short-billed Dowitcher (*Limnodromus griseus*); American Whimbrel (*Numenius phaeopus hudsonicus*); American Woodcock (*Scolopax minor*); Wilson's Phalarope (*Steganopus tricolor*); Lesser Yellowlegs (*Tringa flavipes*); Greater Yellowlegs (*T. melanoleuca*); Willet (*T. semipalmata*); and Solitary Sandpiper (*T. solitaria*).

For the non-breeding season, range extents are greater during the late Pleistocene and early Holocene (*ca.* 14 ka BP to 8 ka BP), following a similar pattern to the breeding range extents as deglaciation led to greater areas with suitable climatic conditions becoming available. Only three species showed greater range extents during the late Pleistocene (26 ka BP to 13 ka BP): Surfbird (*C. virgata*); Long-billed Dowitcher (*L. scolopaceus*); and Wandering Tattler (*T. incana*). This can be related to their current preference for colder climates, their breeding ranges being in Arctic tundra in western and northern Alaska and

along the north coast of Canada (Van Gils et al. 2018a, Van Gils et al. 2018b). See Figure 5.4(b) as an example of this.

There is also a pattern of greater non-breeding range extent between 3 ka BP and 1 ka BP for most of the species; the more stable climatic conditions of the Holocene seem to lead an increase in the range extent for the non-breeding season with no apparent effects of the drier conditions *ca.* 2 ka BP and 1 ka BP (Mayewski et al 2004).

Non-breeding range extents are reduced during Heinrich events for most of the Scolopacidae, contrasting with the breeding range extents. This may reflect the different expression of the Heinrich events beyond higher latitudes of the Northern Hemisphere, including in the tropics, also known as the bipolar seesaw effect (Stocker 1998, Shakun and Carlson 2010), resulting from the reduced strength of the Meridional Overturning Circulation or AMOC during these events (Shakun and Carlson 2010, van Ommen 2015).

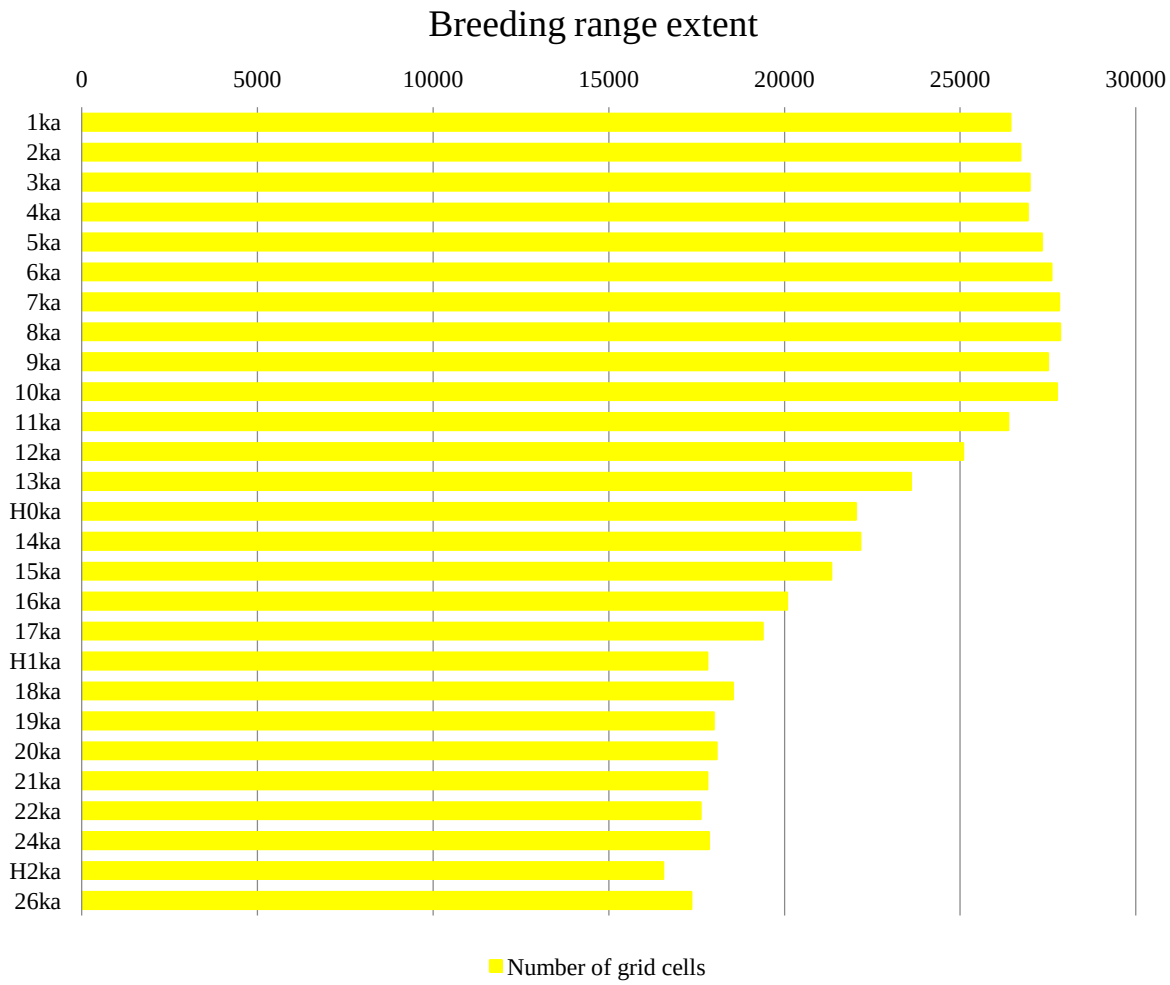

Figure 5.4(a). Changing extent of the Spotted Sandpiper (*A. macularius*) breeding range during the late-Pleistocene and Holocene.

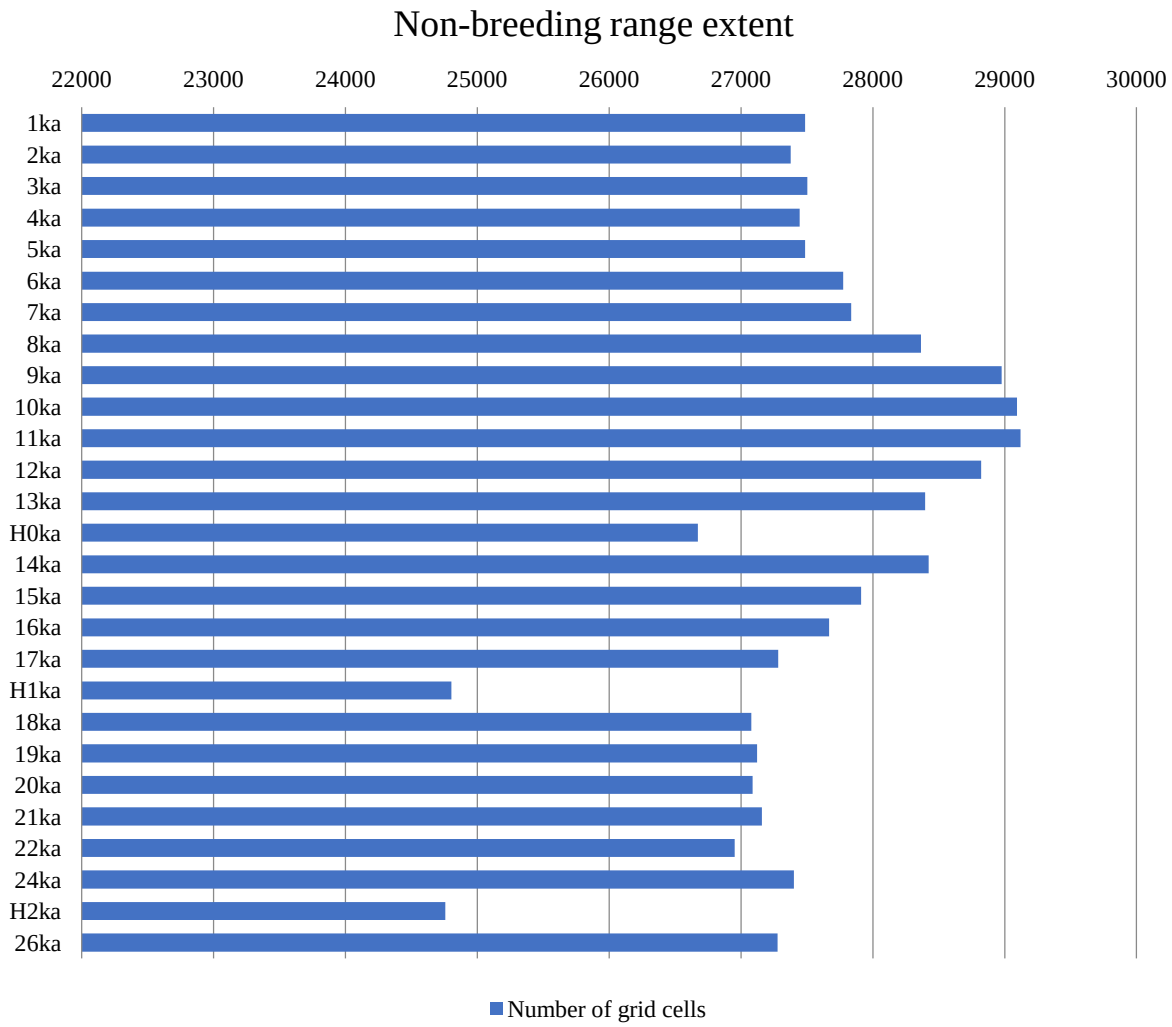

Figure 5.4(b). Changing extent of the Spotted Sandpiper (*A. macularius*) non-breeding range during the late-Pleistocene and Holocene.

The highest species richness for the breeding season is observed at the beginning of the Holocene, specifically on the 8 ka BP projection, supporting the response of species to more stable and warming temperatures of the Holocene climatic optimum and to the deglaciation that allowed previously ice-covered areas of Canada and the USA to be occupied (Borzenkova et al. 2015, Lowe and Walker 2015). See Figure 5.4.1.

The lowest species richness for the breeding season is observed on the 19 ka BP projection that could be an indicator of the effects of the ice sheet covering a large part of North America during the LGM (Clark et al. 2009). See Figure 5.4.2.

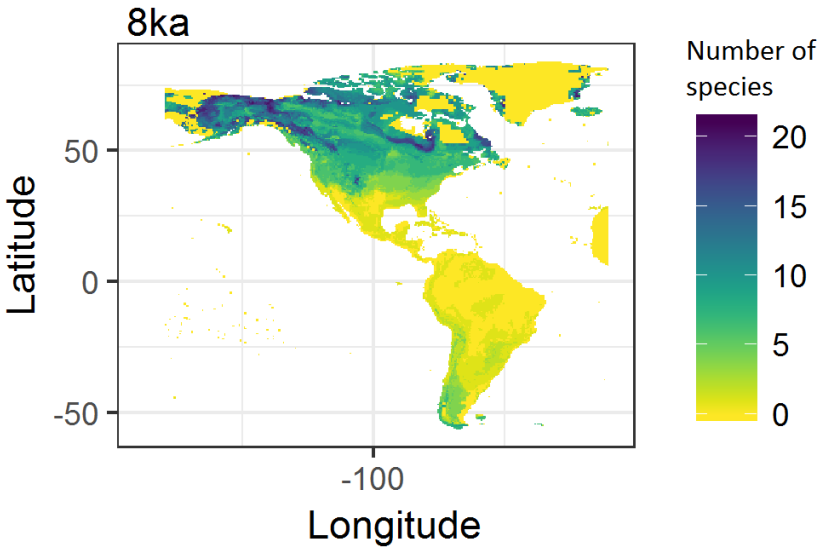

Figure 5.4.1. Projection of breeding-season species richness of Scolopacidae for 8 ka BP, when projected species richness was generally higher.

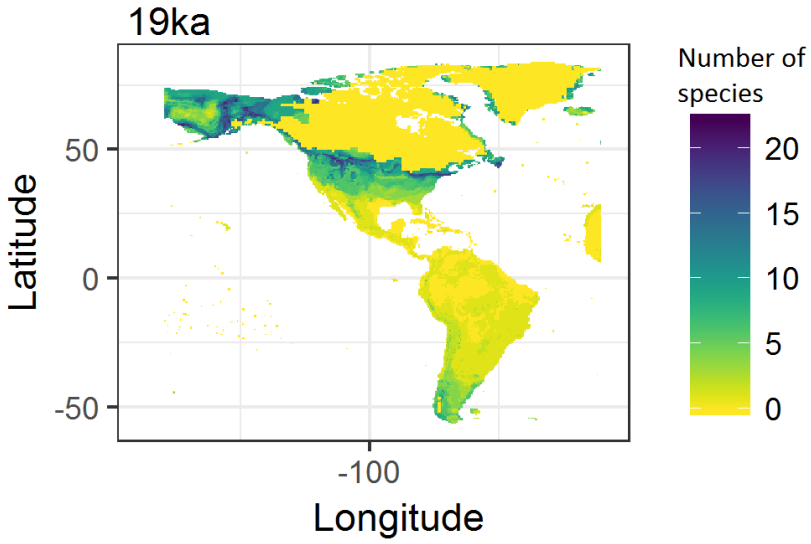

Figure 5.4.2. Projection of breeding-season species richness of Scolopacidae for 19 ka BP, when projected species richness was generally lower.

For the non-breeding season higher species richness of the Scolopacidae is observed on the 11 ka BP and 10 ka BP projections. The warmer and more stable climate of the early Holocene, compared to the late Pleistocene, may be reflected here, rendering greater areas

suitable and thus increasing the range extent of the majority of members of the family. See Figure 5.4.3.

Reduced species richness during the non-breeding season is projected for the Heinrich events, particularly the H1 projection. This may be related to evidence of warmer temperatures and drier conditions in the Southern Hemisphere during Heinrich events as a result of the bipolar seesaw effect and the disruption of the AMOC (McManus et al. 2004, Handiani et al. 2012). See Figure 5.4.3.

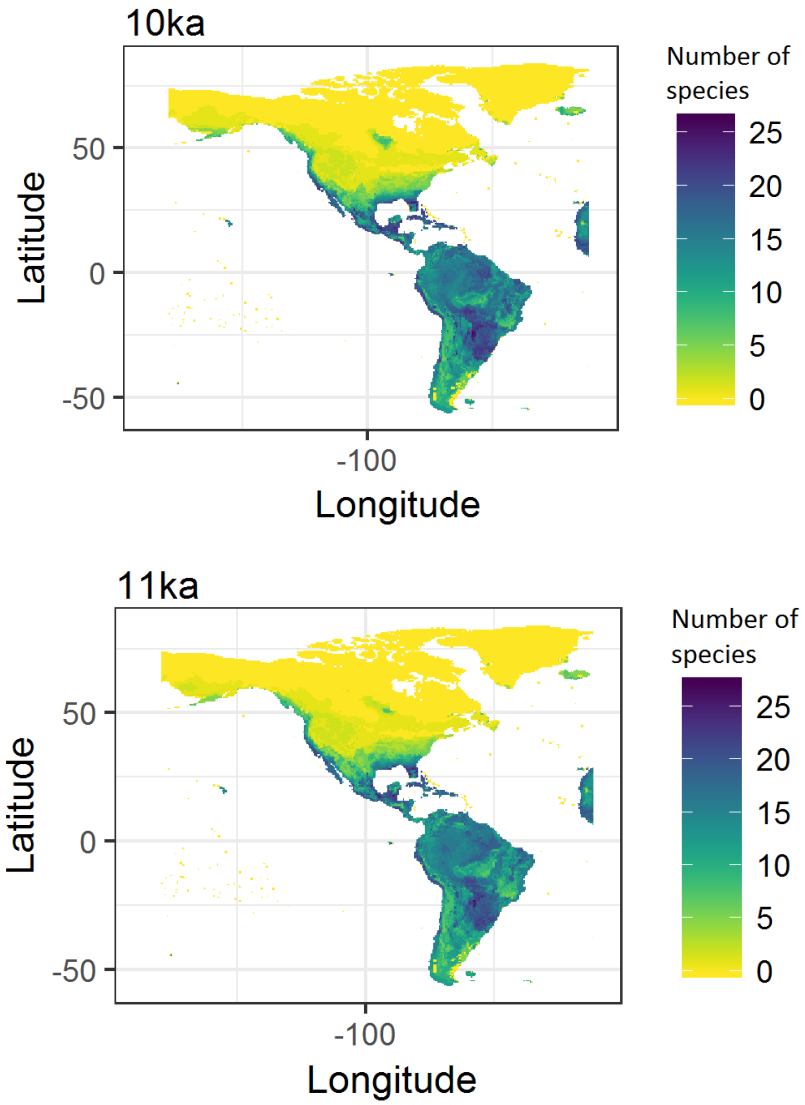

Figure 5.4.3. Projections of non-breeding-season species richness of Scolopacidae for 10 ka BP (above) and 11 ka BP (below), times when projected species richness was generally higher.

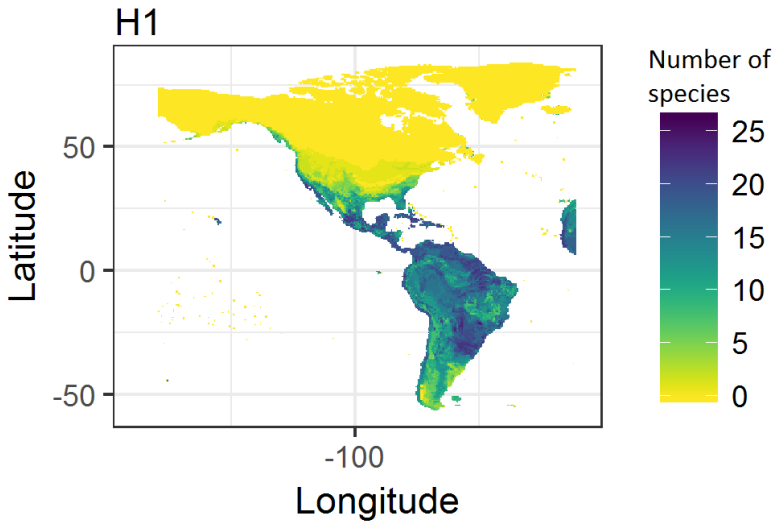

Figure 5.4.4. Projection of non-breeding-season species richness of Scolopacidae for H1 (17 ka BP), when projected species richness was generally lower.

Overall for the Scolopacidae patterns can be detected in both breeding and non-breeding range projections, with greater range extents at the beginning of the Holocene related to the deglaciation process that allowed areas of Canada and the USA to be occupied, as well as improving the climatic suitability with warmer conditions and a more stable climate.

Heinrich events showed contrasting patterns between the breeding and non-breeding season projections, breeding season range extents increasing whereas non-breeding range extents were reduced. This probably reflects the contrasting climatic signature of Heinrich events in the Northern and Southern Hemispheres. Palaeoclimatic evidence shows that whereas conditions were cooler in the Northern Hemisphere, near the tropics there was an aridity effect, species' non-breeding ranges consequently moving to the Southern Hemisphere where conditions were more humid.

5.3.5 Family Trochilidae

Projected range extents for both the breeding and non-breeding seasons were analysed for the 14 species of Trochilidae examined. Projected breeding range extents are higher during the late Pleistocene period from 26 ka BP to 12 ka BP; the colder and more humid conditions during this time for regions in lower latitudes (Metcalfe et al. 2000) seem to have resulted in a greater extent of suitable climate for most of the Hummingbirds. The greater breeding range extents continue between 9 ka BP and 8 ka BP, which also corresponds to a period of wetter and colder conditions as found in paleo-records in Mexico, having an opposite climatic signal that in higher latitudes (Metcalfe et al. 2000).

The colder and more humid conditions in the Northern Hemisphere during Heinrich events (Handiani et al. 2012) provide increased extents of suitable conditions with greater breeding range extents for half of the species of this family: Black-chinned Hummingbird (*Archilochus alexandri*); Ruby-throated Hummingbird (*A. colubris*); Costa's Hummingbird (*Calypte costae*); Broad-billed Hummingbird (*Cynanthus latirostris*); Blue-throated Hummingbird (*Lampornis clemenciae*); Calliope Hummingbird (*Selasphorus calliope*); and the Broad-tailed Hummingbird (*S. platycercus*). These species' current breeding ranges are located throughout the USA and the Sierra Madre Occidental of Mexico, occupying woodland and colder areas (Schuchmann and Bonan 2016).

The remaining species have projected reductions in breeding range extent during Heinrich events: Violet-crowned Hummingbird (*Amazilia violiceps*), Buff-bellied Hummingbird (*A. yucatanensis*), Lucifer Hummingbird (*Calothorax lucifer*), Anna's Hummingbird (*Calypte anna*), Magnificent Hummingbird (*Eugenes fulgens*), Rufous Hummingbird (*Selasphorus rufus*), Allen's Hummingbird (*S. sasin*). This could be due to drier conditions in central and southern Mexico (Metcalfe et al. 2000) where most of these species breed, and to colder conditions in the more northern breeding range of the Rufous Hummingbird (Hostetler et al. 1999). See Figure 5.5(a) as an example of this.

The non-breeding range extents mainly do not display severe fluctuations, with most of the species maintaining similar range extents throughout the projections. For most of the species, the greatest non-breeding range extent is seen in the 10 ka BP and 9 ka BP projections,

during the beginning of the Holocene climate optimum (Borzenkova et al. 2015). Only three species show substantial fluctuations in their non-breeding range extents. Anna's Hummingbird (*C. anna*), Costa's Hummingbird (*C. costae*) and Rufous Hummingbird (*S. rufus*) have projected reduced non-breeding range extents during the late Pleistocene. See Figure 5.5(b) as an example of this.

Most members of the Trochilidae examined are projected to have reduced non-breeding range extents during Heinrich events. This may reflect the location of most species current wintering grounds in central-southern Mexico, a region that as discussed previously experienced drier conditions during these events (Metcalfe et al. 2000).

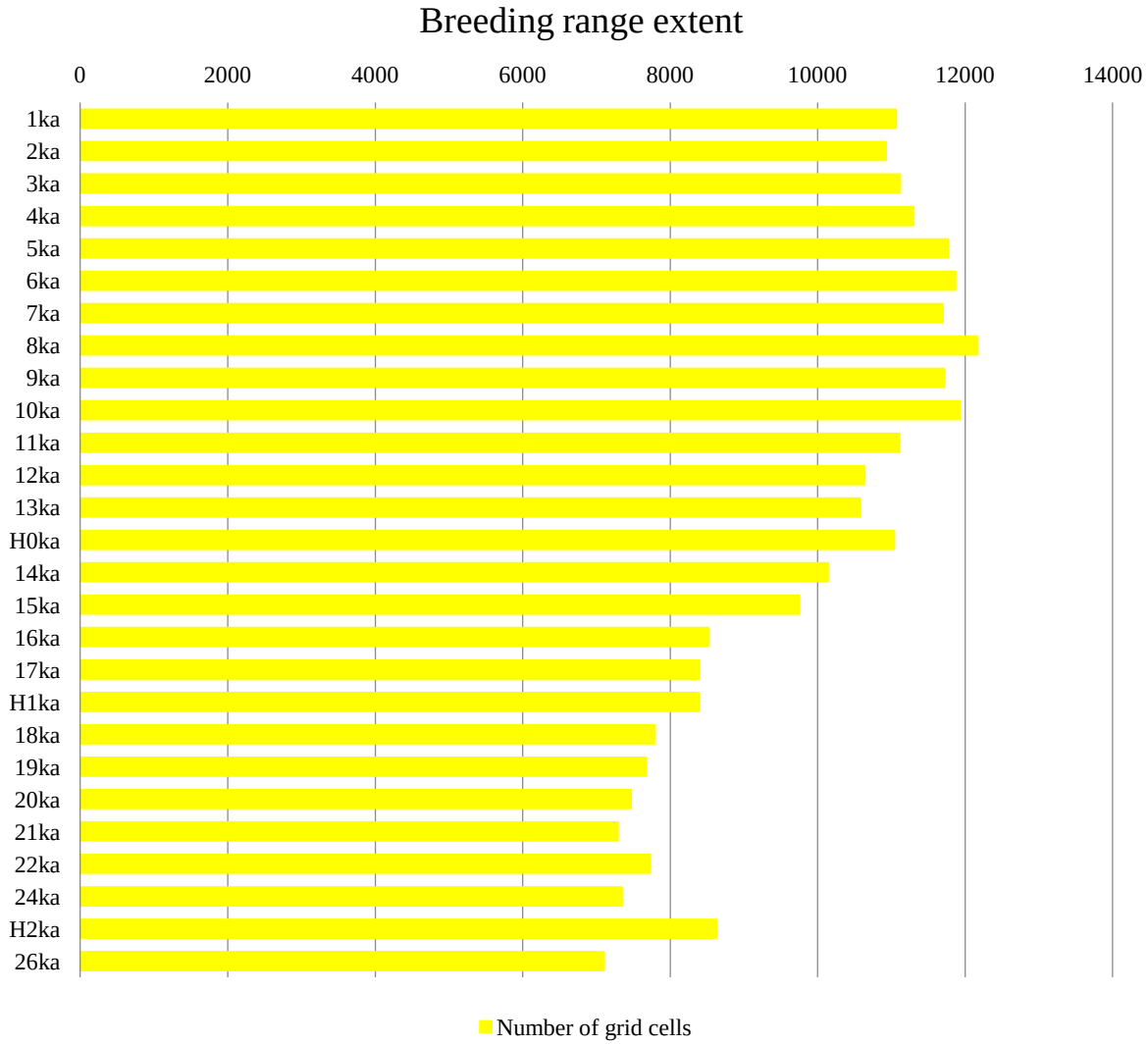

Figure 5.5(a). Changing extent of the Ruby-throated Hummingbird (*A. colubris*) breeding range during the late-Pleistocene and Holocene.

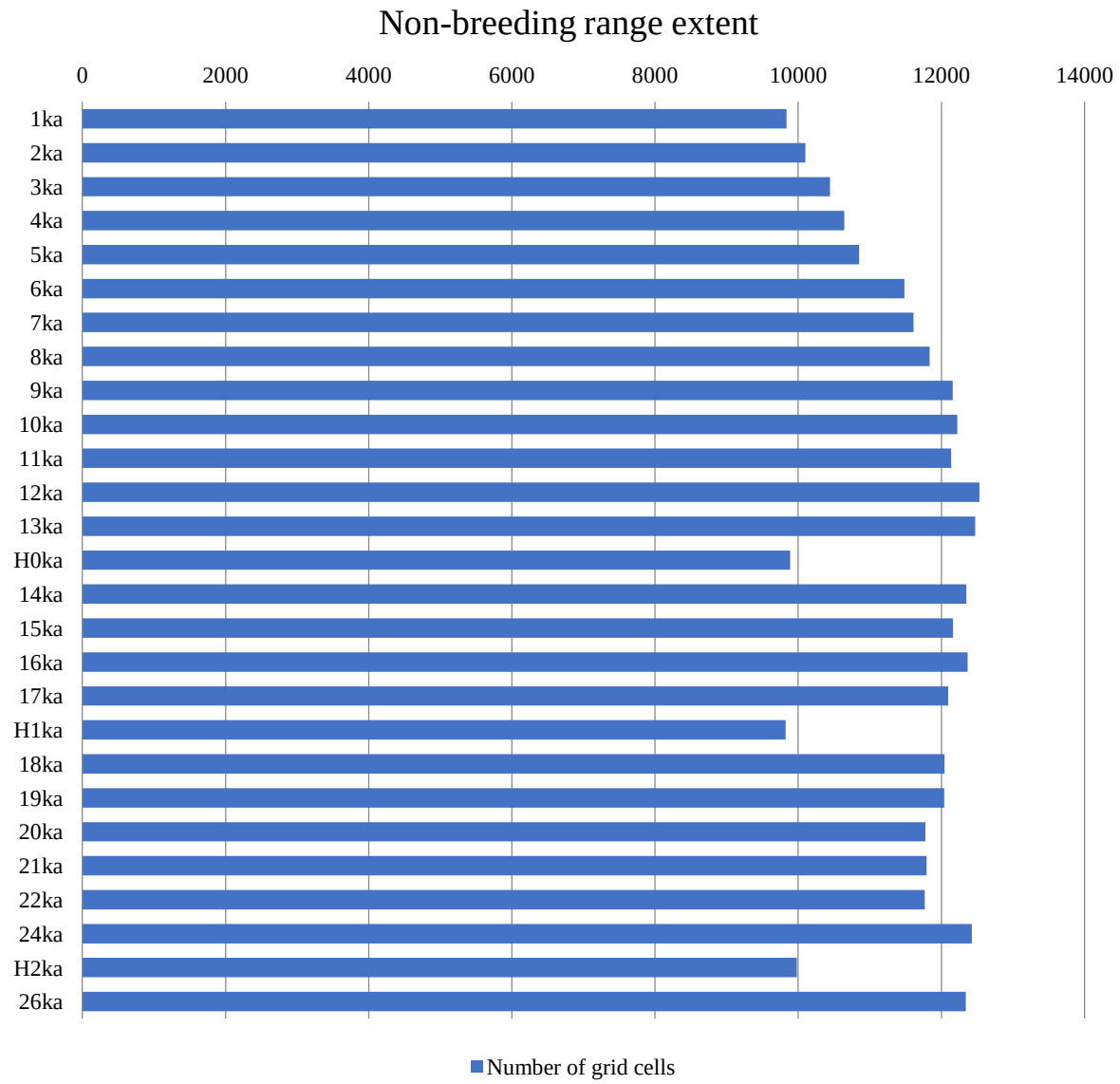

Figure 5.5(b). Changing extent of the Ruby-throated Hummingbird (*A. colubris*) non-breeding range during the late-Pleistocene and Holocene.

Breeding season species richness is greater in the projection for 9 ka BP, reflecting the increased extent of suitable climatic conditions following deglaciation and the developing Altithermal (Mayewski et al. 2004, Borzenkova et al. 2015). See Figure 5.5.1.

Species richness during the breeding season is reduced in the 1 ka BP projection, probably as a result of the colder and drier conditions recorded for that period (Mayewski et al. 2004). See Figure 5.5.2.

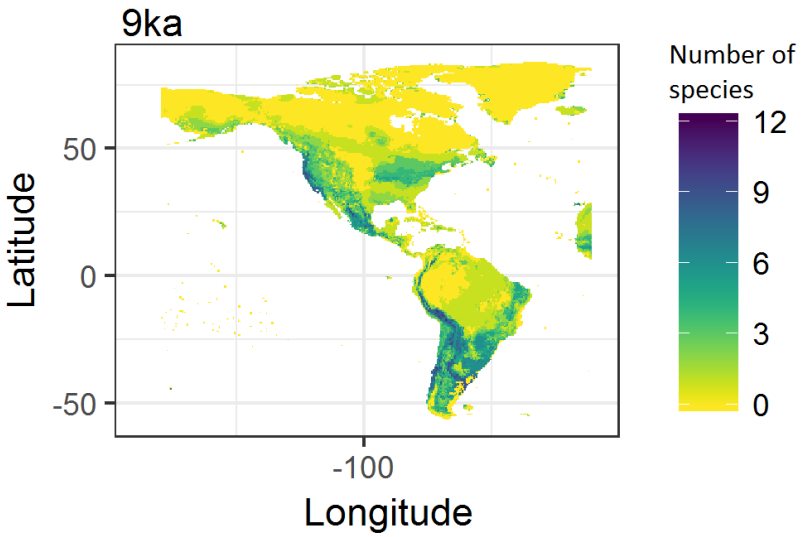

Figure 5.5.1. Projection of breeding-season species richness of Trochilidae for 9 ka BP, when projected species richness was generally higher.

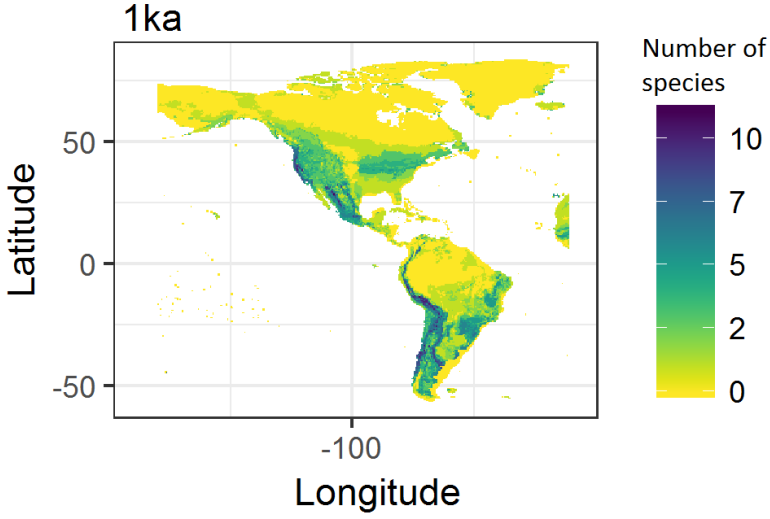

Figure 5.5.2. Projection of breeding-season species richness of Trochilidae for 1 ka BP, when projected species richness was generally lower.

Non-breeding season species richness was higher at 26 ka BP and 16 ka BP. The colder and more humid conditions of these periods (Metcalfe et al. 2000, Clark et al. 2009) apparently influenced positively the non-breeding season range extents of members of the Trochilidae, as most of their non-breeding ranges are located in the southern USA, Mexico and Central America. See Figure 5.5.3.

Lower non-breeding season species richness is projected for 1 ka BP, following a similar pattern to the breeding season and probably also reflecting the drier conditions during that time (Mayewski et al. 2014). See Figure 5.5.4.

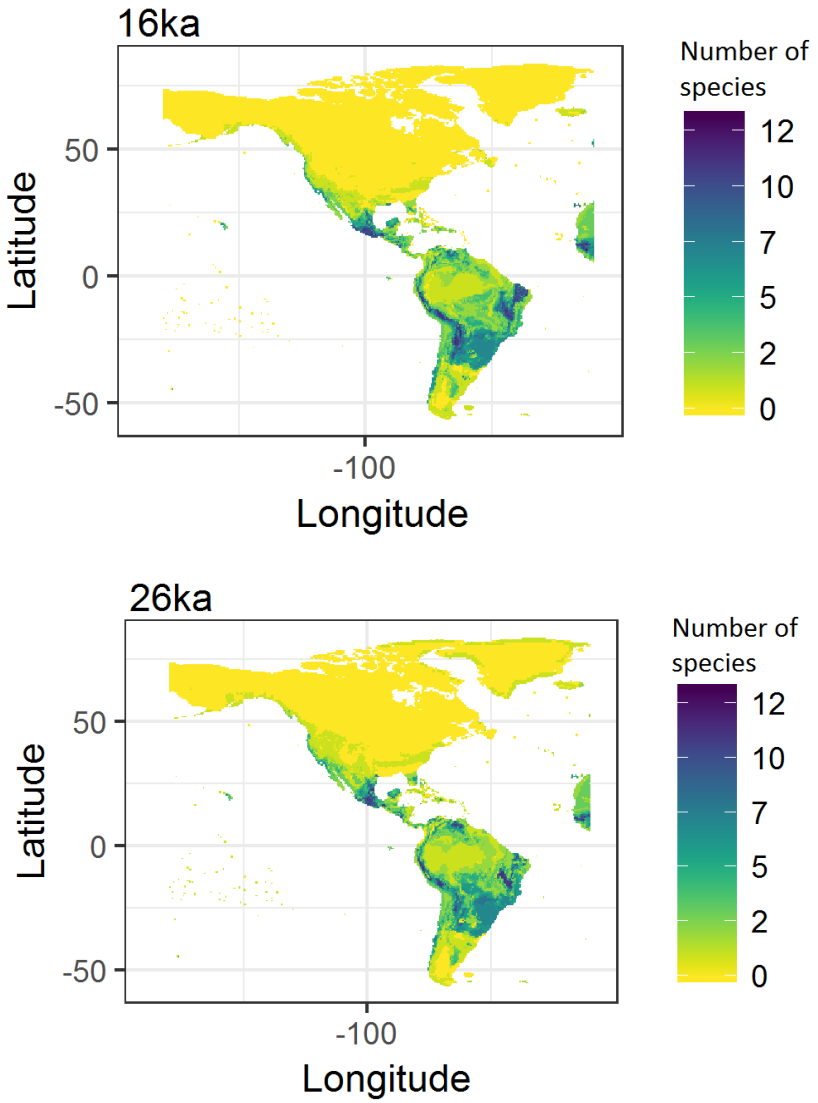

Figure 5.5.3. Projections of non-breeding-season species richness of Trochilidae for 16 ka BP (above) and 26 ka BP (below), when projected species richness was generally higher.

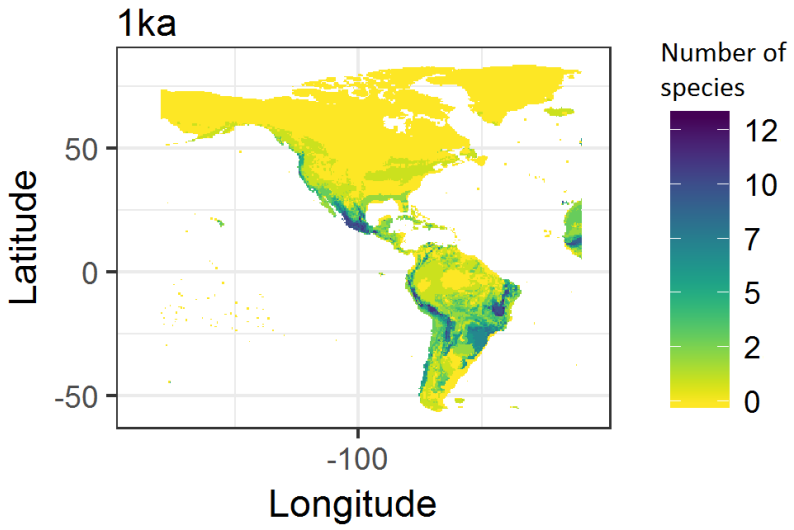

Figure 5.5.4. Projection of non-breeding-season species richness of Trochilidae for 1 ka BP, when projected species richness was generally lower.

Overall for the Trochilidae the shifts in climate between the late Pleistocene glacial and Holocene interglacial periods are projected not to have had a strong impact on species' range extents, either during the breeding or the non-breeding season. For most species the glacial period of cold and humid conditions allowed expansion of their range; only in the case of species with ranges near the tropics was an opposite effect seen during the regionally drier periods, supporting the bipolar seesaw effect as well as the AMOC alteration as discussed before with previous families. As the majority of the species are located today in Mexico, the projections during the Holocene, from 7 ka BP to 1 ka BP display a similar pattern of a declining range extent that may be the result of drier and warmer conditions in this region during the interglacial (Metcalfe et al. 2000, Acosta et al. 2018), differing from wetter and cooler conditions found in higher latitudes after 8 ka BP.

5.3.6 General species richness for all families (Charadriidae, Haematopodidae, Recurvirostridae, Scolopacidae and Trochilidae).

There are several general patterns shown across the families studied. For the Charadriidae, Haematopodidae, Recurvirostridae and Trochilidae most of the projections showed a similar tendency, with no extreme fluctuations. This allows an understanding of the history of their range extent, which seems to have been established before the LGM and that, has not been severely impacted even by the large magnitude and rapid climatic changes since that time.

For species breeding in the Arctic (most of the Scolopacidae family), their ranges were projected to be of greater extent during the Holocene, as a result of the deglaciation of the Laurentide ice sheet leading to increased land area being available at higher latitudes. In contrast, species breeding nearer to the tropics were projected to have reduced range extents during the Holocene as a result of the drier and warmer conditions of that region. Overall the non-breeding season species richness was greater than that of the breeding season, perhaps indicating a generally greater degree of climatic niche differentiation between species during the breeding season resulting in less climatic niche overlap than during the non-breeding season.

It seems that the general pattern for the families reflects the location of their breeding and non-breeding ranges. Families with most species having their current breeding range located in the Northern Hemisphere were projected to have lower species richness during the late Pleistocene, species richness increasing at the beginning of the Holocene and especially during the Altithermal. In contrast to this, families with species having current non-breeding ranges in southern areas of the Northern Hemisphere and near the tropics tended to be projected to have greater species richness during the late Pleistocene and reduced species richness during the Holocene.

Whether or not species were able to realise their past potential distributions, as determined by climatic changes alone, depends upon a number of other factors, notably whether or not suitable habitat also was available in climatically suitable areas. Palaeovegetation data and model simulations of past vegetation offer evidence that allows assessment of this in general terms. Prentice et al. (2011) simulated LGM vegetation using the Land Processes and eXchanges (LPX) dynamic global vegetation model (DGVM), driven by the results of four

GCM simulations for the LGM made as part of the second Paleoclimate Model Intercomparison Project (PMIP II). They present their results as mapped biomes and compare these with biome inferences from palaeovegetation data, showing a generally good match. They show that the tundra habitat required by many of the Shorebirds examined here was more extensive at the LGM than today, whereas the boreal forests used by others in this group were very much reduced in extent, as were the temperate forests favoured by some of the migratory Hummingbirds. Grasslands, shrublands and desert were also less extensive in North America than today in their simulations. O'ishi and Abe-Ouchi (2013) used the MIROC-LPJ coupled atmosphere–ocean–vegetation model (AOVGCM) to simulate the climate and vegetation of the LGM. Their results are broadly similar to those of Prentice et al. (2011), although they simulate somewhat greater extents of boreal forest, grassland and desert in North America. However, direct comparison is difficult, by the recognition of different biomes in the two studies, and by the mapping of large areas as 'uncertain' by Prentice et al. (2011) where results obtained from the four GCMs differed. Overall, such modelling and palaeovegetation evidence suggests that most of the bird species examined would have found suitable habitat in climatically suitable areas, at least at the LGM. Habitat availability is thus unlikely to have limited birds' ability to realise their potential past climatically-determined distributions.

5.4 Comparisons with previous studies

AUC values for the models for the majority of the species examined were above 0.950, paralleling previous studies (Huntley et al. 2007, Bagchi et al. 2013, Distler et al. 2015) and indicating generally a good model performance. Although uncertainties should be considered given that there was no cross-validation for the study.

As in previous studies, the ranges of species that are restricted to coasts, including marine species that breed on coasts as well as Shorebirds that rely principally upon coastal resources and/or habitats, cannot in most cases successfully be modelled using only variables relating to the terrestrial climate. Huntley et al. (2007) circumvented this problem by using data only from coastal grid squares when fitting models for such species, and by limiting the range projections for such species to coastal grid cells. In a study focused upon seabirds, Russell et al. (2015) also used data only from coastal grid squares, but in addition used the winter–spring (December–May) sea surface temperature for the adjacent ocean as one of the bioclimatic variables used to fit their models.

The Shorebirds' projections indicate a different behaviour from that of the Hummingbirds, with a greater susceptibility to climatic change, especially in species that breed in the Arctic regions of North America, these species' ranges decreasing in extent with warmer temperatures. Similar patterns have been observed in previous studies where the climatic variability of the Late Pleistocene is projected to have led to changes in species' distributions (Nogues-Bravo et al. 2010). Furthermore, the susceptibility of species to past climatic changes can give insight to assist in prioritising the species to protect from projected future climatic changes, according to the species' tendency to shift to new regions instead of persisting (Nogues-Bravo 2009).

It is important to mention that the susceptibility to climatic change has also been modelled for the birds of North America under future climatic conditions, with dramatic results for most species, 50% of species losing their habitat by 2080 (Distler et al. 2015, Langham et al. 2015, Schuetz et al. 2015). The hindcasts made in this study show the susceptibility that species have had to climatic changes during the last 26,000 years. This can be helpful when projecting to future climatic scenarios.

It has been stated before that species that spend the breeding season in the Northern Hemisphere are susceptible to projected future climatic changes that will result in the reduction of their habitat ((Huntley et al. 2008, Huntley et al. 2012, Huntley and Green 2012). This, however, does not mean that species that spend the breeding and/or non-breeding season in South America are not affected by climatic change.

There are several species included in the Audubon Bird's and Climate Change Report (2014) that are climatically endangered by 2080, with a threat of losing more than 30% of their current range. The hindcasting of species distribution can be useful when this type of study is presented, given that the reconstructions are made by using palaeo-climates that have a robust evidence of fossil data. A comparison with this study is made with the purpose of showing the validation of this study results. See Table 7a for the breeding season and Table 7b for the non-breeding season.

Table 7a. Qualitative comparison between the past projections of the present study and the forecast projections from the Audubon Bird Climate Change Report.

Breeding range		
Species threatened	**Current study results**	**2080 climate projection***
Piping Plover (*C. melodus*)	Suitable areas in northern NA	62% loss of range
Mountain Plover (*C. montanus*)	Suitable areas at the north-eastern USA	68% decrease on breeding grounds
Semipalmated Plover (*C. semipalmatus*)	Only suitable areas in northern NA	24% decrease in summer range
American Golden Plover (*P. dominica*)	Northern suitable areas of NA	74% decrease on summer areas
Blackish Oystercatcher (*H. ater*)	Eastern USA suitable areas only during LGM	Decrease of 31% summer
Dunlin (*C. alpina*)	Restricted suitable climate in northern NA	94% decrease of breeding grounds
Marbled Godwit (*L. fedoa*)	Expanded range during late Pleistocene in central NA only	100% loss on breeding areas
Long-billed Curlew (*N. americanus*)	Patchy suitable areas in northern Canada	99% decrease on breeding grounds
American Woodcock (*S. minor*)	Suitable areas on eastern NA during Holocene (Alti-thermal)	35% decrease of breeding areas
Wilson's Phalarope (*S. tricolor*)	No suitable areas outside its current range	100% decline on breeding range

Information taken from the Audubon Bird Climate Change Report. *NA=North America, SMO= Sierra Madre Occidental, USA=United States of America, LGM= Last Glacial Maximum.

Table 7a. Qualitative comparison between the past projections of the present study and the forecast projections from the Audubon Bird Climate Change Report (continued**).**

Breeding range		
Species threatened	**Current study results**	**2080 climate projection***
Lesser Yellowlegs (*Tringa flavipes*)	Mostly suitable areas in northern NA as current range	83% loss of summer grounds
Greater Yellowlegs (*T. melanoleuca*)	Suitable climatic areas during the LGM in central NA	97% increase on inland summer areas
Solitary Sandpiper (*T. solitaria*)	Restricted range to northern NA	93% loss of summer areas
Black-chinned Hummingbird (*Archilochus alexandri*)	Suitable areas in central and north-western Mexico	128% increase on inland summer grounds
Calliope Hummingbird (*Selasphorus calliope*)	Suitable climatic areas in central-eastern USA	17% increase of the inland breeding areas
Allen's Hummingbird (*S. sasin*)	Scarce suitable areas in central Mexico and eastern USA during late Pleistocene	90% decline of the breeding range

Information taken from the Audubon Bird Climate Change Report. *NA=North America, SMO= Sierra Madre Occidental, USA=United States of America, LGM= Last Glacial Maximum.

For the species Piping Plover when comparing with the Audubon study, they do not show an expansion on the current change after the Pleistocene, with the range maintained in central USA and with potential suitable areas in northern and central Canada. If the species is likely to lose range, our results show that it could potentially find suitable areas to the north of its current range.

The Mountain Plover past projections show a decrease on the breeding range from the Holocene until ka BP, which can potentially continue when comparing it with the Audubon study, with no alternative suitable climatic areas.

Following the past projection form species Semipalmated Plover and the American Golden Plover that display similar projections, there is potential range in central-northern USA, however this range is near the ice sheet, which can be interpreted as the species affinity to colder weathers as this changes during the Holocene with a northern breeding range. If the

temperature of Earth continues to increase it is possible that both species could lose its current range as stated in the Audubon study.

For species Blackish Oystercatcher the past projections show suitable climatic areas in eastern USA during the late Pleistocene but disappearing after the Holocene. This could be because of the specialized species coastal range.

Dunlin breeding range is only considered with both sub-species in the Audubon study, with a decreasing range when comparing with the past projections of the study, there is no meaningful suitable range across the projections, which could mean that the species is climatically threatened.

For species Marbled Godwit it seems that there are no climatically suitable areas outside its current range as it is shown in the past projections that the breeding range increased during the LGM and near the ice sheet, but was reduced after the beginning of the Holocene. A similar scenario is shown for species Long-billed Curlew.

In the past projections of the American Woodcock there is a suitable climatic area projected in eastern North America that could potentially be used by the species if climatically threatened. Wilson's Phalarope also displays a concise breeding range in the past projections that could be under threat if climatic conditions continue changing.

For both species Lesser Yellowlegs, Greater Yellowlegs, and Solitary Sandpiper, the past projections kept shifting north after the deglaciation in the late Pleistocene which can indicate that the species' suitable climate is in colder and northern regions. This can be under threat as well with the arising of temperatures.

For the Hummingbirds, species Black-chinned Hummingbird past projections show a northern growth during the beginning of the Holocene which can be interpreted as potential suitable areas for the species.

Calliope Hummingbird past projection present suitable areas in central to eastern USA, which is not found in its current breeding range. This can support the modelled projection for future conditions by the Audubon study, showing that the species could occupy suitable areas inland of North America.

As for species Allen's Hummingbird the past projections do not show suitable climatic areas outside its current breeding range, which can mean that the species is under climatic threat. This also supports the statement from the Audubon study.

Table 7b. Qualitative comparison between the past projections of the present study and the forecast projections from the Audubon Bird Climate Change Report.

Non-breeding range		
Species threatened	**Current study results**	**2080 climate projection***
Piping Plover (*C. melodus*)	No suitable areas outside current range	29% decrease on wintering grounds
Mountain Plover (*C. montanus*)	Lower suitable areas than current known range	26% inland expansion of wintering areas
Snowy Plover (*C. nivosus*)	Potential inland growth in Mexico	56% loss of wintering grounds
Semipalmated Plover (*C. semipalmatus*)	Potential inland growth in Mexico, CA and SA	43% decrease in winter
Wilson's Plover (*C. wilsonia*)	Potential growth in Mexico, CA and SA	77% loss of non-breeding areas
Grey Plover (*P. squatarola cynosurae*)	Potential growth in Mexico, CA and SA	97% inland increase on wintering grounds
Blackish Oystercatcher (*H. ater*)	Inland range during LGM in USA	Decrease of 14% for winter
American Oystercatcher (*Haematopus palliatus*)	Potential inland range in Mexico, CA and SA	34% decrease of winter grounds
American Avocet (*R. americana*)	Small inland range during LGM	Increase of 33% on winter inland expansion
Spotted Sandpiper (*A. macularius*)	No inland suitable areas outside current range	133% expansion of inland wintering grounds
Surfbird (*C. virgata*)	SMO inland suitable areas outside current range	75% loss on non-breeding areas
Short-billed Dowitcher (*Limnodromus griseus*)	Suitable areas inland of Mexico, CA and SA	34% decrease on wintering grounds
Whimbrel (*N. phaeopus*)	Suitable areas inland of Mexico, CA and SA	78% loss of wintering areas
Greater Yellowlegs (*T. melanoleuca*)	Suitable climate areas at Holocene in northern USA	11% increase on wintering areas
Willet (*T. semipalmata*)	Suitable areas inland	70% decrease on wintering areas
Rufous Hummingbird (*S. rufus*)	No potential areas outside current range	100% loss of wintering grounds

Information taken from the Audubon Bird Climate Change Report. *NA=North America, SMO= Sierra Madre Occidental, LGM= Last Glacial Maximum.

For species Piping Plover the non-breeding range projections show a consistent range that does not have other suitable climatic areas outside its known range; this of course, can be compared with the results of the Audubon study stating that the range will decrease by 2080.

In a contrasting way, species Mountain Plover shows differences from the past projections and the Audubon study, with a small and fragmented inland range in Mexico and no expansion as mentioned in the future projections from the Audubon study.

For species Snowy Plover there is are potential suitable climatic areas in the past projections, however this cannot be compared with the Audubon study as it is restricted only to North America, with the suitable areas being mostly in Mexico. A similar pattern is shown for species Semipalmated Plover and Wilson's Plover with no increase on inland areas for North America being mostly focused to southern regions.

A similar comparison between the past projections and future projections can be made with species Grey Plover, with suitable climatic areas inland in Mexico, Central and South America.

The Blackish Oystercatcher's past projections show suitable areas in eastern USA during the late Pleistocene and disappear after the beginning of the Holocene. This can be compared to the Audubon study, with a growth on inland areas of the USA that might be due to colder conditions.

For the American Oystercatcher the past projections show suitable climatic areas in Mexico, Central and South America. Even though the future projections do not show suitable climate in the USA does not mean that the species could potentially move to southern regions to find them.

The American Avocet's past projections show small suitable climatic areas during the late Pleistocene that disappears after the beginning of the Holocene. As stated by the Audubon study there is a potential growth of the range to inland areas, but this is not easily compared to the results of this study. A similar scenario is also displayed by the Spotted Sandpiper.

For species Surfbird the past projections show an inland growth mainly to the south of North America, along the Sierra Madre Occidental during the Holocene which can potentially be compared with the Audubon study results for this species, that could lose habitat along the coast but does presents suitable climate inland. A similar pattern is shown for species Short-

billed Dowitcher and Whimbrel, with suitable areas inland of Mexico, Central and South America.

Interestingly, for species Greater Yellowlegs the past projection at the beginning of the Holocene (10ka) shows the Greater Lakes from USA as suitable climatic areas. This could potentially support the information stated by the Audubon study that the species could potentially shift to that area.

For species Willet past projections with suitable climatic areas projected in Central America and South America differed from the future projections from the Audubon study. However, it is important to remember that the study is limited to North America and does not considered the whole species non-breeding range.

At last for species Rufous Hummingbird the future projections predict a loss of 100%, this is a serious statement and following the past projections from this study there are no suitable areas outside the known range; however, suitable conditions are projected for southern regions as Central and South America.

From the last paragraphs it is possible to assume that several relations can be made when comparing to the future projections of the Audubon study and, that studies such as this can potentially increase the understanding of future projections. Even when both modelling approaches have uncertainties, such as currently not having cross-validation, some patterns are shown for the more vulnerable species and this could be significant when deciding to act for conservation purposes.

The results of the present study indicate different patterns of range change in the Southern Hemisphere; this reflects the complexity of climatic history that differs between regions, and especially between the Northern and Southern Hemispheres. The direct impact of extensive continental ice sheets in the Northern Hemisphere results in substantial reductions in projected range extent for species of higher latitudes, with potential for genetic bottlenecks; this pattern is not paralleled in the Southern Hemisphere. On the other hand, the bi-polar see-saw phenomenon results in markedly differing patterns of climatic change, and hence in species' projected ranges, during the Heinrich event stadials.

CHAPTER 6 CONCLUSIONS

The objective of this study was to understand how the breeding and non-breeding areas of suitable climate for Shorebirds are Hummingbirds were influenced by the climatic variations of the last 26,000 years, a period spanning the Last Glacial Maximum, Heinrich events H2 at 24 ka BP, H1 at 17 ka BP and H0 at 13 ka BP, which corresponds to the Younger Dryas, as well as the Little Ice Age of the last millennium. This was achieved by using the CRS modelling approach, fitting models that were then used to simulate the ranges of 64 species from the five families studied for 28-time slices from 26 ka BP to 1 ka BP and including the current range.

Using the values of AUC, TSS and Kappa the overall CRS model accuracy was assessed as excellent, which indicates that the projected ranges for Shorebirds and Hummingbirds present a good representation of the areas of suitable climate, however importance must be considered to the fact that no cross-validation was done in the study, but an attempt to reduce over-projections was made when selecting the variables to use in the CRS model as shown by previous studies (Huntley et al. 2007). In the case of species with ranges restricted to coasts, however, there was systematic projection of inland areas of potential range, reflecting the models' limitations that result from the inclusion only of climatic variables.

The results of the study indicate that the Shorebirds that breed in Arctic areas of North America could have been more susceptible to past climatic variability, with the potential for a population bottleneck when species' suitable ranges were most restricted in extent during the glacial. Deglaciation permitted these species to expand their distribution in northern regions, at the same time disappearing from more southern areas of North America potentially occupied during the glacial. However, for species that breed and spend the non-breeding season in South America, the pattern is different, with a more 'stable' projected range than for species in North America. This reflects the different climatic history in the Southern Hemisphere, including a lack of extensive continental ice sheets and relative warming at higher latitudes during Heinrich events associated with the bi-polar see-saw phenomenon.

The Hummingbirds also presented differences from the Shorebirds, with a continuous pattern during the glacial periods and increases during the deglaciation and the Alti-thermal of the Holocene. There was also projected climatic suitability in South America, although the species examined have a distribution restricted to North and/or Central America. This reflects

the combination of biogeographical or other barriers preventing these species from colonising climatically suitable areas of South America, and the use of data only from the species' range and surrounding regions when fitting the models. Similar problems are illustrated by a circumpolar range projection for White-tailed Ptarmigan (*Lagopus leucura*) made using a model fitted to this North American species' global range, in the study projections were made far from the known current range of the species, which led to a restriction on the analysis of this species (Huntley and Green 2012).

For the Heinrich events, projections in North America are similar to those for the corresponding 'normal' time slices, especially for the Shorebirds; however, the projections in South America for the Heinrich events are different with more extensive suitable areas often projected in several regions. This reflects the complex geographical patterns of climatic changes associated with Heinrich events.

Overall many species' projected ranges in the Northern Hemisphere have decreased considerably in extent since the LGM and the deglaciation of the Late Pleistocene. It was also during the Holocene Alti-thermal that most species shaped their range to a similar pattern as their current known range. Also, most of the birds had an increase at ka BP, indicating the Little Ice Age.

As shown in studies with future projections, the current ranges are decreasing, however, with the past projections, there is an analytical factor, where the response to climate change can be observed, inferring with colder conditions a glacial bottleneck might occur, and with warmer conditions the species tend to restrict their range to northern regions.

It is also important to consider several modelling approaches as well as several variables, to not have a limited performance for the species with coastal regions, and over-projected in inland regions where the species cannot occur.

On the sub-species level, as a recommendation I would consider projecting the species range from the Early Pleistocene, to also have an indicator of where the species divided their range and to understand the role of the glacial and inter-glacial periods.

REFERENCES

Acosta, G., L. E. Beramendi, G. Gonzalez, I. Rivera, I. Eudave, E. Hernandez, S. Sanchez, P. Morales, E. Cienfuegos, and F. Otero. 2018. Climate change and peopling of the Neotropics during the Pleistocene-Holocene transition. Boletin De La Sociedad Geologica Mexicana **70**:1-19.

Adams, J., M. Maslin, and E. Thomas. 1999. Sudden climate transitions during the Quaternary. Progress in Physical Geography **23**:1-36.

Adams, J. M. 1996. Towards a better vegetation scheme for global mapping and monitoring. Global Ecology and Biogeography Letters **5**:3-6.

Allen, J. R. M., T. Hickler, J. S. Singarayer, M. T. Sykes, P. J. Valdes, and B. Huntley. 2010. Last glacial vegetation of northern Eurasia. Quaternary Science Reviews **29**:2604-2618.

Allouche, O., A. Tsoar, and R. Kadmon. 2006. Assessing the accuracy of species distribution models: prevalence, kappa and the true skill statistic (TSS). Journal of Applied Ecology **43**:1223-1232.

Alvarado-Serrano, D. F. and L. L. Knowles. 2014. Ecological niche models in phylogeographic studies: applications, advances and precautions. Molecular Ecology Resources **14**:233-248.

Anisimov, O. A., D. G. Vaughan, T. V. Callaghan, C. Furgal, H. Marchant, T. D. Prowse, V. H., and W. J. E. 2007. Polar regions (Arctic and Antarctic). Pages 653-685 *in* O. F. C. M.L. Parry, J.P. Palutikof, P.J. van der Linden and C.E. and Hanson, editors. Climate Change 2007: Impacts, Adaptation and Vulnerability. Contribution of Working Group II to the Fourth Assessment Report of the Intergovernmental Panel on Climate change. Cambridge University Press, Cambridge.

Araujo, M. B., R. G. Pearson, W. Thuiller, and M. Erhard. 2005. Validation of species-climate impact models under climate change. Global Change Biology **11**:1504-1513.

Arizmendi, M. C. and H. Berlanga. 2014. Colibríes de México y Norteamérica. Hummingbirds of Mexico and North America. CONABIO, Mexico city.

Bagchi, R., M. Crosby, B. Huntley, D. G. Hole, S. H. M. Butchart, Y. Collingham, M. Kalra, J. Rajkumar, A. Rahmani, M. Pandey, H. Gurung, L. T. Trai, N. V. Quang, and S. G. Willis. 2013. Evaluating the effectiveness of conservation site networks under climate change: accounting for uncertainty. Global Change Biology **19**:1236-1248.

Baker, D. J., A. J. Hartley, N. D. Burgess, S. H. M. Butchart, J. A. Carr, R. J. Smith, E. Belle, and S. G. Willis. 2015. Assessing climate change impacts for vertebrate fauna across the West African protected area network using regionally appropriate climate projections. Diversity and Distributions **21**:991-1003.

Baker, D. J., A. J. Hartley, S. H. M. Butchart, and S. G. Willis. 2016. Choice of baseline climate data impacts projected species' responses to climate change. Global Change Biology **22**:2392-2404.

Barnsley, M. J. 2007. Environmental Modeling: A Practical Introduction. Taylor & Francis.

Bartlein, P. J. 1997. Past environmental changes: Characteristic features of quaternary climate variations. Pages 11-29 *in* B. Huntley, W. Cramer, A. V. Morgan, H. C. Prentice, and J. R. M. Allen, editors. Past and Future Rapid Environmental Changes: The Spatial and Evolutionary Responses of Terrestrial Biota. Springer-Verlag Berlin, Berlin.

Bartlein, P. J., S. W. Hostetler, and J. R. Alder. 2014. Paleoclimate. Springer Int Publishing Ag, Cham.

Bartlein, P. J. and I. C. Prentice. 1989. Orbital variations, Climate and Paleoecology. Trends in Ecology & Evolution **4**:195-199.

Beaman, M. and S. Madge. 1998. The handbook of bird identification for Europe and the Western Palearctic.

Beerling, D. J., B. Huntley, and J. P. Bailey. 1995. Climate and the distribuion of *Fallopia japonica*: use of an introduced species to test the predictive capacity of response surfaces. Journal of Vegetation Science **6**:269-282.

Betancourt, J. L., T. R. Van Devender, and P. S. Martiin. 1990. Packrat Middens: The last 4000 years of biotic change.

Bond, G., B. Kromer, J. Beer, R. Muscheler, M. N. Evans, W. Showers, S. Hoffmann, R. Lotti-Bond, I. Hajdas, and G. Bonani. 2001. Persistent solar influence on north Atlantic climate during the Holocene. Science **294**:2130-2136.

Bond, G., W. Showers, M. Cheseby, R. Lotti, P. Almasi, P. deMenocal, P. Priore, H. Cullen, I. Hajdas, and G. Bonani. 1997. A pervasive millennial-scale cycle in North Atlantic Holocene and glacial climates. Science **278**:1257-1266.

Booth, T. H., H. A. Nix, J. R. Busby, and M. F. Hutchinson. 2014. BIOCLIM: the first species distribution modelling package, its early applications and relevance to most current MAXENT studies. Diversity and Distributions **20**:1-9.

Borzenkova, I., E. Zorita, O. Borisova, L. Kalniņa, D. Kisielienė, T. Koff, D. Kuznetsov, G. Lemdahl, T. Sapelko, M. Stančikaitė, and D. Subetto. 2015. Climate Change During the Holocene (Past 12,000 Years). Pages 25-49 *in* B. I. I. A. T. The, editor. Second Assessment of Climate Change for the Baltic Sea Basin. Springer International Publishing, Cham.

Bradbury, J. P. 1989. Late Quaternary lacustrine paleoenvironments in the Cuenca de Mexico. Quaternary Science Reviews **8**:75-100.

Bradley, R. S. 2011. High-Resolution Paleoclimatology. Pages 3-15 *in* M. K. Hughes, T. W. Swetnam, and H. F. Diaz, editors. Dendroclimatology: Progress and Prospects.

Bradley, R. S. 2014. Paleoclimatology: Reconstructing Climates of the Quaternary. 3rd edition. edition. Academic Press, Amherst.

Brambilla, M. and G. F. Ficetola. 2012. Species distribution models as a tool to estimate reproductive parameters: a case study with a passerine bird species. Journal of Animal Ecology **81**:781-787.

Broecker, W. S. 2001. Paleoclimate - Was the medieval warm period global? Science **291**:1497-1499.

Broecker, W. S., G. H. Denton, R. L. Edwards, H. Cheng, R. B. Alley, and A. E. Putnam. 2010. Putting the Younger Dryas cold event into context. Quaternary Science Reviews **29**:1078-1081.

Broecker, W. S., J. P. Kennett, B. P. Flower, J. T. Teller, S. Trumbore, G. Bonani, and W. Wolfli. 1989. Routing of meltwater from the Laurentide Ice Sheet during the Younger Dryas cold episode. Nature **341**:318-321.

Brunelle, A., T. A. Minckley, S. Blissett, S. K. Cobabe, and B. L. Guzman. 2010. A nearly 8000 year fire history from an Arizona/Sonora borderland cienega. Journal of Arid Environments **74**:475-481.

Carlson, A. E. 2013. Paleoclimate | The Younger Dryas Climate Event A2 - Elias, Scott A. Pages 126-134 *in* C. J. Mock, editor. Encyclopedia of Quaternary Science (Second Edition). Elsevier, Amsterdam.

Clapperton, C. M. 1993. Nature of environmental changes in South America at the Last Glacial Maximum. Palaeogeography Palaeoclimatology Palaeoecology **101**:189-208.

Clark, J. S. 2007. Models for ecological data: an introduction.

Clark, P. U. and P. J. Bartlein. 1995. Correlation of Late Pleistocene glaciation in the western United States with North Atlantic Heinrich events. Geology **23**:483-486.

Clark, P. U., A. S. Dyke, J. D. Shakun, A. E. Carlson, J. Clark, B. Wohlfarth, J. X. Mitrovica, S. W. Hostetler, and A. M. McCabe. 2009. The Last Glacial Maximum. Science **325**:710-714.

Clark, P. U. and A. C. Mix. 2002. Ice sheets and sea level of the Last Glacial Maximum. Quaternary Science Reviews **21**:1-7.

Clark, P. U., J. D. Shakun, P. A. Baker, P. J. Bartlein, S. Brewer, E. Brook, A. E. Carlson, H. Cheng, D. S. Kaufman, Z. Y. Liu, T. M. Marchitto, A. C. Mix, C. Morrill, B. L. Otto-Bliesner, K. Pahnke, J. M. Russell, C. Whitlock, J. F. Adkins, J. L. Blois, J. Clark, S. M. Colman, W. B. Curry, B. P. Flower, F. He, T. C. Johnson, J. Lynch-Stieglitz, V. Markgraf, J. McManus, J. X. Mitrovica, P. I. Moreno, and J. W. Williams. 2012. Global climate evolution during the last deglaciation. Proceedings of the National Academy of Sciences of the United States of America **109**:E1134-E1142.

Cohen, J. 1960. A Coefficient of Agreement for Nominal Scales. Educational and Psychological Measurement **20**:37-46.

Coltrinari, L. 1993. Global Quaternary changes in South America. Global and Planetary Change **7**:11-23.

Coronato, A. and J. Rabassa. 2011. Pleistocene Glaciations in Southern Patagonia and Tierra del Fuego. Pages 715-727 *in* J. Ehlers, P. L. Gibbard, and P. D. Hughes, editors. Quaternary Glaciations - Extent and Chronology: A Closer Look.

Correa-Metrio, A., M. B. Bush, K. R. Cabrera, S. Sully, M. Brenner, D. A. Hodell, J. Escobar, and T. Guilderson. 2012. Rapid climate change and no-analog vegetation in lowland Central America during the last 86,000 years. Quaternary Science Reviews **38**:63-75.

Cowardin, L. M., V. Carter, F. C. Golet, and E. T. LaRoe. 1992. Classification of wetlands and deepwater habitats of the United States., Department of the Interior., Washington.

Cox, G. W. 2010. Bird Migration and Global Change. Island Press.

Davis, M. B. and R. G. Shaw. 2001. Range shifts and adaptive responses to Quaternary climate change. Science **292**:673-679.

Davis, O. K. and D. S. Shafer. 1992. A Holocene climatic record for the Sonoran desert from pollen analysis of Montezuma well, Arizona, USA. Palaeogeography Palaeoclimatology Palaeoecology **92**:107-119.

Delcourt, H. R. and P. A. Delcourt. 1988. Quaternary landscape ecology: Relevant scales in space and time. Landscape Ecology **2**:23-44.

Dingle, H. 1996. Migration: the biology of life on the move.

Distler, T., J. G. Schuetz, J. Velasquez-Tibata, and G. M. Langham. 2015. Stacked species distribution models and macroecological models provide congruent projections of avian species richness under climate change. Journal of Biogeography **42**:976-988.

Elith, J., C. H. Graham, R. P. Anderson, M. Dudík, S. Ferrier, A. Guisan, R. J. Hijmans, F. Huettmann, J. R. Leathwick, A. Lehmann, J. Li, L. G. Lohmann, B. A. Loiselle, G. Manion, C. Moritz, M. Nakamura, Y. Nakazawa, J. M. M. Overton, A. T. Peterson, S. J. Phillips, K. Richardson, R. Scachetti-Pereira, R. E. Schapire, J. Soberón, S. Williams, M. S. Wisz, and N. E. Zimmermann. 2006. Novel methods improve prediction of species' distributions from occurrence data. Ecography **29**:129-151.

Elith, J. and J. R. Leathwick. 2009. Species Distribution Models: Ecological Explanation and Prediction Across Space and Time. Pages 677-697 Annual Review of Ecology Evolution and Systematics.

Farner, D. S., J. R. King, and K. C. Parkes. 1985. Avian Biology Vol. VIII.

Farrera, I., S. P. Harrison, I. C. Prentice, G. Ramstein, J. Guiot, P. J. Bartlein, R. Bonnefille, M. Bush, W. Cramer, U. von Grafenstein, K. Holmgren, H. Hooghiemstra, G. Hope, D. Jolly, S.-E. Lauritzen, Y. Ono, S. Pinot, M. Stute, and G. Yu. 1999. Tropical climates at the Last Glacial Maximum: a new synthesis of terrestrial palaeoclimate data. I. Vegetation, lake-levels and geochemistry. Climate Dynamics **15**:823-856.

Floyd, T. 2008. Smithsonian Field Guide to the Birds of North America. HarperCollins.

Fritz, S. C., S. E. Metcalfe, and W. Dean. 2001. Chapter 15 - Holocene Climate Patterns in the Americas Inferred from Paleolimnological Records A2 - Markgraf, Vera. Pages 241-263 Interhemispheric Climate Linkages. Academic Press, San Diego.

Gill, F. and D. Donsker. 2018. IOC World Bird List (v8.2).

Graham, C. H., S. R. Ron, J. C. Santos, C. J. Schneider, C. Moritz, and C. Cunningham. 2004. Integrating Phylogenetics and Environmental Niche Models to explore speciation mechanisms in Dendrobatid Frogs. Evolution **58**:1781-1793.

Graham, R. W. and E. C. Grimm. 1990. Effects of global climate change in the patterns of terrestrial biological communities. Trends in Ecology & Evolution **5**:289-292.

Grayson, D. K. 1991. Late Pleistocene mammalian extinctions in North America: Taxonomy, chronology, and explanations. Journal of World Prehistory **5**:193-231.

Green, R. E., Y. C. Collingham, S. G. Willis, R. D. Gregory, K. W. Smith, and B. Huntley. 2008. Performance of climate envelope models in retrodicting recent changes in bird population size from observed climatic change. Biology Letters **4**:599-602.

Grove, J. M. and R. Switsur. 1994. Glacial geological evidence for the Medieval Warm Period. Climatic Change **26**:143-169.

Guisan, A., T. C. Edwards, and T. Hastie. 2002. Generalized linear and generalized additive models in studies of species distributions: setting the scene. Ecological Modelling **157**:89-100.

Guisan, A. and W. Thuiller. 2005. Predicting species distribution: offering more than simple habitat models. Ecology Letters **8**:993-1009.

Gurgel Costa, M. d. S., R. d. C. Batista, and R. Gurgel-Goncalves. 2014. Predicting geographic distributions of Phacellodomus species (Aves: Furnariidae) in South America based on ecological niche modeling. Acta Scientiarum Biological Sciences **36**:299-306.

Handiani, D., A. Paul, and L. Dupont. 2012. Tropical climate and vegetation changes during Heinrich Event 1: a model-data comparison. Climate of the Past **8**:37-57.

Hannes, G. 1998. Climate, history and the modern world, 2nd ed. Professional Geographer **50**:276-276.

Hawkins, B. A. and E. E. Porter. 2003. Relative influences of current and historical factors on mammal and bird diversity patterns in deglaciated North America. Global Ecology and Biogeography **12**:475-481.

Hayman, P., J. Marchant, T. Prater, and R. T. Peterson. 1991. Shorebirds: An Identification Guide to the Waders of the World. Houghton Mifflin.

Hays, J. D., J. Imbrie, and N. J. Shackleton. 1976. Variations in earth's orbit - pacemaker of Ice Ages. Science **194**:1121-1132.

Heinrich, H. 1988. Origin and consequences of cycling ice rafting in the Northeast Atlantic ocean during the past 130,000 years. Quaternary Research **29**:142-152.

Hemming, S. R. 2004. Heinrich events: Massive late pleistocene detritus layers of the North Atlantic and their global climate imprint. Reviews of Geophysics **42**.

Hendrickson, D. and W. L. Minckley. 1985. Ciénegas - Vanishing Climax Communities of the American Southwest.

Hobbs, R. J., E. Higgs, and J. A. Harris. 2009. Novel ecosystems: implications for conservation and restoration. Trends in Ecology & Evolution **24**:599-605.

Hockey, P., C. J. Sharpe, and A. Bonan. 2018. Oystercatchers (Haematopodidae).*in* J. del Hoyo, A. Elliott, J. Sargatal, D. A. Christie, and E. de Juana, editors. Handbook of the Birds of the World Alive. Lynx Edicions, Barcelona.

Hodell, D. A., J. H. Curtis, and M. Brenner. 1995. Possible role of climate in the collapse of Classic Maya civilization. Nature **375**:391.

Hostetler, S. W., P. U. Clark, P. J. Bartlein, A. C. Mix, and N. J. Pisias. 1999. Atmospheric transmission of North Atlantic Heinrich events. Journal of Geophysical Research-Atmospheres **104**:3947-3952.

Hughes, L. 2000. Biological consequences of global warming: is the signal already apparent? Trends in Ecology & Evolution **15**:56-61.

Hughes, M. K. and H. F. Diaz. 1994. Was there a Medieval Warm Period, and if so, where and when? Climatic Change **26**:109-142.

Huntley, B., J. R. M. Allen, Y. C. Collingham, T. Hickler, A. M. Lister, J. Singarayer, A. J. Stuart, M. T. Sykes, and P. J. Valdes. 2013. Millennial Climatic Fluctuations Are Key to the Structure of Last Glacial Ecosystems. Plos One **8**.

Huntley, B., R. Altwegg, P. Barnard, Y. C. Collingham, and D. G. Hole. 2012. Modelling relationships between species spatial abundance patterns and climate. Global Ecology and Biogeography **21**:668-681.

Huntley, B., Y. C. Collingham, S. G. Willis, and R. E. Green. 2008. Potential Impacts of Climatic Change on European Breeding Birds. Plos One **3**.

Huntley, B. and R. E. Green. 2012. Bioclimatic models of the distributions of Gyrfalcons and ptarmigan.

Huntley, B., R. E. Green, Y. C. Collingham, J. K. Hill, S. G. Willis, P. J. Bartlein, W. Cramer, W. J. M. Hagemeijer, and C. J. Thomas. 2004. The performance of models relating species geographical distributions to climate is independent of trophic level. Ecology Letters **7**:417-426.

Huntley, B., R. E. Green, Y. C. Collingham, and S. G. Willis. 2007. A climatic atlas of European breeding birds.

Huntley, B., G. F. Midgley, P. Barnard, and P. J. Valdes. 2014. Suborbital climatic variability and centres of biological diversity in the Cape region of southern Africa. Journal of Biogeography **41**:1338-1351.

Huntley, B. and T. Webb. 1989. Migration: Species' response to climatic variations caused by changes in the earth's orbit. Journal of Biogeography **16**:5-19.

Jongsomjit, D., D. Stralberg, T. Gardali, L. Salas, and J. Wiens. 2013. Between a rock and a hard place: the impacts of climate change and housing development on breeding birds in California. Landscape Ecology **28**:187-200.

Kaufman, K., R. Bowers, and N. Bowers. 2005. Kaufman Field Guide to Birds of North America. Houghton Mifflin.

Labeyrie, L., L. Skinner, and E. Cortijo. 2007. Paleoclimate reconstruction | Sub-Milankovitch (DO/Heinrich) Events A2 - Elias, Scott A. Pages 1964-1974 Encyclopedia of Quaternary Science. Elsevier, Oxford.

Lambeck, K., Y. Yokoyama, P. Johnston, and A. Purcell. 2000. Global ice volumes at the Last Glacial Maximum and early Lateglacial. Earth and Planetary Science Letters **181**:513-527.

Langham, G. M., J. G. Schuetz, T. Distler, C. U. Soykan, and C. Wilsey. 2015. Conservation Status of North American Birds in the Face of Future Climate Change. Plos One **10**.

Liu, C., M. White, and G. Newell. 2013. Selecting thresholds for the prediction of species occurrence with presence-only data. Journal of Biogeography **40**:778-789.

Liu, C. R., P. M. Berry, T. P. Dawson, and R. G. Pearson. 2005. Selecting thresholds of occurrence in the prediction of species distributions. Ecography **28**:385-393.

Loiselle, B. A., C. A. Howell, C. H. Graham, J. M. Goerck, T. Brooks, K. G. Smith, and P. H. Williams. 2003. Avoiding pitfalls of using species distribution models in conservation planning. Conservation Biology **17**:1591-1600.

Lowe, J. and M. Walker. 2015. Reconstructing Quaternary Environments, 3rd Edition. Routledge, Abingdon.

MacDonald, G. M., K. D. Bennett, S. T. Jackson, L. Parducci, F. A. Smith, J. P. Smol, and K. J. Willis. 2008. Impacts of climate change on species, populations and communities: palaeobiogeographical insights and frontiers. Progress in Physical Geography **32**:139-172.

Mann, M. E. 2007. Paleoclimate Reconstruction | The Last Millennium A2 - Elias, Scott A. Pages 1993-2002 Encyclopedia of Quaternary Science. Elsevier, Oxford.

Marchant, J., P. Hayman, and T. Prater. 2010. Shorebirds. Bloomsbury Publishing.

Marchant, R., A. Cleef, S. P. Harrison, H. Hooghiemstra, V. Markgraf, J. van Boxel, T. Ager, L. Almeida, R. Anderson, C. Baied, H. Behling, J. C. Berrio, R. Burbridge, S. Bjorck, R. Byrne, M. Bush, J. Duivenvoorden, J. Flenley, P. De Oliveira, B. van Geel, K. Graf, W. D. Gosling, S. Harbele, T. van der Hammen, B. Hansen, S. Horn, P. Kuhry, M. P. Ledru, F. Mayle, B. Leyden, S. Lozano-Garcia, A. M. Melief, P. Moreno, N. T. Moar, A. Prieto, G. van Reenen, M. Salgado-Labouriau, F. Schabitz, E. J. Schreve-Brinkman, and M. Wille. 2009. Pollen-based biome reconstructions for Latin America at 0, 6000 and 18 000 radiocarbon years ago. Climate of the Past **5**:725-767.

Markgraf, V. 1993. Climatic history of central and South America since 18,000 yr B.P.: Comparison of pollen records and model simulations. University of Minnesota Press, 2037 University Ave. S. E., Minneapolis, Minnesota 55455, USA; University of Minnesota Press, London, England.

Marshall, J. and R. A. Plumb. 2008. Atmosphere, Ocean, and Climate Dynamics: An introductory text. Elsevier Academic Press, Cambridge, Massachusetts.

Martin, P. S. 2005. Twilight of the mammoths: ice age extinctions and the rewilding of America. University of California Press.

Martin, P. S. and P. J. Mehringer. 1966. Pleistocene pollen analysis and biogeography of the southwest. Princeton Univ. Press, Princeton, New Jersey,1965433-451, 6 figs.

Mayewski, P. A., E. E. Rohling, J. Curt Stager, W. Karlén, K. A. Maasch, L. David Meeker, E. A. Meyerson, F. Gasse, S. van Kreveld, K. Holmgren, J. Lee-Thorp, G. Rosqvist, F. Rack, M. Staubwasser, R. R. Schneider, and E. J. Steig. 2004. Holocene climate variability. Quaternary Research **62**:243-255.

McManus, J. F., R. Francois, J. M. Gherardi, L. D. Keigwin, and S. Brown-Leger. 2004. Collapse and rapid resumption of Atlantic meridional circulation linked to deglacial climate changes. Nature **428**:834.

Message, S. and D. W. Taylor. 2016. Waders of Europe, Asia and North America. Bloomsbury Publishing.

Metcalfe, S. E., S. L. O'Hara, M. Caballero, and S. J. Davies. 2000. Records of Late Pleistocene–Holocene climatic change in Mexico — a review. Quaternary Science Reviews **19**:699-721.

Meyer, E. R. 1973. Late-Quaternary paleoecology of Cuatro Ciénegas Basin, Coahuila, Mexico. Ecology **54**:983-995.

Moreno-Torres, J. G., J. A. Saez, and F. Herrera. 2012. Study on the Impact of Partition-Induced Dataset Shift on k-fold Cross-Validation. Ieee Transactions on Neural Networks and Learning Systems **23**:1304-1312.

Myers, J. P. 1983. Conservation of migrating shorebirds: staging areas, geographic bottlenecks, and regional movements. American Birds **37**:23-25.

Newton, I. 2003. The speciation and biogeography of birds.

Newton, I. 2007. Population limitation in birds: the last 100 years. British Birds **100**:518-539.

Nogues-Bravo, D. 2009. Predicting the past distribution of species climatic niches. Global Ecology and Biogeography **18**:521-531.

Nogues-Bravo, D., R. Ohlemuller, P. Batra, and M. B. Araujo. 2010. Climate predictors of late Quaternary extinctions. Evolution **64**:2442-2449.

O'Ishi, R. and A. Abe-Ouchi. 2013. Influence of dynamic vegetation on climate change and terrestrial carbon storage in the Last Glacial Maximum. Climate of the Past **9**:1571-1587.

Pearson, R. G., C. J. Raxworthy, M. Nakamura, and A. T. Peterson. 2007. Predicting species distributions from small numbers of occurrence records: a test case using cryptic geckos in Madagascar. Journal of Biogeography **34**:102-117.

Pearson, R. G., W. Thuiller, M. B. Araujo, E. Martinez-Meyer, L. Brotons, C. McClean, L. Miles, P. Segurado, T. P. Dawson, and D. C. Lees. 2006. Model-based uncertainty in species range prediction. Journal of Biogeography **33**:1704-1711.

Peterson, R. T. 1960. A Field Guide to the Birds of Texas: And Adjacent States. Texas Game and Fish Commission.

Peterson, R. T. and E. L. Chalif. 1999. A Field Guide to Mexican Birds: Mexico, Guatemala, Belize, El Salvador. Houghton Mifflin.

Pierce, R. J. and A. Bonan. 2016. Avocets, Stilts (Recurvirostridae).*in* E. A. In: del Hoyo J., Sargatal J., Christie D.A. & de Juana E. (eds.). editor. Handbook of the Birds of the World Alive. Lynx Edicions, Barcelona.

Piersma, T. and A. Bonan. 2018. Plover (*Charadriidae).in* J. del Hoyo, A. Elliot, J. Sargatal, D. A. Christie, and E. de Juana, editors. Handbook of the Birds of the World Alive. Lynx Edicions, Barcelona.

Prentice, I. C., P. J. Bartlein, and T. Webb. 1991. Vegetation and climate change in eastern North-America since the Last Glacial Maximum. Ecology **72**:2038-2056.

Prentice, I. C., W. Cramer, S. P. Harrison, R. Leemans, R. A. Monserud, and A. M. Solomon. 1992. A global biome model base on plant physiology and dominance, soil properties and climate. Journal of Biogeography **19**:117-134.

Prentice, I. C., S. P. Harrison, and P. J. Bartlein. 2011. Global vegetation and terrestrial carbon cycle changes after the last ice age. New Phytologist **189**:988-998.

Prentice, I. C. and T. Webb. 1998. BIOME 6000: reconstructing global mid-Holocene vegetation patterns from palaeoecological records. Journal of Biogeography **25**:997-1005.

Reeder, L. A., J. M. Erlandson, and T. C. Rick. 2011. Younger Dryas environments and human adaptations on the West Coast of the United States and Baja California. Quaternary International **242**:463-478.

Ruben, J. 2010. Paleobiology and the origins of avian flight. Proceedings of the National Academy of Sciences of the United States of America **107**:2723-2734.

Russell, D. J. F., S. Wanless, Y. C. Collingham, B. Huntley, and K. C. Hamer. 2015. Predicting Future European Breeding Distributions of British Seabird Species under Climate Change and Unlimited/ No Dispersal Scenarios. Diversity-Basel **7**:342-359.

Rutter, N., A. Coronato, K. Helmens, J. Rabassa, and M. Zárate. 2012. The Glacial and Loess Record of Southern South America. Pages 1-23 Glaciations in North and South America from the Miocene to the Last Glacial Maximum: Comparisons, Linkages and Uncertainties. Springer Netherlands, Dordrecht.

Samaniego-Herrera, A., A. Peralta-García, J. Valdez-Villavicencio, and L. Luna-Mendoza. 2007. Vertebrados de las islas del Pacífico de Baja California. Guía de campo.

Schuchmann, K. L. and A. Bonan. 2016. Hummingbirds (Trochilidae).*in* del Hoyo J., Elliott A., Sargatal J., C. D.A., and d. J. E., editors. Handbook of the Birds of the World Alive. . Lynx Edicions, Barcelona.

Schuetz, J. G., G. M. Langham, C. U. Soykan, C. B. Wilsey, T. Auer, and C. C. Sanchez. 2015. Making spatial prioritizations robust to climate change uncertainties: a case study with North American birds. Ecological Applications **25**:1819-1831.

Shakun, J. D. and A. E. Carlson. 2010. A global perspective on Last Glacial Maximum to Holocene climate change. Quaternary Science Reviews **29**:1801-1816.

Sibley, D. A. 2014. The Sibley guide to birds. Second edition edition. Alfred A. Knopf, New York.

Sinclair, S. J., M. D. White, and G. R. Newell. 2010. How Useful Are Species Distribution Models for Managing Biodiversity under Future Climates? Ecology and Society **15**.

Singarayer, J. S. and T. Davies-Barnard. 2012. Regional climate change mitigation with crops: context and assessment. Philosophical Transactions of the Royal Society a-Mathematical Physical and Engineering Sciences **370**:4301-4316.

Singarayer, J. S. and P. J. Valdes. 2010. High-latitude climate sensitivity to ice-sheet forcing over the last 120 kyr. Quaternary Science Reviews **29**:43-55.

Stocker, T. F. 1998. The Seesaw Effect. Science **282**:61-62.

Stralberg, D., S. M. Matsuoka, A. Hamann, E. M. Bayne, P. Solymos, F. K. A. Schmiegelow, X. Wang, S. G. Cumming, and S. J. Song. 2015. Projecting boreal bird responses to climate change: the signal exceeds the noise. Ecological Applications **25**:52-69.

Straus, L. and T. Goebel. 2011. Humans and Younger Dryas: Dead end, short detour, or open road to the Holocene? Quaternary International **242**:259-261.

Svenning, J. C., C. Flojgaard, K. A. Marske, D. Nogues-Bravo, and S. Normand. 2011. Applications of species distribution modeling to paleobiology. Quaternary Science Reviews **30**:2930-2947.

Sylvestre, F. 2009. Moisture Pattern During the Last Glacial Maximum in South America. Pages 3-27 *in* F. Vimeux, F. Sylvestre, and M. Khodri, editors. Past Climate Variability in South America and Surrounding Regions: From the Last Glacial Maximum to the Holocene. Springer, Dordrecht.

Teller, J. T., D. W. Leverington, and J. D. Mann. 2002. Freshwater outbursts to the oceans from glacial Lake Agassiz and their role in climate change during the last deglaciation. Quaternary Science Reviews **21**:879-887.

Thomas, C. D., A. Cameron, R. E. Green, M. Bakkenes, L. J. Beaumont, Y. C. Collingham, B. F. N. Erasmus, M. F. de Siqueira, A. Grainger, L. Hannah, L. Hughes, B. Huntley, A. S. van Jaarsveld, G. F. Midgley, L. Miles, M. A. Ortega-Huerta, A. T. Peterson, O. L. Phillips, and S. E. Williams. 2004. Extinction risk from climate change. Nature **427**:145-148.

Thuiller, W. 2003. BIOMOD - optimizing predictions of species distributions and projecting potential future shifts under global change. Global Change Biology **9**:1353-1362.

Thuiller, W., S. Pironon, A. Psomas, M. Barbet-Massin, F. Jiguet, S. Lavergne, P. B. Pearman, J. Renaud, L. Zupan, and N. E. Zimmermann. 2014. The European functional tree of bird life in the face of global change. Nature Communications **5**.

Uriarte-Cantolla, A. 2003. Historia del clima de la Tierra. Editorial Gobierno Vasco, España.
Van Gils, J., P. Wiersma, and G. M. Kirwan. 2018a. Long-billed Dowitcher (*Limnodromus scolopaceus*).*in* J. del Hoyo, A. Elliott, J. Sargatal, D. A. Christie, and E. de Juana, editors. Handbook of the Birds of the World Alive. Lynx Edicions, Barcelona.
Van Gils, J., P. Wiersma, and G. M. Kirwan. 2018b. Surfbird (*Calidris virgata*).*in* J. del Hoyo, A. Elliott, J. Sargatal, D. A. Christie, and E. de Juana, editors. Handbook of the Birds of the World Alive. Linx Edicions, Barcelona.
van Ommen, T. 2015. Northern push for the bipolar see-saw. Nature **520**:630.
Virkkala, R. and A. Lehikoinen. 2017. Birds on the move in the face of climate change: High species turnover in northern Europe. Ecology and Evolution **7**:8201-8209.
Wang, J., L. Sun, L. Chen, L. Xu, Y. Wang, and X. Wang. 2016. The abrupt climate change near 4,400 yr BP on the cultural transition in Yuchisi, China and its global linkage. Scientific Reports **6**:27723.
Wanner, H., O. Solomina, M. Grosjean, S. P. Ritz, and M. Jetel. 2011. Structure and origin of Holocene cold events. Quaternary Science Reviews **30**:3109-3123.
Watts, W. A. and M. Stuiver. 1980. Late Wisconsin climate of northern Florida and the origin of species-rich deciduous forest. Science **210**:325-327.
Whitlock, C. and P. J. Bartlein. 1997. Vegetation and climate change in northwest America during the past 125 kyr. Nature **388**:57-61.
Williams, J. W. and S. T. Jackson. 2007. Novel climates, no-analog communities, and ecological surprises. Frontiers in Ecology and the Environment **5**:475-482.
Williamson, S. 2001. A Field Guide to Hummingbirds of North America. Houghton Mifflin.
Xu, X., H. You, K. Du, and F. Han. 2011. An Archaeopteryx-like theropod from China and the origin of Avialae. Nature **475**:465-470.
Zhang, J.-X., C.-Z. Zhao, C.-Q. Yin, L.-L. Li, Z.-J. Hou, and J. Zhang. 2012. Relationship between the spatial pattern of nymph and adult abundance of Oedaleus asiaticus (Orthoptera: Acrididae) and topography in the alpine grassland in the upper reaches of Heihe River analyzed with the GAM model. Acta Entomologica Sinica **55**:1368-1375.